U.S. DEPARTMENT OF COMMERCE
National Technical Information Service

PB-256 320

Proceedings of the Stationary Source Combustion Symposium. Volume I. Fundamental Research

Industrial Environmental Research Lab.

June 1976

KEEP UP TO DATE

Between the time you ordered this report—which is only one of the hundreds of thousands in the NTIS information collection available to you—and the time you are reading this message, several *new* reports relevant to your interests probably have entered the collection.

Subscribe to the **Weekly Government Abstracts** series that will bring you summaries of new reports *as soon as they are received by NTIS* from the originators of the research. The WGA's are an NTIS weekly newsletter service covering the most recent research findings in 25 areas of industrial, technological, and sociological interest—invaluable information for executives and professionals who must keep up to date.

The executive and professional information service provided by NTIS in the **Weekly Government Abstracts** newsletters will give you thorough and comprehensive coverage of government-conducted or sponsored research activities. And you'll get this important information within two weeks of the time it's released by originating agencies.

WGA newsletters are computer produced and electronically photocomposed to slash the time gap between the release of a report and its availability. You can learn about technical innovations immediately—and use them in the most meaningful and productive ways possible for your organization. Please request NTIS-PR-205/PCW for more information.

The weekly newsletter series will keep you current. But *learn what you have missed in the past* by ordering a computer **NTISearch** of all the research reports in your area of interest, dating as far back as 1964, if you wish. Please request NTIS-PR-186/PCN for more information.

WRITE: Managing Editor
5285 Port Royal Road
Springfield, VA 22161

Keep Up To Date With SRIM

SRIM (Selected Research in Microfiche) provides you with regular, automatic distribution of the complete texts of NTIS research reports *only* in the subject areas you select. SRIM covers almost all Government research reports by subject area and/or the originating Federal or local government agency. You may subscribe by any category or subcategory of our WGA **(Weekly Government Abstracts)** or **Government Reports Announcements and Index** categories, or to the reports issued by a particular agency such as the Department of Defense, Federal Energy Administration, or Environmental Protection Agency. Other options that will give you greater selectivity are available on request.

The cost of SRIM service is only 45¢ domestic (60¢ foreign) for each complete microfiched report. Your SRIM service begins as soon as your order is received and processed and you will receive biweekly shipments thereafter. If you wish, your service will be backdated to furnish you microfiche of reports issued earlier.

Because of contractual arrangements with several Special Technology Groups, not all NTIS reports are distributed in the SRIM program. You will receive a notice in your microfiche shipments identifying the exceptionally priced reports not available through SRIM.

A deposit account with NTIS is required before this service can be initiated. If you have specific questions concerning this service, please call (703) 451-1558, or write NTIS, attention SRIM Product Manager.

This information product distributed by

NTIS U.S. DEPARTMENT OF COMMERCE
National Technical Information Service
5285 Port Royal Road
Springfield, Virginia 22161

[illegible]

[illegible]

PB 256 320

Environmental Protection Technology Series

REPRODUCED BY
NATIONAL TECHNICAL
INFORMATION SERVICE
U. S. DEPARTMENT OF COMMERCE
SPRINGFIELD, VA. 22161

RESEARCH REPORTING SERIES

Research reports of the Office of Research and Development, U.S. Environmental Protection Agency, have been grouped into five series. These five broad categories were established to facilitate further development and application of environmental technology. Elimination of traditional grouping was consciously planned to foster technology transfer and a maximum interface in related fields. The five series are:

1. Environmental Health Effects Research
2. Environmental Protection Technology
3. Ecological Research
4. Environmental Monitoring
5. Socioeconomic Environmental Studies

This report has been assigned to the ENVIRONMENTAL PROTECTION TECHNOLOGY series. This series describes research performed to develop and demonstrate instrumentation, equipment, and methodology to repair or prevent environmental degradation from point and non-point sources of pollution. This work provides the new or improved technology required for the control and treatment of pollution sources to meet environmental quality standards.

EPA REVIEW NOTICE

This report has been reviewed by the U.S. Environmental Protection Agency, and approved for publication. Approval does not signify that the contents necessarily reflect the views and policy of the Agency, nor does mention of trade names or commercial products constitute endorsement or recommendation for use.

This document is available to the public through the National Technical Information Service, Springfield, Virginia 22161.

TECHNICAL REPORT DATA

(Please read Instructions on the reverse before completing)

1. REPORT NO. EPA-600/2-76-152a	2.	3. RECIPIENT'S ACCESSION NO.
4. TITLE AND SUBTITLE Proceedings of the Stationary Source Combustion Symposium; Volume I--Fundamental Research		5. REPORT DATE June 1976 6. PERFORMING ORGANIZATION CODE
7. AUTHOR(S) Miscellaneous		8. PERFORMING ORGANIZATION REPORT NO.
9. PERFORMING ORGANIZATION NAME AND ADDRESS NA		10. PROGRAM ELEMENT NO. 1AB014; ROAP 21BCC 11. CONTRACT/GRANT NO. NA (In-house)
12. SPONSORING AGENCY NAME AND ADDRESS EPA, Office of Research and Development Industrial Environmental Research Laboratory Research Triangle Park, NC 27711		13. TYPE OF REPORT AND PERIOD COVERED Proceedings; 9/24-26/75 14. SPONSORING AGENCY CODE EPA-ORD

15. SUPPLEMENTARY NOTES Symposium Chairman J.S. Bowen, Vice-Chairman R.E. Hall, Mail Drop 65, Ext. 2470/2477.

16. ABSTRACT

The proceedings document the 37 presentations made during the Stationary Source Combustion Symposium held in Atlanta, Ga., September 24-26, 1975. Sponsored by the Combustion Research Branch of EPA's Industrial Environmental Research Laboratory--RTP, the symposium dealt with subjects related both to developing improved combustion technology for the reduction of air pollutant emissions from stationary sources, and to improving equipment efficiency. The symposium was divided into four parts and the proceedings were issued in three volumes: Volume I--Fundamental Research, Volume II--Fuels and Process Research and Development, and Volume III--Field Testing and Surveys. The symposium was intended to provide contractor, industrial, and Government representatives with the latest information on EPA in-house and contract combustion research projects related to pollution control, with emphasis on reducing nitrogen oxides.

PRICES SUBJECT TO CHANGE

17. KEY WORDS AND DOCUMENT ANALYSIS

a. DESCRIPTORS	b. IDENTIFIERS/OPEN ENDED TERMS	c. COSATI Field/Group
Air Pollution, Combustion, Field Tests	Air Pollution Control	13B 21B 14B
Combustion Control, Coal, Oils	Stationary Sources	21D 11H
Natural Gas, Nitrogen Oxides, Carbon	Combustion Modification	07B
Carbon Monoxide, Hydrocarbons, Boilers	Unburned Hydrocarbons	07C 13A
Pulverized Fuels, Fossil Fuels, Utilities	Fundamental Research	
Gas Turbines, Efficiency	Fuel Nitrogen	13G 14A
	Burner Tests	

18. DISTRIBUTION STATEMENT Unlimited	19. SECURITY CLASS *(This Report)* Unclassified	21. NO. OF PAGES
	20. SECURITY CLASS *(This page)* Unclassified	22. PRICE $12.00-2.25

EPA Form 2220-1 (9-73)

EPA-600/2-76-152a
June 1976

PROCEEDINGS OF THE STATIONARY SOURCE COMBUSTION SYMPOSIUM

VOLUME I--FUNDAMENTAL RESEARCH

Joshua S. Bowen, Chairman
Robert E. Hall, Vice-Chairman

Industrial Environmental Research Laboratory
Office of Energy, Minerals, and Industry
Research Triangle Park, NC 27711

ROAP No. 21BCC
Program Element No. 1AB014

Prepared for

U.S. ENVIRONMENTAL PROTECTION AGENCY
Office of Research and Development
Washington, DC 20460

PREFACE

The Stationary Source Combustion Symposium was held on September 24-26, 1975, at the Fairmont Colony Square Hotel in Atlanta, Georgia. The symposium was sponsored by the Combustion Research Branch of E.P.A.'s Industrial Environmental Research Laboratory (IERL). The Combustion Research Branch has been involved in developing improved combustion technology for the reduction of air pollutant emissions from stationary sources, and improving equipment efficiency.

Dr. Joshua S. Bowen, Chief, Combustion Research Branch, was Symposium Chairman; Robert E. Hall, Research Mechanical Engineer, Combustion Research Branch, was Symposium Vice Chairman and Project Officer. The Welcome Address was delivered by Dr. John K. Burchard, Director of the Industrial Environmental Research Laboratory. Frank Princiotta, Acting Director of the Energy Processes Division of E.P.A.'s Office of Energy, Minerals, and Industry, was the Keynote Speaker.

The Symposium consisted of four Sessions:

Session I: Fundamental Research

Co-chairmen: Dr. Joshua A. Bowen
W. Steven Lanier, Research Mechanical Engineer, E.P.A., IERL, Combustion Research Branch

Session II: Fuels Research and Development

Chairman: G. Blair Martin, Chemical Engineer, E.P.A., IERL,
Combustion Research Branch

Session III: Process Research and Development

Chairman: David G. Lachapelle, Research Chemical Engineer,
E.P.A., IERL, Combustion Research Branch

Session IV: Field Testing and Surveys

Co-chairmen: Robert E. Hall
John H. Wasser, Research Chemical Engineer, E.P.A.,
Combustion Research Branch

These Session Chairmen have reviewed the transcriptions of the question and answer sessions, and, in addition, have worked with authors to clarify and revise presentations, where appropriate, and to make them clear and meaningful for these printed proceedings.

We are grateful for the cooperation of Marjorie Maws, Project Leader; Anita Lord, Symposium Administrator; and Margaret Kilburn, Program Director, of Arthur D. Little, Inc., who coordinated the symposium for E.P.A.

CONTENTS

Preface iii

Welcome Address - J.K. Burchard I-1

Keynote Address - F.T. Princiotta I-3

SESSION I - FUNDAMENTAL RESEARCH

Formation of Soot and Polycyclic Aromatic Hydrocarbons (PCAH) in Combustion Systems I-18

J.D. Bittner, G.P. Prado, J.B. Howard, R.A. Hites

Questions and Answers I-32

Effects of Fuel Sulfur on Nitrogen Oxide Emissions. I-35

J.O.L. Wendt, J.M. Ekmann

Questions and Answers I-88

Two-Dimensional Combustor Modeling I-91

R.C. Buggeln, H. McDonald

Questions and Answers . . . . (n/a)

Effects of Interaction Between Fluid Dynamics and Chemistry on Pollutant Formation in Combustion I-109

C.T. Bowman, L.S. Cohen, L.J. Spadaccini, F.K. Owen

Questions and Answers I-119

Fate of Coal Nitrogen During Pyrolysis and Oxidation I-125

J.H. Pohl, A.F. Sarofim

Questions and Answers I-147

A Detailed Approach to the Chemistry of Methane/Air Combustion: Critical Survey of Rates and Applications I-153

V.S. Engleman

Questions and Answers I-182

Chemical Reactions in the Conversion of Fuel Nitrogen to NOx I-185

A.E. Axworthy, G.R. Schneider, V.H. Dayan

Questions and Answers I-211

Prediction of Premixed Laminar Flat Flame Kinetics, Including the Effects of Diffusion I-217

R.M. Kendall, J.T. Kelly, W.S. Lanier

Questions and Answers I-266

Estimation of Rate Constants I-267

S.W. Benson, R. Shaw, R.W. Woolfolk

Questions and Answers . . . . (n/a)

Production of Oxides of Nitrogen in Interacting Flames I-291

C. England

Questions and Answers I-316

Concurrent Panel Discussions:

1. Combustion Chemistry and Modeling: An Overview

A.F. Sarofim - Combustion Chemistry and Modeling I-325

Questions and Answers I-345

T.J. Tyson - The Mathematical Modeling of Combustion Devices I-347

Questions and Answers I-410

2. Federal, Regional, State, and Local Air Pollution Regulations: An Overview

S. Cuffe - Federal I-413
G.T. Helms - Regional I-429
R.H. Collum - State I-443
H.W. Poston - Local I-447

SESSION II - FUELS RESEARCH AND DEVELOPMENT

Assessment of Combustion and Emission Characteristics of Methanol and Other Alternate Fuels II-3

G.B. Martin

Questions and Answers II-30

Burner Design Criteria for Control of Pollutant Emissions from Natural Gas Flames II-31

D.F. Shoffstall

Questions and Answers . . . . (n/a)

Integrated Low Emission Residential Furnace II-81

L.P. Combs, W.H. Nurick, A.S. Okuda

Questions and Answers II-101

The Control of Pollutant Emissions from Oil Fired Package Boilers II-109

M.P. Heap, T.J. Tyson, E. Cichanowicz, R.E. McMillan, F.D. Zoldak

Questions and Answers II-160

Pilot Scale Investigation of Catalytic Combustion Concepts for Industrial and Residential Applications II-163

J.P. Kesselring, R.M. Kendall, C.B. Moyer, G.B. Martin

Questions and Answers II-196

The Optimization of Burner Design Parameters to Reduce NOx Formation in Pulverized Coal and Heavy Oil Flames II-197

M.P. Heap, T.J. Tyson, G.P. Carver, G.B. Martin, T.M. Lowes

Questions and Answers II-239

Pilot Scale Investigation of Combustion Modification Techniques for NOx Control in Industrial and Utility Boilers II-241

R.E. Brown, C.B. Moyer, H.B. Mason, D.G. Lachapelle

Questions and Answers II-267

SESSION III - PROCESS RESEARCH AND DEVELOPMENT

Overfire Air as an NOx Control Technique for Tangential Coal-Fired Boilers III-3

A.P. Selker

Questions and Answers III-26

Control of NOx Formation in Wall Coal-Fired Boilers III-31

G.A. Hollinden, J.R. Crooks, N.D. Moore, R.L. Zielke, C. Gottschalk

Questions and Answers III-77

The Effect of Additives in Reducing Particulate Emissions from Residual Oil Combustion III-83

R.D. Giammar, H.H. Krause, A.E. Weller, D.W. Locklin

Questions and Answers III-115

System Design for Power Generation from Low Btu Gas Boilers III-119

M.P. Heap, T.J. Tyson, N.D. Brown

Questions and Answers . . . . (n/a)

SESSION IV - FIELD TESTING AND SURVEYS

The Effect of Combustion Modification on Pollutants and Equipment Performance of Power Generation Equipment IV-3

A.R. Crawford, E.H. Manny, M.W. Gregory, W. Bartok

Questions and Answers IV-109

Analysis of Gas-, Oil-, and Coal-Fired Utility Boiler Test Data IV-115

O.W. Dykema, R.E. Hall

Questions and Answers IV-161

Influence of Combustion Modifications on Pollutant Emissions from Industrial Boilers IV-163

G.A. Cato, L.J. Muzio, R.E. Hall

Questions and Answers IV-219

Emission Characteristics of Small Gas Turbine Engines IV-227

J.H. Wasser

Questions and Answers IV-252

Systems Evaluation of the Use of Low-Sulfur Western Coal in Existing Small- and Intermediate-Sized Boilers IV-255

K.L. Maloney

Questions and Answers IV-316

A Survey of Emissions Control and Combustion Equipment Data in Industrial Process Heating IV-321

P.A. Ketels, J.D. Nesbitt, D.R. Shoffstall, M.E. Fejer

Questions and Answers . . . . (n/a)

POM and Particulate Emissions from Small Commercial Stoker-Fired Boilers IV-411

R.D. Giammar, R.B. Engdahl, R.E. Barrett

Questions and Answers IV-439

Concluding Remarks - J.S. Bowen IV-441

Appendix

List of Speakers A-1
List of Participants
    Alphabetically by Name A-2
    Alphabetically by Organization A-6

WELCOME ADDRESS

U.S. E.P.A. STATIONARY SOURCE COMBUSTION SYMPOSIU

September 24, 1975

Atlanta, Georgia

Dr. John K. Burchard
Director, E.P.A. Industrial
Environmental Research Laboratory

I see by the program that I have just given the welcoming speech. I think one of the chief virtues of welcoming speeches is that they be brief, so I will be.

On behalf of the Environmental Protection Agency and particularly the Industrial Environmental Research Laboratory, I would like to welcome you to this symposium. I still have trouble saying IERL, because up until our recent reorganization we were known as the Control Systems Laboratory, but we are basically the same bunch of people. Our mission now is enlarged slightly in that whereas we used to be strictly confined to air pollution activities, we will now be involved in certain water pollution and solid waste activities, so the scope of our activities has broadened some. I would like to emphasize that we want to engage in technology transfer in these kind of symposia. We'd like to tell you what we're doing, what people that we are sponsoring are doing, and we'd like to get feedback from you on questions you have and things that you would like to know more about. There is a special questionnaire in the program booklet for this kind of thing.

As is shown in the program, Day One will focus primarily on fundamental research and development. The second day will be on fuels research and development and process R&D, and the last day will focus on field testing surveys. At the end of today there will be a concurrent panel discussion, and I hope you can decide on which one to attend. One is on air pollution regulations and the other on combustion chemistry.

Well, as I said, I'd like to keep it brief. Again, it's a pleasure to have you here. We, after all, feel that the major purpose of all our work is to try to spread the results of our work amongst the technical and user community and those are you people; so, I hope this will be a worthwhile and productive few days.

Thank you.

Keynote Address at EPA's
Stationary Source Combustion Symposium

Atlanta, Georgia
September 24, 1975

Frank T. Princiotta
Acting Director, Energy Processes Division
Office of Energy, Minerals & Industry
Office of Research & Development
Environmental Protection Agency
Washington, D.C.

I welcome you to the Industrial Environmental Research Laboratory's (IERL) Stationary Source Combustion Symposium. I am pleased that I have been asked to present the Keynote address, and trust that my remarks will be relevant and informative. I believe the most fruitful approach for my 10-minute address is to briefly explain the EPA research and development organization and show where EPA-sponsored stationary source combustion efforts fit in. Also, even more importantly, I will touch upon the status of EPA's NO_x emission control strategy, since this represents the driving forces for utilization of much of the technology we will hear about at this Symposium.

Recently, the EPA's Office of Research and Development has been reorganized under the direction of the newly appointed Assistant Administrator (AA), Dr. Wilson Talley, and his Associate Assistant Administrator, Carl Gerber. Briefly, the new organization calls for each of the 15 field laboratories to report directly to one of the four headquarters Office Directors, who in turn report directly to Dr. Talley. Figure 1 shows each office and its performing laboratories.

Generally, the headquarters staff performs strategic planning with emphasis on resource allocation by major technical category; the laboratory implements the research and development program through extramural and intramural efforts. As you can see, the IERL-RTP reports to Dr. Stephen Gage's Office of Energy, Minerals and Industry. This office has two headquarters staff Divisions: the Energy Processes Division of which I am Acting Director, and the Industrial and Extractive Processes Division under the directorship of Dr. Peter Lederman. As you may have guessed by now, all control technology development work for energy and industrial sources falls within the responsibility of OEMI and its two IERL laboratories. Generally, the assignment of R,D&D implementing responsibilities between the two IERL laboratories is based on assigning specific industries (and their pollutants) to each laboratory. Since IERL-RTP has been assigned the utility and industrial boiler "industries," essentially the total stationary source combustion control technology program is performed under their auspices. As many of you know, Josh Bowen's Combustion Research Branch reporting to Bob Hangebrouck's Energy Assessment and Control Division is the group within IERL-RTP responsible for the stationary source combustion program.

It is important to note that the funding for the NO_x control technology part of EPA's program is based upon a special Congressional energy appropriation which is supplemental to the Office of Research and Development's Base Program. This supplementary appropriation, which was initiated in fiscal year 1975, includes funding for a comprehensive energy/environmental research and development program involving control technology development and process and effects research related to conventional and second-generation energy sources. The energy appropriations was $134 million in FY 1975 of which $81 million was for control technology development. In fiscal year 1976, the funding leveal was reduced to $100 million of which $59 million is for control technology development. We are hopeful that the FY 77 appropriation will be close to the FY 76 funding levels. Despite the reduction in control technology funding from FY 75 to FY 76, energy funding for the NO_x control technology program increased from $3.8 million in FY 75 to $7.7 million in FY 76. Further increases in funding are considered likely. Funding will continue to increase in this area since NO_x control from stationary sources is growing in importance. This is an appropriate lead-in to the next subject I would like to briefly discuss--the overall EPA strategy--attaining acceptable ambient air quality with regard to NO_2 concentrations.

As many of you know, there has not been substantial progress made toward attainment of the national ambient air quality standard for NO_2 since it was discovered in 1972 that the Federal reference method (Jacobs-Hochheiser technique) for measuring ambient NO_2 was unreliable. As a result of this discovery, 43 of the 47 Air Quality Control Regions which were originally thought to have a serious NO_2 problem (Priority I) were reclassified to Priority III, since alternative* NO_2 measurement techniques indicated that standards were not exceeded in these regions. This left Los Angeles, New York, Chicago and Salt Lake City AQCR's which are presently classified as Priority I. However, recent data which the EPA Administrator presented at his May 1975 news conference indicate that now at least 16 AQCR's are presently exceeding the NO_2 standard and that several other regions may have difficulty in maintaining the NO_2 standard. It is apparent that the NO_2 problem is getting more serious, and more stringent stationary and mobile source NO_x control will be required.

---

* EPA has activated a schedule which will designate reference NO_2 measurement methods by June 1976; this should help clarify the NO_2 situation and allow a more aggressive NO_x control strategy to be undertaken.

At the present time, only modest NO_x control emission standards have been applied to both new mobile and stationary sources on a national basis. It appears that the existing 3.1 gm/mile emission standard for automobiles and New Source Performance Standards (NSPS) for coal, oil and gas-fired steam generators and nitric acid plants will not be adequate to meet and maintain ambient air quality standards in many parts of the country. Presently, additional NSPS for additional sources are being considered and appear likely for: Stationary gas turbines, lignite steam generators, stationary internal combustion engines and intermediate-size coal, oil and gas-fired boilers. But again, these additional NSPS, even if combined with a more stringent (2.0 gm/mile) auto standard, may not provide an adequate level of control for many regions.

The most definitive document evaluating various NO_x mobile and stationary control strategies which I am familiar with, is the Air Quality, Noise and Health Panel Report of the Department of Transportation Study on Mobile Source Goals Beyond 1980. This report is only in a draft version and is not yet available for publication. The basic analytical approach utilized was to estimate the incremental cost of various levels of emission controls for a variety of mobile and stationary sources needed to decrease emissions from assumed 1980 levels. The incremental costs are then used to determine the cost-effectiveness of each level of control. It was assumed that baseline emissions in 1980 would be as follows:

Source	1980 Emissions	1980 Control Technology Assumed
light-duty vehicles	3.8×10^6 tons NO_x/yr	2.0 gm/mile (catalytic converter)
heavy-duty vehicles	4.8×10^6	10.0 gm/mile
stationary sources	25.5×10^6	Based on NSPS constraints, an average of 25% emission control from all sources
Total	34.1×10^6	

Based on these baseline emissions, and the best available information regarding the effectiveness and cost for various second-generation mobile and stationary control technologies, these technologies were evaluated for their cost-effectiveness and impact on NO_x emissions. Table 1 summarizes the results of this exercise.

The implications of this study are as follows:

- The most cost-effective NO_x control approaches, which can control up to 27% of baseline emissions, involve second-generation combustion modification techniques for utility and industrial boilers and stationary IC engines. Such control can be achieved for an investment of only $100-225/ton of NO_x removed.
- The cumulative control of baseline emissions can be increased from 27 to 44% with heavy-duty vehicular control tightened from 10 gm/mile to 2 gm/mile and for automobile control tightened to 1.0 gm/mile. Such incremental control will cost about $450/ton.
- The next major reduction of NO_x emissions can be attained by more stringent control of utility boilers using the expensive

flue gas cleaning techniques estimated at $1200/ton. Such technology used in conjunction with the aforementioned technique can yield overall cumulative control of baseline emissions to 63%.

- Further emission control beyond the utilization of flue gas cleaning may be prohibitively expensive and will only increase overall control from 63 to 69%. This would require increasing control from stationary IC engines from 75 to 90% control ($1700/ton) and further control of auto emissions to 0.4 gm/mile.

The implications of this study are displayed graphically in Figure 2 using cost as a function of tons of NO_x removed. Three categories are shown: (1) a mobile source approach; (2) a stationary source approach; and (3) most cost-effective approach for combined stationary and mobile source control.

Although such a study is only as good as the many assumptions made regarding effectiveness and cost of second-generation control technologies, I believe it clearly indicates the major role that stationary source control will play in the years ahead. I have no doubt that many of the control techniques described at this Symposium will help us achieve acceptable NO_2 ambient levels.

Table 1
COST-EFFECTIVE STRATEGIES FOR CONTROL OF NO_x EMISSIONS DURING YEAR 2000

CONTROL STRATEGY	CONTROL TECHNOLOGY (PROJECTED)	NO_x REMOVED (10^6 tons)	% OF BASELINE EMISSIONS**	CUL % OF BASELINE	COST-EFFECTIVENESS ($/ton)	ANNUAL COST OF STRATEGY (billion $)	CUL-ANNUAL COST (billion $)	CUL NO_x REMOVED (10^6 tons)
New Utility Boilers From 25% to 50% Control	Low Excess Air (LEA) & Staged Comb. (SC) (or Flue Gas Retrc.) (FGR)	3.52	10	10	100	0.35	0.35	3.5
Industrial Boilers From 25% to 65% Control	LEA & SC (or FGR)	2.46	7	17	150	0.37	0.72	6.0
Exist. Util. Boilers from 25% to 50% Control	LEA & SC (or FGR)	0.62	2	19	225	0.14	0.86	6.6
Sta. IC Engines From 25% to 75% Control	Not Well Defined at Present Time	2.87	8	27	340	0.98	1.84	9.5
Other Mobile From 10 gm/mile to 80% Control	Catalytic Converter	3.82	11	3	450	1.72	3.56	13.3
LDV From 2.0 to 1.0 gm/mile	Adv. Catalytic Converter and/or New Engines	1.91	6	44	450	0.86	4.42	15.2
Util. Boilers From 50% to 90% Control	Flue Gas Cleaning	6.62	19	63	1200	7.94	12.36	21.8
Sta. IC Engines From 75% to 90% Control*	Not Well Defined at Present Time	0.86	3	66	1700	1.46	13.82	22.7
LDV to 0.4 gm/mile	Adv. Catalytic Converter and/or New Engines	1.15	3	69	2300	2.65	16.47	23.8

* STA IC ENG Control Does Not Include Small Engines

** Baseline Emissions = 34.1 X 10 Tons in 2000 and is Based Upon - LDV Standard 2.0 gm/mile Other Mobile 10 gm/mile, 25% Control of All Stationary Source Emissions.

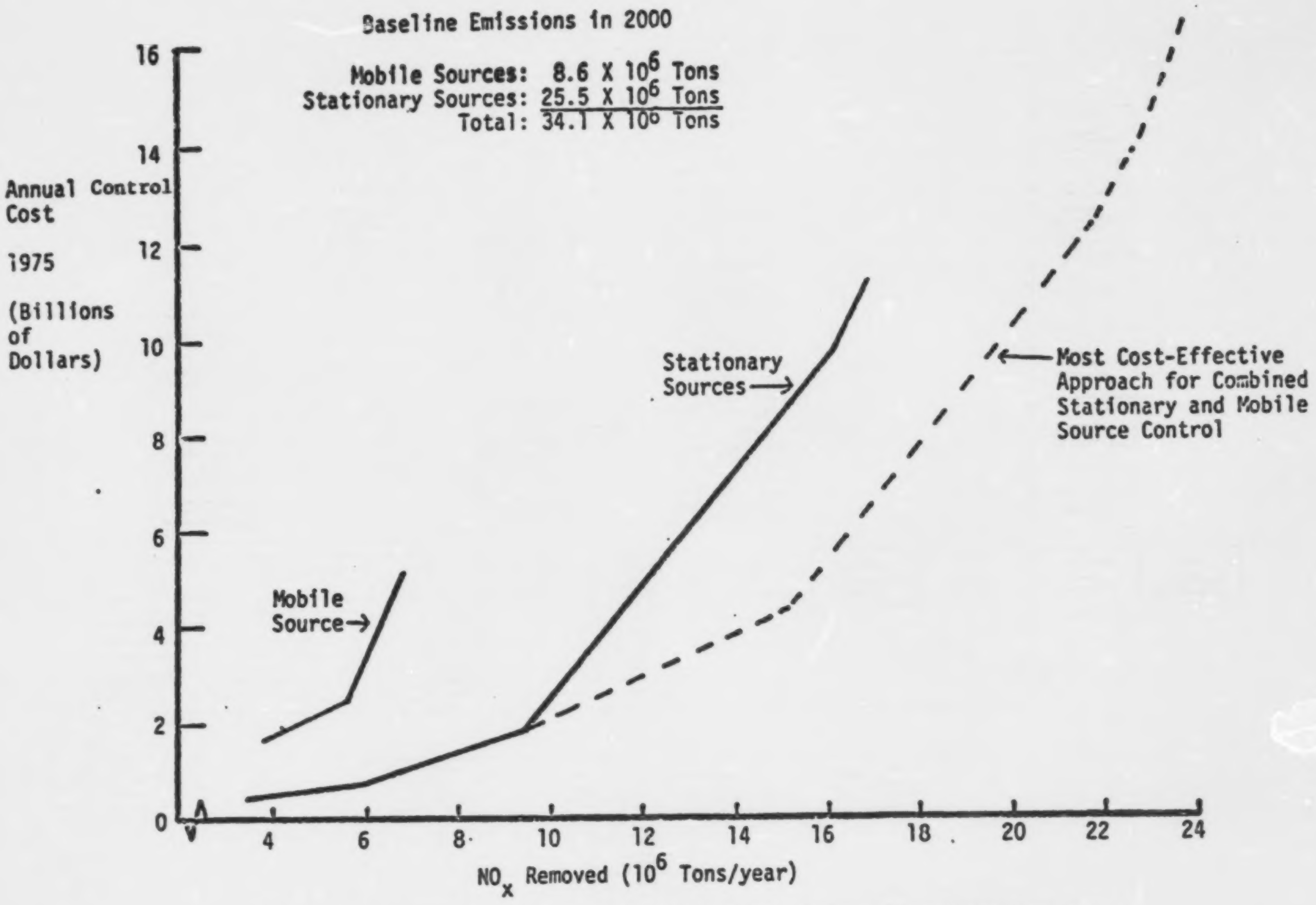

Figure 2 Comparison of Cost VS Tons of NO_x Removed From Baseline Case for Mobile Sources, Stationary Sources, and Optimum Cost-Effective Strategy, For The Year 2000.

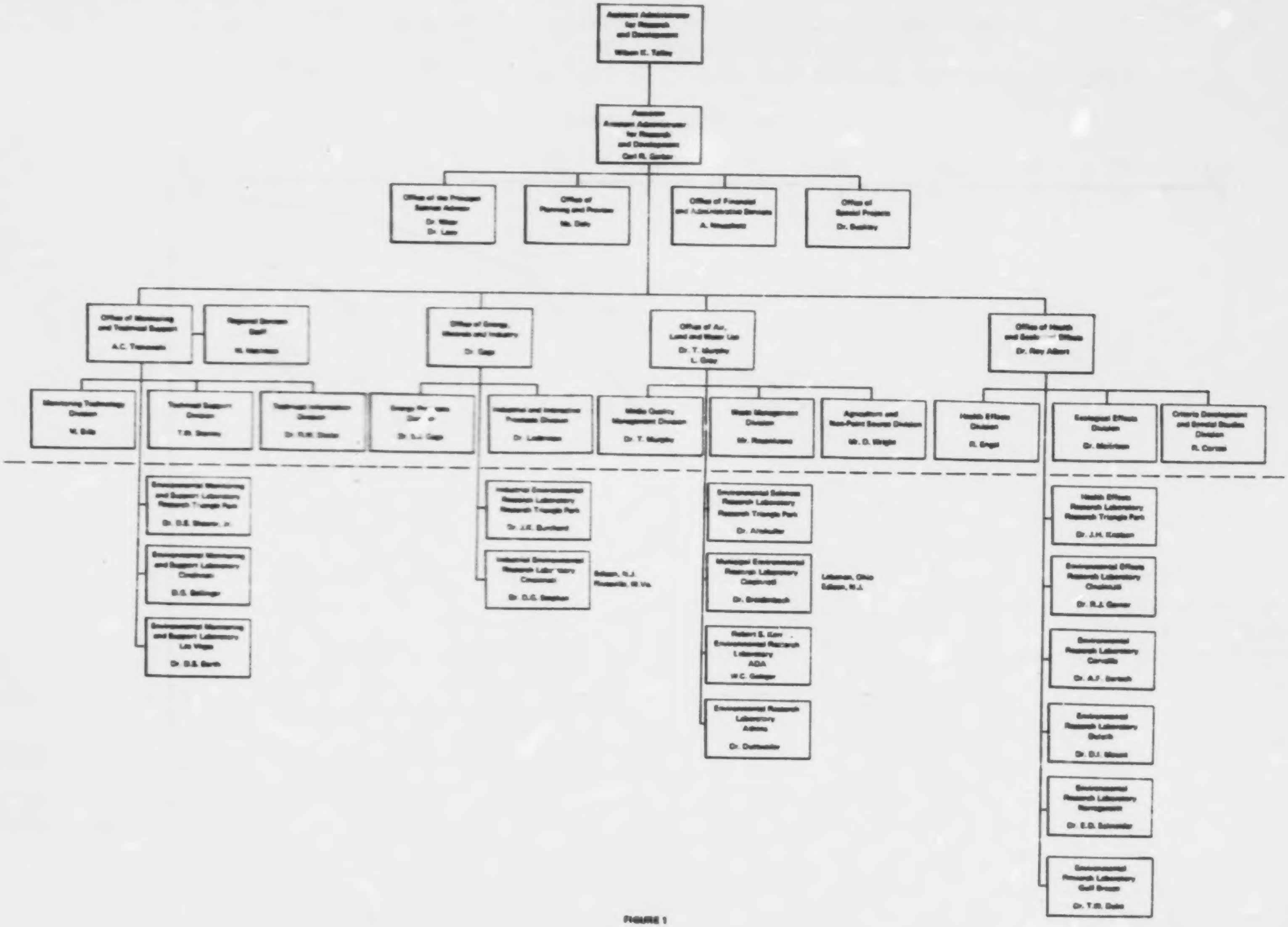
Assistant Administrator
for Research
and Development
Wilson K. Talley
Associate
Assistant Administrator
for Research
and Development
Carl R. Gerber
Office of the Principal
Science Advisor
Dr. Wiser
Dr. Lee
Office of
Planning and Review
Ms. Daly
Office of Financial
and Administrative Services
A. Neustadt
Office of
Special Projects
Dr. Buckley
Office of Monitoring
and Technical Support
A.C. Trakowski
Regional Services
Staff
H. Harrison
Office of Energy,
Minerals and Industry
Dr. Gage
Office of Air,
Land and Water Use
Dr. T. Murphy
L. Gray
Office of Health
and Ecological Effects
Dr. Roy Albert
Monitoring Technology
Division
H. Bills
Technical Support
Division
T.R. Stanley
Technical Information
Division
Dr. R.M. Dobbs
Energy Processes
Division
Dr. S.J. Gage
Industrial and Extractive
Processes Division
Dr. Ludemann
Media Quality
Management Division
Dr. T. Murphy
Waste Management
Division
Mr. Rosenkranz
Agriculture and
Non-Point Source Division
Mr. D. Wright
Health Effects
Division
R. Engel
Ecological Effects
Division
Dr. McIntosh
Criteria Development
and Special Studies
Division
R. Cortesi
Environmental Monitoring
and Support Laboratory
Research Triangle Park
Dr. D.E. Shearer, Jr.
Environmental Monitoring
and Support Laboratory
Cincinnati
D.G. Ballinger
Environmental Monitoring
and Support Laboratory
Las Vegas
Dr. D.S. Barth
Industrial Environmental
Research Laboratory
Research Triangle Park
Dr. J.K. Burchard
Industrial Environmental
Research Laboratory
Cincinnati
Dr. D.G. Stephan
Edison, N.J.
Rockville, W.Va.
Environmental Sciences
Research Laboratory
Research Triangle Park
Dr. Altshuller
Municipal Environmental
Research Laboratory
Cincinnati
Dr. Breidenbach
Lebanon, Ohio
Edison, N.J.
Robert S. Kerr
Environmental Research
Laboratory
ADA
W.C. Galegar
Environmental Research
Laboratory
Athens
Dr. Duttweiler
Health Effects
Research Laboratory
Research Triangle Park
Dr. J.H. Knelson
Environmental Effects
Research Laboratory
Cincinnati
Dr. R.J. Garner
Environmental
Research Laboratory
Corvallis
Dr. A.F. Bartsch
Environmental
Research Laboratory
Duluth
Dr. D.I. Mount
Environmental
Research Laboratory
Narragansett
Dr. E.D. Schneider
Environmental
Research Laboratory
Gulf Breeze
Dr. T.W. Duke

FIGURE 1

8:35 a.m.
Keynote Address
Frank Princiotta

Q: On the column where it said percent of control, say it was 10%, did that mean that you could control 10% of the emissions or reduce them to 10%?

A: No, that is 10% control of the base line emissions. In other words, I gave you the number of 34,000,000 tons per year assumed in 1980. That very first level of control would mean that roughly 3.4 million tons could be controlled utilizing the technology, then as you add these other strategies you are able to increase that percentage to, at the very most, roughly 2/3 of all the emissions. I might point out that obviously this is a somewhat simplified analysis and one has got to be worried about ambient air quality in specific locations; one has got to be worried about nitrates as probably being an important pollutant, perhaps as important as NO_2. There are many complications through an analysis of this type. I don't want to imply that, by any means, this will be the sole basis of EPA policies; it certainly will not.

Q: You use a dollar per ton basis; what's the unit? Is that tons of coal used?

A: It's tons of NO_x removed by the control process.

Q: Would you care to comment on these 1980's standards that you are hinting at, in terms of pounds per million Btu's fired for stationary power plants of the 500 megawatt variety - what the implications were? For example, at the moment it is .7 pounds of NO_x per million Btu's fired for coal. Do you contemplate a tighter restriction than that?

A: It's a very complex issue. I can just give you a personal opinion and that is that we will, within the next decade, see tighter standards on the big sources. In my own opinion, the only question is will it be a tighter standard than a combustion modification technology would allow. As you may know, in Japan, which is primarily an oil burning country, there are standards so tight that combustion modifications are not sufficient. Controls beyond 50-60% are required in some areas and there they have to go to flue gas cleaning. Whether or not this will happen in this country I don't know, but I personally think it's likely that within the foreseeable future, within the next 10 years, we may see a tightening up on coal-fired steam generators. It's apparent that our present strategy is not good enough.

Q: I don't want to totally quote Dr. Bowen out of context, but in the April 14 American Flame Research Committee meeting he quoted coal standards for 1980 around 200 ppm and for 1985 around 100 ppm; do you know if these are still good numbers?

[Dr. Bowen]

A: I don't believe I quoted these as standards that we would be achieving. These were targets that we would be aiming for in our technology development effort.

Q: In noting the numbers you have on the chart there, it was emission tons controlled and certainly the thing we're all concerned with is ambient concentrations. Do you intend to expand your study to relate the control to tons at an ambient level rather than a ton emission level? We see in our area that a certain amount of control on the mobile sources can take care of a great deal more of the ambient level concentrations of NO_x than control on the industrial sources.

A: Yes, as I mentioned before I think this is right. Analysis is continuing in this area and our Office of Air Quality, Planning and Standards is doing these kinds of analyses. Clearly they'll have to do it on a regional basis and will have to take into account transport phenomena. My presentation was based on a superficial study indicating the relative priorities of control for stationary versus mobile sources.

Q: I wonder if you were able to look at the energy impact of the various options you had listed.

A: No, I'm afraid this particular study from the Department of Transportation, to my knowledge, did not look at the energy impact. I think we will probably be hearing at this symposium a little bit about what the energy situation might be with combustion modification technology associated with so many strategies. As far as flue gas cleaning is concerned, that is a fairly energy-intensive operation, and some of the systems in Japan would probably require several percentage points of a total power plant output to run their flue gas cleaning units; probably energy usage is not quite as high but in the same ball park as FCD scrubbers.

SESSION I

FUNDAMENTAL RESEARCH

Dr. J. S. Bowen; W. S. Lanier
Co-Chairmen

Preceding page blank

THE FORMATION OF SOOT AND POLYCYCLIC AROMATIC HYDROCARBONS (PCAH) IN COMBUSTION SYSTEMS

By:

J.D. Bittner, G.P. Prado, J.B. Howard, R.A. Hites

Fuels Research Laboratory

Department of Chemical Engineering

Massachusetts Institute of Technology

Cambridge, Massachusetts

Introduction

Soot formation in combustion systems has been studied for many years with the long range objective of attaining a working knowledge of the process to aid in predicting flame emissivities for radiative heat transfer problems. However, recently concern has been expressed that soot and some of the organic compounds associated with incomplete combustion may become pollution problems that will have to be controlled. It is known that some polycyclic aromatic hydrocarbons (PCAH) produced in flames and adsorbed on soot particles are carcinogenic. Soot and other organic particulate matter may not be the most abundant particulates emitted, but because the small particles (< 0.2 μm) are easily injested deep into the respiratory system, they may be one of the types of particulates most hazardous to human health. The NOx control strategies such as lower temperature combustion and staged combustion presently being considered work to increase PCAH and soot formation. Another change in combustion practices that could increase the emissions of particulate organic matter is the predicted increased use of coal as a solid or heavy liquid since highly aromatic fuels are known to be troublesome in this respect.

The mechanism of soot formation in combustion systems is not well understood. Some of the mechanisms proposed over the years and the confusion surrounding the role of PCAH in the process are illustrated in Figure 1. Since soot particles contain many more carbon atoms and a much lower H/C ratio than the fuel molecules, soot formation must involve processes of aggregration (top to bottom) and dehydrogenation (left to right). The extreme routes, the C_2 route and the saturated polymer route, are unlikely to occur under typical combustion conditions.[1] The C_2 route may be important at high temperatures around 3000°K, and below 700°K and at long reaction times the saturated polymer route may occur. But, around 2000°K most mechanisms can be represented by the central portion of Figure 1. From this figure it is seen that PCAH species have been postulated to serve as nuclei for soot growth by surface decomposition of any number of hydrocarbon species (including themselves). They have been postulated to be of sufficiently low vapor pressure to physically condense to liquid droplets, which then form soot. They have also been postulated to be stable byproducts of the soot formation process.

Project Objectives

In light of the concern over particulate organic matter as a pollutant and the confusion surrounding soot formation mechanisms and the role of PCAH, the overall objective of the project is to assess qualitatively and quantitatively the production of particulate organic matter (soot and organic compounds) in well-defined yet relevant combustion systems. To that end two types of information are of interest: the identities of PCAH and concentrations of soot and PCAH i) emitted from the flame and ii) at different stages of the combustion process.

To obtain the information on PCAH and soot emissions measurements on both laminar and turbulent atmospheric pressure diffusion flames are being made. Extensive measurements on the turbulent diffusion flame are being made possible by interaction with the Mechanical Engineering Department at M.I.T. on soot and other emissions research. One benefit of this type of collaboration is the opportunity to study the role of turbulent mixing on soot and PCAH emissions and the resulting interdependencies with NOx and CO emissions. In prior research efforts measurements of CO and NOx emissions have been made on this burner system and a model to characterize the mixing process has been developed and tested.[9-11]

To obtain the information on factors that govern PCAH and soot emissions a low pressure laminar flat premixed flame was chosen. In such a flame the kinetic processes are easily studied because the different stages are well resolved in time and space. The low pressure system allows the use of on-line mass spectrometry which is difficult with high pressure particle-laden gases because of clogging of the sampling probe orifice.

Low Pressure Flat Flame Study

A schematic of the apparatus to be used in the low pressure flat flame study is shown in Figure 2. A modulated molecular beam mass spectrometer system will be used for on-line analysis of gas phase species over the atomic mass range of 1 - 1000 a.m.u. A major advantage of this sampling-analysis technique over other techniques is that the excellent quenching possible with molecular beam sampling allows detection of reactive free radical species. Other advantages are the extension of the mass range beyond that usually studied with gas chromatography (< 400 a.m.u., limited by volatility) and the quick analysis of species of all molecular weights within the extended mass range. One disadvantage of mass spectrometry is that it cannot distinguish between isomers. To help sort out the isomer problem a cryogenic sample collector has been designed to trap the beam of gas for combined gas chromatography - mass spectrometry (G.C.-M.S.) analysis.

Samples of soot particles will be collected by placing electron microscope grids into the beam. From the electron microscope analysis particle number concentrations and size distributions will be obtained.

Data to be taken are concentration profiles of low and high molecular weight species, temperature profiles and particle number concentrations and size distributions as a function of position in the flame. Acetylene-oxygen flames of several fuel equivalence ratios and burner exit velocities will be investigated over the pressure range 2 to 5.33 kN/m^2 (15 to 40 torr). The particle data will be reduced to rates of particle nucleation, growth and coagulation with an existing model.[2,3] These rates will then be used with the organic species gas phase concentration data to investigate the factors governing PCAH and soot formation.

Turbulent Diffusion Flame Study

The burner being used for the atmospheric pressure turbulent diffusion flame study is shown in Figure 3. This burner can be operated with either liquid or gaseous fuel, and a selection of nozzles with and without atomizing air. Gas and soot samples are collected with the water-flushed sampling probe shown in Figure 4. The water injection design has several advantages over conventional water-cooled probes. The injected water prevents soot deposition and clogging thereby allowing quantitative collection of the soot without having to perform the tedious task of scraping the probe after each sample is taken. After passing through the probe, the water, gas and particulates pass through a tightly packed glass fiber filter where the soot is deposited. The water and gas then pass through a condenser for cooling. The water is collected in a large flask and the gas flow is measured by a wet test meter after passing through an ice bath condensate trap and vacuum pump. The amount of soot collected is determined by weighing the dried filter before and after collection. The filter with the soot deposit is then extracted with methylene dichloride. The filter is again dried and weighed. The soot is thus classified as carbonaceous residue and methylene dichloride soluble material. The methylene dichloride soluble portion is then concentrated by evaporation and analyzed by G.C.-M.S. for PCAH compounds. The carbonaceous residue is then removed from the filter and dispersed in an ultrasonic bath and deposited on electron microscope grids for particle size distribution analysis.

The G.C.-M.S. systems used in this study have both high and low resolution mass spectrometry interfaced with an IBM 1800 computer for data storage and processing. The details of the system and its use for identification of PCAH are described elsewhere.[4-8]

The data being collected on this burner system are the mass loadings of soot, the number concentration and size distribution of soot particles and concentrations of individual PCAH species. This information is being obtained at different positions along the axis of the burner as well as in the exhaust gases. Formation of particulate organic matter is being studied for several fuel equivalence ratios and fuel injection modes. Kerosene is currently being used as the fuel. Future plans are to study different liquid and gaseous fuels.

Preliminary Measurements of Soot Mass Loadings

Preliminary scoping runs to measure soot loadings with kerosene and air have yielded some interesting results. The soot loadings in units of mg of soot per standard cubic meter of gas for a fuel equivalence ratio, $\phi = 1.0$ and three atomizing air pressures are shown in Figure 5. Profiles along the axis of the burner for atomizing air pressures of P = 205 kN/m^2 (15 psig) and P = 239 kN/m^2 (20 psig) show decreasing soot loadings beyond 10 cm from the nozzle. The interesting point, however, is the strong dependence that the soot loading at the exhaust (53 cm) has on the atomizing air pressure. The soot emission increases four orders of magnitude for a decrease in atomizing air pressure from P = 239 kN/m^2 (20 psig) to 205 kN/m^2 (10 psig). Flagan and Appleton[9] measured NOx emissions from this burner under similar conditions (ϕ = 0.99, pyridine doped kerosene fuel) and found NOx concentrations in the exhaust to be reduced by a factor of two when the atomizing air pressure was decreased from 301 kN/m^2 (29 psig) to 184 kN/m^2 (12 psig). This illustrates the extreme sensitivity of soot emissions and possibly PCAH emissions to changes in combustor firing practices in efforts to reduce NOx formation. The importance of studying soot particle and hydrocarbon formation and their oxidation for modelling staged combustors is apparent.

Acknowledgements

We are grateful to Dr. Richard C. Flagan for valuable collaboration. One of us (G.P.P.) received financial support from a N.A.T.O. Fellowship, Honeywell Inc., and Center National de la Richerche Scientifique, Ministère de L'Éducation Nationale (France); the major fraction of support is from EPA grant no. R803242.

References

1. Palmer, H.B. and C.F. Cullis, "The Formation of Carbon from Gases" in "Chemistry and Physics of Carbon," Vol. 1, P.L. Walker, ed., pp. 265-325, Marcel Dekker, Inc., N.Y. (1965).

2. Wersborg, B.L., J.B. Howard and G.C. Williams, Fifteenth Symposium (International) on Combustion, The Combustion Institute, Pittsburgh, p. 929, (1973).

3. Wersborg, B.L., J.B. Howard and G.C. Williams, Faraday Symposia of the Chemical Society, No. 7, 109 (1973).

4. Hites, R.A. and K. Biemann, Anal. Chem., 39, 965 (1967).

5. Hites, R.A. and K. Biemann, Anal. Chem., 40, 1217 (1968).

6. Hites, R.A. and K. Biemann, Anal. Chem., 42, 855 (1970).

7. Hertz, H.S., R.A. Hites and K. Biemann, Anal. Chem., 43, 681 (1971).

8. Hites, R.A., A.C.S. Division of Petroleum Chemistry Preprints 20, 824 (1975).

9. Flagan, R.C. and J.P. Appleton, Combustion and Flame, 23, 249 (1974).

10. Appleton, J.P. and J.B. Heywood, The Fourteenth Symposium (International) on Combustion, The Combustion Institute, Pittsburgh, p. 777 (1973).

11. Pompei, F. and Heywood, J.B., Combustion and Flame, 19, 407 (1972).

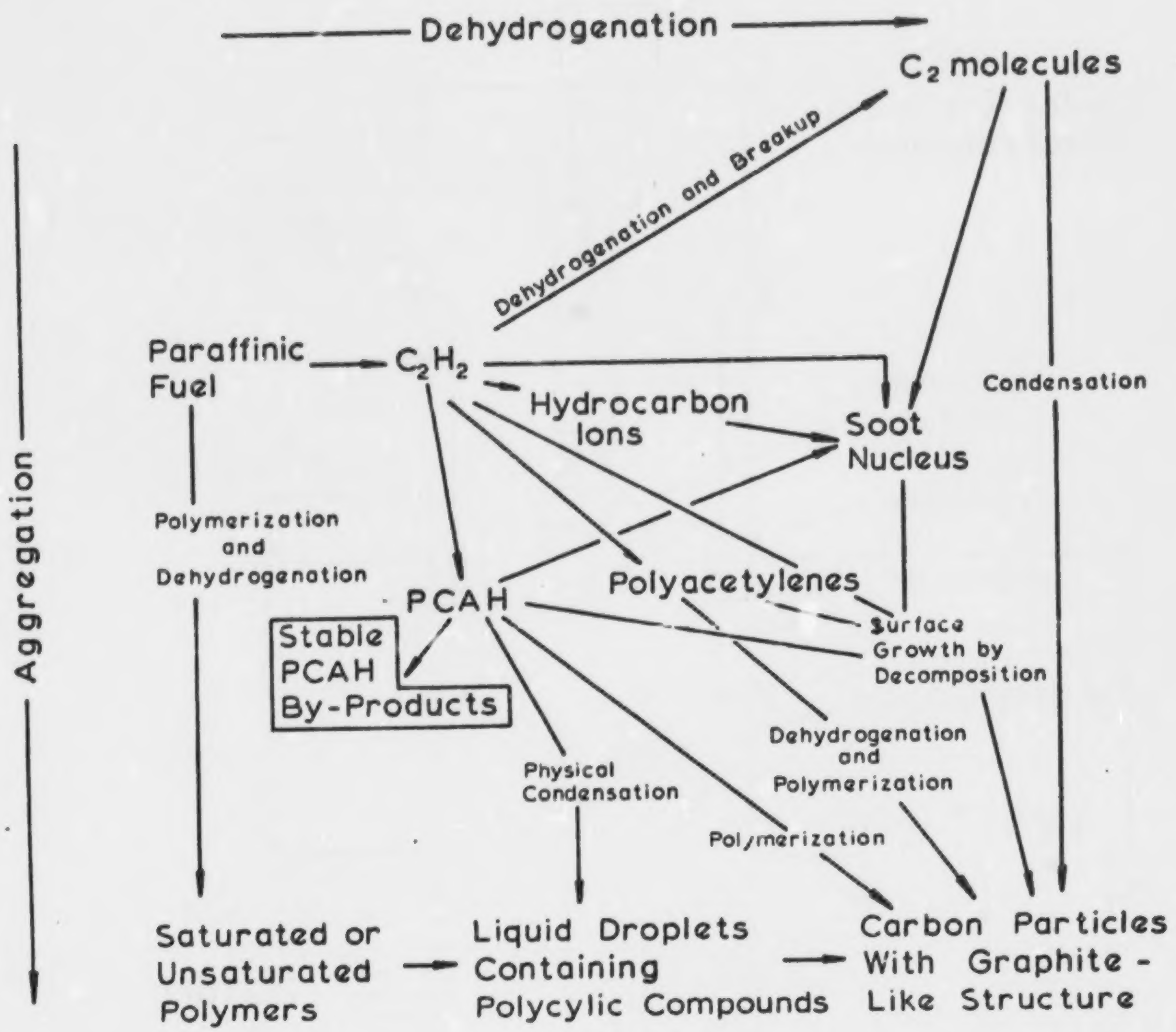
Dehydrogenation
C₂ molecules
Dehydrogenation and Breakup
Aggregation
Paraffinic Fuel
C2H2
Hydrocarbon Ions
Soot Nucleus
Condensation
Polymerization and Dehydrogenation
PCAH
Polyacetylenes
Stable PCAH By-Products
Surface Growth by Decomposition
Physical Condensation
Dehydrogenation and Polymerization
Polymerization
Saturated or Unsaturated Polymers
Liquid Droplets Containing Polycylic Compounds
Carbon Particles With Graphite - Like Structure

Figure 1 Summary of proposed mechanisms of soot formation

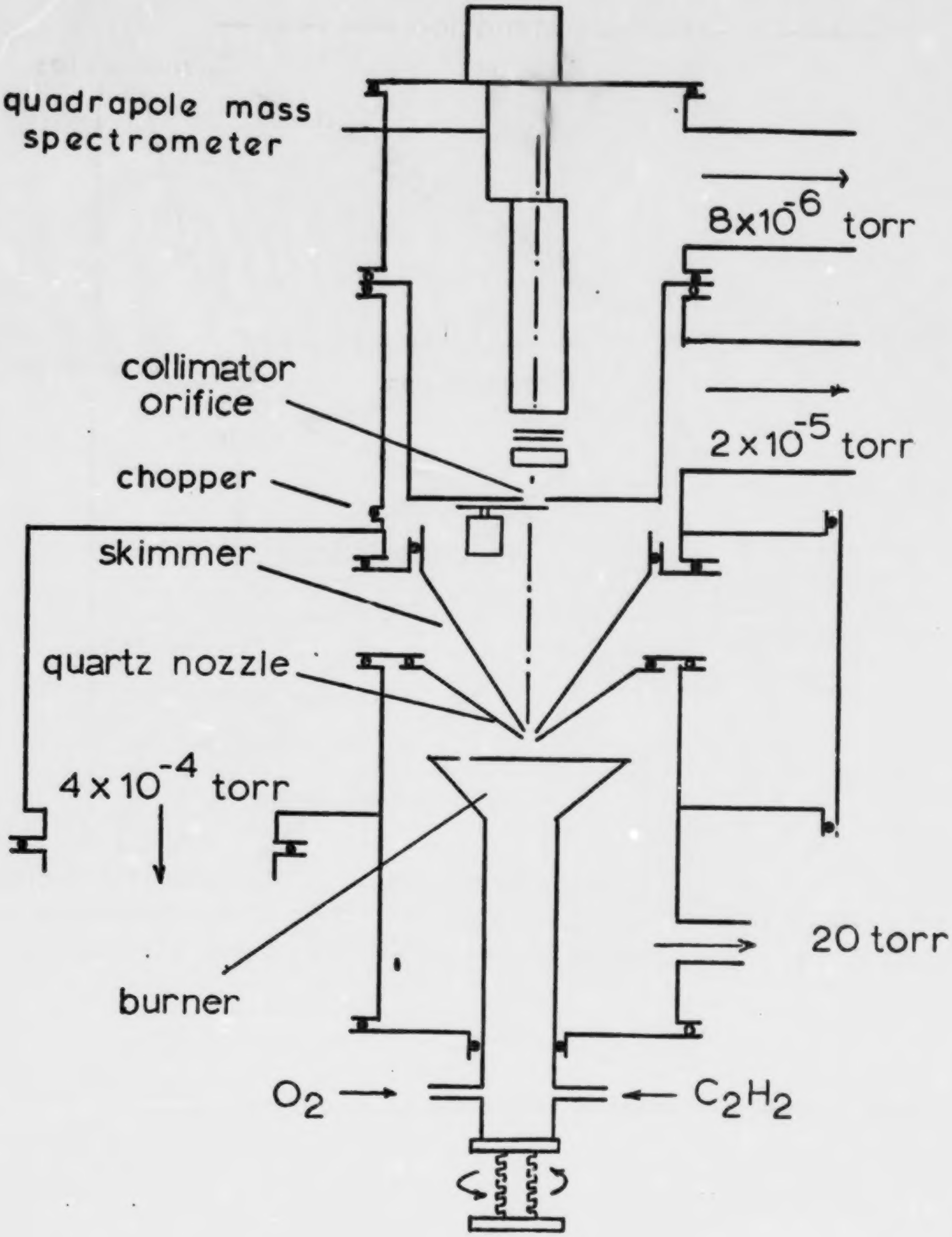
quadrapole mass spectrometer
8x10^{-6} torr
collimator orifice
2x10^{-5} torr
chopper
skimmer
quartz nozzle
4x10^{-4} torr
burner
20 torr
O_2
C_2H_2

Figure 2 Modulated beam - mass spectrometer sampling apparatus

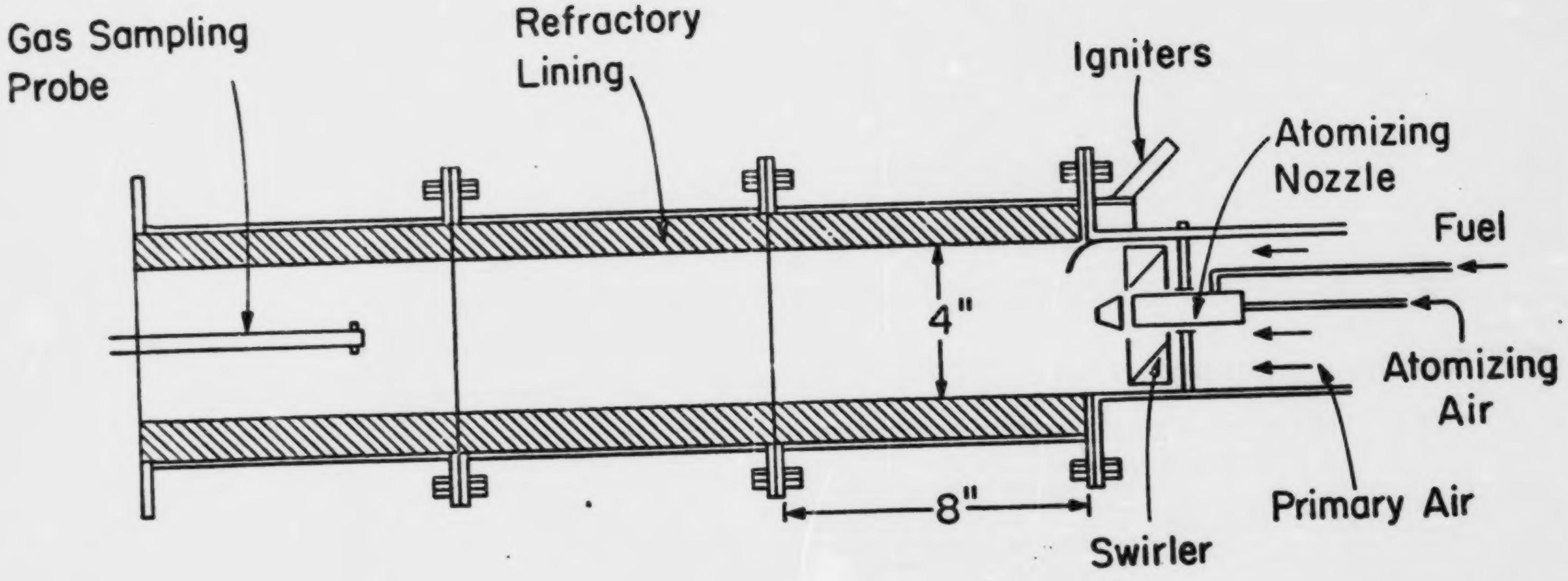
Gas Sampling Probe
Refractory Lining
Igniters
Atomizing Nozzle
Fuel
Atomizing Air
Primary Air
Swirler
4"
8"

Figure 3 Turbulent Diffusion Flame Burner

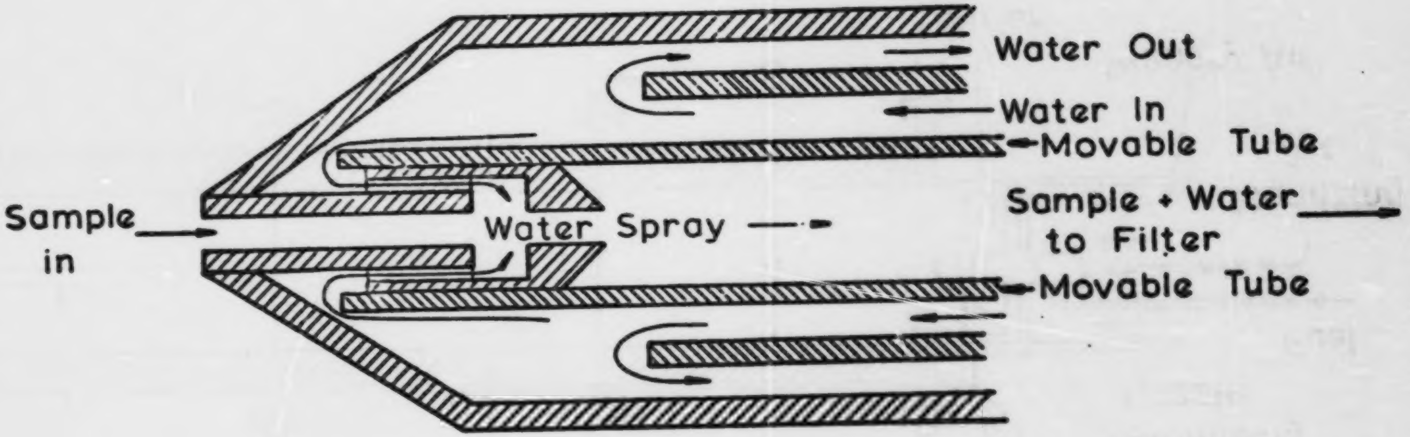
Water Out
Water In
Movable Tube
Sample + Water to Filter
Movable Tube
Sample in
Water Spray

Figure 4 Water-flushed soot sampling probe

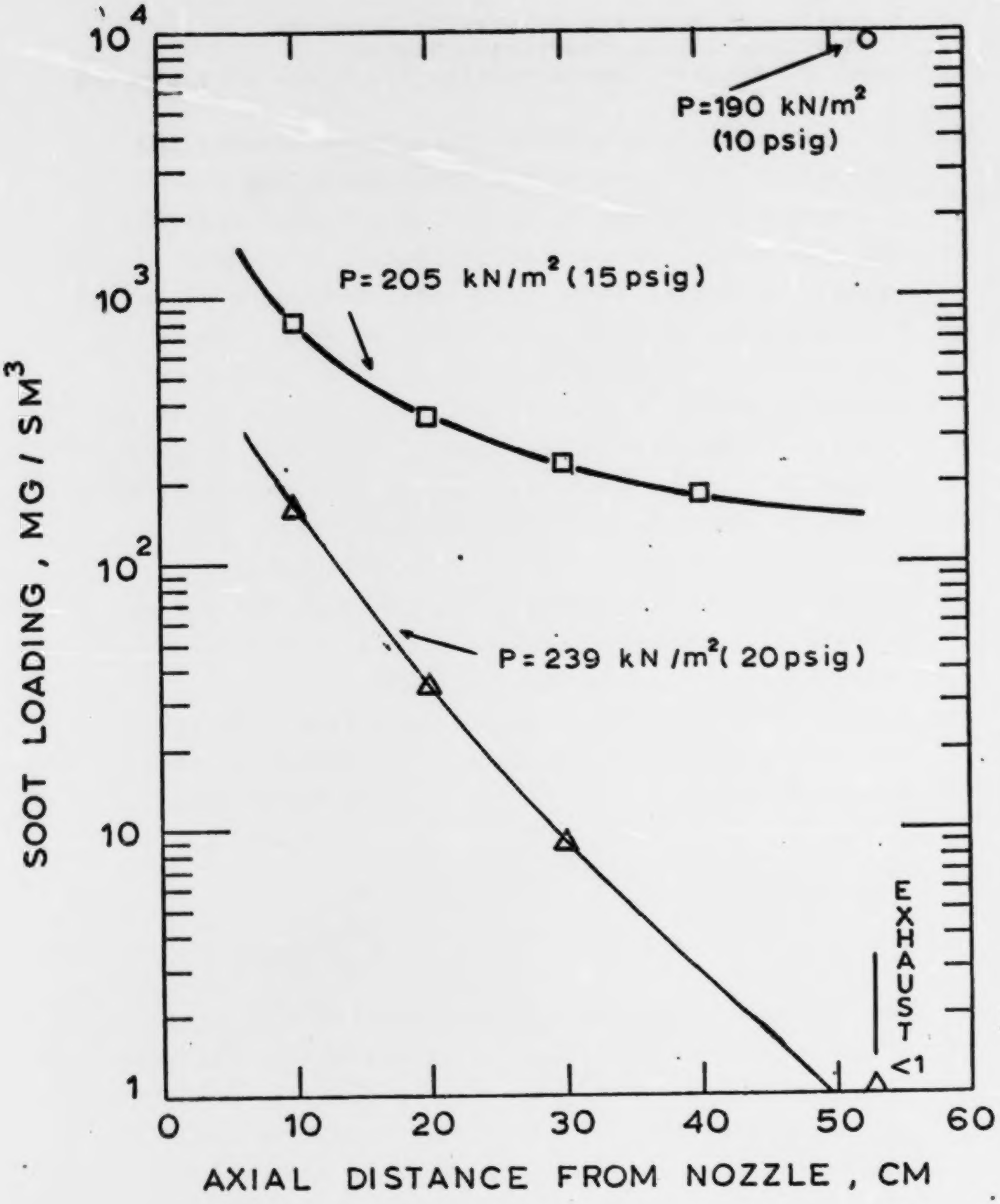

Figure 5 Preliminary results of soot loading as a function of axial position and atomizing air pressure. For conversion from mg/sm^3 to the mass fraction of soot in the combustion gases multiply by 7.81 x 10^{-7} $\frac{\text{g C}}{\text{g products}}$/mg/sm^3.

8:45 a.m.

Formation of Soot and Polycyclic Aromatic Hydrocarbons in Combustion Systems

James D. Bittner, Massachusetts Institute of Technology

Q: Is there any correlation to experience between the laboratory condition of low atmospheric and sub-atmospheric pressure where you obtain your radicals and your small, semi-solid particles, and the reality of actual combustion and atmospheric pressure?

A: Your question is, are conditions the same. Peak temperatures for acetylene oxygen flame are around 2000° K. I have no evidence on production of radicals' effect on temperature. We really haven't gotten to the study of hydrocarbon free radicals; that system is still in the construction stages.

Q: What type of liquid fuels are you using in the atmospheric furnace and are you studying the effects of varying asphaltene concentrations or various sulphur concentrations in the fuel?

A: Currently we are using aviation kerosene. There are some plans of investigating the effect of the degree of varomaticity of the fuel on hydrocarbon and polycyclic aromatic formation; we haven't looked into sulphur effects.

Q: You mentioned that the carbonaceous residue, which is insoluble, is dispersed in an ultrasonic bath and then particle size distribution is measured with the electro-microscope. I was wondering if you would comment on the potential irreversible agglomeration that might occur and affect your results. If agglomeration occurs which can be reversed with the ultrasonic bath, then the distribution you're measuring may not be the field distribution.

A: Yes, I have to agree with that. We've had some problems in getting good dispersions, and rather than a bath or a tub, we've gone to an ultrasonic probe which seems to provide much more intense agitation; but you're right, we have no guarantee that we can completely re-disperse the material.

EFFECTS OF FUEL SULFUR ON
NITROGEN OXIDE EMISSIONS

By:

J.O.L. Wendt and J.M. Ekmann
Department of Chemical Engineering
University of Arizona
Tucson, Arizona 85721

Presented at EPA Symposium on Stationary Source Combustion
Atlanta, Georgia, September 24-26, 1975

Preceding page blank

ABSTRACT

The effect of some fuel sulfur compounds on NO_x emissions arising from thermal fixation was investigated. Laboratory experiments, using a methane-air flat flame doped with either SO_2 or H_2S, showed that fuel sulfur can inhibit the formation of nitrogen oxides, and that this inhibition is significant at all air fuel ratios and especially at high air preheats. A mathematical simulation of a flat flame was developed and this showed that the observed effect could be explained by a kinetic mechanism involving the catalysis of atom recombination reactions by SO_2.

The experimental and theoretical results obtained are especially significant from a practical point of view, since they indicate that fuel desulfurization may lead to increased NO_x.

INTRODUCTION

One of the roles of fundamental combustion research is to help identify new problem areas of concern to EPA. A potential area of concern is the interrelationship between sulfur oxide and nitrogen oxide abatement. Sulfur oxide pollution may be abated by either fuel desulfurization or stack gas scrubbing. The choice of abatement method is usually dictated by economic considerations. However, in calculating the cost effectiveness of various sulfur oxide abatement strategies, it is important to determine the extent to which the technology used has an adverse effect on other pollutants such as NO_x. Should sulfur compounds in the flame front have an inhibitory influence on the formation of NO_x, this would indicate that fuel desulfurization might require additional NO_x abatement methods to be implemented, and that this would involve additional costs which would not occur with stack gas scrubbing, where the sulfur species are removed after the combustion process.

That sulfur and nitrogen oxides interact at low temperatures is not new and has been studied exhaustively (1,2). This interaction results in the catalysis, by NO, of the oxidation of SO_2 to SO_3. At higher temperatures, under combustion conditions, the situation is quite different and a clear distinction should be drawn between low temperature interactions. At high temperatures under combustion conditions, free radicals are produced in superequilibrium amounts and this fact has been shown to be important in explaining high NO production rates(3,4) where the NO is formed by atmospheric fixation (Thermal NO). Since it has been shown(5,6) that sulfur dioxide is an effective catalyst in reducing superequilibrium free radical concentrations, it is reasonable to expect that sulfur dioxide and possibly other fuel sulfur compounds inhibit the formation of NO in flames. In order to explore this possibility further, it is necessary to focus on certain fundamental aspects of NO formation mechanisms.

In spite of much research in the area, there is even now no general agreement on the kinetic mechanisms of thermal NO production. Most widely recognized is the mechanism proposed by Zeldovich(7)

$$N_2 + O \rightarrow NO + N \qquad (I)$$

$$N + O_2 \rightarrow NO + O \qquad (II)$$

with the modification

$$N + OH \rightarrow NO + H \qquad (III)$$

and with the free radicals necessary for these reactions being produced through the combustion process. It should be noted that the free radicals so produced can have concentrations many fold in excess of those determined by equilibrium and that the decay of these radicals towards equilibrium is relatively slow and occurs downstream from the flame front. It is in this region of free radical decay that the bulk of the NO is formed through reactions (1) through (3). Thompson and Beer(3) have shown that, indeed, superequilibrium concentrations of oxygen atoms are responsible for high rates of NO formed in their apparatus and their conclusion was corroborated by other workers, (4,8) especially as regards NO formation in the fuel lean regime. In the fuel rich regime, however, it appears that for hydrocarbon flames, an NO formation mechanism involving cyanide compounds as intermediates may be applicable (4,9), and under these conditions the role of superequilibrium atom and radical concentrations is unclear. It is generally recognized, however, that high rates of NO formation can result from superequilibrium atom concentrations, and it would therefore appear that catalysts and other impurities, such as SO_2, that have been shown to decrease radical concentrations, should tend to lower thermal NO formation rates.

In order to determine the effect of fuel sulfur on thermal NO it is necessary to devise a well defined laboratory experiment to answer the following questions:

- Does SO_2 have an inhibitory effect on thermal NO emissions?
- Under which conditions is any inhibition of NO formation by SO_2 most significant?
- Does SO_2 affect the formation of "prompt NO" and if so what conclusions can be drawn about the role of superequilibrium atom concentrations and "prompt NO"?
- With H_2S in the fuel, is conversion of the fuel sulfur to SO_2 sufficiently rapid to allow the SO_2 formed to have the same effect as when added directly to the fuel?

In order for laboratory results to be extrapolated to other conditions, it is also necessary to develop theoretical mathematical models that describe the appropriate kinetic mechanisms, and that can be used to determine the significance of the results in other, more real world combustion environments. In particular, mathematical models will give insight into fundamental questions such as

- Can the observed effect be explained by catalysis of atom and radical recombination rates by SO_2?
- What can be expected under different time temperature histories?

- **What can be expected in real furnace flames?**

EXPERIMENTAL APPARATUS

Combustion Rig

A schematic of the premixed combustion rig and supporting equipment used is shown in Figure 1 and a diagram of the burner itself in Figure 2. Metered amounts of methane (Matheson, C.P.) preheated house air, and when applicable, SO_2 or H_2S (Matheson, C.P.), were allowed to mix, then preheated further before being fed into a modified Meker burner. The temperature of the gas mixture entering the burner was controlled. The Meker burner was modified so that an approximately flat flame could be supported above the burner grid. The burner was at atmospheric pressure and enclosed in a pyrex glass chimney.

The combustion rig was designed primarily for a large number of input/output measurements rather than for detailed in-flame probing. However, some detailed probing was successfully attempted, and this showed that the flame could be considered flat to within our experimental error.

Partial temperature profiles showed that the flame had temperatures in excess of 2000°K, even with no air preheat. This means that heat loss to the surroundings was

Figures 1 and 2 follow

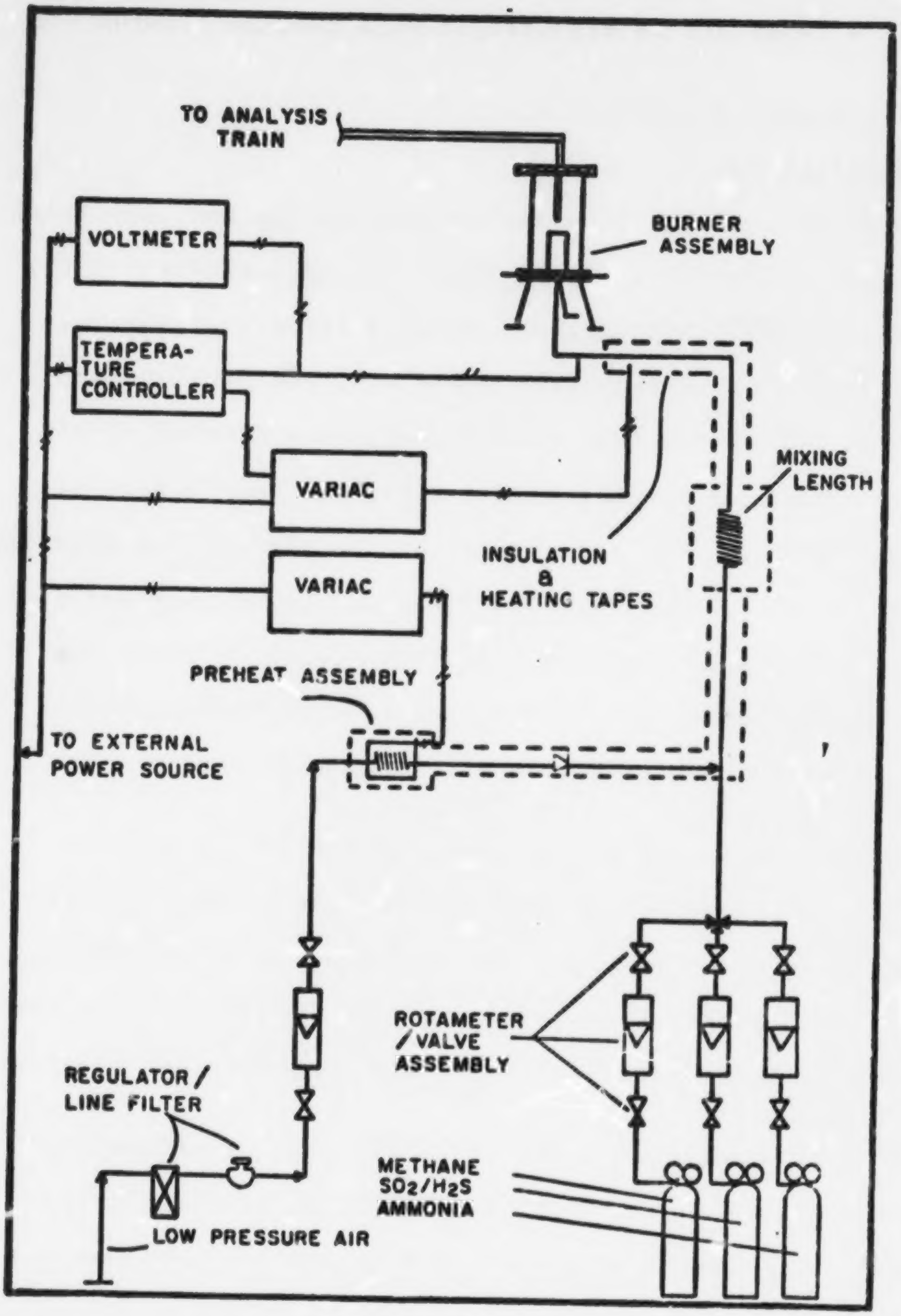
TO ANALYSIS TRAIN
BURNER ASSEMBLY
VOLTMETER
TEMPERA-TURE CONTROLLER
VARIAC
VARIAC
MIXING LENGTH
INSULATION & HEATING TAPES
PREHEAT ASSEMBLY
TO EXTERNAL POWER SOURCE
ROTAMETER / VALVE ASSEMBLY
REGULATOR / LINE FILTER
METHANE
SO2/H2S
AMMONIA
LOW PRESSURE AIR

FIGURE 1. SCHEMATIC OF APPARATUS

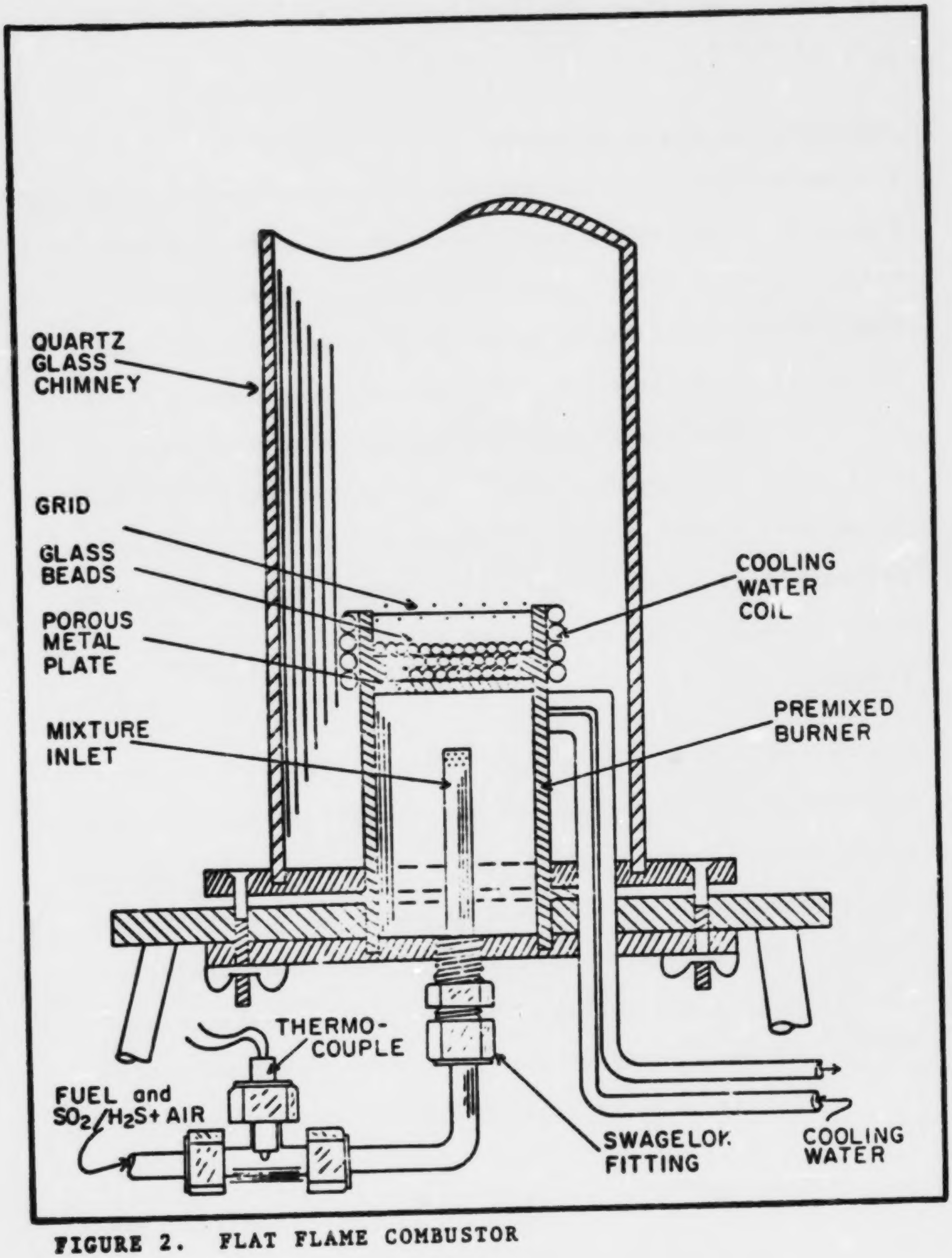
QUARTZ GLASS CHIMNEY
GRID
GLASS BEADS
POROUS METAL PLATE
COOLING WATER COIL
PREMIXED BURNER
MIXTURE INLET
THERMO-COUPLE
FUEL and SO2/H2S+AIR
SWAGELOK FITTING
COOLING WATER

FIGURE 2. FLAT FLAME COMBUSTOR

not great, and might distinguish this flat flame from others(10,11).

Sampling and Analysis Train

A schematic of the sampling and analysis train is shown in Figure 3. The sample was drawn through a 1mm diameter orifice into a 6mm OD, uncooled, quartz sampling tube. Preliminary experiments in which the sampling rate was varied by a factor of four showed that our data did not depend on sampling rate and this, together with data from other experimentalists(12), indicates that all reactions were effectively rapidly quenched and no further reaction took place in the tube. The height of the sampling tube could be positioned accurately to within 0.03mm.

Quartz and teflon tubing were used throughout the sampling and analysis train since stainless steel tubing has been shown to interfere with NO analysis under rich conditions. A cooled knockout pot removed moisture in the burned gas sample. The analysis train had the following features:

- NO/NO_x analysis by Thermoelectron Chemiluminescence Analyzer with stainless steel convertor
- O_2 analysis by Beckman Model 715 (Electrochemical) O_2 Monitor

Figure 3 follows

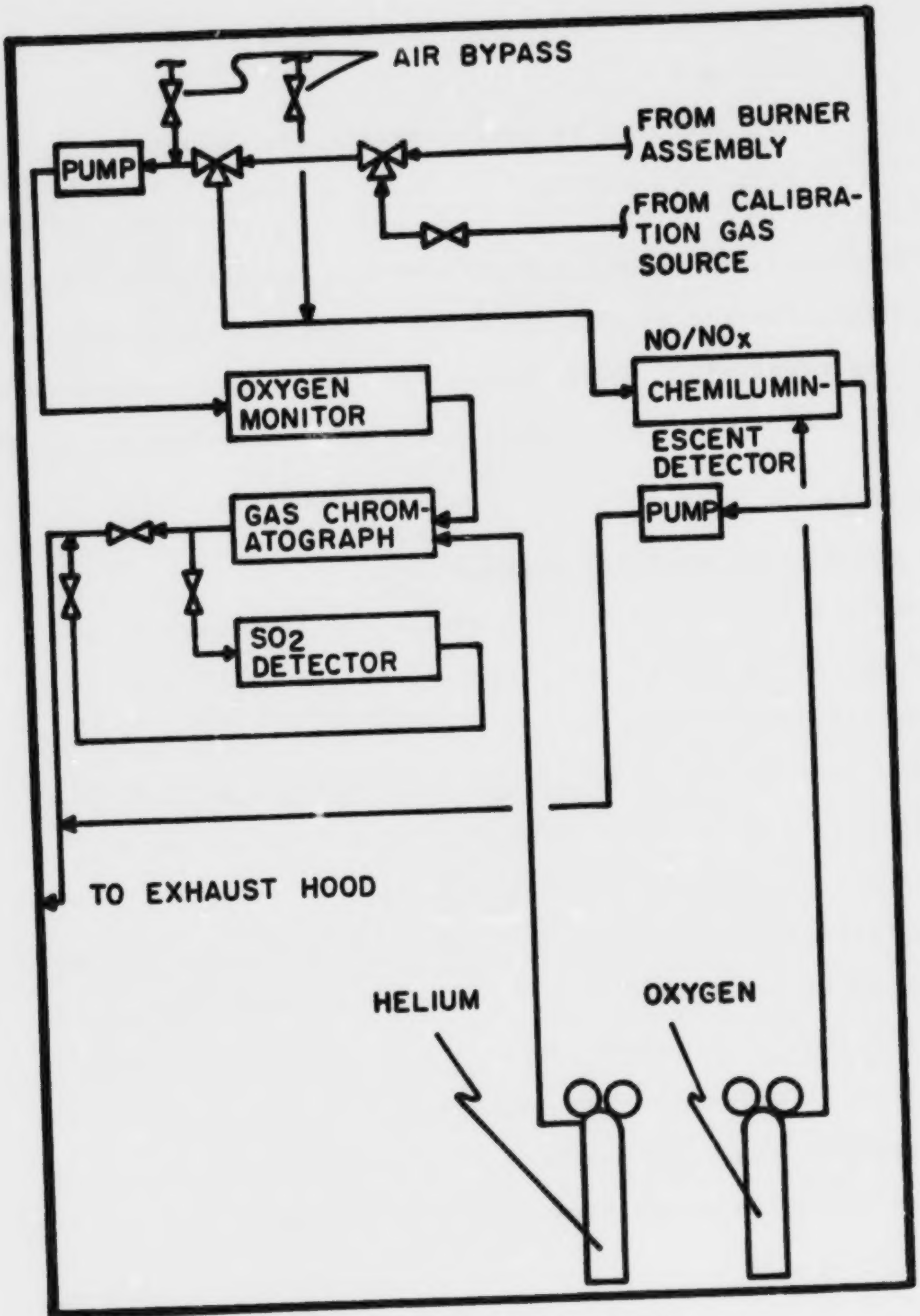
AIR BYPASS
FROM BURNER ASSEMBLY
PUMP
FROM CALIBRATION GAS SOURCE
NO/NOx
CHEMILUMINESCENT DETECTOR
OXYGEN MONITOR
GAS CHROMATOGRAPH
PUMP
SO2 DETECTOR
TO EXHAUST HOOD
HELIUM
OXYGEN

FIGURE 3. SCHEMATIC OF ANALYSIS SYSTEM

- CO analysis by chromatograph with Porapak Q column
- SO_2 analysis by Theta Sensors SO_2 (Electrochemical) Monitor.

The chemiluminescence analyzer worked perfectly and showed no interference by SO_2, O_2 or CO. This confirmed previous results(13) which showed that SO_2 does not interfere with (Thermoelectron) chemiluminescence measurements of NO.

RESULTS

Premixed Combustor Performance

Figure 4 and Figure 5 show results obtained with no SO_2 or H_2S added to the fuel. These are the base cases showing exhaust NO emissions as functions of air fuel ratio, air preheat (Figure 4) and NO concentration within the flame as a function of residence time from the burner (Figure 5). Figure 4 shows that with no preheat a maximum of 152 ppm (dry, reduced to 100% stoichiometric air) NO was obtained at 104% stoichiometric air while with 240°C air preheat the maximum was 232 ppm. There is also a strong dependence on air fuel ratio. Figure 5 shows that formation of NO was complete at 6 cm above the burner grid or after a residence time of approximately 20 milliseconds

Figures 4 and 5 follow

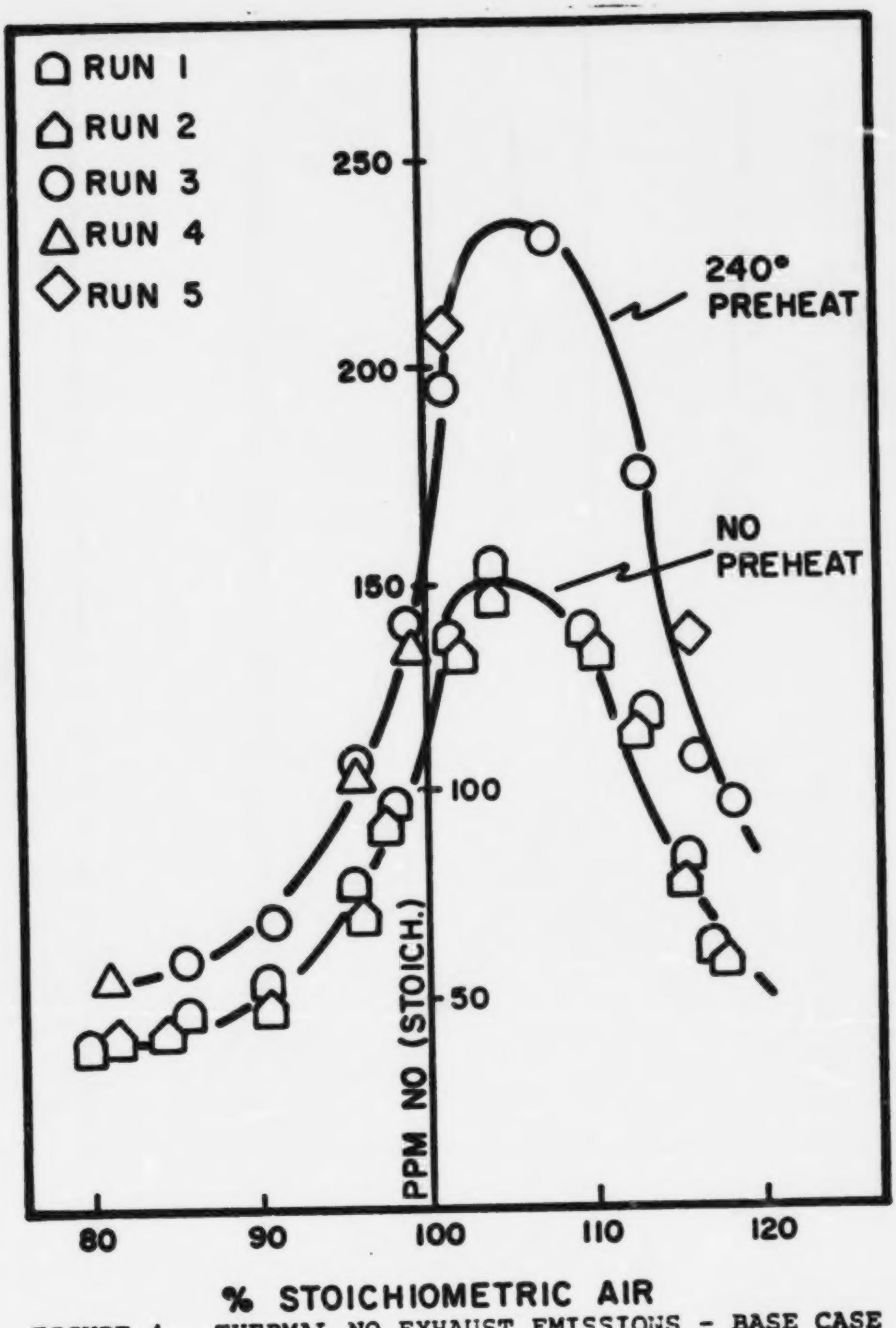

FIGURE 4. THERMAL NO EXHAUST EMISSIONS - BASE CASE

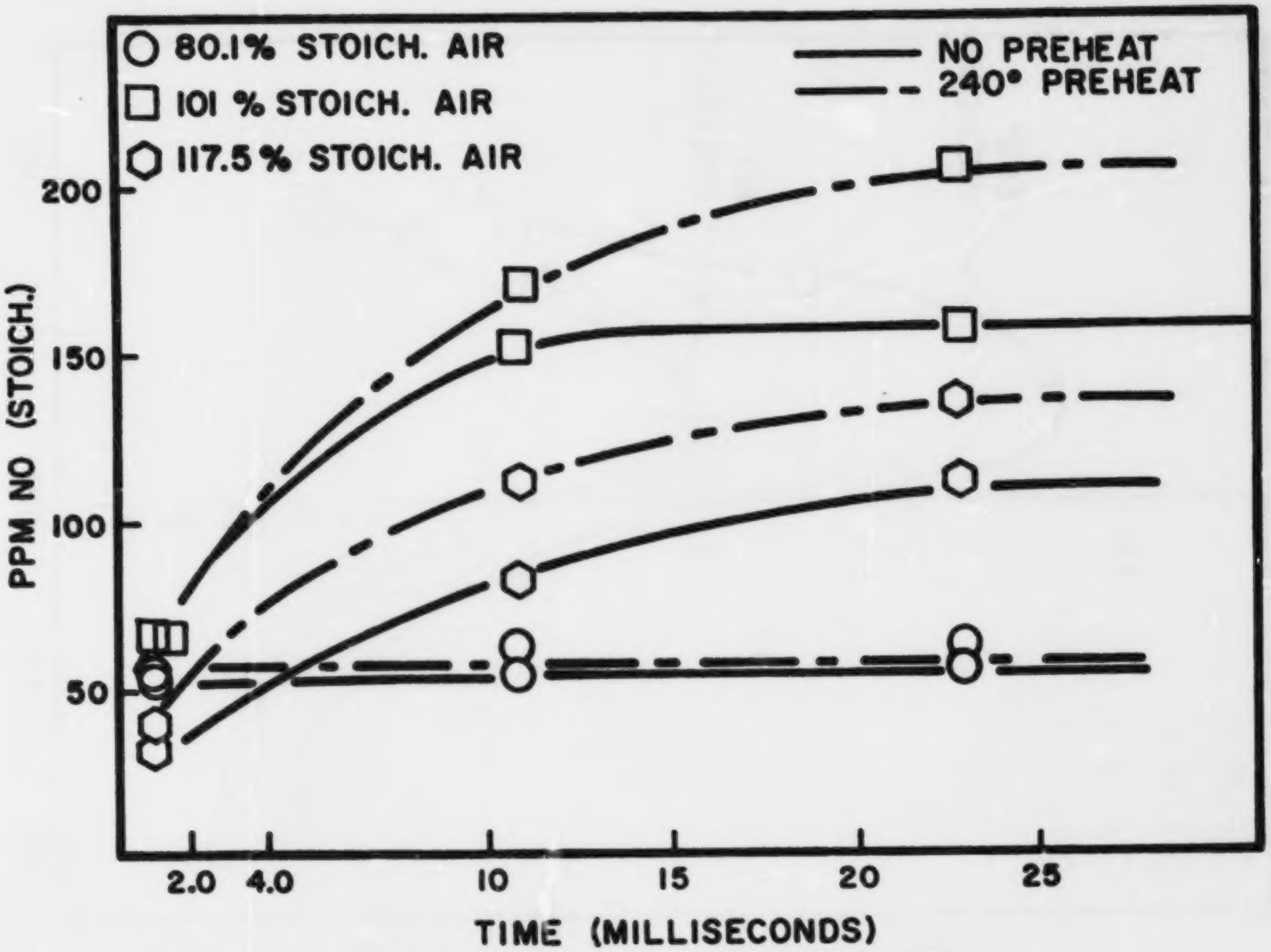

FIGURE 5. EXHAUST LEVELS OF NO ACHIEVED RAPIDLY

and that sampling at that point was truly representative of exhaust NO emissions. Figure 5 also shows that under fuel rich conditions all the NO is formed very early in the flame and that this "prompt NO" was not a strong function of air preheat and that more "prompt NO" was formed under fuel rich conditions than under fuel lean conditions. These results agree somewhat with those of Fenimore(9).

The ppm NO measured, under no preheat conditions, is substantially greater than that measured by other workers in flat flames(11). This is probably due to the low heat loss rate in our system, and by the resulting high temperatures. The existence of temperatures well above 2000°K was confirmed by (incomplete) temperature measurements(14).

At each point (Figure 5) under fuel lean conditions both NO and NO_x were measured by the chemiluminescence analyzer. At most 3 ppm NO_2 were observed, and then only under very fuel lean conditions. We thus did not observe any early NO_2 formation as reported by Merryman and Levy(15).

Additional runs were also made to investigate whether the addition of a fuel additive, such as SO_2, would lower NO emissions significantly by virtue of dilution alone. With molecular N_2 as the fuel diluent at zero preheat, 104% stoichiometric air, it was found that 10% N_2 in the fuel led to a reduction of less than 7 ppm NO in the exhaust. This means that any effect (larger than this) due to addition of up to 5% SO_2 to the fuel is due to kinetic interactions and not just simple dilution and temperature reduction.

Effect of SO_2 on NO_x Emissions

The effect of SO_2 as an additive in the fuel on the exhaust emissions of nitrogen oxide is shown in Figures 6 and 7. In Figure 6 the ppm NO (dry, reduced to stoichiometric) in the exhaust is shown in the absence of air preheat with and without 4.9 percent by volume SO_2 in the fuel. 4.9 percent by volume SO_2 in methane leads to approximately 6800 ppm SO_2 in the exhaust. It can be seen that at approximately 101% stoichiometric air, 4.9% SO_2 in the fuel lowers NO exhaust emissions by 50 ppm or by about 36%. At other air/fuel ratios the percent reduction is somewhat less as shown on Table 1. At a preheat of 240°C (Figure 7) and at 101.% stoichiometric air the addition of 4.9% of SO_2 in the fuel lowers NO_x emissions by about 60 ppm or 30%. Conversely, looking at the

Table 1, Figures 6 and 7
follow

TABLE 1. REDUCTION IN NO_x EMISSIONS BY SO_2 ADDITION TO FUEL

Percent Stoichiometric Air	Reduction in NOx Emissions							
	2.5% SO_2 in Fuel				4.9% SO_2 in Fuel			
	no preheat		240°C preheat		no preheat		240°C preheat	
	ppm	%	ppm	%	ppm	%	ppm	%
80.1	7	12.6	6.0	10.7	6.0	16.0	13.0	24.6
90.0	--	--	--	--	9.0	17.3	15.0	23.1
101.3	22.0	14.0	21.0	10.7	50.0	35.7	60.0	30.9
103.0	--	--	--	--	40.0	26.0	68.0	30.4
110.0	--	--	--	--	27.0	24.5	60.0	26.4
117.4	12.0	11.7	37.0	27.4	16.0	13.9	22.0	21.6

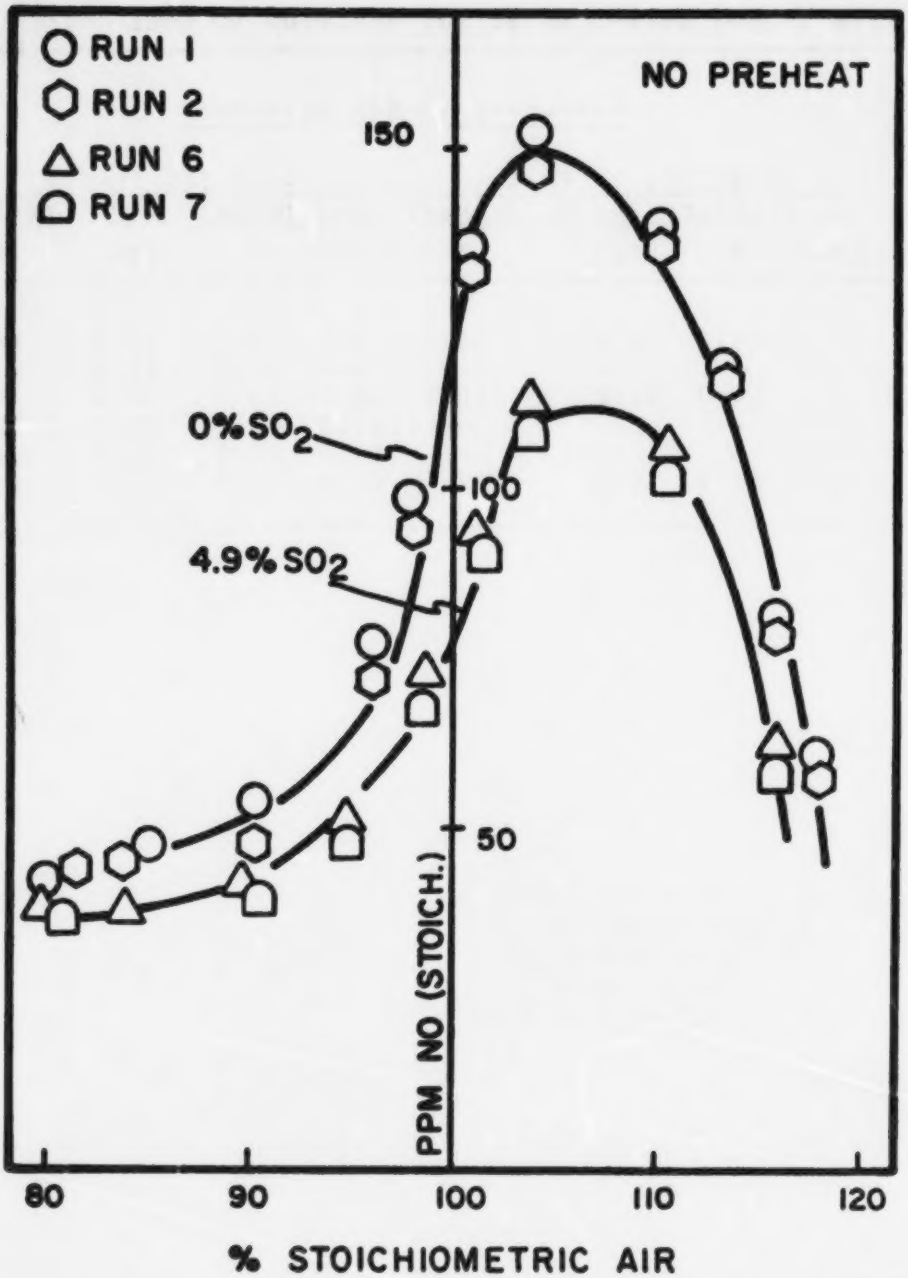

FIGURE 6. SO_2 INHIBITS NO FORMATION AT ZERO PREHEAT

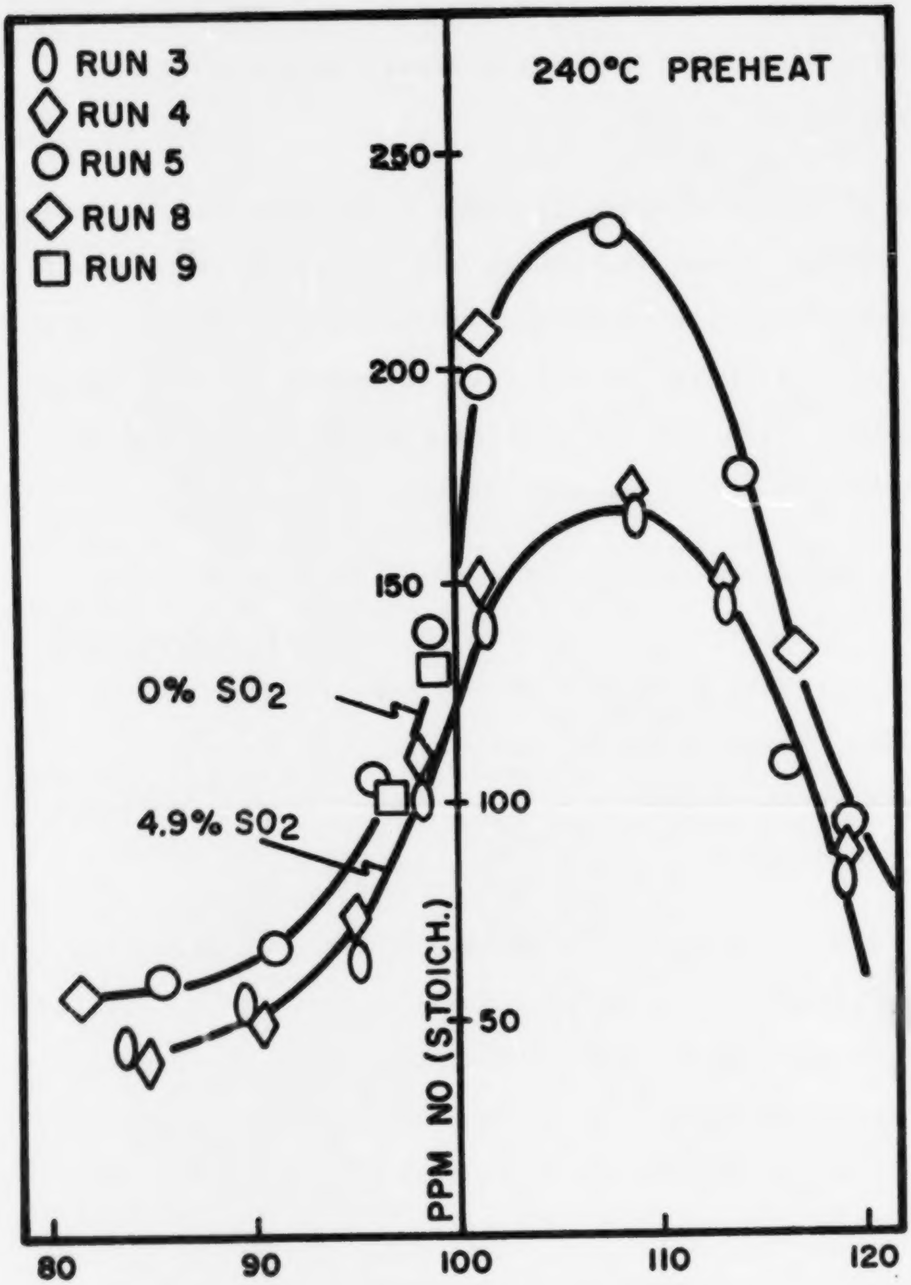

FIGURE 7. SO_2 INHIBITS NO FORMATION AT HIGH PREHEAT

effect of removal of SO_2 from the fuel one can say in this case, fuel desulfurization caused increases in NO_x emissions of up to 55%.

Further details are shown in Table 1 in which results from two different flames are presented. (Flame 1 has slightly lower base case NO emissions.) These results clearly show that as the SO_2 level in the fuel decreases so does reduction in NO_x emissions. With less than 1% SO_2 in the fuel any inhibition effect was not significant.

Figure 8 shows the results of probing within the flame (118.5% stoichiometric air, 4.9% SO_2 in Fuel) and clearly demonstrates that at both preheats the effect of SO_2 is to quench the formation of NO fairly early in the flame. This data gives insight into a probable kinetic mechanism as described later.

In Figure 9 the effect of 2.5% and 4.9% SO_2 on the formation of "prompt NO" is shown, where "prompt NO" is defined in this case as that formed within 0.3 cm of the burner grid. It can be seen that at both preheats and at all air fuel ratios, the effect of increasing SO_2 is to decrease "prompt NO" formation. This indicates that superequilibrium concentrations of atoms and free radicals might be

Figures 8 and 9 follow

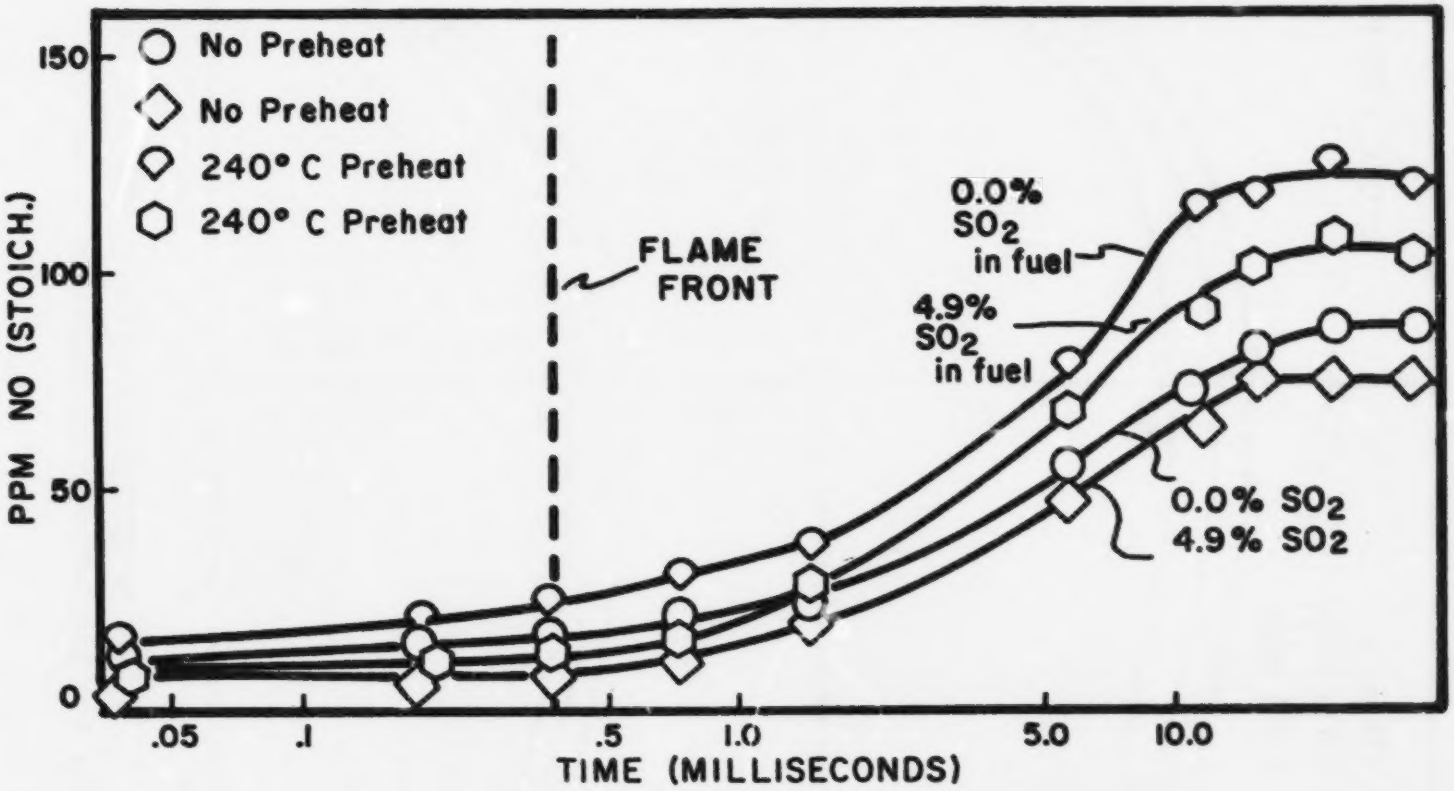

FIGURE 8. SO_2 DECREASES RATE OF NO FORMATION NEAR THE FLAME

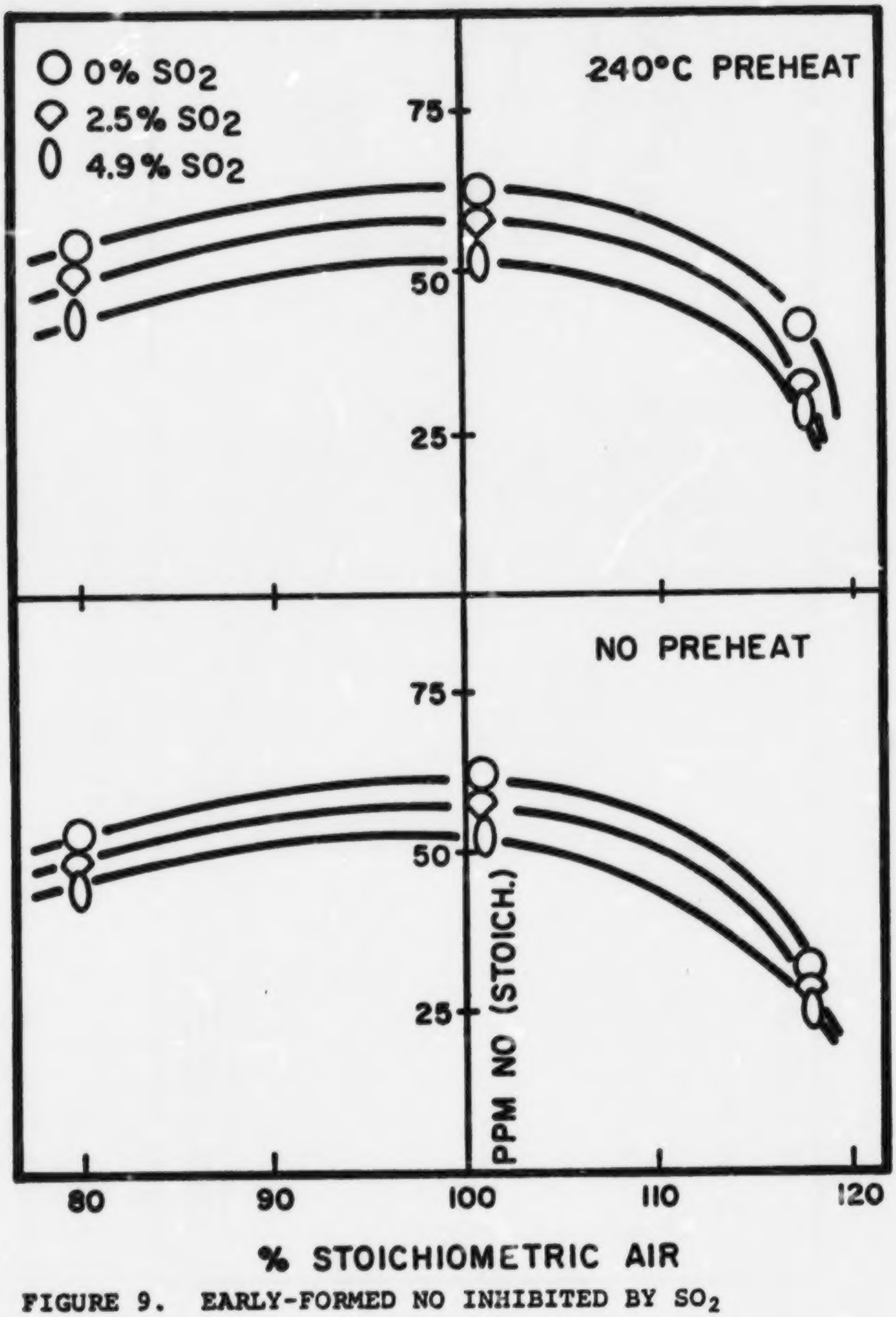

FIGURE 9. EARLY-FORMED NO INHIBITED BY SO_2

important under all air/fuel ratio conditions.

Effect of H_2S on NO_x Emissions

In fossil fuels, sulfur is normally present in the reduced state. Thus, some experiments were completed with H_2S as the fuel additive, in order to determine whether fuel sulfur in this form has an effect on thermal NO_x formation.

Figures 10 and 11 show the effect of H_2S addition at two levels of mixture preheat. Since H_2S is a fuel, addition of this compound changes the air fuel ratio, and this has been taken into account in labeling the abscissa axis. In Figure 10 it is clear that both 2.6% and 5.0% H_2S in the fuel, with no mixture preheat, inhibit the formation of NO_x. NO_x emissions were reduced up to 31.6% under fuel lean conditions as shown on Table 2. With 250°C mixture preheat, H_2S inhibits NO_x formation on the average by an even greater extent as shown on Figure 11 and Table 2.

It is instructive to compare the inhibition of NO_x formation by SO_2 and by H_2S. Comparison of Table 1 and Table 2 show that without preheat SO_2 had a greater effect while with 240°C mixture preheat the effects of H_2S and SO_2 addition are roughly the same. This is probably due to

Table 2 and
Figures 10 and 11 follow

TABLE 2. REDUCTION IN NO_x EMISSIONS BY H_2S ADDITION TO FUEL

Percent Stoichiometric Air	Reduction in NO_x Emissions							
	2.6% H_2S in Fuel				5.0% H_2S in Fuel			
	No Preheat		240°C Preheat		No Preheat		240°C Preheat	
	ppm	%	ppm	%	ppm	%	ppm	%
80	5.0	11.4	7.0	13.2	5.0	11.4	13.0	24.6
90	8.0	14.6	10.0	15.4	8.0	14.6	20.0	30.8
100	28.0	23.3	26.0	17.1	28.0	23.2	42.0	27.7
103	17.0	11.4	50.0	22.8	28.0	18.9	75.0	34.0
110	15.0	11.1	44.0	19.1	26.0	19.4	63.0	28.0
115	15.0	15.8	23.0	14.1	30.0	31.6	48.0	29.4

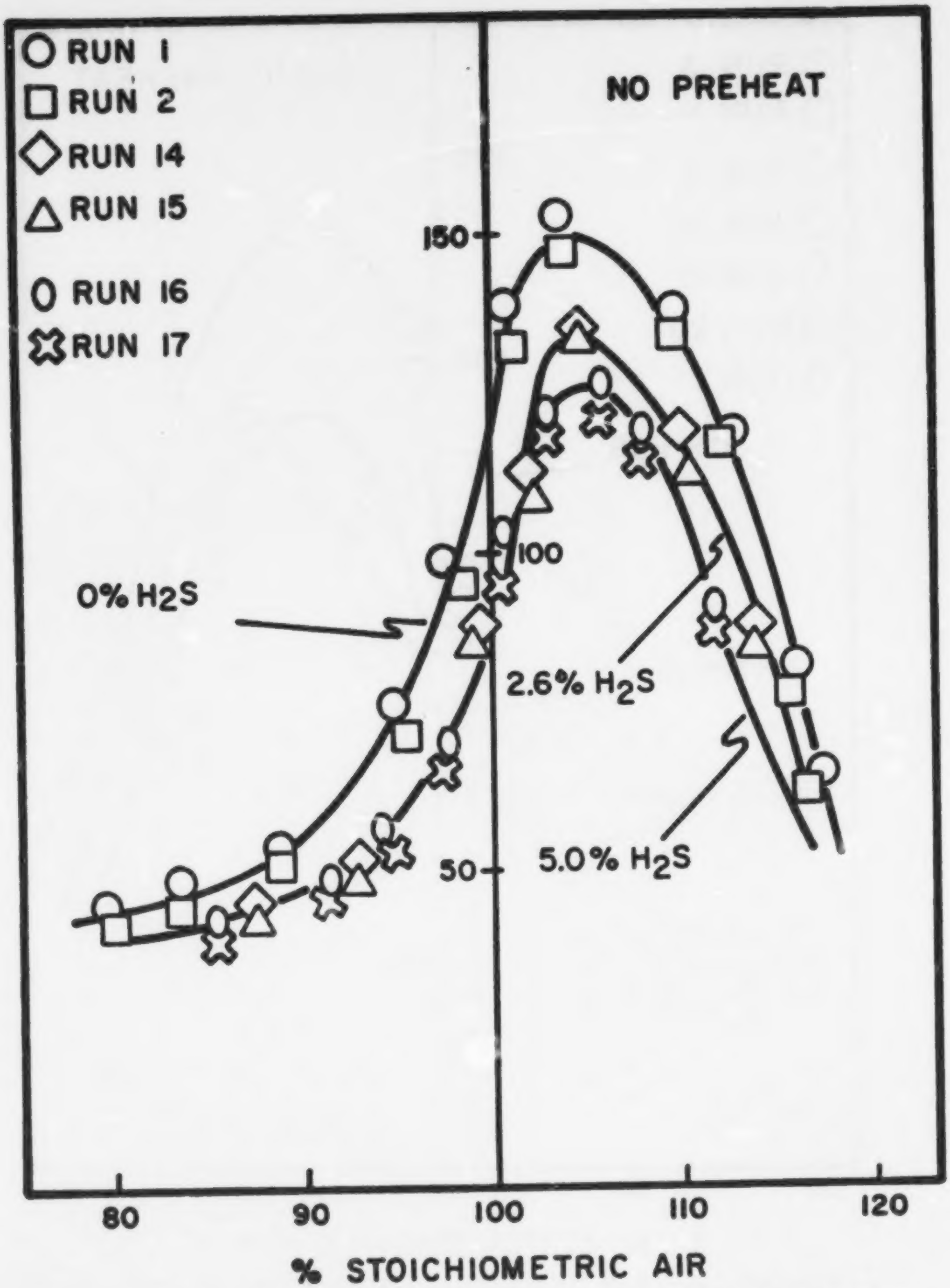

FIGURE 10. H_2S INHIBITS NO FORMATION AT ZERO PREHEAT

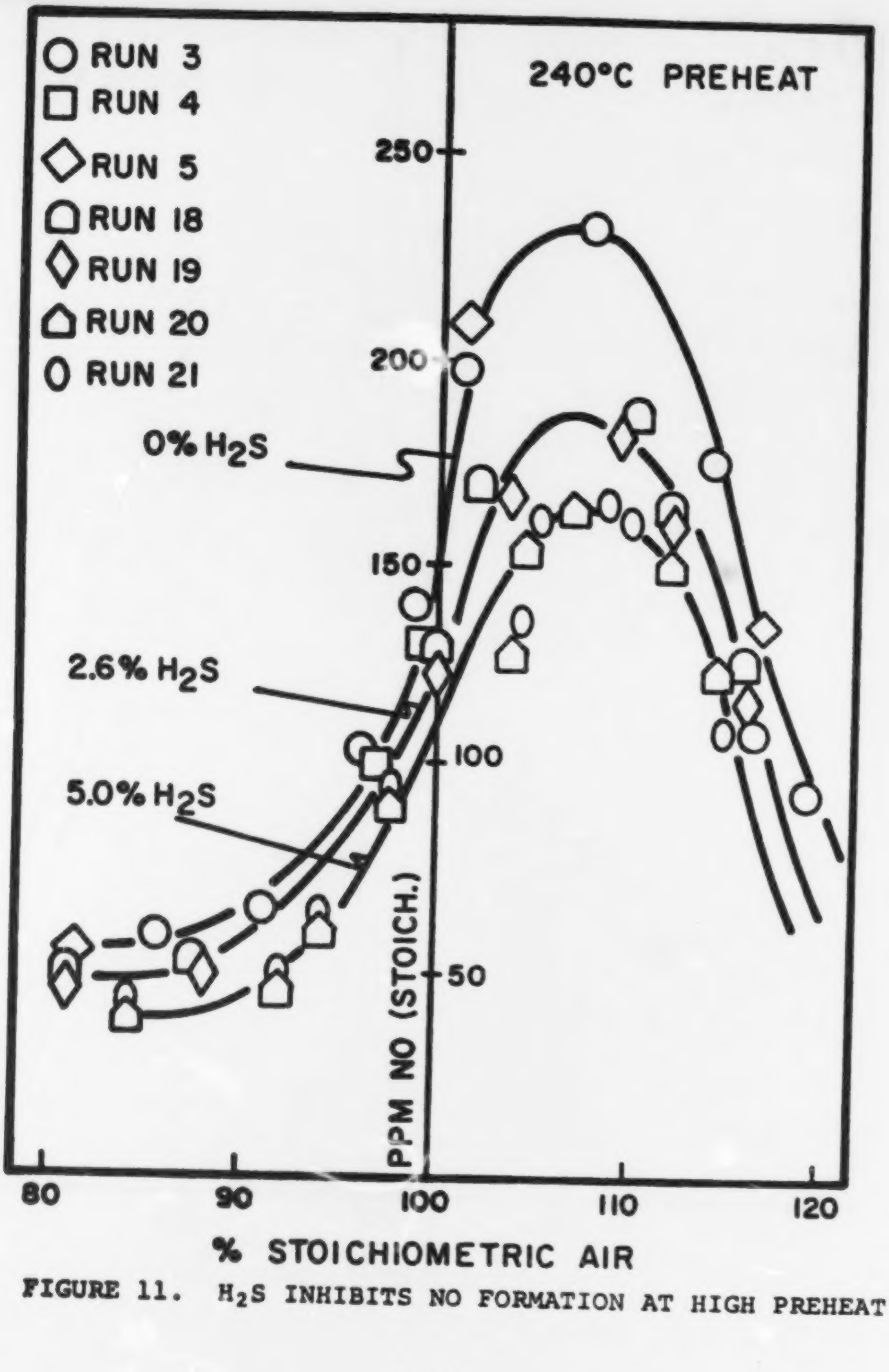

FIGURE 11. H_2S INHIBITS NO FORMATION AT HIGH PREHEAT

the effect of temperature on conversion rates of H_2S to SO_2.

Figure 12 shows the effect of H_2S on "prompt NO", and indicates that under fuel lean conditions the presence of H_2S does lower "prompt NO" formation rates. Under fuel rich conditions, where conversion of H_2S to SO_2 is not complete, there is little effect of H_2S on "prompt NO".

The foregoing indicates that H_2S must be converted to SO_2 before inhibition of NO is important, and that this occurs rapidly under fuel lean conditions. This is confirmed in Figures 13 and 14 in which SO_2, NO, and O_2 concentrations are plotted as functions of time for zero preheat. At 98% stoichiometric air (Figure 13) H_2S conversion to SO_2 is essentially complete when NO has attained 70% of its final value; at 113.5% stoichiometric air the conversion of H_2S to SO_2 is essentially complete when the NO has attained only 34% of its final value. Since H_2S has a greater inhibiting effect in the fuel lean case, it would appear that inhibition of NO formation occurs through the rapid conversion of H_2S to SO_2 and by the subsequent inhibiting effect of SO_2. Thus, under fuel lean conditions, a kinetic model simulating fuel sulfur as SO_2, rather than as H_2S, would be adequate.

Figures 12, 13 and 14
follow

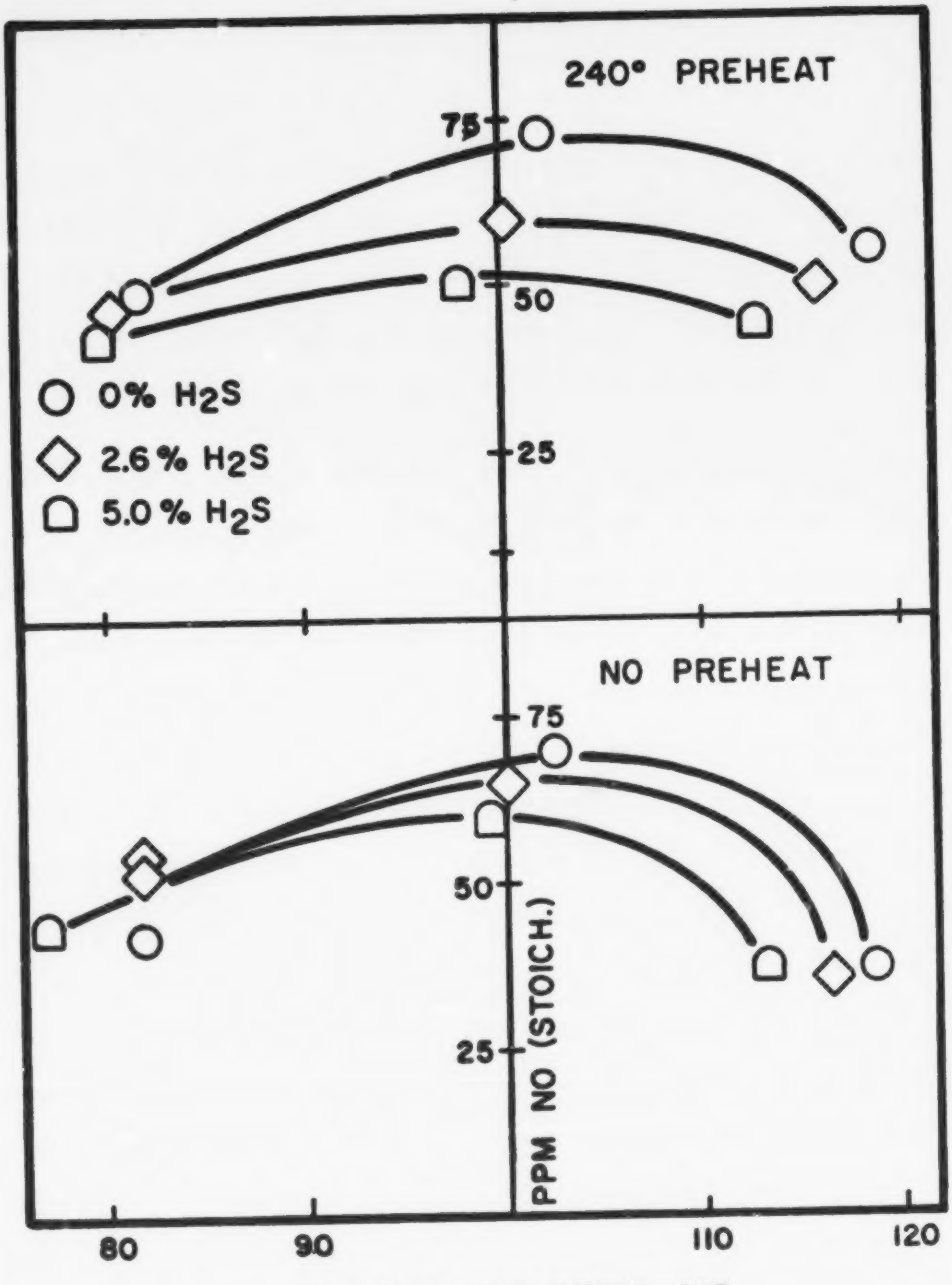

FIGURE 12. EARLY-FORMED NO INHIBITED BY H_2S

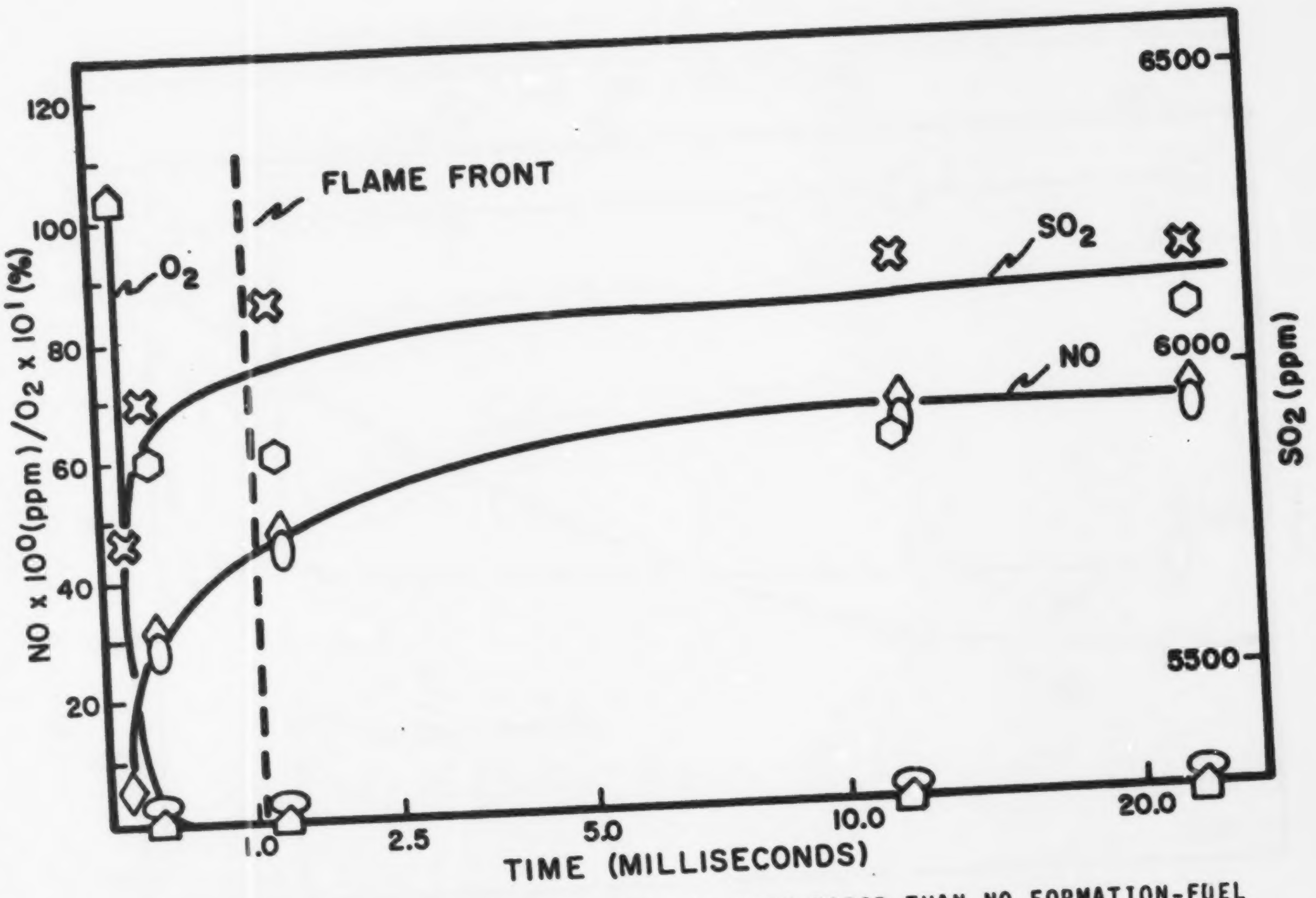

FIGURE 13. CONVERSION OF H_2S TO SO_2 IS MORE RAPID THAN NO FORMATION-FUEL RICH CONDITIONS

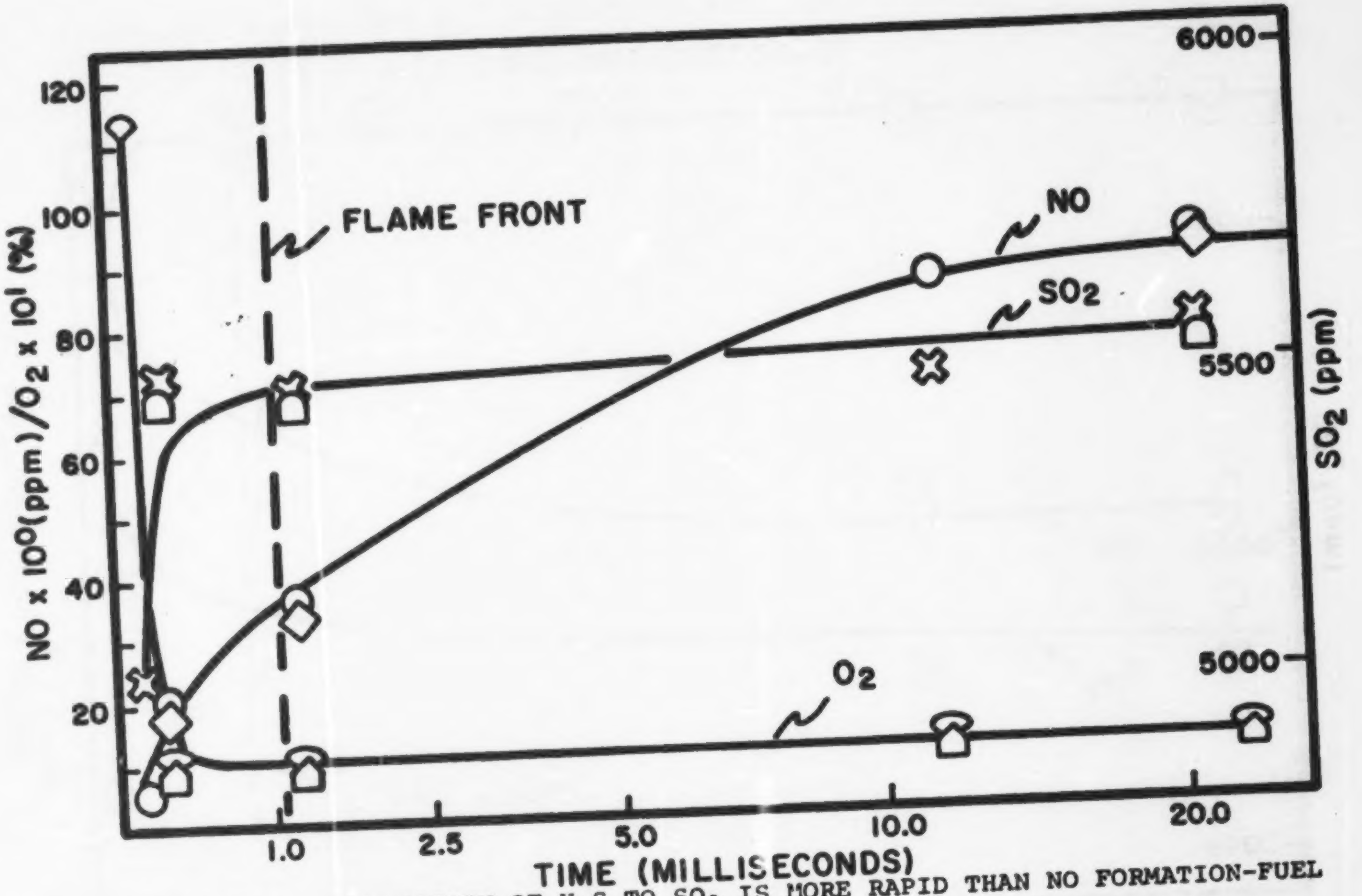

FIGURE 14. CONVERSION OF H_2S TO SO_2 IS MORE RAPID THAN NO FORMATION-FUEL LEAN CONDITIONS

MATHEMATICAL MODELING

In order to model the kinetic mechanisms of the sulfur-nitrogen oxide interactions experimentally observed it is first necessary to model the physical environment of a flat flame in which the reaction chemistry occurs. In a flat flame the physical processes of convection and diffusion are important and simple plug flow models are inadequate. Indeed a substantial amount of back diffusion into the unburned gases is crucial in allowing a stable flame front to be maintained, and in allowing ignition to occur. Simple models that impose a specified time temperature-history on the kinetics environment can be misleading, especially in the case examined here, where temperature, free radical concentrations and nitrogen oxide kinetics are intimately coupled. For example, high superequilibrium concentrations of atoms and free radicals necessarily lead to significantly lower temperatures because of the enthalpy of disassociation of oxygen, hydrogen and water molecules. Thus a substance that catalyzes atom recombination rates and lowers free radical concentrations will also raise the flame temperature at that point and this rise in temperature may offset, in some degree, the effect of lower oxygen atom concentrations as regards NO formation. Thus any reasonable model describing the observed effects must

a) calculate the resulting temperature from a heat balance and

b) properly take account of diffusion in the flame front.

Unfortunately, no model of a flat flame is generally available and so it was necessary to develop a very approximate simulation to be used in this study. It is recognized that substantial improvements in such a simulation are desirable. However, our model is an improvement on others that take no account of diffusion in the flame front. The approach used here was to develop a simplified premixed flat flame model that takes account of diffusion, then to calibrate this model against

a) literature data on free radical concentrations and

b) our own base case of NO formation without sulfur present.

It should be noted that the model therefore used only two unknown parameters, one of which was obtained from the open literature, the other of which uses our own base case data. This model was then used to test kinetic mechanisms of sulfur oxide - nitrogen oxide interactions, and the resulting mechanism was then used to determine the effect of different environments and different heat loss rates corresponding to those likely in a furnace.

Premixed Flat Flame Model

The salient features of our preliminary flat flame model is that the diffusion in the ignition zone is assumed to be such that it can be simulated by a (hypothetical) well stirred stage or pointwise calculation. The ignition zone is then followed by a plug flow calculation. This model can be shown to be exact(16) only when the true concentration profiles are parabolic. Since this is seldom the case, the model should be regarded as only an approximate simulation of our flat flame. The volume of the hypothetical stirred stage is determined by that which allows a certain fraction of a species (designated "fuel") to be converted.

The basic tool used was computer program REKINET which integrates the conservation equations for well stirred and plug flow reactors both with and without a heat balance. In addition, this program allows the volume of the well stirred stage to vary until a specified fraction of a specified species is converted.

The basic approach used to model the flat flame investigated here consisted of the following steps:

- choose a kinetic mechanism for CH_4/air combustion
- determine which value of percent CH_4 consumed (denoted by χ) during pointwise calculation led to measured atom concentrations of Peeters and Mahnen(17)
- use this value of χ to simulate our flat flame and calibrate the heat loss parameters in the model until the predicted and measured base case NO profiles matched
- investigate changes due to SO_2 addition, assuming atom recombination catalysis with mechanisms and rates proposed by Halstead and Jenkins(5) and Merryman and Levy(18). No other parameters should be altered in this phase.

Kinetic Mechanism

The methane air reactions used were those suggested by Waldman *et al.*,(4) in an EPA sponsored investigation of kinetic mechanisms of methane/air combustion with pollutant formation. A list of reactions is shown on Table 3. The reaction named ULT36 through ULT143 denote the reactions numbered 36 through 143 in Table 7.5 of Reference (4).

In addition, for the runs simulating sulfur addition, the atom recombination catalysis is described by reactions shown in Table 4. Those reactions named MERL7 and MERL3A are reactions numbered 7 and 3A by Merryman and Levy(18) while those labeled JENKI are from Halstead and Jenkins(5). Reaction JOHN11 is from Johnston's review of O atom kinetics(19). These reactions demonstrate the catalysis of O atom recombination by SO_2 via SO_3 as an intermediate as well as the catalysis of H atom and OH radical recombination to form H_2O, with HSO_2 as an intermediate. No adjustment of rate coefficient values from those suggested by the original authors was made and it was assumed throughout that:

$$k_f/k_r = K_{equil}.$$

An important result obtained from this kinetic model is to determine whether this atom recombination catalysis is sufficient to account for the drop in NO emissions caused by SO_2 addition. In addition, a kinetic calculation of this type allows the separate effects of temperature profile changes and radical concentration changes to be investigated. This should lead to greater insight into the salient features involved.

Tables 3 and 4 follow

TABLE 3. METHANE COMBUSTION MECHANISM

ULT36	CHO	+M		=CO	+H	+M
ULT77	CO2	+M		=CO	+O	+M
ULT84	H2O	+M		=OH	+H	+M
ULT99	H	+O	+M	=OH	+M	
ULT101	H	+O2	+M	=HO2	+M	
ULT140	N2O	+M		=N2	+O	+M
ULT44	CHO	+H		=CO	+H2	
ULT46	CH2O	+O		=CHO	+OH	
ULT47	CHO	+OH		=CO	+H2O	
ULT52	CHO	+O		=CO	+OH	
ULT59	CH3	+O		=CH2O	+H	
ULT63	CH4	+O		=CH3	+OH	
ULT65	CH4	+H		=CH3	+H2	
ULT66	CH4	+OH		=CH3	+H2O	
ULT70	CO	+OH		=CO2	+H	
ULT83	H	+OH		=H2	+O	
ULT85	H	+HO2		=OH	+OH	
ULT88	OH	+H2		=H	+H2O	
ULT91	OH	+N		=H	+NO	
ULT98	H	+N2O		=OH	+N2	
ULT100	OH	+O		=H	+O2	
ULT117	OH	+OH		=H2O	+O	
ULT125	N	+NO		=N2	+O	
ULT133	N	+O2		=NO	+O	
ULT135	N2O	+O		=NO	+NO	
ULT143	CHO	+O2		=CO	+HO2	
JOHN11	O2	+M		=O	+O	

TABLE 4. SO_2 CATALYZED RECOMBINATION OF ATOMS AND RADICALS

MERL1	SO2	+O	+M	=SO3	+M
MERL3A	SO3	+O		=SO2	+O2
JENKI1	H	+SO2	+M	=HSO2	+M
JENKI2	HSO2	+OH		=H2O	+SO2

Calibration of Flat Flame Simulation with Data of Peeters

In our simulation of a flat flame the ignition zone is simulated by a well stirred stage or pointwise calculation where the hypothetical volume is determined by that volume which will convert a certain fraction χ of the primary fuel. This is followed by a plug flow heat balanced calculation. We settled on a value of χ by calibrating our simulation with the data of Peeters and Mahnen(17). Heat loss in the ignition zone was assumed to be negligible. A value of

$$\chi = 0.98$$

was chosen because, as shown in Table 5:

- the maximum CH_4 consumption rate was then similar to that measured
- the peak O atom mole fraction (0.048) was of the same order as that measured (0.025) compared to the equilibrium O_2 mole fraction which was two orders of magnitude lower
- the temperature of the hypothetical well stirred stage matched that measured at the maximum CH_4 consumption rate.

Table 5 follows

TABLE 5. SIMULATION OF FLAME OF PEETERS et al. (1973)

	Simulation	Experiment
Temperature at Ignition Zone Exit	1569°K	1550°K
Max. Rate of CH_4 Consumption	5.53×10^{-5} $\frac{\text{moles}}{\text{cc sec}}$	8.4×10^{-5} $\frac{\text{moles}}{\text{cc sec}}$
Ignition Zone Exit, Mole Fractions		
CO	0.0336	0.042
O	0.0343	0.011
OH	0.0173	0.015
CH_2O	0.00126	0.001
Max. O Atom Mole Fraction	0.0474	0.025

The simulation did over predict the atom concentration by a factor of two and also tended to under predict the rate of temperature increase. Obviously the simulation does not give a true picture of the flat flame at this stage, and the discrepancies are probably due to inaccuracies in both the model and the kinetic mechanism. Nevertheless, the simulation was considered sufficiently adequate to investigate the kinetic mechanism appropriate to SO_2 inhibition of nitrogen oxides.

This calculation also demonstrated that the kinetic mechanism of methane combustion proposed by Waldman(4) did contain the salient features observed by Peeters and Mahnen(17). For example, the predicted formaldehyde, hydroxyl and carbon monoxide profiles were reasonably close to those measured. This gives both the kinetic mechanism and the simulation some credence.

Calibration with Base Case NO Measured

The base cases used to test the kinetic model were those with 104% stoichiometric air at both zero and 240°C mixture preheat. We restricted our investigation to the fuel lean regime because the dominant NO formation kinetics are there better understood. Using the value of $\chi = 0.98$ determined previously and the kinetic mechanism for methane combustion shown on Table 3 it was found that the NO measurements in our flat flame could be matched by the simulation with a radiative heat loss coefficient

$$\sigma = 3.45 \times 10^{-14} \quad \text{cal/sec cm}^3\ ^\circ\text{K}^4$$

for the case with no preheat, and with

$$\sigma = 8.0 \times 10^{-14} \quad \text{cal/sec cm}^3\ ^\circ\text{K}^4$$

for the case with 240°C mixture preheat.

The discrepancy between these two values indicate shortcomings in our model. However, since the purpose of our model is to predict the change in NO due to SO_2 addition, it is reasonable to calibrate against both the zero and high preheat base cases individually. Obviously an improved model should be able to predict the effect of mixture preheat, without additional calibration.

Effect of SO_2 in Fuel

With 4.9% SO_2 in the fuel the simulation showed a drop of 49 ppm NO in the exhaust for the case with no preheat. This compares with a measured drop of 40 ppm as shown in Table 6. At 240°C preheat the simulation predicted a drop of 51 ppm NO compared to a measured reduction of 70 ppm. Given the inaccuracies of the physical model, the kinetic

Table 6 follows

TABLE 6. EFFECT OF SO_2 on NO_x EMITTED: SIMULATION AND MEASURED VALUES

	Simulation	Measured
Base case, 104% stoich.air, zero preheat, NO ppm	148	150
4.9% SO_2 in fuel, NO ppm	99	110
Reduction in NO ppm	49	40
Percent reduction in NO	33	27
Base case, 104% stoich air, 240°C preheat, NO ppm	232	232
4.9% SO_2 in fuel, NO ppm	181	160
Reduction in NO ppm	51	72
Percent reduction in NO	22	30

rate coefficients, the simulation predicts the correct effect of SO_2 addition with remarkable accuracy, especially for the no preheat case. The discrepancy between theory and experiment in the high preheat case may be due to an inaccurate simulation of the heat loss under that condition. It is clear, therefore, that the SO_2 catalysis of atoms and free radicals as described by Reactions MERL7 through JENK12 on Table 4 can explain the observed inhibition NO formation by SO_2.

Analysis of Simulation and Application

Calculated profiles of oxygen atom concentration, NO concentration and temperature are shown on Figure 15 for the zero preheat case. It is clear that the addition of SO_2 to the fuel changes both the oxygen atom and the temperature profiles (assuming that the radiative heat transfer coefficient remains unchanged). In the presence of SO_2 the higher temperature at early times is intimately coupled with the drop in atom concentration, which is significant. This indicates that before 10^{-4} seconds the NO formation rate is actually slightly higher with SO_2 than with no SO_2. However, during the time when most of the NO is being formed and when radiative heat loss is important, the drop in O atom concentration dominates, and the resultant NO formed is significantly lower. It is clear,

Figure 15 follows

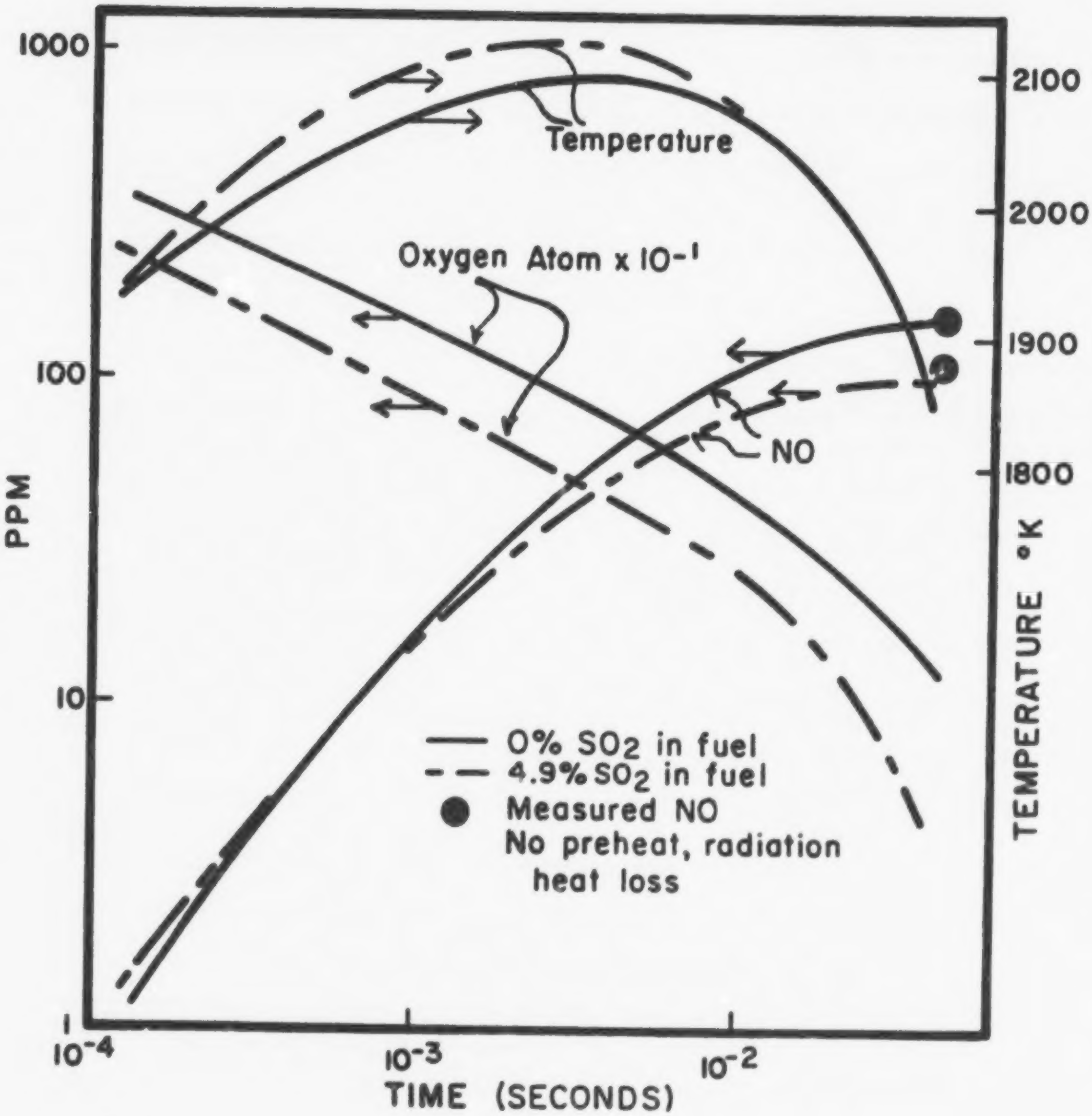

FIGURE 15. SO_2 ADDITION AFFECTS BOTH OXYGEN ATOM AND TEMPERATURE PROFILES, BUT LOWERS NO

therefore, that the reason behind the observed effect is that the presence of SO_2 catalyzes the recombination of oxygen atoms, and that the drop in oxygen atom concentration is sufficient to lower the NO formation rate.

There is, however, a qualitative discrepancy between the predicted profile of NO shown on Figure 15 and that measured (at a different air/fuel ratio) and shown on Figure 8. In general, the measured profile showed a more rapid formation of prompt NO than that predicted. The qualitative discrepancy is probably due to unknown features in the mechanism of prompt NO formation. It is felt, however, that this discrepancy is not serious and does not detract from the point that O atom recombination catalysis by SO_2 can explain the drop in exhaust NO measured, with no adjustment to known rate coefficients being necessary. Further details of the results from the model are shown on Table 7 for the no preheat case. These tables show the early formation of superequilibrium concentrations of SO_3, which is an intermediate species in the recombination catalysis scheme, followed by a decline to relatively low values, corresponding to approximately 1% conversion of SO_2 to SO_3. Surprisingly, the calculations also indicate that the addition of SO_2 also appear to hasten the CO burnout rate, although low CO levels were

Table 7 follows

TABLE 7. SIMULATION DETAILS - NO PREHEAT

	Mole Fractions				Temp.
Time (sec)	NO	O	SO_3	CO	T°K
0% SO_2 in Fuel					
Ignition Zone Exit	0.479E-7	0.458E-2	--	0.408E-1	1659
0.11×10^{-5}	0.488E-7	0.484E-2	--	0.414E-1	1678
0.125×10^{-4}	0.720E-7	0.555E-2	--	0.364E-1	1754
0.482×10^{-4}	0.253E-6	0.465E-2	--	0.267E-1	1850
0.329×10^{-3}	0.404E-5	0.236E-2	--	0.183E-1	2003
0.133×10^{-3}	0.112E-5	0.343E-2	--	0.216E-1	1935
0.780×10^{-3}	0.118E-4	0.158E-2	--	0.151E-1	2055
0.140×10^{-2}	0.223E-4	0.119E-2	--	0.129E-1	2081
0.365×10^{-2}	0.537E-4	0.749E-3	--	0.979E-2	2099
0.996×10^{-2}	0.103E-3	0.454E-3	--	0.686E-2	2064
0.280×10^{-1}	0.140E-3	0.197E-3	--	0.338E-2	1939
0.425×10^{-1}	0.145E-3	0.119E-3	--	0.208E-2	1852
4.9% SO_2 in Fuel					
Ignition Zone Exit	0.622E-7	0.396E-2	0.384E-3	0.400E-1	1686
0.104×10^{-5}	0.632E-7	0.415E-2	0.387E-3	0.406E-1	1704
0.118×10^{-4}	0.883E-7	0.466E-2	0.325E-3	0.362E-1	1783
0.347×10^{-4}	0.204E-6	0.386E-2	0.221E-3	0.286E-1	1864
0.298×10^{-3}	0.388E-5	0.158E-2	0.321E-4	0.154E-1	2046
0.723×10^{-3}	0.106E-4	0.994E-3	0.136E-4	0.118E-1	2094
0.123×10^{-2}	0.178E-4	0.755E-3	0.887E-5	0.100E-1	2113
0.303×10^{-2}	0.377E-4	0.480E-3	0.519E-5	0.740E-2	2123
0.835×10^{-2}	0.701E-4	0.282E-3	0.425E-5	0.494E-2	2090
0.123×10^{-1}	0.819E-4	0.212E-3	0.438E-5	0.389E-2	2058
0.256×10^{-1}	0.956E-4	0.903E-4	0.534E-5	0.180E-2	1959
0.372×10^{-1}	0.978E-4	0.457E-4	0.650E-5	0.916E-3	1882

obtained in all cases.

It is instructive to examine the effect of SO_2 in the fuel on NO formation rates when there is zero radiative heat loss, i.e., under adiabatic conditions. This is shown in Figure 16 where it is apparent that under adiabatic conditions the presence of SO_2 causes NO to reach its equilibrium value more slowly. This simulation also indicated that SO_2 causes a change in the time temperature history, but that the primary effect was due to lower O atom concentrations.

In order to separate out kinetic and temperature effects it is useful to determine the role of SO_2 under a specified time-temperature history. In this case there is no attempt made to satisfy the heat balance, but rather, it is assumed that the temperature and heat transfer are controlled by the furnace configuration. A realistic temperature history is one with an exponential temperature drop from 2100°K to 1050°K in one second. This time-temperature history is roughly representative of that felt by a labeled volume of premixed gas and fuel as it combusts and moves through the convection section of a furnace. Thus this simulation can give some indication of what might happen in a utility boiler, under conditions where

Figure 16 follows

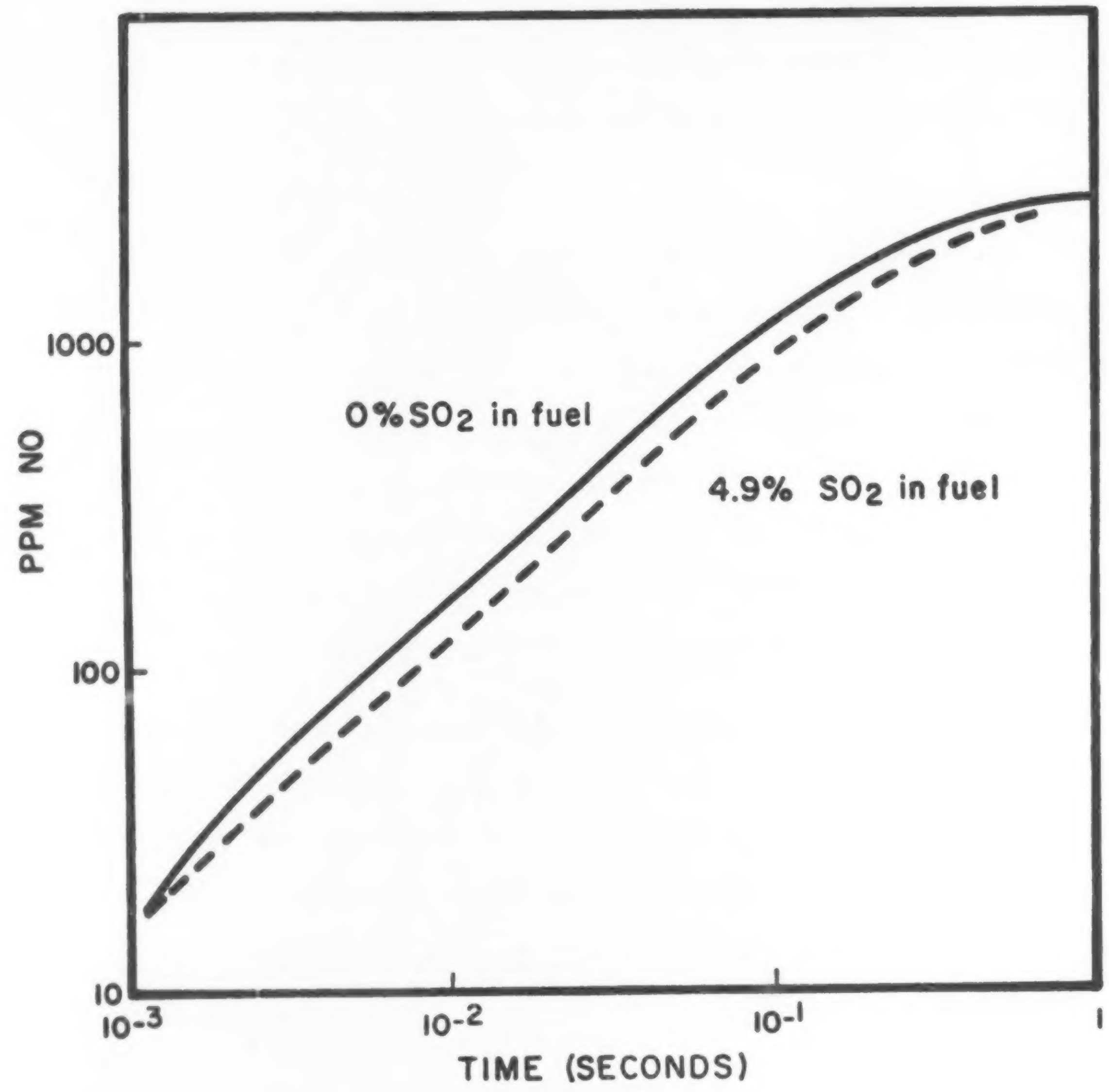

FIGURE 16. UNDER ADIABATIC CONDITIONS SO_2 DELAYS NO FORMATION

fuel and air mixing is very rapid. Results are shown on Table 8, and indicate that under such conditions fuel sulfur is likely to inhibit the formation of NO_x.

CONCLUSIONS

It was found that both sulfur dioxide and hydrogen sulfide, when added to a gaseous fuel, had a significant inhibition effect on thermal NO_x emissions. The presence of sulfur to make about 6800 ppm SO_2 in the exhaust lowered NO_x emissions by up to 36%. Although it should be noted that these results are valid for premixed gaseous flames, they do imply that fuel desulfurization may lead to increased (thermal) NO_x emissions from combustion processes.

It appears to make very little difference whether the fuel sulfur is introduced into the fuel as SO_2 or H_2S, except under fuel rich conditions where conversion of H_2S to SO_2 is not rapid. This indicates that the inhibition of NO formation by fuel sulfur occurs through mechanisms involving SO_2.

A preliminary model of a premixed flat flame showed that this inhibition effect could be explained by the homogeneous catalysis of free radical recombination rates by sulfur dioxide. This mechanism lowers the oxygen atom

Table 8 follows

TABLE 8. FURNACE SIMULATION-PREMIXED MIXTURE, SPECIFIED TEMPERATURE FALLING FROM 2100°K to 1050°K IN ONE SECOND. APPROXIMATELY 4% EXCESS AIR

	NO ppm	
Approximate Time	Without sulfur	With sulfur (4.9% SO_2 Fuel)
0.4 m sec	33.6	24.5
1 m sec	63.0	38.8
2.5 m sec	218.0	125.0
Exhaust	339.0	189.0

concentration and, for a given radiative heat loss, lowers NO formation rates. The effect of lower atom concentrations is greater than the ensuing (coupled) temperature increase. Under conditions where the temperature was fixed as an independent variable the predicted inhibitory effect of SO_2 on NO_x emissions was even larger.

Observations involving inhibition of NO formation by SO_2 can therefore be used to arrive at conclusions concerning the role of superequilibrium oxygen atoms. Since inhibition was observed under fuel rich and fuel lean conditions it appears that superequilibrium oxygen atoms play an important role in both regimes. The effect of SO_2 was especially pronounced on "prompt" NO formation, and this supports theories that superequilibrium concentrations oxygen atoms are a factor in the rapid formation of NO early in the flame.

In addition, the experimental results showed that "prompt" NO accounted for essentially all the NO_x emissions under fuel rich conditions and that it was not a strong function of mixture preheat. This implies that NO_x formation mechanisms other than those of Zeldovich are controlling early in the flame.

Current efforts at the University of Arizona are focused on the effect of fuel sulfur on Fuel NO emissions and on sulfur oxide nitrogen oxide interactions in more practical oil diffusion flames. Results are expected shortly. Then it will be possible to gauge the practical importance of adverse effects of fuel desulfurization.

ACKNOWEDGMENTS

This research was supported by the U.S. Environmental Protection Agency under Grant R-802204. However, the opinions and results presented do not necessarily reflect the views of the Environmental Protection Agency. The help and advice of W. Steven Lanier is gratefully acknowledged.

REFERENCES

1. Cullis, C.F., R.M. Henson, and D.L. Trimm, Proc. Roy. Soc. (London) A295, 72 (1966).

2. Wendt, J.O.L., and C.V. Sternling, Comb. & Flame, 21, 387 (1973)

3. Thompson, D., T.D. Brown and J.M. Beer, Fourteenth Symposium (International) on Combustion, p.787, The Combustion Institute, (1973).

4. Waldman, C.H., R.P. Wilson, Jr., and K.L. Maloney, "Kinetic Mechanism of Methane/Air Combustion with Pollutant Formation". Environmental Protection Technology Series Report EPA-650/2-74-045 (1974).

5. Halstead, D.J., and D.R. Jenkins, Trans. Faraday Soc., 65, 3013 (1969).

6. Durie, R.A., G.M. Johnson, and M.V. Smith, Comb. & Flame, 17, 197 (1971).

7. Zeldovich, Y., Acta Physiochim. URSS 21, 577 (1946).

8. Bowman, C.T., Fourteenth Symposium (International) on Combustion, p.729, The Combustion Institute, (1973).

9. Fenimore, C.P., Thirteenth Symposium (International) on Combustion, p.373, The Combustion Institute, (1971).

10. Wendt, J.O.L., C.V. Sternling, and M.A. Matovich, Fourteenth Symposium (International) on Combustion, p.897, The Combustion Institute (1973).

11. Sarofim, A.F., and J.H. Pohl, Fourteenth Symposium (International) on Combustion, p.739, The Combustion Institute (1973).

12. Fristrom, R., and A. Westenberg, "Flame Structure".

13. Brown, J.W., D.W. Pershing, J.H. Wasser, and E.E. Berkau, "Interactions of Stack Gas Sulfur and Nitrogen Oxides on Dry Sorbents", U.S. Environmental Protection Series No. EPA-650/2-73-029 (1973).

14. Ekmann, J.J., M.S. Thesis, Department of Chemical Engineering, University of Arizona (1974).

15. Merryman, E.L., and A. Levy, "Nitrogen Oxide Formation in Flames: The Roles of NO_2 and Fuel Nitrogen". Presented at Fifteenth Symposium (International) on Combustion, Tokyo, (August 1974).

16. Sternling, C.V., and J.O.L. Wendt, "Kinetic Mechanisms Governing the Fate of Chemically Bound Sulfur and Nitrogen in Combustion". Environmental Protection Technology Series, Report EPA-650/2-74-017 (1972).

17. Peeters, J., and G. Mahnen, Fourteenth Symposium (International) on Combustion, p.133, The Combustion Institute, (1971).

19. Johnston, H.S., "Gas Phase Reaction Kinetics of Neutral Oxygen Species", National Stand. Ref. Data Ser., NBS 20 (1968).

9:25 a.m.
Effects of Fuel Sulfur on
Nitrogen Oxide Emissions
Dr. Jost O.L. Wendt, University of Arizona

Q: Jost, are you implying that your reduction is also going to follow the same mechanism for the prompt NO?

A: Well, what I am implying is that superequilibrium atom and free radical concentrations are important in the formation of prompt NO, but I am not implying that, for example, the Zeldovich mechanism is the mechanism to form prompt NO.

Q: You're right, because I wonder if for your prompt NO, there may be more likelihood of an OH type mechanism accounting for the oxidation.

A: Absolutely. In fact, I should point out that when you lower the oxygen atom concentration by whatever mechanism, you tend to lower the free radical concentrations of all other species as well, and so there are secondary effects that may be important.

Q: In all your reported measurements you report NO_x as NO; are those actually just simple NO measurements or measurements of total NO_x reported as NO?

A: Those measurements are NO. It turns out we did look for NO_2; unfortunately we only had a stainless steel converter on our chemaluminescent analyzer so we could only do this in the fuel lean regime, and at most we only found 3% of the NO_x was NO_2. So we found very little NO_2.

Q: Jost, did you say that the effect of added sulfur was to reduce the oxygen atom concentration but to increase the temperature, so that the overall effect was almost none?

A: No. I didn't say that. It turns out that your temperature profile is a function of both the composition of a mixture at a point and of the radiative heat loss that your flame sees as a function of time. Now as you lower the oxygen atom concentration, the initial temperature early on in the profile will increase, but then the heat loss more than compensates for that, so the drop in the O-atom concentration more than offsets any increase in temperature that you get. That's what the calculations showed as well.

Q: I didn't quite get how you measure your oxygen atom concentration; or do you just assume a level for them?

A: No, we did not measure that.

Q: Basically then, what you're saying is that if you don't really know that, you also don't know whether or not you're really catalyzing the recombination; I mean that's an assumption.

A: Well, I think you're thinking about that second to last slide, and that is the result of a calculation that we made in which we modelled the chemical and physical processes occurring in the flat flame. We used a fairly detailed set of chemical reactions, actually those recommended by Ultrasystems Corporation. So those curves that you saw were the results of a calculation. What we did was to calibrate a model with our base case and we left it alone and used Merryman's and Levy's and Halstad and Jenkin's data on SO_2 atom recombination rates and wanted to see what the effect of that would be. The effect predicted is to lower the atom concentrations -- theoretically, that is.

Q: I want to just establish that all you really know for fact is that addition of SO_2 lowered your NO_2 or NO.

A: As an experimental fact that is all we know.

Q: In reading some of those charts, although I couldn't see them too clearly, the fifth or fourth one before the end looked to me like the NO concentration peaked at about 5% excess air.

A: Right.

Q: And that reading out to about 20% excess air, it looked to me like the concentration was approximately half. It looked like the addition of the 20% excess air dropped the concentration much more radically. This would imply a lot more free oxygen and yet the results you foundwere that the reduction of the free oxygen reduced the NO; I do not quite put those two facts together.

A: The first thing you have to realize is that these results are for pre-mixed laminar flames; in other words, you can't compare our results with results from diffusion flames or typical burners. The base case results are in line with what other people have gotten. It's quite normal to see the nitrogen oxides be decreased rapidly as you increase the excess air. This is a thermal temperature effect. In terms of your other question about free oxygen, I think we will have to discuss that later.

TWO-DIMENSIONAL COMBUSTOR MODELING*

By:

R. C. Buggeln and H. McDonald
United Technologies Research Center
East Hartford, Connecticut 06108

---

*Work sponsored in part by the Environmental Protection Agency, Research Triangle Park, North Carolina under Contracts 68-02-1092 and 68-02-1873

ABSTRACT

The equations that describe the conservation of mass, momentum, and energy in the flow fields of industrial furnaces are presented and the concepts of stream function and vorticity are introduced. The stream function-vorticity formulation reduces the number of governing equations to be solved by one, and at the same time removes the troublesome pressure terms. In the present formulation each equation has the same general form, a feature which is convenient for ease of solution. A numerical procedure is then described which transforms each equation into a series of linear algebraic equations suitable for solution on a high-speed computer. Coupling and nonlinear effects are accounted for by using an iterative technique. Once the solution of the flow field is completed, the same numerical procedure is utilized to solve for the NO levels.

INTRODUCTION

Events of the last decade, especially in the areas of pollution control and fuel consumption, have placed a considerable burden on the present-day designers of industrial furnaces. Prediction of industrial furnace performance and pollutant emission characteristics require modeling procedures possessing a high degree of sophistication in the areas of chemistry and fluid dynamics. Methods of modeling furnaces have generally been less than completely satisfactory largely due to a lack of understanding of the fundamental flow processes which, through heat, mass, and momentum exchange, directly effect pollutant emission and combustion efficiency. For example, it has been shown (Refs. 1 and 2) that stability and combustion intensity of flames as well as residence time in furnaces are strongly influenced by swirling flow. Residence times and flame stability and intensity are, in turn, related to furnace performance and efficiency as well as to pollutant emission formation (Refs. 3 and 4). Thus, because of the strong influence of flow processes on combustion characteristics, it is particularly important that the fluid mechanics be properly taken into account in the development of furnace modeling techniques.

Most previous procedures employed for modeling combustion processes have generally been highly simplified, particularly in regard to flow modeling where stirred reactor concepts and one-dimensional assumptions are employed. As a general criticism, it seems that these previous methods are lacking in their ability to properly account for mixing and reverse flow phenomena occurring in the recirculation zone of an industrial furnace. In contrast to these one-dimensional, stirred reactor models, the recently developed computational method of Gosman, et al., (Refs. 5 and 6) has demonstrated the feasibility of making computations in combustors that have recirculation zones. However, the Gosman procedure utilizes a relatively inefficient point-by-point (Ref. 5) or line-by-line (Ref. 6) relation technique rather than a field relaxation procedure. In order to achieve a more efficient computational scheme a field relaxation technique, the field relaxation elliptic procedure (FREP), was developed at United Technologies Research Center (UTRC).

GOVERNING EQUATIONS

The set of elliptic partial differential equations that describe the combustion system under consideration are based on the conservation laws of mass, chemical species, momentum and energy (Ref. 7). For simplicity and generality, these equations are expressed in vector notation below; however, since the present study is concerned in particular with axisymmetric flow, future discussion will concentrate on the axisymmetric form of these equations. In the present effort, effects of thermal diffusion, pressure diffusion, and forced diffusion upon mass transport as well as the effects of bulk viscosity in the momentum equations are assumed to be negligible. Fick's law is presumed to be valid throughout, implying equal binary diffusion coefficients. With these assumptions in mind, the governing equations can be written as:

Continuity

$$\nabla \cdot \rho \vec{v} = 0 \tag{1}$$

Conservation of Gas Phase Species

$$\nabla \cdot \rho m_i \vec{v} - \nabla \cdot \left(\frac{\mu_{eff}}{Sc} \nabla m_i \right) - \dot{r}_i = 0 \tag{2}$$

Conservation of Liquid Phase Species

$$\nabla \cdot \rho f_j \vec{v} - \nabla \cdot \left(\frac{\mu_{eff}}{Sc} \nabla f_j \right) - \dot{r}_j = 0 \tag{3}$$

Conservation of Momentum

$$\nabla \cdot \rho \vec{v}\vec{v} - \mu_{eff} \left[\nabla \vec{v} + \nabla \vec{v}^{+} - \frac{2}{3} (\nabla \cdot \vec{v}) \delta \right] + \nabla P = 0 \tag{4}$$

Conservation of Energy

$$\nabla \cdot \rho \vec{V} H - \nabla \cdot \left(\frac{\mu_{eff}}{P_r} c_p \nabla T \right) - \nabla \cdot \left(\sum_i \frac{\mu_{eff}}{Sc} h_i \nabla m_i \right) - \nabla \cdot \left[\mu_{eff} \nabla \left(\frac{|\vec{V}|^2}{2} \right) \right] + Q_R = 0 \tag{5}$$

In addition to the above conservation equations, it is necessary to specify a gas law which in the present procedure is given by

$$P = \frac{\rho R T}{M} \tag{6}$$

where the mixture molecular weight, M, is defined by

$$M = \frac{1}{\sum_i \frac{m_i}{M_i}} \tag{7}$$

Finally, the stagnation enthalpy, H, is defined by

$$H = \frac{|\vec{V}|^2}{2} + \sum_i m_i \left[\int_{T_0}^{T} c_{p_i} \, dT + h_{f_i} \right] \tag{8}$$

where $|\vec{V}|$ is the magnitude of the velocity and m_i, c_{p_i}, and h_{f_i} are the mass fraction, specific heat, and the heat of formation of the ith chemical species. T_0 refers to an arbitrary reference temperature. The equations are written for variable fluid properties and embody mass diffusion, thermal conduction, chemical reactions, radiative heat transfer, and viscous dissipations. Solution of these governing equations requires values of the effective turbulent transport coefficients; i.e., a value for the effective viscosity and turbulent Schmidt and Prandtl numbers. In the present procedure, the effective viscosity is calculated by means of either an algebraic mixing length model or by the solution of one or more partial differential equations and the use of Prandtl-Kolmogorov assumption (Ref. 8). Values of the turbulent Prandtl and Schmidt numbers are based upon an empirical knowledge of these parameters in turbulent flows of gases.

When the primitive flow variables, ρ, $\vec{V}$, and P are employed, experience has shown the explicit appearance of the pressure terms in the momenta equations can lead to numerical difficulties. The problems associated with pressure have often been eliminated (for two-dimensional and axisymmetric flows) by the formation of the vorticity transport equation, an equation obtained by taking the derivative of the first momentum equation with respect to the second coordinate direction and taking the derivative of the second momentum equation with respect to the first coordinate direction, and then subtracting the first equation from the second. In this manner the explicit appearance of the pressure terms is eliminated as the momenta conservation equations are replaced by a transport equation for the vorticity, ω, where, by definition, $\omega = \nabla \times \vec{V}$. For axisymmetric flow the vorticity vector is in the azimuthal direction and is given by

$$\omega = \frac{\partial v}{\partial x} - \frac{\partial u}{\partial r} \tag{9}$$

After much rearrangement, the vorticity equation emerges in the form

$$\begin{aligned} r^2 \left[\frac{\partial}{\partial x} (\rho u \omega) - \frac{\partial}{\partial r} (\rho v \omega) \right] - \frac{\partial}{\partial x} \left[r^3 \frac{\partial}{\partial x} \left(\mu_{eff} \frac{\omega}{r} \right) \right] \\ - \frac{\partial}{\partial r} \left[r^3 \frac{\partial}{\partial r} \left(\mu_{eff} \frac{\omega}{r} \right) \right] = r \frac{\partial}{\partial x} (\rho w^2) \\ + r^2 \left[\frac{\partial}{\partial x} \left(\frac{u^2 + v^2}{2} \right) \frac{\partial \rho}{\partial r} + \frac{\partial}{\partial r} \left(\frac{u^2 + v^2}{2} \right) \frac{\partial \rho}{\partial x} \right] + r^3 S_\omega \end{aligned} \tag{10}$$

where S_ω is defined by

$$\begin{aligned} S_\omega = \frac{2}{r} \Big[\nabla (\vec{I}_r \cdot \vec{v}) \cdot (\nabla \vec{I}_x \cdot \nabla \mu_{eff}) \\ + \nabla (\vec{I}_r \cdot \vec{v}) \cdot \nabla (\vec{I}_r \cdot \nabla \mu_{eff}) - \nabla (\nabla \cdot \vec{v} \cdot \nabla_{eff}) \Big] \end{aligned} \tag{11}$$

and where $\vec{1}_x$ and $\vec{1}_r$ are unit vectors in the axial and radial directions. It may appear that little has been achieved by introducing the concept of vorticity since Eq. (10) still has the two velocity components as unknowns. However, it should be noted that the inconvenient pressure terms have been eliminated through the introduction of an additional unknown, the vorticity. Further advantage of this formulation is obtained by introducing the stream function relationships to close the system. The stream function, ψ, is related to the velocity components u and v by

$$\rho u = \frac{1}{r} \frac{\partial \psi}{\partial r} \tag{12}$$

and

$$\rho v = \frac{1}{r} \frac{\partial \psi}{\partial x} \tag{13}$$

Substitution of Eqs. (12) and (13) into Eq. (1) shows that the stream function by definition satisfies the continuity equation, while the combination of Eq. (9) with Eqs. (12) and (13) yields the stream function equation

$$\frac{\partial}{\partial x} \left(\frac{1}{\rho r} \frac{\partial \psi}{\partial r} \right) + \frac{\partial}{\partial r} \left(\frac{1}{\rho r} \frac{\partial \psi}{\partial x} \right) = - \frac{\omega}{r} \tag{14}$$

When Eqs. (10) and (14) are used to replace the continuity and the axial and radial momentum equations there is thus a dual beneficial effect: (i) the awkward pressure terms are eliminated and (ii) the number of equations is reduced by one, i.e., three equations are equivalently replaced by two. After solving Eqs. (10) and (14) (and Eqs. (2), (3), (5), and Eq. (4) for the swirl component of velocity), the variables that were eliminated by the introduction of stream function and vorticity, u, v, and P can be reconstructed. The axial and radial velocity components are computed from Eqs. (12) and (13). The pressure gradients are calculated from Eq. (4), the conservation form of the momentum equation, and then integrated to yield the pressure distribution.

It is also convenient to replace the axial and radial velocity components in the species conservation equations, Eqs. (2) and (3), the swirl equation, Eq. (4), and the energy equation, Eq. (5), by the stream function formulation of velocity. When this is done, it is seen that all of the partial differential equations solved in this study are of the general form

$$a_\phi\left[\frac{\partial}{\partial x}\left(\phi\frac{\partial\psi}{\partial r}\right)-\frac{\partial}{\partial r}\left(\phi\frac{\partial\psi}{\partial x}\right)\right]-\frac{\partial}{\partial x}\left[b_{\phi_1}r\frac{\partial}{\partial x}\left(c_\phi\phi\right)\right]-\frac{\partial}{\partial r}\left[b_{\phi_2}r\frac{\partial}{\partial r}\left(c_\phi\phi\right)\right]+rS_\phi=0 \quad (15)$$

where the nonlinear coefficients a_ϕ, b_{ϕ_1}, b_{ϕ_2}, and c_ϕ and the source term S_ϕ are tabulated in TABLE I for each of the dependent variables, ϕ, under consideration. The generalized form of all the equations to be solved is a very convenient feature for ease of application to any numerical technique. The general form given above was first suggested by Gosman, et al.,(Ref. 5) and for convenience was adopted for use in the present work.

COMPUTATIONAL ANALYSIS

In the present study, solution of the set of coupled elliptic partial differential equations describing the flow inside a furnace is achieved through a field residual relaxation procedure. The procedure is discussed in detail in a soon to be published EPA report and is reviewed briefly here. In the procedure a finite difference analogy is first constructed at interior grid points for each solution variable by replacing the derivatives of Eq. (15) by second-order central difference formulae and rearranging the difference equations into the form

$$c_1\phi_{i-1,j}+c_2\phi_{i+1,j}+c_3\phi_{i,j}+c_4\phi_{i,j-1}+c_5\phi_{i,j+1}+rS_\phi=0 \quad (16)$$

TABLE I

COEFFICIENTS OF GENERAL ELLIPTIC EQUATION

ϕ	a_ϕ	b_{ϕ_1}	b_{ϕ_2}	c_ϕ	S_ϕ
ψ	0	$\frac{1}{\rho r^2}$	$\frac{1}{\rho r^2}$	1.0	$-\frac{\omega}{r}$
$\frac{\omega}{r}$	r^2	r^2	r^2	μ_{eff}	$-\frac{\partial}{\partial x}(\rho w^2) - r\left[\frac{\partial}{\partial x}\left(\frac{u^2+v^2}{2}\right)\frac{\partial \rho}{\partial r} - \frac{\partial}{\partial r}\left(\frac{u^2+v^2}{2}\right)\frac{\partial \rho}{\partial x}\right] - r^2 S_\omega$
rw	1.0	$\mu_{eff} r^2$	$\mu_{eff} r^2$	$\frac{1}{r^2}$	0
m_i	1.0	$\frac{\mu_{eff}}{Sc}$	$\frac{\mu_{eff}}{Sc}$	1.0	$-\mathring{r}_i$
f_j	1.0	$\frac{\mu_{eff}}{Sc}$	$\frac{\mu_{eff}}{Sc}$	1.0	$-\mathring{r}_j$
H	1.0	$\frac{\mu_{eff}}{Pr}$	$\frac{\mu_{eff}}{Pr}$	1.0	$-\frac{1}{r}\frac{\partial}{\partial x}\left[\mu_{eff} r \left\{\left(1-\frac{1}{Pr}\right)\frac{\partial}{\partial x}\left(\frac{v^2}{2}\right) + \sum_i\left(\frac{1}{Sc}-\frac{1}{Pr}\right) h_i \frac{\partial m_i}{\partial x}\right\}\right] - \frac{1}{r}\frac{\partial}{\partial r}\left[\mu_{eff} r \left\{\left(1-\frac{1}{Pr}\right)\frac{\partial}{\partial r}\left(\frac{v^2}{2}\right) + \sum_i\left(\frac{1}{Sc}-\frac{1}{Pr}\right) h_i \frac{\partial m_i}{\partial r}\right\}\right] + Q_R$

The c's represent a collection of terms that account for the convection and diffusion of the variable ϕ throughout the mesh system. In general, the c's may be functions of the ϕ's as well as other dependent variables. Thus, Eq. (16) represents a system of nonlinear coupled equations. Linearization of Eq. (16) is accomplished by the utilization of a Newton-Raphson procedure, as follows. First a guess, $\phi^n_{i,j}$, is made for each solution variable at each grid point. Using this guess, a residual of the form

$$R^n_{i,j} = c^n_1 \phi^n_{i-1,j} + c^n_2 \phi_{i+1,j} + c^n_3 \phi^n_{i,j} + c^n_4 \phi^n_{i,j-1} + c^n_5 \phi^n_{i,j+1} \qquad (17)$$

is defined. The Newton-Raphson procedure seeks to drive the residual at the n+1st level to zero by expanding the residual in a Taylor series about the residual level n. This results in the equation

$$\begin{aligned} -R^n_{i,j} = {} & \left(\frac{\partial r}{\partial \phi_{i-1,j}}\right)^n \left(\phi^{n+1}_{i-1,j} - \phi^n_{i-1,j}\right) + \left(\frac{\partial R}{\partial \phi_{i+1,j}}\right)^n \left(\phi^{n+1}_{i+1,j} - \phi^n_{i+1,j}\right) \\ & + \left(\frac{\partial R}{\partial \phi_{i,j}}\right)^n \left(\phi^{n+1}_{i,j} - \phi^n_{i,j}\right) + \left(\frac{\partial R}{\partial \phi_{i,j-1}}\right)^n \left(\phi^{n+1}_{i,j-1} - \phi^n_{i,j-1}\right) \qquad (18) \\ & + \left(\frac{\partial R}{\partial \phi_{i,j+1}}\right)^n \left(\phi^{n+1}_{i,j+1} - \phi^n_{i,j+1}\right) \end{aligned}$$

Derivatives of the residual with respect to the solution variables are replaced with the appropriate c's, e.g.,

$$\left(\frac{\partial R}{\partial \phi_{i-1,j}}\right)^n = c^n_1$$

for which n-level values are available. Substitution and rearranging leads to a linear form of Eq. (18), viz.

$$\begin{aligned} & c^n_1 \phi^{n+1}_{i-1,j} + c^n_2 \phi^{n+1}_{i+1,j} + c^n_3 \phi^{n+1}_{i,j} + c^n_4 \phi^{n+1}_{i,j-1} + c^n_5 \phi^{n+1}_{i,j+1} \qquad (19) \\ & = \left\{ c_1 \phi_{i-1,j} + c_2 \phi_{i+1,j} + c_3 \phi_{i,j} + c_4 \phi_{i,j-1} + c_5 \phi_{i,j+1} - R_{i,j} \right\}^n \end{aligned}$$

Equation (19) is constructed at interior grid points for each selection variable. If the grid mesh were of size MxN, this would result in the need to solve MxN simultaneous linear equations to update each solution variable, ϕ, to the n+1 st iteration level. For small values of M and N this could readily be accomplished; however, for larger values of M and N a more efficient means is the Alternating Direction Implicit (ADI) procedure (Ref. 9). Once each solution variable is updated to the n+1 st level, new mesh values of the c's can be calculated for each equation and the overall solution procedure can be performed to update the variables to the n+2 nd iteration level. This overall solution procedure is repeated until the desired degree of convergence is achieved.

CALCULATION OF NO LEVELS

Once a converged flow field solution is available, it is now possible to solve the NO mass fraction equation for the nitric oxide levels. The form of this mass fraction equation is the same as the form of Eq. (15), hence the same general solution technique can be utilized. The source term of this mass fraction equation, $\dot{r}_{NO}$, requires an expression for the rate of creation of nitric oxide. A generally accepted reaction model for nitric oxide formation and decomposition in post-flame gases is that proposed by Lavoie, at al., (Ref. 10) which consists of the following six reactions:

$$N_2 + O \rightleftharpoons NO + N \tag{20}$$

$$N + O_2 \rightleftharpoons NO + O \tag{21}$$

$$N + OH \rightleftharpoons NO + H \tag{22}$$

$$H + N_2O \rightleftharpoons N_2 + OH \tag{23}$$

$$O + N_2O \rightleftharpoons N_2 + O_2 \tag{24}$$

$$O + N_2O \rightleftharpoons NO + NO \tag{25}$$

The first two reactions, Eqs. (20) and (21), form the Zeldovitch mechanism (Ref. 11) and are considered to be the principal nitric oxide formation reaction mechanism. The two reactions together with the third reaction, Eq. (22), which assumes minor importance under fuel-rich conditions, form the extended Zeldovitch mechanism which is employed in the present study. At low temperatures, when nitric oxide concentrations are much greater than equilibrium values, the fourth, fifth, and sixth reactions, Eqs. (23) through (25), involving N_2O as an intermediary, may become important; however, because overall reaction rates are so low, the net effects of these reactions are probably negligible. Therefore, these last three reactions are neglected in the present study. The results of Bowman and Seery (Ref. 12), as well as other investigators (Ref. 13) in investigation of nitric oxide formation kinetics in combustion processes, lend support to this nitric oxide formation model.

Use of the above information or the 'Law of Mass Action' enables one to derive an expression for the term $\dot{r}_{NO}$. $\dot{r}_{NO}$ is a function of the temperature (which at this point is assumed to be unaffected by the level of NO) and the concentrations of N_2, O, N, and O_2 (which are assumed to be the equilibrium values). Since the velocity, temperature, diffusion coefficient, etc. do not vary during the solution of this equation, there is no coupling; however, nonlinear effects enter the equation through the source term and hence an iterative procedure must also be used to solve this equation.

Solution of the NO equation along with the previously solved flow field thus gives the designer the capability of being able to predict both the efficiency and pollutant levels from industrial furnaces. For typical cases, a converged solution can be achieved in approximately one hour of UNIVAC 1110 computer time. Wide ranges of flow conditions can be considered at a relatively low cost, certainly much more inexpensively than by performing an experiment. The numerical procedure is very general and additional equations, geometrical considerations, etc. can be included in a relatively short period of time.

LIST OF SYMBOLS

a	Coefficient in general elliptic equation, Eq. (15)
b	Coefficient in general elliptic equation, Eq. (15)
c	Coefficient in general elliptic equation, Eq. (15); collection of convection and diffusion terms
c_p	Species specific heat
C_p	Mixture specific heat
f	Liquid particle mass fraction
h_f	Heat of formation
H	Stagnation enthalpy
$\vec{I}_x$	Unit vector in axial direction
$\vec{I}_r$	Unit vector in radial direction
m	Gaseous mass fraction
M	Mixture molecular weight; axial grid locations
M_i	species molecular weight
N	Radial grid locations
P	Pressure
Pr	Prandtl number
Q_R	Radiation flux
r	Radial coordinate
$\overset{\circ}{r}$	Production term in species conservation equation

R	Universal gas constant; residual
S	Source term
Sc	Schmidt number
S_{ω}	Group of terms in vorticity equation (see Eq. (11))
T	Absolute temperature
u	Axial velocity
v	Radial velocity
$\vec{V}$	Time-averaged velocity
w	Swirl velocity
x	Axial coordinate

Greek Symbols

δ	Kronecker delta
ζ	Normalized vorticity (ω/r)
μ	Viscosity
ρ	Density
ϕ	General function
ψ	Stream function
ω	Vorticity
∇	Nabla operator

Subscripts

eff	Imparts molecular (laminar) and turbulent characteristics
i	Gas phase component; axial grid node
j	Liquid phase component; radial grid node
o	Reference
ϕ	General function
ϕ_1	General function axial component
ϕ_2	General function radial component

Superscripts

n	Iteration level
o	Reference
$\dagger$	Transpose of a tensor

REFERENCES

1. Beer, J. M. and N. A. Chigier: Stability and Combustion Intensity of Pulverized Coal Flames - Effect of Swirl and Impingement. Journal of the Institute of Fuel, December 1969.

2. Beer, J. M. and W. Leucker: Turbulent Flames in Rotating Flow Systems. Paper No. Inst. F-NAFTC-7, North American Fuel Technology Conference, Ottawa, Canada, 1970.

3. Beer, J. M. and J. B. Lee: The Effects of Residence Time Distribution on the Performance and Efficiency of Combustors. The Combustion Institute, 1965, pp. 1187-1202.

4. Marteney, P. J.: Analytical Study of the Kinetics of Formation of Nitrogen Oxide in Hydrocarbon - Air Combustion. Combustion Science and Technology, Vol. 1, 1970, pp. 37-45.

5. Gosman, A. D., W. M. Pun, A. K. Runchal, D. B. Spalding, and M. Wolfshtein: Heat and Mass Transfer in Recirculating Flows. Academic Press, New York, New York, 1969.

6. Gosman, A. D. and W. M. Pun: Calculation of Recirculating Flows. Lecture notes, Imperical College of Science and Technology, London, England, 1973.

7. Bird, R. B., W. E. Stewart, and E. N. Lightfoot: Transport Phenomena. John Wiley & Sons, Inc., New York, New York, 1960.

8. Launder, B. E. and D. B. Spalding: Turbulence Models and Their Application to the Prediction of Internal Flows. Imperial College of London, Technical Engineering Department Report No. TM/TN/A/18, 1971.

9. Smith, G. D.: Numerical Solution of Partial Differential Equations. Oxford University Press, London, England, 1965.

10. Lavoie, G. A., J. B. Heywood, and J. C. Keck: Experimental and Theoretical Study of Nitric Oxide Formation in Internal Combustion Engines. Combustion Science and Technology, Vol. 1, 1970, pp. 313-326.

11. Zeldovitch, Ya. B., P. Ya Sadounikov, and D. A. Frank-Kamenetskll: Oxidation of Nitrogen in Combustion. Academy of Sciences of USSR, Institute of Chemical Physics, Moscow-Leningrad, 1947.

12. Bowman, C. T. and D. J. Seery: Investigation of NO Formation Kinetics in Combustion Process: The Methane-Oxygen-Nitrogen Reaction, Emissions from Continuous Combustion Systems. Plenum Publishing Company, New York, New York, 1972.

13. Caretto, L. S., L. H. Muzio, R. T. Sawyer, and E. S. Starkman: The Role of Kinetics in Engine Emission of Nitric Oxide. Combustion Sciences and Technology, Vol. 3, 1971.

EFFECTS OF INTERACTION BETWEEN FLUID DYNAMICS AND CHEMISTRY ON POLLUTANT FORMATION IN COMBUSTION*

by

C. T. Bowman, L. S. Cohen
L. J. Spadaccini and F. K. Owen
United Technologies Research Center
East Hartford, Connecticut 06108

*Work sponsored in part by the Environmental Protection Agency Research Triangle Park, North Carolina under Contracts 68-02-1092 and 68-02-1873

Preceding page blank

ABSTRACT

Average concentration levels of the pollutants NO, NO_2, CO and unburned hydrocarbons (THC) were measured at the exhaust of an axisymmetric combustor over a significant range of operating conditions. In addition, detailed species concentration, temperature and velocity maps were obtained throughout the combustor for representative operating conditions. Major combustor input parameters were varied over the following ranges: overall fuel/air equivalence ratio 0.5 - 1.3, air-fuel velocity ratio 0.1 - 40, inlet air swirl number 0 - 0.6, air flow rate 0.09 - 0.14 kg/sec, inlet air temperature 730 - 860 K and combustor pressure 1 - 7 atm. Water-cooled probes were used to remove samples from the flow for on-line concentration analysis and to measure temperature. Velocity and flow direction were measured using both an impact-static pressure probe and a laser velocimeter.

Elevated pressure and introduction of swirl to the extent considered in the experiments creates "unmixedness" in the combustor flow field, producing high local temperatures, which in turn result in enhanced NO formation and consumption of hydrocarbons. Aerodynamic flame stabilization, achieved without benefit of swirl or physical flameholders in systems having large air-fuel momentum flux ratios, produces strong stirring which results in reduced temperatures and in relatively low NO formation and hydrocarbon consumption rates.

INTRODUCTION

Recent experimental investigations of factors affecting pollutant emissions from various continuous combustion devices (Refs. 1-4) have shown that changes in operating conditions, which alter the flow pattern in the combustion chamber, can have a substantial effect on pollutant emissions. These observations suggest that coupling between fluid dynamic and chemical processes inside the combustion chamber is a major factor in governing pollutant emissions from many combustion devices. Analytical studies of reacting flow fields (Refs. 5-8) have indicated in a qualitative manner how mixing and turbulence can influence pollutant formation. However, at the present time our understanding of the nature of the coupling between fluid dynamic and chemical processes is insufficient to permit extrapolation of results obtained from one combustion device to other devices or to allow a priori determination of the effects of changes in operating conditions on pollutant emissions.

An experimental investigation of the interaction between fluid dynamics and chemistry in a combustor and the subsequent effects on pollutant formation and destruction has been carried out. The overall objectives of this investigation are:

(i) To examine experimentally the interaction between fluid dynamic and chemical processes inside a model combustor as operating conditions are varied, and to correlate changes in pollutant emissions with these variations.

(ii) To compare the experimental results with results from a combustor flow analysis to assist in interpretation of the experimental results and to evaluate and calibrate the theoretical model.

EXPERIMENTAL APPARATUS

The experimental configuration consists of an axisymmetric combustor in which a central gaseous fuel stream mixes with a coaxial annular air stream. In this configuration, which resembles the primary combustion zone in many practical combustion devices, the resulting flame will not be stabilized in general, and blow-off will occur. In order to stabilize a flame in such a system, it is necessary to provide a continuous ignition source either by means of a pilot flame or through creation of zones of hot recirculating combustion gases. These stabilizing recirculation zones may be created by the introduction of physical flameholders into the flow or by imparting a swirl component to the flow. Swirl stabilization techniques have been used extensively in continuous flow combustion devices such as furnaces and gas turbines. Hence, a significant portion of the current effort focuses on swirl-stabilized flames.

A new approach to flame stabilization also was employed. A review of recent literature on mixing of coaxial non-reacting jets indicated that flame stabilization might be achieved in gaseous-fueled systems by judicious selection of the momentum flux ratio of the fuel and air streams. This flameholding approach relies neither on a physical flameholder nor on swirl. Rather, it makes use of the observation that a recirculation zone is formed in the initial region of coaxial streams when the outer, annular stream (air stream) is moving very rapidly relative to the central (fuel) jet. The aerodynamic flameholding technique, in principle, should result in a simplified determination of inlet conditions and also should provide a unique opportunity to contrast swirling and non-swirling flow fields without the disruptive presence of a physical flameholder.

Tests were conducted in an instrumented, water-cooled combustion system, Fig. 1. The facility design placed particular emphasis on acquisition of species concentration, temperature and velocity distributions throughout the reacting flow field. Air from an electrical heater section flows around a replaceable fuel injector. Swirl may be imparted to the air stream by inserting various swirl vanes into the annular air passage. Observation of the combusting flow is made through window ports in the entry and combustor sections, Fig. 1. The combustor probes used to make these measurements are compatible with all ports and may be replaced by a quartz window for laser velocimetry measurements. The 12.23 cm diameter, 100 cm long instrumented combustor is divided into three water-cooling zones of approximately equal length. Flow exhausts from the combustor to the facility exhaust stack. Chokes can be installed downstream of the extender to raise the pressure in the combustor.

An exhaust probe rake is placed at the exit of the combustor to determine concentrations of pollutant species in the exhaust flow. Gas composition is determined on-line using redundant sampling instrumentation. Temperature distributions in the combustor were obtained using both a traversing calibrated-heat-loss thermocouple probe and a double-sonic-orifice probe. Flow velocity and direction in the combustor were determined using a five-hole impact-static pressure probe. This probe performed satisfactorily throughout the combustor flow field except in those regions, near the injector, with high turbulence levels or reverse flow. In these regions, flow velocity and direction were measured using a laser velocimeter.

EXPERIMENTAL RESULTS

The experimental program was comprised of input-output tests and flow-field mapping tests. In the input-output tests, the influence of various combustor input parameters on pollutant concentration levels in the exhaust flow was determined. Generally, for a particular fuel injector and swirl vane insert, the overall fuel-air equivalence ratio was varied from fuel-lean to fuel-rich conditions at two or more levels of inlet air temperature, air flow rate and combustor pressure, and the composition of the exhaust flow was measured for each operating condition.

Results from the input-output tests, discussed in detail in Ref. 9, indicate that the pollutant emission levels are particularly sensitive to certain combustor input parameters. NO and THC emissions are strongly dependent on swirl and pressure and also are dependent on air-fuel velocity ratio. Over most of the ranges of combustor input parameters investigated, exhaust CO concentrations are the equilibrium levels; however, for non-swirling flows and for swirling flows with low air-fuel velocity ratios, exhaust CO levels can significantly exceed equilibrium levels. To investigate how changes in these significant input parameters influence the combustor flow field and subsequent pollutant formation, detailed maps of the flow field properties were obtained.

In these mapping experiments, radial distributions of flow velocity and direction, temperature and species concentration were acquired at a number of axial locations in the combustor. Based on results from these experiments, several general observations were made concerning the interaction between the flow field and the pollutant formation and destruction processes, Ref. 9. For the conditions investigated, the primary hydrocarbon combustion zone, where most of the hydrocarbon fuel reacts to form CO, is located relatively close to the injector. In this zone, which contains the stabilizing recirculation zone, a significant fraction of the total available chemical energy is released, and high levels of CO and NO are established. Peak CO levels in the primary zone are significantly larger than final equilibrium levels. Measured NO_2 concentrations in the primary combustion zone are relatively large. Near the injection plane, NO_2 concentrations in excess of the NO concentrations were measured in the shear region separating the inner and outer flows. Downstream from the primary combustion zone, the remaining hydrocarbon fuel and the CO oxidize. There are no significant increases in temperature in this post-combustion zone due to heat loss to the combustor walls; however, because of the relatively high temperatures, significant additional NO formation occurs. In the post-combustion zone, the NO_2/NO ratio decreases, primarily because of the increasing NO concentration.

In the present experiments, the reacting flows can be characterized roughly as chemistry-limited or mixing-limited, depending on the relative rates of chemical reaction and mixing. In non-swirling, atmospheric pressure flames, large scale fluctuations of the stabilizing recirculation zone enhance mixing of the fuel and air streams and result in a primary combustion zone which resembles a stirred reactor. Downstream from the primary zone, the flow resembles plug flow. These flows appear to be chemistry-limited in that mixing rates are rapid relative to chemical reaction rates. As a result of the well-mixed nature of the flow, temperatures are moderated so that hydrocarbon and CO oxidation rates and NO formation rates are relatively slow. Hence, chemistry-limited flows are characterized by relatively high THC and CO emissions and relatively low NO emissions.

Increasing combustor pressure or imparting swirl to the inlet air stream results in a shift from chemistry-limited to mixing-limited behavior. In mixing-limited flows, the time-mean flow field exhibits the characteristics of a diffusion flame, with separation of the fuel and air streams and with chemical reaction occurring principally in an annular region surrounding the combustor centerline. Maximum temperatures in the region are considerably larger than found in the chemistry-limited flows, resulting in increased hydrocarbon and CO oxidation rates and NO formation rates. Hence, mixing-limited flows are characterized by relatively low THC and CO emissions and relatively high NO emissions.

Laser velocimeter data and high-speed motion picture films of the reacting flow field in the vicinity of the injection plane reveal significant fluctuations in the flame structure. Recent analytical studies of turbulent flames (Ref. 5) suggest that these fluctuations will significantly influence pollutant formation in the combustor.

Initial comparisons of measured distributions of mean velocity and mean temperature with those obtained from the combustor flow analysis show relatively good agreement. However, the agreement of measured and calculated pollutant species concentration profiles in the combustor is less satisfactory. The poorer agreement may result from the effect of turbulent fluctuations on pollutant formation and destruction, discussed above, or from the use of a relatively simple hydrocarbon combustion model in the combustor flow analysis.

REFERENCES

1. a) M. P. Heap, T. M. Lowes and R. Walmsley: The Effect of Burner Parameters on Nitric Oxide Formation in Natural Gas and Pulverized Fuel Flames, Paper presented at First American Flame Days Meeting, Chicago, Illinois, September 1972.

b) M. P. Heap, T. M. Lowes and R. Walmsley: Emission of Nitric Oxide From Large Turbulent Diffusion Flames, Fourteenth Symposium (International) on Combustion (The Combustion Institute, Pittsburgh, 1973), p. 883.

2. D. R. Shoffstall and L. H. Larson: Aerodynamic Control of Nitrogen Oxides and Other Pollutants from Fossil Fuel Combustion, EPA Report 650/2-73-033a, October 1973.

3. a) A. M. Mellor, R. D. Anderson, R. A. Altenkirch and J. H. Tuttle: Emissions from and within an Allison J-33 Combustor, Combust. Sci. and Tech. 6, 169 (1972).

b) J. H. Tuttle, R. A. Altenkirch and A. M. Mellor: Emissions from and within an Allison J-33 Combustor II: The Effect of Inlet Air Temperature, Combust. Sci. and Tech. 7, 125 (1973).

4. R. E. Jones and J. Grobman: Design and Evaluation of Combustors for Reducing Aircraft Engine Pollution, AGARD Document CP-125, April 1973.

5. F. C. Gouldin: Role of Turbulent Fluctuations in NO Formations, Combust. Sci. and Tech. 9, 17 (1974).

6. R. F. Anasoulis and H. McDonald: A Study of Combustor Flow Computations and Comparison with Experiment, EPA Report 650/2-73-045, December 1973.

7. L. S. Caretto: Modeling Pollutant Formation in Combustion Processes, Fourteenth Symposium (International) on Combustion (The Combustion Institute, Pittsburgh, 1973), p. 803.

8. D. B. Spalding: Mathematical Models on Continuous Combustion, *Proceedings of the Symposium on Emissions from Continuous Combustion Systems* (Plenum Press, New York, 1972) p. 3.

9. C. T. Bowman and L. S. Cohen: Influence of Aerodynamic Phenomena on Pollutant Formation in Combustion, EPA Report 650/2-75-061a, July 1975.

FLUID DYNAMICS/CHEMISTRY INTERACTION IN COMBUSTORS

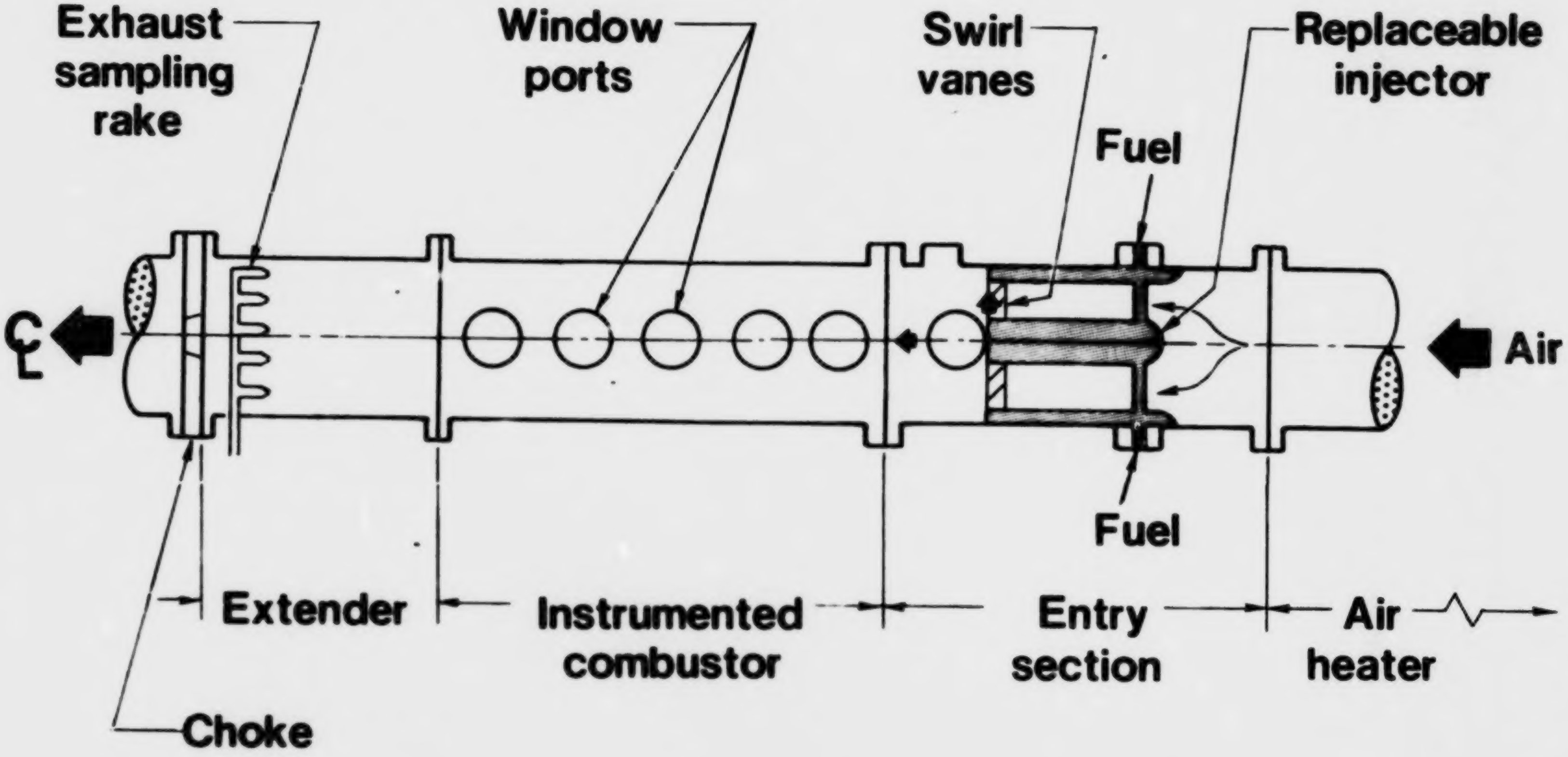
Exhaust sampling rake
Window ports
Swirl vanes
Replaceable injector
Fuel
Air
Fuel
Extender
Instrumented combustor
Entry section
Air heater
Choke
℄

UNITED TECHNOLOGIES RESEARCH CENTER

R06-34-3

Fig. 1

10:20 a.m.
Effects of Interaction Between
Fluid Dynamics and Chemistry
on Pollutant Formation in
Combustion
Dr. Craig T. Bowman, United Technology Research Center

Q: The question is related to the interpretation of these fine experimental results, in a sense that, if we take the swirl for instance, you show for the highest swirl the NO concentrations are reduced.

A: No, increased.

Q: Then, the question is what kind of heat transfer did you have on your combustor? Was it a hot refractory wall or was it a water-cooled wall?

A: It is a water-cooled segmented combustor; we have three segments along the combustor, we measure the temperature in, the termperature out, and we measure the wall temperature as well. The amount of transport that is out of this particular combustion is rather small. We maintain a hot wall but not an adiabatic wall, and we feel that we are taking out something on the order of 5-10% of the total enthalpy of the flow over the entire length of the combustor for these conditions.

* * *

Q: There have been a number of cases in the literature of periodicity of flow patterns such as precessing vortices. Tom, you mentioned how important it is to allow for turbulence; I wonder if you see any evidence of periodicity of flow and if there are periodic flows, how do you see the model handling these?

A: Yes, we have seen the precessing vortex core which has been reported by Syrec, Beer and others. What

Adel is referring to here is that with the swirling flow there is a vortex which precesses around the fuel injector, goes around and around at some well-defined frequencies, and in fact the flame itself stabilizes on that precessed vortexing core. The high speed motion picture films which we have taken show, in fact, that in swirling flow the flame is helical, and that it is precessing at a rate which is equal to the precession rate of the core. In most of the flows which we have examined, this rate of precessing has been between 20 and 150 hertz. We have seen it very clearly on the high speed films. It means that what is normally a time mean-steady flow is really not that at all. It's actually three-dimensional and time dependent. So this is going to have a very significant impact on analytical modeling. I am going to beg the issue by saying that what one would do is probably best answered by Harry McDonald. Do you want to comment on that, Harry?

[Mr. McDonald]
The only observation I can make at this point is that the turbulent fluctuations can be represented in terms of correlation coefficients in the various chemical reaction equations and in the various equations of fluid mechanics. The central problem of most of the active research in this area at the present time is how to adequately model these correlations and that particular subject is one that has to be measured at great length.

Q: Tom, you mentioned that the measured CO_2 concentrations were those given by chemical equilibrium.

A: Very nearly.

Q: Could you comment on how this could be and what significance it might have?

A: Under certain conditions we find that the CO concentration is its equilibrium value, and specifically we find this under the fuel rich combustion conditions. In the case of fuel lean combustion, we find that the CO concentrations are greater than equilibrium; however, the actual levels of CO within the flow under lean conditions are very, very much lower than they are under rich conditions. So whereas the CO concentration itself is not in equilibrium, the CO_2 is very nearly its equilibrium. Obviously it's not exactly equilibrium because you have carbon tied up in both species, so I was trying to deal with it in a more simplistic sense. Obviously, there has to be a carbon balance within the flow.

Q: Could you tell us briefly what this Laser Raman technique of measuring temperature is?

A: This work is going on in our laboratory and elsewhere. In our lab, Dr. Alan Eckbreth is heading up this effort. This is a technique which is based on the Raman principle of scattering of radiation off of a characteristic molecule. In our case, the characteristic molecule is nitrogen, since that is the most plentiful species. This involves irradiating the gas with a well-collimated, well-defined laser beam of a given energy and a given wave length, and observing the scattered radiation that comes off of the molecule. There are two types of scattering in the Raman technique. One is Stokes and one is anti-Stokes. It really means you are scattering off of a higher and a lower energy state, and by ratioing those two signals and assuming the Boltzman distribution within the nitrogen molecule, one can get a measure of temperature. This is highly valuable in turbulent flows. The technique we are using involves a pulsed di-laser, microsecond pulse in, and by running hundreds of pulses in and tracing out the probability distribution of the temperature measurements you can get an awful lot of information about the turbulent fluctuations in temperature as well, which is very important.

Q: I have a question on velocity measurements. Have you observed isotropic behavior in the flow or not?

A: I do not think we have had a chance to do the level of comparison with the laser velocimeter data to allow us to answer that question. The slides which I showed were generated yesterday from data which has been taken over the past several weeks. This is one question which is important, and I think we will be able to address it based on the data which we have taken.

Q: Tom, you alluded to the difficulty of measuring total oxides of nitrogen and mentioned that the resolution of the actual ratio of NO to NO_2 remains to be solved. You have referred in your paper to your findings as NO rather than oxides of nitrogen. Is that a prejudgment on your part that you are seeing NO or is it for the sake of simplicity that you are presenting your data in this form?

A: I would say it is for the sake of simplicity and accuracy. We have a great deal of confidence in being able to measure NO. We have a certain lack of confidence in our ability to measure total oxides of nitrogen using chemaluminescent detectors and the sampling trains which exist today. I think there is a substantial uncertainty in the types of measurement I am talking about. NO is one of the species for which we know the analytical measurement is good. We are less certain of the analytical measurement of NO_2; however, we don't know whether we've lost some of that NO in coming down our sampling probe and into our device. It could best be viewed as a lower limit, if you will, of the amount of NO that exists in the system or lower limit to the nitrogen oxides. This quantifying of nitrogen oxides within reacting flow fields, I think, is a topic area that really requires attention.

Q: Tom, did you say why increasing the total pressure increases NO?

A: I didn't say, but I think we know why. There are actually two effects. If we keep the total mass input into the combustor constant and increase the pressure, the velocity levels within the combustor will decrease because of the increasing density; so, increasing pressure first of all increases combustor residence time, but it does more than that. I didn't have a chance to show it today, but it also changes the structure of the flow field considerably and results in higher peak temperatures than in low pressure cases. So it's really a combined effect; higher temperatures coupling with increased combustor residence times, both of which serve to provide high NO emissions.

FATE OF COAL NITROGEN DURING PYROLYSIS AND OXIDATION

By:

J. H. Pohl and A. F. Sarofim

Fuels Research Laboratory

Massachusetts Institute of Technology

Cambridge, Massachusetts 02139

Preceding page blank

ABSTRACT

U.S. coals contain 0.5 to 2.0% nitrogen by weight, of which about 10 to 50% is converted to nitric oxide in combustors. Little information is available, however, on whether the conversion occurs by oxidation of nitrogen compounds devolatilized from the coal or by oxidation of nitrogen in the char. In order to provide a better understanding of the factors influencing fuel nitrogen conversion, and to obtain guidance for control strategies, a laboratory furnace has been designed for studies of devolatilization and oxidation of coal under simulated combustor conditions. Preliminary results show a decrease in nitrogen retention in the char with increasing exposure temperature and time, the conversion of part of the nitrogen devolatilized in inert atmospheres to N_2, HCN, NH_3, and the decrease in NO_x emissions with increases in the fuel equivalence ratio.

Introduction

A major obstacle preventing the widespread utilization of the extensive U.S. coal reserves is that the emissions of sulfur and nitrogen oxides from coal-burning facilities of current design are often unacceptable. Examination of the composition of U.S. coals shows that if their nitrogen and sulfur contents were quantitatively converted to their corresponding oxides the resulting emissions would be in excess of the EPA New Source Performance standards for NO_x for most U.S. coals and in excess of the SO_x standards for approximately 70 percent of U.S. reserves (see Fig. 1, prepared from a statistical sampling of U.S. coal reserves).

Fortunately, only a fraction of the fuel nitrogen is converted to NO_x as shown in Fig. 2. The limited data on the conversion of fuel nitrogen in coal is supplemented in the figure with some of the more extensive measurements on oils and synthetic mixtures. The fuel nitrogen conversion to NO_x in general decreases with increases in both fuel/air ratio and fuel nitrogen content. The data in Fig. 2 for coal represent uncontrolled emissions and are seen often to lie above the EPA standards, even without the incremental NO_x contribution from atmospheric nitrogen fixation.

The potential exists for reducing the fuel nitrogen conversion by combustion process modification but the development of an optimum strategy must depend on a better understanding of the mechanism of fuel nitrogen behavior in flames. Some of the processes that occur during coal com-

Fig. 1 NITROGEN & SULFUR CONTENT OF US COAL RESERVES

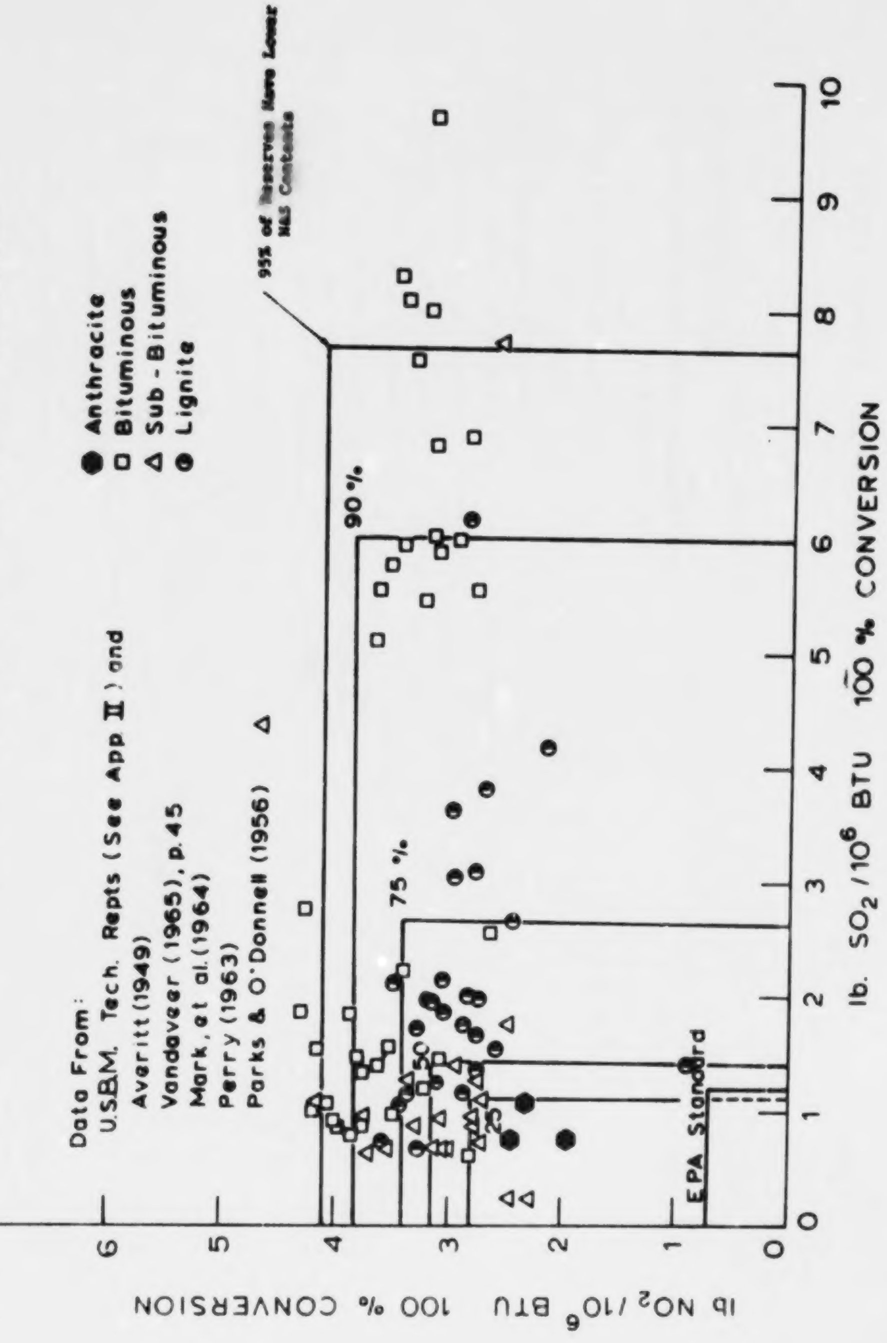

Fig. 2 CONVERSION OF FUEL N IN PRACTICAL COMBUSTORS

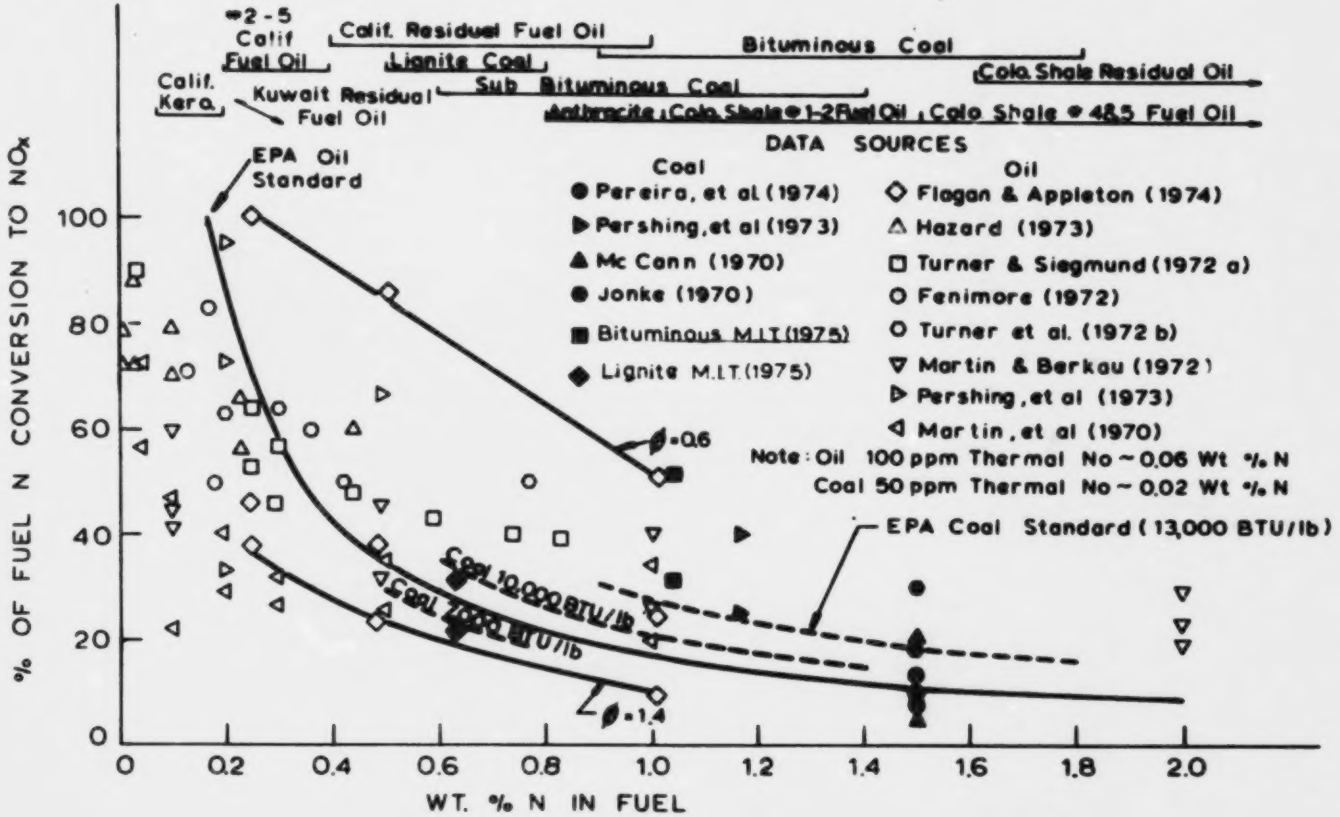

bustion are depicted schematically in Fig. 3. Coal may undergo rapid devolatization by heating in the products of combustion recirculated to the burner, the volatiles may subsequently burn either in the boundary layers of individual particles or in the flames engulfing clouds of particles, and the char will ultimately burn out in the tail of the flame. Alternatively, ignition may precede complete devolatization and char and volatiles may burn contemporaneously. The extent of volatilization prior to ignition and the distribution of nitrogen between char and volatiles will undoubtedly influence NO_x emissions. For example, if the nitrogen can be retained in the char and allowed to burn in the diffusion limited regime, the fuel nitrogen will be subjected to locally reducing conditions which should suppress NO_x formation.

The present study has as its long-term objective the determination of the distribution of fuel nitrogen between char and volatiles and the fate of the char and volatiles under simulated combustion conditions. Preliminary findings are reported below.

Apparatus

The apparatus consists of an essentially isothermal furnace with a controlled atmosphere into which coal can be injected through a narrow water-cooled feeder. The pyrolysis or oxidation products can be withdrawn through a water-cooled probe, and the samples quenched by water injection at the inlet of the probe. The solids are collected on a bronze filter and the gases withdrawn for analysis. For studies at short residence times a high gas flow rate preheated to furnace temperatures by a plasma-gun is utilized. Data at longer residence times can be obtained by allowing the particles to free-fall through the furnace or by heating the coal in crucibles raised into the furnace. A schematic of the furnace set up for use in the short residence time studies is shown in Fig. 4.

Coals Studied

A Pittsburgh seam bituminous coal and a Montana lignite were chosen as representative of swelling and non-swelling coals. The proximate analyses (moisture, ASTM volatiles, and ASTM ash), ultimate analyses (carbon, hydrogen, nitrogen, sulfur), and sulfur forms (pyritic, organic and sulfate) are reported for each coal in Table I. The coals were sieved to yield 38-45μ and 75-90μ fractions. Representative scanning

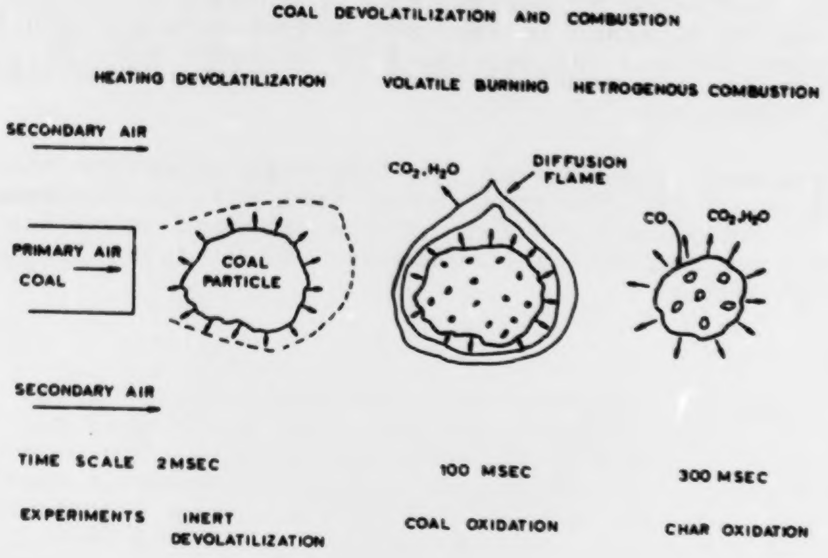
COAL DEVOLATILIZATION AND COMBUSTION
HEATING DEVOLATILIZATION
VOLATILE BURNING
HETROGENOUS COMBUSTION
SECONDARY AIR
CO₂,H₂O
DIFFUSION FLAME
CO
CO₂,H₂O
PRIMARY AIR
COAL
COAL PARTICLE
SECONDARY AIR
TIME SCALE 2MSEC
100 MSEC
300 MSEC
EXPERIMENTS
INERT DEVOLATILIZATION
COAL OXIDATION
CHAR OXIDATION

Fig. 3 Schematic of processes occurring in pulverized coal flame

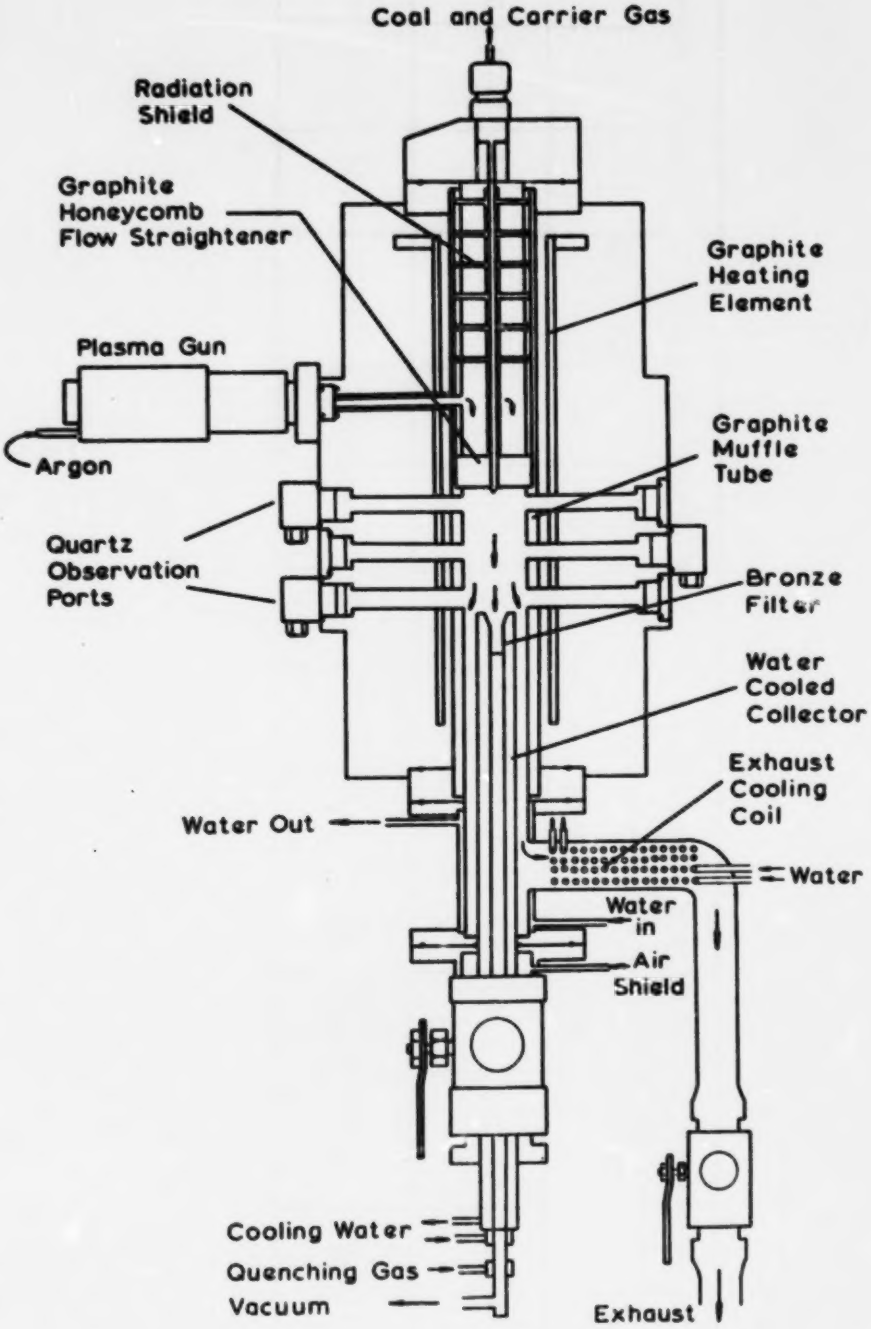
Coal and Carrier Gas
Radiation Shield
Graphite Honeycomb Flow Straightener
Graphite Heating Element
Plasma Gun
Argon
Graphite Muffle Tube
Quartz Observation Ports
Bronze Filter
Water Cooled Collector
Exhaust Cooling Coil
Water Out
Water
Water in
Air Shield
Cooling Water
Quenching Gas
Vacuum
Exhaust

Fig. 4 Schematic of short-residence-time furnace

Table I. COAL CHARACTERIZATION

COAL	MINE	BTU/lb MOIST MM*FREE	PROXIMATE ANALYSIS AR, WT%			ULTIMATE ANALYSIS					SULFUR FORMS		
			H_2O	VM	ASH	C	H	N	S	BY DIFF O			
PITTSBURG SEAM #8 hvA-b	IRELAND	13,900	1.70	40.7	10.7	67.80	5.00	1.04	5.03	8.73	2.61	1.70	0.72
MONTANA LIGNITE-A	SAVAGE	8,800	13.60	36.2	8.3	55.21	4.93	0.61	0.85	16.50	0.16	0.63	0.06

*DULONG

electronmicrographs of the coals are presented in Fig. 5.

Results

Physical Behavior

Figure 6 shows a bituminous coal particle after devolatization (approx. 1 second residence time) in an inert (argon) atmosphere at 1250°K. The particle has swelled from an original size of about 40μ to 400μ, an approximately tenfold expansion in linear dimensions. Examination of the electromicrographs in Fig. 6 show holes in the surface through which the volatiles escaped; high magnification of the surface suggests that the coal has passed through a plastic stage as a consequence of which some of the open pore structure is lost (this is confirmed by a decrease in adsorption surface areas for coals that have been heated above about 1250°K). Focussing on the inside of one of the holes shows the shell-like structure of the coal particle, further evidence of this is provided by the photomicrograph of a polished section (see Fig. 8). Electronmicrographs in Fig. 7 of lignite particles devolatilized under inert conditions at 1750°K show evidence of little swelling.

The marked contrast in behavior of the bituminous and lignite coals is shown by the photomicrographs in Fig. 8 of particles devolatilized in an inert atmosphere at 1750°K. The particles were originally about 40μ in size. The top photomicrograph in Fig. 8 shows that for a devolatilized bituminous coal the organic matter is distributed in a thin circumferential shell whereas the lower photomicrograph shows that for devolatilized lignite particles the organic matter is distributed throughout the particles. Under oxidation conditions the organic matter is burned away leaving fused spherical ash particles for both coals (Fig. 9).

Kinetics of Pyrolysis

The selective loss of different species during the rapid pyrolysis step is shown in Fig. 10. The data on the figure were obtained on the char samples collected after the coals had been devolatized for periods of 10 to 100 milliseconds in the flow furnace, for approximately a second in the free fall furnace, and for periods up to ten minutes in crucibles. The furnace temperatures were set at 1000, 1500, and 1750°K. The results show the expected progressive loss in the different elemental components of the coal. The carbon results at long times show anomolously low losses.

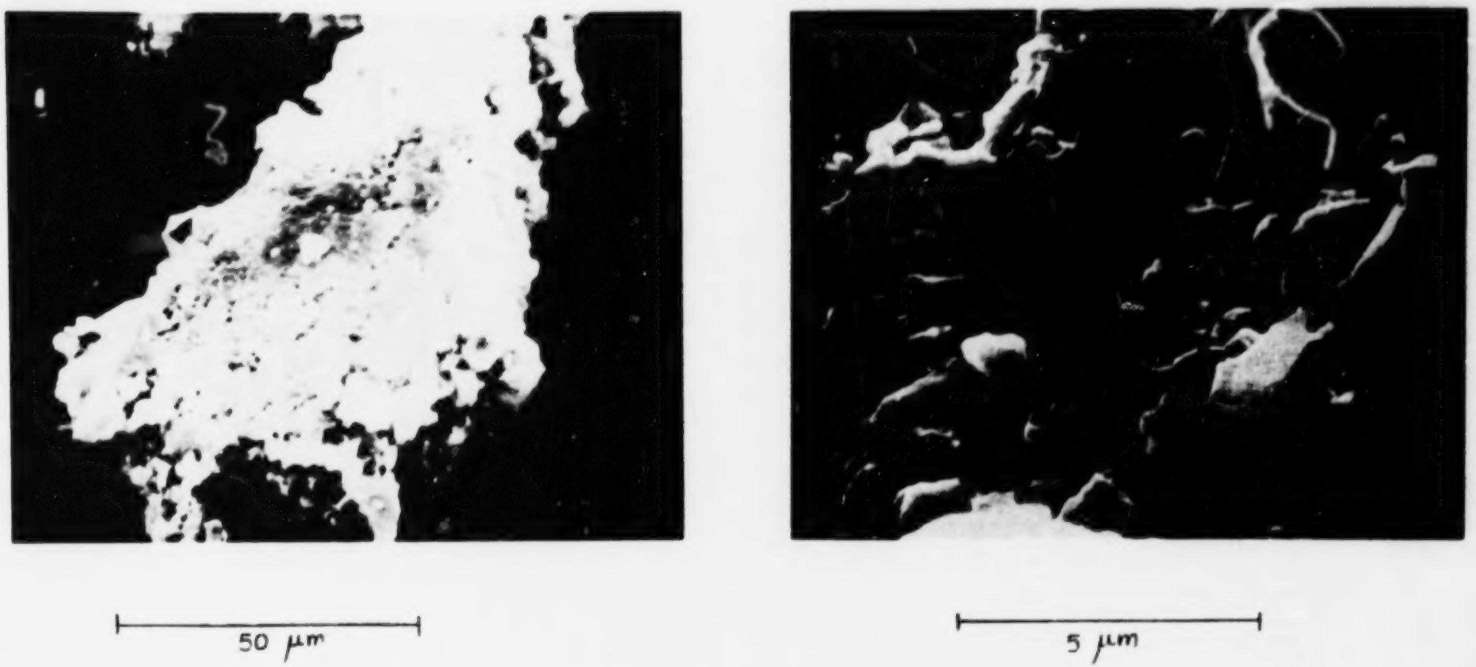

Pulverized BITUMINOUS COAL PARTICLES
(75-90 μm size range)

(A)

Surface of one Particle at higher magnification

(B)

Plate-2

Fig. 5 A. Electronmicrographs of Pittsburgh Seam #8 Coal

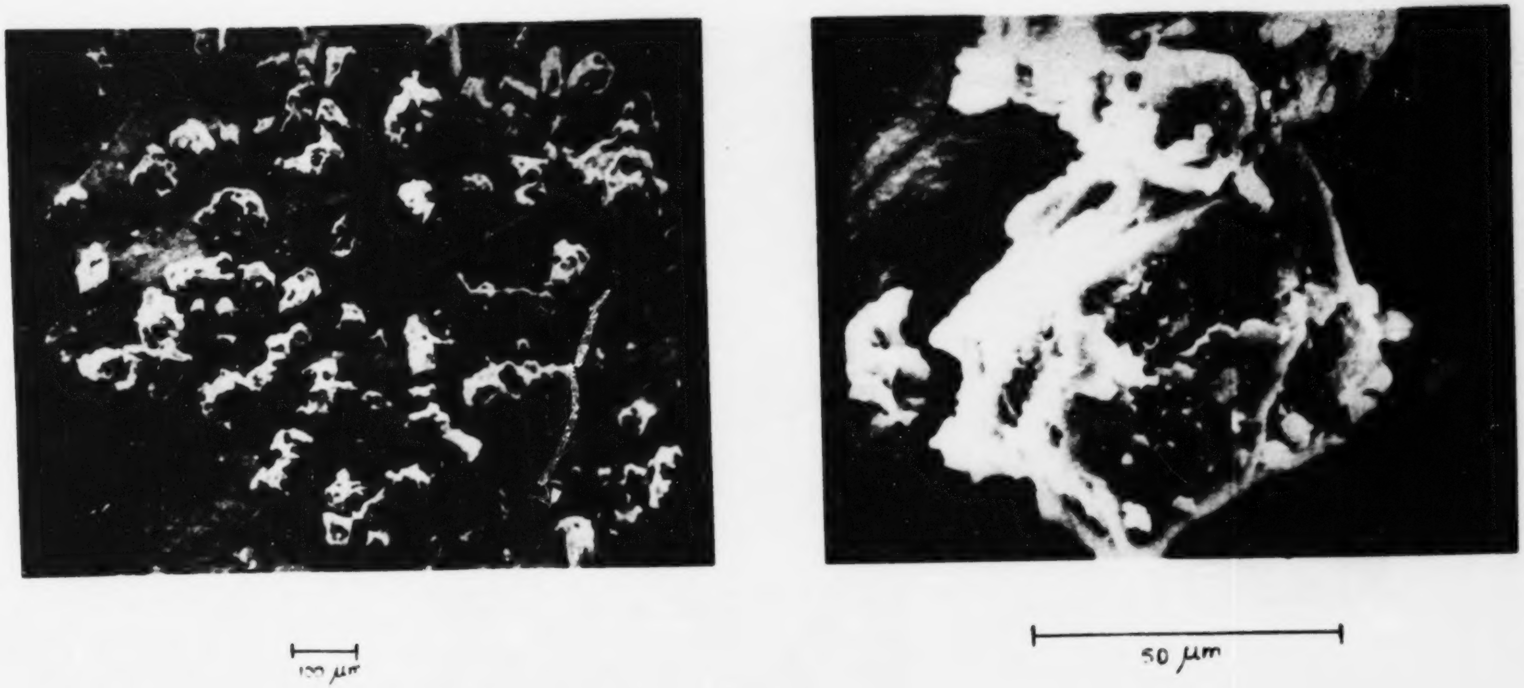

SEM Photograph of PULVERIZED LIGNITE COAL PARTICLES
(75-90 μm size range)

(A)

ONE PARTICLE AT HIGHER MAGNIFICATION

(B)

Plate-1

Fig. 5 B. Electronmicrographs of Montana lignite

DEVOLATILIZED BITUMINOUS COAL 1250K

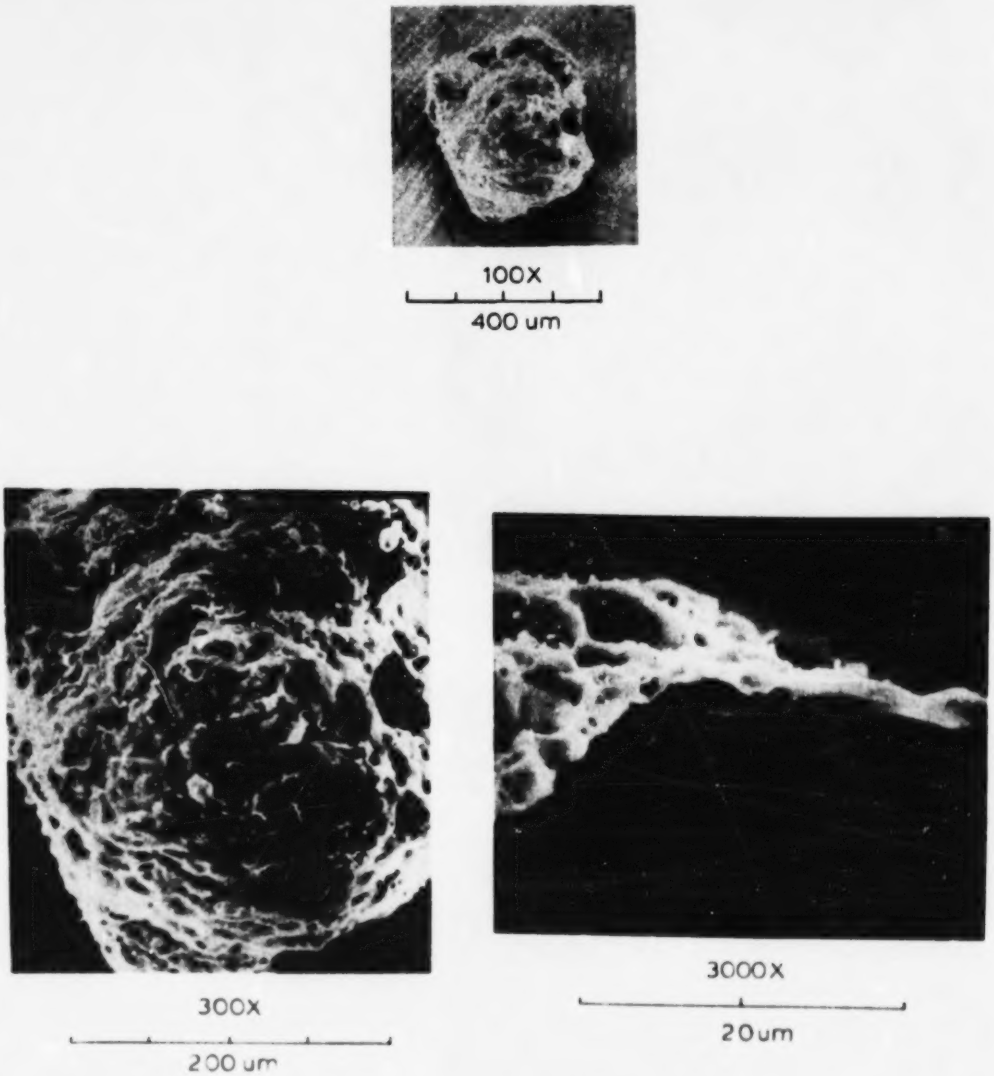
100X
400 um
300X
200 um
3000X
20um

Fig. 6 Electronmicrographs of a devolatilized bituminous coal particle

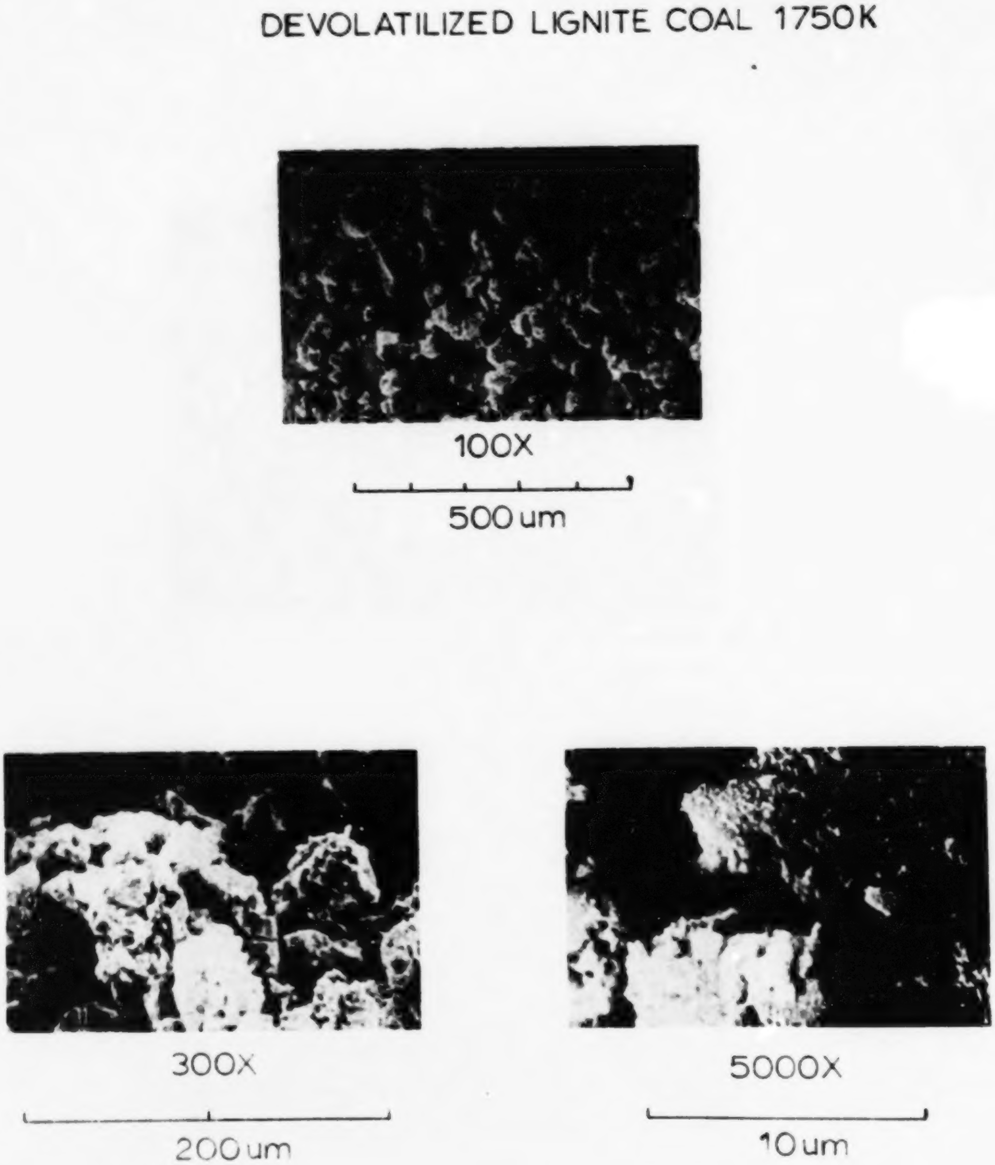
DEVOLATILIZED LIGNITE COAL 1750K
100X
500 um
300X
200 um
5000X
10 um

Fig. 7 Electronmicrographs of devolatilized lignite particles

POLISHED DEVOLATILIZED COAL 1750 K

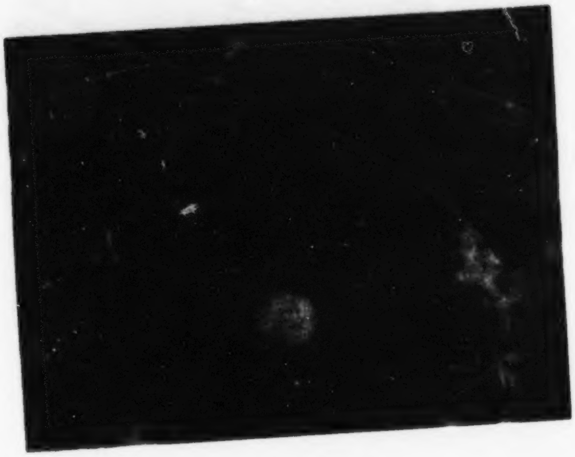

BITUMINOUS

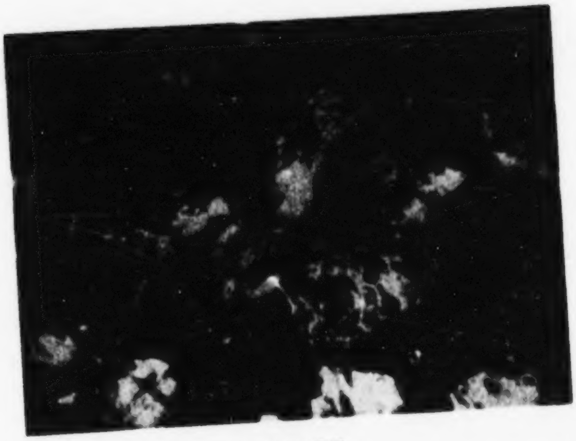

LIGNITE
450X

50 um

Fig. 8 Photomicrographs of a devolatilized coal: a single bituminous coal particle (top), a collection of lignite particles (bottom)

ASH FROM COAL COMBUSTION

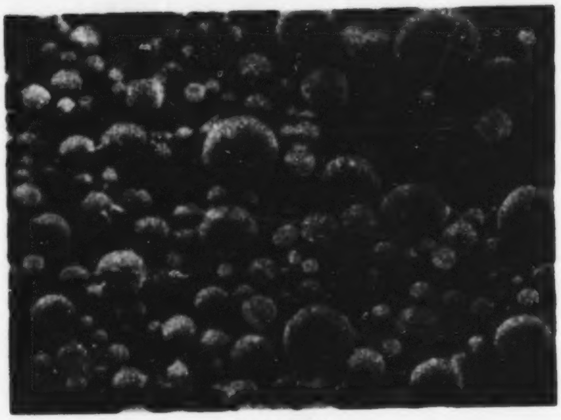
2000X
20 um
BITUMINOUS

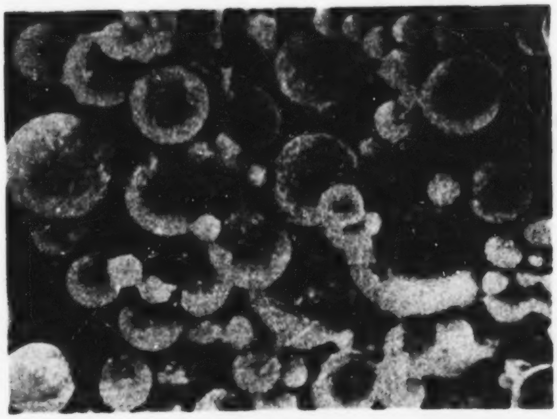
2000X
20um
LIGNITE

Fig. 9 Electronmicrograph of ash obtained on the complete combustion of bituminous coal (top), lignite (bottom)

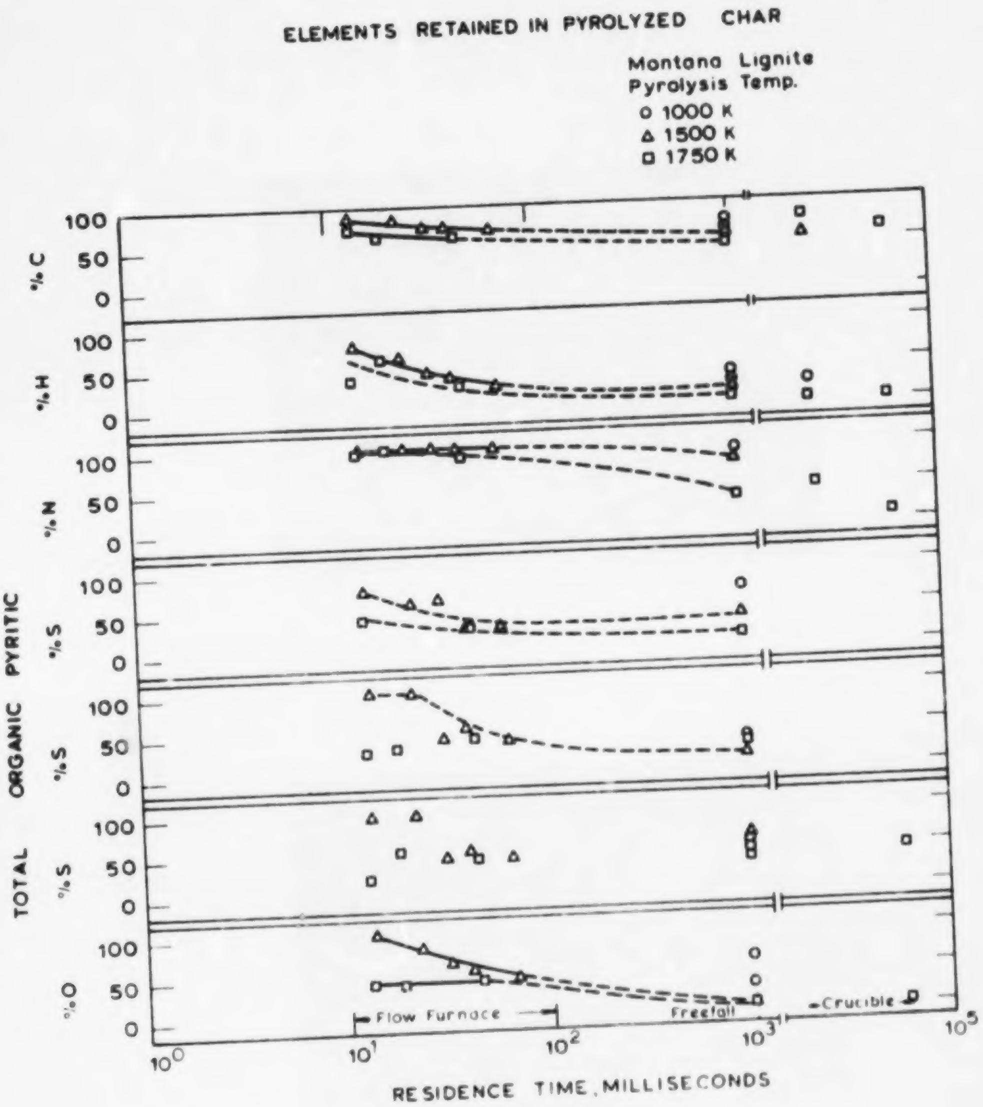

Fig. 10 Percent retention of elemental components of lignite in char produced by pyrolysis at temperatures of 1000 to 1750°K

This may be explained in part by the low heating rates experienced in the crucible experiments and by the deposition of pyrolysis products on the crucible walls and the char over which the volatiles flowed. The major element of interest to this study is nitrogen, which is found to be retained by the char in amounts that depend on both temperature and time (see Fig. 11, for details). At 1000°K less than 8 percent of the nitrogen in lignite (20% in bituminous coal) is devolatilized for exposure times less than a second. At 1500°K the amounts of nitrogen devolatized increase to about 20% for lignite and 45% for bituminous coal, and at 1700°K, measurements were obtained only for the lignite coal; these showed a 70% nitrogen volatile yield for an exposure time of a second. Prolonged heating in a crucible at 1750°K yielded 90% devolatilization of the nitrogen content of the coals. From these results it is apparent that the distribution of nitrogen between char and volatiles is determined by kinetics and that the rate of devolatilization of nitrogen compounds is a function of coal type. The studies are being extended to obtain the kinetic parameters needed for the modelling of fuel nitrogen behavior.

Only exploratory data are available at this stage of the present study on the composition of the nitrogen-containing volatile species. To place the problem in perspective, data reported in the literature on the nitrogen distribution between products obtained during coking are summarized in Fig. 12. For coking conditions the nitrogen retained in the coke falls from about 80% at 600°C to about 40% at 1100°C. The nitrogen evolved appears predominantly as ammonia at the lower temperatures but molecular nitrogen becomes the dominant gaseous product at higher temperatures. Small amounts of nitrogen are evolved as HCN, heterocyclic compounds, and in tars. The nitrogen retained in the chars from the present crucible experiments follow the extrapolation to higher temperatures of the coking data. Analysis of gas phase constituents in the present study show that relatively little of the coal nitrogen was converted to ammonia (under 5 percent), up to 15 percent was evolved as molecular nitrogen, and up to 10 percent as hydrogen cyanide. More quantitative information on the distribution of nitrogen in the gaseous pyrolysis products will be obtained in the continuation of the study.

The behavior of the fuel nitrogen when the coal was injected into an air stream (or a helium oxygen mixture simulating air) is shown in Fig. 13 as a function of the over-all fuel/air equivalence ratio. Under very lean conditions about

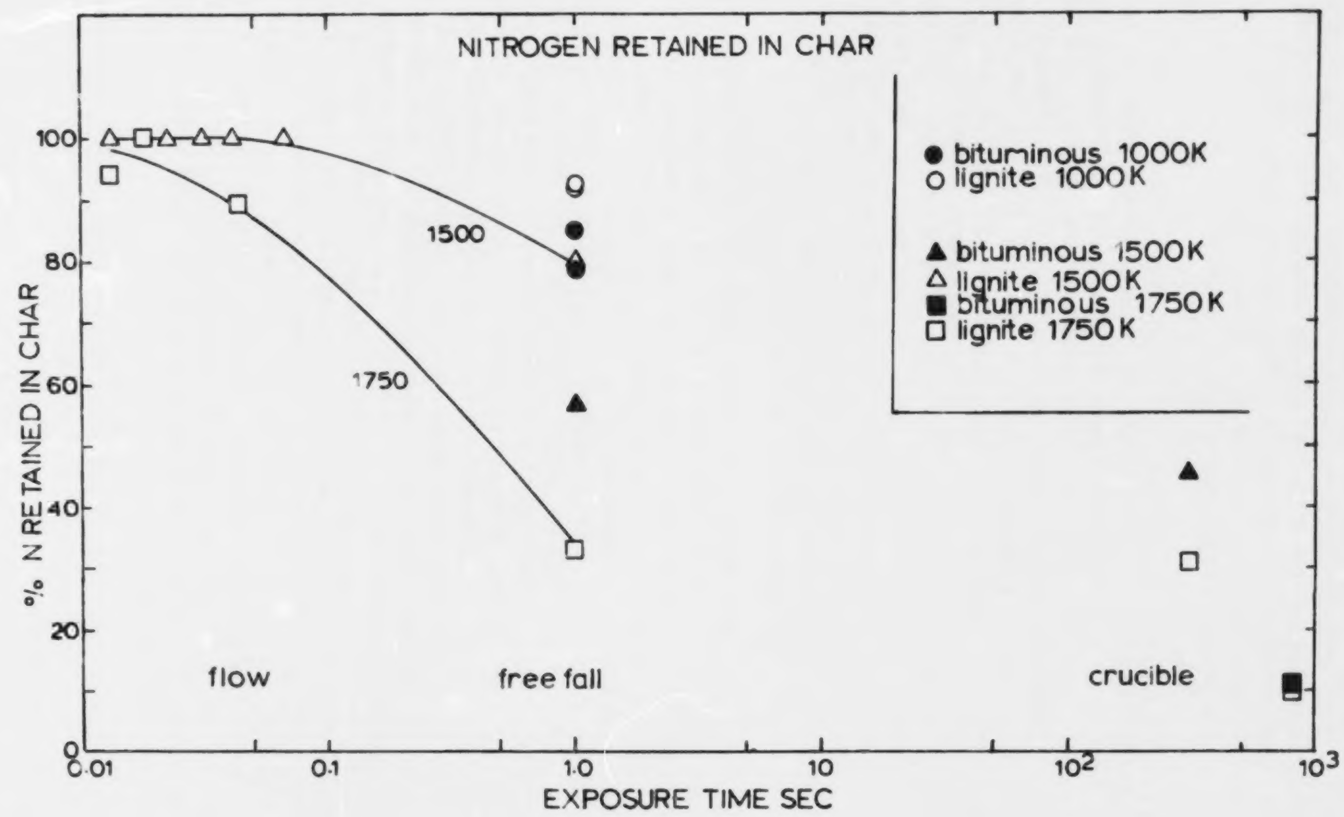

Fig. 11 Percent retention of nitrogen in chars produced by the pyrolysis of a bituminous coal and lignite

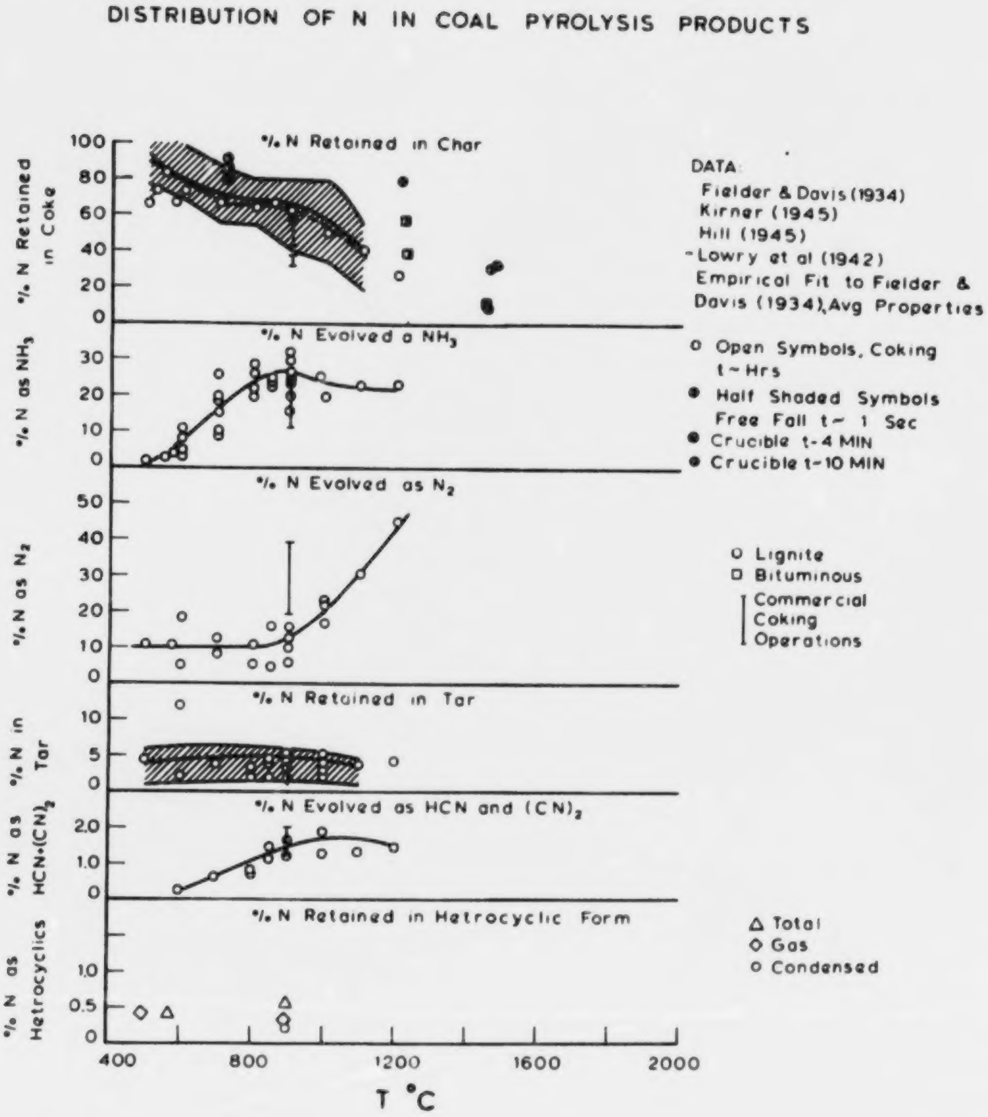

Fig. 12 Fate of fuel nitrogen during coal pyrolysis. Data below 1200°C correspond to coking conditions

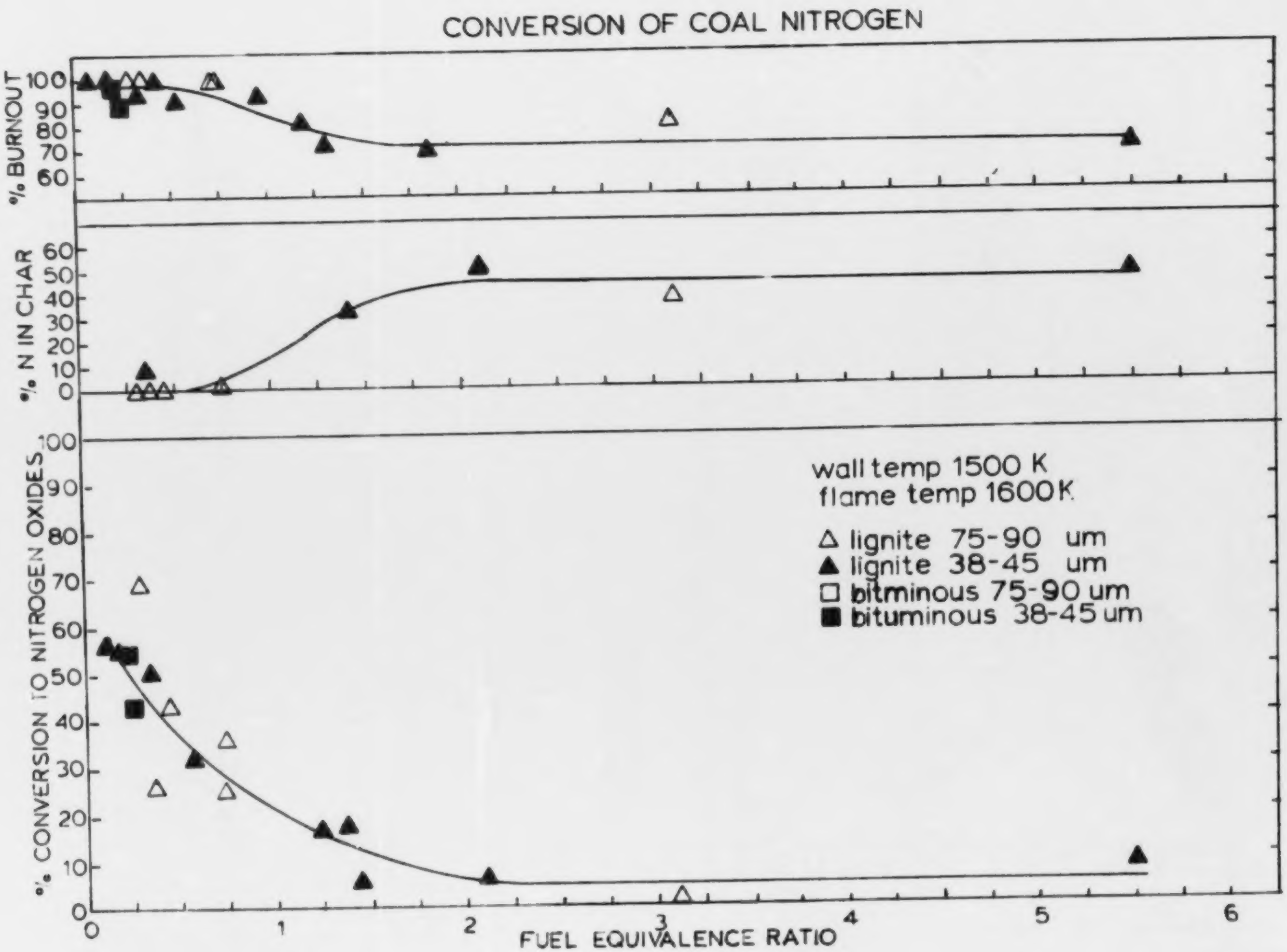

Fig. 13 Conversion to NO_x (bottom plot) and retention in char (middle plot) of nitrogen in coal

60 percent of the fuel nitrogen was converted to nitric oxide. As the fuel/air equivalence ratio increased the conversion efficiency decreased to values under 10 ten percent for equivalence ratios greater than about 1.5. At fuel/air equivalence ratios of 0.7 to 0.8, the range of interest for many utility boilers, the fraction of the nitrogen converted to NO_x was found to be about 25 to 30 percent, a value in agreement with estimates derived from field data. It should be noted that as the fuel/air equivalence ratio increased beyond 0.8 the fraction of the carbon unreacted increased reaching an asymptotic value of about 30 percent at a fuel/air equivalence ratio of 1.5. This unreacted carbon was found to contain up to 40 percent of the nitrogen content of the original coal. The fate of the nitrogen retained in the char during oxidation will determine the maximum potential for reducing fuel NO_x formation by use of staged combustion.

The above results are preliminary and were obtained with a coal flame stabilized on the coal feeder. Subsequent tests will examine the effect on nitric oxide yields of operating under conditions favoring combustion of coals in a dispersed phase and will also attempt to close a nitrogen material balance by measuring the molecular nitrogen formed during combustion in helium/oxygen mixtures.

Concluding Comments

Preliminary experiments on the behavior of fuel nitrogen under simulated combustion conditions indicate that (1) fuel nitrogen devolatization is kinetically controlled; (2) significant amounts of nitrogen (about 70% at 1750°K) may remain in the char after devolatilization. Since the nitrogen retained in the char will be oxidized heterogenously, optimum strategies for control of fuel nitrogen in coals may differ from those for oils; (3) nitric oxide yields decrease monotically with increasing fuel/air equivalence ratios; (4) at fuel/air equivalence ratios greater than 1.5 as much as forty percent of the nitrogen content of the coal may be retained in the char. From these findings, the current data indicate oxidation of nitrogen in the char may contribute significantly to NO_x emissions at temperatures below 1750°K but less at higher temperatures. Complete models of nitric oxide formation from coal flames should include the kinetics of nitrogen devolatilization from char.

Acknowledgements

The results presented in this paper were obtained under EPA Grant No. R-803242-01-0. The data were obtained on equipment developed jointly with a parallel OCR study on coal devolatization and ash behavior. The authors wish to acknowledge that the results reported here are part of a larger collaborative activity involving A. Padia, H. Kobayashi, G. Mandel, and Professor J. B. Howard. The authors also wish to acknowledge early recognition by Dr. J. Wendt of the University of Arizona that oxidation of the nitrogen retained in the char could contribute significantly to nitric oxide emissions.

11:00 a.m.
Fate of Coal Nitrogen During
Pyrolysis and Oxidation
John H. Pohl, Massachusetts
Institute of Technology

Q: I noticed on one of your early charts you made mention of crude oil and residual fuels' conversion rates of bound nitrogen. Have you made any comparisons as to how effective the conversion is of these liquid fuels compared to solids?

A: That data was not mine. It was gathered from a number of different sources, some of it was in fact from the Environmental Protection Agency data - Martin's, for instance - and, they appeared to lie on the same curve is my best answer to that. There is another parameter in that curve in terms of fuel equivalence ratio and if you looked at it, there is a .6 at the top and a 1.4 at the bottom and so there was a variation, but they seem to go about in the same way. If we wanted to look at the slide again it shows about 40-50% conversion. It is a little bit higher as we go down on the lower nitrogen concentrations.

Q: At this time, do you have any idea of how much of the volatilized nitrogen will be converted to NO_X and how much of the nitrogen remaining in the char will be burned to NO_x?

A: Are you asking in terms of how much nitric oxide is included in the devolatilized char or in the oxidized?

Q: No. What percent of the volatalized nitrogen?

A: We don't have direct measurements on that but by going to the very rich fuel equivalent ratios you can see that there is less than 5% from strict devolatilization. There is some oxygen particularly in the lignite -- it's up to about 16%.

Q: Have you passed HCN through your furnace to see if the N_2 that you observed could be the HCN decomposition?

A: Not as yet.

Q: We run into that in our system all the time and we have to be sure that doesn't happen if we run an experiment.

A: I was aware that you had that problem.

Q: You indicated that as you increased your heating rates --

A: The heating rates are fixed by the geometry of the furnace; the maximum temperature we can vary.

Q: Okay, but you did seem to indicate that as you changed your derivative of temperature with respect to time for every little particle as you increased that, that more nitrogen went into the char. How do you interpret your results as a function of heating rate of your particle?

A: We really haven't investigated the heating rate at all; I can't answer that but if you want me to speculate on what I would think, that is, if I increased the heating rate, I would expect that I would remove more nitrogen from the char.

Q: But as you lowered your residence time, you increased the percent of nitrogen retained in the char, and as you lower your residence time ...

A: That might also have an effect on the heating rate, certainly. As we lower the residence time what we do is lower the quenching apparatus up towards the probe so that the heating times are smaller but the heating rates should be approximately the same.

Q: You mentioned that the bituminous coal particles swell while the lignite particles do not; can you comment on whether you expect any gross changes in the ability of a bituminous particle to burn, compared to the lignite as a result of the expansion of the particle and the bursting of it, and increase the surface area?

A: We haven't seen any bursting yet;there has been, apparently, some speculation that they do, but my conclusion at this time would be they are molten enough so that they don't burst. They just form a plastic sphere which then when we cool down goes that way. The answer is that, apparently, people have been relatively successful in modeling oxidation of coal as a diffusion model so that it doesn't appear to make too much difference.

* * *

Q: Did I read one of your charts correctly - that under stoichiometric conditions that 50% of the N involved would transform into N_2?

A: I think you are referring to the pyrolysis chart. That was the Bureau of Mines data; we have not achieved that high. We do put a lot of nitrogen into the N_2 but we have not gotten to 50% yet, and yes, you did read it right.

Q: Would this indicate a trend for design in which the fuel bed should be pyrolyzed before the admission of combustion air?

A: Well, I would wonder what you would do with the nitrogen which is retained in the char which would still be a relatively large fraction.

Q: ...to allow for the N to N_2 conversion, just an opinion...

A: I think that the N to N_2 conversion is of course favored by rich conditions and long residence time, and I think there's some indication that it is also favored by possibly an increase in temperature.

Q: There's some difficulty in measuring fuel nitrogen when the nitrogen is partially oxidized in the fuel. Could you just tell me how you measured fuel nitrogen and how you are sure that you got it all?

A: We did it two ways and it didn't seem to make much difference. First, I didn't mention the furnace wall temperatures were about 1500°K. Optical pyrometer measurements of the flame temperature showed them to be about 100-150° higher. We ran with air as an oxidizer; we ran the air through the furnace and saw no nitric oxide; we then went back and repeated the experiments using helium oxygen mixtures which eliminates, of course, the problems of thermal fixation-and we saw essentially the same results.

Q: I'd like to make one cautionary remark and solicit your response to it; I think you are going to agree with me. I think you have to be very careful in correlating nitric oxide yields from fuel nitrogen in terms of overall equivalence ratios because the actual conversion which takes place is strongly dependent upon the local fuel air equivalence ratio, and so we don't want to be misled into thinking that you are going to get a fixed number for a fixed overall fuel-air equivalence ratio.

A: Tom is certainly right and we have thought about this problem a bit. He's approaching the problem from the turbulence standpoint where he would have a mixture of different fuel equivalence ratios as he looked across his system. Our system is essentially a laminar diffusion flame when we burn the coal and we get a gross fuel equivalence ratio. What it amounts to is how much of the nitric oxide passes through a region where they can be reduced by other reactive species such as ammonia, hydrogen cyanide and hydrocarbon species.

Q: I'd just like to comment on the question that was asked about the conversion of N to N_2. It seems to me that it makes sense that it would be favored by high temperatures because the formation of N_2 from nitrogen in the coal is most likely to be single atoms of nitrogen and you have to get them to go to N_2. That process is bound to be favored by high concentrations of nitrogen-containing species. The high temperatures would, I think, cause the high concentrations. My own guess, and there is very little information on the reactions of these free radicals and species containing a nitrogen atom, is that the effect of temperature on the kinetics of these individual reactions would be minimal. I should imagine that they are mostly low activation energy processes; so, the effect of temperature would be to increase the concentration of the species.

A DETAILED APPROACH TO THE CHEMISTRY OF METHANE/AIR COMBUSTION: CRITICAL SURVEY OF RATES AND APPLICATIONS

By:

Victor S. Engleman

Exxon Research and Engineering Company

Government Research Laboratories

Linden, New Jersey

A DETAILED APPROACH TO THE CHEMISTRY OF METHANE/AIR COMBUSTION

Modeling of full-scale combustion systems will require considerations of chemical kinetics, fluid mechanics and heat transfer. Progress is being made on all three fronts to develop fundamental understanding which may ultimately lead to a practical model. In the area of chemical kinetics, much progress has been made in recent years in rate measurements, critical evaluations, and estimation techniques. One of the potential difficulties in the establishment of chemical mechanisms is in oversimplification or neglect of important reactions in such a fashion that cancelling errors result in apparent agreement with "theory". In the past such simplifications were justified on the grounds that rate data were not available. However, the situation is improving sufficiently so that an investigation of a detailed approach to the chemistry of methane/air combustion is fully warranted.

The objective of this paper, which discusses a detailed approach to the chemistry of methane/air combustion, is threefold:

(1) To describe the approach itself
(2) To disseminate the results of the kinetics evaluation
(3) To discuss applications and examples

The work described here was part of a larger effort, under EPA Contract 68-02-0224, to study the coupling between NO_x formation and combustion reactions under normal and combustion modification conditions. Experimental studies with flat flames, diffusion flames, and stirred reactors under both adiabatic and non-adiabatic conditions, as well as theoretical calculations using the approach described here were accomplished in this program. Detailed results of calculations using this approach and the comparison with experimental data which were obtained in the overall study will be discussed elsewhere.

There are basically five steps in the approach to be described:

(1) Selection of species
(2) Construction of reactions
(3) Evaluation of probable relative importance
(4) Survey of kinetics data
(5) Evaluation and selection of rates

When the above steps have been accomplished the results can be applied to the problem with appropriate knowledge of both the utility of the approach and the hazards in its application.

Selection of Species

The selection of species determines the order of magnitude of the problem. The fewer species, the simpler the problem; however, it is clearly undesirable to eliminate important species. Therefore, in the methane/air system, one should seek the carbon- hydrogen- nitrogen- and oxygen-containing species of potential importance. In this case, such an evaluation was made for species of potential importance for the interaction between combustion and NO_x formation processes for methene/air at one atmosphere between 80 and 125 percent stoichiometric air and between 1500 and 2500 K. Fewer species could be considered if NO_x formation were not of importance, but additional species might be needed if one were to venture outside the specified limits (to more fuel-rich conditions, for example). Giving consideration to thermochemical parameters, the nature of the problem (hydrocarbon combustion with NO_x formation), and critical species proposed in the literature to be of importance, a list of 25 primary species was chosen (Table 1).* As will be seen in the next section, this list of species results in a very large number of potential reactions. While these species were considered to be of primary importance, 14 additional species were considered to be of secondary importance; that is, unlikely to be of importance within the range of conditions considered but possibly important outside that range. These species are listed in Table 2.* Charged species and excited species were not considered for the purpose of this study.

Construction of Reactions and Filing Order

A computer program was developed to construct all mathematically possible unimolecular and bimolecular reactions among a selected list of species. The program is dimensioned to accept up to 99 species with each species containing up to four different kinds of atoms (for the purpose of this study they were carbon, hydrogen, nitrogen and oxygen) although the dimensioning is easily expanded. The program produces a master list containing all of the reactions for the selected species in a filing order consistent with the alphanumeric sequence used in the JANNAF Thermochemical Tables. That is, each side of the reaction is listed in alphanumeric sequence and the side of the reaction with earliest alphanumeric species is listed first.

---

* The alphanumeric name for a given species does not necessarily represent structure. Consideration should be given to the likelihood of alternative structures. In most cases one structure will be the most likely.

Table 1

Primary Species for Methane-Air Combustion

Species	Log KP at 2000K	Considerations	JANNAF Reference
CH	-10	hydrocarbon radical	12/67
CHN	-2	possible role in prompt NO	12/69
CHO	+1	stable radical	12/70
CH_2	-7	hydrocarbon radical	12/72
CH_2O	+1	combustion intermediate	3/61
CH_3	+5	hydrocarbon radical	6/69
CH_3O	-6	possible role in ignition	constructed from CH_2F 12/63
CH_4	-3	starting material	3/61
CN	-6	possible role in prompt NO	6/69
CO	+7	combustion product	3/61
CO_2	+10	combustion product	9/65
H	-3	combustion intermediate	9/65
HN	-9	possible role in prompt NO	7/72
HNO	-5	possible role in prompt NO	3/63
HO	0	combustion intermediate	12/70
HO_2	-3	combustion intermediate	3/64
H_2	0	combustion product	3/61
H_2O	+4	combustion product	3/61
N	-9	important role NO formation	3/61
NO	-2	of prime interest	6/63
NO_2	-4	oxidation of NO	9/64
N_2	0	starting material	3/61
N_2O	-6	possible role NO formation	12/64
O	-3	combustion intermediate	6/62
O_2	0	starting material	3/61

Table 2

Secondary Species for Methane-Air Combustion

Species	Log KP at 2000K	Considerations
C	-10	possible role in soot formation
CNO		possible role NO/HC interaction
C_2	-12	possible role in soot formation
C_2H	-6	C_2 intermediates possibly important for fuel rich methane or higher hydrocarbons
C_2H_2	-3	
C_2H_3		
C_2H_4	-5	
C_2H_5		
C_2H_6		
H_2N	-6	possible intermediate
H_2O_2		possible role in ignition
H_3N	-5	possible role fuel rich
NO_3	-10	higher oxidation of NO
O_3	-7	possible role in ignition

As an example, the reaction N + OH = NO + H is frequently of interest for NO_x formation. To find its location in the master list three steps would be required:

(1) Make sure each of the species is written according to the alphanumeric sequence

N + HO = NO + H

(2) Sort each side into alphanumeric order

HO + N = H + NO

(3) Switch left and right side of the reaction if necessary to put the earliest sorted species on the left

H + NO = HO + N

In the master list of reactions every reaction is listed, but each reaction is listed only once. That is, the reverse of a given reaction does not appear elsewhere in the master list. The program also produces an auxiliary list in which each species in each reaction is listed first in turn. Thus each reaction may appear up to four times in the auxiliary list. This auxiliary list is useful for cross-comparisons of relative reaction rates and for evaluation of probable relative importance of reactions.

The 25 primary species selected for consideration resulted in the construction of 322 unimolecular and bimolecular reactions (double that number if one considers both the forward and reverse reactions). These reactions are listed in the Appendix along with additional information which will be discussed below. To give an appreciation of the rapid growth in the number of reactions with additional species, when the 14 secondary species are added to the list of 25 primary species, the number of reactions increases to 1078.

Evaluation of Probable Relative Importance

As discouraging and formidable as the task may seem with 322 reactions (worse yet with 1078) an evaluation can be made of the probable relative importance of the reactions based on thermochemical and stereochemical considerations to drastically reduce the number of reactions. It should be emphasized that the reaction lists constructed by the computer are mathematical constructions and many of them are not likely to be elementary reactions. In addition many of them are likely to be slow compared to competing reactions among the same species.

Such an evaluation was made for the methane/air system and the results are shown in the Appendix. The evaluation divides the reactions into three groups (1) those that are probably important (2) those that are possibly important and (3) those that are probably unimportant. Those in the first group are reactions that are likely to be important for combustion or NO_x formation across the range of conditions considered. Those in the second group consist of those reactions that may become important under specific conditions, or those reactions that may be important for species of marginal importance, or those reactions that have been proposed in the literature as important but appear to be marginal. Those in the third group are reactions that can be screened out as not being elementary or as being too slow to be of importance under the conditions of interest. As a result of the evaluation, 28 reactions were judged to be of probable importance, 73 reactions of possible importance, and 221 reactions probably unimportant. This evaluation aids in determining potentially important reactions that have not been reported in the literature.

Survey of Kinetic Data

The literature was surveyed for data on reactions of the 25 primary species*. The data in the literature and prior evaluations of those data were considered in establishing recommendations for rates to be used for the combustion calculations. In a number of cases, data for reactions of potential importance was unavailable or was clearly unreliable. In those case estimates were either made by the author or estimates were requested through EPA to be made by Stanford Research Institute under EPA Grant R 800798. The results of the recommendations are presented in the Appendix. Further details on the survey and evaluation will be found in a forthcoming EPA report by the author.

---

* only a cursory survey was made for reactions of CH_3O

Applications and Examples

The approach described in this paper can be applied for several purposes related to reaction mechanisms. There is, of course, the ultimate purpose of screening reactions for importance under specific conditions,but this goal has potential pitfalls which will be discussed shortly. The approach is useful for the evaluation of competitive reactions. By listing competitive reactions on a common basis, the thermochemistry and stereochemistry can be compared with experimental or theoretical rate constants in order to judge whether their relative values are consistent. By knowing that all competitive reactions among considered species have been included, the chances of oversight are minimized. The approach can be used to identify important reactions that require further study. In many cases, a reaction that is found to be of key importance will have a large uncertainty or may not have been studied at all. In that case, further study of such reactions is warranted. As a corrollary to establishing reaction mechanisms, the approach can be useful to establish "global" behavior. If it can be established that a sequence of elementary reactions leads from the same reactants to the same products over the entire range of conditions of interest, then that sequence would behave as if it were a single reaction over that range. Establishing such global behavior is desirable to simplify the complexity of reaction models. However,the more detailed the predictions one wishes to make, the less likely one is to find such global behavior.

There are a number of dangers in applying this detailed approach if one is lulled into a false sense of security. Although all of the reactions for the species selected are constructed by the computer program, the decision to include enough species must be made first. While including too many species makes the job more laborious and time consuming, the unimportant species will be weeded out eventually. Including too few species, on the other hand, will result in neglecting important reactions. Even if all the important reactions are constructed, care must be taken not to eliminate too many too soon. A good example of such a temptation might be one of the Zeldovich reactions:

$$N_2 + O \longrightarrow N + NO$$

With an activation energy of 75 kcal, one might be tempted to eliminate this reaction because it is quite endothermic. But it is still one of only two reactions between N_2 and O, which are important species in hydrocarbon/air combustion. The other reaction is

$$N_2 + O + M = N_2O + M$$

and N_2O can decompose rapidly at high temperatures.

Two other pitfalls are very closely related. In view of the complicated nature of the calculations using a large number of rate constants there is a temptation to overlook the uncertainties in the individual rates. Placing too heavy a reliance on uncertain rates can lead to a serious hazard in the construction of minimum reaction sets, a hazard which I shall call the quasi-detailed mechanism. Chemical kinetics has made substantial progress in recent years and with the development of improved diagnostic techniques, improvements should continue. But in the kinetics of methane/air combustion, a number of key reactions still have large uncertainties (some of these will be discussed below). While the detailed approach can point out critical reactions, and an assessment of the sensitivity of the calculations to the uncertainty of the rates can be made, minimum sets can be considered only quasi-detailed until sufficient accuracy in the key rates is obtained. Another hazard to be avoided in the construction of minimum sets is extrapolation beyond the range studied.

Two examples of the application of this detailed approach to the chemical kinetics of combustion problems of current interest are (1) NO/NO_2 conversion and (2) reactions between N_2 and carbon-containing species. In the case of NO/NO_2 conversion there are twelve reactions from the 25 species list:

43. NO + CHO = CH + NO2
161. NO + CH2O = CH2 + NO2
203. NO + CH3O = CH3 + NO2
227. NO + CO2 = CO + NO2
268. NO + HNO = HN + NO2
248. NO + HO = H + NO2
295. NO + HO2 = HO + NO2
300. NO + H2O = H2 + NO2
307. NO + NO = N + NO2
317. NO + N2O = NO2 + N2
318. NO + O + M = NO2 + M
319. NO + O2 = NO2 + O

For a well-stirred reactor burning methane/air between 80 and 125 percent stoichiometric air, calculations indicate that the main reactions producing NO_2 are

$$NO + O + M \longrightarrow NO_2 + M$$

and

$$NO + HO_2 \longrightarrow NO_2 + HO$$

and the main reaction destroying NO_2 is

$$NO_2 + H \longrightarrow NO + HO$$

For this case the rate constants are such that no substantial amount of NO_2 (< 1 ppm) is calculated even though the concentrations of NO ($\sim$ 100 ppm) and O atom ($\sim$ 2,000 ppm) are substantial. Other species with NO bonds (such as HNO, N_2O and possibly CNO) could conceivably lead to formation of "prompt" NO_2 without going through the NO molecule itself but these do not appear to be of importance for stirred reactor calculations.

Twelve reactions are also found between N_2 and carbon-containing species:

47. N2 + CH = CHN + N
48. N2 + CH = CN + HN
50. N2 + CHO = CH + N2O
82. N2 + CHO = CHN + NO
132. N2 + CHO = CN + HNO
65. N2 + CH2 = CHN + HN
67. N2 + CH2O = CHN + HNO
162. N2 + CH2O = CH2 + N2O
204. N2 + CH3O = CH3 + N2O
216. N2 + CO = CN + NO
218. N2 + CO2 = CN + NO2
228. N2 + CO2 = CO + N2O

For the same stirred reactor case the reaction that appears to play a major role is

$$CH + N_2 = CHN + N$$

Further details on the complete calculations will be provided elsewhere.

All of the reactions mentioned as important in the above examples have a fairly high degree of uncertainty in the 1500-2500K temperature range and bear further study. It is recommended that these reactions receive attention in studies of elementary rate constants.

Conclusions and Recommendations

The detailed approach to the chemistry of methane-air combustion is useful for

- Guidance in establishing reaction mechanisms
- Evaluation of competitive reactions
- Establishing global behavior
- Identifying critical reactions

Caution should be exercised when applying the approach to avoid the pitfalls of

- Insufficient species
- Overelimination of reactions
- Overreliance on uncertain rate constants
- Construction of minimum sets which are actually quasi-detailed mechanisms

The following reactions or their reverse bear further study in the temperature range 1500-2500K to help answer questions of current interest

$NO + O + M \longrightarrow NO_2 + M$

$HO_2 + NO \longrightarrow HO + NO_2$

$H + NO_2 \longrightarrow HO + NO$

$CH + N_2 \longrightarrow CHN + N$

APPENDIX

SUMMARY OF INFORMATION ON REACTIONS IN KINETICS SURVEY

This Appendix contains a summary of the probable relative importance and recommended rates for reactions in methane/air combustion. The format of the tables in this Appendix and the range of applicability intended for those data is explained in the notes below and to the right. The notes below refer to the left hand side of the tables and the notes on the right refer to the right hand side of the tables. More detailed information will be found in a forthcoming EPA report entitled "Survey and Evaluation of Kinetic Data on Reactions in Methane-Air Combustion" by Victor S. Engleman.

EVALUATION OF PROBABLE RELATIVE REACTION IMPORTANCE

This section contains a reaction-by-reaction evaluation of the potential importance of each of the 322 reactions considered in this study. It is extremely important to understand the groundrules for the evaluation and scope of its applicability. The comments found in this section refer only to the combustion of methane-air from 80-125% stoichiometric air, from 1500-2500K. This has been stated elsewhere in this report, but bears repeating. The use of the information in this section outside the limits mentioned, may be valid, but should be approached with caution. Not only would the relative importance of the given reactions require evaluation for specific conditions but other species and, therefore, additional reactions might have to be considered outside those limits. And of course, other reaction systems such as higher hydrocarbons or fuel-nitrogen containing systems would bear their own evaluations.

The headings in this section are as follows:

Headings	Description
REACTION	Written in both directions Reaction number indicated F = Forward R = Reverse
HR	ΔH_r for both directions given at 2000K (mid-range of 1500-2500K) note: in the thermochemical tables ΔH_r298 is used in the expression for log K_c in Section 4 of the full survey
NOTES	A Probably important B Possibly important C Probably unimportant * Flag indicating reaction was rated either A or B
COMMENTS	Notes explaining reasons for ranking

RECOMMENDED RATES FOR REACTIONS FOUND IN THE LITERATURE AND ADDITIONAL REACTIONS OF POTENTIAL IMPORTANCE

In assembling recommendations for rates to be used, every attempt was made to use existing critical evaluations. This was done so as not to impose an additional layer of "slightly different" rate parameters to an already confusing array of differing opinions. Where alterations were required the nature of the change has been carefully indicated. Where critical evaluations were not available, use was made of reliable experimental data in the appropriate temperature range. Where data in the appropriate range were not available, reliable data outside the temperature range were extrapolated to the range of interest with a reasonable temperature dependence. Where no such data were available, literature estimates that seemed reasonable were used. And finally, where no literature estimates were available, reasonable estimates were made or were requested to be made as indicated.

In all cases, an attempt has been made to make the rates self consistent; i.e., to bring relative rates of competing reactions into line. While a number of rates have been altered for this purpose, there may still exist some that are not yet consistent with other similar reactions. In many cases, recently revised thermochemistry has an influence on estimated activation energies of reactions. In cases where older estimates have activation energies significantly below the endothermicity currently calculated, appropriate adjustments have been made.

The rates given are recommendations as of December 31, 1974.

The headings in this section are as follows:

Headings	Description
REACTION	Written in the direction of the recommendation. Each reaction is recommended in one direction only. Reverse rate may be obtained by using the expression for K_c in Section 4 of the full survey $K_c = k_f/k_r$ Each reaction is numbered and direction indicated F = Forward of master reaction R = Reverse of master reaction * Flag to indicate that reaction should be considered in initial screening for combustion of methane/air at one atmosphere between 1500-2500K and 80-125% stoichiometric air.
LOG A	Common logarithm of constant preexponential term. Uncertainty in parenthesis.
B	Exponent of T
C	Activation energy (kcal/mole) Uncertainty in parenthesis.
note:	$k = 10^{LOG\ A}\ T^B\ e^{-C/RT}$
COMMENTS	Basis for selection of recommendation. References listed in Section 7 of the full survey Explanation of notes: Note A - No experimental data in literature, given rate selected as most reliable. Note B - No other estimate available in literature. Note C - No literature estimate available, estimated as indicated. Note D - Limited experimental data available, use with caution. (J-P) - Johnston-Parr method. (EST) - Order of magnitude estimate. (EVAL) - Evaluation. (EXP) - Based on experimental determinations.
LOG K	Calculated from recommended rate expression at temperatures of 300, 1500, 2000 and 2500K (note: 300K is outside considered range, provided for reference only).

REACTION	HR	NOTES	COMMENTS
1F. CH + CHN = CH2 + CN 1R. CH2 + CN = CH + CHN	20.3 -20.3	B * B *	CONSIDER BOTH DIRECTIONS, FUEL RICH POSSIBLE ROLE CN/HCN PROBABLY MINOR
2F. CH + CHO = CH2 + CO 2R. CH2 + CO = CH + CHO	-85.5 85.5	C C	FORWARD UNIMPORTANT FOR CHO REMOVAL H, O, NO MORE LIKELY REACTION PARTNERS REVERSE ENDOTHERMIC
3F. CH + CH2O = CHO + CH2 3R. CHO + CH2 = CH + CH2O	-15.6 15.6	C C	CH, CH2 MINOR RX PARTNERS FOR CHO, CH2O
4F. CH + CH2O = CH3 + CO 4R. CH3 + CO = CH + CH2O	-108.6 108.6	C C	CH MINOR RX PARTNER FOR CH2O REVERSE HIGHLY ENDOTHERMIC
5F. CH + CH3 = CH2 + CH2 5R. CH2 + CH2 = CH + CH3	7.4 -7.4	C C	(CH)(CH3) AND (CH2)(CH2) LIKELY SMALL POSSIBLE FUEL RICH
6F. CH + CH3O = CHO + CH3 6R. CHO + CH3 = CH + CH3O	-102.7 102.7	C C	LOW CONCENTRATIONS FORWARD REVERSE HIGHLY ENDOTHERMIC
7F. CH + CH3O = CH2 + CH2O 7R. CH2 + CH2O = CH + CH3O	-79.6 79.6	C C	LOW CONCENTRATIONS FORWARD REVERSE ENDOTHERMIC
8F. CH + CH3O = CH4 + CO 8R. CH4 + CO = CH + CH3O	-191.3 191.3	C C	NOT LIKELY TO BE ELEMENTARY REACTION
9F. CH + CH4 = CH2 + CH3 9R. CH2 + CH3 = CH + CH4	3.0 -3.0	B * B *	CONSIDER BOTH DIRECTIONS, FUEL RICH CH4 STARTING MATL, CH3 INITIAL INTERMED THERMALLY NEUTRAL
10F. CH + CO2 = CHO + CO 10R. CHO + CO = CH + CO2	-68.3 68.3	B * C	CONSIDER FORWARD, FUEL RICH (CO2) HIGH, PATH FROM CH TO CO REVERSE ENDOTHERMIC

REACTION	LOG A	B	C	COMMENTS	300	TEMP, KELVIN 1500	2000	2500
						LOG K		
1R. CH2 + CN = CH + CHN	* 12.5	0.	5.	SAI ESTIMATE	8.9	11.8	12.0	12.1
2F. CH + CHO = CH2 + CO	10.5 (0.5)	0.7	1. (5.)	BASED ON T1 (J-P) NOTE A	11.5	12.6	12.7	12.8
3F. CH + CH2O = CH2 + CHO	11.0 (0.5)	0.7	4. (5.)	BASED ON T1 (J-P) NOTE A	9.8	12.6	12.9	13.0
4F. CH + CH2O = CH3 + CO				NO RATE DATA				
5R. CH2 + CH2 = CH + CH3	11.7 (0.5)	0.5	6. (5.)	BASED ON T1 (EST) NOTE B	8.6	12.4	12.7	12.9
6F. CH + CH3O = CHO + CH3				NO RATE DATA				
7F. CH + CH3O = CH2 + CH2O				NO RATE DATA				
8F. CH + CH3O = CH4 + CO				NO RATE DATA				
9F. CH +CH4 = CH2 + CH3	* 11.4 (0.5)	0.7	6. (5.)	BASED ON T1 (J-P) NOTE A	8.8	12.7	13.1	13.3
10F. CH + CO2 = CHO + CO	* 10.0 (0.5)	0.5	6. (5.)	BASED ON T1 (EST) NOTE B	6.9	10.7	11.0	11.2

REACTION	HR	NOTES	COMMENTS
11F. CH + H + M = CH2 + M 11R. CH2 + M = CH + H + M	-105.1 105.1	C C	THIRD ORDER, LOW CONC IN FORWARD REVERSE HIGHLY ENDOTHERMIC
12F. CH + HN = CHN + H 12R. CHN + H = CH + HN	-145.4 145.4	C C	LOW CONCENTRATIONS FORWARD HIGHLY ENDOTHERMIC REVERSE
13F. CH + HN = CH2 + N 13R. CH2 + N = CH + HN	-26.2 26.2	C C	LOW CONCENTRATIONS BOTH DIRECTIONS
14F. CH + HN = CN + H2 14R. CN + H2 = CH + HN	-128.4 128.4	C C	LOW CONCENTRATIONS FORWARD REVERSE HIGHLY ENDOTHERMIC FOUR-CENTER REACTION
15F. CH + HNO = CHN + NO 15R. CHN + NO = CH + HNO	-123.8 123.8	C C	FORWARD POSSIBLE FOR NOH STRUCTURE CONCENTRATIONS LOW REVERSE HIGHLY ENDOTHERMIC
16F. CH + HNO = CHO + HN 16R. CHO + HN = CH + HNO	-67.8 67.8	C C	LOW CONCENTRATIONS BOTH DIRECTIONS REVERSE ENDOTHERMIC
17F. CH + HNO = CH2 + NO 17R. CH2 + NO = CH + HNO	-52.4 52.4	C C	LOW CONCENTRATIONS FORWARD CH2 + NO = CH2O + N MORE LIKELY REVERSE
18F. CH + HNO = CH2O + N 18R. CH2O + N = CH + HNO	-78.4 78.4	C C	LOW CONCENTRATIONS FORWARD REVERSE ENDOTHERMIC
19F. CH + HNO = CN + H2O 19R. CN + H2O = CH + HNO	-121.7 121.7	C C	LOW CONCENTRATIONS FORWARD REVERSE HIGHLY ENDOTHERMIC FOUR-CENTER REACTION FOR NOH STRUCTURE
20F. CH + NO = CHO + N 20R. CHO + N = CH + NO	-89.4 89.4	B * C	CONSIDER FORWARD REVERSE ENDOTHERMIC

REACTION	LOG A	B	C	COMMENTS	300	TEMP, KELVIN 1500	2000	2500
						LOG K		
11F. CH + H + M = CH2 + M	19.0 (0.5)	-1.	0.	EST BY METHOD OF BBS NOTE C	16.5	15.8	15.7	15.6
12F. CH + HN = CHN + H				NO RATE DATA				
13R. CH2 + N = CH + HN	11.8 (0.5)	0.67	40.5 (5.)	BASED ON HB (J-P) NOTE B	-16.0	8.0	9.6	10.5
14F. CH + HN = CN + H2				NO RATE DATA				
15F. CH + HNO = CHN + NO				NO RATE DATA				
16F. CH + HNO = CHO + HN				NO RATE DATA				
17F. CH + HNO = CH2 + NO	11.8 (0.5)	0.5	0. (5.)	BASED ON T1 (EST) NOTE B	13.0	13.4	13.5	13.5
18F. CH + HNO = CH2O + N				NO RATE DATA				
19F. CH + HNO = CN + H2O				NO RATE DATA				
20F. CH + NO = CHO + H	* 11.7 (0.5)	0.5	10. (5.)	BASED ON T1 (EST) NOTE B	5.7	11.8	12.3	12.5

REACTION	HR	NOTES	COMMENTS
21F. CH + HO = CH2 + O 21R. CH2 + O = CH + HO	1.2 -1.2	C C	CH + HO = CHO + H MORE LIKELY FORWARD CH2 + O = CHO + H MORE LIKELY REVERSE
22F. CH + HO + M = CH2O + M 22R. CH2O + M = CH + HO + M	-178.9 178.9	C C	THIRD ORDER, LOW CONCENTRATION FORWARD REVERSE HIGHLY ENDOTHERMIC NOT LIKELY TO BE ELEMENTARY REACTION
23F. CH + HO = CO + H2 23R. CO + H2 = CH + HO	-178.3 178.3	C C	FOUR-CENTER REACTION CH + HO = CHO + H MORE LIKELY FORWARD REVERSE HIGHLY ENDOTHERMIC
24F. CH + HO2 = CHO + HO 24R. CHO + HO = CH + HO2	-129.6 129.6	C C	H-O2 WEAKER THAN HO-O CH + HO2 = CH2 + HO2 MORE LIKELY FORWARD REVERSE HIGHLY ENDOTHERMIC
25F. CH + HO2 = CH2+ O2 25R. CH2+ O2 = CH + HO2	-54.7 54.7	B * C	CONSIDER FORWARD REVERSE ENDOTHERMIC
26F. CH + HO2 = CH2O + O 26R. CH2O + O = CH + HO2	-112.8 112.8	C C	NOT LIKELY TO BE ELEMENTARY REACTION
27F. CH + HO2 = CO + H2O 27R. CO + H2O = CH + HO2	-233.4 233.4	C C	FOUR-CENTER REACTION CH + HO2 = CH2 + O2 MORE LIKELY FORWARD REVERSE HIGHLY ENDOTHERMIC
28F. CH + HO2 = CO2 + H2 28R. CO2 + H2 = CH + HO2	-259.7 259.7	C C	NOT LIKELY TO BE ELEMENTARY REACTION
29F. CH + H2 = CH2 + H 29R. CH2 + H = CH + H2	3.4 -3.4	B * B *	CONSIDER BOTH DIRECTIONS FUEL RICH
30F. CH + H2 + M = CH3 + M 30R. CH3 + M = CH + H2 + M	-109.2 109.2	C C	NOT LIKELY TO BE ELEMENTARY REACTION

REACTION	LOG A	B	C	COMMENTS	300	TEMP, KELVIN 1500	 2000	2500
						LOG K		
21R. CH2 + O = CH + HO	11.3 (0.5)	0.7	26. (5.)	BASED ON HB (J-P) NOTE A	-5.9	9.7	10.8	11.4
22F. CH + HO + M = CH2O + M				NO RATE DATA				
23F. CH + HO = CO + H2				NO RATE DATA				
24F. CH + HO2 = CHO + HO	11.7 (0.5)	0.5	6. (5.)	BASED ON T1 (EST) NOTE B	8.6	12.4	12.7	12.9
25F. CH + HO2 = CH2 + O2	* 10.0 (0.5)	0.5	19. (5.)	BASED ON T1 (EST) NOTE B	0.3	9.4	10.0	10.4
26F. CH + HO2 = CH2O + O				NO RATE DATA				
27F. CH + HO2 = CO + H2O				NO RATE DATA				
28F. CH + HO2 = CO2 + H2				NO RATE DATA				
29R. CH2 + H = CH + H2	* 11.5 (0.5)	0.7	5. (5.)	BASED ON HB,T1 (J-P) WITH C=5 NOTE A	9.6	13.0	13.3	13.4
30F. CH + H2 + M = CH3 + M				NO RATE DATA				

REACTION	HR	NOTES	COMMENTS
31F. CH + H2O = CHO + H2 31R. CHO + H2 = CH + H2O	-74.5 74.5	C C	NOT LIKELY TO BE ELEMENTARY REACTION
32F. CH + H2O = CH2+ HO 32R. CH2+ HO = CH + H2O	18.2 -18.2	B * B *	CONSIDER BOTH DIRECTIONS FUEL RICH
33F. CH + H2O = CH2O + H 33R. CH2O + H = CH + H2O	-55.6 55.6	C C	NOT LIKELY TO BE ELEMENTARY REACTION
34F. CH + H2O = CH3 + O 34R. CH3 + O = CH + H2O	12.0 -12.0	C C	NOT LIKELY TO BE ELEMENTARY REACTION
35F. CH + H2O + M = CH3O + M 35R. CH3O + M = CH + H2O + M	-81.1 81.1	C C	NOT LIKELY TO BE ELEMENTARY REACTION
36F. CH + N + M = CHN + M 36R. CHN + M = CH + N + M	-224.3 224.3	C C	THIRD ORDER, LOW CONCENTRATIONS FORWARD REVERSE HIGHLY ENDOTHERMIC
37F. CH + N = CN + H 37R. CN + H = CH + N	-98.9 98.9	C C	LOW CONCENTRATIONS FORWARD REVERSE HIGHLY ENDOTHERMIC
38F. CH + NO = CHN + O 38R. CHN + O = CH + NO	-70.2 70.2	B * C	CONSIDER FORWARD FUEL RICH REVERSE ENDOTHERMIC
39F. CH + NO = CHO + N 39R. CHO + N = CH + NO	-41.6 41.6	B * C	CONSIDER FORWARD FUEL RICH REVERSE ENDOTHERMIC
40F. CH + NO = CN + HO 40R. CN + HO = CH + NO	-51.1 51.1	C C	FOUR-CENTER REACTION

REACTION	LOG A	B	C	COMMENTS	300	TEMP, KELVIN 1500	 2000	2500
						LOG K		
31F. CH + H2O = CHO + H2				NO RATE DATA				
32R. CH2 + HO = CH + H2O	* 11.7 (0.5)	0.5	6. (5.)	BASED ON T1 (EST) NOTE B	8.6	12.4	12.7	12.9
33F. CH + H2O = CH2O + H				NO RATE DATA				
34F. CH + H2O = CH3 + O				NO RATE DATA				
35F. CH + H2O + M = CH3O + M				NO RATE DATA				
36F. CH + N + M = CHN + M				NO RATE DATA				
37F. CH + N = CN + H				NO RATE DATA				
38F. CH + NO = CHN + O	* 12.3	0.	0.	SRI ESTIMATE	12.3	12.3	12.3	12.3
39F. CH + NO = CHO + N	* 13.2	0.	10.	SRI ESTIMATE SPIN RETARDED	5.9	11.7	12.1	12.3
40F. CH + NO = CN + HO				NO RATE DATA				

```
         REACTION              HR     NOTES              COMMENTS                                       REACTION             LOG A    B      C        COMMENTS            300     TEMP, KELVIN      2500
                                                                                                                                                                                1500    2000
                                                                                                                                                                                    LOG K
41F. CH + NO = CO + HN       -101.0    C     FOUR-CENTER REACTION                           41F. CH + NO = CO + HN                           NO RATE DATA
41R. CO + HN = CH + NO        101.0    C

42F. CH + NO2 = CHN + O2     -117.5    C     NOT LIKELY TO BE ELEMENTARY REACTION           42F. CH + NO2 = CHN + O2                         NO RATE DATA
42R. CHN + O2 = CH + NO2      117.5    C

43F. CH + NO2 = CHO + NO     -121.0    C     LOW CONCENTRATIONS FORWARD                     43F. CH + NO2 = CHO + NO                         NO RATE DATA
43R. CHO + NO = CH + NO2      121.0    C     REVERSE HIGHLY ENDOTHERMIC

44F. CH + NO2 = CN + HO2      -42.6    C     NOT LIKELY TO B2 ELEMENTARY REACTION           44F. CH + NO2 = CN + HO2                         NO RATE DATA
44R. CN + HO2 = CH + NO2       42.6    C

45F. CH + NO2 = CO + HNO     -156.1    C     LOW CONCENTRATIONS FORWARD                     45F. CH + NO2 = CO + HNO                         NO RATE DATA
45R. CO + HNO = CH + NO2      156.1    C     REVERSE HIGHLY ENDOTHERMIC

46F. CH + NO2 = CO2 + HN     -153.7    C     NOT LIKELY TO BE ELEMENTARY REACTION           46F. CH + NO2 = CO2 + HN                         NO RATE DATA
46R. CO2 + HN = CH + NO2      153.7    C

47F. CH + N2 = CHN + N          5.1    A *   FORWARD IS LOW ENERGY N-N BREAKING             47F. CH + N2 = CHN + N     * 13.3    0.    13.   ORIG SRI ESTIMATE      3.8    11.4    11.9    12.2
47R. CHN + N = CH + N2         -5.1    B *   POTENTIALLY VERY IMPORTANT                                                                         SPIN RETARDED
                                             SPIN RETARDED                                                                11.0    0.    19.   REVISED SRI ESTIMATE  -2.8     8.2     8.9     9.3
                                             CONSIDER BOTH DIRECTIONS                                                     13.3    0.    40.   ALT FROM COMB CALC   -21.7     6.3     8.1     9.1
48F. CH + N2 = CN + HN         51.6    B *   FOUR-CENTER REACTION                           48F. CH + N2 = CN + HN     * 14.5    0.    92.   SRI ESTIMATE         -52.5     1.1     4.4     6.5
48R. CN + HN = CH + N2        -51.6    B *   FORWARD IS MODERATE ENERGY N-N BREAKING                                                            FOUR-CENTER
                                             CONSIDER BOTH DIRECTIONS FOR SCREENING                                                             BASED ON EST ACTIV
                                                                                                                                                ENERGY 40. FOR REV
49F. CH + N2O = CHN + NO     -109.1    C     LOW CONCENTRATIONS FORWARD                     49F. CH + N2O = CHN + NO                         NO RATE DATA
49R. CHN + NO = CH + N2O      109.1    C     REVERSE HIGHLY ENDOTHERMIC

50F. CH + N2O = CHO + N2     -155.0    C     LOW CONCENTRATIONS FORWARD                     50F. CH + N2O = CHO + N2                         NO RATE DATA
50R. CHO + N2 = CH + N2O      155.0    C     REVERSE HIGHLY ENDOTHERMIC


         REACTION              HR     NOTES              COMMENTS                                       REACTION             LOG A    B      C        COMMENTS            300     TEMP, KELVIN      2500
                                                                                                                                                                                1500    2000
                                                                                                                                                                                    LOG K
51F. CH + N2O = CN + HNO      -16.4    C     LOW CONCENTRATIONS BOTH DIRECTIONS             51F. CH + N2O = CN + HNO                         NO RATE DATA
51R. CN + HNO = CH + N2O       16.4    C

52F. CH + O + M = CHO + M    -195.7    C     THIRD ORDER, LOW CONCENTRATIONS FORWARD        52F. CH + O + M = CHO + M   16.   -0.5    0.   BASED ON T1 (EST)     14.0    14.4    14.3    14.3
52R. CHO + M = CH + O + M     195.7    C     REVERSE HIGHLY ENDOTHERMIC                                                (0.5 )       ( 5. ) NOTE B

53F. CH + O = CO + H         -176.2    B *   CONSIDER FORWARD                               53F. CH + O = CO + H      * 11.7    0.5    0.   BASED ON T1 (EST)     12.9    13.3    13.4    13.4
53R. CO + H = CH + O          176.2    C     REVERSE HIGHLY ENDOTHERMIC                                                (0.5 )       ( 5. ) C=O BASED ON OBS
                                                                                                                                                NOTE B
54F. CH + O2 = CHO + O        -75.7    B *   CONSIDER FORWARD                               54F. CH + O2 = CHO + O    * 11.7    0.5    6.   BASED ON T1 (EST)      8.6    12.4    12.7    12.9
54R. CHO + O = CH + O2         75.7    C     REVERSE ENDOTHERMIC                                                       (0.5 )       ( 5. ) NOTE B

55F. CH + O2 = CO + HO       -160.4    C     FOUR-CENTER REACTION                           55F. CH + O2 = CO + HO                           NO RATE DATA
55R. CO + HO = CH + O2        160.4    C     CH + O2 = CHO + O MORE LIKELY FORWARD
                                             REVERSE HIGHLY ENDOTHERMIC
56F. CH + O2 = CO2 + H       -181.6    C     NOT LIKELY TO BE ELEMENTARY REACTION           56F. CH + O2 = CO2 + H                           NO RATE DATA
56R. CO2 + H = CH + O2        181.6    C

57F. CHN + M = CN + H + M     125.4    C     FORWARD HIGHLY ENDOTHERMIC                     57R. CN + H + M = CHN + M   16.5   -0.5    0.   BASED ON T1 (EST)     15.3    14.9    14.8    14.8
57R. CN + H + M = CHN + M    -125.4    C     THIRD ORDER, LOW CONCENTRATIONS REVERSE                                   (0.5 )       ( 5. ) NOTE B

58F. CHN + CHO = CH2O + CN     35.9    C     LOW CONCENTRATIONS, STERIC HINDRANCE           58R. CH2O + CN = CHN + CHO  11.1    0.7    3.   BASED ON T1 (J-P)     10.6    12.9    13.1    13.2
58R. CH2O + CN = CHN + CHO    -35.9    C                                                                               (0.5 )       ( 5. ) NOTE B

59F. CHN + CH2 = CH3 + CN      12.9    B *   CONSIDER FUEL RICH                             59R. CH3 + CN = CHN + CH2 * 11.0    0.7    3.   BASED ON T1 (J-P)     10.5    12.8    13.0    13.1
59R. CH3 + CN = CHN + CH2     -12.9    B *   REVERSE POSSIBLE DURING EARLY STAGES                                      (0.5 )       ( 5. ) NOTE B

60F. CHN + CH2O = CH3O + CN    99.9    C     STERIC HINDRANCE, LOW CONCENTRATIONS           60F. CHN + CH2O = CH3O + CN                      NO RATE DATA
60R. CH3O + CN = CHN + CH2O   -99.9    C     BOTH DIRECTIONS
```

REACTION	HR	NOTES	COMMENTS
61F. CHN + CH3 = CH4 + CN 61R. CH4 + CN = CHN + CH3	17.3 -17.3	B * B *	CONSIDER BOTH DIRECTIONS FUEL RICH REVERSE POSSIBLE DURING EARLY STAGES
62F. CHN + CO = CHO + CN 62R. CHO + CN = CHN + CO	105.9 -105.9	C C	FORWARD HIGHLY ENDOTHERMIC LOW CONCENTRATIONS REVERSE
63F. CHN + H = CH2 + N 63R. CH2 + N = CHN + H	119.2 -119.2	C C	FORWARD HIGHLY ENDOTHERMIC LOW CONCENTRATIONS REVERSE
64F. CHN + H = CN + H2 64R. CN + H2 = CHN + H	17.0 -17.0	B * B *	CONSIDER BOTH DIRECTIONS FUEL RICH
65F. CHN + HN = CH2 + N2 65R. CH2 + N2 = CHN + HN	-11.3 11.3	C B *	LOW CONCENTRATIONS FORWARD CONSIDER REVERSE FOR N-N BREAKING FOUR-CENTER REACTION
66F. CHN + HNO = CH2 + N2O 66R. CH2 + N2O = CHN + HNO	56.0 -56.0	C C	LOW CONCENTRATIONS BOTH DIRECTIONS FOUR-CENTER REACTION
67F. CHN + HNO = CH2O + N2 67R. CH2O + N2 = CHN + HNO	-83.5 83.5	C C	NOT LIKELY TO BE ELEMENTARY REACTION
68F. CHN + HO = CHO + HN 68R. CHO + HN = CHN + HO	56.0 -56.0	C C	FOUR-CENTER REACTION FORWARD ENDOTHERMIC LOW CONCENTRATIONS REVERSE
69F. CHN + HO = CH2 + NO 69R. CH2 + NO = CHN + HO	71.4 -71.4	C C	FOUR-CENTER REACTION FORWARD ENDOTHERMIC CH2 + NO = CH2O + N MORE LIKELY REVERSE
70F. CHN + HO = CH2O + N 70R. CH2O + N = CHN + HO	45.6 -45.6	C C	NOT LIKELY TO BE ELEMENTARY REACTION

REACTION	LOG A	B	C	COMMENTS	300	TEMP, KELVIN 1500	 2000 LOG K	 2500
61R. CH4 + CN = CHN + CH3	* 11.5 (10.5)	0.7	5. (5.)	BASED ON TI (J-P) GOOD AGRMT W/B78	9.6	13.0	13.3	13.4
62R. CHO + CN = CHN + CO	11.3 (10.5)	0.5	0. (5.)	BASED ON TI (EST) NOTE B	12.5	12.9	13.0	13.0
63F. CHN + H = CH2 + N				NO RATE DATA				
64R. CN + H2 = CHN + H	* 12.5	0.	5.	SRI ESTIMATE	8.9	11.8	12.0	12.1
65R. CH2 + N2 = CHN + HN	* 14.0	0.	70.	SRI ESTIMATE BASED ON EST ACTIV ENERGY 40. FOR REV	-37.0	3.8	6.4	7.9
66F. CHN + HNO = CH2 + N2O				NO RATE DATA				
67F. CHN + HNO = CH2O + N2				NO RATE DATA				
68F. CHN + HO = CHO + HN				NO RATE DATA				
69F. CHN + HO = CH2 + NO				NO RATE DATA				
70F. CHN + HO = CH2O + N				NO RATE DATA				

REACTION	HR	NOTES	COMMENTS
71F. CHN + HO = CN + H2O 71R. CN + H2O = CHN + HO	2.1 -2.1	B * B *	CONSIDER BOTH DIRECTIONS FUEL RICH
72F. CHN + HO2 = CHO + HNO 72R. CHO + HNO = CHN + HO2	-5.0 5.0	C C	UNLIKELY TO BE ELEMENTARY REACTION FOUR-CENTER REACTION STERIC HINDRANCE
73F. CHN + HO2 = CH2 + NO2 73R. CH2 + NO2 = CHN + HO2	62.8 -62.8	C C	FOUR-CENTER REACTION FORWARD ENDOTHERMIC LOW CONCENTRATIONS REVERSE
74F. CHN + HO2 = CH2O + NO 74R. CH2O + NO = CHN + HO2	-42.6 42.6	C C	NOT LIKELY TO BE ELEMENTARY REACTION
75F. CHN + H2 = CH2 + HN 75R. CH2 + HN = CHN + H2	148.8 -148.8	C C	FOUR-CENTER REACTION C-N BOND STRONG REVERSE HIGHLY ENDOTHERMIC
76F. CHN + H2 = CH3 + N 76R. CH3 + N = CHN + H2	115.1 -115.1	C C	NOT LIKELY TO BE ELEMENTARY REACTION
77F. CHN + H2O = CH2 + HNO 77R. CH2 + HNO = CHN + H2O	142.0 -142.0	C C	NOT LIKELY TO BE ELEMENTARY REACTION STERIC HINDRANCE
78F. CHN + H2O = CH2O + HN 78R. CH2O + HN = CHN + H2O	89.0 -89.0	C C	NOT LIKELY TO BE ELEMENTARY REACTION
79F. CHN + H2O = CH3 + NO 79R. CH3 + NO = CHN + H2O	82.2 -82.2	C C	NOT LIKELY TO BE ELEMENTARY REACTION
80F. CHN + H2O = CH3O + N 80R. CH3O + N = CHN + H2O	143.3 -143.3	C C	NOT LIKELY TO BE ELEMENTARY REACTION

REACTION	LOG A	B	C	COMMENTS	300	TEMP, KELVIN 1500	 2000 LOG K	 2500
71F. CHN + HO = CN + H2O	* 11.3 (10.5)	0.6	5. (5.)	BASED ON TI (J-P) NOTE B	9.1	12.5	12.7	12.9
72F. CHN + HO2 = CHO + HNO				NO RATE DATA				
73F. CHN + HO2 = CH2 + NO2				NO RATE DATA				
74F. CHN + HO2 = CH2O + NO				NO RATE DATA				
75F. CHN + H2 = CH2 + HN				NO RATE DATA				
76F. CHN + H2 = CH3 + N				NO RATE DATA				
77F. CHN + H2O = CH2 + HNO				NO RATE DATA				
78F. CHN + H2O = CH2O + HN				NO RATE DATA				
79F. CHN + H2O = CH3 + NO				NO RATE DATA				
80F. CHN + H2O = CH3O + N				NO RATE DATA				

REACTION	HR	NOTES	COMMENTS
81F. CHN + N = CN + HN	46.5	C	LOW CONCENTRATIONS BOTH DIRECTIONS
81R. CN + HN = CHN + N	-46.5	C	
82F. CHN + NO = CHO + N2	-46.7	C	FOUR-CENTER REACTION LOW CONCENTRATIONS FORWARD REVERSE ENDOTHERMIC
82R. CHO + N2 = CHN + NO	46.7	C	
83F. CHN + NO = CN + HNO	72.7	C	FORWARD ENDOTHERMIC
83R. CN + HNO = CHN + NO	-72.7	C	LOW CONCENTRATIONS REVERSE
84F. CHN + NO2 = CHO + N2O	-11.8	C	FOUR-CENTER REACTION
84R. CHO + N2O = CHN + NO2	11.8	C	STERIC HINDRANCE
85F. CHN + O = CHO + N	28.6	B *	CONSIDER BOTH DIRECTIONS FUEL RICH
85R. CHO + N = CHN + O	-28.6	B *	
86F. CHN + O = CN + HO	19.1	B *	CONSIDER BOTH DIRECTIONS FUEL RICH
86R. CN + HO = CHN + O	-19.1	B *	NOTE- CNO POSSIBLE PRODUCT REVERSE
87F. CHN + O = CO + HN	-30.8	C	NOT LIKELY TO BE ELEMENTARY REACTION
87R. CO + HN = CHN + O	30.8	C	
88F. CHN + O2 = CHO + NO	-3.4	C	FOUR-CENTER REACTION
88R. CHO + NO = CHN + O2	3.4	C	CHN AND O2 NOT LIKELY HI SIMULTANEOUSLY
89F. CHN + O2 = CN + HO2	75.1	C	FORWARD ENDOTHERMIC
89R. CN + HO2 = CHN + O2	-75.1	C	LOW CONCENTRATIONS REVERSE
90F. CHN + O2 = CO + HNO	-36.6	C	NOT LIKELY TO BE ELEMENTARY REACTION
90R. CO + HNO = CHN + O2	36.6	C	

REACTION	LOG A	B	C	COMMENTS		TEMP, KELVIN		
					300	1500	2000	2500
						LOG K		
81R. CN + HN = CHN + N	11.0 (10.5)	0.5	2. (5.)	BASED ON T1 (EST) NOTE B	10.8	12.3	12.4	12.5
82F. CHN + NO = CHO + N2				NO RATE DATA				
83R. CN + HNO = CHN + NO	11.6 (10.5)	0.5	0. (5.)	BASED ON T1 (EST) NOTE B	12.8	13.2	13.3	13.3
84F. CHN + NO2 = CHO + N2O				NO RATE DATA				
85R. CHO + N = CHN + O	* 14.0	0.	0.	SRI ESTIMATE	14.0	14.0	14.0	14.0
86R. CN + HO = CHN + O	* 12.5	0.	3.	SRI ESTIMATE	10.3	12.1	12.2	12.2
87F. CHN + O = CO + HN				NO RATE DATA				
88F. CHN + O2 = CHO + NO				NO RATE DATA				
89F. CHN + O2 = CN + HO2				NO RATE DATA				
90F. CHN + O2 = CO + HNO				NO RATE DATA				

REACTION	HR	NOTES	COMMENTS
91F. CHN + O2 = CO2 + HN	-36.2	C	NOT LIKELY TO BE ELEMENTARY REACTION
91R. CO2 + HN = CHN + O2	36.2	C	
92F. CHO + M = CO + H + M	19.6	B *	WEAK BOND FORWARD
92R. CO + H + M = CHO + M	-19.6	C	THIRD ORDER REVERSE
93F. CHO + CHO = CH2 + CO2	-17.3	C	FOUR-CENTER REACTION
93R. CH2 + CO2 = CHO + CHO	17.3	C	STERIC HINDRANCE
94F. CHO + CHO = CH2O + CO	-69.9	B *	WEAK BOND FORWARD
94R. CH2O + CO = CHO + CHO	69.9	C	REVERSE ENDOTHERMIC
95F. CHO + CH2 = CH3 + CO	-93.0	B *	WEAK BOND FORWARD
95R. CH3 + CO = CHO + CH2	93.0	C	REVERSE ENDOTHERMIC
96F. CHO + CH2O = CH3 + CO2	-40.3	C	NOT LIKELY TO BE ELEMENTARY REACTION
96R. CH3 + CO2 = CHO + CH2O	40.3	C	
97F. CHO + CH2O = CH3O + CO	-5.9	C	LARGE MOLECULES, LOW CONCENTRATIONS
97R. CH3O + CO = CHO + CH2O	5.9	C	LIKELY TO BE UNIMPORTANT
98F. CHO + CH3 = CH2 + CH2O	23.0	B *	RETAIN FORWARD FOR COMPARISON WITH
98R. CH2 + CH2O = CHO + CH3	-23.0	C	CHO + CH3 = CH4 + CO LOW CONCENTRATIONS REVERSE
99F. CHO + CH3 = CH4 + CO	-88.6	B *	WEAK BOND FORWARD
99R. CH4 + CO = CHO + CH3	88.6	C	REVERSE ENDOTHERMIC
100F. CHO + CH3O = CH2O + CH2O	-64.0	C	LARGE MOLECULES, LOW CONCENTRATIONS
100R. CH2O + CH2O = CHO + CH3O	64.0	C	LIKELY TO BE SLOW

REACTION	LOG A	B	C	COMMENTS		TEMP, KELVIN		
					300	1500	2000	2500
						LOG K		
91F. CHN + O2 = CO2 + HN				NO RATE DATA				
92R. CO + H + M = CHO + M	* 20.2 (10.5)	-1.5	0.	EST BY METHOD OF BBS AGREES W/ EST OF JI	16.5	15.4	15.2	15.1
93F. CHO + CHO = CH2 + CO2				NO RATE DATA				
94F. CHO + CHO = CH2O + CO	* 11.2 (10.5)	0.5	0. (5.)	BASED ON T1 (EST) NOTE B	12.4	12.8	12.9	12.9
95F. CHO + CH2 = CH3 + CO	* 10.5 (10.5)	0.7	1. (5.)	BASED ON T1 (J-P) NOTE B	11.5	12.6	12.7	12.8
96F. CHO + CH2O = CH3 + CO2				NO RATE DATA				
97F. CHO + CH2O = CH3O + CO				NO RATE DATA				
98R. CH2 + CH2O = CHO + CH3	* 10.5 (10.5)	0.5	6. (5.)	BASED ON T1 (EST) NOTE A	7.4	11.2	11.5	11.7
99F. CHO + CH3 = CH4 + CO	* 11.5 (10.5)	0.5	0. (5.)	BASED ON T1 (EST) NOTE B	12.7	13.1	13.2	13.2
100F. CHO + CH3O = CH2O + CH2O				NO RATE DATA				

REACTION	HR	NOTES	COMMENTS
101F. CHO + CH3O = CH4 + CO2 101R. CH4 + CO2 = CHO + CH3O	-129.0 129.0	C C	NOT LIKELY TO BE ELEMENTARY REACTION
102F. CHO + CH4 = CH2 + CH3O 102R. CH2 + CH3O = CHO + CH4	105.7 -105.7	C C	NOT LIKELY TO BE ELEMENTARY REACTION
103F. CHO + CH4 = CH2O + CH3 103R. CH2O + CH3 = CHO + CH4	18.6 -18.6	B * B *	CONSIDER BOTH DIRECTIONS FUEL RICH
104F. CHO + H = CH2 + O 104R. CH2 + O = CHO + H	90.6 -90.6	C B *	FORWARD ENDOTHERMIC CONSIDER REVERSE
105F. CHO + H + M = CH2O + M 105R. CH2O + M = CHO + H + M	-89.5 89.5	C C	THIRD ORDER FORWARD REVERSE ENDOTHERMIC
106F. CHO + H = CO + H2 106R. CO + H2 = CHO + H	-88.9 88.9	A * C	CONSIDER FORWARD FOR CHO BREAKDOWN REVERSE ENDOTHERMIC
107F. CHO + HN = CH2 + NO 107R. CH2 + NO = CHO + HN	15.4 -15.4	C C	FOUR-CENTER REACTION LOW CONCENTRATIONS BOTH DIRECTIONS
108F. CHO + HN = CH2O + N 108R. CH2O + N = CHO + HN	-10.6 10.6	C C	LOW CONCENTRATIONS BOTH DIRECTIONS
109F. CHO + HN = CN + H2O 109R. CN + H2O = CHO + HN	-53.9 53.9	C C	NOT LIKELY TO BE ELEMENTARY REACTION
110F. CHO + HNO = CH2 + NO2 110R. CH2 + NO2 = CHO + HNO	68.6 -68.6	C C	FOUR-CENTER REACTION ENDOTHERMIC FORWARD LOW CONCENTRATIONS REVERSEHO AND CH2O

REACTION	LOG A	B	C	COMMENTS	300	TEMP. KELVIN 1500	2000 LOG K	2500
101F. CHO + CH3O = CH4 + CO2				NO RATE DATA				
102F. CHO + CH4 = CH2 + CH3O				NO RATE DATA				
103R. CH2O + CH3 = CHO + CH4	* 10.0 10.5)	0.5	6. (5.)	BASED ON T1 (EST) NOTE A	6.9	10.7	11.0	11.2
104R. CH2 + O = CHO + H	* 11.7 10.5)	0.5	4. (5.)	BASED ON T1 (EST) NOTE B	10.0	12.7	12.9	13.0
105R. CH2O + M = CHO + H + M	17.5 10.5)	0.	87. (5.)	BASED ON T1 (EST) NOTE B	-45.9	6.8	8.0	9.9
106F. CHO + H = CO + H2	* 12.2 10.5)	0.5	0. (5.)	BASED ON T1 (EST) NOTE A	13.4	13.8	13.9	13.9
107F. CHO + HN = CH2 + NO				NO RATE DATA				
108F. CHO + HN = CH2O + N				NO RATE DATA				
109F. CHO + HN = CN + H2O				NO RATE DATA				
110F. CHO + HNO = CH2 + NO2				NO RATE DATA				

REACTION	HR	NOTES	COMMENTS
111F. CHO + HNO = CH2O + NO 111R. CH2O + NO = CHO + HNO	-36.8 36.8	C C	UNIMPORTANT PATH BETWEEN CHO AND CH2O BETWEEN HNO AND NO
112F. CHO + HO = CH2 + O2 112R. CH2 + O2 = CHO + HO	74.9 -74.9	C C	FOUR CENTER REACTION CHO + HO = CO + H2O FASTER THAN FORWARD CH2 + O2 = CH2O + O FASTER THAN REVERSE
113F. CHO + HO = CH2O + O 113R. CH2O + O = CHO + HO	10.8 -10.8	C A *	CHO + HO = CO + H2O FASTER THAN FORWARD CONSIDER REVERSE FOR CH2O BREAKDOWN
114F. CHO + HO = CO + H2O 114R. CO + H2O = CHO + HO	-103.8 103.8	A * C	CONSIDER FORWARD FOR CHO BREAKDOWN REVERSE HIGHLY ENDOTHERMIC
115F. CHO + HO = CO2 + H2 115R. CO2 + H2 = CHO + HO	-110.0 110.0	C C	FOUR-CENTER REACTION CHO + HO = CO + H2O FASTER THAN FORWARD REVERSE HIGHLY ENDOTHERMIC
116F. CHO + HO2 = CH2O + O2 116R. CH2O + O2 = CHO + HO2	-39.1 39.1	B * B *	CONSIDER BOTH DIRECTIONS
117F. CHO + HO2 = CO2 + H2O 117R. CO2 + H2O = CHO + HO2	-165.1 165.1	C C	FOUR-CENTER REACTION CHO + HO2 = CH2O + O2 FASTER THAN FWD REVERSE HIGHLY ENDOTHERMIC
118F. CHO + H2 = CH2 + HO 118R. CH2 + HO = CHO + H2	92.8 -92.8	C C	FOUR-CENTER REACTION FORWARD ENDOTHERMIC CH3 + O AND CH2O + O MORE LIKELY PRODUCTS FROM REVERSE
119F. CHO + H2 = CH2O + H 119R. CH2O + H = CHO + H2	19.0 -19.0	B * A *	CONSIDER BOTH DIRECTIONS REVERSE MORE LIKELY TO BE IMPORTANT CH2O BREAKDOWN
120F. CHO + H2 = CH3 + O 120R. CH3 + O = CHO + H2	86.5 -86.5	C C	NOT LIKELY TO BE ELEMENTARY REACTION

REACTION	LOG A	B	C	COMMENTS	300	TEMP. KELVIN 1500	2000 LOG K	2500
111F. CHO + HNO = CH2O + NO	11.5 10.5)	0.5	0. (5.)	BASED ON T1 (EST) NOTE B	12.7	13.1	13.2	13.2
112F. CHO + HO = CH2 + O2				NO RATE DATA				
113R. CH2O + O = CHO + HO	* 11.0 10.3)	1.	3.5 (2.)	BASED ON D22,H33,H27 FIT MODIF ARRHENIUS 300-2600K	10.9	13.7	13.9	14.1
114F. CHO + HO = CO + H2O	* 10.5	1.	0.	SRI ESTIMATE	13.0	13.7	13.8	13.9
115F. CHO + HO = CO2 + H2				NO RATE DATA				
116F. CHO + HO2 = CH2O + O2	* 14.0	0.	5.	SRI ESTIMATE	11.8	13.6	13.7	13.7
117F. CHO + HO2 = CO2 + H2O				NO RATE DATA				
118F. CHO + H2 = CH2 + HO				NO RATE DATA				
119R. CH2O + H = CHO + H2	* 10.1 10.5)	1.	3.2	BASED ON H40 USING B=1 FOR EXTRAP NO DATA ABOVE 1000K	10.2	12.8	13.1	13.2
120F. CHO + H2 = CH3 + O				NO RATE DATA				

REACTION	HR	NOTES	COMMENTS	REACTION	LOG A	B	C	COMMENTS	300	TEMP, KELVIN 1500	2000	2500
										LOG K		
121F. CHO + H2 + M = CH3O + M 121R. CH3O + M = CHO + H2 + M	-6.5 6.5	C C	NOT LIKELY TO BE ELEMENTARY REACTION	121F. CHO + H2 + M = CH3O + M				NO RATE DATA				
122F. CHO + H2O = CH2 + HO2 122R. CH2 + HO2 = CHO + H2O	147.8 -147.8	C C	FOUR-CENTER REACTION FORWARD HIGHLY ENDOTHERMIC CH2 + HO2 = CH3 + O2 FASTER THAN REVERSE	122F. CHO + H2O = CH2 + HO2				NO RATE DATA				
123F. CHO + H2O = CH2O + HO 123R. CH2O + HO = CHO + H2O	33.8 -33.8	C A *	CHO + M = CO + H + M FASTER THAN FORWARD CONSIDER REVERSE FOR CH2O BREAKDOWN	123R. CH2O + HO = CHO + H2O	* 10.5 (0.3)	1.	0. (3.)	BASED ON H30,P13,H2 K=13.0 AT 300 (H30) K=13.8 AT 1500 (H2) K=13.6 AT 1600 (P13)	13.0	13.7	13.8	13.9
124F. CHO + H2O = CH3 + O2 124R. CH3 + O2 = CHO + H2O	85.7 -85.7	C C	NOT LIKELY TO BE ELEMENTARY REACTION	124F. CHO + H2O = CH3 + O2				NO RATE DATA				
125F. CHO + H2O = CH3O + O 125R. CH3O + O = CHO + H2O	114.6 -114.6	C C	NOT LIKELY TO BE ELEMENTARY REACTION	125F. CHO + H2O = CH3O + O				NO RATE DATA				
126F. CHO + N = CN + HO 126R. CN + HO = CHO + N	-9.5 9.5	C C	NOT LIKELY TO BE ELEMENTARY REACTION	126F. CHO + N = CN + HO				NO RATE DATA				
127F. CHO + N = CO + NH 127R. CO + NH = CHO + N	-59.4 59.4	B * C	CONSIDER FORWARD REVERSE ENDOTHERMIC	127F. CHO + N = CO + NH	* 11.3 (0.5)	0.5	2. (5.)	BASED ON T1 (EST) NOTE B	11.1	12.6	12.7	12.8
128F. CHO + NO = CN + HO2 128R. CN + HO2 = CHO + NO	78.5 -78.5	C C	NOT LIKELY TO BE ELEMENTARY REACTION	128F. CHO + NO = CN + HO2				NO RATE DATA				
129F. CHO + NO = CO + HNO 129R. CO + HNO = CHO + NO	-33.2 33.2	B * B *	CONSIDER BOTH DIRECTIONS PROBABLY NOT MAJOR IMPORTANCE	129F. CHO + NO = CO + HNO	* 11.3 (0.5)	0.5	2. (5.)	BASED ON T1 (EST) NOTE B	11.1	12.6	12.7	12.8
130F. CHO + NO = CO2 + NH 130R. CO2 + NH = CHO + NO	-32.7 32.7	C C	FOUR-CENTER REACTION CHO + NO = CO + HNO FASTER THAN FORWARD REVERSE MINOR	130F. CHO + NO = CO2 + NH				NO RATE DATA				

REACTION	HR	NOTES	COMMENTS	REACTION	LOG A	B	C	COMMENTS	300	TEMP, KELVIN 1500	2000	2500
										LOG K		
131F. CHO + NO2 = CO2 + HNO 131R. CO2 + HNO = CHO + NO2	-85.9 85.9	C C	FOUR-CENTER STERIC HINDRANCE	131F. CHO + NO2 = CO2 + HNO				NO RATE DATA				
132F. CHO + N2 = CN + HNO 132R. CN + HNO = CHO + N2	119.4 -119.4	C C	NOT LIKELY TO BE ELEMENTARY REACTION	132F. CHO + N2 = CN + HNO				NO RATE DATA				
133F. CHO + O = CO + HO 133R. CO + HO = CHO + O	-86.8 86.8	A * C	CONSIDER FORWARD FOR CHO BREAKDOWN REVERSE ENDOTHERMIC	133F. CHO + O = CO + HO	* 11.5	1.	0.5	SRI ESTIMATE	13.6	14.6	14.7	14.9
134F. CHO + O = CO2 + H 134R. CO2 + H = CHO + O	-107.9 107.9	B * C	CONSIDER FORWARD REVERSE HIGHLY ENDOTHERMIC	134F. CHO + O = CO2 + H	* 11.5	0.	0.	SRI ESTIMATE	11.5	11.5	11.5	11.5
135F. CHO + O2 = CO + HO2 135R. CO + HO2 = CHO + O2	-30.8 30.8	B * B *	CONSIDER BOTH DIRECTIONS FORWARD FOR CHO BREAKDOWN REVERSE PROBABLY LESS IMPORTANT	135F. CHO + O2 = CO + HO2	* 12.2	0.	7.	SRI ESTIMATE	7.1	11.2	11.4	11.6
136F. CHO + O2 = CO2 + HO 136R. CO2 + HO = CHO + O2	-92.2 92.2	C C	FOUR-CENTER REACTION CHO + O2 = CO + HO2 FASTER THAN FORWARD REVERSE ENDOTHERMIC	136F. CHO + O2 = CO2 + HO				NO RATE DATA				
137F. CH2 + CH2O = CH4 + CO 137R. CH4 + CO = CH2 + CH2O	-111.6 111.6	C C	NOT LIKELY TO BE ELEMENTARY REACTION	137F. CH2 + CH2O = CH4 + CO				NO RATE DATA				
138F. CH2 + CH3O = CH2O + CH3 138R. CH2O + CH3 = CH2 + CH3O	-87.0 87.0	C C	LARGE MOLECULES, LOW CONCENTRATIONS REVERSE ENDOTHERMIC LIKELY TO BE UNIMPORTANT	138F. CH2 + CH3O = CH2O + CH3				NO RATE DATA				
139F. CH2 + CH4 = CH3 + CH3 139R. CH3 + CH3 = CH2 + CH4	-4.4 4.4	B * B *	CONSIDER BOTH DIRECTIONS FUEL RICH MAY BE IMPORTANT EARLY STAGES	139F. CH2 + CH4 = CH3 + CH3	* 12.1 (0.5)	0.7	20. (5.)	BASED ON T1 (J-P) NOTE B	-0.7	11.4	12.2	12.7
140F. CH2 + CO2 = CH2O + CO 140R. CH2O + CO = CH2 + CO2	-52.7 52.7	C C	FORWARD RX UNIMPORTANT FOR CH2 OR CO2 REVERSE ENDOTHERMIC	140F. CH2 + CO2 = CH2O + CO				NO RATE DATA				

REACTION	HR	NOTES	COMMENTS	REACTION	LOG A	B	C	COMMENTS	300	TEMP, KELVIN 1500	2000	2500
										LOG K		
141F. CH2 + H + M = CH3 + M	-112.5	C	THIRD ORDER, LOW CONCENTRATIONS FORWARD	141F. CH2 + H + M = CH3 + M				NO RATE DATA				
141R. CH3 + M = CH2 + H + M	112.5	C	REVERSE HIGHLY ENDOTHERMIC									
142F. CH2 + HN = CH3 + N	-33.6	C	LOW CONCENTRATIONS BOTH DIRECTIONS	142F. CH2 + HN = CH3 + N				NO RATE DATA				
142R. CH3 + N = CH2 + HN	33.6	C										
143F. CH2 + HNO = CH2O + HN	-52.2	C	CH2 + HNO = CH3 + NO MORE LIKELY FORWARD	143F. CH2 + HNO = CH2O + HN				NO RATE DATA				
143R. CH2O + HN = CH2 + HNO	52.2	C	REVERSE ENDOTHERMIC									
144F. CH2 + HNO = CH3 + NO	-59.8	C	FORWARD RX UNIMPORTANT FOR CH2 OR HNO	144F. CH2 + HNO = CH3 + NO	11.8 (10.5)	0.5	0. (5.)	BASED ON TI (EST) NOTE B	13.0	13.4	13.5	13.5
144R. CH3 + NO = CH2 + HNO	59.8	C	REVERSE ENDOTHERMIC									
145F. CH2 + HNO = CH3O + N	1.2	C	NOT LIKELY TO BE ELEMENTARY REACTION	145F. CH2 + HNO = CH3O + N				NO RATE DATA				
145R. CH3O + N = CH2 + HNO	-1.2	C										
146F. CH2 + HO = CH2O + H	-75.8	B *	CONSIDER FORWARD	146F. CH2 + HO = CH2O + H	* 13.	0.	5.	ESTIMATED NO RATE DATA	9.4	12.3	12.5	12.6
146R. CH2O + H = CH2 + HO	75.8	C	REVERSE ENDOTHERMIC									
147F. CH2 + HO = CH3 + O	-6.2	B *	CONSIDER BOTH DIRECTIONS	147F. CH2 + HO = CH3 + O	* 11.7 (10.5)	0.5	6. (5.)	BASED ON TI (EST) NOTE B	8.6	12.4	12.7	12.9
147R. CH3 + O = CH2 + HO	6.2	B *	REVERSE FOR CH3 BREAKDOWN									
148F. CH2 + HO + M = CH3O + M	-94.5	C	CH2O + H OR CH3 + O MORE LIKELY PRODUCTS	148F. CH2 + HO + M = CH3O + M				NO RATE DATA				
148R. CH3O + M = CH2 + HO + M	94.5	C	REVERSE ENDOTHERMIC									
149F. CH2 + HO2 = CH2O + HO	-114.0	C	CH2 + HO2 = CH3 + O2 MORE LIKELY FORWARD	149F. CH2 + HO2 = CH2O + HO				NO RATE DATA				
149R. CH2O + HO = CH2 + HO2	114.0	C	REVERSE HIGHLY ENDOTHERMIC									
150F. CH2 + HO2 = CH3 + O2	-62.2	B *	CONSIDER FORWARD	150R. CH3 + O2 = CH2 + HO2	* 12.5	0.	69.5	SRI ESTIMATE BASED ON EST ACTIV ENERGY 7. FOR REV	-38.1	2.4	4.9	6.4
150R. CH3 + O2 = CH2 + HO2	62.2	C	REVERSE ENDOTHERMIC									

REACTION	HR	NOTES	COMMENTS	REACTION	LOG A	B	C	COMMENTS	300	TEMP, KELVIN 1500	2000	2500
										LOG K		
151F. CH2 + HO2 = CH3O + O	-33.2	C	NOT LIKELY TO BE ELEMENTARY REACTION	151F. CH2 + HO2 = CH3O + O				NO RATE DATA				
151R. CH3O + O = CH2 + HO2	33.2	C										
152F. CH2 + H2 = CH3 + H	-4.1	B *	CONSIDER BOTH DIRECTIONS	152F. CH2 + H2 = CH3 + H	* 12.5	0.	7.	SRI ESTIMATE	7.4	11.5	11.7	11.9
152R. CH3 + H = CH2 + H2	4.1	A *	REVERSE FOR CH3 BREAKDOWN FUEL RICH									
153F. CH2 + H2 + M = CH4 + M	-112.2	C	NOT LIKELY TO BE ELEMENTARY REACTION	153F. CH2 + H2 + M = CH4 + M				NO RATE DATA				
153R. CH4 + M = CH2 + H2 + M	112.2	C										
154F. CH2 + H2O = CH2O + H2	-58.9	C	NOT LIKELY TO BE ELEMENTARY REACTION	154F. CH2 + H2O = CH2O + H2				NO RATE DATA				
154R. CH2O + H2 = CH2 + H2O	58.9	C	MIGHT BE FOUR-CENTER STERICALLY HINDERED									
155F. CH2 + H2O = CH3 + HO	10.8	B *	CONSIDER BOTH DIRECTIONS	155R. CH3 + HO = CH2 + H2O	* 10.8 (10.5)	0.7	2. (5.)	BASED ON TI (J-P) NOTE A	11.1	12.7	12.9	13.0
155R. CH3 + HO = CH2 + H2O	-10.8	A *	REVERSE FOR CH3 BREAKDOWN									
156F. CH2 + H2O = CH3O + H	24.0	C	NOT LIKELY TO BE ELEMENTARY REACTION	156F. CH2 + H2O = CH3O + H				NO RATE DATA				
156R. CH3O + H = CH2 + H2O	-24.0	C										
157F. CH2 + H2O = CH4 + O	9.0	C	NOT LIKELY TO BE ELEMENTARY REACTION	157F. CH2 + H2O = CH4 + O				NO RATE DATA				
157R. CH4 + O = CH2 + H2O	-9.0	C										
158F. CH2 + N = CN + H2	-102.3	C	NOT LIKELY TO BE ELEMENTARY REACTION	158F. CH2 + N = CN + H2				NO RATE DATA				
158R. CN + H2 = CH2 + N	102.3	C										
159F. CH2 + NO = CH2O + N	-26.0	B *	CONSIDER FORWARD FUEL RICH	159F. CH2 + NO = CH2O + N	* 12.2	0.	7.	SRI ESTIMATE	7.1	11.2	11.4	11.6
159R. CH2O + N = CH2 + NO	26.0	C	REVERSE NOT LIKELY TO BE IMPORTANT									
160F. CH2 + NO = CN + H2O	-69.3	C	NOT LIKELY TO BE ELEMENTARY REACTION	160F. CH2 + NO = CN + H2O				NO RATE DATA				
160R. CN + H2O = CH2 + NO	69.3	C										

REACTION	HR	NOTES	COMMENTS
161F. CH2 + NO2 = CH2O + NO 161R. CH2O + NO = CH2 + NO2	-105.4 105.4	C C	LOW CONCENTRATIONS FORWARD REVERSE HIGHLY ENDOTHERMIC
162F. CH2 + N2O = CH2O + N2 162R. CH2O + N2 = CH2 + N2O	-140.2 140.2	C C	LOW CONCENTRATIONS FORWARD REVERSE HIGHLY ENDOTHERMIC
163F. CH2 + O + M = CH2O + M 163R. CH2O + M = CH2 + O + M	-180.1 180.1	C C	THIRD ORDER FORWARD REVERSE HIGHLY ENDOTHERMIC
164F. CH2 + O = CO + H2 164R. CO + H2 = CH2 + O	-179.5 179.5	C C	NOT LIKELY TO BE ELEMENTARY REACTION
165F. CH2 + O2 = CH2O + O 165R. CH2O + O = CH2 + O2	-58.1 58.1	B * C	CONSIDER FORWARD REVERSE ENDOTHERMIC
166F. CH2 + O2 = CO + H2O 166R. CO + H2O = CH2 + O2	-178.6 178.6	C C	NOT LIKELY TO BE ELEMENTARY REACTION
167F. CH2 + O2 = CO2 + H2 167R. CO2 + H2 = CH2 + O2	-184.9 184.9	C C	NOT LIKELY TO BE ELEMENTARY REACTION
168F. CH2O + M = CO + H2 + M 168R. CO + H2 + M = CH2O + M	0.6 -0.6	C C	NOT LIKELY TO BE ELEMENTARY REACTION
169F. CH2O + CH2O = CH4 + CO2 169R. CH4 + CO2 = CH2O + CH2O	-59.0 59.0	C C	NOT LIKELY TO BE ELEMENTARY REACTION
170F. CH2O + CH4 = CH3 + CH3O 170R. CH3 + CH3O = CH2O + CH4	82.7 -82.7	C C	FORWARD ENDOTHERMIC LARGE MOLECULES LOW CONCENTRATIONS REV

REACTION	LOG A	B	C	COMMENTS	300	TEMP, KELVIN 1500	2000	2500
						LOG K		
161F. CH2 + NO2 = CH2O + NO				NO RATE DATA				
162F. CH2 + N2O = CH2O + N2				NO RATE DATA				
163F. CH2 + O + M = CH2O + M				NO RATE DATA				
164F. CH2 + O = CO + H2				NO RATE DATA				
165F. CH2 + O2 = CH2O + O	* 11.7 (0.5)	0.5	7. (5.)	BASED ON T1 (EST) NOTE B	7.8	12.3	12.6	12.8
166F. CH2 + O2 = CO + H2O				NO RATE DATA				
167F. CH2 + O2 = CO2 + H2				NO RATE DATA				
168F. CH2O + M = CO + H2 + M				NO RATE DATA				
169F. CH2O + CH2O = CH4 + CO2				NO RATE DATA				
170F. CH2O + CH4 = CH3 + CH3O				NO RATE DATA				

REACTION	HR	NOTES	COMMENTS
171F. CH2O + H = CH3 + O 171R. CH3 + O = CH2O + H	67.6 -67.6	C A *	FORWARD ENDOTHERMIC CONSIDER REVERSE FOR CH3 BREAKDOWN
172F. CH2O + H + M = CH3O + M 172R. CH3O + M = CH2O + H + M	-25.5 25.5	B * B *	CONSIDER BOTH DIRECTIONS REVERSE MAY BE IMPORTANT CH3O BREAKDOWN
173F. CH2O + HN = CH3 + NO 173R. CH3 + NO = CH2O + HN	-7.6 7.6	C C	FOUR-CENTER, STERIC HINDRANCE
174F. CH2O + HN = CH3O + N 174R. CH3O + N = CH2O + HN	53.4 -53.4	C B *	FORWARD ENDOTHERMIC CONSIDER REVERSE FOR CH3O BREAKDOWN PROBABLY MINOR
175F. CH2O + HNO = CH3 + NO2 175R. CH3 + NO2 = CH2O + HNO	45.6 -45.6	C C	FOUR-CENTER, STERIC HINDRANCE
176F. CH2O + HNO = CH3O + NO 176R. CH3O + NO = CH2O + HNO	27.2 -27.2	C C	LOW CONCENTRATIONS BOTH DIRECTIONS
177F. CH2O + HO = CH3 + O2 177R. CH3 + O2 = CH2O + HO	51.8 -51.8	C B *	FORWARD ENDOTHERMIC CONSIDER REVERSE FOR CH3 BREAKDOWN FOUR-CENTER REACTION
178F. CH2O + HO = CH3O + O 178R. CH3O + O = CH2O + HO	80.8 -80.8	C B *	FORWARD ENDOTHERMIC CONSIDER REVERSE FOR CH3O BREAKDOWN
179F. CH2O + HO2 = CH3O + O2 179R. CH3O + O2 = CH2O + HO2	24.9 -24.9	C B *	LOW CONCENTRATIONS FORWARD CONSIDER REVERSE FOR CH3O BREAKDOWN
180F. CH2O + H2 = CH3 + HO 180R. CH3 + HO = CH2O + H2	69.7 -69.7	C C	FOUR-CENTER REACTION FORWARD ENDOTHERMIC CH3 + HO = CH4 + O AND CH3 + HO = CH2 + H2O MORE LIKELY REVERSE

REACTION	LOG A	B	C	COMMENTS	300	TEMP, KELVIN 1500	2000	2500
						LOG K		
171R. CH3 + O = CH2O + H	* 13.7 (0.3)	0.	0.	BASED ON D22,H25,P13 K=13.7 AT 300 (H25) K=13.8 AT 1500 (P13) K=13.8 AT 2000 (D22)	13.7	13.7	13.7	13.7
172R. CH3O + M = CH2O + H + M	* 40.6	-7.5	22.6	SRI ESTIMATE BASED ON HINSHELWOOD -LINDEMAN THEORY	5.6	13.5	13.4	13.1
173F. CH2O + HN = CH3 + NO				NO RATE DATA				
174R. CH3O + N = CH2O + HN	* 14.0	0.	0.	SRI ESTIMATE	14.0	14.0	14.0	14.0
175F. CH2O + HNO = CH3 + NO2				NO RATE DATA				
176F. CH2O + HNO = CH3O + NO				NO RATE DATA				
177R. CH3 + O2 = CH2O + HO	* 13.5 (0.5)	0.	20. (10.)	BASED ON B45,B64,B76 W/ EST ACTIV ENERGY	-1.1	10.6	11.3	11.8
178R. CH3O + O = CH2O + HO	* 14.0	0.	0.	SRI ESTIMATE	14.0	14.0	14.0	14.0
179R. CH3O + O2 = CH2O + HO2	* 12.0	0.	6.	SRI ESTIMATE	7.6	11.1	11.3	11.5
180F. CH2O + H2 = CH3 + HO				NO RATE DATA				

REACTION	HR	NOTES	COMMENTS
181F. CH2O + H2 = CH3O + H	83.0	C	FORWARD ENDOTHERMIC
181R. CH3O + H = CH2O + H2	-83.0	B *	CONSIDER REVERSE FOR CH3O BREAKDOWN
182F. CH2O + H2 = CH4 + O	67.9	C	NOT LIKELY TO BE ELEMENTARY REACTION
182R. CH4 + O = CH2O + H2	-67.9	C	
183F. CH2O + H2O = CH3 + HO2	124.8	C	FOUR-CENTER REACTION
183R. CH3 + HO2 = CH2O + H2O	-124.8	C	STERIC HINDRANCE
184F. CH2O + H2O = CH3O + HO	97.8	C	FORWARD ENDOTHERMIC
184R. CH3O + HO = CH2O + H2O	-97.8	B *	CONSIDER REVERSE FOR CH3O BREAKDOWN
185F. CH2O + H2O = CH4 + O2	67.0	C	NOT LIKELY TO BE ELEMENTARY REACTION
185R. CH4 + O2 = CH2O + H2O	-67.0	C	
186F. CH2O + N = CN + H2O	-61.3	C	NOT LIKELY TO BE ELEMENTARY REACTION
186R. CN + H2O = CH2O + N	61.3	C	
187F. CH2O + O = CO + H2O	-120.6	C	NOT LIKELY TO BE ELEMENTARY REACTION
187R. CO + H2O = CH2O + O	120.6	C	
188F. CH2O + O = CO2 + H2	-126.8	C	NOT LIKELY TO BE ELEMENTARY REACTION
188R. CO2 + H2 = CH2O + O	126.8	C	
189F. CH2O + O2 = CO2 + H2O	-126.0	C	NOT LIKELY TO BE ELEMENTARY REACTION
189R. CO2 + H2O = CH2O + O2	126.0	C	
190F. CH3 + CO2 = CH3O + CO	34.6	C	LARGE MOLECULES
190R. CH3O + CO = CH3 + CO2	-34.6	C	LIKELY TO BE UNIMPORTANT

REACTION	LOG A	B	C	COMMENTS	300	TEMP, KELVIN 1500	 2000	2500
						LOG K		
181R. CH3O + H = CH2O + H2	* 14.0	0.	0.	SRI ESTIMATE	14.0	14.0	14.0	14.0
182F. CH2O + H2 = CH4 + O				NO RATE DATA				
183F. CH2O + H2O = CH3 + HO2				NO RATE DATA				
184R. CH3O + HO = CH2O + H2O	* 13.9	0.	0.	SRI ESTIMATE	13.9	13.9	13.9	13.9
185F. CH2O + H2O = CH4 + O2				NO RATE DATA				
186F. CH2O + N = CN + H2O				NO RATE DATA				
187F. CH2O + O = CO + H2O				NO RATE DATA				
188F. CH2O + O = CO2 + H2				NO RATE DATA				
189F. CH2O + O2 = CO2 + H2O				NO RATE DATA				
190F. CH3 + CO2 = CH3O + CO				NO RATE DATA				

REACTION	HR	NOTES	COMMENTS
191F. CH3 + H + M = CH4 + M	-108.2	B *	MAY BE IMPORTANT EARLY STAGES
191R. CH4 + M = CH3 + H + M	108.2	B *	
192F. CH3 + NH = CH4 + N	-29.2	C	LOW CONCENTRATIONS
192R. CH4 + N = CH3 + NH	29.2	C	
193F. CH3 + HNO = CH3O + NH	34.8	C	LOW CONCENTRATIONS
193R. CH3O + NH = CH3 + HNO	-34.8	C	
194F. CH3 + HNO = CH4 + NO	-59.4	C	LOW CONCENTRATIONS FORWARD
194R. CH4 + NO = CH3 + HNO	59.4	C	REVERSE ENDOTHERMIC
195F. CH3 + HO = CH3O + H	13.2	B *	CONSIDER BOTH DIRECTIONS FOR RULE CH3O
195R. CH3O + H = CH3 + HO	-13.2	B *	
196F. CH3 + HO = CH4 + O	-1.8	A *	CONSIDER BOTH DIRECTIONS
196R. CH4 + O = CH3 + HO	1.8	A *	ROLE IN INITIAL CH4 BREAKDOWN
197F. CH3 + HO2 = CH3O + HO	-27.0	C	CH3 + HO2 = CH4 + O2 MORE LIKELY FORWARD
197R. CH3O + HO = CH3 + HO2	27.0	C	CH3O + HO = CH2O + H2O MORE LIKELY REV
198F. CH3 + HO2 = CH4 + O2	-57.8	B *	CONSIDER FORWARD
198R. CH4 + O2 = CH3 + HO2	57.8	C	REVERSE ENDOTHERMIC
199F. CH3 + H2 = CH4 + H	0.3	A *	CONSIDER BOTH DIRECTIONS
199R. CH4 + H = CH3 + H2	-0.3	A *	ROLE IN INITIAL CH4 BREAKDOWN
200F. CH3 + H2O = CH3O + H2	28.1	C	NOT LIKELY TO BE ELEMENTARY REACTION
200R. CH3O + H2 = CH3 + H2O	-28.1	C	

REACTION	LOG A	B	C	COMMENTS	300	TEMP, KELVIN 1500	 2000	2500
						LOG K		
191R. CH4 + M = CH3 + H + M	* 17.3 (0.3)	0.	87.5 (2.)	BASED ON H32 RECENT EXPERIMENT	-46.4	4.6	7.7	9.7
192F. CH3 + NH = CH4 + N				NO RATE DATA				
193F. CH3 + HNO = CH3O + NH				NO RATE DATA				
194F. CH3 + HNO = CH4 + NO	11.7 (0.5)	0.5	0. (5.)	BASED ON T1 (EST) NOTE B	12.9	13.3	13.4	13.4
195F. CH3 + HO = CH3O + H	* 12.8	0.	0.	COMPARES W/ 195R NO RATE DATA	12.8	12.8	12.8	12.8
196R. CH4 + O = CH3 + HO	* 13.3 (0.2)	0.	9. (1.)	BASED ON H25 CRIT EVAL 350-2000K	6.7	12.0	12.3	12.5
197F. CH3 + HO2 = CH3O + HO				NO RATE DATA				
198F. CH3 + HO2 = CH4 + O2	* 11.0 (0.5)	0.5	6. (5.)	BASED ON T1 (EST)	7.9	11.7	12.0	12.2
199R. CH4 + H = CH3 + H2	* 13.8 (0.3)	0.	11.9 (0.3)	BASED ON REFS B64,K34,S1,S33,W30	5.1	12.1	12.5	12.8
200F. CH3 + H2O = CH3O + H2				NO RATE DATA				

REACTION	HR	NOTES	COMMENTS	REACTION	LOG A	B	C	COMMENTS	300	1500	2000	2500
										TEMP, KELVIN		
										LOG K		
201F. $CH_3 + H_2O = CH_4 + HO$ 201R. $CH_4 + HO = CH_3 + H_2O$	15.2 -15.2	A * A *	CONSIDER BOTH DIRECTIONS ROLE IN INITIAL CH_4 BREAKDOWN	201R. $CH_4 + HO = CH_3 + H_2O$	* 13.5 (0.3)	0.	5. (0.5)	BASED ON REFS 864,025,533,W31	9.9	12.8	13.0	13.1
202F. $CH_3 + NO = CH_3O + N$ 202R. $CH_3O + N = CH_3 + NO$	61.0 -61.0	C C	FORWARD ENDOTHERMIC $CH_3O + N = CH_2O + HN$ MORE LIKELY REVERSE	202F. $CH_3 + NO = CH_3O + N$				NO RATE DATA				
203F. $CH_3 + NO_2 = CH_3O + NO$ 203R. $CH_3O + NO = CH_3 + NO_2$	-18.3 18.3	C C	LOW CONCENTRATIONS BOTH DIRECTIONS	203F. $CH_3 + NO_2 = CH_3O + NO$				NO RATE DATA				
204F. $CH_3 + N_2O = CH_3O + N_2$ 204R. $CH_3O + N_2 = CH_3 + N_2O$	-53.2 53.2	C C	LARGE MOLECULES STERIC HINDRANCE FORWARD REVERSE ENDOTHERMIC	204F. $CH_3 + N_2O = CH_3O + N_2$				NO RATE DATA				
205F. $CH_3 + O + M = CH_3O + M$ 205R. $CH_3O + M = CH_3 + O + M$	-93.1 93.1	C C	THIRD ORDER FORWARD STABILIZATION UNLIKELY REVERSE ENDOTHERMIC	205F. $CH_3 + O + M = CH_3O + M$				NO RATE DATA				
206F. $CH_3 + O_2 = CH_3O + O$ 206R. $CH_3O + O = CH_3 + O_2$	29.0 -29.0	B * B *	CONSIDER BOTH DIRECTIONS FORWARD FOR CH_3 BREAKDOWN	206F. $CH_3 + O_2 = CH_3O + O$	* 12.5	0.	30.	SRI ESTIMATE	-9.4	8.1	9.2	9.9
207F. $CH_3O + H = CH_4 + O$ 207R. $CH_4 + O = CH_3O + H$	-15.1 15.1	C C	$CH_3O + H = CH_2O + H_2$ MORE LIKELY FORWARD $CH_4 + O = CH_3 + HO$ MORE LIKELY REVERSE	207F. $CH_3O + H = CH_4 + O$				NO RATE DATA				
208F. $CH_3O + HN = CH_4 + NO$ 208R. $CH_4 + NO = CH_3O + HN$	-90.3 90.3	C C	LOW CONCENTRATIONS FORWARD REVERSE ENDOTHERMIC	208F. $CH_3O + HN = CH_4 + NO$				NO RATE DATA				
209F. $CH_3O + HNO = CH_4 + NO_2$ 209R. $CH_4 + NO_2 = CH_3O + HNO$	-37.1 37.1	C C	LOW CONCENTRATIONS BOTH DIRECTIONS FOUR-CENTER, STERIC HINDRANCE	209F. $CH_3O + HNO = CH_4 + NO_2$				NO RATE DATA				
210F. $CH_3O + HO = CH_4 + O_2$ 210R. $CH_4 + O_2 = CH_3O + HO$	-30.8 30.8	C C	FOUR-CENTER, STERIC HINDRANCE	210F. $CH_3O + HO = CH_4 + O_2$				NO RATE DATA				

REACTION	HR	NOTES	COMMENTS	REACTION	LOG A	B	C	COMMENTS	300	1500	2000	2500
										TEMP, KELVIN		
										LOG K		
211F. $CH_3O + H_2 = CH_4 + HO$ 211R. $CH_4 + HO = CH_3O + H_2$	-12.9 12.9	C C	FOUR-CENTER, STERIC HINDRANCE	211F. $CH_3O + H_2 = CH_4 + HO$				NO RATE DATA				
212F. $CH_3O + H_2O = CH_4 + HO_2$ 212R. $CH_4 + HO_2 = CH_3O + H_2O$	42.1 -42.1	C C	FOUR-CENTER, STERIC HINDRANCE	212F. $CH_3O + H_2O = CH_4 + HO_2$				NO RATE DATA				
213F. $CN + HO = CO + HN$ 213R. $CO + HN = CN + HO$	-69.9 69.9	C C	FOUR-CENTER REACTION $CN + HO = CHN + O$ MORE LIKELY FORWARD REVERSE ENDOTHERMIC	213F. $CN + HO = CO + HN$				NO RATE DATA				
214F. $CN + HO_2 = CO + HNO$ 214R. $CO + HNO = CN + HO_2$	-111.7 111.7	C C	FOUR-CENTER FOR HON STRUCTURE REVERSE HIGHLY ENDOTHERMIC	214F. $CN + HO_2 = CO + HNO$				NO RATE DATA				
215F. $CN + HO_2 = CO_2 + HN$ 215R. $CO_2 + HN = CN + HO_2$	-111.2 111.2	C C	NOT LIKELY TO BE ELEMENTARY REACTION	215F. $CN + HO_2 = CO_2 + HN$				NO RATE DATA				
216F. $CN + NO = CO + N_2$ 216R. $CO + N_2 = CN + NO$	-152.6 152.6	B * C	CONSIDER FORWARD FOR NO DESTRUCTION REVERSE HIGHLY ENDOTHERMIC FOUR-CENTER REACTION	216F. $CN + NO = CO + N_2$	* 11.5 (0.5)	0.	0. (5.)	BASED ON B78 (XPT) ASSUME ACT ENERGY=0 NOTE D	11.5	11.5	11.5	11.5
217F. $CN + NO_2 = CO + N_2O$ 217R. $CO + N_2O = CN + NO_2$	-117.7 117.7	C C	FOUR-CENTER, STERIC HINDRANCE REVERSE HIGHLY ENDOTHERMIC	217F. $CN + NO_2 = CO + N_2O$				NO RATE DATA				
218F. $CN + NO_2 = CO_2 + N_2$ 218R. $CO_2 + N_2 = CN + NO_2$	-205.3 205.3	C C	NOT LIKELY TO BE ELEMENTARY REACTION	218F. $CN + NO_2 = CO_2 + N_2$				NO RATE DATA				
219F. $CN + O = CO + N$ 219R. $CO + N = CN + O$	-77.2 77.2	B * C	CONSIDER FORWARD REVERSE ENDOTHERMIC	219F. $CN + O = CO + N$	* 12. (0.5)	0.	0. (5.)	BASED ON B78,R5 ASSUME ACT ENERGY=0 NOTE D	12.0	12.0	12.0	12.0
220F. $CN + O_2 = CO + NO$ 220R. $CO + NO = CN + O_2$	-109.3 109.3	B * C	FOUR-CENTER REACTION, PROBABLY SLOW REVERSE HIGHLY ENDOTHERMIC	220F. $CN + O_2 = CO + NO$	* 11.5 (0.5)	0.	0. (10.)	BASED ON B86 (XPT) UPPER LIMIT AT 298K ASSUME ACT ENERGY=0 NOTE B	11.5	11.5	11.5	

REACTION	HR	NOTES	COMMENTS
221F. CN + O2 = CO2 + N 221R. CO2 + N = CN + O2	-82.6 82.6	C C	NOT LIKELY TO BE ELEMENTARY REACTION
222F. CO + HNO = CO2 + HN 222R. CO2 + HN = CO + HNO	0.4 -0.4	C C	HNO, HN MINOR RX PARTNERS FOR CO, CO2
223F. CO + HO = CO2 + H 223R. CO2 + H = CO + HO	-21.1 21.1	A * B *	FORWARD MAIN PATH FROM CO TO CO2 CONSIDER BOTH DIRECTIONS
224F. CO + HO2 = CO2 + HO 224R. CO2 + HO = CO + HO2	-61.9 61.9	C C	CO + HO = CO2 + H MORE IMPORTANT FORWARD MAY HAVE MINOR ROLE FORWARD REVERSE ENDOTHERMIC
225F. CO + H2O = CO2 + H2 225R. CO2 + H2 = CO + H2O	-6.3 6.3	C C	NOT LIKELY TO BE ELEMENTARY REACTION
226F. CO + NO = CO2 + N 226R. CO2 + N = CO + NO	26.7 -26.7	C C	SPIN HINDERED EXPERIMENT INDICATES REACTION SLOW
227F. CO + NO2 = CO2 + NO 227R. CO2 + NO = CO + NO2	-52.7 52.7	C C	LOW CONCENTRATIONS FORWARD REVERSE ENDOTHERMIC
228F. CO + N2O = CO2 + N2 228R. CO2 + N2 = CO + N2O	-87.6 87.6	C C	CO, N2O MINOR REACTION PARTNERS REVERSE ENDOTHERMIC
229F. CO + O + M = CO2 + M 229R. CO2 + M = CO + O + M	-127.4 127.4	B * C	FORWARD TERMINATION REACTION REVERSE HIGHLY ENDOTHERMIC
230F. CO + O2 = CO2 + O 230R. CO2 + O = CO + O2	-5.6 5.6	B * B *	CONSIDER BOTH DIRECTIONS PROBABLY SLOWER THAN CO + HO = CO2 + H

REACTION	LOG A	B	C	COMMENTS	300	TEMP, KELVIN 1500	 2000	2500
						LOG K		
221F. CN + O2 = CO2 + N				NO RATE DATA				
222F. CO + HNO = CO2 + HN	11.0 (0.5)	0.5	7. (5.)	BASED ON T1 (EST) NOTE B	7.1	11.6	11.9	12.1
223F. CO + HO = CO2 + H	* 7.18	1.3	0.76	BASED ON B98 FIT TO EXPTL DATA FROM 300-2000K	9.8	11.2	11.4	11.5
224F. CO + HO2 = CO2 + HO	11. (0.5)	0.	10. (3.)	BASED ON L16 (EVAL)	3.7	9.5	9.9	10.1
225R. CO2 + H2 = CO + H2O	9.0 (0.5)	0.5	15. (5.)	BASED ON T1 (EST) NOTE B	-0.7	8.6	9.0	9.4
226R. CO2 + N = CO + NO	11.3 (1.)	0.5	30. (20.)	BASED ON T1 WITH HIGHER C SPIN HINDERED	-9.3	8.5	9.7	10.4
227F. CO + NO2 = CO2 + NO	12.3 (0.3)	0.	30. (3.)	BASED ON K45	-9.6	7.9	9.0	9.7
228F. CO + N2O = CO2 + N2	11.0 (0.3)	0.	20. (3.)	BASED ON L9,M29 NOTE D	-3.6	8.1	8.8	9.3
229R. CO2 + M = CO + O + M	* 15. (0.3)	0.	100. (5.)	BASED ON C26,O1 COMPLEX REACTION	-57.9	0.4	4.1	6.3
230F. CO + O2 = CO2 + O	* 12.5 (0.5)	0.	50. (10.)	BASED ON D20,D22,S10 HI T DATA FAIR AGRMT	-23.9	5.2	7.0	8.1

REACTION	HR	NOTES	COMMENTS
231F. H + H + M = H2 + M 231R. H2 + M = H + H + M	-108.4 108.4	A * C	FORWARD TERMINATION REACTION REVERSE HIGHLY ENDOTHERMIC
232F. H + HN = H2 + N 232R. H2 + N = H + HN	-29.5 29.5	B * B *	CONSIDER BOTH DIRECTIONS
233F. H + HNO = HN + HO 233R. HN + HO = H + HNO	21.6 -21.6	B * B *	CONSIDER BOTH DIRECTIONS PROBABLY MINOR
234F. H + HNO = H2 + NO 234R. H2 + NO = H + HNO	-55.7 55.7	B * C	CONSIDER FORWARD, PROBABLY MINOR REVERSE ENDOTHERMIC
235F. H + HNO = H2O + N 235R. H2O + N = H + HNO	-22.8 22.8	C C	POSSIBLE FOR NOH STRUCTURE PROBABLY MINOR
236F. H + HO = H2 + O 236R. H2 + O = H + HO	-2.2 2.2	A * A *	CONSIDER BOTH DIRECTIONS
237F. H + HO + M = H2O + M 237R. H2O + M = H + HO + M	-123.3 123.3	A * C	FORWARD TERMINATION REACTION REVERSE HIGHLY ENDOTHERMIC
238F. H + HO2 = HO + HO 238R. HO + HO = H + HO2	-40.2 40.2	B * C	CONSIDER FORWARD FOR HO2 REMOVAL HO + HO = H2O + O FASTER THAN REVERSE
239F. H + HO2 = H2 + O2 239R. H2 + O2 = H + HO2	-56.1 56.1	B * C	CONSIDER FORWARD FOR HO2 REMOVAL REVERSE ENDOTHERMIC
240F. H + HO2 = H2O + O 240R. H2O + O = H + HO2	-57.2 57.2	C C	FORWARD PRODUCTS MORE LIKELY TO BE HO + HO OR H2 + O2

REACTION	LOG A	B	C	COMMENTS	300	TEMP, KELVIN 1500	 2000	2500
						LOG K		
231R. H2 + M = H + H + M	* 14.3 (0.3)	0.	96. (4.)	BASED ON B88, M = AR CRITICAL EVALUATION	-55.6	0.3	3.8	5.9
232F. H + HN = H2 + N	* 11.8 (0.2)	0.5	0. (5.)	BASED ON B97 (EST) TRANS STATE CORLAT	7.2	12.2	12.6	12.8
233F. H + HNO = HN + HO	* 11.3 (0.5)	0.5	23. (5.)	BASED ON T1 (EST) W/ HIGHER C NOTE B	-4.2	9.5	10.4	11.0
234F. H + HNO = H2 + NO	* 13. (0.2)	0.	2.5 (2.)	BASED ON S1 EVALUATION 200-2000K	11.2	12.6	12.7	12.8
235F. H + HNO = H2O + N				NO RATE DATA				
236F. H + HO = H2 + O	* 9.9 (0.2)	1.	7. (0.3)	BASED ON B88 EVALUATION 400-2000K	7.3	12.1	12.4	12.7
237F. H + HO + M = H2O + M	* 22.3 (0.3)	-2.	0.	BASED ON B88, M = N2 CRIT EVAL 1000-3000K	17.3	15.9	15.7	15.5
238F. H + HO2 = HO + HO	* 14.4 (0.3)	0.	1.9 (1.)	BASED ON L16 EVALUATION 300-1000K	13.0	14.1	14.2	14.2
239F. H + HO2 = H2 + O2	* 13.4 (0.3)	0.	0.7 (1.)	BASED ON L16 EVALUATION 300-1000K	12.9	13.3	13.3	13.3
240F. H + HO2 = H2O + O	13.0 (1.)	0.	1. (1.)	BASED ON L16 EVALUATION 300-1000K	12.3	12.9	12.9	12.9

REACTION	DH	NOTES	COMMENTS
241F. H + H2O = HO + H2 241R. HO + H2 = H + H2O	14.9 -14.9	A * A *	CONSIDER BOTH DIRECTIONS
242F. H + N + M = HN + M 242R. HN + M = H + N + M	-78.9 78.9	C C	THIRD ORDER, LOW CONCENTRATIONS FORWARD REVERSE ENDOTHERMIC
243F. H + NO = HN + O 243R. HN + O = H + NO	75.9 -75.9	C B *	FORWARD ENDOTHERMIC CONSIDER REVERSE
244F. H + NO + M = HNO + M 244R. HNO + M = H + NO + M	-52.7 52.7	C C	THIRD ORDER FORWARD REVERSE ENDOTHERMIC
245F. H + NO = HO + N 245R. HO + N = H + NO	47.8 -47.8	B * A *	CONSIDER BOTH DIRECTIONS REVERSE PART OF MODIFIED ZELDOVICH
246F. H + NO2 = HN + O2 246R. HN + O2 = H + NO2	27.8 -27.8	C C	STERIC HINDRANCE OTHER PRODUCTS MORE LIKELY
247F. H + NO2 = HNO + O 247R. HNO + O = H + NO2	22.0 -22.0	C C	POSSIBLE FOR NOH STRUCTURE OTHER PRODUCTS MORE LIKELY
248F. H + NO2 = HO + NO 248R. HO + NO = H + NO2	-31.6 31.6	B * B *	CONSIDER BOTH DIRECTIONS PROBABLY UNIMPORTANT
249F. H + NO2 = HO2 + N 249R. HO2 + N = H + NO2	56.6 -56.6	C C	NOT LIKELY TO BE ELEMENTARY REACTION
250F. H + N2 = HN + N 250R. HN + N = H + N2	150.5 -150.5	C C	FORWARD HIGHLY ENDOTHERMIC LOW CONCENTRATIONS REVERSE

REACTION	LOG A	B	C	COMMENTS	300	TEMP, KELVIN 1500 LOG K	2000	2500
241R. HO + H2 = H + H2O	* 13.4 (0.1)	0.	9.2 (0.2)	BASED ON B88 EVALUATION 300-2900K	9.6	12.6	12.8	12.9
242F. H + N + M = HN + M	17.6 (1.)	-0.5	0. (2.)	BASED ON TI (EST) AND B91 (XPT)	16.2	15.8	15.7	15.7
243R. HN + O = H + NO	* 11.8 (0.2)	0.5	0. (5.)	BASED ON B97 TRANS STATE CORELAT	13.0	13.4	13.5	13.5
244F. H + NO + M = HNO + M	15.7 (0.3)	0.	-0.6 (0.3)	BASED ON B90, M = H2 EVALUATION 230-700K	16.1	15.8	15.8	15.8
245R. HO + N = H + NO	* 11.8 (0.3)	0.5	0. (3.)	BASED ON B97 TRANS STATE COREL AGREES W/ REF C8 XPT	13.0	13.4	13.5	13.5
246F. H + NO2 = HN + O2				NO RATE DATA				
247R. HNO + O = H + NO2	10.7 (0.5)	0.5	0. (5.)	BASED ON TI (EST) NOTE B	11.9	12.3	12.4	12.4
248F. H + NO2 = HO + NO	* 14.5 (0.3)	0.	1.5 (1.)	BASED ON B90 EVALUATION 300-630K	13.4	14.3	14.3	14.4
249F. H + NO2 = HO2 + N				NO RATE DATA				
250R. HN + N = H + N2	11.8 (0.2)	0.5	0. (3.)	BASED ON B97 TRANS STATE CORELAT	13.0	13.4	13.5	13.5

REACTION	DH	NOTES	COMMENTS
251F. H + N2O = HN + NO 251R. HN + NO = H + N2O	36.2 -36.2	C C	H + N2O = HO + N2 FASTER FORWARD LOW CONCENTRATIONS REVERSE
252F. H + N2O = HNO + N 252R. HNO + N = H + N2O	62.5 -62.5	C C	FORWARD ENDOTHERMIC LOW CONCENTRATIONS REVERSE
253F. H + N2O = HO + N2 253R. HO + N2 = H + N2O	-66.4 66.4	B * C	CONSIDER FORWARD REVERSE ENDOTHERMIC
254F. H + O + M = HO + M 254R. HO + M = H + O + M	-106.3 106.3	A * C	FORWARD REMOVES ACTIVE CENTERS REVERSE HIGHLY ENDOTHERMIC
255F. H + O2 = HO + O 255R. HO + O = H + O2	15.7 -15.7	A * A *	CONSIDER BOTH DIRECTIONS
256F. H + O2 + M = HO2 + M 256R. HO2 + M = H + O2 + M	-50.6 50.6	B * C	CONSIDER FORWARD REVERSE ENDOTHERMIC
257F. HN + HN = H2 + N2 257R. H2 + N2 = HN + HN	-180.0 180.0	C C	FOUR-CENTER REACTION LOW CONCENTRATIONS FORWARD REVERSE HIGHLY ENDOTHERMIC
258F. HN + HNO = H2 + N2O 258R. H2 + N2O = HN + HNO	-92.0 92.0	C C	FOUR-CENTER, STERIC HINDRANCE LOW CONCENTRATIONS FORWARD REVERSE ENDOTHERMIC
259F. HN + HNO = H2O + N2 259R. H2O + N2 = HN + HNO	-173.3 173.3	C C	FOUR-CENTER, STERIC HINDRANCE
260F. HN + HO = H2 + NO 260R. H2 + NO = HN + HO	-77.3 77.3	C C	FOUR-CENTER REACTION HN + HO = H2O + N MORE LIKELY FORWARD REVERSE ENDOTHERMIC

REACTION	LOG A	B	C	COMMENTS	300	TEMP, KELVIN 1500 LOG K	2000	2500
251F. H + N2O = HN + NO	11.0 (0.5)	0.5	30. (5.)	BASED ON TI (EST) NOTE B	-9.6	8.2	9.4	10.1
252R. HNO + N = H + N2O	10.7 (0.5)	0.5	3. (5.)	BASED ON TI (EST) NOTE B	9.8	11.9	12.0	12.1
253F. H + N2O = HO + N2	* 13.9 (0.2)	0.	15. (1.)	BASED ON B90 EVALUATION 700-2500K	3.0	11.7	12.3	12.6
254F. H + O + M = HO + M	* 15.9 (1.)	0.	0.	BASED ON S30 LIMITED DATA	15.9	15.9	15.9	15.9
255R. HO + O = H + O2	* 13.4 (0.3)	0.	0.	BASED ON M31 EVALUATION 300-2000K	13.4	13.4	13.4	13.4
256F. H + O2 + M = HO2 + M	* 15.3 (0.1)	0.	1. (0.5)	BASED ON B88, M = N2 EVALUATION 300-2000K	16.0	15.2	15.2	15.2
257F. HN + HN = H2 + N2	13.0 (1.)	0.	0.	ESTIMATE OF D8 REDUCED BY 10X	13.0	13.0	13.0	13.0
258F. HN + HNO = H2 + N2O				NO RATE DATA				
259F. HN + HNO = H2O + N2				NO RATE DATA				
260F. HN + HO = H2 + NO				NO RATE DATA				

REACTION	HR	NOTES	COMMENTS
261F. $HN + NO = N_2O + H$ 261R. $N_2O + H = HN + NO$	-44.4 44.4	B * C	CONSIDER FORWARD REVERSE ENDOTHERMIC
262F. $HN + HO_2 = HNO + HO$ 262R. $HNO + HO = HN + HO_2$	-61.8 61.8	C C	LOW CONCENTRATIONS FORWARD REVERSE ENDOTHERMIC
263F. $HN + HO_2 = H_2 + NO_2$ 263R. $H_2 + NO_2 = HN + HO_2$	-86.0 86.0	C C	NOT LIKELY TO BE ELEMENTARY REACTION
264F. $HN + HO_2 = H_2O + NO$ 264R. $H_2O + NO = HN + HO_2$	-132.4 132.4	C C	FOUR-CENTER REACTION, STERIC HINDRANCE
265F. $HN + H_2O = HNO + H_2$ 265R. $HNO + H_2 = HN + H_2O$	-6.7 6.7	C C	FOUR-CENTER REACTION STERIC HINDRANCE NOH STRUCTURE
266F. $HN + NO = HNO + N$ 266R. $HNO + N = HN + NO$	26.2 -26.2	C C	LOW CONCENTRATIONS BOTH DIRECTIONS
267F. $HN + NO = HO + N_2$ 267R. $HO + N_2 = HN + NO$	-102.7 102.7	C C	FOUR-CENTER REACTION LOW CONCENTRATIONS FORWARD REVERSE HIGHLY ENDOTHERMIC
268F. $HN + NO_2 = HNO + NO$ 268R. $HNO + NO = HN + NO_2$	-53.2 53.2	C C	LOW CONCENTRATIONS BOTH DIRECTIONS
269F. $HN + NO_2 = HO + N_2O$ 269R. $HO + N_2O = HN + NO_2$	-67.8 67.8	C C	FOUR-CENTER REACTION, STERIC HINDRANCE LOW CONCENTRATIONS FORWARD REVERSE ENDOTHERMIC
270F. $HN + NO_2 = HO_2 + N_2$ 270R. $HO_2 + N_2 = HN + NO_2$	-94.0 94.0	C C	NOT LIKELY TO BE ELEMENTARY REACTION

REACTION	LOG A	B	C	COMMENTS	300	TEMP, KELVIN 1500	2000 LOG K	2500
261F. $HN + NO = N_2O + H$	* 11.7 (10.5)	0.5	2. (5.)	BASED ON T1 (EST) NOTE B	11.5	13.0	13.1	13.2
262F. $HN + HO_2 = HNO + HO$				NO RATE DATA				
263F. $HN + HO_2 = H_2 + NO_2$				NO RATE DATA				
264F. $HN + HO_2 = H_2O + NO$				NO RATE DATA				
265F. $HN + H_2O = HNO + H_2$				NO RATE DATA				
266R. $HNO + N = HN + NO$	11.0 10.5)	0.5	2. (5.)	BASED ON T1 (EST) NOTE B	10.8	12.3	12.4	12.5
267F. $HN + NO = HO + N_2$				NO RATE DATA				
268F. $HN + NO_2 = HNO + NO$	11.3 (10.5)	0.5	5. (5.)	BASED ON T1 (EST) NOTE B	8.9	12.2	12.4	12.6
269F. $HN + NO_2 = HO + N_2O$				NO RATE DATA				
270F. $HN + NO_2 = HO_2 + N_2$				NO RATE DATA				

REACTION	HR	NOTES	COMMENTS
271F. $HN + N_2O = HNO + N_2$ 271R. $HNO + N_2 = HN + N_2O$	-88.0 88.0	C C	LOW CONCENTRATIONS FORWARD REVERSE ENDOTHERMIC
272F. $HN + O + M = HNO + M$ 272R. $HNO + M = HN + O + M$	-127.9 127.9	C C	THIRD ORDER FORWARD REVERSE HIGHLY ENDOTHERMIC
273F. $HN + O = HO + N$ 273R. $HO + N = HN + O$	-27.4 27.4	C C	$HN + O + M = HNO + M$ MORE LIKELY FORWARD $HO + N + M = HNO + M$ MORE LIKELY REVERSE
274F. $HN + O_2 = HNO + O$ 274R. $HNO + O = HN + O_2$	-5.8 5.8	B * B *	CONSIDER BOTH DIRECTIONS PROBABLY MINOR
275F. $HN + O_2 = HO + NO$ 275R. $HO + NO = HN + O_2$	-59.4 59.4	C C	FOUR-CENTER REACTION $HN + O_2 = HNO + O$ FASTER FORWARD REVERSE ENDOTHERMIC
276F. $HN + O_2 = HO_2 + N$ 276R. $HO_2 + N = HN + O_2$	28.6 -28.6	C C	$HN + O_2 = HNO + O$ FASTER FORWARD LOW CONCENTRATIONS REVERSE
277F. $HNO + M = HO + N + M$ 277R. $HO + N + M = HNO + M$	100.5 -100.5	C C	FORWARD HIGHLY ENDOTHERMIC THIRD ORDER REVERSE NOH STRUCTURE
278F. $HNO + HNO = H_2O + N_2O$ 278R. $H_2O + N_2O = HNO + HNO$	-85.3 85.3	C C	FOUR-CENTER REACTION, STERIC HINDRANCE
279F. $HNO + HO = H_2 + NO_2$ 279R. $H_2 + NO_2 = HNO + HO$	-24.2 24.2	C C	FOUR-CENTER REACTION $HNO + HO = H_2O + NO$ MORE LIKELY FORWARD LOW CONCENTRATIONS REVERSE
280F. $HNO + HO = H_2O + NO$ 280R. $H_2O + NO = HNO + HO$	-70.6 70.6	B * C	CONSIDER FORWARD REVERSE ENDOTHERMIC

REACTION	LOG A	B	C	COMMENTS	300	TEMP, KELVIN 1500	2000 LOG K	2500
271F. $HN + N_2O = HNO + N_2$	11.0 (10.5)	0.5	3. (5.)	BASED ON T1 (EST) NOTE B	10.1	12.2	12.3	12.4
272F. $HN + O + M = HNO + M$	16.0 (10.5)	-0.5	0. (5.)	BASED ON T1 (EST) NOTE B	14.8	14.4	14.3	14.3
273F. $HN + O = HO + N$	11.5 (10.3)	0.5	8. (3.)	BASED ON B97 TRANS STATE CORELAT	6.9	11.9	12.3	12.5
274R. $HNO + O = HN + O_2$	* 11.0 (10.5)	0.5	7. (5.)	BASED ON T1 (EST) NOTE B	7.1	11.6	11.9	12.1
275F. $HN + O_2 = HO + NO$				NO RATE DATA				
276R. $HO_2 + N = HN + O_2$	11.0 (10.5)	0.	0. (5.)	BASED ON K25 (EXPT) LOWER LIMIT AT 300K NOTE D	11.0	11.0	11.0	11.0
277R. $HO + N + M = HNO + M$	15.0	-0.5	0.	BASED ON T1 (EST) NOTE B	13.8	13.4	13.3	13.3
278F. $HNO + HNO = H_2O + N_2O$				NO RATE DATA				
279F. $HNO + HO = H_2 + NO_2$				NO RATE DATA				
280F. $HNO + HO = H_2O + NO$	* 13.5 (10.5)	0.	0. (2.)	BASED ON B46,N39	13.5	13.5	13.5	13.5

REACTION	HR	NOTES	COMMENTS
281F. HNO + HO2 = H2O + NO2 281R. H2O + NO2 = HNO + HO2	-79.2 79.2	C C	FOUR-CENTER REACTION, STERIC HINDRANCE
282F. HNO + N = HO + N2 282R. HO + N2 = HNO + N	-128.9 128.9	C C	LOW CONCENTRATIONS FORWARD REVERSE HIGHLY ENDOTHERMIC
283F. HNO + NO = HO + N2O 283R. HO + N2O = HNO + NO	-14.7 14.7	C C	FOUR-CENTER REACTION, STERIC HINDRANCE
284F. HNO + NO = HO2 + N2 284R. HO2 + N2 = HNO + NO	-40.9 40.9	C C	FOUR-CENTER REACTION, NEW STRUCTURE LOW CONCENTRATIONS FORWARD REVERSE ENDOTHERMIC
285F. HNO + NO2 = HO2 + N2O 285R. HO2 + N2O = HNO + NO2	-6.0 6.0	C C	FOUR-CENTER REACTION, STERIC HINDRANCE
286F. HNO + O = HO + NO 286R. HO + NO = HNO + O	-53.6 53.6	B * C	CONSIDER FORWARD REVERSE ENDOTHERMIC
287F. HNO + O = HO2 + N 287R. HO2 + N = HNO + O	34.6 -34.6	C C	HNO + O = HO + NO FASTER FORWARD LOW CONCENTRATIONS REVERSE
288F. HNO + O2 = HO + NO2 288R. HO + NO2 = HNO + O2	-6.3 6.3	C C	FOUR-CENTER REACTION, STERIC HINDRANCE
289F. HNO + O2 = HO2 + NO 289R. HO2 + NO = HNO + O2	2.4 -2.4	C C	FOUR-CENTER REACTION, STERIC HINDRANCE
290F. HO + HO = H2 + O2 290R. H2 + O2 = HO + HO	-17.9 17.9	C C	FOUR-CENTER REACTION HO + HO = H2O + O FASTER FORWARD REVERSE MAY HAVE ROLE IN H2/O2 IGNITION

REACTION	LOG A	B	C	COMMENTS	300	TEMP, KELVIN 1500	2000 LOG K	2500
281F. HNO + HO2 = H2O + NO2				NO RATE DATA				
282F. HNO + N = HO + N2				NO RATE DATA				
283F. HNO + NO = HO + N2O	12.3 (0.3)	0.	26. (5.)	BASED ON H23 REEVALUATION OF EXISTING H2-NO DATA	-6.6	8.5	9.5	10.0
284F. HNO + NO = HO2 + N2				NO RATE DATA				
285F. HNO + NO2 = HO2 + N2O				NO RATE DATA				
286F. HNO + O = HO + NO	* 11.7 (0.5)	0.5	0. (5.)	BASED ON TL (EST) NOTE B	12.9	13.3	13.4	13.4
287F. HNO + O = HO2 + N				NO RATE DATA				
288F. HNO + O2 = HO + NO2				NO RATE DATA				
289F. HNO + O2 = HO2 + NO				NO RATE DATA				
290R. H2 + O2 = HO + HO	12.4 (1.)	0.	39. (10.)	BASED ON K2 (EXPT) NOTE D	-16.0	6.7	8.1	9.0

REACTION	HR	NOTES	COMMENTS
291F. HO + HO = H2O + O 291R. H2O + O = HO + HO	-17.0 17.0	A * A *	CONSIDER BOTH DIRECTIONS
292F. HO + HO2 = H2O + O2 292R. H2O + O2 = HO + HO2	-73.0 73.0	A * C	CONSIDER FORWARD FOR HO2 REMOVAL REVERSE ENDOTHERMIC
293F. HO + H2O = HO2 + H2 293R. HO2 + H2 = HO + H2O	55.1 -55.1	C C	FOUR-CENTER REACTION FORWARD ENDOTHERMIC
294F. HO + HO = HO2 + H 294R. HO2 + H = HO + HO	38.0 -38.0	C C	FORWARD ENDOTHERMIC LOW CONCENTRATIONS REVERSE
295F. HO + NO2 = HO2 + NO 295R. HO2 + NO = HO + NO2	8.6 -8.6	B * B *	CONSIDER BOTH DIRECTIONS REVERSE HAS BEEN CONSIDERED FOR EARLY NO2 FORMATION
296F. HO + N2O = HO2 + N2 296R. HO2 + N2 = HO + N2O	-26.2 26.2	B * B *	CONSIDER BOTH DIRECTIONS PROBABLY MINOR
297F. HO + O + M = HO2 + M 297R. HO2 + M = HO + O + M	-66.1 66.1	B * C	CONSIDER FORWARD REVERSE ENDOTHERMIC
298F. HO + O2 = HO2 + O 298R. HO2 + O = HO + O2	55.9 -55.9	C A *	FORWARD ENDOTHERMIC CONSIDER REVERSE FOR HO2 REMOVAL
299F. H2 + NO = H2O + N 299R. H2O + N = H2 + NO	32.9 -32.9	C C	NOT LIKELY TO BE ELEMENTARY REACTION
300F. H2 + NO2 = H2O + NO 300R. H2O + NO = H2 + NO2	-46.4 46.4	C C	NOT LIKELY TO BE ELEMENTARY REACTION

REACTION	LOG A	B	C	COMMENTS	300	TEMP, KELVIN 1500	2000 LOG K	2500
291F. HO + HO = H2O + O	* 12.8 (0.3)	0.	1. (0.5)	BASED ON BBB EVALUATION 300-2000K	12.1	12.7	12.7	12.7
292F. HO + HO2 = H2O + O2	* 13.7 (0.5)	0.	1. (1.)	BASED ON L16 EVALUATION 300-1000K	13.0	13.6	13.6	13.6
293F. HO + H2O = HO2 + H2				NO RATE DATA				
294F. HO + HO = HO2 + H				NO RATE DATA				
295R. HO2 + NO = HO + NO2	* 13.0 (0.3)	0.	3. (3.)	BASED ON L16 USING ACTIV ENERGY=3	10.8	12.6	12.7	12.7
296F. HO + N2O = HO2 + N2	* 13.5	0.	15.	ESTIMATE NO RATE DATA	2.6	11.3	11.9	12.2
297F. HO + O + M = HO2 + M	* 17.0 (2.)	0.	0.	BASED ON REF B24 NO VALID DATA (BBB)	17.0	17.0	17.0	17.0
298R. HO2 + O = HO + O2	* 13.7 (0.3)	0.	1. (1.)	BASED ON L16 LIMITED DATA	13.0	13.6	13.6	13.6
299F. H2 + NO = H2O + N				NO RATE DATA				
300F. H2 + NO2 = H2O + NO				NO RATE DATA				

REACTION	HR	NOTES	COMMENTS
301F. $H_2 + N_2O = H_2O + N_2$ 301R. $H_2O + N_2 = H_2 + N_2O$	-81.3 81.3	C C	NOT LIKELY TO BE ELEMENTARY REACTION
302F. $H_2 + O + M = H_2O + M$ 302R. $H_2O + M = H_2 + O + M$	-121.2 121.2	C C	NOT LIKELY TO BE ELEMENTARY REACTION
303F. $H_2 + O_2 = H_2O + O$ 303R. $H_2O + O = H_2 + O_2$	0.9 -0.9	C C	NOT LIKELY TO BE ELEMENTARY REACTION
304F. $N + N + M = N_2 + M$ 304R. $N_2 + M = N + N + M$	-229.4 229.4	C C	THIRD ORDER, LOW CONCENTRATIONS FORWARD REVERSE HIGHLY ENDOTHERMIC
305F. $N + NO = N_2 + O$ 305R. $N_2 + O = N + NO$	-75.3 75.3	B * A *	CONSIDER BOTH DIRECTIONS REVERSE PART OF ZELDOVICH MECHANISM
306F. $N + NO + M = N_2O + M$ 306R. $N_2O + M = N + NO + M$	-115.2 115.2	C C	THIRD ORDER, LOW CONCENTRATIONS FORWARD REVERSE HIGHLY ENDOTHERMIC
307F. $N + NO_2 = NO + NO$ 307R. $NO + NO = N + NO_2$	-79.6 79.6	B * C	CONSIDER FORWARD (LOW CONCENTRATIONS) REVERSE ENDOTHERMIC
308F. $N + NO_2 = N_2 + O_2$ 308R. $N_2 + O_2 = N + NO_2$	-122.6 122.6	C C	NOT LIKELY TO BE ELEMENTARY REACTION
309F. $N + NO_2 = N_2O + O$ 309R. $N_2O + O = N + NO_2$	-40.4 40.4	C C	N + NO2 = NO + NO MORE LIKELY FORWARD REVERSE ENDOTHERMIC
310F. $N + N_2O = NO + N_2$ 310R. $NO + N_2 = N + N_2O$	-114.2 114.2	C C	LOW CONCENTRATIONS FORWARD REVERSE HIGHLY ENDOTHERMIC

REACTION	LOG A	B	C	COMMENTS	300	TEMP, KELVIN 1500	LOG K 2000	2500
301F. $H_2 + N_2O = H_2O + N_2$				NO RATE DATA				
302F. $H_2 + O + M = H_2O + M$				NO RATE DATA				
303F. $H_2 + O_2 = H_2O + O$				NO RATE DATA				
304R. $N_2 + M = N + N + M$	21.6 (0.5)	-1.6	225. (1.)	BASED ON B90, M = N2 EVALUATION	-146.3	-16.3	-8.3	-3.5
305F. $N + NO = N_2 + O$	* 13.2 (0.3)	0.	0.	BASED ON B90 EVALUATION 300-5000K	13.2	13.2	13.2	13.2
306F. $N + NO + M = N_2O + M$				NO EVIDENCE OF IT REF S30	0.0	0.0	0.0	0.0
307F. $N + NO_2 = NO + NO$	* 12.6 (0.7)	0.	0. (3.)	BASED ON P10 (XPT) ASSUME ACT ENERGY=0 NOTE D	12.6	12.6	12.6	12.6
308F. $N + NO_2 = N_2 + O_2$	12.0 (0.3)	0.	0. (3.)	BASED ON P10 (XPT) ASSUME ACT ENERGY=0 NOTE D	12.0	12.0	12.0	12.0
309F. $N + NO_2 = N_2O + O$	12.7 (0.3)	0.	0. (3.)	BASED ON P10 (XPT) ASSUME ACT ENERGY=0 NOTE D	12.7	12.7	12.7	12.7
310F. $N + N_2O = NO + N_2$	8.7 (0.5)	0.	10. (5.)	BASED ON B19 (EST) NOTE A	1.4	7.2	7.6	7.8

REACTION	HR	NOTES	COMMENTS
311F. $N + O + M = NO + M$ 311R. $NO + M = N + O + M$	-154.1 154.1	C C	THIRD ORDER, LOW CONCENTRATION FORWARD REVERSE HIGHLY ENDOTHERMIC
312F. $N + O_2 = NO + O$ 312R. $NO + O = N + O_2$	-32.1 32.1	A * B *	CONSIDER BOTH DIRECTIONS FORWARD PART OF ZELDOVICH MECHANISM
313F. $N + O_2 + M = NO_2 + M$ 313R. $NO_2 + M = N + O_2 + M$	-106.8 106.8	C C	NOT LIKELY TO BE ELEMENTARY REACTION
314F. $NO + NO = N_2 + O_2$ 314R. $N_2 + O_2 = NO + NO$	-43.2 43.2	C C	FOUR-CENTER REACTION, SPIN HINDERED NO + NO = N2O + O FASTER EXPERIMENTALLY POSSIBLY BY AT LEAST A FACTOR OF 10
315F. $NO + NO = N_2O + O$ 315R. $N_2O + O = NO + NO$	38.9 -38.9	B * B *	CONSIDER BOTH DIRECTIONS
316F. $NO + NO_2 = N_2O + O_2$ 316R. $N_2O + O_2 = NO + NO_2$	-8.4 8.4	C C	NOT LIKELY TO BE ELEMENTARY REACTION
317F. $NO + N_2O = NO_2 + N_2$ 317R. $NO_2 + N_2 = NO + N_2O$	-34.9 34.9	C C	FORWARD SLOW EXPERIMENTALLY REVERSE EVEN SLOWER
318F. $NO + O + M = NO_2 + M$ 318R. $NO_2 + M = NO + O + M$	-74.7 74.7	B * C	CONSIDER FORWARD REVERSE ENDOTHERMIC
319F. $NO + O_2 = NO_2 + O$ 319R. $NO_2 + O = NO + O_2$	47.3 -47.3	B * B *	CONSIDER BOTH DIRECTIONS FORWARD ENDOTHERMIC
320F. $N_2 + O + M = N_2O + M$ 320R. $N_2O + M = N_2 + O + M$	-39.9 39.9	B * B *	CONSIDER BOTH DIRECTIONS FOR ROLE OF N2O

REACTION	LOG A	B	C	COMMENTS	300	TEMP, KELVIN 1500	LOG K 2000	2500
311R. $NO + M = N + O + M$	20.6 (0.5)	-1.5	150. (5.)	BASED ON C19, W6 M = AR, N2, O2 USE WITH CAUTION	-92.4	-6.0	-0.7	2.4
312F. $N + O_2 = NO + O$	* 9.8 (0.3)	1.	6.3 (0.3)	BASED ON B90 EVALUATION 300-3000K	7.7	12.1	12.4	12.6
313F. $N + O_2 + M = NO_2 + M$				NO RATE DATA				
314F. $NO + NO = N_2 + O_2$				SPIN HINDERED OLD EXPERIMENTS ACTUALLY MEASURED NO + NO = N2O + O	0.0	0.0	0.0	0.0
315R. $N_2O + O = NO + NO$	* 14.0 (0.3)	0.	28. (3.)	BASED ON B90 EVAL 1200-200K SAME RATE AS N2O + O = N2 + O2	-6.4	9.9	10.9	11.6
316F. $NO + NO_2 = N_2O + O_2$	12.0 (2.)	0.	60.	BASED ON B19 (EST) NOTE A	-31.7	3.3	5.4	6.8
317F. $NO + N_2O = NO_2 + N_2$	14.3 (1.)	0.	50.	BASED ON F20,R30 NOTE D	-22.1	7.0	8.0	9.0
318R. $NO_2 + M = NO + O + M$	* 16.0 (0.1)	0.	65. (1.5)	BASED ON B90, T4 M=AR,O2 1400-2400K	-31.4	6.5	8.9	10.3
319R. $NO_2 + O = NO + O_2$	* 13.0 (0.3)	0.	1. (0.5)	BASED ON B90 EVALUATION 300-600K NO HI TEMP DATA	12.3	12.9	12.9	12.9
320R. $N_2O + M = N_2 + O + M$	* 14.7 (0.2)	0.	58. (3.)	BASED ON B90, M = AR EVAL 1300-2500K	-27.6	6.2	8.4	9.6

REACTION	HR	NOTES	COMMENTS
321F. N2 + O2 = N2O + O	82.2	C	FORWARD ENDOTHERMIC
321R. N2O + O = N2 + O2	-82.2	B *	CONSIDER REVERSE
322F. O + O + M = O2 + M	-122.0	A *	FORWARD TERMINATION REACTION
322R. O2 + M = O + O + M	122.0	C	REVERSE HIGHLY ENDOTHERMIC

					TEMP, KELVIN			
REACTION	LOG A	B	C	COMMENTS	300	1500	2000	2500
					LOG K			
321R. N2O + O = N2 + O2	* 14. (0.4)	0.	28. (4.)	BASED ON 890 EVAL 1200-2500K SAME RATE AS N2O + O = NO + NO	-6.4	9.9	10.9	11.6
322R. O2 + M = O + O + M	* 18.4 19.4 (0.3)	-1. -1.	118.7 118.7	BASED ON J4, M = AR BASED ON J4, M = O2 CRITICAL EVALUATION WIDE TEMP RANGE	-70.6	-2.1	2.1	4.6

11:40 a.m.
A Detailed Approach to the Chemistry of Methane/Air Combustion: Critical Survey of Rates and Applications
Dr. Victor S. Engleman, Exxon Research and Engineering

Q: With respect to that NO_2 formation right in the flame zone, we have data that shows that NO_2 is formed right after the flame zone, and it is mostly by OH radicals rather than by any other species. We have quantitative profiles both for NO formation as well as NO_2 formation right through the flame zone.

A: Are those probe or optical?

Q: These are obtained by a supersonic mass spectrometry probe. The analysis has data for all the hydrocarbon radicals as well as NO species like HO, HO_2, hydrogen peroxide, formyl radical, etc.

A: I would really like to see some optical evidence, some non-interfering evidence. Whenever you stick a probe into a flame there's always a chance of interference. I know how good molecular beam mass spec sampling is as well. I have a lot of faith in it, but I would really like to see some unequivocal optical evidence for early NO_2 formation.

[Questioner:]

I would argue against the skepticism against such probing. We have studied probing extensively in various systems just to establish this as a technique. Let's put it this way, there are a number of ways that you can test where in fact you are perturbing your flame; the obvious ones are to you look at your flame, and see if you perturb it, if it's lifting or attaching itself to the probe. We don't see that; but also, then, it may perturb the temperature and thus the reaction rates; we don't see that either. Of course ultimately the probe perturbation, indeed, I agree with you in that respect and for the intermediate species it should be independently checked. We have done that for our data, but if you compare the estimates that have been made by other methods, they come embarrassingly close, so there is correspondence, and if perturbation is present it is certainly not very major.

Q: Vic, we've known which rate constants we would like measurements of for some time. As modelers we haven't really convinced anybody to go out and measure them. I wonder if you had any recommendations of what might be done in terms of supplying some stimulus to this.

A: Well, I am sure EPA is always responsive to unsolicited proposals from anyone in the audience who would be anxious to measure these rates. I think there is more and more evidence from some of the basic studies, especially when you want to get to low NO_x concentrations, some of the flame phenomena are quite important in NO_x formation.

Q: I'd like to add to your comment on the uncertainty of the rate coefficients. When we were doing the simple Zeldovitch mechanism without the OH reaction and doing the literature search for the complete sets of coefficients, we found that, depending on the source, you get variations of a factor of 1000 in the rate coefficient between one source and another. I am not going to point any fingers. The results in calculating your thermal NO_x are reasonably spectacular.

Q: Vic, I wonder if you would comment about the Zeldovich rate constant. Leeds has readjusted the values down; what is your own particular opinion on that?

A: Well, I'm glad you asked that question because it just so happens that Bob Shaw will be talking about estimating rate constants a little later on. SRI has come up with a very neat way of estimating reactions between unimolecular and bimolecular species, and it turns out, without scooping Bob too much, that the estimates come very, very close to the rates that are measured in the literature, and in this particular case, for that particular class of reactions (and the Zeldovich mechanism does fall into that class), that technique is applicable. I'll leave it at that and I'll let Bob tell you what the real answer is.

CHEMICAL REACTIONS IN THE CONVERSION OF FUEL NITROGEN TO NO_X

By:

A. E. Axworthy, G. R. Schneider, and V. H. Dayan
Rockwell International, Rocketdyne Division
Canoga Park, California

INTRODUCTION

An experimental and analytical program was conducted to investigate the chemical and physical processes involved in the conversion of fuel-bound nitrogen to NO_x in combustion.* To study the types of reactions volatile fuel nitrogen species can undergo near the surface of a burning coal particle or oil droplet, model fuel nitrogen compounds were pyrolyzed in helium at elevated temperatures. Fuel oils and coals were then pyrolyzed under similar conditions and the fate of the nitrogen species determined. This study demonstrated that HCN and, to a much smaller extent, NH_3 are likely to form from nitrogen compounds in the preflame stages of combustion. A premixed, flat-flame burner study was then carried out to investigate the combustion kinetics involved in the conversion of HCN and NH_3 to NO and N_2 in rich and lean CH_4-O_2-Ar flames.

INERT PYROLYSIS OF MODEL NITROGEN COMPOUNDS

Pyrolysis rates for pyridine and picolines calculated from available data (Ref. 1) are shown in Fig. 1. The picolines are less thermally stable than pyridine at lower temperatures, suggesting that hydrogen abstraction from the substituted methyl group is rate determining. However, the decomposition rate of pyridine approaches that of the picolines at higher temperatures. It appears, therefore, that a direct attack on the N-heterocyclic ring will be rate-determining at the high heating rates involved in combustion. This is the rationale for employing low-molecular-weight nitrogen compounds, such as pyridine, to study the higher-molecular-weight analogs present in fossil fuels.

Previous studies of the pyrolysis of organic nitrogen compounds have not emphasized determination of the fate of the nitrogen (Ref. 1). HCN has been reported as a product, but there has been no indication as to whether it is a major or minor product, although the amount of HCN formed is stated to increase at higher pyrolysis temperatures.

The model compound pyrolysis experiments were carried out in a quartz flow reactor at the nominal conditions listed in Table 1. The unreacted model compound and the organic products were measured by temperature-programmed gas chromatography. The inorganic nitrogen products

---

*The details of the work described here can be found in the final report for EPA Contract 68-02-0635. The effort on modeling particle and droplet combustion is not included in this presentation.

HCN, NH_3, and N_2 were determined by sensitive GC and colorimetric chemical analysis techniques.

PYROLYSIS RATES

The results obtained on the thermal stabilities of the model compounds pyridine, quinoline, benzonitrile, and pyrrole are compared in Fig. 2, which shows percent undecomposed as a function of reaction temperature at constant pressure and mass flowrate. The relative thermal stabilities of these compounds vary with temperature. For example, benzonitrile decomposed to a greater extent than did pyridine below 1020 C, but appreciable benzonitrile remained unreacted even at 1100 C.

The decomposition curves shown in Fig. 2 were fitted to empirical rate expressions by integrating the rate expression through the reactor and varying the kinetic parameters (reaction order, pre-exponential factor, and activation energy) until the predicted percent-undecomposed curve followed the experimental curve. The integration procedure took into account the reactor temperature profile and the change in residence time with temperature as well as the change in rate with reactant concentration and temperature. The data obtained for pyridine, pyrrole, and quinoline were found to fit the first-order rate expressions listed in Table 2. The pre-exponential factors for pyridine and pyrrole suggest that the rate-determining step may be a homogeneous unimolecular reaction. However, the pre-exponential factor for pyridine was found to vary with the initial pyridine concentration (decreasing with decreasing concentration).* The rate expression for quinoline indicates a possible heterogeneous or chain reaction, and the benzonitrile data do not appear to fit any simple-order rate expression.

The inert pyrolysis rate expression assigned to pyridine in Table 2 predicts the decomposition half-life denoted by the solid line in Fig. 3. It can be seen that when an N-heterocyclic fuel nitrogen compound approaches the flame front around a droplet or particle, its decomposition rate will become very rapid and it should decompose or react before entering the flame zone. Oxidative pyrolysis and oxidation may become competitive with thermal decomposition as the flame front is approached. Preliminary oxidative pyrolysis experiments with pyridine and benzonitrile have shown that oxygen markedly increases the reaction rate under the conditions of this study. It can be seen from Fig. 3, however, that if the activation energy for oxidative pyrolysis were only one-half of that of the thermal decomposition process, thermal decomposition could be the predominate initial preflame reaction of organic nitrogen compounds at sufficiently high heating rates even though oxidative pyrolysis is faster at lower temperatures.

---

*Pyridine was the only compound for which the initial reactant concentration was varied.

PYROLYSIS PRODUCTS

The organic products from the inert pyrolysis of pyridine are shown in Fig. 4. The more thermally stable products predominate at the higher temperatures. This suggests that the primary product distribution may approximate that obtained at 950 C, but the less stable products react at the higher temperatures before exiting the reactor. More data on product decomposition rates would be required before the product distributions could be modeled in enough detail to substantiate this hypothesis. The nitrogen-containing organic products recovered from pyridine pyrolysis (solid curves in Fig. 4) contain a maximum of about 10 percent of the nitrogen from the decomposed pyridine.

HCN was found to be the major nitrogen-containing product from the inert pyrolysis of pyridine and benzonitrile (Table 3). The amount of HCN formed increased with temperature, and the HCN yield from pyridine was about 100 percent at 1100 C. No detectable N_2 (i.e., less than 1 percent) was formed in the pyrolysis of these two model compounds. The extent of conversion at 960 C of model compound-N to NH_3 was 2 to 8 percent for pyridine, and 3 to 5 percent for benzonitrile. The carbonaceous residue that formed on the reactor wall was analyzed for nitrogen in a single experiment with pyridine at 960 C. It contained 49 percent of the nitrogen from the portion of the pyridine that had decomposed. As shown in Table 4, these data permit the nitrogen mass balance for pyridine to be closed at both 960 and 1100 C.

INERT PYROLYSIS OF FOSSIL FUELS

Samples of fuel oils and coals were pyrolyzed in helium under conditions similar to those employed with the model compounds and the inorganic products measured. The fuel sample (about 1.5 mg) was placed in a small quartz boat that was rapidly moved into a preheated quartz reactor, and the volatile products were swept from the reactor in a flowing carrier gas stream. HCN was collected in Na_2CO_3 solution as before and measured colorimetrically. Because the fuel reactor promoted decomposition of NH_3 to N_2, the sum of any NH_3 and N_2 formed in fuel pyrolysis was determined by measuring by GC the N_2 present in the carrier gas stream. A converter was placed upstream of the GC to convert any NH_3 that escaped the reactor to N_2, and an ascarite trap preceded this to remove HCN, which would also have been converted to N_2.

Listed in Table 5 are the HCN yields from six No. 6 fuel oils and from Wilmington crude oil. From 23 to 50 percent of the nitrogen in the samples formed HCN at 1100 C. The amount of HCN formed at 950 C for each sample was from one-half to two-thirds of the amount formed at 1100 C. The sums of $NH_3 + N_2$ formed from four of these oils are listed in Table 6 as percent of fuel-N. The $NH_3 + N_2$ measured at 1100 C represented 28 percent of the fuel nitrogen contained in the lowest N-content oil but only 6 percent in the oil with the highest N content. Table 7 shows that the amount $NH_3 + N_2$ formed was relatively independent of the N-content of the fuel when expressed as micrograms of N_2 per milligram of oil suggesting that part of the measured N_2 might be dissolved nitrogen actually present as molecular nitrogen in the sample.

The HCN and $NH_3 + N_2$ yields obtained from two coals are summarized in Table 8. The results were similar to those obtained with the fuel oils. Since the residues formed in the fuel pyrolysis experiments were not analyzed, it is not known if the remainder of the fuel-N was contained in the residue or if some unmeasured volatile products were formed.

FLAT-FLAME BURNER EXPERIMENTS

HCN and NH_3 were added to premixed CH_4-O_2-Ar flames to investigate the combustion kinetics involved in the formation of NO from these combustion intermediates. NO was added initially in some experiments to determine its fate once formed. The design of the water-cooled burner is shown in Fig. 5. An uncooled quartz probe and an Al_2O_3-coated thermocouple were used to measure species concentrations and temperature along the centerline of the burner. The burner was enclosed in a glass envelope so that a pressure of 0.1 atm could be maintained to spread the flame and permit more detailed probing. The mole fractions of the major stable species were measured by mass spectrometry. A chemiluminescent analyzer (CA) was used to measure NO directly and NO_2, HCN, and NH_3 by conversion of these species to NO. A molybdenum catalyst converter was used at 400 C to convert NO_2 and at 800 C to convert HCN (60- to 90-percent conversion to NO, depending on the concentration) and NH_3 (45- to 60-percent conversion). Air was added to the gas sample upstream of the converter. The nominal burner conditions employed in this study are listed in Table 9. The detailed probing experiments were conducted at equivalence ratios, ϕ, of 0.8 (fuel-lean) and 1.5.

SCREENING EXPERIMENTS

A series of screening experiments were conducted with the probes positioned well downstream (80 mm above the burner) to study the effects of various parameters on the overall NO yield. The overall yields of NO were nearly the same from HCN and NH_3 when the conditions were identical (Fig. 6).

High NO yields on the order of 80 percent* were obtained in fuel-lean flames, but the yield dropped off continually when the flame was made more and more fuel rich. Varying the pressure, burner feed rate, or Ar/O_2 ratio usually affected the flame temperature apparently by changing the position of the flame front and thereby the rate of heat loss to the burner. (Argon dilution also decreased the adiabatic flame temperature, and the effects were partially compensating because the lower temperature and reaction rates moved the flame further from the burner decreasing the heat loss.) The NO yield appeared to be related to but not directly proportional to flame temperature, i.e., increasing somewhat with increasing temperature. Changing the reactant concentrations by varying the pressure or Ar/O_2 ratio had little effect on the final NO yield if the effect of the attendant temperature change was taken into account. This indicates that the reactions that form NO and N_2 are of the same order--undoubtedly second. The rate of NO formation is presumably a strong function of species concentration even though the yield apparently is not.

DETAILED PROBING EXPERIMENTS

The measured profile of species mole fraction vs distance from the burner is affected by both the species reaction rate at various positions and the axial diffusion of the species. The probe data were analyzed by the procedure of Fristrom and Westenberg (Ref. 2) to separate the chemical reaction rates from the effects of diffusion. For each species of interest, the species diffusion velocity, V_i, relative to the velocity of the total gas stream was calculated at various points from an approximation of the equation:

$$-V_i = \mathcal{D}_{i,j}\left(\frac{1}{C_i}\right)\frac{dC_i}{dx}$$

The species flux was then obtained at each point by adding the species diffusion velocity to the main gas velocity and multiplying by the species concentration. Unlike the mole fraction profiles, the flux profiles only change as the result of chemical reaction, and the slope of the flux curve (on a distance plot) gives directly the species reaction rate at that point (in moles/cm^3-sec). Flux plots will, therefore, be employed in the following discussion. The flux profiles are plotted on a time scale (obtained by integrating the gas velocity as a function of distance) to indicate the relative times required for the various chemical processes to occur. The zeros on the time scales were defined as the point where the temperature reached 1250 K in fuel-rich flames (ϕ = 1.5) and 1550 K (ϕ = 0.8).

---

*The results of other studies of fuel NO formation suggest that even higher NO yields would have been obtained at lower additive concentrations.

The importance of the diffusion correction is demonstrated in Fig. 7 (NH_3 additive, ϕ = 0.8). The NO mole fraction profile suggests that most of the NO forms in and below the luminous zone. The NO flux profile, however, demonstrates that nearly all of the NO exiting the burner was formed just above the luminous zone. Most of the NO present in the luminous zone was formed above the flame zone and diffused upstream. A small amount of NO does form near the bottom of the luminous zone and then reacts farther up in the zone. Likewise, the CH_4 mole fraction is about one-half of its initial value at the bottom of the luminous zone, but the flux curve demonstrates that CH_4 reaction does not begin until just at that point. The decrease in CH_4 mole fraction below the luminous zone results solely from downstream diffusion of CH_4 toward the flame front.

The typical temperature profile shown in Fig. 8 increases rapidly through the luminous zone, where the CH_4 reacts, continues to increase above the luminous zone as CO oxidation occurs, reaches a maximum about 8 mm above the burner, and then decays slowly.

Before discussing each of the four selected conditions in more detail, the NO flux yields are compared on a single plot in Fig. 9. The time scales were adjusted so that the tops of the luminous zones coincide in this figure. In the fuel-rich flames (ϕ = 0.8), the NO forms rapidly and in high yield just above the luminous zone. With NH_3 additive, the NO forms more rapidly than with HCN (reaching its maximum rate of formation just before CO_2 formation reaches its maximum in the case of NH_3 and just after with HCN). In fuel-rich flames, the NO forms in low yield from either additive, and most of the NO forms far above the luminous zone. An apparent surge of NO formation occurs just above the top of the luminous zone. The final NO yields obtained in the screening experiments (Fig. 6) were about 82 percent at ϕ = 0.8 and 32 percent at ϕ = 1.5. The NH_3 flux yield at ϕ = 0.8 leveled off at 77 percent in Fig. 9, which is slightly less than was obtained in the screening experiments. The other flux yield curves were still increasing at the last measurement point and could have reached their expected values farther above the flame front.

More detailed flux plots are presented in Fig. 10 through 13 for these four conditions. Shown on each plot are (1) the initial fluxes of CH_4 and additive (calculated from the metered flowrates to the burner); (2) CH_4 and NO flux profiles; (3) "NH_3" or "HCN" flux profile, which is put in quotes because the converter-CA system could not distinguish directly between NH_3, HCN, and NO_2;* (4) an N-BAL flux profile that represents a nitrogen mass balance and was calculated at each point by subtracting the measured NO flux and the "NH_3" or "HCN" flux from the initial additive flux, and (5) temperatures at selected positions. The N-BAL curve includes the N_2 flux (multiplied by 2) and the fluxes of any other nitrogen-containing species that do not form NO upon passing through the quartz probe and the molybdenum catalyst converter (at 800 C with added air) before entering the CA reactor.

NH_3, $\phi = 0.8$ (Fig. 10)

In the fuel-lean flame, NH_3 reacts in and possibly below the luminous zone. At the top of the luminous zone, the "NH_3" flux, as well as the measured "NH_3" mole fraction, is nearly zero, and the NO flux is zero (although the mole fraction of NO is large at this point, (Fig. 7)). These results indicate that, within the accuracy of the rather large NO diffusion correction, nearly all of the added NH_3 is converted in the luminous zone to nitrogen species that are not measurable in the probe-converter-CA system. Only a small fraction of these "N-BAL" species can be N_2, because the final yield of N_2 at $\phi = 0.8$ is only 18 percent, and N_2 is not expected to react in these moderate-temperature flames. Small amounts of NO_2 were observed under these conditions, but the maximum NO_2 flux, which occurred at the center of the luminous zone, was only 0.3 percent of the initial NH_3 flux. Thus, all of the NO forms from an unidentified reaction intermediate.

HCN, $\phi = 0.8$ (Fig. 11)

In contrast to NH_3, most of the added HCN apparently survived the luminous zone in the fuel-lean flame. The "HCN" reacts rapidly just above the luminous zone, and NO forms in high yield, reaching its maximum rate about 0.1 msec after the reaction of HCN reaches its maximum. (The rate of CO_2 formation reaches a maximum between these two maxima.) The relatively slow reaction of HCN appears to be the cause of the NO forming more slowly from HCN than from NH_3 (Fig. 9).

---

*"NH_3" and "HCN" denote the amount of NO formed in the converter multiplied by the converter calibration factor for either NH_3 or HCN.

In the fuel-lean flame with HCN addition, it can be shown that much and possibly all of the NO is formed from an intermediate (N-BAL species) that builds up above the luminous zone. In particular, the maximum rate of NO formation is more than twice the rate of HCN consumption at the point where the NO maximum rate occurs.

HCN, $\phi = 1.5$ (Fig. 12)

In the fuel-rich flame, part of the HCN reacts in the luminous zone (in two surges), but most of the HCN apparently again survives the luminous zone but then reacts slowly, forming NO in low yield far above the flame front. A small surge in NO formation occurs just at the top of the luminous zone. Because of the low yield of NO, it is not possible to determine how directly the NO forms from HCN in the rich flame (i.e., if a time delay is involved with the NO forming from a relatively long-lived intermediate as was the case in the fuel-lean flame). In the rich flame, the NO formation rate never exceeds the HCN consumption rate except just above the luminous zone.

NH_3, $\phi = 1.5$ (Fig. 13)

The results obtained with NH_3 addition are quite interesting. As discussed, all of the NH_3 reacts below the top of the luminous in the lean flame forming only N-BAL nitrogen species (Fig. 10). In the fuel-rich flame, the NH_3 apparently reacts in or below the luminous zone with about one-half forming HCN and one-half forming N-BAL species. Some indirect reasoning was employed in concluding that the "HCN" flux curve represents mainly HCN, because the converter-CA system could not distinguish directly between HCN and NH_3. However, the differences in conversion efficiencies for HCN and NH_3 did permit this tentative conclusion to be drawn from the experimental flux curves for "NH_3" (not shown in Fig. 13) and "HCN."

De Soete (Ref. 3) has reported that NH_3 is partially converted to HCN in a fuel-rich C_2H_4-O_2-Ar flame at atmospheric pressure. Another strong argument for the conversion NH_3 to HCN in our study is the similarity of the flux profiles above the luminous zone in Fig. 12 and 13. Thus the mechanism of NO formation in the fuel-rich flame appears to be the same whether the additive is NH_3 or HCN, and involves the formation of NO from HCN.

Comparison of Results

The conclusions drawn from the addition of NH_3 and HCN to lean and rich methane flames are compared in Table 10. NH_3 reacts much more rapidly than does HCN in both flames. The similarity of the overall NO yields from NH_3 and HCN in the rich flame (Fig. 6) apparently results from the fact that the NO forms from HCN with either additive. The reason for the similarity of the NO yields in the lean flame is not as apparent, since a common stable intermediate is not formed. However, a common free radical intermediate could be involved.

Effect of Argon Dilution

An experiment (not shown) was conducted with HCN addition at $\phi = 0.8$ in which the Ar/O_2 ratio was increased by 40 percent, and the total burner feed rate was reduced to increase the heat loss to the burner. Although these conditions reduced the maximum flame temperature by 150 degrees and the initial reactant concentrations by 23 percent, the maximum reaction rates for NO, HCN, CH_4, and CO_2 only decreased by 30, 8, 42, and 29 percent, respectively. An analysis of these results, presented in the final report, indicates that certain compensating effects control the maximum reaction rates, but that the measured rates do have a normal dependency on temperature and species concentration.

Effect of NO Addition

When NO was added initially (at 625 ppm) to the fuel-rich flame, together with HCN (Fig. 14) or alone (Fig. 15), the rapid consumption of NO occurred just below the top of luminous zone. NO then formed rapidly just above the luminous zone and decayed rapidly again farther downstream. The magnitude of the NO surge was greater with HCN present, but the shape of the NO flux profile in this region is highly dependent on the diffusion correction (i.e., on the exact shape of the NO mole fraction curve). In the absence of added HCN, the consumed NO was partially converted (40 percent) to a measurable nitrogen species that was presumably HCN. When NO was added to the fuel-lean flame, together with HCN (not shown), a small consumption of NO occurred in the luminous zone before the formation of NO from HCN obscured any further reaction of the added NO. These results, with added NO, are in general agreement with the results of De Soete (Ref. 4) that are summarized in Table 2.

Reaction Mechanism and Conclusions

A possible reaction mechanism for the formation of NO and N_2 from NH_3 is presented in Table 12. The experimental results indicate that a rather long-lived nitrogen intermediate forms in high concentration in the fuel-lean flame. A likely candidate that could have the required characteristics of (1) low reactivity in the luminous zone and (2) not forming NO in the probe-converter system is the NCO radical.* Bosco

---

*NCO could form N_2 in the probe via $2\ NCO = N_2 + 2\ CO$.

(Ref. 5) has shown that CN radicals react with O_2 to form NCO and O atom. The competing reaction to form CO and NO is slower by a factor of more than 7 at room temperature. Davies and Thrush (Ref. 6) have proposed that NCO is an intermediate in the formation of NO from the reaction of oxygen atom with HCN. More recently, Mulvihill and Phillips have proposed NCO as the precursor to NO formation from cyanogen added to a low-temperature H_2-N_2-O_2 flame (Ref. 7).

According to the proposed reaction scheme, CN radicals form in fuel-lean flames from NH_3 and (more slowly) from HCN, and then react to form NCO:

$$CN + O_2 = NCO + O$$

$$CN + OH = NCO + H.$$

The NCO radical is postulated to be relatively stable and react rapidly with oxygen atoms above the luminous zone to form NO:

$$NCO + O = NO + CO.$$

The most likely path for N_2 formation appears to be the reaction proposed by Mui and Back (Ref. 8):

$$NCO + NCO = N_2 + 2\ CO.$$

The amount of N_2 that can form via the reverse Zeldovich reaction:

$$N + NO = N_2 + O$$

is limited by the competing reaction

$$N + O_2 = NO + O.$$

The mechanism of NO formation in fuel-rich flames may also involve the NCO radical, but there is little evidence relating to this point. The rapid consumption of NO in the fuel-rich flame must result from reaction with hydrocarbon radicals. It can be shown that the reverse Zeldovich reaction

$$O + NO = N + O_2$$

is much too slow to cause the observed consumption of NO. Additional data and theoretical modeling are required to test this somewhat speculative overall mechanism for the formation of fuel NO.

The conclusions from the burner experiments are outlined in Table 13. The major conclusion is that the formation of NO from NH_3 and HCN is a relatively slow process even under fuel-lean conditions where the NO yields are high. The NO forms in lean premixed flames in the same region that CO oxidation occurs.

CONVERSION TO SI UNITS

To Convert From	To	Multiply
atm	pascal (Pa)	1.013×10^5
inch	metre (m)	2.54×10^{-2}
kilocalorie (Kcal)	joule (J)	4184
mil	metre (m)	2.54×10^{-5}
psi	pascal (Pa)	6894
torr	pascal (Pa)	133.3

and

Pressure (Pa) = 9864* + 6894 x Pressure (psig)

REFERENCES

1. Hurd, C. D., and J. I. Simon, J. Amer. Chem. Soc., 84, 4519 (1962).
2. Fristrom, R. M., and A. A. Westenberg, Flame Structure, McGraw-Hill, New York, 1965.
3. De Soete, G., Rev. Inst. Fr. du Petr. Ann. Combustion Liquide, 28(1), 96 (1973).
4. De Soete, G., and A. Querand, Preprint, Inst. Fr. du Petrole, 1973.
5. Bosco, N., Proc. Roy. Soc. (London), 283A, 291 (1965).
6. Davies, P. B., and B. A. Thrush, Trans. Far. Soc., 64, 1836 (1968).
7. Mulvihill, J. N., and L. F. Phillips, 15th Combustion Symposium (International), Tokyo, 1974.
8. Mui, J.Y.P., and R. A. Back, Can. J. Chem., 41, 826 (1963).

---

*At local barometric pressure of 74 torr.

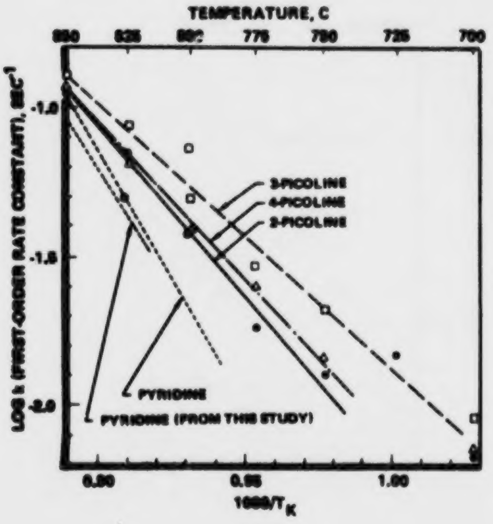

Figure 1. Arrhenius Plots of Pyrolysis Rates for Picolines and Pyridine Obtained by Hurd and Simon

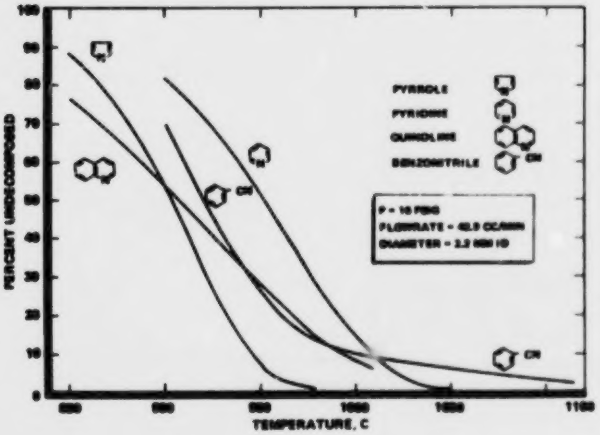

Figure 2. Comparison of Model Compound Decomposition Rates in Helium

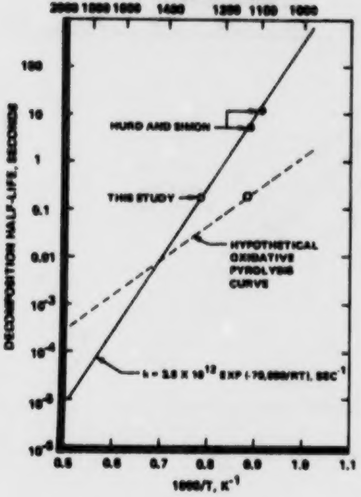

Figure 3. Calculated Decomposition Half-life for Inert Pyrolysis of Pyridine

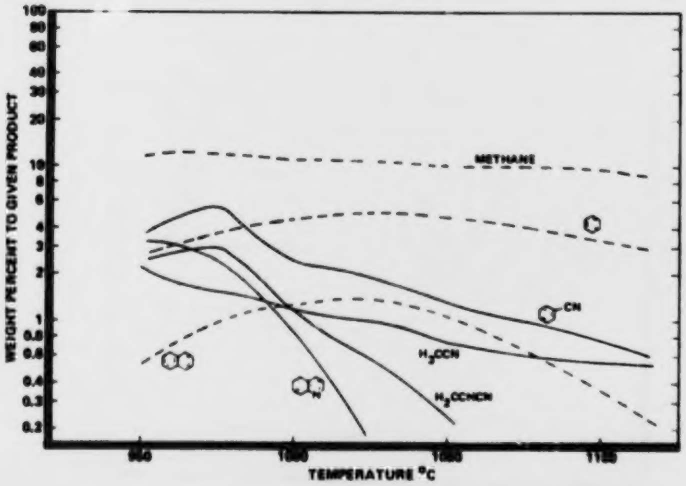

Figure 4. Organic Products From Inert Pyrolysis of Pyridine

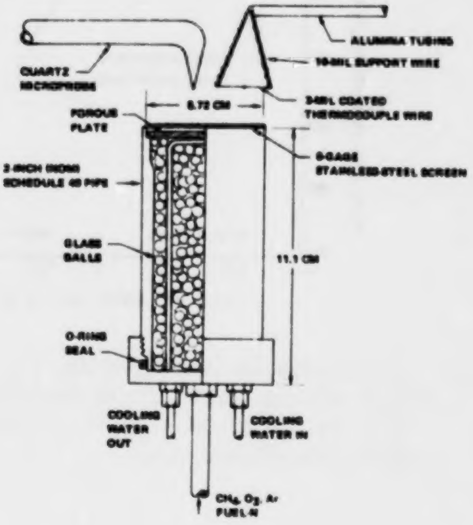
QUARTZ MICROPROBE
ALUMINA TUBING
10-MIL SUPPORT WIRE
3-MIL COATED THERMOCOUPLE WIRE
5.72 CM
POROUS PLATE
8-GAGE STAINLESS-STEEL SCREEN
2-INCH (NOM) SCHEDULE 40 PIPE
GLASS BALLS
11.1 CM
O-RING SEAL
COOLING WATER OUT
COOLING WATER IN
CH4, O2, Ar FUEL N

Figure 5. Flat-Flame Burner

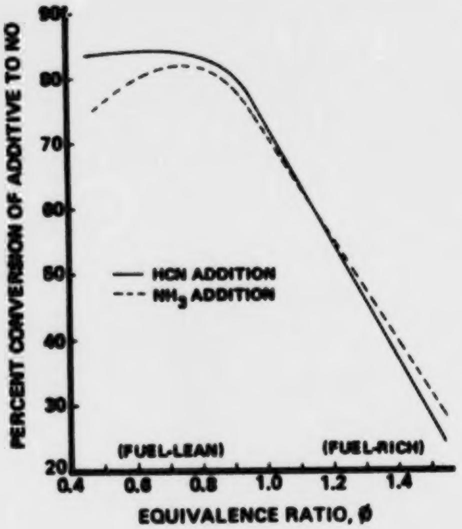

Figure 6. Conversion of Additive to NO_x as a Function of Equivalence Ratio in Screening Experiments ($P = 76$ torr, $DR = 1$, $\dot{w} = 7520$ cc/min and Additive = 2500 ppm)

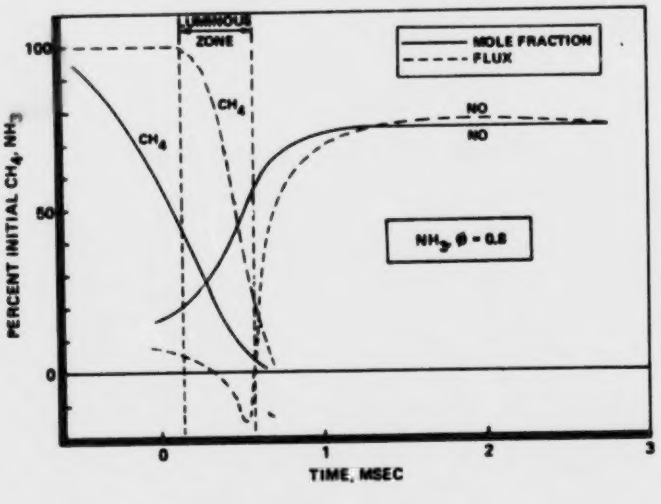

Figure 7. Effect of Diffusion Correction on CH_4 and NO Profiles

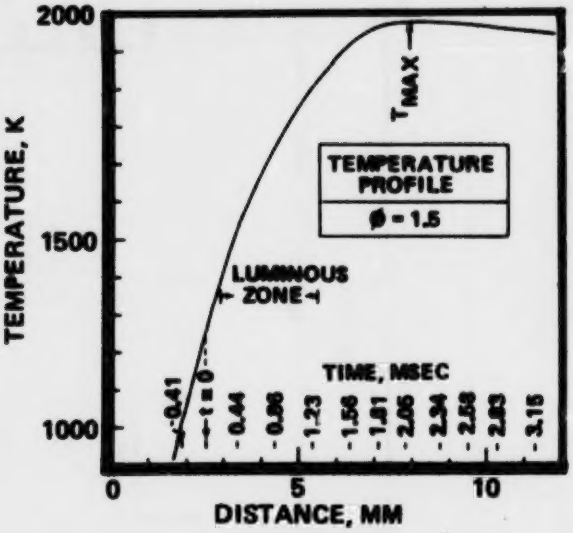

Figure 8. Typical Temperature Profile

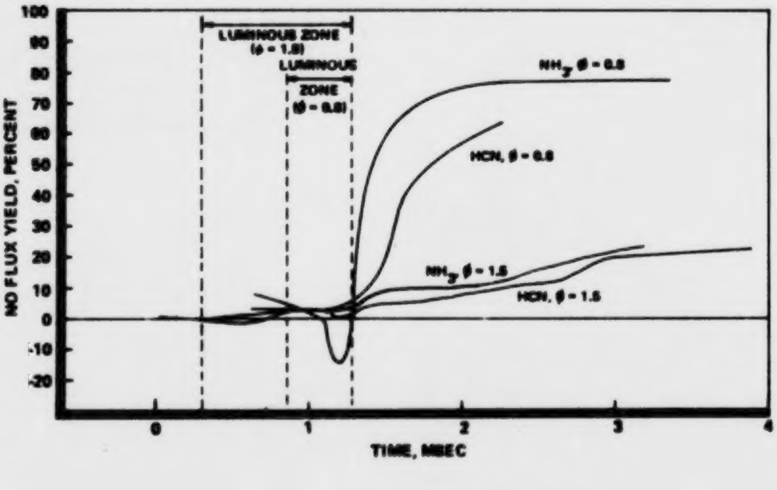

Figure 9. Comparison of NO Flux Yield Profiles at Various Conditions

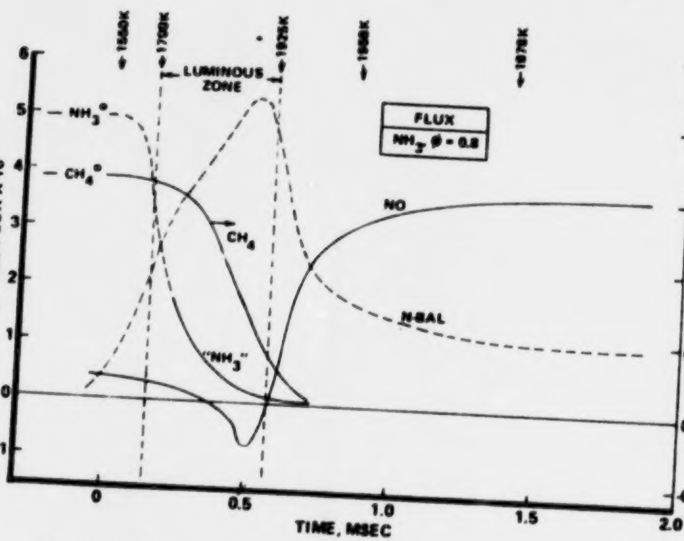

Figure 10. Flux Profiles (NH_3, lean flame)

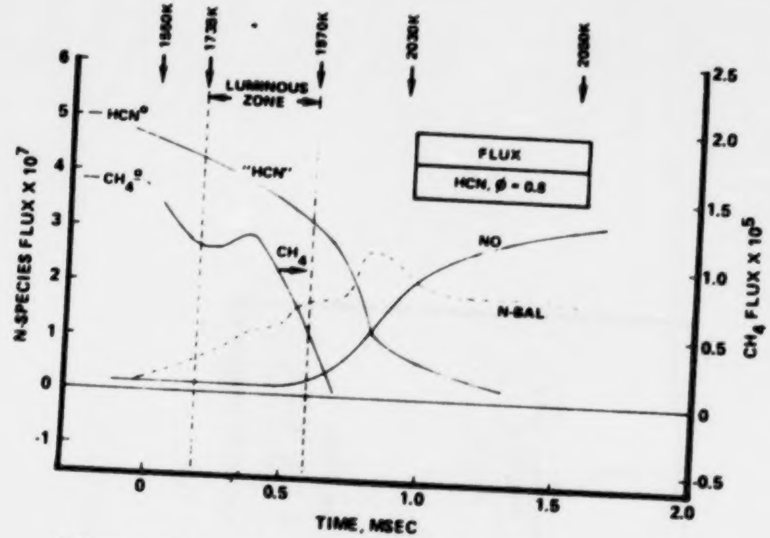

Figure 11. Flux Profiles (HCN, lean flame)

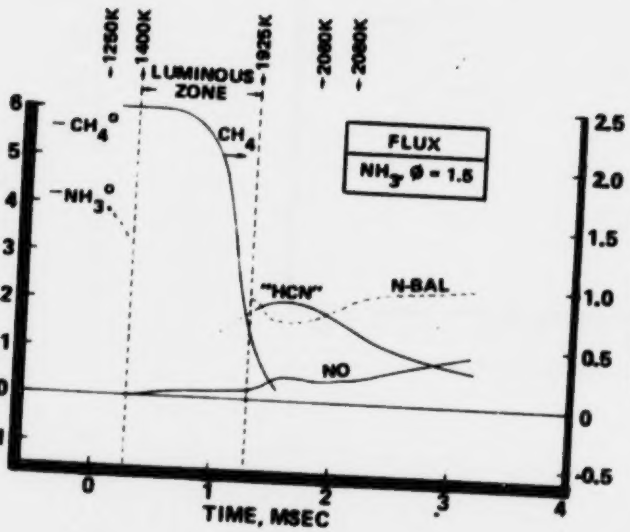

Figure 13. Flux Profiles (NH_3, rich flame)

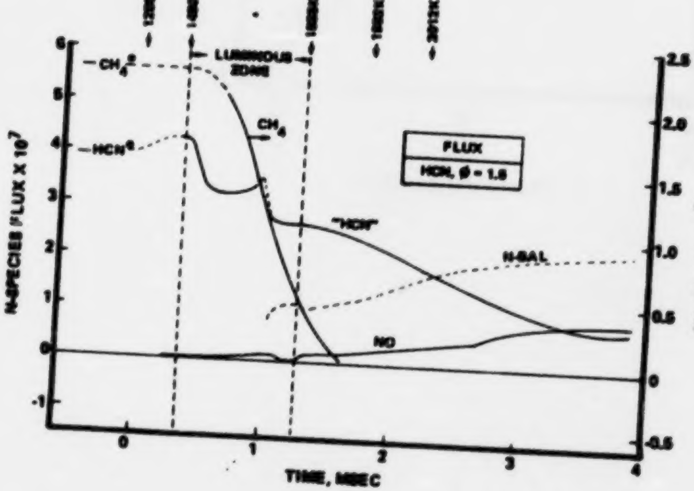

Figure 12. Flux Profiles (HCN, rich flame)

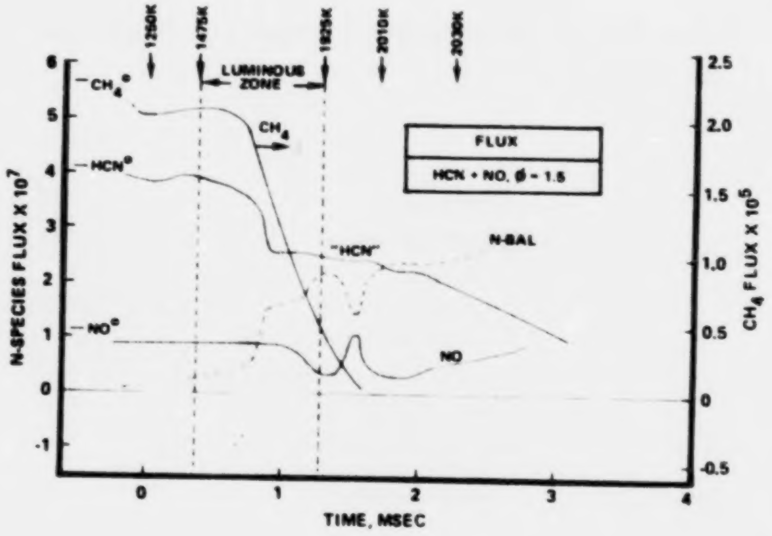

Figure 14. Flux Profiles (NO and HCN, rich flame)

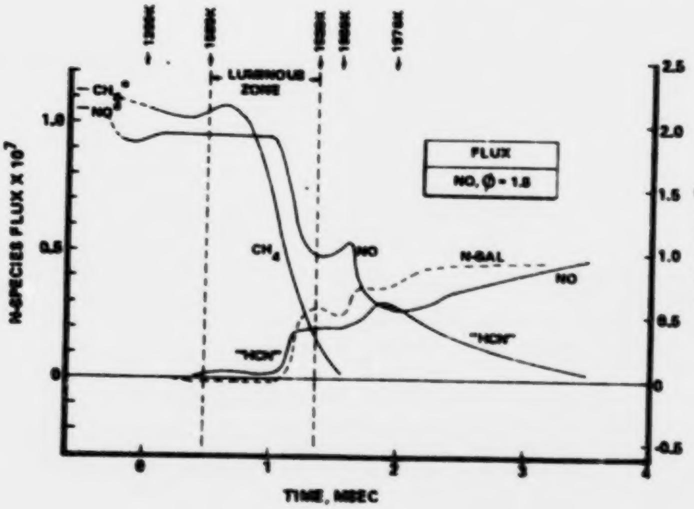

Figure 15. Flux Profiles (NO alone, rich flame)

TABLE I. MODEL COMPOUND PYROLYSIS CONDITIONS

- 850 TO 1100 C
- QUARTZ REACTOR
  - 2 MM ID
  - 1 CC VOLUME
  - 0.5 SEC RESIDENCE TIME
- HELIUM OR HE-O_2 CARRIER GAS
- SAMPLE INJECTION
  - 0.2 μL PREVAPORIZED AT 160 C OR 1 CC CARRIER GAS SATURATED WITH PYRIDINE

TABLE II. KINETIC PARAMETERS FOR MODEL COMPOUND PYROLYSIS

$$-dC/dt = k(C)^N = A \cdot (C)^N \cdot \exp(-E/RT)$$

	N	A, SEC^{-1}	E, KCAL/MOLE
PYRIDINE	1	3.8×10^{12}	70
PYRROLE	1	7.5×10^{15}	85
QUINOLINE	1	2.4×10^{8}	45

TABLE III. HCN YIELD FROM MODEL COMPOUNDS

	TEMPERATURE, C	PERCENT DECOMPOSED	PERCENT N CONVERTED TO HCN*
PYRIDINE	956	(62)	35.6
	960	65	45.7
	959	65	36.8
PYRIDINE	1102	100	106
	1106	100	98
	1107	100	98
	1107	100	105
BENZONITRILE	957	(71)	45
	955	69	53
BENZONITRILE	1107	98.0	82
	1106	98.0	81

*BASED ON N CONTENT OF DECOMPOSED PORTION OF SAMPLE

TABLE IV. NITROGEN BALANCE IN PYRIDINE PRODUCTS

PRODUCT	PERCENT N IN PRODUCT*	
	960 C	1100 C
RESIDUE	49	NM†
HCN	40	102
BENZONITRILE	5	0.5
QUINOLINE	3	< 0.1
ACRYLONITRILE	3	< 0.1
NH_3	< 8	NM
N_2	< 0.1	NM
	≈100	102

*BASED ON N IN DECOMPOSED PORTION OF SAMPLE (65 PERCENT AT 960 C AND 99.9 PERCENT AT 1100 C)

†NM = NOT MEASURED

TABLE V. HCN YIELDS FROM OIL PYROLYSIS

SAMPLE	% N	% S	% N TO HCN		HCN (950 C)/HCN (1100 C)
			(1100 C)	(950 C)	
GULF NO. 6 FUEL OIL (VENEZUELAN CRUDE)	0.43	2.3	32.9	19.4	0.59
GULF NO. 6 FUEL OIL (VARIOUS CRUDES)	0.44	0.73	38.8	23.2	0.60
GULF NO. 6 FUEL OIL (MAINLY CALIFORNIA)	1.41	1.6	23.2	14.5	0.63
CONOCO NO. 6 FUEL OIL	0.3	0.7	42.0	20.4	0.49
"EPA" NO. 6 FUEL OIL (IN HOUSE)	0.22	0.9	37.0	24.6	0.67
NO. 6 FUEL OIL (ULTRASYSTEMS)	0.38	0.3	35.2	17.8	0.51
WILMINGTON CRUDE OIL	0.63	1.6	49.8	30.3	0.61

TABLE VI. PERCENTAGE YIELDS OF $NH_3 + N_2$ FROM OIL PYROLYSIS

OIL SAMPLE	% N	950 C	1100 C
EPA NO. 6	0.22	23.8 ±0.5	28.2 ±1.0
WILMINGTON CRUDE	0.63	10.5 ±0.8	10.9 ±0.2
GULF NO. 6	1.41	5.2 ±0.8	5.9 ±0.4
ULTRASYSTEM NO. 6	0.38	...	16.1

TABLE VII. $NH_3 + N_2$ YIELDS FROM OIL PYROLYSIS CALCULATED AS μg of N_2 RECOVERED PER MG OF OIL

OIL SAMPLE	% N	950 C	1100 C
EPA NO. 6	0.22	0.52 ±0.01	0.62 ±0.02
WILMINGTON CRUDE	0.63	0.66 ±0.05	0.75 ±0.01
GULF NO. 6	1.41	0.73 ±0.10	0.83 ±0.05
ULTRASYSTEM NO. 6	0.38		0.61

TABLE VIII. INORGANIC PRODUCTS OF COAL PYROLYSIS

	955 C	1106 C
PERCENT FUEL-N TO HCN:		
EPA COAL (1.17% N)	20.3, 18.0	29.8, 30.2
IFRF-N (1.8% N)	---	26.2, 22.7
$NH_3 + N_2$, % OF FUEL-N		
EPA COAL (1.17% N)	8.3, 10.5	---
$NH_3 + N_2$, μGM/MG		
EPA COAL (1.17% N)	0.97, 1.23	

TABLE IX. BURNER CONDITIONS (NOMINAL)

- PREMIXED CH_4-O_2-AR FLAT FLAME
- DILUENT RATIO = 1

  $$DR = \frac{AR}{O_2} \bullet \left(\frac{O_2}{N_2}\right) \text{ AIR}$$

- 0.1 ATM
- EQUIVALENCE RATIO (FUEL/AIR), ϕ = 0.5 TO 1.5
- ADIABATIC FLAME TEMPERATURE CALCULATED
  2230 K (ϕ = 1.5) 2300 K (ϕ = 0.8)
- MEASURED TEMPERATURE (CORRECTED FOR RADIATION)
  1980 K TO 2080 K
- VELOCITY AT T_{MAX} = 240 TO 340 CM/SEC
- ADDITIVES HCN (2500 PPM), NH_3 (2500 PPM), NO (625 PPM)
- EQUIVALENT WT % N IN CH_4 FOR 2500 PPM ADDITIVE
  ϕ = 1.5, 1.6% ϕ = 1.0, 2.3% ϕ = 0.8, 2.8%

TABLE X. COMPARISON OF RESULTS OF HCN AND NH_3 ADDITION

ADDITIVE	ϕ = 0.8 (HIGH NO YIELDS)	ϕ = 1.5 (LOW NO YIELDS)
HCN	65% HCN SURVIVES LZ*	70% HCN SURVIVES LZ
	HCN REACTS RAPIDLY ABOVE LZ	HCN REACTS SLOWLY ABOVE LZ
	ALL NO FORMS RAPIDLY ABOVE LZ	ALL NO FORMS SLOWLY ABOVE LZ
	NO FROM INTERMEDIATE	NO FROM INTERMEDIATE AND/OR HCN
NH_3	ALL NH_3 REACTS BELOW TOP LZ	ALL NH_3 REACTS BELOW TOP LZ (ONE-HALF CONVERTED TO HCN)
		"HCN" REACTS SLOWLY ABOVE LZ
	NO FORMS RAPIDLY ABOVE LZ	MOST NO FORMS SLOWLY ABOVE LZ
	ALL NO FORMS FROM INTERMEDIATE	NO FROM INTERMEDIATE AND/OR HCN

*LZ DENOTES LUMINOUS ZONE

TABLE XI. NO ADDITION RESULTS OF DE SOETE

- $C_2H_4 \cdot O_2$ - AR, 1 ATM, PREMIXED
- Ø = 0.7 (2300-2400 K)
  NO = 215 PPM → 160 PPM → 210 PPM

- Ø = 1.5
  NO = 200 PPM → 50 PPM → 75 PPM
  NO = 265 PPM → 60 PPM → 70 PPM
  (HCN = 180 PPM WHEN NO = 60 PPM)

TABLE XII. PROPOSED MECHANISM FOR NO FORMATION FROM HCN AND NH_3

	ΔH_{298}, KCAL/MOLE
$NH_3 \rightarrow NH_2 \rightarrow NH \rightarrow N$	
$N + R^* \rightarrow$ HCN OR CN	
$HCN + O \rightarrow NCO + H$	-1.7
$HCN + OH \rightarrow CN + H_2O$	+4.4
$CN + O_2 \rightarrow NCO + O$	-6.3
$CN + OH \rightarrow NCO + H$	-23.3
$NCO + O \rightarrow NO + CO$	-102.5
$CN + O \rightarrow CO + N$	-77.0
$N + NO \rightarrow N_2 + O$	-75.0
$N + O_2 \rightarrow NO + O$	-31.8
$NCO + NCO \rightarrow N_2 + 2\,CO$	-129.0
$NCO + N \rightarrow N_2 + CO$	-177.5

TABLE XIII. CONCLUSIONS FROM BURNER STUDIES

- MOST HCN SURVIVES THE LUMINOUS ZONE OF LEAN OR RICH FLAMES
- LEAN FLAMES: NO FORMS RAPIDLY JUST ABOVE THE LUMINOUS ZONE FROM A REACTION INTERMEDIATE (PROBABLY NCO). NH_3 REACTS MUCH FASTER THAN HCN. N_2 FORMS FROM NCO.
- RICH FLAMES: ADDED NH_3 REACTS RAPIDLY IN THE FLAME FORMING HCN, SOME NO AND N_2. HCN (ADDED OR FORMED FROM NH_3) REACTS SLOWLY IN THE POST-FLAME GASES FORMING NO IN LOW YIELD.
- IN LEAN FLAMES, FUEL-NO FORMS IN THE SAME REGION AS DOES CO_2. NO FORMS MUCH LATER IN RICH FLAMES.
- NO ADDED TO RICH FLAMES IS PARTLY CONVERTED TO HCN AND OTHER SPECIES IN AND ABOVE THE LUMINOUS ZONE. THE HCN REACTS SLOWLY IN THE POST-FLAME GASES TO FORM NO AND N_2. NO CONSUMPTION IS NOT INITIATED BY REVERSE ZELDOVICH MECHANISM.

1:15 p.m.
Chemical Reactions in the Conversion
of Fuel Nitrogen to NO_x
Dr. Arthur E. Axworthy - Rocketdyne

Q: I think there is some support for your NCO thinking, Art, but I can't remember the reference now . . . .

A: Moba, Hill, and Phillips at the 15th meeting of the Combustion Institute proposed NCO as an intermediate when they added cyenogen into what I believe was a methane flame; at least it was a hydrocarbon flame.

Q: But there is an older reference. Somebody did, I think, a spectroscopic study on the oxidation of HCN where 85% of it went to NCO plus OH.

A: Norish did some work that showed NCO radicals, then Davies and Thrush on the O atom reaction with HCN where they proposed NCO as an intermediate. Yes, there is a lot of background for it.

Q: We were trying to justify the possibility of the NCO to even explain our early NO_2 on the basis that we would not require NO as a precursor. One reaction you don't have there, and maybe it's quite legitimate not to have it, is NCO plus O where if the O_2 came from the back side you may form NO_2 but you'd have to go through a kind of shifting around. It's probably something that Bob wouldn't put up with anyway.

A: He doesn't like, at least on the last meeting, the O atom plus NCO because of the spin conservation.

Q: On your early slides I missed a particular thing. Were you using a platinum resistance wire when you were heating your medium in the quartz, that 1 cc quartz reactor?

A: It was just quartz, the wire was on the outside of the quartz. Just a heated quartz tube. We were passing the helium carrier gas.

Q: Those ups and downs that you have for your flux profiles there...how do you know that for those very reactive intermediates those are really not computational artifacts?

A: I'll try to discuss that. It turns out that the flux curves are extremely sensitive to the shape that you drew through your measured mole fractions; so the method we used, the Tristrum and Westenburg method, is open to these types of artifacts.

Q: The very computational method is dependent on the fact that the species diffuses and doesn't react. Yet those species that you report your profiles for are highly reactive. It is questionable; can they really diffuse as far as this sort of a simple diffusion computation will indicate, and that's where you draw your flux profiles from?

A: No, the method takes that all into account accurately, and we think the diffusion coeffients are absent.

Q: The reactive term is absent in diffusion/velocity computations. All you have there -- the capital V_i -- does not have any reactive term.

A: O.K., right, we correct for that.

Q: So, therefore, for very reactive species, you are really undercompensating for any possibility that the species does not go as far as this indicates.

A: Obviously, if something reacts and the flame is consumed, diffusion can affect where it reacts. I'll agree to that, and the method could be inaccurate in either direction, but I can't see how you say it undercompensates in one direction.

Q: If you compute diffusion velocity, the capital V_i, as was first formulated by Hirshfielder and Curtis, and then taken up in Tristrum and Westenburg's book, has no reactive term in it. In other words, you compute or assume a diffusion coefficient for the species in question. For some of the reactive species, you don't even have anything to take from literature. You just make one up. Well, that's the least of the errors that you produce in there. But when you then compute just the diffusive term there, then, this assumes that the particle is completely free to go as if it would be going in a completely inert surrounding. And that is not the case.

A: Well, so what actually happens is that it will diffuse in and will reach steady state. It'll be reacting, if it does react; or if it doesn't react, it'll just diffuse and reach a concentration where diffusion equals the flow, and it will just level off. But, that's a subtle thing -- I could be wrong. Maybe you could give me some insight into it. But the way I look at it is that it could be off in either direction.

Q: It is a minor point, but on an earlier slide, you speculated that if you had oxygen presence in pyrolysis rather than nitrogen, the rates would change and the activation energies would change. And you show at higher temperatures that the rate of pyrolysis in oxygen is lower than in inert.

A: That was a hypothetical curve assuming that the activation energy was about half.

Q: I'd just like to take a quick poke at this if I can and maybe get a comment from you now or perhaps later. Your mechanism for ammonia addition had the reaction N + R going on to other things. Ammonia breaking down to N, then N + R going on to other things, and then NO eventually forming from some NCO reaction with O_2. Now, my question is why in these flames do you feel that the N atom would preferentially react with some radical R to form these species rather than hydroxyl radical, which has a very rapid rate constant at these temperatures -- on the order of 1×10^{14} cm cubed per mole second? I don't understand why you've left that reaction out of consideration.

A: Well, I didn't show it really -- I showed N atom before we got more reactions, but I had N* on that second one. It could have been NH. It may only go to NH and then react with the CH or C_2. It may never get the N atom.

Q: Well, there are some data on ammonia flames by Kesken and Hughes which suggest that our whole nitrogen pool equilibrates very rapidly in these flames, and if that's the case, then I would question that assumption. I'm having some trouble accepting conceptually your method.

A: The reason we did it that way is because our results showed that. The ammonia decays and NO doesn't form in our flame, so we have to assume that it went by that path. And I say this is just a possible route that has to be modeled.

Q: I would say your experimental results are controversial because there are other data out with ammonia added to flames and ammonia reactions in shock tubes which show the NO coming out much earlier.

A: Yes, I realize that. Sawyer said it can't be, you must make NO when ammonia reacts. But I just have to report what I think we see.

Q: Just a quick comment, Art. Bob Woolfolk and I have done some thermodynamic calculations on solvent refined coal and peradine which overlap, particularly the peradine calculations overlap yours. These are thermodynamic calculations, not kinetic. But these show that thermodynamically, at equilibrium, most of the fuel nitrogen ends up as N_2; 98% of it. There is only about 1 or 2% ammonia and HCN.

PREDICTION OF PREMIXED LAMINAR FLAT FLAME KINETICS, INCLUDING THE EFFECTS OF DIFFUSION

by

R. M. Kendall
J. T. Kelly

Aerotherm/Acurex Corporation
Mountain View, Cal[illegible]nia

W. Steven Lan[illegible]

Environmental Protection Agency
Combustion Research Section
Research Triangle Park, N.C.

Preceding page blank

PREDICTION OF PREMIXED LAMINAR FLAT FLAME KINETICS, INCLUDING THE EFFECTS OF DIFFUSION

R. M. Kendall and J. T. Kelly
Aerotherm Division/Acurex Corporation
Mountain View, California

W. Steven Lanier
Environmental Protection Agency
Combustion Research Section
Research Triangle Park, N.C.

Pollutant formation in flames depends on the interaction of complex chemical and physical processes. Comprehensive theoretical treatment of these processes requires the application of multivariable boundary value problem solution procedures. The PRemixed One-dimensional Flame computer code (PROF), described herein, has been developed to treat this difficult class of boundary value problems in an efficient manner. The technique is based on a matrix or quasilinearization solution procedure which employs predictor and linearized corrector steps to solve the finite difference form of the flame conservation equations. The method includes a general chemical kinetics formulation and unequal diffusion of all species.

Several initial flame system calculations, with up to 42 kinetic reactions and 19 species, are presented to demonstrate the speed, reliability and accuracy of the PROF code in predicting complex combustion and pollutant formation chemistry. In particular, CH_4/AIR and H_2/AIR flames are calculated and their laminar flame velocities are favorably

compared with experimental data. $H_2/O_2/N_2$ and $CO/O_2/N_2/H_2O$ flame calculations with NO_x pollutant formation kinetics are also presented and species concentration results are favorably compared with experimental data. The H_2 and CO flame predictions suggest that the rapid formation of NO in the flame zone is a result of the presence of super-equilibrium O atom concentrations which generate NO through the reaction:

$$N_2 + O \rightarrow NO + N$$

Results of a $CO/O_2/N_2/H_2O$ flame calculation to which NO is initially added are also presented. Agreement of predicted and experimental detailed species concentrations is good. The numerical results indicate that HO_2 plays a major role in flame zone NO, NO_2 kinetics through the reactions:

$$NO + HO_2 \rightarrow NO_2 + OH$$

and

$$NO_2 + O \rightarrow NO + O_2$$

INTRODUCTION

Experimental probing of flat flame burners has yielded considerable information on the formation of pollutants in flames. However, in many cases a clear interpretation of the data is not possible due to (1) lack of fundamental knowledge of elementary reaction steps,

(ii) insufficient amount of specie concentration data, (iii) unknown experimental probe effects, and (iv) obscuration of chemical events due to the complex interaction of chemical and physical (i.e., diffusion) processes. Utilizing elementary kinetic reaction and diffusion data, comprehensive theoretical predictions of flame combustion and pollutant formation processes can be a valuable aid in the interpretation of data previously obscured by effects (ii) to (iv). Further, having established the validity of the theoretical flame model through comparison with data at a single condition, several calculations may be carried out to determine the effect of variation of pressure, preheat or initial species concentrations on pollutant formation in flames. Even though the advantages of theoretical modeling of flames is clear, only recently has significant progress been made towards a comprehensive treatment of flames. This delay is partly due to the difficulty in solving the multivariable boundary value flame problem formed as a result of the mathematical modeling of coupled chemical kinetic and diffusion processes. The PRemixed One-dimensional Flame computer code (PROF), described herein, has been developed to treat this difficult class of boundary value problems in an efficient manner.

Several mathematical approaches have been applied to the solution of the flame equations. In Reference 1 a "shooting" method is described where, beginning at the burned gas state (presumed known), the calculation marches upstream until a match of the unburned state is realized.

For simple systems, this approach can be successful but is unwieldy for complex systems. Others (References 2, 3, 4, 5) have utilized time dependent solutions, seeking the steady state solution as the time asymptote. Although relatively simple to formulate, some of these procedures suffer when complex coupled chemistry is introduced due to the inevitable "stiffness" of the resulting equations. Also, several hundred time steps are required to reach the steady state resulting in lengthy computer runs.

In the treatment of "stiff" boundary value problems, a class of procedures, variously described by "quasilinearization", "Newton-Raphson" or simply "matrix", have achieved considerable success. Wilde (Reference 6) presents such a method and utilizes it with considerable success to calculate several flame velocities. Matrix methods (e.g., Reference 7) have been widely used for boundary and shock layer solutions including coupled field effects, chemical nonequilibrium, and complex interactive boundary conditions.

The efficient matrix procedures applied in the PROF code consist of:

1. Reduction of the differential equations to sets of algebraic equations through finite difference relationships
2. Solution of these algebraic equations by an iterative linearization procedure. This solution is performed simultaneously

over the entire domain of interest and includes additional constraints (eigen-functions) which allows the easy determination of flame speed.

In the next section the PROF code formulation is briefly discussed. Following this, several initial flame system calculations are presented which demonstrate the speed, reliability and accuracy of the PROF code in predicting complex combustion and pollutant formation chemistry.

FORMULATION

The flow model for the PRemixed One-dimensional Flame (PROF) code is depicted in the schematic below. Flow, $\dot{m}$, is presumed to be uniform across plans perpendicular to the axis. Diffusion of species, J_i, and heat, q, occur only in the axial direction.

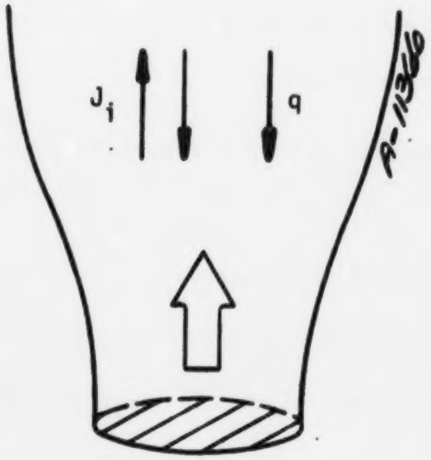

Several simplifying assumptions have been utilized in the PROF code formulation, including steady state one-dimensional flow, perfect gas behavior, mean Lewis number of unity, negligible pressure drop, radiation and thermal and pressure diffusion. Also, heat and species losses at the flameholder are neglected. Applying these simplifying assumptions and standard reduction procedures, the mass, momentum and energy conservation equations can be reduced to a set of equations for the conservation of species and enthalpy along the flame axis. Since the formulation of the enthalpy conservation equation follows a development similar to the species conservation equation, only development of the latter is presented.

The species conservation equation for the flame problem is:

$$\dot{m} \frac{dY_i}{ds} - AW_i = \frac{d}{ds}\left[A\rho D_{im} \frac{dY_i}{ds} \right] \tag{1}$$

where

$\dot{m}$ = total mass flow in flame, gm/sec

A = cross sectional area of flame, cm^2

s = axial distance

X_i = mole fraction of species i

Y_i = mass fraction of species i

W_i = kinetic production rate of species i, $gm/cm^3 sec$

Pm = pressure molecular weight product, atm gm/mole

ρ = density, gm/cm^3

M_i = molecular weight of i

$\mathcal{D}_{im}$ = diffusion coefficient for species i into the mixture of other species

Introducing

r_i = mole kinetic rate of production of species i, gm-mole/cm^{3}sec

α_i = gm-mole of species i per gm of system

and dividing Equation (1) by M_i, yields

$$\dot{m}\frac{d\alpha_i}{ds} - Ar_i = \frac{d}{ds}\left[A\rho\, \mathcal{D}_{im}\frac{d\alpha_i}{ds}\right] \tag{2}$$

In the development of the diffusional flux term, the bifurcation approximation developed in NASA CR-1063 (Reference 8) has been adopted. Basically, the approximation assumes that the contributions of species i and j to the binary diffusion coefficient, $\mathcal{D}_{ij}$, can be separated via:

$$\mathcal{D}_{ij} \simeq \frac{\overline{D}}{F_iF_j} \tag{3}$$

where $\overline{D}$ is a reference diffusion coefficient and F_i and F_j might be termed diffusion factors.* The primary advantage of this approximation is that it permits an explicit formulation for diffusional mass flux, j_i, to be developed from the Stefan-Maxwell relations

---

*Equation (3) is exact for binary and ternary systems and should be thought of as a good correlating function of diffusion data for larger systems.

$$j_i = -\frac{\rho\bar{D}}{\mu_1 F_i}\left[\frac{dY_i}{ds} + \frac{Y_i}{M}\left(\frac{dM}{ds} - F_i\,\frac{d\mu_2}{ds}\right)\right] \tag{4}$$

where $\mu_1 = \sum X_i F_i$ and $\mu_2 = \sum Y_i/F_i$

In calculating multicomponent diffusion this formulation results in a considerable increase of computational efficiency over approaches which apply the full Stefan-Maxwell implicit equations. For Y_i approaching zero or unity or equal F_i's:

$$j_i = -\frac{\rho\bar{D}}{\mu_1 F_i}\frac{dY_i}{ds} = -\rho\mathcal{D}_{im}\frac{dY_i}{ds} \tag{5}$$

and is typically a good approximation otherwise. Equation (5) will be used as the defining relation for $\mathcal{D}_{im}$.

In Equation (3), $\bar{D}$ is typically taken as the self diffusion coefficient of some reference species, e.g., O_2. The F_i are then found to be constants effectively independent of temperature and pressure. From References 8 and 9 the $\bar{D}$ value, with O_2 as the reference species, is found to be

$$\bar{D} = 0.172 \times 10^{-4}\ T^{1.659}/P \quad (\text{cm}^2/\text{sec}) \tag{6}$$

$$= \hat{D}\mu_1 T^{1.659}$$

Introducing Equations (5) and (6) and the normalized distance coordinate $\bar{s}$, defined by $d\bar{s} = ds/A\rho T^{1.659}$, into equation (2)

$$\dot{m}\, d\alpha_i - A^2 r_i \rho T^{1.659} \cdot d\bar{s} = d\left[\frac{\hat{D}}{F_i}\,\frac{d\alpha_i}{d\bar{s}}\right] \qquad (7)$$

The finite difference form of Equation (7) is:

$$\left(\alpha_{i_n} - \alpha_{i_{n-1}}\right) - a_n\left(\frac{Pm}{RT}\, r_i T^{1.659}\right)_n \left(\frac{\sigma_{n-1} + \sigma_n}{2}\right) = b_i\left[\frac{\alpha_{i_{n+1}}}{\sigma_n} + \frac{\alpha_{i_{n-1}}}{\sigma_{n-1}} - \alpha_{i_n}\left(\frac{1}{\sigma_n} + \frac{1}{\sigma_{n-1}}\right)\right] \qquad (8)$$

where n denotes axial grid location index and the composite quantities are defined as

$$a_n \equiv \frac{A^2\delta}{\dot{m}}$$

$$b_i \equiv \frac{\hat{D}}{F_i \dot{m}\delta}$$

$$\bar{s}_{n+1} - \bar{s}_n = \sigma_n \cdot \delta$$

In this equation, well stirred reactor control volumes are assumed to exist between axial stations $\frac{Sn + Sn+1}{2}$ and $\frac{Sn-1 + Sn}{2}$.

Equation (8) can also be arranged to yield an equation for α_{i_n} in terms of a composite convection and diffusion "initial" concentration, $\alpha^o_{i_n}$.

$$\alpha_{i_n} - (Pm)_n \left(\frac{r_i T^{1.659}}{R} \right)_n \frac{a_n(\sigma_{n-1} + \sigma_n)}{2\left[1 + b_i\left(\frac{1}{\sigma_n} + \frac{1}{\sigma_{n-1}}\right)\right]}$$

$$= \frac{\left(1 + \frac{b_i}{\sigma_{n-1}}\right)\alpha_{i_{n-1}} + \frac{b_i}{\sigma_n}\alpha_{i_{n+1}}}{1 + b_i\left(\frac{1}{\sigma_n} + \frac{1}{\sigma_{n-1}}\right)} \equiv \alpha^o_{i,n} \tag{9}$$

It is this set of relations that is solved in the kinetic subroutine to PROF, given values $\alpha^o_{i,n}$ and the necessary state parameters or equations, e.g., an energy equation and assigned pressure. The energy equation can be developed in a similar manner and leads to

$$h_n - a_n \left(\frac{PmT^{0.659}}{R} \frac{Q}{r_n} \right)_n \frac{\sigma_{n-1} + \sigma_n}{2\left[1 + b_i\left(\frac{1}{\sigma_n} + \frac{1}{\sigma_{n-1}}\right)\right]}$$

$$= \frac{\left(1 + \frac{b_i}{\sigma_{n-1}}\right)h_{n-1} + \frac{b_i}{\sigma_n} \cdot h_{n+1}}{1 + b_i\left(\frac{1}{\sigma_n} + \frac{1}{\sigma_{n-1}}\right)} \equiv h^o_n \tag{10}$$

where Q is the heat loss to the environment per unit volume of the reacting gases. Implicit in this equation is the use of a mean Lewis number that leads to a heat flux relation of the form

$$q = -\frac{k}{C_p}\frac{dh}{ds} = \frac{\rho\overline{D}}{F_T\mu_1}\frac{dh}{ds}$$

where F_T is the Lewis number for O_2.

The procedure whereby Equations (9) and (10) are solved with the appropriate kinetic relations is the key to the success of the technique. This procedure is discussed in detail in References 10 and 11 and only a brief description of the approach will be presented herein.

The kinetic production term, r_i, in Equation (9) can be written as:

$$r_i = \sum_m \left(\mu_{im}^P - \mu_{im}^R\right) k_{f_m} \left[e^{\sum \mu_j^R \ell n\, P_j} - e^{\sum \mu_j^P \ell n\, P_j - \ell n\, K_{p_m}} \right] \sum \mu_j^T P_j \quad (11)$$

where for reaction m

k_{f_m} = forward rate constant in moles — atm units

μ_j^T = third body efficiency of species j

K_{p_m} = equilibrium constant for reaction m

In the Newton-Raphson solution procedure for the species conservation Equation (9), the errors in all equations are calculated and a matrix indicating the variation of these errors with respect to all variables is calculated. This matrix is inverted and multiplied by the errors to give a set of variable corrections. When the initial guess is close to the answer, or, the equations are fairly linear, the procedure is rarely defeated. However, as discussed at some length in References 10 and 11 the solution of these equations is subject to several pitfalls which need to be carefully circumvented if efficient and reliable coupled kinetics/diffusion boundary value problem solutions are to be achieved. The most discussed problem is associated with k_{f_m} becoming very large, forcing the bracketed term in Equation (11) to zero to maintain a finite net contribution of the term to the species conservation Equation (9). The forcing of the bracketed term toward zero is equivalent to imposing equilibirum. Through experience, it has been found that a combination of gradual recharacterization of equations and damping has proved highly successful at overcoming the difficulties associated with chemical systems near equilibrium.

A side benefit of the Newton-Raphson procedure is the immediate accessibility of a linearized representation of the chemical equations. Referring to Equation (9), one can obtain its linearized replacement

$$\alpha_{i,C} = \alpha_{i,P} + \left(\frac{\partial \alpha_i}{\partial \alpha_j^o}\right) \left(\alpha_{j,C}^o - \alpha_{j,P}^o\right) + \frac{\partial \alpha_i}{\partial \dot{m}} (\dot{m}_C - \dot{m}_p) \qquad (12)$$

where the subscripts C and P refer to the corrector and predictor steps, respectively, and the repeated j index implies summation.

Thus, the solution procedure becomes:

1. Initial values are selected for all α_i. (To date a crude linear interpolation between the initial and equilibrium compositions are used at all n.)
2. At each n:
   a. Evaluate α_i^o from Equation (9) using only the guessed value of $\alpha_{i,n+1}$.
   b. Solve Equations (9) and (10) in the chemistry routine and evaluate the $(\partial\alpha_i/\partial\alpha_j^o)$ matrix and the $(\partial\alpha_i/\partial\dot{m})$ vector.
3. Formulate the block tri-diagonal matrix resulting from the substitution of Equation (9) into Equation (12), and solve it simultaneously for all $\alpha_{i,C}$ in terms of $\dot{m}_C$.
4. Introduce constraint to determine $\dot{m}_C$ and thus all $\alpha_{i,C}$.
5. Using these $\alpha_{i,C}$ as new guesses, repeat the predictor step (Step 2).

Although solutions have been achieved by simply repeating the predictor step, the addition of the matrix corrector step has reduced the number of required passes by factors of from 2 to 10. The constraint introduced at Step 4 to calculate the mass velocity can be an assigned temperature or an α_i at some grid point. By requiring some value intermediate between the inlet and equilibrium state to exist at a grid point well removed from the inlet, flame speed calculations can be achieved.

The proof of any procedure is in its application to problems. This application is presented in the next section.

DISCUSSION OF RESULTS

Several preliminary calculations are presented which demonstrate the speed, reliability and accuracy of the PROF code in predicting complex combustion and pollutant formation chemistry. Comparison with data is shown to be good for all the results presented.

Even though the calculation of flame speed is not an extremely sensitive function of most reaction rates, correct predictions of flame speed provide a means of indirectly validating the combined diffusive/chemical kinetic procedures which are applied in the code. Of course, a more complete test of the technique is the comparison, with experimental data, of predictions of individual specie concentration distributions through the flame. In the following discussion comparisons of experimental and predicted $H_2/O_2/N_2$ and $CH_4/O_2/N_2$ flame speeds and some $CO/O_2/N_2/H_2O$ flame specie concentrations are presented.

Figures 1 and 2 present the results of a hydrogen rich (50 percent H_2, 10.5 percent O_2, 39.5 percent N_2) premixed laminar flat flame calculation. This flame was studied by Wilde (Reference 6) and provides a convenient point of comparison between flame calculational

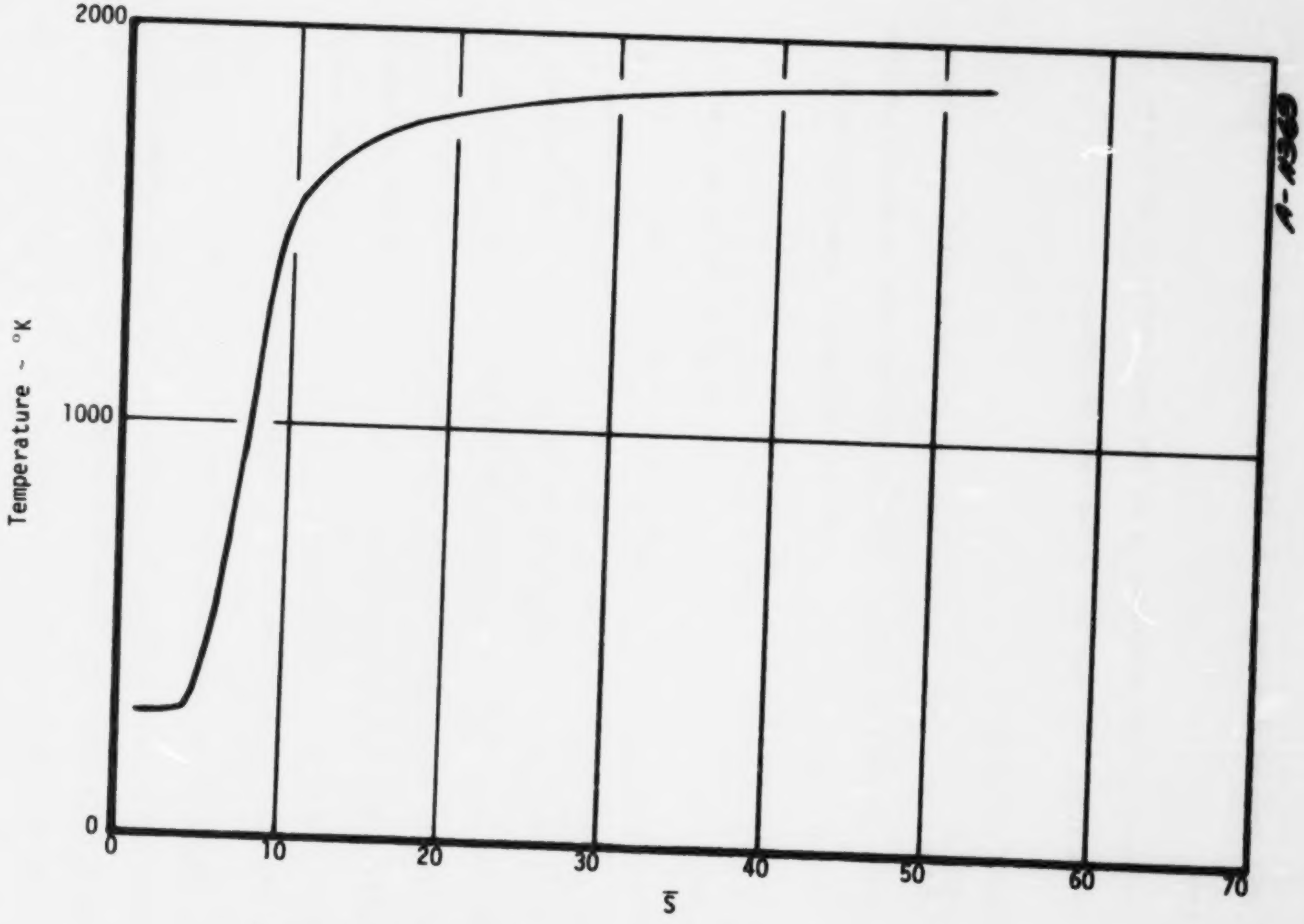

Figure 1. Temperature distribution through a $H_2/O_2/N_2$ flat flame as a function of normalized distance.

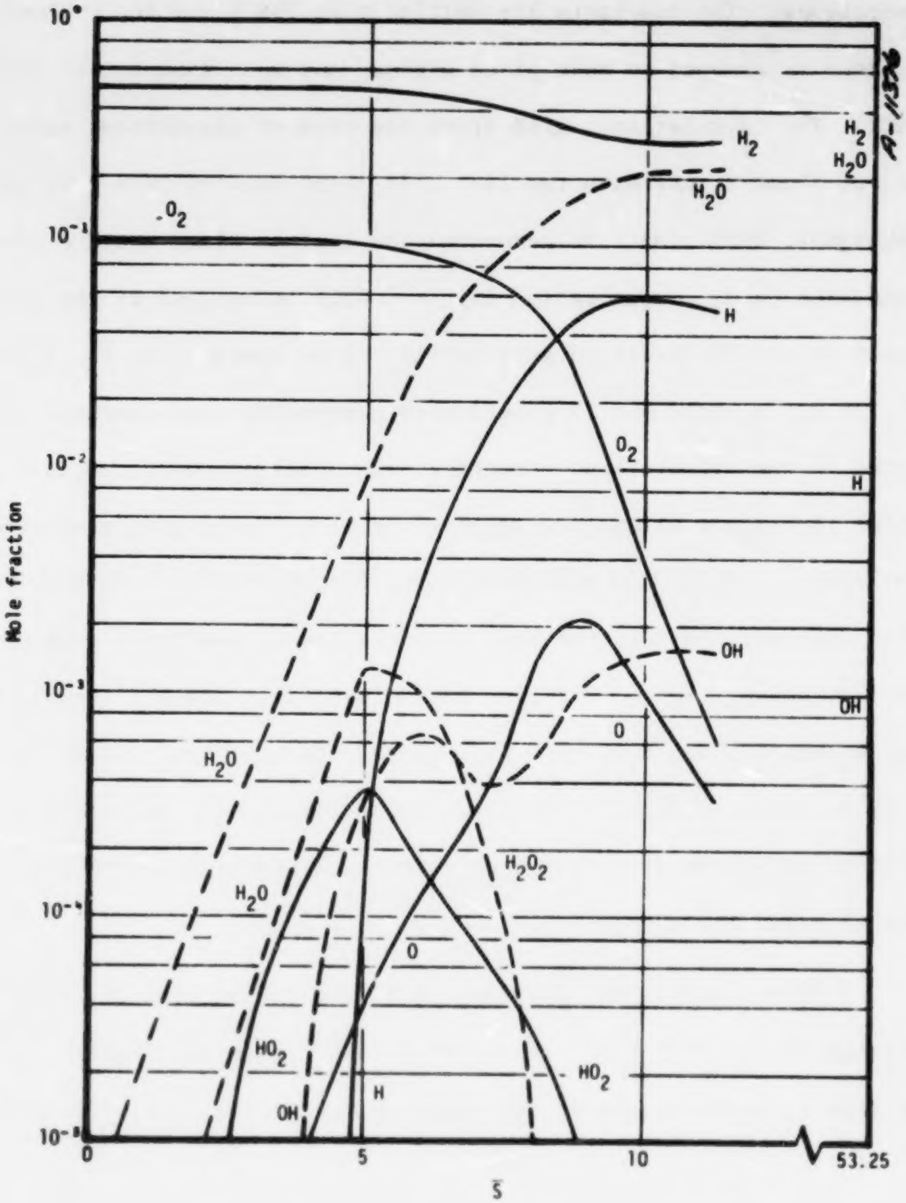

Figure 2. Specie concentrations through a $H_2/O_2/N_2$ flat flame as a function of normalized distance.

techniques. The reactants are initially at 298°K and the combustion process is assumed to take place without any heat loss to the environment. The calculational grid spans the zone of significant reaction (i.e., flame front) with the last grid point located in a zone of negligible diffusion. To determine the laminar flame speed a constraint condition on O_2 concentration ($\alpha_{O_2} = 0.002$) is applied at the 10th point of the 21 specified grid points. Nine species, H, H_2, H_2O, N_2, O_2 HO_2, H_2O_2, O, OH), and 13 kinetically controlled reactions are considered in the calculation. Reaction rate constants were obtained from Wilde (Reference 6) and are given along with their associated reactions in Table 1. Of the 15 reactions specified in Reference 6, one has been deleted* and two combined† to yield the 13 reactions used in the present computation. Diffusion parameters $1/F_i$, for the species H_2, O_2, H, OH, O, HO_2, H_2O_2, H_2O and N_2 are, respectively, 3.0, 1.0, 5.0, 1.5, 1.5, 1.0, 0.8, 1.2, and 1.0. These values were specified by Wilde (Reference 6) and are consistent with the bifurcation approximation values given in Reference 8.

Figure 1 shows the characteristic temperature distribution through the laminar flat flame. From this figure and Figure 2 it can be seen that the length of the rapid change region, i.e., flame front,

---

*A duplicate reaction cast in the reverse manner

†Present technique can include individual third bodies and their efficiencies for a general reaction.

TABLE 1. KINETIC REACTIONS AND ARRHENIUS COEFFICIENTS FOR HYDROGEN/AIR FLAT FLAME
(Reference 6)

					Pre-exp mole-cm-sec	T-exp	Activation Energy kcal/mole	Individual 3rd Body
OH	H2		H2O	H	2.2 +13		5.15	
H	O2		OH	O	2.2 +14		16.8	
O	H2		OH	H	1.7 +13		9.45	
H	H	M	H2		2.00+18	-1.		
O	H2O		OH	OH	5.75+13		18.0	
H	OH	M	H2O		1.30+16		-1.28	H2O 13.077
H	O2	M	HO2		2.40+15		-1.0	
H2	HO2		H2O2	H	9.60+12		24.0	
H2O2		M	OH	OH	1.17+17		45.5	
H	HO2		OH	OH	7.00+13			
H	H2O2		H2O	OH	3.20+14		9.00	
OH	H2O2		H2O	HO2	1.00+13		1.8	
HO2	HO2		H2O2	O2	1.80+12			

is confined to roughly one-fourth of the specified total grid length. This result substantiates the application of the no diffusion boundary condition at the last grid point. Besides the species concentrations illustrated in Figure 2, detailed information on the contributions of kinetic reactions to the individual species mass balances are output for each grid point. Examining this output it appears that, for the reaction mechanism specified:

1. In the early part of the flame (T < 1000°K) significant heat release occurs through the following chain reaction

$$H + O_2 + M \rightarrow HO_2 + M$$

$$H + HO_2 \rightarrow 2OH$$

$$OH + H_2 \rightarrow H_2O + H$$

   where the initial H diffued from the hot flame zone. Also, H_2O_2 plays an insignificant role compared to the above HO_2 mechanism. These observations are in line with other investigators (References 1 and 5).

2. In the latter part of the flame (T > 1000°K) water is produced via the branching mechanism

$$OH + H_2 \rightarrow H_2O + H$$

$$H + O_2 \rightarrow OH + O$$

$$O + H_2 \rightarrow OH + H$$

followed primarily by the recombination

$$H + OH + M \rightarrow H_2O + M$$

This observation is also consistent with other investigators (Reference 5).

These brief observations are an example of the value of the PROF code where, for a given reaction mechanism, an in-depth study of the detailed chemical events can be carried out to elucidate the important reaction paths in the mechanism. A comparable experimental program would require the measurement of all major and minor chemical species through the flame. This latter approach is rarely achieved and then only at great expense.

It should be mentioned that, for the H_2 flame, each sweep of the 21 grid points, including the corrector step, required 6 seconds of computer time on a UNIVAC 1108. If a good first guess is utilized, under five sweeps are required to achieve a fully converged solution, resulting in a total computer run time of about 30 seconds.

The calculated flame speed for this flame was 268 cm/sec which is close to the 241 cm/sec predicted by Wilde (Reference 6). As indicated in his paper, Wilde, besides making several simplifying assumptions, roughly equivalent to those made in the present analysis, also assumes a linear enthalpy variation with temperature. This difference combined with the extraction of a duplicate reaction from his reaction set could easily account for the difference in flame speed noted.

The reaction and species sets for this problem were applied in several calculations to determine flame speed as a function of percent hydrogen and preheat in the unburnt gas. The predictions of 1 atm zero preheat (T_i = 298°K) flame speeds as a function of percent hydrogen are compared in Figure 3 with experimental results from several sources (References 12, 13, 14, 15, 16, 17). Though scatter in the data is wide, the trends of the predicted flame speeds are consistent with those found experimentally. On an absolute level comparison, the predictions fall intermediate to some recent (Reference 13, 17) and past (Reference 15) data. Most of the data shown suffer from inaccuracies due to heat and reactive specie losses to the burner, curvature of the flame surface, smallness of the flame being measured, etc. Gunther and Janisch (Reference 13) suggest that their data might be 10 percent high due to the smallness of the flame measured. Even the recent "double kernel" flame data of Andrews and Bradley (Reference 17) is not completely satisfactory since only 8 of 30 H_2 flame experiments were usable. As indicated by them the data is particularly suspect near the maximum velocity point where they measured a velocity which falls at the high end of their recent compilation of flame speed data (Reference 16). Recognizing the limitations of the experimental data, the present inherent inadequacies of the code (e.g., mean Lewis number of unity,

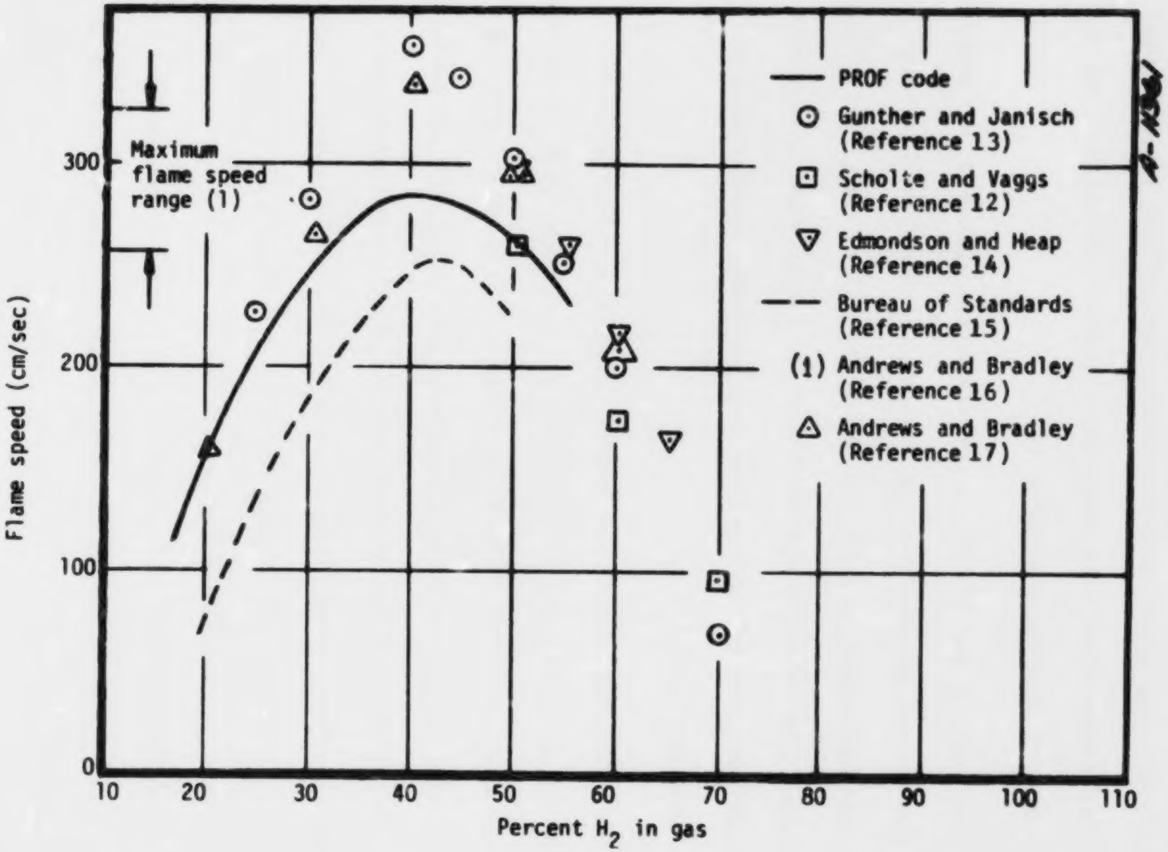

A-11361

Figure 3. Comparison of predicted and experimental H_2/air flame speed variation with percent H_2 in gas.

thermal diffusion neglected) and the limitations of the kinetic models and associated rates input, the agreement between predictions and experimental data is certainly acceptable.

For this problem and all those subsequently discussed, it should be noted that no attempt was made to adjust the reaction rate coefficients or diffusion data in order to bring the calculations into line with the data. The calculations were made to simply demonstrate the capability of the code in calculating complex flame combustion and pollutant formation chemistry.

Several years ago Padley and Sugden (Reference 18) noted that flame speed correlated quite precisely as a linear function of the maximum H concentration found in $H_2/O_2/N_2$ flames. This correlation of flame speed with radical concentration was first suggested by Tanford and Pease (Reference 19) who on much simplified theoretical grounds argued that the flame speed should be proportional to the square root of the radical concentration. Whatever the true form of the flame speed variation with maximum H concentration, it was felt that the comparison of PROF predicted flame speed as a function of maximum H concentration with the data of Reference 18 would provide an interesting further test of codes capability in calculating premixed flame properties.

Figure 4 shows the good correspondence achieved between the measured values and PROF predictions as well as the linear variation* of flame speeds with maximum H atom concentration. The various predicted maximum H atom concentrations were obtained either by adding more H_2 to the initial gas than stoichiometrically needed (equivalence ratios from 2.0 to 3.0) or by preheating the reactants (T initial varied from 298°K to 735°K) for an initial composition equivalence ratio of 2.38.

Having established some confidence in the combustion mechanism of $H_2/O_2/N_2$ flames through favorable comparison of predicted flame speed and maximum H atoms concentration with data, NO_x chemistry was added to the reaction set to determine pollutant formation in flames. Previously, predictions of pollutant formation could only be carried out on post-flame gases where diffusion effects are negligible and available plug flow reactor codes are applicable. These calculations could provide estimates of rates of production of NO in the post-flame gases. However, in many cases the absolute level of NO predicted fell short of the measured value. This difference, which remained constant all along the flame axis, was termed "prompt" NO by Fenimore (Reference 21). Various mechanisms for the rapid formation of NO in the flame

---

*Only stoichiometric or fuel rich flame velocities vary linearly with H atom concentration.

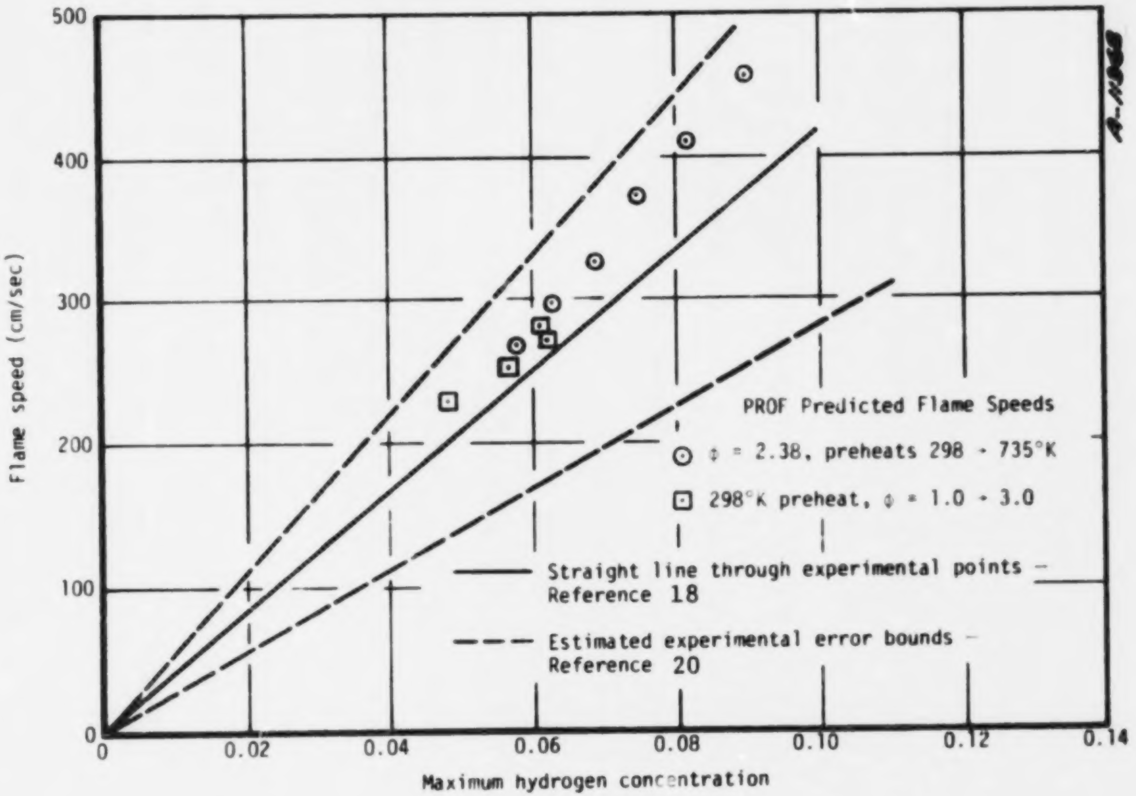

Figure 4. Comparison of predicted and experimental H_2/air flame speed variation with maximum H atom concentration in flame.

zone have been postulated (e.g., see Reference 21). A likely mechanism has been the presence of superequilibrium O atom concentrations in the flame zone which through the reaction

$$N_2 + O \rightarrow NO + N$$

results in a rapid formation of NO. Homer and Sutton (Reference 22) attempted to establish a proof for this conjecture through measurement and calculations of NO concentration through $H_2/O_2/N_2$ flames. They employed a plug flow reactor calculational technique to the post-flame gases. The reaction scheme made use of the burnt gas equilibrium composition plus an assumed O atom concentration.* It was hoped that the specification of O atom concentration would model the effect of superequilibrium O atom concentration on NO formation in the flame zone. The results achieved indicated that the level of NO in $H_2/O_2/N_2$ flames could be accounted for utilizing the O atom overshoot mechanism. However, the O atom specification was arbitrary and the growth rates of NO did not correspond to data very well. Exercising the PROF code with NO_x formation chemistry removes the arbitrariness of the above approach and allows the simultaneous prediction of all species concentrations through the flame zone as well as the post-flame gases. Results of a

---

*The other radical concentrations were determined through exchange reactions.

PROF calculation which utilized the same initial conditions as Homer and Suttons flame 1 are presented in Figure 5 ($H_2/O_2/N_2$ initial volume ratios were 2/1.4/4.6, at 1 atm and 298°K. Reactions and rates applied are given in Table 2). Correspondence with the data is reasonable with the rapid production of NO (i.e., "prompt" NO) clearly shown followed by a more gradual rise indicative of the post-flame NO production. The rapid rise in NO formation follows the peaking of the O atom concentrations and from the detailed PROF output it is evident that the primary production of flame region NO is through the presence of superequilibrium O atom concentration and the reaction

$$N_2 + O \rightarrow NO + N$$

As a further test of the code's capability in predicting complex flame chemistry, an atmospheric pressure stoichiometric methane/air flame calculation was carried out. Fifteen species (CH_4, O_2, CO_2, H_2O, H_2, CO, CH_3, CH_2O, CHO, HO_2, H, O, HO, CH_2, and N_2) were considered along with 30 reactions which model approximately the processes of methane decomposition and partial oxidation, methyl conversion to formaldehyde, formation and depletion of formyl and finally carbon monoxide, hydrogen, oxygen combustion. The reactions and their associated rates, extracted from Reference 23, are given in Table 3. Results of the calculation are given in Figures 6 and 7 where some major specie concentrations are plotted as a function of distance through the flame. The calculated flame speed was 48.7 cm/sec which, considering the

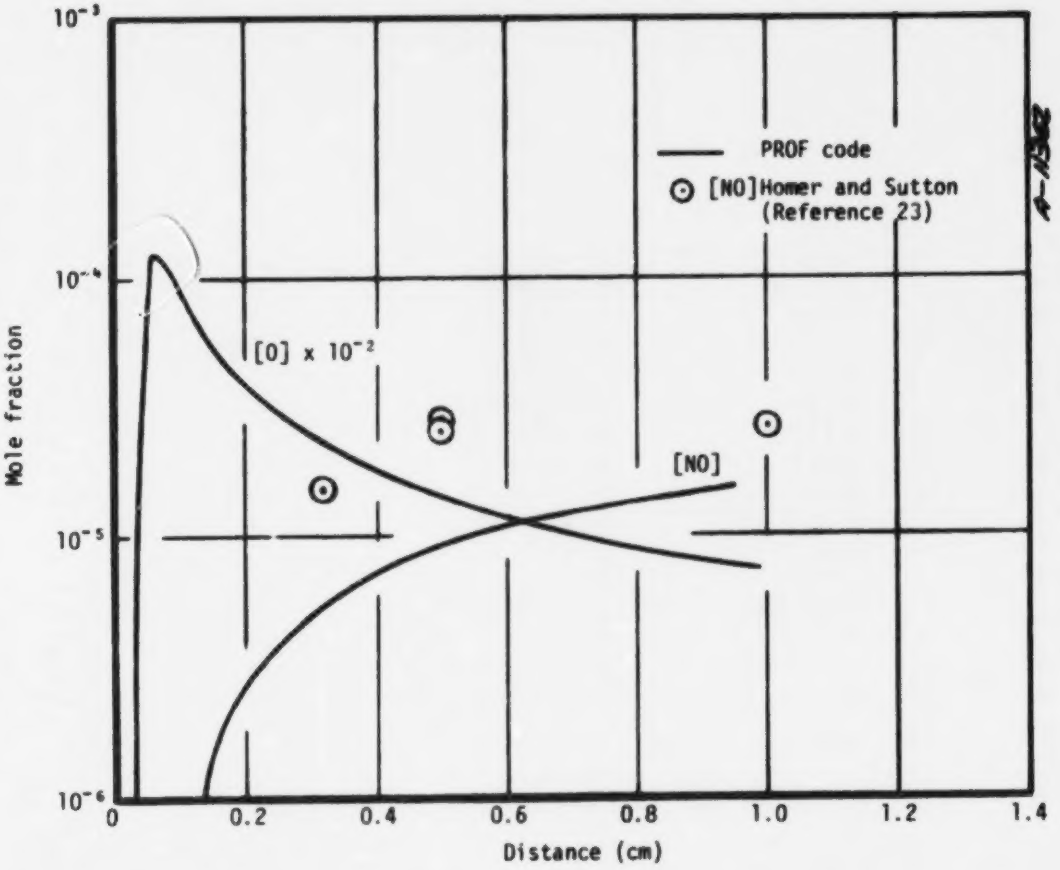

Figure 5. Comparison of predicted and experimental NO concentrations through a $H_2/O_2/N_2$ flame.

TABLE 2. KINETIC REACTIONS AND ARRHENIUS COEFFICIENTS FOR $H_2/O_2/N_2$ FLAMES INCLUDING NO FORMATION

(References 6 and 23)

	Pre-exp. mole-cm-sec	T-exp	Activation Energy kcal/mole
OH +H2 + --> H2O +H	.2200+14	.000	5.1500
H +O2 + --> OH +O	.2200+15	.000	16.8000
O +H2 + --> OH +H	.1700+14	.000	9.4500
H +H +M --> H2 +	.2000+19	-1.000	.0000
O +H2O + --> OH +OH	.5750+14	.000	18.0000
H +OH +M --> H2O +	.1300+17	.000	-1.2800
H +O2 +M --> HO2 +	.2400+16	.000	-1.0000
H2 +HO2 + --> H2O2+H	.9600+13	.000	24.0000
H2O2+ +M --> OH +OH	.1170+18	.000	45.5000
H +HO2 + --> OH +OH	.7000+14	.000	.0000
H +H2O2+ --> H2O +OH	.3200+15	.000	9.0000
OH +H2O2+ --> H2O +HO2	.1000+14	.000	1.8000
HO2 +HO2 + --> H2O2+O2	.1800+13	.000	.0000
OH +N + --> H +NO	.6000+12	.500	8.0000
N +O2 + --> NO +O	.6000+10	1.000	6.3000
N +NO + --> N2 +O	.6310+12	.500	.0000

TABLE 3. KINETIC REACTIONS AND ARRHENIUS COEFFICIENTS FOR METHANE/AIR FLAMES
(Reference 23)

					Pre-exp mole-cm-sec	T-exp	Activation Energy kcal/mole
CH4	O		CH3	HO	1.00+10	1.	8.00
CH4	H		CH3	H2	5.00+10	1.	16.0
CH4	HO		CH3	H2O	3.00+13	0.0	5.00
CH4		M	CH3	H	2.00+17	0.	88.
CH3	HO2		CH4	O2	1.00+11	.5	6.0
CH3	H		CH2	H2	2.00+11	.7	3.0
CH3	HO		CH2	H2O	6.00+10	.7	2.0
CH3	O		CH2O	H	2.00+12	.5	-.30
CH3	O2		CH2O	HO	3.00+13	0.0	30.
CH2O		M	CO	H2	2.10+16	0.0	35.
CH2O	HO		CHO	H2O	3.00+09	1.0	1.0
CH2O	H		CHO	H2	1.25+10	1.0	3.2
CH2O	O		CHO	HO	2.00+11	1.	4.40
CHO	H		CO	H2	3.00+10	1.0	0.0
CHO	O2		CO	HO2	8.00+12	.0	0.0
CHO	CH3		CH2	CH2C	1.50+11	.7	4.0
CHO	CH4		CH2O	CH3	8.00+11	.6	9.0
CHO	HO		CO	H2O	3.00+10	1.	0.00
CHO	O		CO	HO	3.00+11	1.	0.50
CHO		M	CO	H	2.50+20	-1.5	16.8
CH2	O2		CH2O	O	5.00+11	.5	7.0
CO2		M	CO	O	1.00+15	0.0	100.
CO	HO		CO2	H	4.00+09	.5	.0
H	O2	M	HO2		1.50+15	0.0	1.00
H	HO		H2	O	8.00+09	1.	7.00
HO	H2		H	H2O	2.50+13	0.0	5.20
HO	O		H	O2	2.50+13	0.0	0.00
HO	HO		H2O	O	6.00+12	0.0	1.00
H2O		M	HO	H	3.00+15	0.0	105.0
H	O	M	HO		8.00+15	0.0	0.0

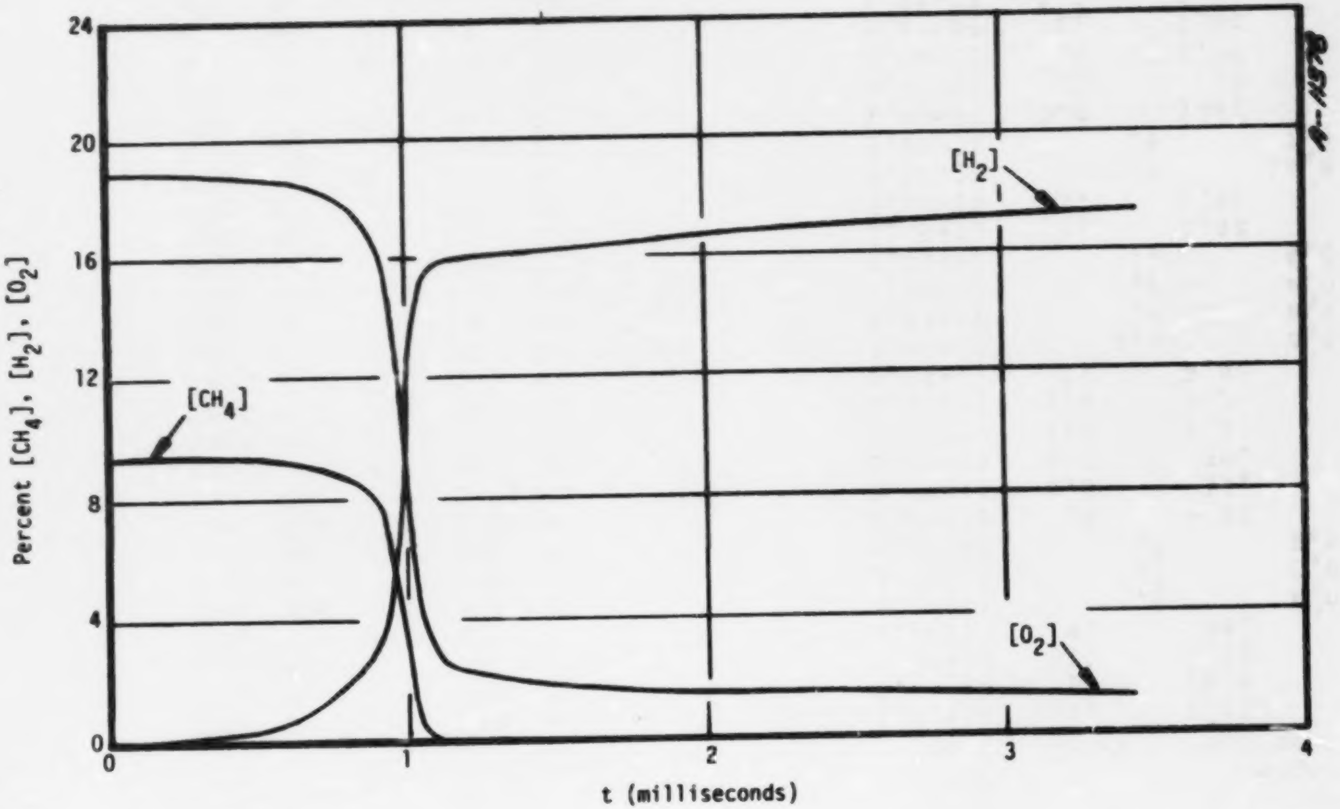

Figure 6. Major specie concentrations through a CH_4/air flame
$P = 1$ atm, $\phi = 1.0$.

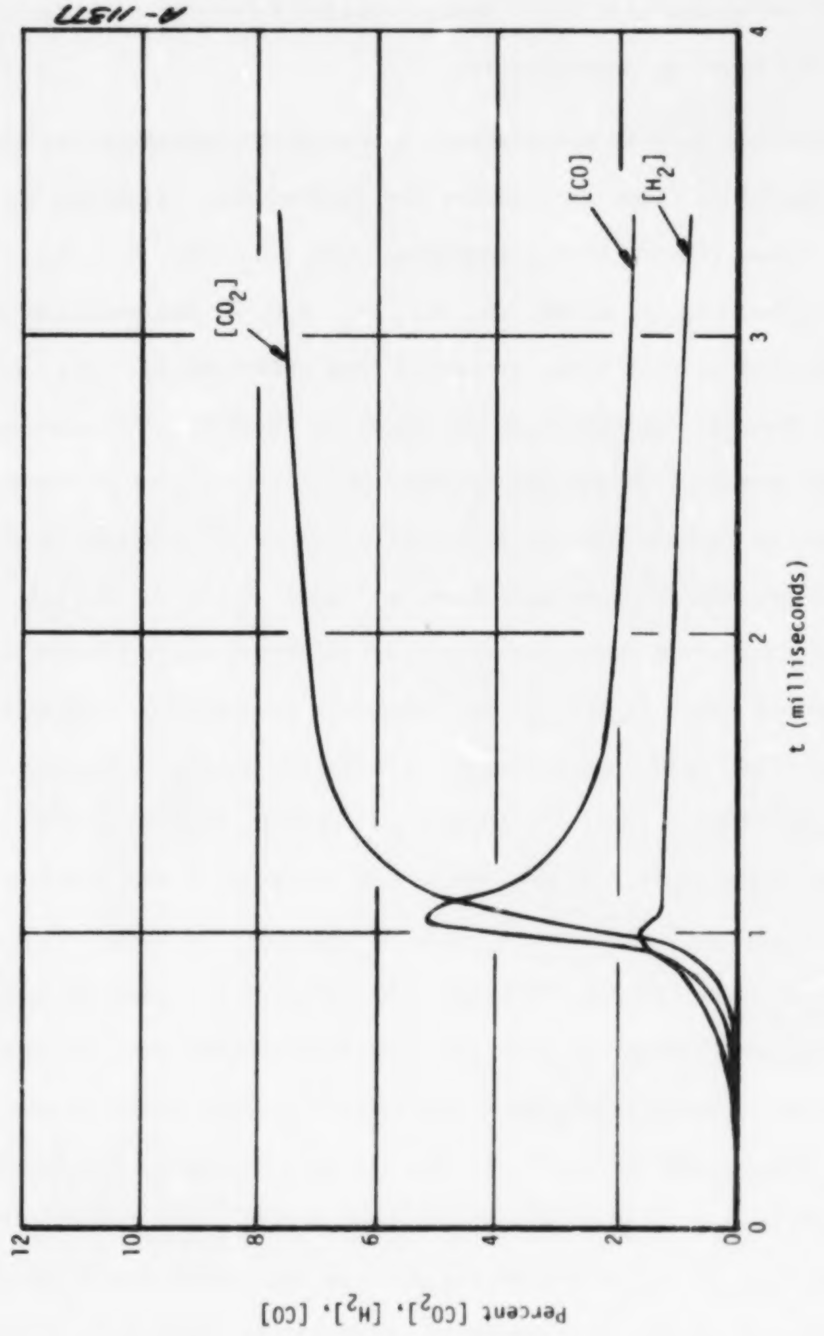

Figure 7. Major specie concentrations through a CH_4/air flame
P = 1, ϕ = 1.0.

uncertainties of the code input data, compares favorably with the value of 42 cm/sec found in Reference 18.

In addition to this calculation, a one-tenth atmosphere stoichiometric methane/air flame calculation was carried out. Nineteen species, including those related to NO_x formation (CH_4, O_2, CO_2, H_2O, H_2, CO, CH_3, CH_2O, CHO, HO_2, H, O, HO, CH_2, N_2, NO_2, N_2O, N, NO), were considered along with 42 reactions, extracted from Reference 23. The reactions and their associated rates are given in Table 4. The calculated flame speed was 62.6 cm/sec which, considering the scatter of experimental data (Reference 24), is a reasonable value. Predicted results from these calculations are presented in Figures 8 and 9. Before proceeding to discuss these results it is necessary to reiterate that the purpose of the calculations was to assess the numerical capabilities of the PROF code. Accordingly, no rigorous attempt has been made to select a definitive set of reaction mechanisms, reaction rates or diffusion coefficients. Indeed, there are a number of reactions not included in the set presented in Table 4, which the authors view as essential to describing NO_x kinetics. In spite of the above disclaimers, this particular PROF calculation predicts several phenomena of significant interest. Shown in Figure 9 are axial profiles of the hydroxyl, oxygen hydrogen, and hydroperoxyl radicals in addition to the NO profile. What is most significant about these profiles are the relative axial positions of appearance of the various radicals. That significant quantities of HO_2 were predicted prior to the appearance of the

TABLE 4. KINETIC REACTIONS AND ARRHENIUS COEFFICIENTS FOR METHANE/AIR FLAMES INCLUDING NO_x FORMATION KINETICS (Reference 23)

					Pre-exp mole-cm-sec	T-exp	Activation Energy keal/mole
CH4	O		CH3	HO	1.00+10	1.	8.00
CH4	H		CH3	H2	5.00+10	1.	10.0
CH4	HO		CH3	H2O	3.00+13	0.0	5.00
CH4		M	CH3	H	2.00+17	0.	88.
CH3	HO2		CH4	O2	1.00+11	.5	6.0
CH3	H		CH2	H2	2.00+11	.7	3.0
CH3	HO		CH2	H2O	6.00+10	.7	2.0
CH3	O		CH2O	H	2.00+12	.5	-.30
CH3	O2		CH2O	HO	3.00+13	0.0	30.
CH2O		M	CO	H2	1.00+12	1.0	65.
CH2O	HO		CHO	H2O	3.00+09	1.0	1.0
CH2O	H		CHO	H2	1.25+10	1.0	3.2
CH2O	O		CHO	HO	2.00+11	1.	4.40
CHO	H		CO	H2	3.00+10	1.0	0.0
CHO	O2		CO	HO2	8.00+12	.0	0.0
CHO	CH3		CH2	CH2O	1.50+11	.7	4.0
CHO	CH4		CH2O	CH3	8.00+11	.6	9.0
CHO	HO		CO	H2O	3.00+10	1.	0.00
CHO	O		CO	HO	3.00+11	1.	0.50
CHO		M	CO	H	2.50+20	-1.5	16.8
CH2	O2		CH2O	O	5.00+11	.5	7.0
CO2		M	CO	O	1.00+15	0.0	100.
CO	HO		CO2	H	4.00+09	.5	.0
H	O2	M	HO2		1.50+15	0.0	1.00
H	HO		H2	O	8.00+09	1.	7.00
HO	H2		H	H2O	2.50+13	0.0	5.20
HO	O		H	O2	2.50+13	0.0	0.00
HO	HO		H2O	O	6.00+12	0.0	1.00
H2O		M	HO	H	3.00+15	0.0	105.0
H	O	M	HO		8.00+15	0.0	0.0
O2		M	O	O	2.50+19	-1.	118.7
H2		M	H	H	2.00+14	0.0	96.
NO	HO2		NO2	HO	2.00+13	0.0	2.86
HO	N		H	NO	6.00+11	.5	.00
N	O2		NO	O	6.00+09	1.	6.30
N	NO		N2	O	1.50+13	.0	.0
NO2		M	NO	O	1.00+16	0.	65.
N2O		M	N2	O	1.00+14	0.0	50.0
N2O	O		N2	O2	1.00+14	0.0	28.0
N2O	O		NO	NO	1.00+14	0.0	28.0
H	N2O		HO	N2	8.00+13	0.0	15.0
NO2	O		NO	O2	1.00+13	0.0	1.0

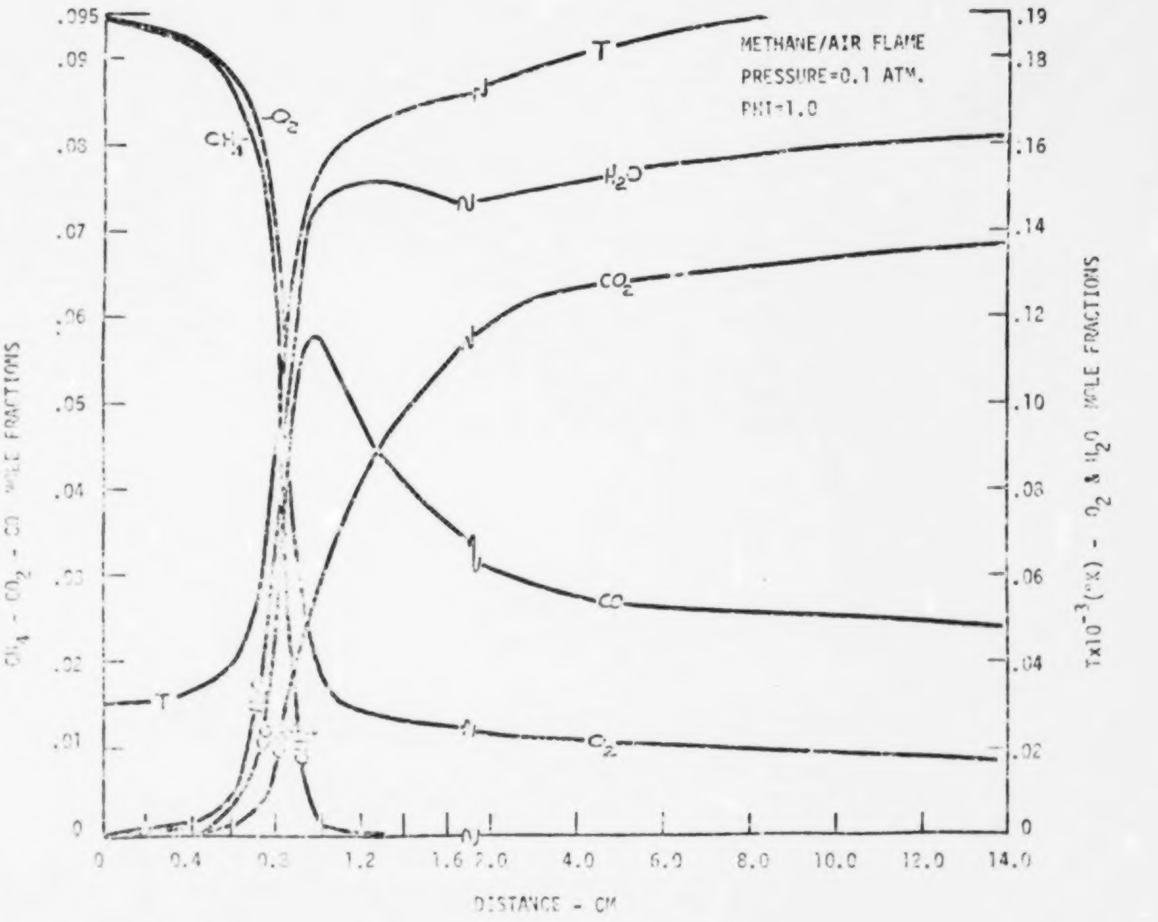

Figure 8. Major specie concentrations and temperature through a CH_4/air flame P = 0.1 atm, ϕ = 1.0.

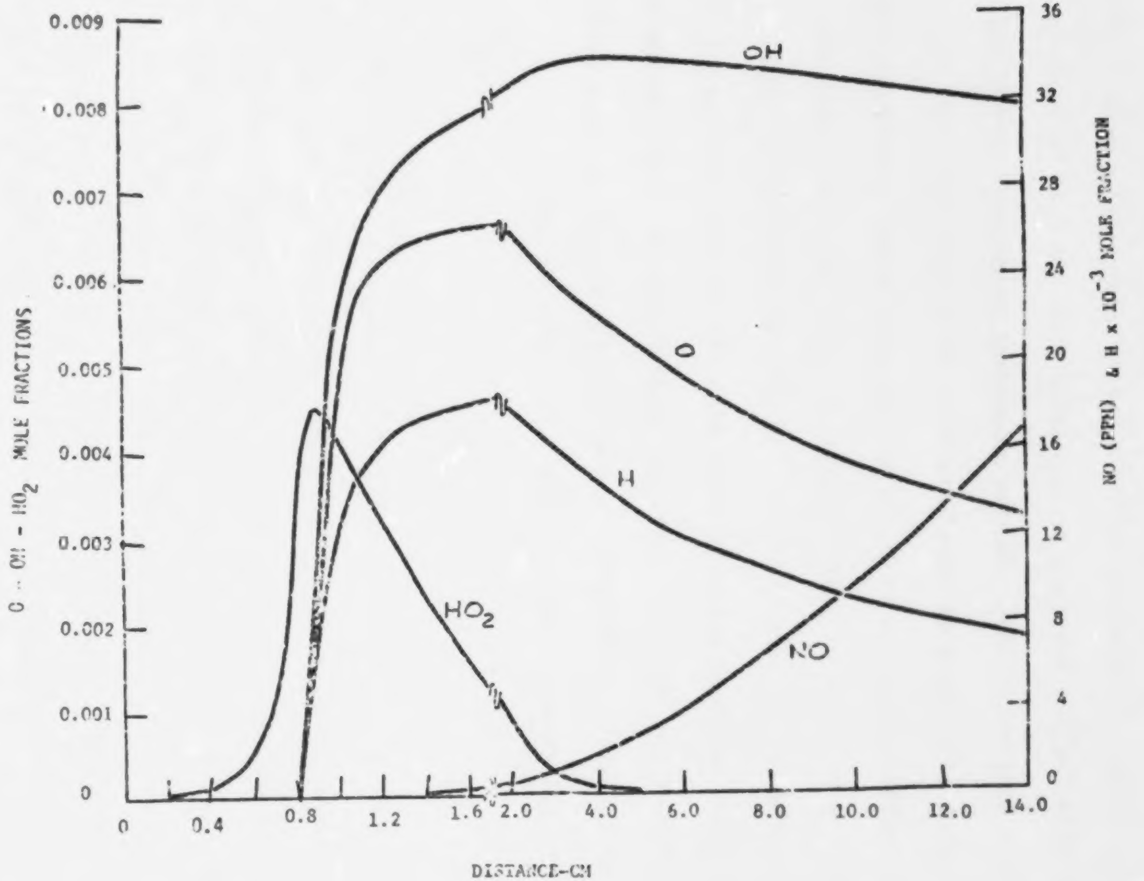

Figure 9. Minor specie concentrations through a CH_4/air flame P = 0.1 atm, ϕ = 1.0.

hydrogen, oxygen or hydroxyl radicals was an unexpected result. This general behavior is, however, in agreement with the data of Peeters and Mahnen (Reference 25). Another phenomena predicted by PROF and in agreement with the data from Reference 25 is that the appearance of substantial quantities of O, H, and OH occur almost simultaneously and that the position of this appearance coincides closely with the point of maximum HO_2 concentration. It should also be noted that these predictions qualitatively agree with the data of Reference 26. Examination of the kinetic production rates yields no clear-cut explanation to the above phenomena. It can be said that the primary path for production of HO_2 is through the third body reaction

$$H + O_2 + M = HO_2 + M$$

Hydrogen atoms are, of course, available through upstream diffusion from the flame front, and from the minute concentrations of H prior to the 0.8 cm location it would appear that the H atoms are rapidly consumed by O_2 as they are stripped from the CH_4 molecule. This would tend to indicate the possibility of describing CH_4 pyrolysis by some type of quasi-global step. This calculation required approximately 47 seconds of UNIVAC 1110 computer time to sweep 21 grid points including the corrector step. A total of four sweeps was required to achieve a fully converged solution resulting in a total computer run time of two and one half minutes.

As mentioned previously, this calculation was performed simply to demonstrate the code's capabilities. The comments made about this particular prediction are, therefore, tentative at best. It should be obvious that the possibilities of the code are many and that phenomena such as those described above can only be predicted by a code which includes diffusional effects in the computations.

To this point in the discussion comparisons of detailed specie concentration predictions with experimental data have been limited to NO concentrations in $H_2/O_2/N_2$ flames. To further substantiate the capability of the code in predicting detailed combustion and pollution chemistry events some predictions of $CO/O_2/N_2/H_2O$ flame specie concentrations are compared with the data of Merryman and Levy (Reference 27). The specie concentrations presented in Figures 10 and 11 correspond to run number 1 of Reference 27. For this case the initial $CO/O_2/N_2/H_2O$ volume ratios were 0.190/0.155/0.638/0.017, respectively. The pressure was 1 atmosphere and the reactants entered the burner at 298°K. For this calculation, 14 species (CO, H_2O, O_2, N_2, CO_2, H, O, HO, H_2, HO_2, NO_2, N_2O, N, NO) and 30 reactions were specified. Table 5 lists the reactions and their associated rates which were extracted from Reference 23. Predictions of CO, CO_2, O_2 and NO species concentrations through the flame are favorably compared with data in Figures 10 and 11. The good agreement between the predicted and measured rates of change of CO, CO_2 and O_2 indicates that, at the very least, gross combustion characteristics are adequately modeled. As in the $H_2/O_2/N_2$ flame, the detailed output indicates that in the early part of the flame HO_2

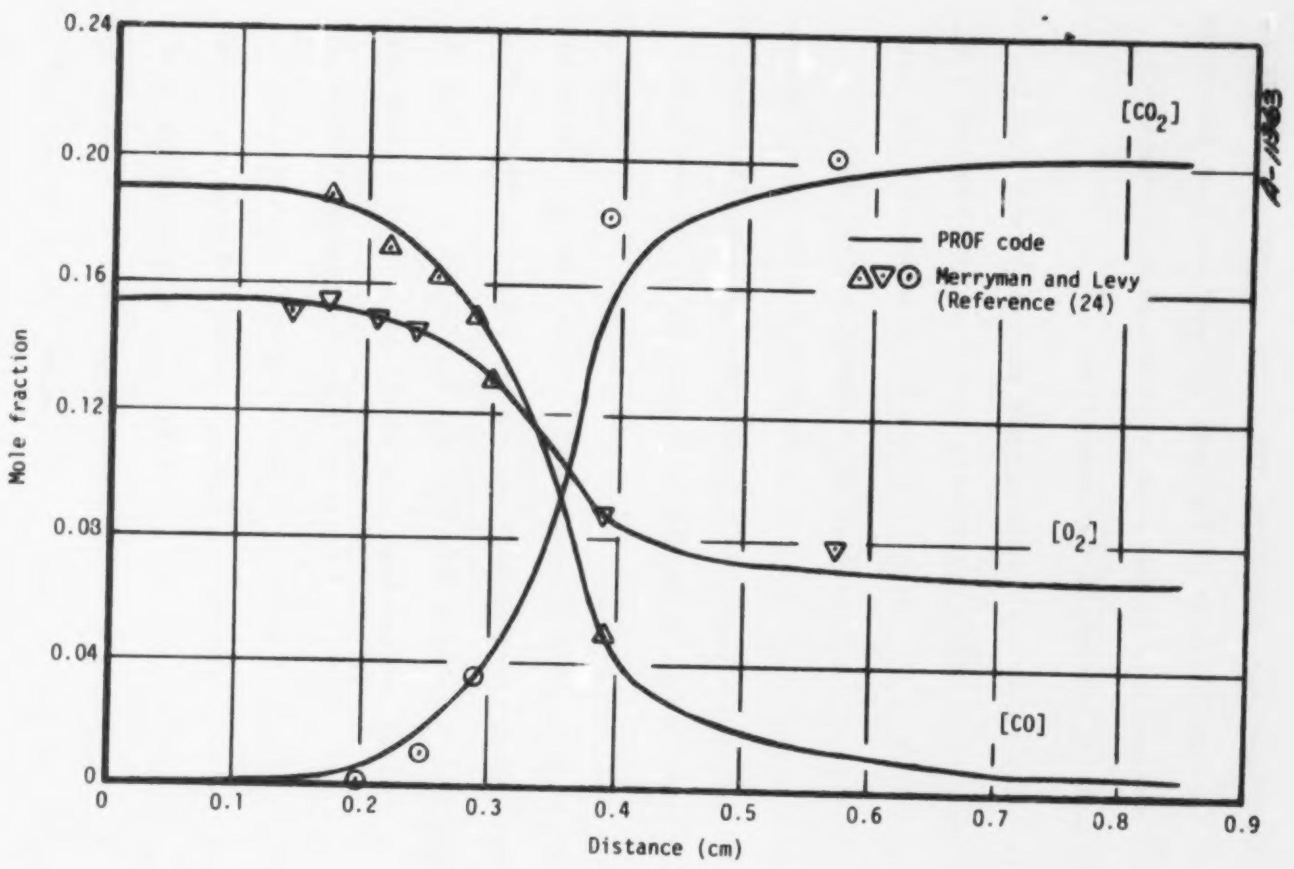

Figure 10. Comparison of predicted and experimental major specie concentrations through a $CO/O_2/N_2/H_2O$ flame.

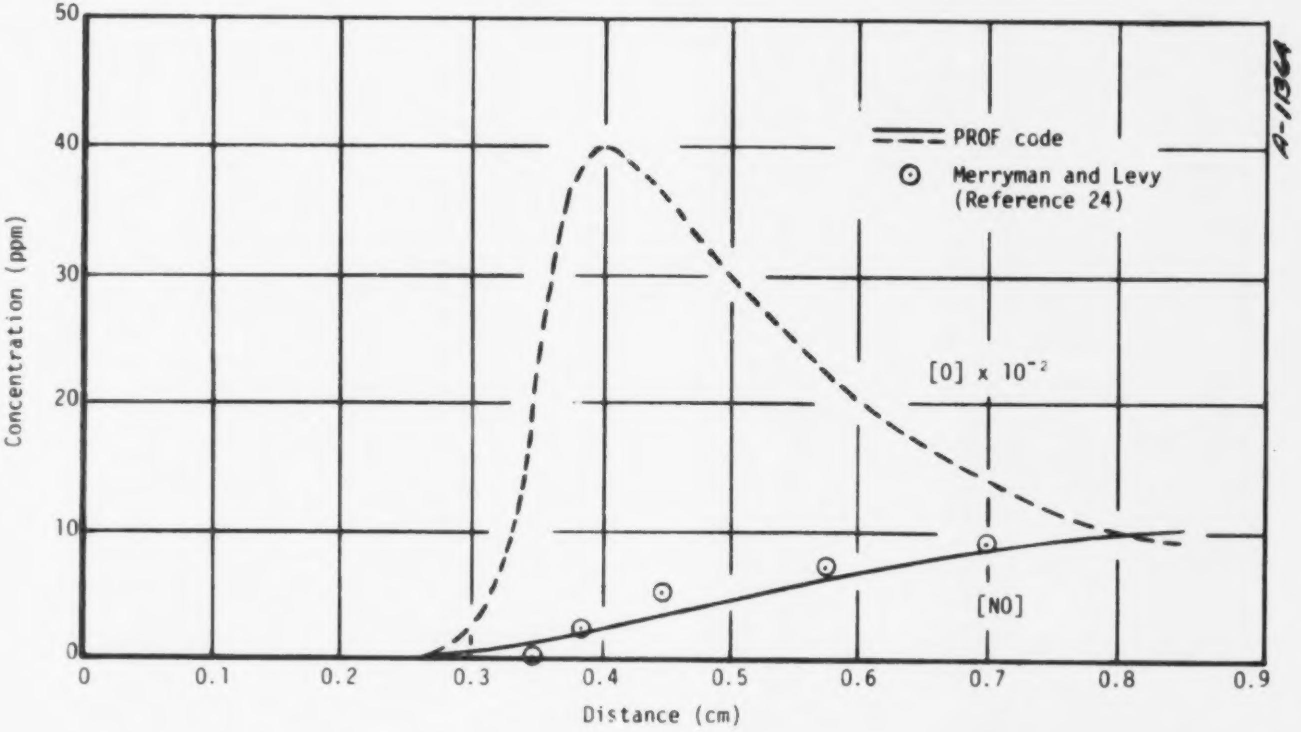

Figure 11. Comparison of predicted and experimental NO concentration through a $CO/O_2/N_2/H_2O$ flame.

TABLE 5. KINETIC REACTIONS AND ARRHENIUS COEFFICIENTS FOR $CO/O_2/N_2/H_2O$ FLAT FLAMES (Reference 23)

					Pre-exp mole-cm-sec	T-exp	Activation Energy kcal/mole
H	+HO2	+	-->	HO +HO	.2500+15	.000	1.9000
HO2	+O	+	-->	HO +O2	.5000+14	.000	1.0000
CO	+HO2	+	-->	CO2 +HO	.1000+13	.000	12.0000
H2	+O2	+	-->	HO +HO	.2500+13	.000	39.0000
CO	+O2	+	-->	CO2 +O	.1000+14	.000	60.0000
O2	+	+M	-->	O +O	.2500+20	-1.000	118.7000
H2	+	+M	-->	H +H	.2000+15	.000	96.0000
H	+O	+M	-->	HO +	.8000+16	.000	.0000
H2O	+	+M	-->	HO +H	.3000+16	.000	105.0000
HO	+HO	+	-->	H2O +O	.6000+13	.000	1.0000
HO	+O	+	-->	H +O2	.2500+14	.000	.0000
HO	+H2	+	-->	H +H2O	.2500+14	.000	5.2000
H	+HO	+	-->	H2 +O	.8000+10	1.000	7.0000
CO	+HO	+	-->	CO2 +H	.4000+10	.500	.0000
H	+O2	+M	-->	HO2 +	.1500+16	.000	1.0000
CO2	+H2	+	-->	CO +H2O	.1000+10	.500	15.0000
H	+HO2	+	-->	H2 +O2	.2500+19	.000	.7000
H	+HO2	+	-->	H2O +O	.1000+14	.000	1.0000
CO	+O	+M	-->	CO2 +	.5050+16	.000	1.8000
NO	+HO2	+	-->	NO2 +HO	.2000+14	.000	2.8600
HO	+N	+	-->	H +NO	.6000+12	.500	8.0000
N	+O2	+	-->	NO +O	.6000+10	1.000	6.3000
N	+NO	+	-->	N2 +O	.1500+14	.000	.0000
NO	+	+M	-->	N +O	.4000+21	-1.500	150.0000
NO2	+	+M	-->	NO +O	.1000+17	.000	65.0000
N2O	+	+M	-->	N2 +O	.1000+15	.000	50.0000
N2O	+O	+	-->	N2 +O2	.1000+15	.000	28.0000
N2O	+O	+	-->	NO +NO	.1000+15	.000	28.0000
H	+N2O	+	-->	HO +N2	.8000+14	.000	15.0000
NO2	+O	+	-->	NO +O2	.1000+14	.000	1.0000

plays a dominant role leading to the formation of CO_2 through the chain reaction

$$H + O_2 + M \rightarrow HO_2 + M$$

$$H + HO_2 \rightarrow 2OH$$

$$CO + OH \rightarrow CO_2 + H$$

In the latter part of the flame the O atom concentration is large enough to produce CO_2 through the reaction

$$CO + O + M \rightarrow CO_2 + M$$

as well as through the reaction

$$CO + OH \rightarrow CO_2 + M$$

Figure 11 shows the good agreement between the predicted and measured NO concentrations as well as the prediction of superequilibrium O atom concentrations in the flame zone. It is primarily the large concentration of O atoms which drives the production of NO in the flame zone through the reaction

$$N_2 + O \rightarrow NO + N$$

Merryman and Levy were interested in NO production through fuel nitrogen oxidation as well as through thermal fixation of air nitrogen. To model the effect of fuel nitrogen on NO production they injected various additives into $CO/O_2/N_2/H_2O$ flames. They postulated that the fuel nitrogen compounds would yield NH and CN type species which subsequently oxidize to NO in the early part of the flame. This NO will then be scavenged by HO_2 radicals producing "early NO_2" which, in the latter part of the flame, is converted back into NO via reactions with excess O atoms. The mechanism for this process can be written

$$NH \text{ (or CN)} + O_2 \rightarrow NO + OH \text{ (or CO)}$$

$$NO + HO_2 \rightarrow NO_2 + OH$$

$$NO_2 + O \rightarrow NO + O_2$$

To test steps 2 and 3 of this mechanism Merryman and Levy in ex-
perimental run three injected NO into a $CO/O_2/N_2/H_2O$ flame. The
hanges in initial conditions from those of run 1 were $CO/O_2/N_2/H_2O$
olume ratios of 0.187/0.154/0.642/0.017 and an initial NO concentra-
ion of 34 ppm. Utilizing the above initial conditions and the species
d reactions of run 1, flame species concentrations were predicted
d are compared with experimental results in Figure 12. Considering
e experimental uncertainties, the inherent inadequacies of the code
the limitations of the kinetic model the agreement is adequate.
detailed output indicates that the proposed kinetic mechanism which
lves NO scavenging by HO_2 and oxidation of the resulting NO_2 via
requilibrium O concentration is indeed operable and yields the
cteristic concentration profile shapes shown in Figure 12.

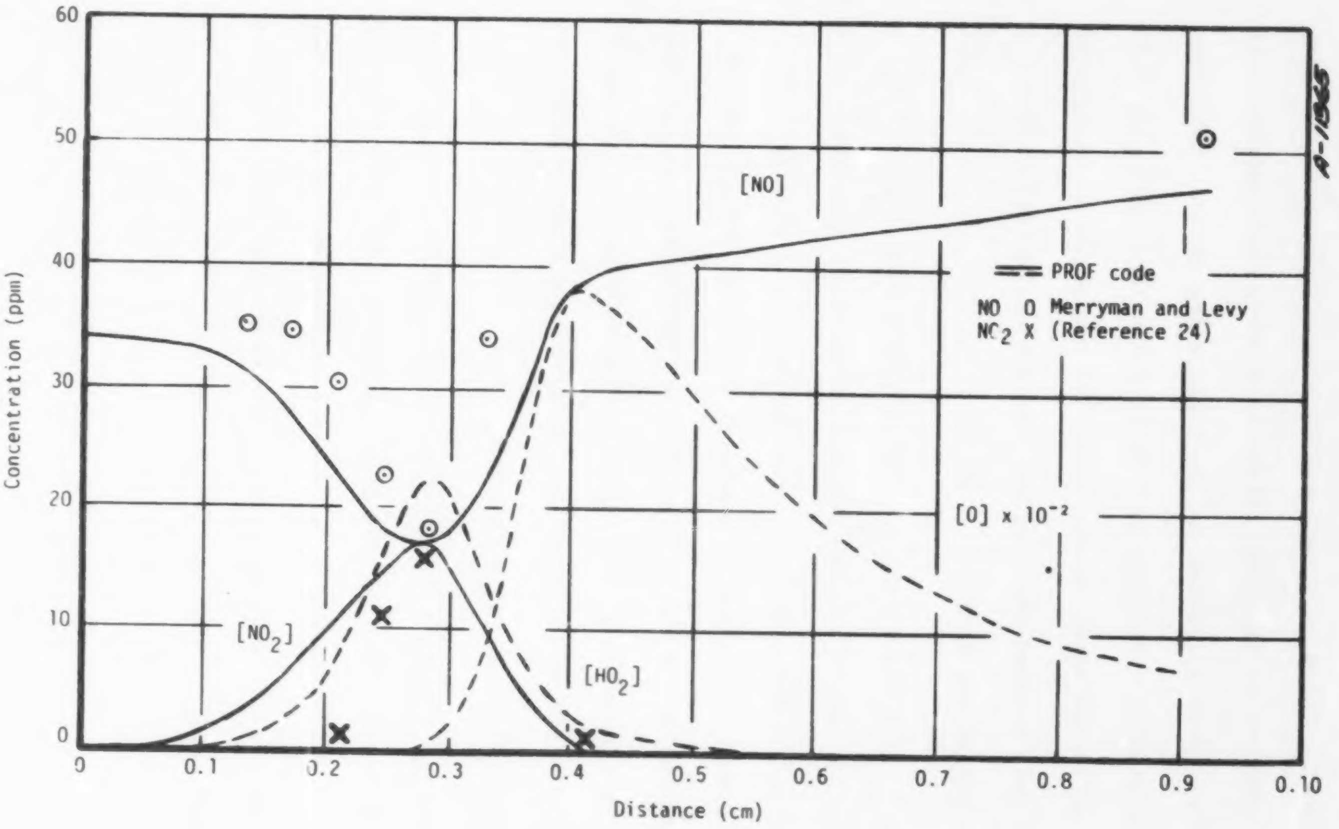

Figure 12. Comparison of predicted and experimental NO_2 and NO concentrations through a $CO/O_2/N_2/H_2O$ flame.

Before leaving these computations, it should be pointed out that they will be repeated in the near future in a series of computer runs which concentrate more attention on the kinetic mechanisms, reaction rates, and diffusional coefficients. It is fully expected that these computations will shed light on the prompt NO and early NO_2 questions as well as to help unravel the complex reaction mechanisms of the hydrocarbon ignition and burnout.

In summary, several preliminary calculations have been carried out to demonstrate the speed, reliability and accuracy of the PROF code in predicting complex combustion and pollutant formation chemistry in flames. In general, the good agreement of predicted quantities and those measured has been encouraging. Further improvement in agreement might be easily accomplished through code modifications to include (i) thermal diffusion (ii) heat losses to the environment (iii) heat and reactive specie losses to the flameholder.

The brief experiences of this program have brought out the power and usefulness of the PROF calculational technique in elucidating the important steps in a proposed flame reaction mechanism. Also, it has been demonstrated that PROF predictions can be an important complement to experimental complex chemistry flame studies.

REFERENCES

1. Dixon-Lewis, G., "Flame Structure and Flame Reaction Kinetics, V. Investigation of Reaction Mechanism in a Rich Hydrogen + Nitrogen + Oxygen Flame by Solution of Conservation Equations," Proc. Roy Soc. Lond., A, Volume 317, 1970, pp. 235-263.

2. Bledjian, L., "Computation of Time-Dependent Laminar Flame Structure," Combustion and Flame, Volume 20, 1973, pp. 5-17.

3. Spalding, D. B., et al., "A Calculation Procedure for the Prediction of Laminar Flame Speeds," Combustion and Flame, Volume 17, 1971, pp. 55-64.

4. Stephenson, P. L. and Taylor, R. G., "Laminar Flame Propagation in Hydrogen, Oxygen, Nitrogen Mixtures," Combustion and Flame. Volume 20, 1973, pp. 231-244.

5. Eberius, K. H., et al., "Experimental and Mathematical Study of a Hydrogen-Oxygen Flame," Thirteenth Symposium (International) on Combustion, The Combustion Institute, 1971, pp. 713-721.

6. Wilde, K. A., "Boundary-Value Solutions of the One-Dimensional Laminar Flame Propagation Equations," Combustion and Flame, Volume 18, 1972, pp. 43-52.

7. Kendall, R. M. and Bartlett, E. P., "Nonsimilar Solution of the Multicomponent Laminar Boundary Layer by an Integral Matrix Method," AIAA Journal, Volume 6, No. 6, June 1968.

8. Bartlett, E. P., Kendall, R. M., and Rindal, R. A., "A Unified Approximation for Mixture Transport Properties for Multicomponent Boundary Layer Applications," Aerotherm Corporation Final Report 66-7, Part IV (also NASA CR-1063), March 14, 1967.

9. Hirschfelder, J. O., Curtiss, C. F., and Bird, R. B., Molecular Theory of Gases and Liquids, Second Printing, Corrected, with notes added, John Wiley and Sons, Inc., New York, 1964.

10. Kendall, R. M., "An Analysis of the Coupled Chemically Reacting Boundary Layer and Charring Ablator, Part V, A General Approach to the Thermochemical Solution of Mixed Equilibrium-Nonequilibrium, Homogeneous or Heterogeneous Systems," NASA CR-1064, June 1968.

11. Kendall, R. M. and Kelly, J. T., "Premixed One-Dimensional Flame Code — Its Formulation Manipulation and Evaluation," Aerotherm Corporation Final Report TR-75-158, July 1975.

12. Scholte, T. G. and Vaags, P. B., "Combustion and Flame," Volume 3, 1959, p. 495.

13. Gunther, R. and Janisch, G., "Measurements of Burning Velocity in a Flat Flame Front," Combustion and Flame, Volume 19, 1972, pp. 49-53.

14. Edmondson, H. and Heap, M. P., "The Burning Velocity of Hydrogen-Air Flame," Combustion and Flame, Volume 16, 1971, pp. 161-165.

15. "Flame Velocities of Various Gas-Air Mixtures," Bureau of Standards J. Research, 17, 7-43, 1936.

16. Andrews, G. E. and Bradley, D., "Determination of Burning Velocities: A Critical Review," Combustion and Flame, Volume 18, 1972, pp. 133-153.

17. Andrews, G. E. and Bradley, D., "Determination of Burning Velocity by Double Ignition in a Closed Vessel," Combustion and Flame, Volume 20, 1973, pp. 77-89.

18. Padley, P. J. and Sugden, T. M., "Chemiluminescence and Radical Recombinations in Hydrogen Flames," Seventh Symposium (International) on Combustion, Butterworths, London, 1959, p. 235.

19. Tanford, C. and Pease, R. N., Journal of Chemical Physics, 15, 1947, p. 861.

20. Brown, N. J., Fristrom, R. M., and Sawyer, R. F., "A Simple Premixed Flame Model Including Application of H_2 + Air Flames," Combustion and Flame, Volume 23, Number 2, October 1974.

21. Fenimore, C. P., "Formation of Nitric Oxide in Premixed Hydrocarbon Flames," Thirteenth Symposium (International) on Combustion, The Combustion Institute, 1971, p. 373.

22. Homer, J. B. and Sutton, M. M., "Nitric Oxide Formation and Radical Overshoot in Premixed Hydrogen Flames," Combustion and Flame, Volume 20, 1973, pp. 71-76.

23. Waldman, C. H., Wilson, R. P., Jr., and Maloney, K. L., "Kinetic Mechanism of Methane/Air Combustion with Pollutant Formation," EPA-650/2-74-045, June 1974.

24. Andrews, C. E. and Bradley, D., "The Burning Velocity of Methane-Air Mixtures," Combustion and Flame, Volume 19, 1972, pp. 275-288.

25. Peters, J. and Mahnen, G., "Reaction Mechanisms and Rate Constants of Elementary Steps in Methane-Oxygen Flames," Fourteenth Symposium (International) on Combustion, The Combustion Institute, Pittsburgh, 1973, pp. 133-146.

26. Lazzaru, C. P., Biordi, J. C., and Papp, J. F., "Concentration Profiles for Radical Species in a Methane-Oxygen-Argon Flame," Combustion and Flame, Volume 21, 1973, pp. 371-382.

27. Merryman, E. L. and Levy, A., "NO_x Formation in CO Flames," in preparation, 1975.

2:10 p.m.

Prediction of Premixed Laminar Flat Flame Kinetics Including the Effects of Diffusion

Dr. Robert M. Kendall, Aerotherm Acurex

Q: Do you have any feeling, Bob, for how important your diffusion correction is? If you were to make the same run, setting all your diffusion coefficients equal to 0, would your predicted curves change very much?

A: Well, actually, in the problems that we were doing, we were usually looking for a flame speed, and there's no way you can solve these problems without diffusion. If diffusion did not exist, the reactions would never get started. So, if there was no diffusion, the thing would never light. Still, there would be no transfer of energy upstream. You have to have the diffusion in there. You could, perhaps, go in and take a measured temperature, and impose that, and leave out the energy equation. And, in that case, you would predict things I would think would be radically different, because the hydrogen atom diffusion upstream is a very important ignition mechanism. Without that, I think quite a few things would be different.

June 1975

ESTIMATION OF RATE CONSTANTS AS A FUNCTION OF TEMPERATURE FOR THE REACTIONS $X + YZ \rightleftharpoons XY + Z$ WHERE X, Y, AND Z ARE ATOMS OF THE ELEMENTS CARBON, HYDROGEN, NITROGEN, OXYGEN, AND SULFUR

Running Title: ESTIMATION OF RATE CONSTANTS

by

S. W. Benson, Robert Shaw, and R. W. Woolfolk

Physical Sciences Division
Stanford Research Institute
Menlo Park, California 94025

ABSTRACT

Estimated rate constants for some reactions of the type $X + YZ \rightarrow XY + Z$ where X, Y, and Z are atoms of the elements carbon, hydrogen, nitrogen, oxygen, and sulfur have been compared with rate constants measured by others. This work completes earlier comparisons for the above reaction where X, Y, and Z were atoms of the elements hydrogen, nitrogen, and oxygen. In all cases except a single experimental value for the reaction $H + HS \rightarrow H_2 + S$, there is good agreement between measured and estimated rate constants. The estimates are empirical, but are based on transition state theory. The technique gives the following expression for the rate constant of the above reactions in the exothermic direction, $k/(\mathrm{cm}^3\ \mathrm{mol}^{-1}\ \mathrm{s}^{-1}) = 10^{11.8}\ T^{0.5}\ \exp[-(\Delta H^{0\ddagger}_{300} + 1)/RT]$, where $\Delta H^{0\ddagger}_{300}$ has the value of -1 kcal/mol for reactions that have a stable XYZ intermediate, or 7 kcal/mol for reactions that are concerted or have an unstable XYZ intermediate.

INTRODUCTION

We have previously shown [1] that all the critically evaluated [2] rate constants for the reactions

$$X + YZ \rightleftarrows XY + Z \qquad (1)$$

where X, Y, and Z are atoms of the elements hydrogen, nitrogen, and oxygen can be fitted in the temperature range 200 to 4000 K by the following equation derived from transition state theory,

$$k/(\mathrm{cm^3\ mol^{-1} s^{-1}}) = AT^{B} \exp(-C/RT) \qquad (2)$$

where $\log_{10}[A/(\mathrm{cm^3\ mol^{-1}s^{-1}})] = 16.6 + [\Delta S^{0\ddagger}_{300}/(2.3R)]$, $B = 0.5$, $C/(\mathrm{kcal/mol}) = \Delta H^{0\ddagger}_{300} + 1$, R = gas constant, T = absolute temperature, $\Delta S^{0\ddagger}_{300}$ = entropy of activation at 300 K, and $\Delta H^{0\ddagger}_{300}$ = enthalpy of activation at 300 K.

In the exothermic direction, $\Delta S^{0\ddagger}_{300}$ has a value of -22 cal/(mol K), and $\Delta H^{0\ddagger}_{300}$ has a value of either -1 kcal/mol for reactions that have a transition state preceded by an intermediate that is stable with respect to the reactants (see Figure 1) or 7 kcal/mol for reactions that are concerted or that have a transition state preceded by an intermediate that is unstable with respect to the reactants (see Figure 2).

We have recently [3] completed estimates of the heat of formation of the intermediate XYZ where X, Y, and Z are atoms of the elements carbon, hydrogen, nitrogen, oxygen, and sulfur, which have enabled us to assign values of $\Delta H^{0\ddagger}_{300}$ to all reactions like Reaction (1) where X, Y, and Z are C, H, N, O and S. The assignments are in Appendices A and B.

The purpose of the present paper is to compare the estimated rate constants with experimental data for reactions involving carbon and sulfur atoms that were not covered previously, and with more recent data for the reaction of hydrogen atoms with nitric oxide and oxygen atoms with nitric oxide. The reactions of interest and the estimated rate parameters are given in Table 1.

RESULTS

For each reaction in Table 1, the experimental and estimated results have been compared. Boden and Thrush [4] have measured the rate of Reaction (3)

$$O + CN \longrightarrow OC + N \qquad (3)$$

between 570 and 687 K. The only rate constant reported by Boden and Thrush was $10^{13.0}$ cm^3 $mol^{-1}s^{-1}$ at 687 K. Albens, Schmatjko, Wagner, and Wolfrum [5] recently reported a rate constant of $10^{13.1}$ cm^3 $mol^{-1}s^{-1}$ independent of temperature at 298, 400, and 500 K. The experimental and estimated values are compared in Figure 3.

Figure 3

Hancock and Smith [6] have studied reaction (4).

$$O + CS \longrightarrow OC + S \qquad (4)$$

They measured a rate constant of $10^{12.8}$ cm^3 $mol^{-1}s^{-1}$ at 298 K and reported a previous measurement of $10^{14.1}$ cm^3 $mol^{-1}s^{-1}$ at 1100 K by Homann, Krome, and Wagner [7]. The experimental results are compared with estimated values in Figure 3.

Flower, Hanson, and Kruger [8] recently completed a study of Reaction (5) in a shock tube between 2400 and 4500 K.

$$H + ON \longrightarrow HO + N \qquad (5)$$

The experimental and estimated results are compared in Figure 4.

Figure 4

Cupitt and and Glass [9] have studied the reaction of atomic oxygen with hydrogen sulfide by esr spectroscopy. The variation in the concentration of free radicals was measured, and the results were interpreted in terms of a mechanism consisting of seven elementary reactions. One of the the reactions was

$$O + SH \longrightarrow OS + H \qquad (6)$$

The experimental results were consistent with a rate constant of $10^{14.5}$ $cm^3\ mol^{-1}s^{-1}$ at 295 K for Reaction (6). This rate constant is compared with the estimated one in Figure 3.

Mihelcic and Schindler [10] have studied the sulfur analog of Reaction (6)

$$S + SH \longrightarrow S_2 + H \qquad (7)$$

by the same method as Cupitt and Glass. The rate constant of Reaction (7) at 300 K was found to be $10^{13.4}$ $cm^3\ mol^{-1}s^{-1}$. This rate constant is compared with the estimated one in Figure 5.

Figure 5

Using the same system as was used to study Reaction (6), Cupitt and Glass measured the rate constant at 295 K for Reaction (8)

$$H + HS \longrightarrow H_2 + S \qquad (8)$$

to be $10^{13.8}$ $cm^3\ mol^{-1}s^{-1}$. This rate constant is compared with the estimated one in Figure 6.

Figure 6

Hanson, Flower, and Kruger [11] recently investigated the decomposition of nitric oxide in a shock tube in the range of 2500 to 4100 K. From their rate measurements, they derived the rate constants for Reaction (9)

$$O + ON \longrightarrow O_2 + N \qquad (9)$$

shown in Figure 7 with rate constants measured by other workers [12 to 15] and with the estimated rate constants.

Figure 7

Reaction (10)

$$S + O_2 \longrightarrow SO + O \qquad (10)$$

has been studied by Cupitt and Glass [9], who found $k_{10} = 10^{11.9}$ cm^3 mol^{-1}s^{-1} at 295 K, and by Fair and Thrush [16], who found $k_{10} = 10^{12.1}$ cm^3 mol^{-1}s^{-1} at 298 K. The experimentally determined rate constants are compared with the estimated ones in Figure 5.

DISCUSSION

The agreement between measured and estimated rate constants for H, N, O reactions is excellent, as shown in Figures 4 and 7. For reactions involving carbon and sulfur atoms, there is enough experimental evidence to suggest that the method of estimation is at least a good first approximation.

Consider reactions of the type

$$O + YZ \longrightarrow OY + Z \tag{11}$$

shown in Figure 3. At first sight it appears that the worst agreement between measured and estimated values is for Reaction (6)

$$O + SH \longrightarrow OS + H \tag{6}$$

However, if all the difference between measured and estimated rate constants is attributed to activation energy, as is likely, then the difference between observed and calculated rate constants for Reaction (6) corresponds to less than 2 kcal/mol, whereas the difference is 3 kcal/mol for Reaction (4)

$$O + CS \longrightarrow CO + S \tag{4}$$

These differences are not large for combustion reactions.

Similarly, for reactions of the type

$$S + YZ \longrightarrow SY + Z \qquad (12)$$

where Y is a sulfur or an oxygen atom, the difference between estimated and observed rate constants at 300 K corresponds to a difference of about 2 kcal/mol, as shown in Figure 5. However, when Y is a hydrogen atom, as in Reaction (-8)

$$S + H_2 \longrightarrow SH + H \qquad (-8)$$

$$H + HS \longrightarrow H_2 + S \qquad (8)$$

there is a big discrepancy (about 7 powers of 10) between the rate constants at 300 K. This discrepancy in the rate constants for Reaction (8) corresponds to about 10 kcal/mol in the activation energies. There is only one experimental value for Reaction (8), but the other two rate constants in the same experiment, namely, for Reactions (6) and (10)

$$O + SH \longrightarrow OS + H \qquad (6)$$

$$S + O_2 \longrightarrow SO + O \qquad (10)$$

are in good agreement with other experimental work and with the estimates. On the other hand, this one value for Reaction (8) is the only example, out of all available experimental data for the CHNOS system, where the estimated and experimental data are not in agreement. There is no room for adjusting the estimated value, because the thermochemistry is too well known for Reaction (8) to be anything other than exothermic. Furthermore, since the atom being transferred is a hydrogen atom, there is no need to estimate the heat of formation of the transition state. Clearly, more work is required on this reaction.

Acknowledgements

We are pleased to acknowledge the support and encouragement of W. Steve Lanier and the very helpful discussions with R. M. Kendall and R. K. Hanson. We thank W. L. Flower, R. K. Hanson, and C. H. Kruger for permission to quote their unpublished results, M. K. Stein and J. J. Hayes for typing and C. J. Reeds for editing the manuscript. The research was made possible by a grant from the U.S. Environmental Protection Agency, with financial assistance from Stanford Research Institute.

REFERENCES

1. Benson, S. W., Golden, D. M., Lawrence, R. W., Shaw, R., and Woolfolk, R. W., Estimation of rate constants as a function of temperature for reactions $X + YZ \rightleftarrows XY + Z$, $X + Y + M \rightleftarrows XY + M$, and $X + YZ + M \rightleftarrows XYZ + M$, where X, Y, and Z are atoms, H, N, and O, presented at the Symposium on Chemical Kinetics Data for the Lower and Upper Atmosphere, September 16-18, 1974, Airlie House, Warrenton, Virginia, U.S.A., to be published in a special issue of the International Journal of Chemical Kinetics.

2. Baulch, D. L., Drysdale, D. D., and Horne, D. G., Evaluated Kinetic Data for High Temperature Reactions, Butterworths, London, 1973.

3. Benson, S. W., Golden, D. M., Lawrence, R. W., Shaw, R., and Woolfolk, R. W., Estimates of kinetics of combustion, especially reactions involving NO_x and SO_x, U.S. Environmental Protection Agency Report 300-00-0000, June 1975.

4. Boden, J. C., and Thrush B. A., Proc. Roy. Soc. (London) 305A, 107 (1968).

5. Albers, E. A., Schmatjko, K. J., Wagner, H. Gg., and Wolfrum, J., 15th Symposium (International) on Combustion, The Combustion Institute, Pittsburgh, Pa., Paper No. 73.

6. Hancock, G., and Smith, I.W.M., Trans. Faraday Soc. 67, 2586 (1971).

7. Homann, K. H., Krome, G., and Wagner, H. Gg., Ber. Bunsenges, Phys. Chem. 72, 998 (1968).

8. Flower, W. L., Hanson, R. K., and Kruger, C. H., 15th Symposium (International) on Combustion, The Combustion Institute, Pittsburgh, Pa., Paper No. 78.

9. Cupitt, L. T., and Glass, G. P., Trans. Faraday Soc. 66, 3007 (1970).

10. Mihelcic, D., and Schindler, R. N., Ber. Bunsenges. Phys. Chem. 74, 1280 (1970).

REFERENCES, (Concluded)

11. Hanson, R. K., Flower, W. L., and Kruger, C. H., *Combustion Sci. Tech.*, in press.

12. Kaufman, F., and Kelso, J. R., *J. Chem. Phys.* 23, 1702 (1955).

13. Kaufman, F., and Decker, L. J., *7th Symposium (International) on Combustion*, the Combustion Institute, Pittsburgh, Pa., 1959, p. 57.

14. Wray, K. L., and Teare, J. D., *J. Chem. Phys.* 36, 2582 (1962).

15. Clark, T. C., Garnett, S. H., and Kistiakowsky, G. B., *J. Chem. Phys.* 51, 2885 (1969).

16. Fair, R. W., and Thrush, B. A., *Trans. Faraday Soc.* *65*, 1557 (1969).

TABLE 1

Estimated rate parameters of the equation $k = AT^{0.5} \exp(-C/RT)$ and rate constants at 1000 K for some reactions of the type $X + YZ \rightarrow XY + Z$, where X, Y, and Z are atoms of the elements carbon, hydrogen, nitrogen, oxygen, and sulfur.

Empirical formula of XYZ	Reaction	$\log[A/(cm^3\ mol^{-1}\ s^{-1})]$	C/(kcal/mol)	$\log[k/(cm^3\ mol^{-1}\ s^{-1})]$ at 1000 K
CNO	$O + CN \rightarrow OC + N$	11.8	0.0	13.4
COS	$O + CS \rightarrow OC + S$	11.8	0.0	13.4
HNO	$H + ON \rightarrow HO + N$	12.4	48.6	6.9
HOS	$O + SH \rightarrow OS + H$	11.8	0.0	13.4
HS_2	$S + SH \rightarrow S_2 + H$	11.8	0.0	13.4
H_2S	$H + HS \rightarrow H_2 + S$	11.8	8.0	12.2
NO_2	$O + ON \rightarrow O_2 + N$	11.1	40.1	6.9
SO_2	$S + O_2 \rightarrow SO + O$	11.8	0.0	13.4

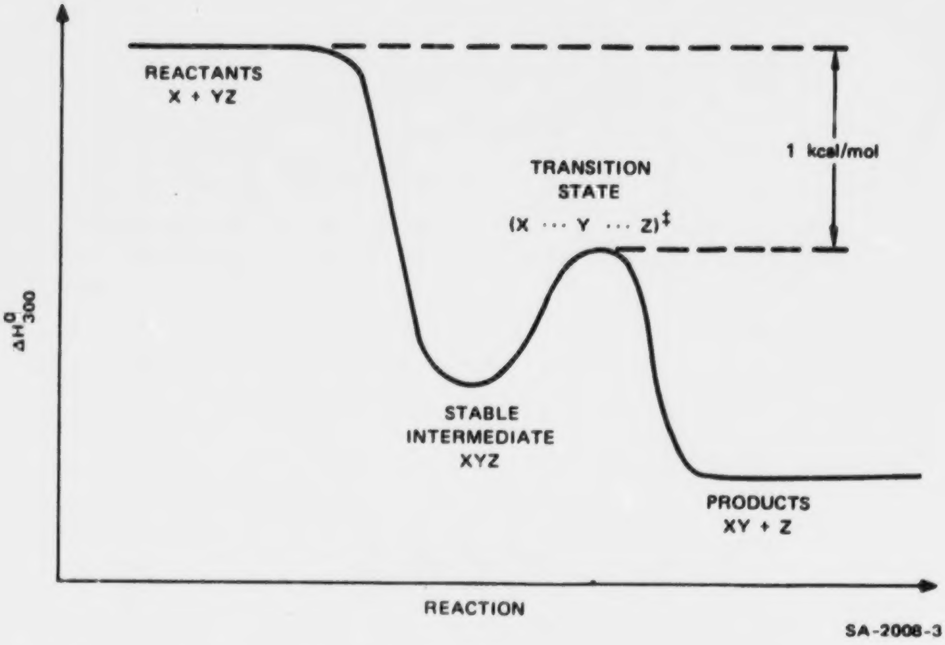
REACTANTS
X + YZ
1 kcal/mol
TRANSITION
STATE
(X ··· Y ··· Z)‡
STABLE
INTERMEDIATE
XYZ
PRODUCTS
XY + Z
ΔH°300
REACTION
SA-2008-3

FIGURE 1 HEAT CHANGES FOR REACTIONS HAVING TRANSITION STATES PRECEDED BY AN INTERMEDIATE THAT IS STABLE WITH RESPECT TO THE REACTANTS

In such cases $\Delta H^{0\ddagger}_{300}$ = -1 kcal/mol.

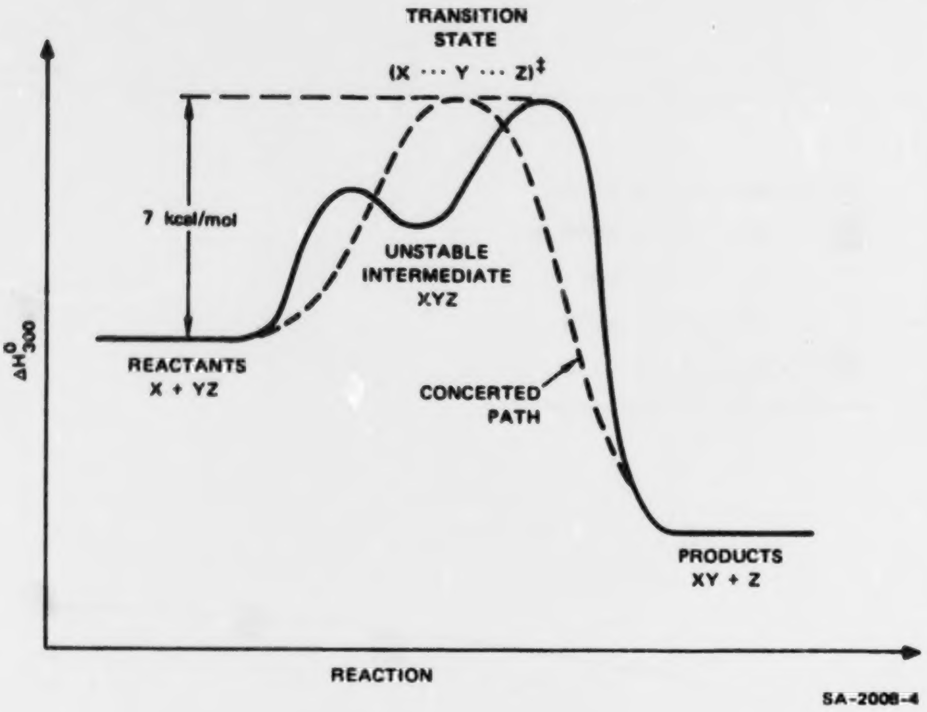
TRANSITION STATE
$(X \cdots Y \cdots Z)^{\ddagger}$
7 kcal/mol
UNSTABLE INTERMEDIATE XYZ
REACTANTS X + YZ
CONCERTED PATH
PRODUCTS XY + Z
ΔH^0_{300}
REACTION
SA-2008-4

FIGURE 2 HEAT CHANGES FOR REACTIONS THAT ARE CONCERTED OR THAT HAVE A TRANSITION STATE THAT IS PRECEDED BY AN INTERMEDIATE THAT IS UNSTABLE WITH RESPECT TO THE REACTANTS

In such cases $\Delta H^{0\ddagger}_{300}$ = 7 kcal/mol.

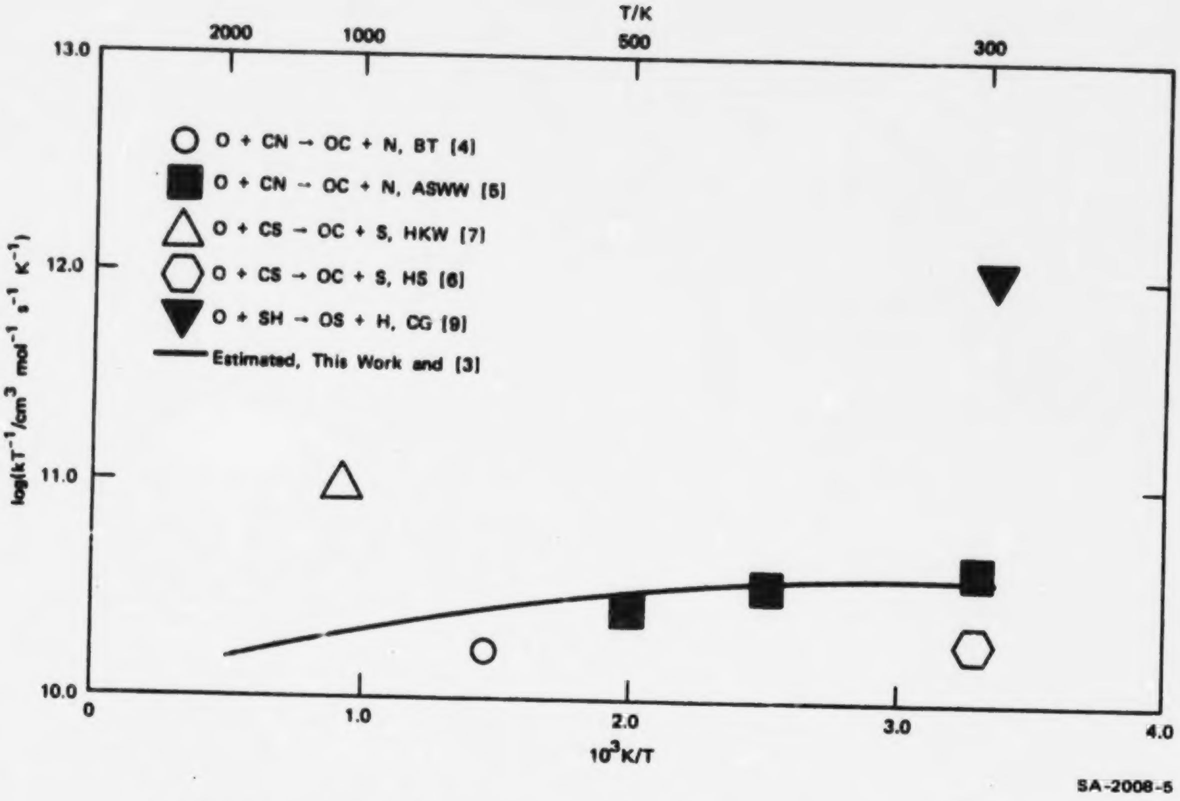

FIGURE 3 COMPARISON OF MEASURED AND ESTIMATED RATE CONSTANTS FOR REACTIONS OF OXYGEN ATOMS

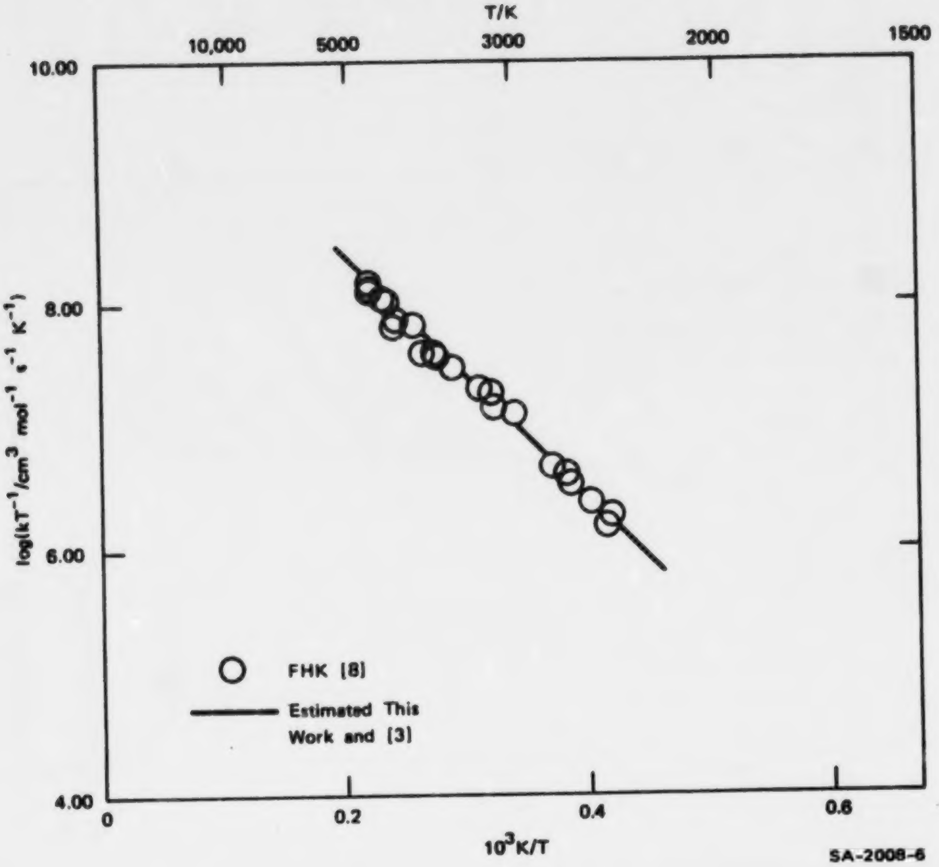

FIGURE 4 COMPARISON OF MEASURED AND ESTIMATED RATE CONSTANTS FOR THE REACTION H + ON → HO + N

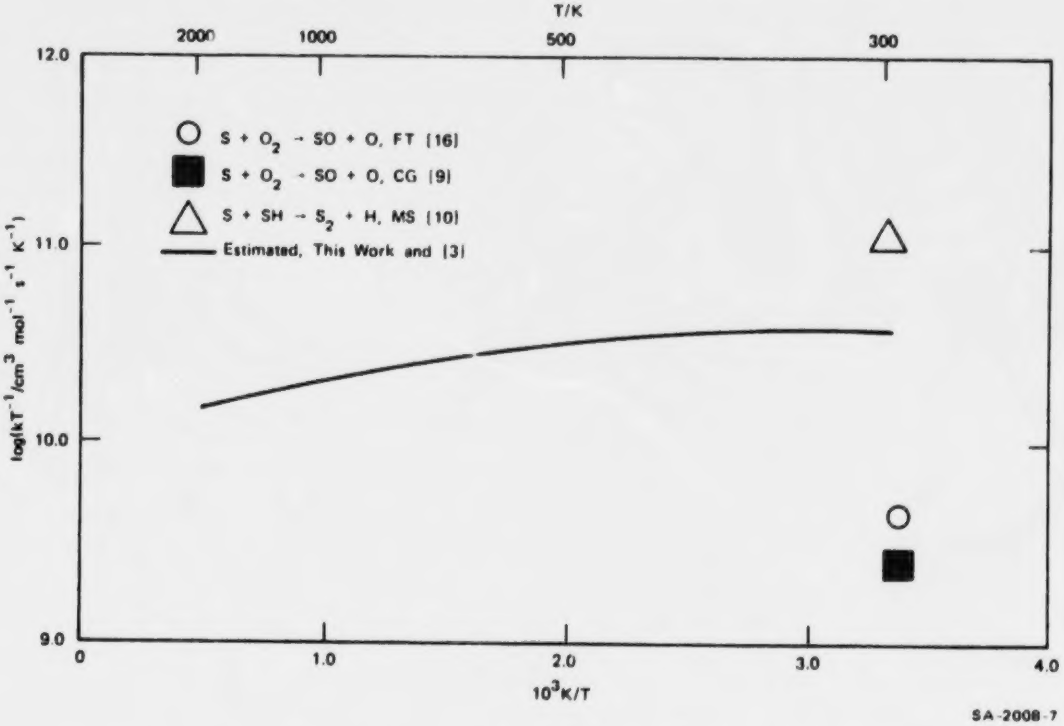

FIGURE 5 COMPARISON OF MEASURED AND ESTIMATED RATE CONSTANTS FOR REACTIONS OF SULFUR ATOMS

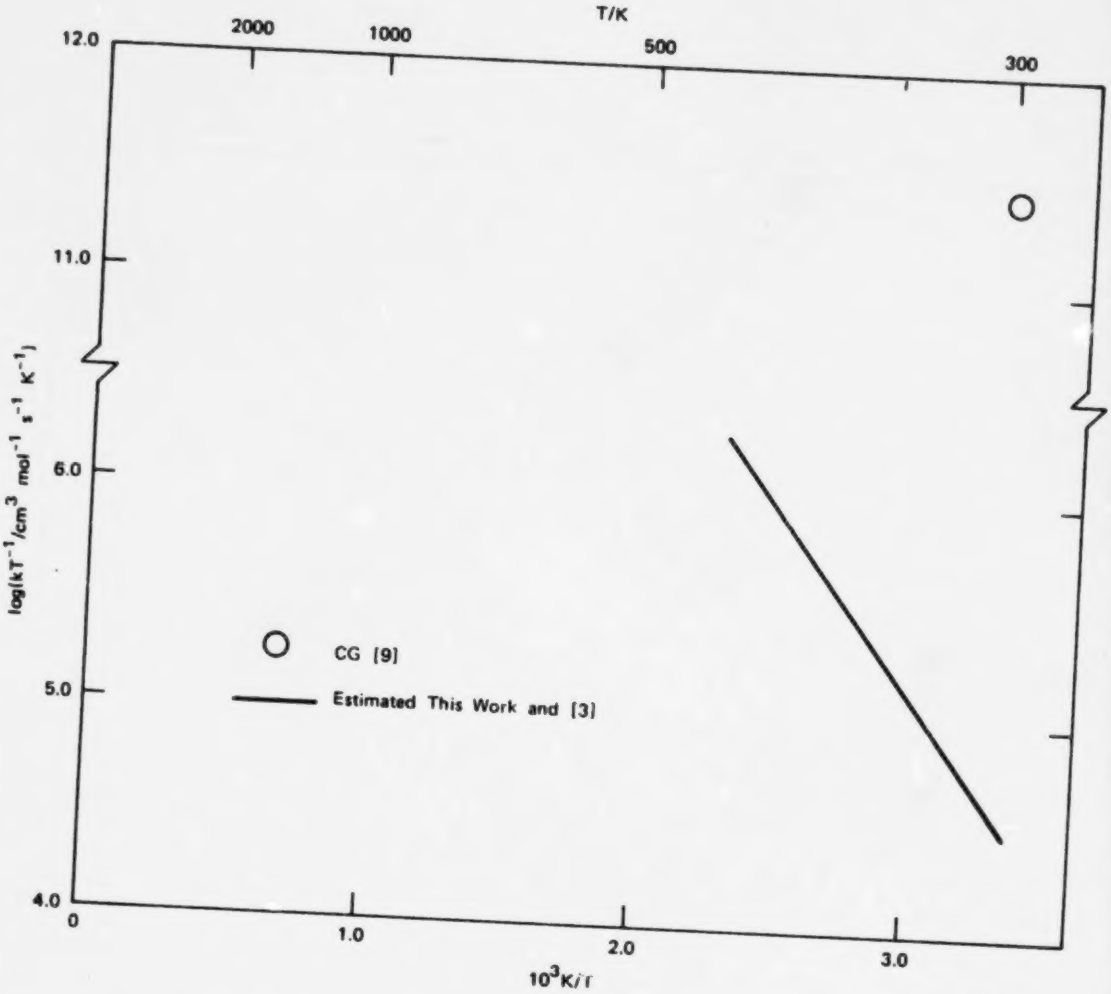

SA-2008-8

FIGURE 6 COMPARISON OF MEASURED AND ESTIMATED RATE CONSTANTS FOR THE REACTION H + HS → H_2 + S

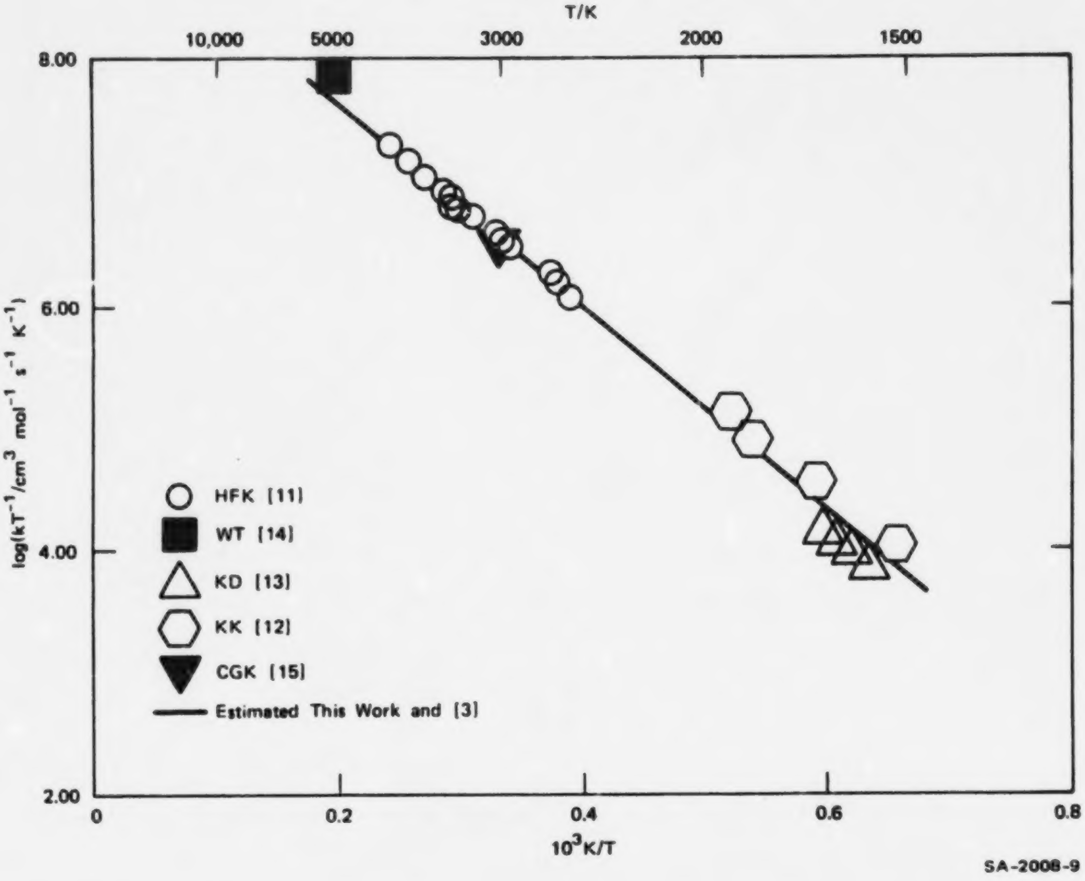

FIGURE 7 COMPARISON OF MEASURED AND ESTIMATED RATE CONSTANTS FOR THE REACTION O + ON → O_2 + N

Appendix A

HYDROGEN TRANSFER REACTIONS[a]

Formula of Triatomic Transition State XYZ		Reaction
Empirical	Structural	
CHN	CHN	$C + NH \rightarrow CH + N$
CHO	OHN	$O + HC \rightarrow OH + C$
CHS	SHC	$S + HC \rightarrow SH + C$
CH_2	HHC	$H + HC \rightarrow H_2 + C$
C_2H	CHC	$C + HC \rightarrow CH + C$
HNO	OHN	$O + HN \rightarrow OH + N$
HNS	SHN	$S + HN \rightarrow SH + N$
HN_2	NHN	$N + HN \rightarrow NH + N$
HOS	OHS	$O + HS \rightarrow OH + S$
HO_2	OHO	$O + HO \rightarrow OH + O$
HS_2	SHS	$S + HS \rightarrow SH + S$
H_2N	HHN	$H + HN \rightarrow H_2 + N$
H_2O	HHO	$H + HO \rightarrow H_2 + O$
H_2S	HHS	$H + HS \rightarrow H_2 + O$
H_3	HHH	$H + H_2 \rightarrow H_2 + H$

---

[a] Reactions $X + HZ \rightarrow XH + Z$ where X and Z are atoms of the elements carbon, hydrogen, nitrogen, oxygen, and sulfur. The rate constant for every reaction is: $k/(cm^3\ mol^{-1}\ s^{-1}) = 10^{11.8}T^{0.5}\ exp(-8/RT)$. Reactions are in the exothermic direction.

Appendix B

ATOM TRANSFER REACTIONS[a]

Formula of Triatomic Intermediate XYZ		Reaction	$[\Delta H_f^o(X) + \Delta H_f^o(YZ)]$	$\Delta H_f^o(XYZ)$	$\Delta H_{300}^{o\ddagger}$
Empirical	Structural				
CHN	CNH	$C + NH \rightarrow NC + H$	155 ± 5	110 ± 3[b]	-1
CHN	NCH	$N + CH \rightarrow NC + H$	255 ± 1	32.3 ± 2[c]	-1
CHO	OCH	$O + CH \rightarrow OC + H$	201.6 ± 0.1	7.2[d] 10.4 ± 2[c]	-1
CHO	COH	$C + OH \rightarrow CO + H$	180 ± 1	81 ± 15[b]	-1
CHS	CSH	$C + SH \rightarrow CS + H$	203 ± 1	123 ± 15[b]	-1
CHS	SCH	$S + CH \rightarrow SC + H$	208.3 ± 0.1	92 ± 8[b]	-1
CH_2	HCH	$H + CH \rightarrow HC + H$	194.1 ± 0.1	92.4 ± 1[c]	-1
CNO	CNO	$C + NO \rightarrow CN + O$	192.5 ± 0.5	145 ± 17[b]	-1
CNO	CON	$C + ON \rightarrow CO + N$	192.5 ± 0.5	215 ± 29[b]	7
CNO	OCN	$O + CN \rightarrow OC + N$	164 ± 3	38 ± 3[c]	-1
CNS	CNS	$C + NS \rightarrow CN + S$	234 ± 10	186 ± 25[b]	-1
CNS	CSN	$C + SN \rightarrow CS + N$	234 ± 10	250 ± 29[b]	7
CNS	SCN	$S + CN \rightarrow SC + N$	170 ± 3	73 ± 3[b]	-1
CN_2	NCN	$N + CN \rightarrow NC + N$	217 ± 4	113 ± 5[c]	-1
CN_2	NNC	$N + NC \rightarrow N_2 + C$	217 ± 4	140 ± 30[c]	-1

[a] Reactions $X + YZ \rightarrow XY + Z$ where Y is not a hydrogen atom and where X and Z are atoms of the elements carbon, hydrogen, nitrogen, oxygen and sulfur. If the heat of formation of the intermediate XYZ is less than the sum of the heats of formation of X and YZ, then $\Delta H_{300}^{o\ddagger} = -1$ kcal/mol in the equation for the rate constant: $k/(cm^3\ mol^{-1}\ s^{-1}) = 10^{11.8}T^{0.5} \exp[-(\Delta H_{300}^{o\ddagger} + 1)/RT]$. If the heat of formation of the intermediate XYZ is greater than the sum of the heats of formation of X and YZ, then $\Delta H_{300}^{o\ddagger} = 7$ kcal/mol. All units are kcal/mol. Reactions are in the exothermic direction.

[b] Estimated value for $\Delta H_f^o(XYZ)$.

[c] Reference 9.

[d] Reference 4.

Appendix B

ATOM TRANSFER REACTIONS (Continued)

Formula of Triatomic Intermediate XYZ		Reaction	$[\Delta H_f^o(X) + \Delta H_f^o(YZ)]$	$\Delta H_f^o(XYZ)$	$\Delta H_{300}^{o\ddagger}$
Empirical	Structural				
COS	COS	$C + OS \rightarrow CO + S$	172.1 ± 0.8	161 ± 36[b]	-1
COS	OCS	$O + CS \rightarrow OC + S$	115 ± 5	-33.1 ± 0.3[a]	-1
COS	CSO	$C + SO \rightarrow CS + O$	172.1 ± 0.8	164 ± 19[b]	-1
CO_2	COO	$C + O_2 \rightarrow CO + O$	170.9 ± 0.5	135 ± 22[b]	-1
CO_2	OCO	$O + CO \rightarrow OC + O$	33.2 ± 0.6	-94.05 ± 0.01[c]	-1
CS_2	CSS	$C + S_2 \rightarrow CS + S$	201.7 ± 0.7	164 ± 19[b]	-1
CS_2	SCS	$S + CS \rightarrow SC + S$	121 ± 5	28.0 ± 0.2[c]	-1
C_2H	CCH	$C + CH \rightarrow C_2 + H$	312.9 ± 0.6	114 ± 7[c]	-1
C_2N	NCC	$N + C_2 \rightarrow NC + C$	313 ± 2	146 ± 16[b]	-1
C_2N	CNC	$C + NC \rightarrow CN + C$	275 ± 4	133 ± 30[c]	-1
C_2O	OCC	$O + C_2 \rightarrow OC + C$	259.7 ± 0.9	69 ± 15[c]	-1
C_2O	COC	$C + OC \rightarrow CO + C$	144.5 ± 1.1	213 ± 30[b]	7
C_2S	SCC	$S + CC \rightarrow SC + C$	266.5 ± 0.9	130 ± 15[b]	-1
C_2S	CSC	$C + SC \rightarrow CS + C$	266 ± 5	248 ± 30[b]	7
C_3	CCC	$C + C_2 \rightarrow C_2 + C$	371 ± 1	196 ± 4[b]	-1
HNO	ONH	$O + NH \rightarrow ON + H$	150 ± 4	23.8[b]	-1
HNO	NOH	$N + OH \rightarrow NO + H$	122 ± 1	77 ± 11[b]	-1
HNS	SNH	$S + NH \rightarrow SN + H$	156 ± 4	65 ± 11[b]	-1
HNS	NSH	$N + SH \rightarrow NS + H$	146 ± 2	112 ± 11[b]	-1
HN_2	HHH	$N + NH \rightarrow N_2 + H$	203 ± 5	152 ± 16[b]	-1
HOS	SOH	$S + OH \rightarrow SO + H$	75.6 ± 0.3	11 ± 13[b]	-1

Appendix B

ATOM TRANSFER REACTIONS (Concluded)

Formula of Triatomic Intermediate XYZ		Reaction	$[\Delta H_f^0(X) + \Delta H_f^0(YZ)]$	$\Delta H_f^0(XYZ)$	$\Delta H^{0\ddagger}_{300}$
Empirical	Structural				
HOS	OSH	$O + SH \rightarrow OS + H$	93 ± 1	23 ± 10[b]	-1
HO_2	OOH	$O + OH \rightarrow O_2 + H$	69.9 ± 0.3	5 ± 2[c]	-1
HS_2	SSH	$S + SH \rightarrow S_2 + H$	99.6 ± 1.2	33 ± 5[b]	-1
H_2N	HNH	$H + NH \rightarrow HN + H$	142 ± 4	46 ± 2[c]	-1
H_2O	HOH	$H + OH \rightarrow HO + H$	61.4 ± 0.3	-57.8 ± 0.001[c]	-1
H_2S	HSH	$H + SH \rightarrow HS + H$	85.4 ± 1.2	-4.9 ± 0.2[c]	-1
NOS	NOS	$N + OS \rightarrow NO + S$	114 ± 1	149 ± 21[b]	7
NOS	OSN	$O + SN \rightarrow OS + N$	123 ± 10	166 ± 39[b]	7
NOS	ONS	$O + NS \rightarrow ON + S$	123 ± 10	49 ± 10[b]	-1
NO_2	NOO	$N + O_2 \rightarrow NO + O$	113 ± 1	136 ± 17[b]	7
NO_2	ONO	$O + NO \rightarrow ON + O$	81.1 ± 0.4	7.9 ± 0.2[c]	-1
NS_2	NSS	$N + S_2 \rightarrow NS + S$	144 ± 1	164 ± 32[b]	7
NS_2	SNS	$S + NS \rightarrow SN + S$	129 ± 10	90 ± 20[b]	-1
N_2O	NNO	$N + NO \rightarrow N_2 + O$	135 ± 1	19.6 ± 0.1[c]	-1
N_2O	NON	$N + ON \rightarrow NO + N$	135 ± 1	209 ± 27[b]	7
N_2S	NNS	$N + NS \rightarrow N_2 + S$	176 ± 11	61 ± 10[b]	-1
N_2S	NSN	$N + SN \rightarrow NS + N$	176 ± 11	244 ± 31[b]	7
N_3	NNN	$N + N_2 \rightarrow N_2 + N$	113 ± 1	171 ± 13[b,c,e]	7
S_2O	OSS	$O + S_2 \rightarrow OS + S$	90.4 ± 0.2	-14 ± 8[c]	-1
S_2O	SOS	$S + OS \rightarrow SO + S$	67.5 ± 0.3	36.5 ± 1.0[b]	-1
SO_2	SOO	$S + O_2 \rightarrow SO + O$	66.29 ± 0.01	35.3 ± 0.7[b]	-1
SO_2	OSO	$O + SO \rightarrow OS + O$	60.8 ± 0.3	-70.95 ± 0.05[c]	-1
O_3	OOO	$O + O_2 \rightarrow O_2 + O$	59.55 ± 0.02	34.1 ± 0.4	-1
S_3	SSS	$S + S_2 \rightarrow S_2 + O$	97.1 ± 0.2	65 ± 1[b]	-1

[e] The $\Delta H_f^0(XYZ)$ includes an additional 60 ± 6 kcal/mol for spin forbidden reaction.

PRODUCTION OF OXIDES OF NITROGEN IN INTERACTING FLAMES

Christopher England
Jet Propulsion Laboratory
Pasadena, California 91106

Paper Presented at the
Symposium on Stationary Source Combustion
Fairmont Colony Square Hotel
Atlanta, Georgia
September 24-26, 1975

Sponsored by
The Combustion Research Section
U.S. Environmental Protection Agency

PRODUCTION OF OXIDES OF NITROGEN IN INTERACTING FLAMES

by

Christopher England

ABSTRACT

Measurements of oxides of nitrogen (NO_x) were made in a 250,000 BTU/h laboratory furnace fired with multiple burners to determine the effects of burner interactions on the effectiveness of NO_x control techniques. Measurements were made with both gas and oil firings. When all burners were operated at equal air-fuel ratios, the behavior of the furnace closely matched that of full-scale boilers with furnace gas temperature and air-fuel ratio the major controlling factors. When burners were operated at widely different air-fuel ratios, NO_x levels were generally higher than at uniform operation, a result which conflicted greatly with predicted values. Tracer measurements indicated a very high degree of mixing in the furnace, a feature which is believed responsible for the anomalous results.

Preceding page blank

Introduction

Techniques to reduce emissions of oxides of nitrogen (NO_x) in boilers are well known and generally center on either lowering peak temperatures in the firebox, or lowering the available oxygen in high temperature zones. In-plant testing has demonstrated the effectiveness of these techniques, and laboratory testing has attempted to quantify the reductions that are possible. Laboratory testing, however, has been confined to the testing of single burner systems, in contrast to commercial practice in which furnaces are often fired with arrays of burners. The purpose of this work is to evaluate NO_x reduction methods on a laboratory scale but in a furnace with arrayed burners that can approximate the interburner interactions that occur in commercial furnaces.

Apparatus

Furnace

Experiments were conducted in a 34.3 cm x 34.3 cm x 81.3 cm (13.5 in x 13.5 in x 32 in) refractory furnace shown in Figures 1 and 2. Burners were placed at the bottom of the furnace in a machined "M"-type refractory block. The walls of the furnace were firebrick with a thickness of 11.4 cm (4.5 in). Covering the brick were sheets of 2.5 cm "M" type refractory which in turn was surrounded by 0.64 cm thick transite board. The ceiling of the furnace was a refractory cast around water-cooled pipes. The ceiling contained exit ports in line with the gas burners followed by a refractory mixing section from which samples of average furnace composition were taken.

Gas Burners

Three types of gas burners were used in the study including a ring-type, a coaxial spud type and a radial spud type as shown schematically in Figure 3. Swirl vanes were also used in conjunction with both spud-type burners to determine the effects of air rotation on the burner interactions.

Technical grade methane 92% CH_4,[30.5 kj/m^3 (1022 btu/ft^3)] from cylinders was throttled through critical flow orifices to meter the flow of fuel to the burners. Air was supplied from the laboratory supply and was also throttled through critical flow devices. Electrical heaters were used to preheat air up to 315°C (600°F).

Two independent controls were maintained on fuel supplies so that the air-fuel ratio of individual or manifolded burners could be operated independently from the others. A single air supply was used, and all tests were conducted with equal air flows in all burners.

Oil Burners

Oil burners were similar to the concentric spud gas burners with 60° solid-cone spray nozzles mounted on spuds which were fitted with swirl vanes as shown in Figure 3. A symmetrical pattern of 5 burners was used including a central burner and a square array of 4 burners, each spaced 14.0 cm (5.5 in) from the burner walls.

The spray nozzles were supplied by Delavan, and had capacities of 1.9 l/min (0.5 gpm) each.

Instrumentation and Sampling

A chemiluminescent analyzer (Thermoelectron) was used for NO_x analysis. Anomalous results due to peculiarities in the instrument were found when measurements were made of total NO_x in fuel-rich flames. This was believed to be caused by the reduction of NO_x by carbon monoxide in the stainless steel converter which was used to thermally decompose NO_2 to NO. Catalytic effects of metals in fuel-rich flames are well known, and in this case, reduction of NO_x was nearly complete. At equivalence ratios of 1.2 where CO concentrations are on the order of 4%, NO_x was reduced to about 5 ppm when NO was measured at concentrations above 400 ppm. As a result, all measurements reported are for NO on a dry basis. Sample gases were dried in successive ice and dry ice baths before measurement. This assured that the same was free of all easily condensable gases.

Sampling was by a water-cooled quartz probe. Problems of poor reproducibility were noted if this probe was exposed to fuel-rich flames prior to use. This apparently was due to chemical reduction of NO_x by carbon near the tip of the probe. As a result, it was necessary to clean the probe after any exposure to flames containing free carbon. Probing the interior of the flames was very difficult because of this phenomena and, while several tests were made to measure centerline NO_x concentrations, the results were not reproducible.

The probe which was used had an orifice diameter of 1.6 mm (0.063 in) and sampled at a rate of 9 l/min giving a sampling velocity of from about 75-100 m/sec depending on the temperature. This apparently was not sufficiently fast to prevent reduction. A better design might have been a thinner quartz interface near the tip where heat transfer and quenching would be faster. This design, however, would not be compatible with sampling of coal flames that the probe was designed to handle.

Operating Procedures

Operating procedures varied with the type of data desired and the type of fuel used. For baseline parametric tests used to characterize the furnace of the burner array, NO_x was measured as a function of equivalence ratio (defined as the actual fuel-air ratio divided by the stoichiometric fuel-air ratio) and temperature by simply firing the furnace and scanning over various air-fuel mixtures. Temperature readings were taken at each data point as the furnace was heated; the resulting data were plotted as NO_x vs temperature at constant equivalence ratio, and cross-plotted to give NO_x vs equivalence ratio.

The temperature of the furnace was taken as the temperature given by a thermocouple imbedded in the furnace wall. This temperature followed closely the temperature of the furnace gases when taken approximately 2.5 cm above the furnace floor between burners, or when taken 25 cm above the furnace floor. Typically, the temperatures were within 8°C of each other, an indication of the high surface-to-volume ratio of the furnace.

When data were desired at a constant temperature, the furnace was heated by firing at an air-fuel ratio at which this temperature was self-sustaining. The furnace was then set at a desired air-fuel setting and an NO_x reading was taken.

Results

Gas Burners

A variety of tests was made with an array of ring burners in which the general characteristics of the furnace with respect to NO_x were measured. Later tests were made with spud-type burners, with and without swirl to determine the sensitivity of emissions to different burner aerodynamics and flame shape.

Baseline Tests

For the ring burners, NO_x-equivalence ratio profiles were taken as a function of air preheat temperature and furnace temperature when all burners in the 9-burner array were held at a uniform equivalence ratio. Figure 4 shows that air preheat temperature had a substantial effect on NO_x with emissions roughly doubling as the temperature of the incoming combustion air was raised from 90° to 315°C (200° to 600°F). Emissions of NO_x were also greatly influenced by furnace temperature as shown in Figure 5. A relatively strong temperature dependence was observed above 1100°C (2000°F) in air-rich flames while a weaker dependence was observed in fuel-rich flames. Figure 6 is a crossplot of Figure 5 which shows more clearly the relative effects of temperature in which lean flames display marked increases in NO_x, especially above 1200°C (2200°F).

Ring Burner Interactions

Tests of the effects of flame interactions were run with the ring burners in which the air-fuel ratios of the individual burners were changed to determine the differences between single burner and arrayed burner systems. "Interactions" were defined simply as deviations from the calculated NO_x-equivalence ratio profiles based on the sum of individual NO_x contributions as determined by plots such as shown in Figure 6.

For example, Figure 7 shows data for a nine-burners array with 3 burners off. The predicted NO_x concentration when six burners are operated at $\phi = 1.0$ and 3 burners are off is:

$$NO_x = \frac{6}{9} NO_{x(\phi = 1.0)} + \frac{3}{9} NO_{x(\phi = 0.0)}$$

or, from Figure 7

$$NO_x = \frac{6}{9}(150) + \frac{3}{9}(0) = 100 \text{ ppm}$$

where the overall furnace equivalence ratio is

$$\phi = \frac{6}{9}(1.0) + \frac{3}{9}(0.0) = 0.67.$$

It is apparent from these calculations that for the particular case of a 6 on/3 off array, the maximum "predicted" NO_x should be two-thirds of the maximum "identical" NO_x, a suggestion which is invalidated by measurement. Either by coincidence or by physics, "identical" burner data corresponds closely with single burner data in smaller systems and with tests with a large (7.62 cm, 3 in) burner in the multiburner furnace.

Concentric Spud Interactions

Figure 8 shows the interactions of concentric spud burners with and without swirl. Again, surprising results were found in that interactions were dominant in NO_x production with near-predicted levels occurring in only very lean systems. The levels of NO_x were substantially higher with the spud-type burner relative to the ring burner, indicating possibly a better mixing pattern in the latter type.

The addition of swirl (a swirl number of approximately 0.5) raised the overall NO_x levels of the concentric spud to peak levels above 1200 ppm although it did not change the interaction effects appreciably. The swirling flames burn with a much greater intensity than non-swirling ones, probably resulting in the higher levels.

Radial Spud Interactions

Figure 9 shows the interactions of radial spud burners with and without swirl. The results were much like those of the concentric spud, although the observed flame intensities were greatest for these burners. Reductions of NO_x below those of uniform burners were not found, and very high levels of NO_x in swirling flames were observed in near-stoichiometric flames. As in the case of ring and concentric spud burners, modest deviations from uniform burner operations, say, operating three burners at an equivalence ratio of 0.4 and six at 1.4, gave very little measurable change from NO_x levels with uniform operation. For this particular case, NO_x levels of 83 ppm would be expected at the overall equivalence ratio of 1.07, while levels of about 1000 ppm were measured.

Oil Burner Interactions

A five-burner array of burners was used in the oil tests, a feature which allowed a greater burner spacing in the vertically-fired furnace. Figure 10 shows the typical NO_x-equivalence characteristic when all burners were operating at equal air-fuel mixtures. With the 60° solid-cone nozzles and swirl vanes (swirl no. 0.5), the NO_x was only influenced by air-fuel mixture ratio in fuel-rich flames, with steady levels of about 400 ppm occurring from equivalence ratios from 0.4 to 1.0. These levels were lower than for gas, a somewhat unexpected result.

Interactions for oil were much more predictable than for gas as shown in Figure 10. Each burner appeared to act relatively independently of the other with respect to NO_x, and, as a result, less interactions were found. Why this should be the case is not clear, but may be related to the insensitivity of the oil burners to stoichiometry. Increased air preheat, however, was capable of NO_x increase comparable to gas, indicating that the burners were not insensitive to incoming enthalpy.

Discussion

The results with gas burners showed that, with the particular geometry selected, the furnace was "resistant" to NO_x control by burner patterning. Some probing of the furnace was done to determine the cause of this resistance and the results are shown in Figure 11. In these tests, done without combustion, helium was added in trace quantities to determine the entrainment of gases between burners. When helium was added to the center burner, it was entrained in the outer burners in a reasonable manner, and the rate of dilution of helium in the center jet was predictable from jet entrainment theory. When helium was added to burners near the wall, extremely high rates of entrainment of gases occurred, and after about 5 diameters, the center jet actually exhibited more helium than the jet that was introducing helium to the furnace.

What these results indicate is the very high degree of mixing in the furnace, a feature that exceeds in importance the actual fuel-air mixtures of the burners. Only a few diameters from the burners, the furnace appears to be almost homogeneous in composition.

That the NO_x production levels tend to follow this composition indicates that NO_x occurs away from the flame and in the plume, possibly greater than 5 diameters from the burner.

By contrast, the oil burners were well-behaved, and relatively predictable NO_x levels occurred when the burners were patterned for low NO_x. The major differences between the gas and oil systems were the burner spacing and, of course, the nature of the fuel. Interburners distances were 11.4 cm (4.5 in) and 14.0 cm (5.5 in.) for gas and oil, respectively. It is possible that a critical burner spacing exists between these two values. A more probable explanation, however, lies in the widely different NO_x characteristics of the two fuels even when all burners are operated with identical fuel-air mixtures. While multiple gas burner data show a sharp peak in NO_x concentration in near-stoichiometric flames, multiple oil burners show no sharp peak. This may indicate that NO_x from the latter burners is formed nearer the burner and is not as influenced by furnace mixing. It is expected that the jet entrainment rates in both oil and gas burners are similar so that bulk mixing phenomena should not be widely different.

The purpose of the tests is to allow the prediction of NO_x levels from commercial furnaces by means of inexpensive laboratory testing and suitable modelling to take into account factors of scale. In the present tests, the laboratory furnace was built to match the volumetric heat release rate of commercial equipment, about 75,000 btu/ft^3. It is not, however, possible in small furnaces to match another important furnace variable, the surface-to-volume ratio. An example of its influence on NO_x lies in the fact that the sub-scale furnace walls take on the temperature of the furnace gases, say, 2200°F, while commercial equipment operates at cooled wall temperatures of 1000°F. This ratio for the laboratory furnace $0.3\ cm^{1}$ $(0.89\ ft^{1})$ is more than 7 times higher than a commercial system.

Further tests have been performed on nitrogen-doped oil and are now being made with a 5-burner array on coal. These results will be reported at a later date.

Acknowledgment

This paper represents the results of one phase of research carried out at the Jet Propulsion Laboratory, California Institute of Technology, under Contract No. NAS 7-100, National Aeronautics and Space Administration, and was sponsored by the Environmental Protection Agency. The author wishes to acknowledge the valuable support by G. Blair Martin of the EPA, and by Robert Silver and Raymond Devlin at JPL.

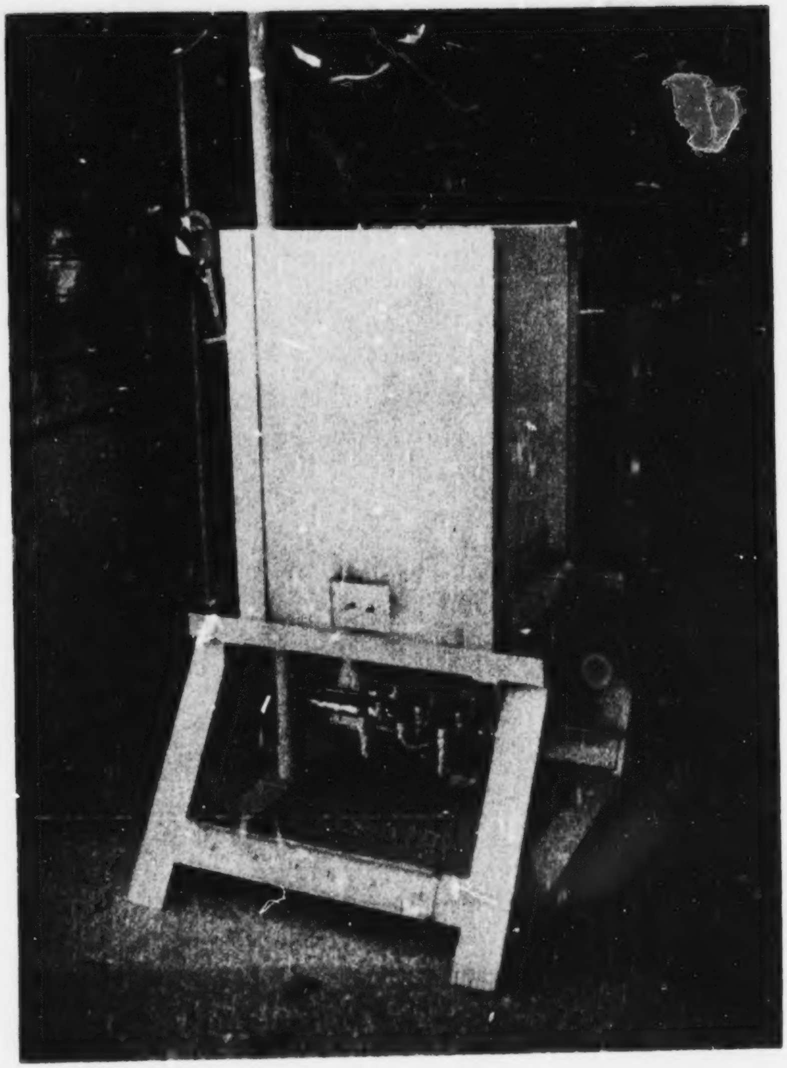

Figure 1. Photograph of the Furnace Used for Flame-Interaction Studies

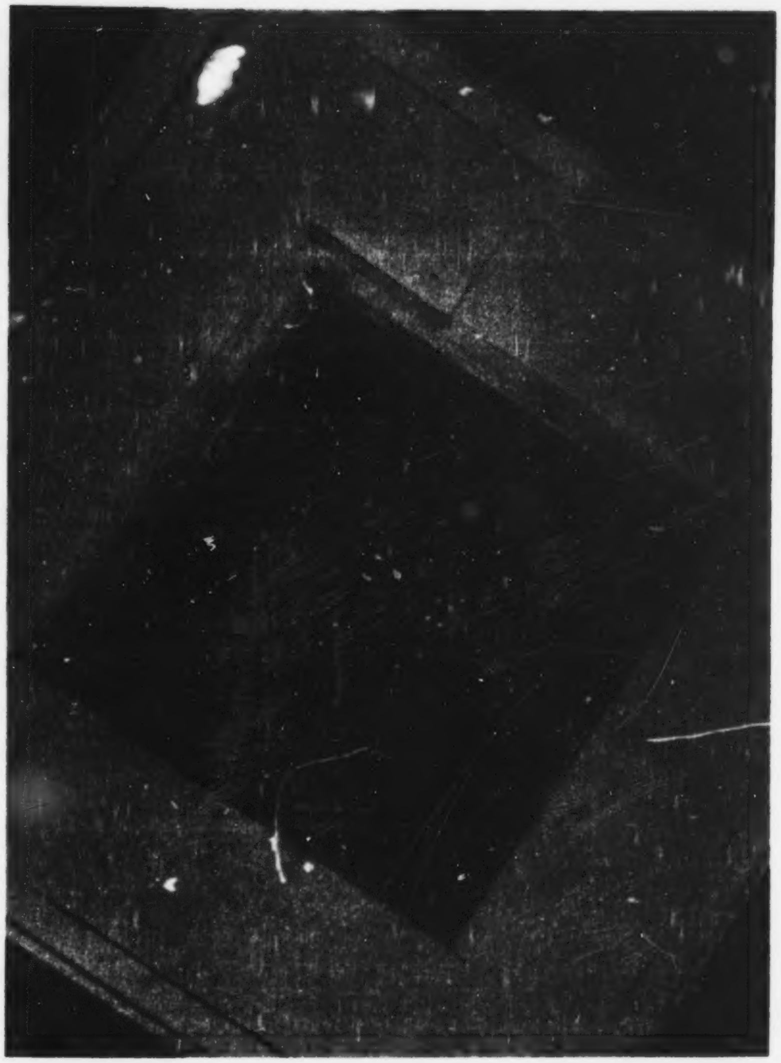

Figure 2. Interior Photograph of the Furnace Installed with an Array of Gas Burners

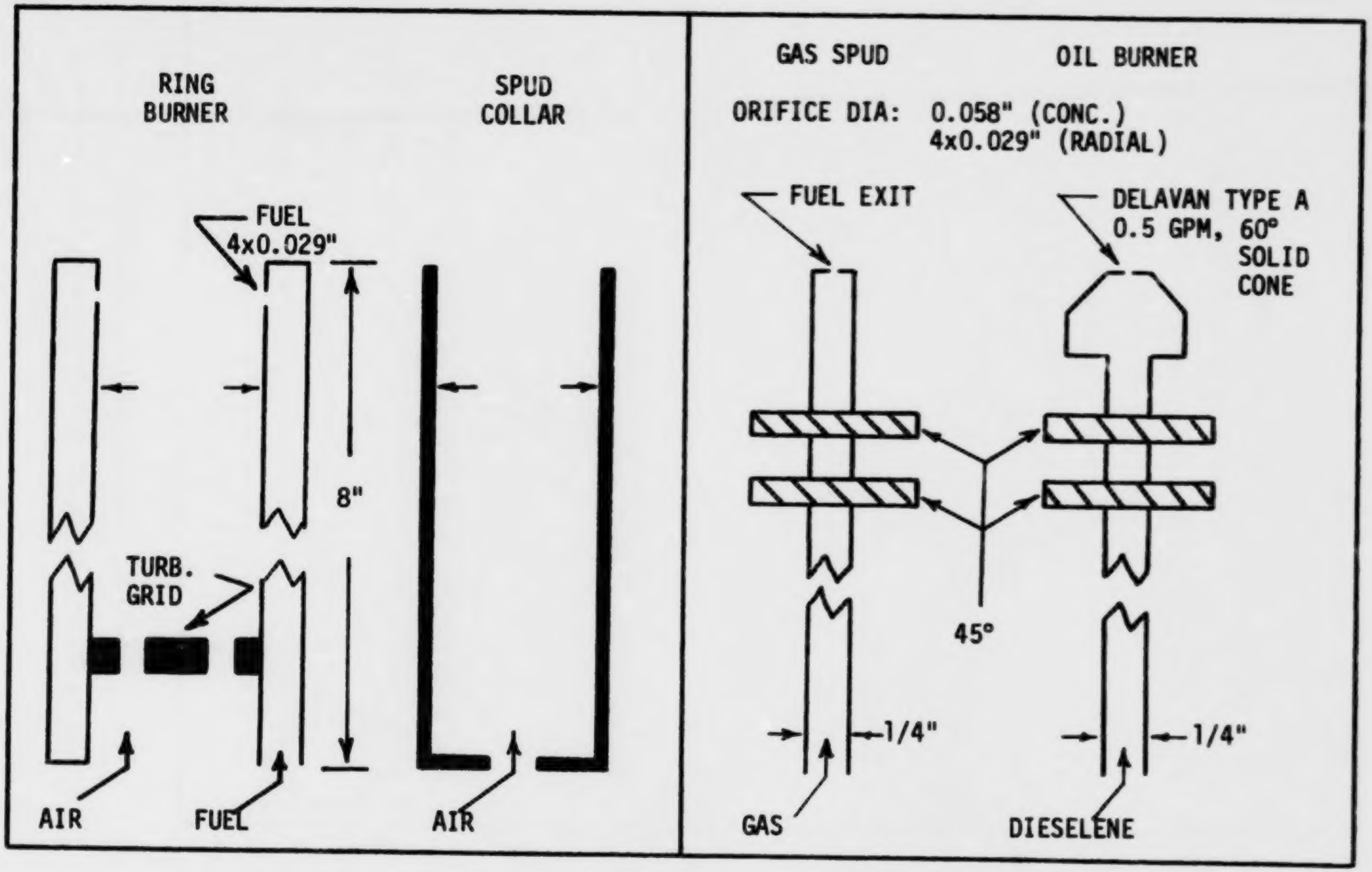
RING BURNER
SPUD COLLAR
GAS SPUD
OIL BURNER
ORIFICE DIA: 0.058" (CONC.)
4x0.029" (RADIAL)
FUEL 4x0.029"
8"
TURB. GRID
AIR
FUEL
AIR
FUEL EXIT
DELAVAN TYPE A 0.5 GPM, 60° SOLID CONE
45°
1/4"
1/4"
GAS
DIESELENE

Figure 3. Schematic of Burner Types for Interaction Studies

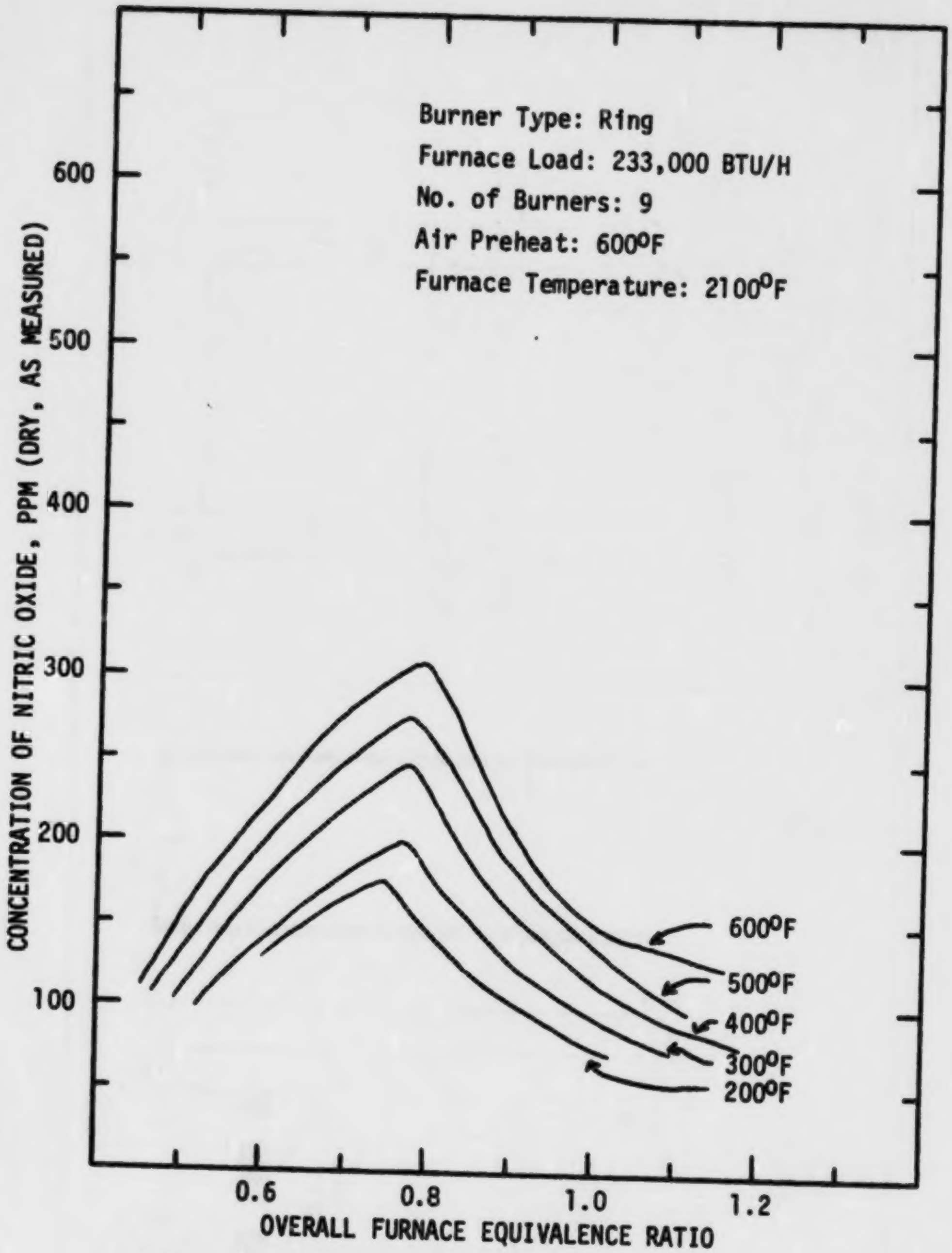

Figure 4. Influence of Air Preheat on NO_x Emissions from the Multiburner Furnace

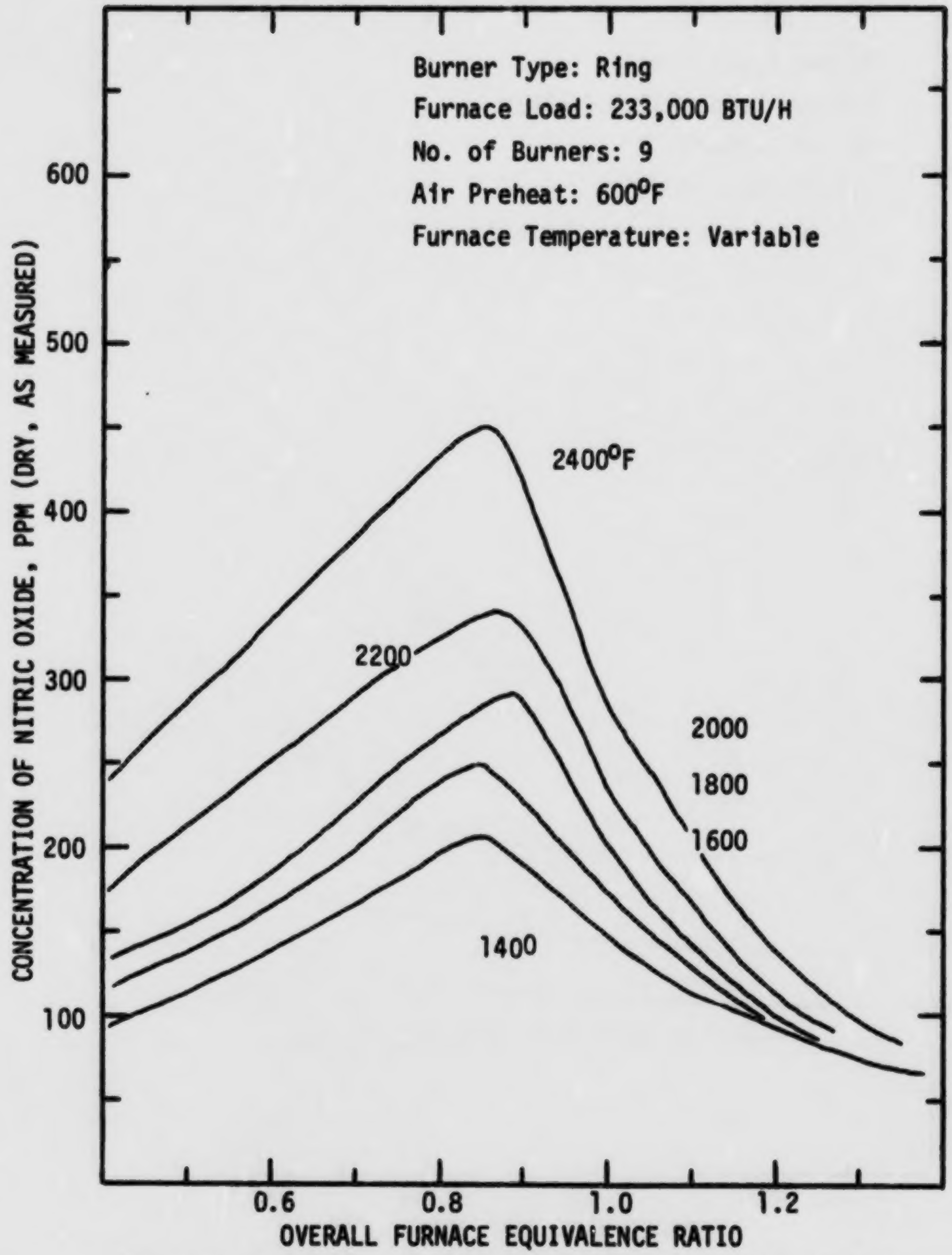

Figure 5. Influence of Equivalence Ratio and Temperature on NO_x Emissions from the Multiburner Furnace

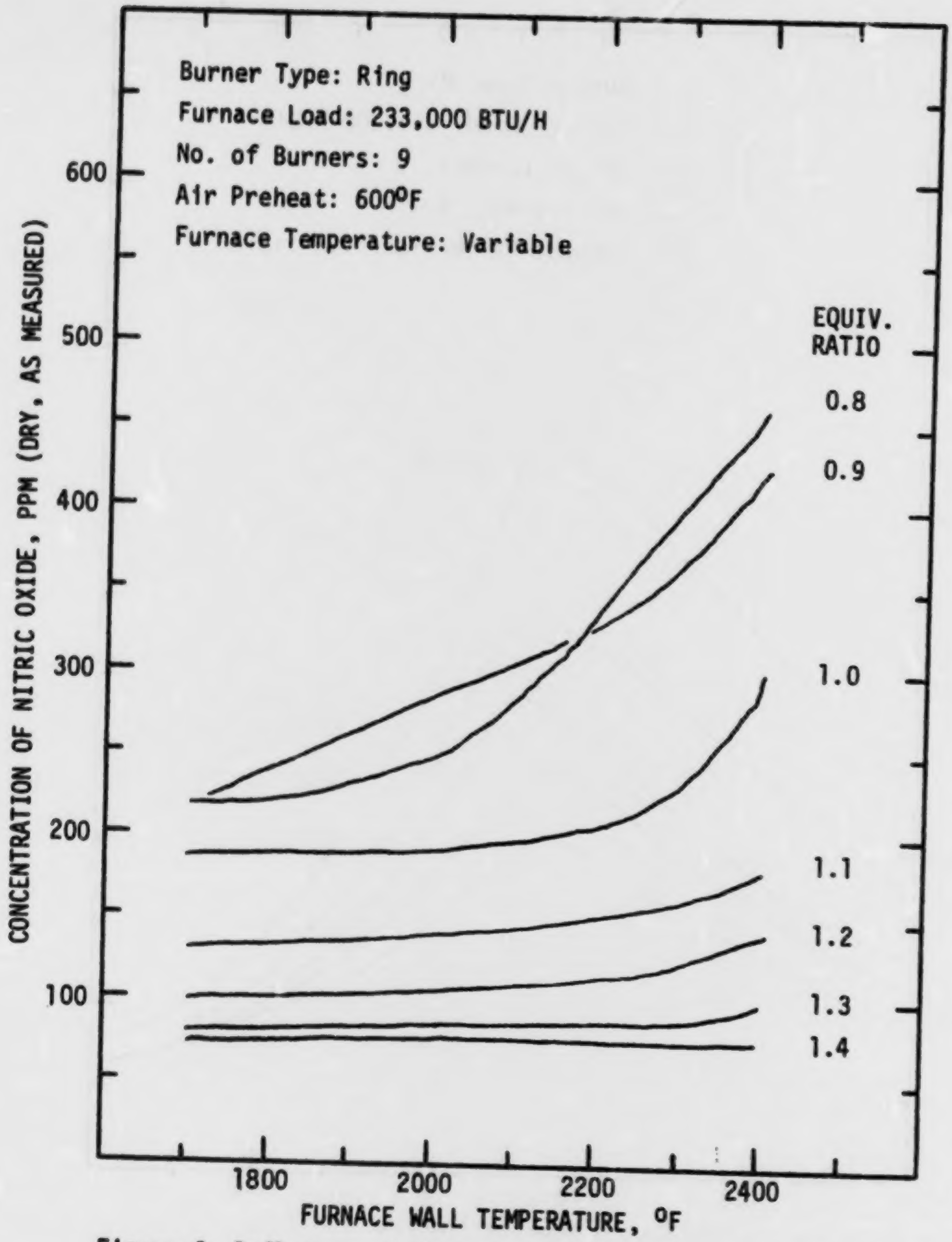

Figure 6. Influence of Furnace Temperature on NO_x Emissions

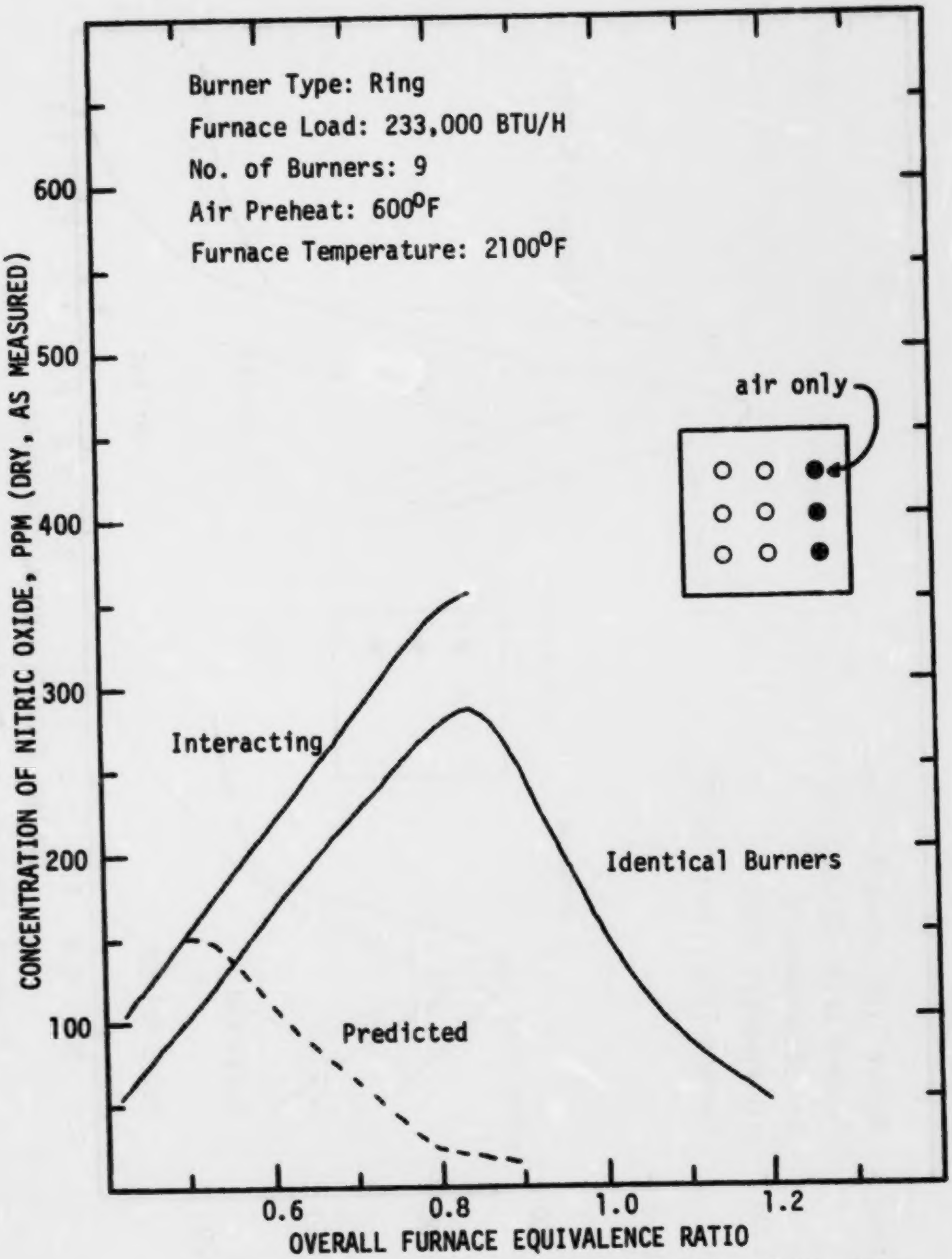

Figure 7. Measured and Predicted Levels of NO_x from an Array of Ring Burners

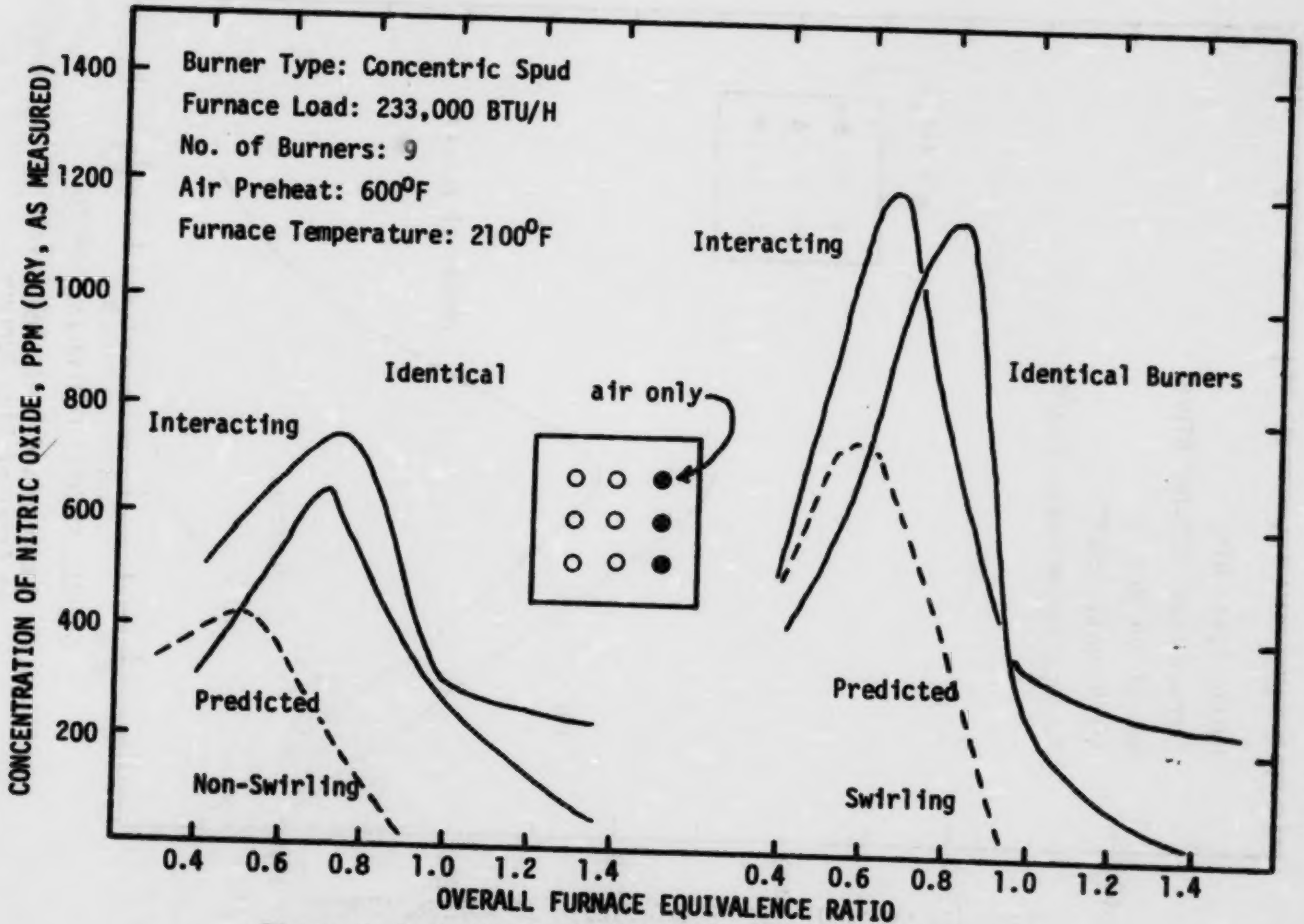

Figure 8. Measured and Predicted Levels of NO_x from an Array of Concentric Spud Burners

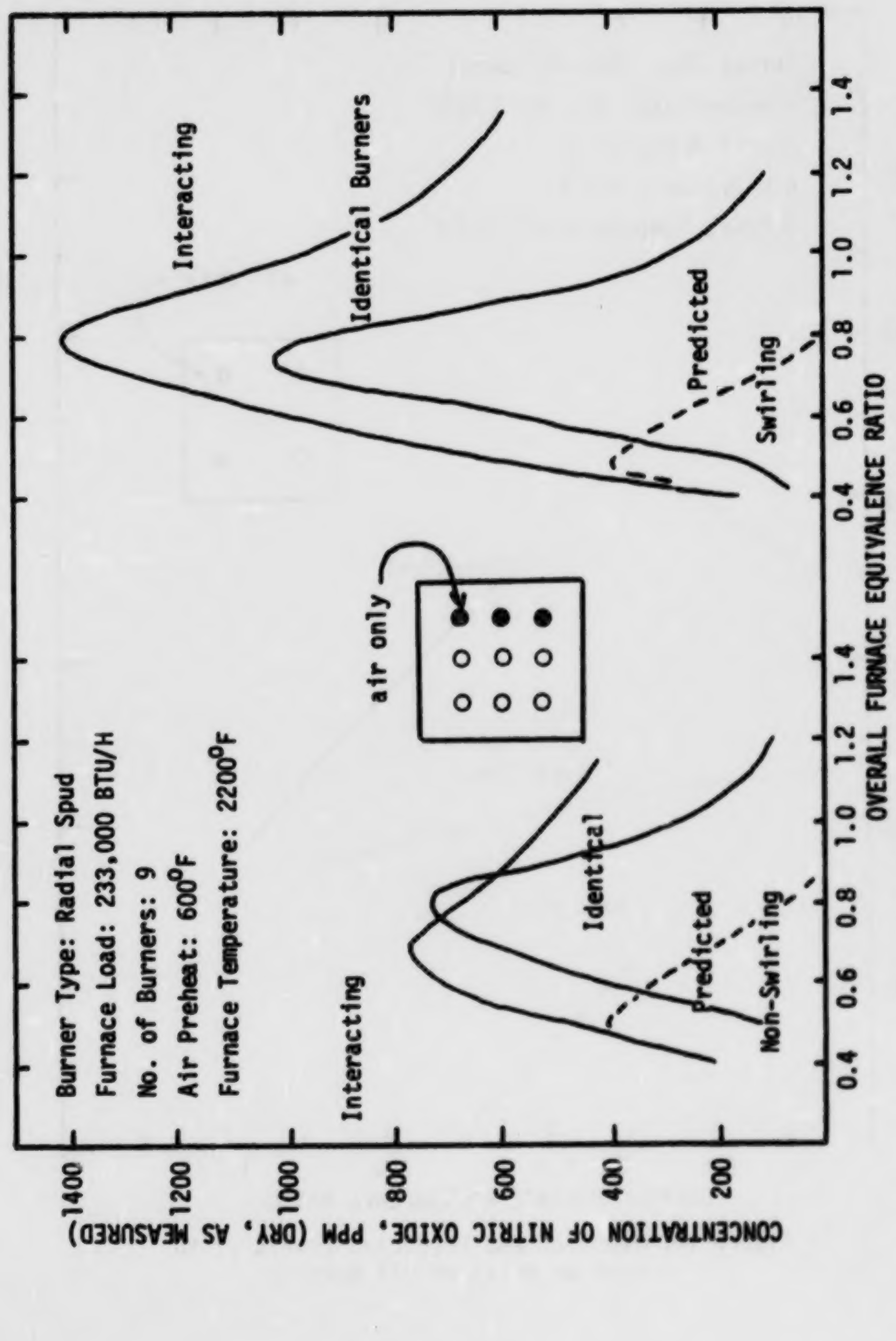

Figure 9. Measured and Predicted Levels of NO_x from an Array of Radial Spud Burners

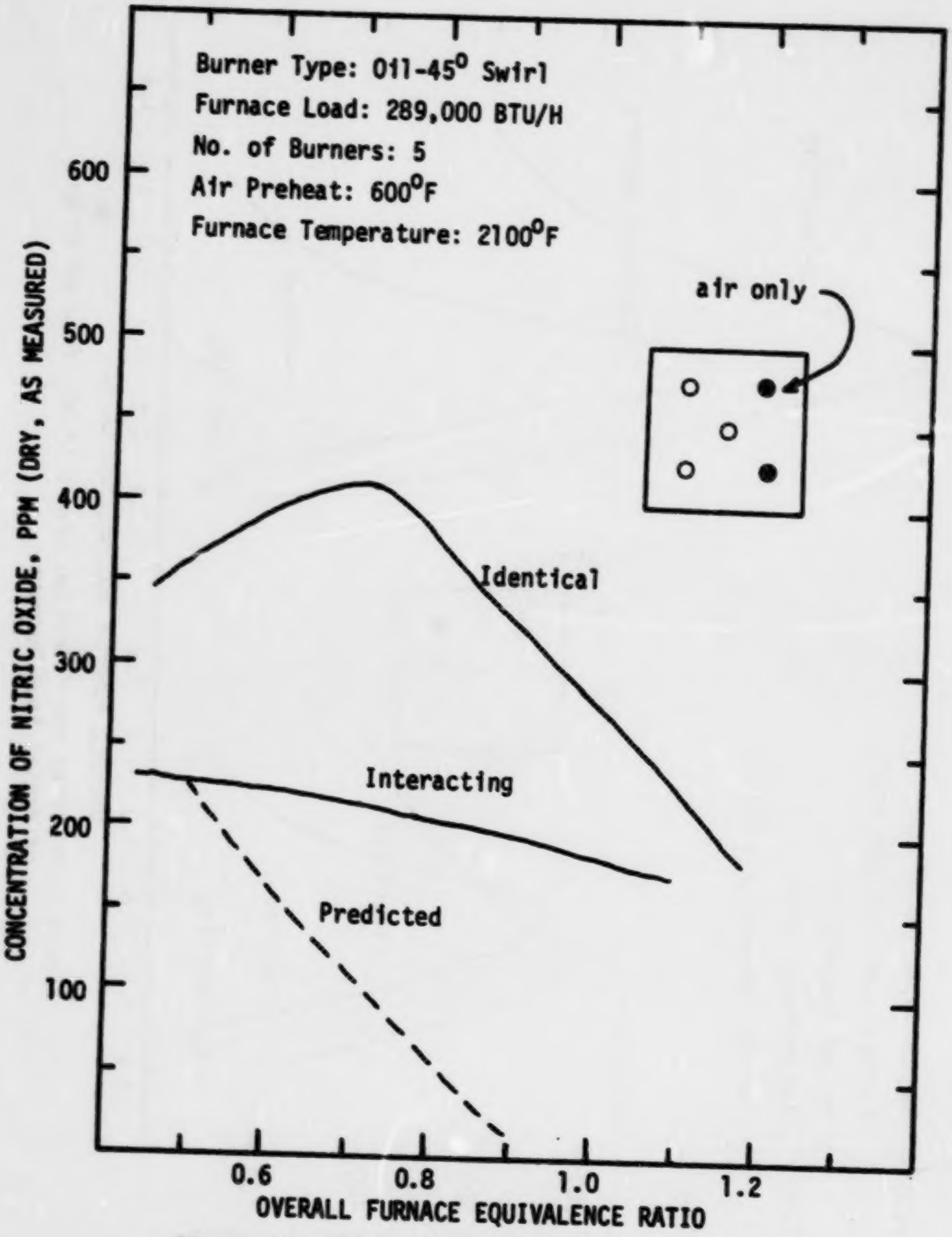

Figure 10. Measured and Predicted Levels of NO_x from an Array of Oil Burners

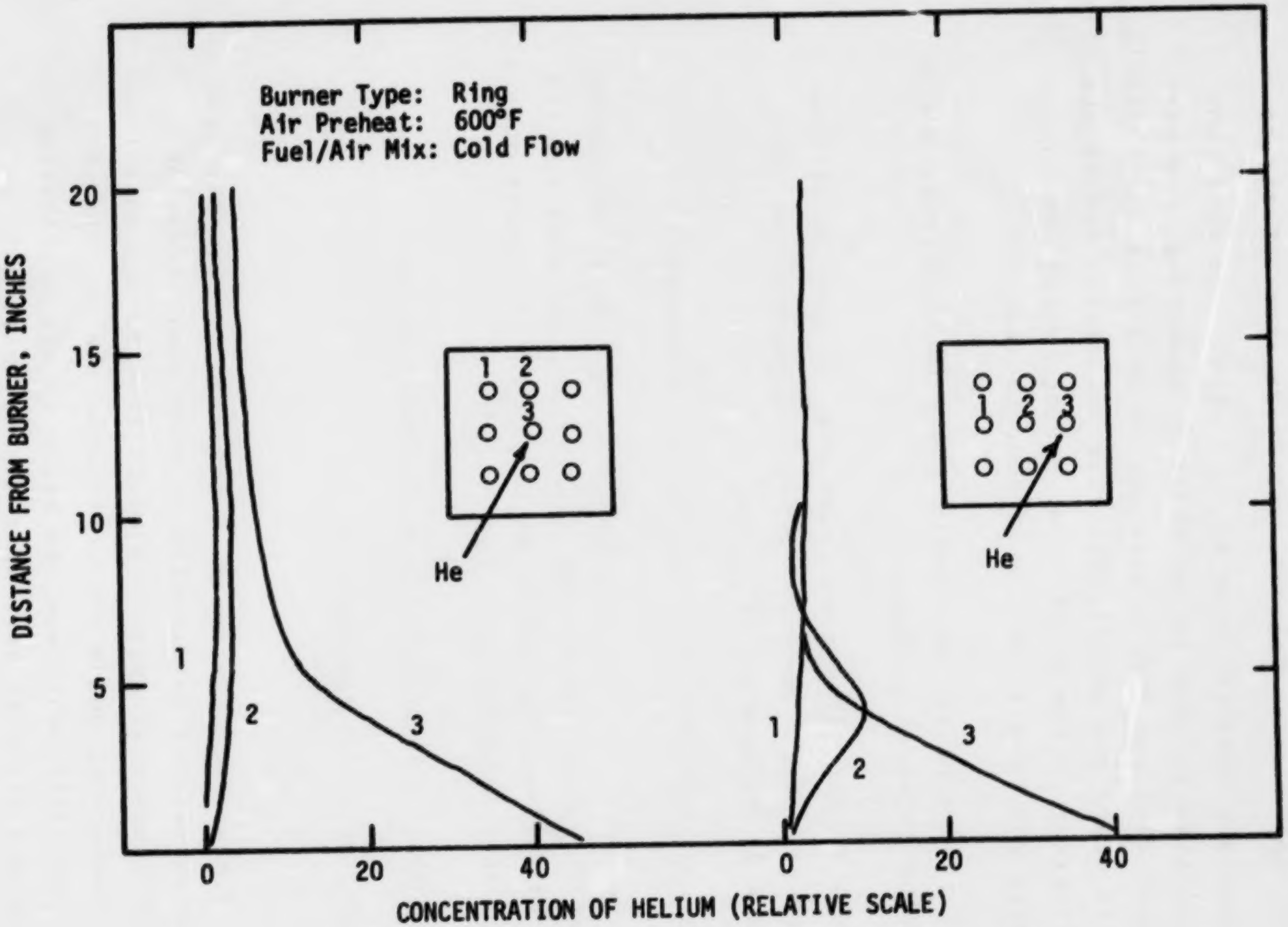

Figure 11. Helium Tracer Studies in the Multiburner System

3:45 p.m.
Production of Oxides of Nitrogen
In Interacting Flames
Dr. Christopher England, Jet Propulsion Laboratory

Q: When you measured your NO_x, I didn't see where you established that at the point of measuring, you were sure that you didn't have any stratification. I didn't see where you established that you really had no stratification at the point of measuring, which can happen when you have a portion of your burners off.

A: If you probe in the furnace after 10 diameters, everything is mixed completely.

Q: That is a general assumption that is made in orifice measurements. However, I don't think you can just take it without establishing it.

A: Oh, no, no -- we have the tracer measurement.

Q: O.K., that was the question I asked. When you probed for NO_x under combustion conditions, not when you had a cold flow, did you probe for NO_x at different points, and show uniformity of your data?

A: Oh, yes. And uniformity of temperature also.

Q: O.K., that was the question.

Q: If I heard you correctly, I believe you said that you had correlated the results of your small-scale unit with commercial units. I would like to ask what type of commercial units you correlated the results with, and secondly, what was the basis of the correlation - - what measurements were made in the small unit -- and what measurements were made in the commercial units?

A: The data I correlated with are data that were taken by Southern California Edison in support of a separate single burner project I had some years ago. The single burner data, at that time, didn't agree --

This is basically the air pre-heat data -- that's the best data. But, it was an old gas-fired Peabody ring burner system, similar in many, many respects to the furnace we operate.

Q: What type of fuel were you firing -- liquid fuel -- and what type of atomization was it?

A: This was with dieselene, using a 60° solid cone, Delzvan nozzle that we operate at full capacity. I don't know what the particles are.

Q: That's mechanical or air atomized?

A: Air atomized.

Q: And how were you determining your equivalence ratio?

A: The equivalence ratio was -- well, for oil?

[Yes.]

See, this is a small system. We had the oil on rotometers and had the air on orifices.

Q: So you were measuring the air flow. You weren't taking O_2 readings.

A: That's correct.

Q: And your probing in the flame -- this was done with probes -- water-cooled probes?

A: The hot stuff was all done with -- well, NO_x was done with a water-cooled quartz probe; the oxygen stuff -- that's just done with a stainless steel probe.

Q: The last question was what type of helium tracing technique did you use?

A: Well, we used just a straight leak detector.

Q: Could you explain the rationale behind taking 2/3 of the emissions for estimating a proportion for your projected or estimated emissions in dealing with concentrations rather than quantities? If I understand correctly, you were expressing your findings in terms of PPM, not mass of NO_x. Could you explain the rationale behind-you know, just taking -- if you take three burners out of action, then you're saying you're dealing with only 6/9 of the total emissions.

A: O.K., we're turning the fuel off - the air is already on -- so the total mass flow through the furnace is comparable when compared on overall equivalence ratio. The mass flow, total fuel flow and the air flow are the same for the two curves for identical equivalence ratio and what we call interacting. Now, we're just trying to define some handle to look at just what the interactions are. That's a convenient way to do it. If you look at the jets as though they're completely independent and you put cooled walls between them or adiabatic walls, you would expect 2/3 of the NO_x. If we operate six at 1.4 and three at air only, you'd expect to get the NO_x atom equivalence ratio of 1.4, 6 x 1.4 and 3 x 0, divide by 9.

Q: I think I'm bothered by the same thing Dr. Bartok is. If you shut off the fuel, and you don't shut off the air, when you're measuring the concentrations, then, actually, you've changed the equivalence ratio on the whole system. You're only putting in 2/3 as much fuel, and if you haven't changed the air, you've changed your equivalence ratio for the whole 9 configuration unit.

A: The abscissa is overall furnace equivalence ratio.

Q: Yes, I think maybe it ought to be plotted against something else.

A: We're trying to compare two different cases, and the overall furnace equivalence ratio is what we're interested in. We're interested in overall stack oxygen levels of 3% or whatever. So that's how they're plotted.

Q: But when you plot on equivalence ratio, then actually you're plotting not against the furnace with nine burners on and the furnace with six burners on; you're plotting against a situation where, in effect, you've transferred that fuel from those three burners to the other six burners. So, the question is whether you release the same amount of heat through nine burners or through six burners. If you release it through six burners, you might have locally higher heat release rates, which could locally up your NO_x generation and explain your results. In that side of the furnace, you're releasing more heat because you're putting all the fuel in only 2/3 of the furnace. You may get higher local temperatures and up your NO_x.

A: Yes, on the first data slide, I showed the effect of load was essentially the effect of heat release. And that is constant in our measurements over a factor of 5 or 6, or whatever -- that's about our turndown ratio. So that probably is not a factor.

Q: Would you care to reidentify the term "identical" with respect to interacting?

A: O.K., the identical is when we took the furnace and we ran all the burners at the same equivalence ratio. This kind of gives us a baseline feeling for what the furnace does as far as NO_x is concerned. Then, what we define as interacting is what happens when we pattern in some pattern. We alternate or otherwise change the equivalence ratios on the different burners, and then we measure the overall furnace NO_x. Originally, what we wanted to do is determine optimum pattern. What we found with gas was that there was no pattern that would help us.

Q: There is evidence from your charts and graphs that high swirl and high NO_x were correlated. Could you identify your observations on the shape of the flame at high swirl numbers? Was it much reduced in volume, for example?

A: It was much reduced in volume, yes.

Q: Getting back to that previous question, I don't know -- I seem to be missing the boat here, but you justify the conclusion by saying, well, you proved it by changing the furnace load. However, if I understood it right when you presented it, when you changed the load, you maintain the equivalence ratio, you just vary the total throughput. O.K., now, the point that the gentleman was making, and the point I was trying to make, is when you shut off three of your burners, and you maintain your overall equivalence ratio, the equivalence ratio on the other burners has, therefore, changed drastically. And I don't know how you can justify it by saying, well, -- I changed the load. . .

with the same equivalence ratio on all burners. I just don't see how to relate it; I think the gentleman's point is very well taken, that when you looked at your total equivalence ratio, and maintain that constant or turning off the gas to three burners, you therefore had to change the other burners, their individual equivalence ratios, and therefore their proportion of NO_x that they released had to be changed for the very data you presented.

A: Yes, but I don't think there is any question that load is a second order factor in NO_x. I don't think that -- our effects aren't second order effects. The other thing is that in an equivalence ratio of 1.4, NO_x should be low, regardless of the heat release.

Q: You know, I am one of those semi-bad hardware guys. There is no question that I can go air-only burners, you know, on a large furnace and drop the NO. And if I saw your photograph correctly, it looks like you have got an adiabatic combustion system. As soon as you do that, the staging doesn't mean a damn thing.

A: It's not adiabatic. The small systems have a small burner ---

Q: Unless you lose heat between the staging, you've got to get the same temperature. And I know I can pull air-only burners on any large size furnace and I know I could change the NO.

A: Well, that is true. That is why I said wall firing helps you; burner spacing helps you. We have a very well mixed system, and in the paper that will be in the proceedings, I point out that the difference of our furnace and the furnaces that you work with is that, in any small system, you have a very high surface to volume ratio. The surface to volume ratio controls the furnace temperature. To keep our furnace temperatures, our gas temperatures up and our NO_x up to a level that is comparable to a utility boiler, we must run wall temperatures of 2200° F. Well, that is substantially lower than adiabatic flame temperature, so there's no way you can contend that it is adiabatic, if there's lots of heat released through the walls. But the furnace's dominant method of heat transfer is convection from the walls. So if you measure the wall temperature, if you measure the gas temperature, if you measure the plume temperature, it's ten diameters away from the plume. Everything is exactly the same. It's a very well mixed system. It's different from a large system in which the wall temperatures may be 1000 or 1500 degrees -- many, many hundred degrees below the temperatures of the gases that are entrained in the plume. That is the difference between small furnaces and large furnaces; it is a tough problem to model.

Q: I think you just responded to the question I was going to ask. I recall from talking to you before that this was an unsteady operation that you were working with, so that when you had a fixed preheat temperature, and a fixed OF ratio, you were able to get variable temperature by variable conditioning of the furnace.

A. That's right . . .

Q: And therefore, locally right at the injectors, or at the burners, you would have conditions that would be perhaps typical of a large system, whereas in the bulk of the flow, you would have conditions that were unique to your own system. Therefore, you had two variables really -- if you were looking at the near burner effects, preheat would be a primary variable and the OF ratio to that burner; whereas if you're looking at post flame, or bulk effects, it became the wall temperature that was controlling. And therefore, your curves almost need an extra parameter in them. It just compounds the confusion, is all I was saying.

A: One of the things our data implies is that the NO_x is formed away from the burners, though.

Combustion Chemistry
and Modeling: An Overview

by

Adel F. Sarofim
Department of Chemical Engineering
Massachusetts Institute of Technology
Cambridge, Mass. 02139

Preceding page blank

ABSTRACT

The current understanding of mechanisms and kinetics of reactions pertinent to the combustion of fossil fuels is reviewed. Special emphasis is placed on reactions leading to pollutant formation.

Introduction

This overview presents a brief and necessarily incomplete coverage of developments in combustion chemistry and modeling that pertain to emissions from stationary sources. Prior to the passage of the Clean Air Act of 1967, in most practical combustion problems the rate of reaction was justifiably treated as being limited by the rate of mixing of fuel and air. In a few cases, such as the blow out of high output combustors or the velocity of flame propagation, the importance of chemical kinetics was recognised but allowance for kinetics was usually made using global rate expressions (1,2). The study of the details of combustion kinetics was mainly the preserve of the scientists interested in mechanism. It is only with the relatively recent recognition of the dominant contribution to air pollution of trace noxious species in combustion products that engineers have become actively interested in modeling combustion kinetics.

As an illustration of the importance of knowledge of flame kinetics on the development of pollution control strategy, the emissions from the first stage of a two-stage combustor burning a nitrogen-containing fuel are reported as a function of fuel/air equivalence ratio in Fig. 1. The nitric oxide emissions decrease, as expected, with increasing fuel/air ratio. Beyond a critical fuel/air equivalence ratio, however, an increasing amount of bound nitrogen escapes from the first stage of the combustor, and is available for oxidation to nitric oxide in the second stage. The maximum reduction in NO_x emissions and the fuel/air equivalence ratio at which it will be attained (1.7 for the example in Fig. 1) will depend on fuel composition, burner type, and air preheat in a manner that depends upon the governing chemical kinetics. Herein lies one practical motivation for studying mechanism and kinetics.

It is of interest to note that the data in Fig. 1 were generated by Smithells and Dent in 1894 (3) using a cyanogen/air mixture in a Smithells burner. Their objective was to demonstrate that the combustion of cyanogen occurred in two

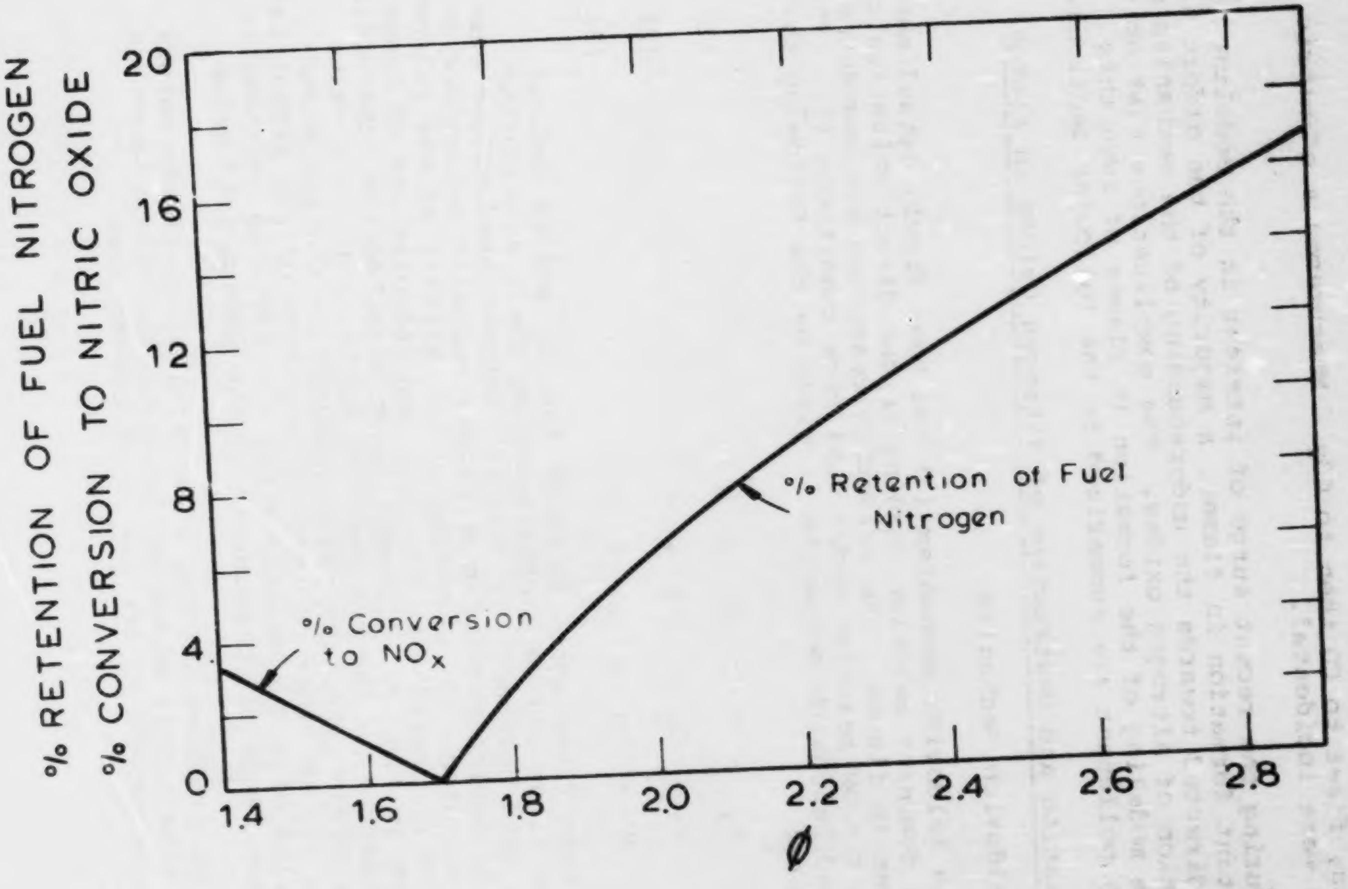

Fig. 1 Conversion of Fuel Nitrogen in First Stage of Two - Stage Combustor

stages, first to CO then to CO_2. Measurements of nitric oxide were incidental.

During the recent surge of interest in the modeling of pollutant formation in flames, a majority of the effort has been directed towards the understanding of the mechanism of formation of nitrogen oxides. The complications that arise in the modeling of the formation in flames of even this simple pollutant are summarized in the following sections.

Formation and Destruction of Nitrogen Oxides in Flames

A. Zeldovich Mechanism

The Zeldovich mechanism (4) has been firmly established as the dominant reaction leading to the direct oxidation of nitrogen in flames. The Zeldovich reactions are augmented by the N + OH reaction under fuel rich conditions (5). The extended Zeldovich mechanism is given by the following three reactions:

$$N_2 + O = NO + N \tag{1}$$

$$N + O_2 = NO + O \tag{2}$$

$$N + OH = NO + H \tag{3}$$

In the post flame zone, in which the O and OH radical concentrations can be approximated by their equilibrium values, good agreement is obtained between predictions based on the Zeldovich mechanism and experimentally determined NO formation rates. An illustration of validity of the Zeldovich mechanism is provided by the data and calculations of Lange (6) shown in Fig. 2. Although Lange adjusted the rate limiting constant (the forward reaction of Eq. (1)) to a value slightly higher than the value reported in the Leeds compilation (7) in order to improve the match of the calculated NO profiles with his measurements, his adjusted constant is within the range of uncertainty of the recommended value.

The NO profiles in Fig. 2 extrapolate to finite values at zero time. This anomalous behavior has become known as Fenimore or prompt NO (8) and is discussed next.

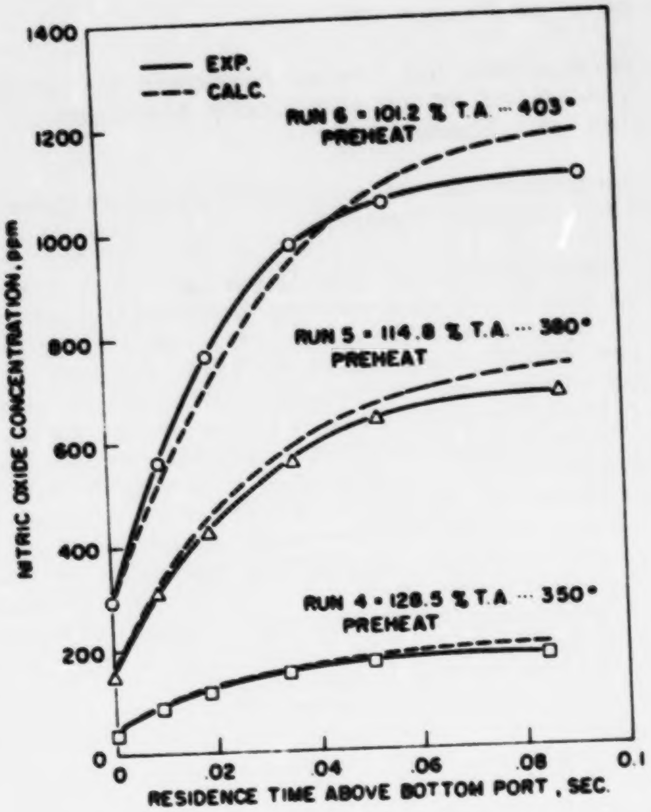

Fig. 2 Comparison of measured NO_x profiles with values calculated using the Zeldovich mechanism (from Ref. 6)

B. Fenimore or Prompt NO

Two mechanisms have been proposed to explain the very rapid build-up of NO in the early portions of premixed hydrocarbon air flames.

(1) The contribution of superequilibrium free radical concentrations to prompt NO

As a consequence of the increase in the number of moles during the early stages of the combustion of hydrocarbon fuels and the relatively slow rate of the termolecular recombination reactions, there exists regimes in flames containing oxygen and hydroxyl radicals in concentrations exceeding their equilibrium values by an order of magnitude or more. This excess radical concentration has been found to be sufficient to explain the prompt NO observed under fuel lean conditions (9,10,11). An example of the effect of the excess radical concentrations is shown in Fig. 3. The lower of the two NO profiles shown was calculated using equilibrium oxygen concentrations and the upper was obtained with allowance for superequilibrium oxygen concentrations (12); the shaded area represents the contribution to prompt NO of superequilibrium radical concentrations. The magnitude of this prompt NO is of the order of 50 ppm, modest by comparison to uncontrolled levels of emissions from large boilers, but significant relative to controlled emissions or emissions from smaller units. The results in Fig. 4 are used to illustrate that the phenomenon of superequilibrium oxidant concentrations is also encountered in laminar diffusion flames (13). Agents such as SO_2 which can scavenge the excess oxidant radicals can be effective in reducing the magnitude of this source of prompt NO as has been shown by Wendt and Ekmann (this Symposium).

(2) The contribution of the formation of fuel nitrogen to prompt NO

Fenimore (8) proposed originally that prompt NO is formed indirectly by the oxidation of an organic nitrogen compound, produced by a reaction such as

$$CH + N_2 = HCN + N \tag{4}$$

Such reactions appear to account for most of the prompt NO encountered under fuel rich conditions. Conclusive evidence for this mechanism is provided by the results of Haynes et al. (14) summarized in Fig. 5 which show the build-up and decay of HCN in a fuel-rich ethylene flame.

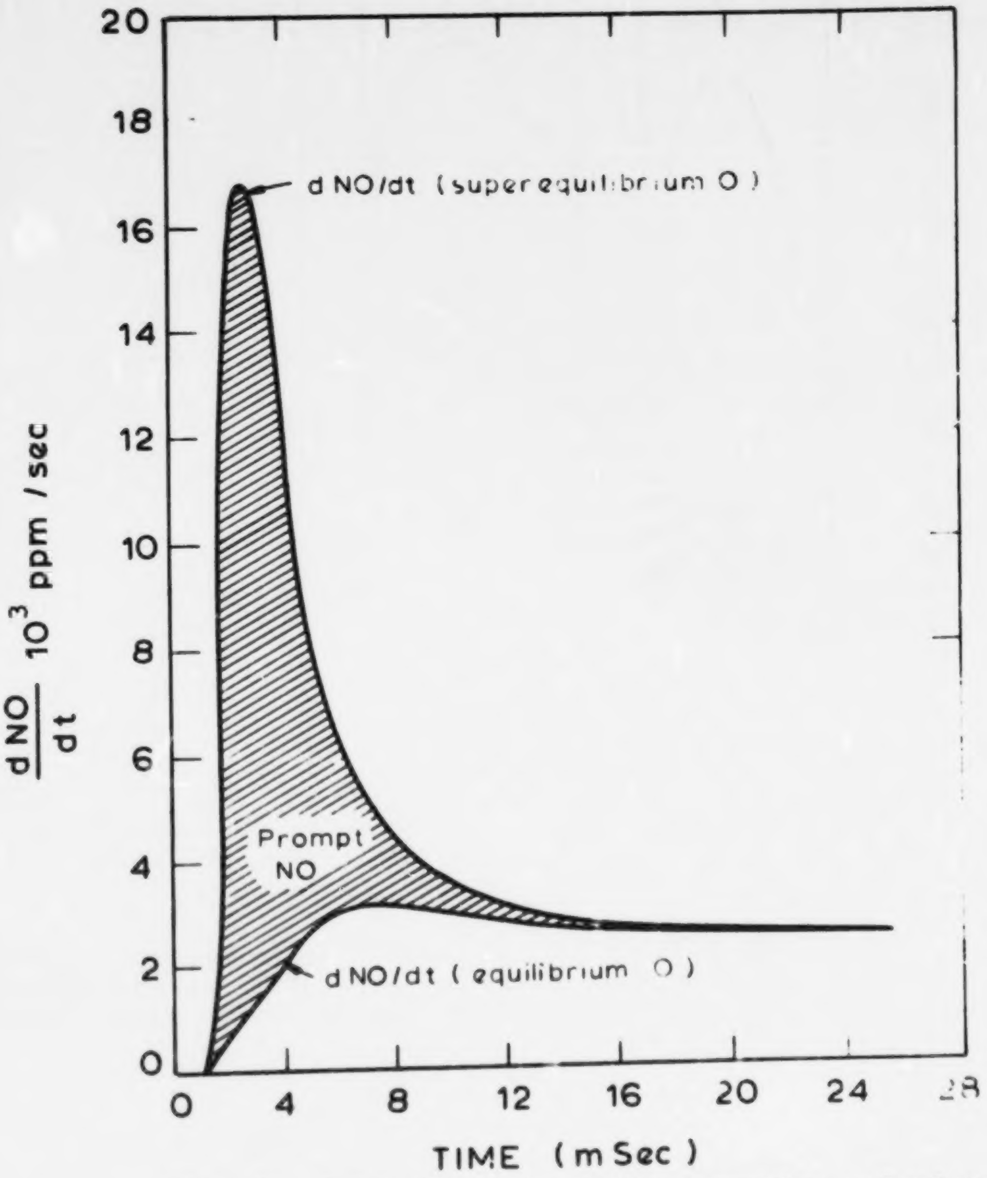

Fig. 3 Rate of nitric oxide formation calculated using equilibrium (bottom curve) and non-equilibrium (top curve) radical concentrations (from Ref. 12)

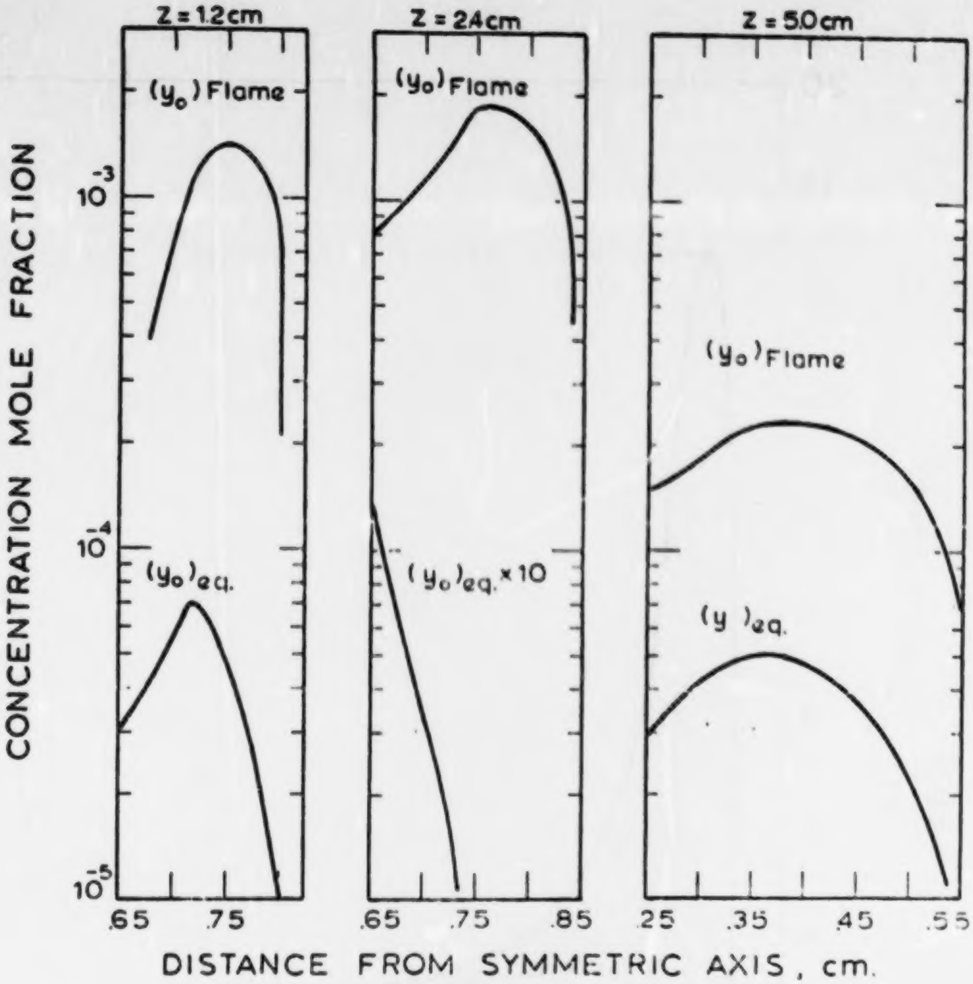

Fig 4 Comparison of equilibrium and nonequilibrium oxygen atom concentrations at three elevations in a methane/air laminar diffusion flame (from Ref. 14)

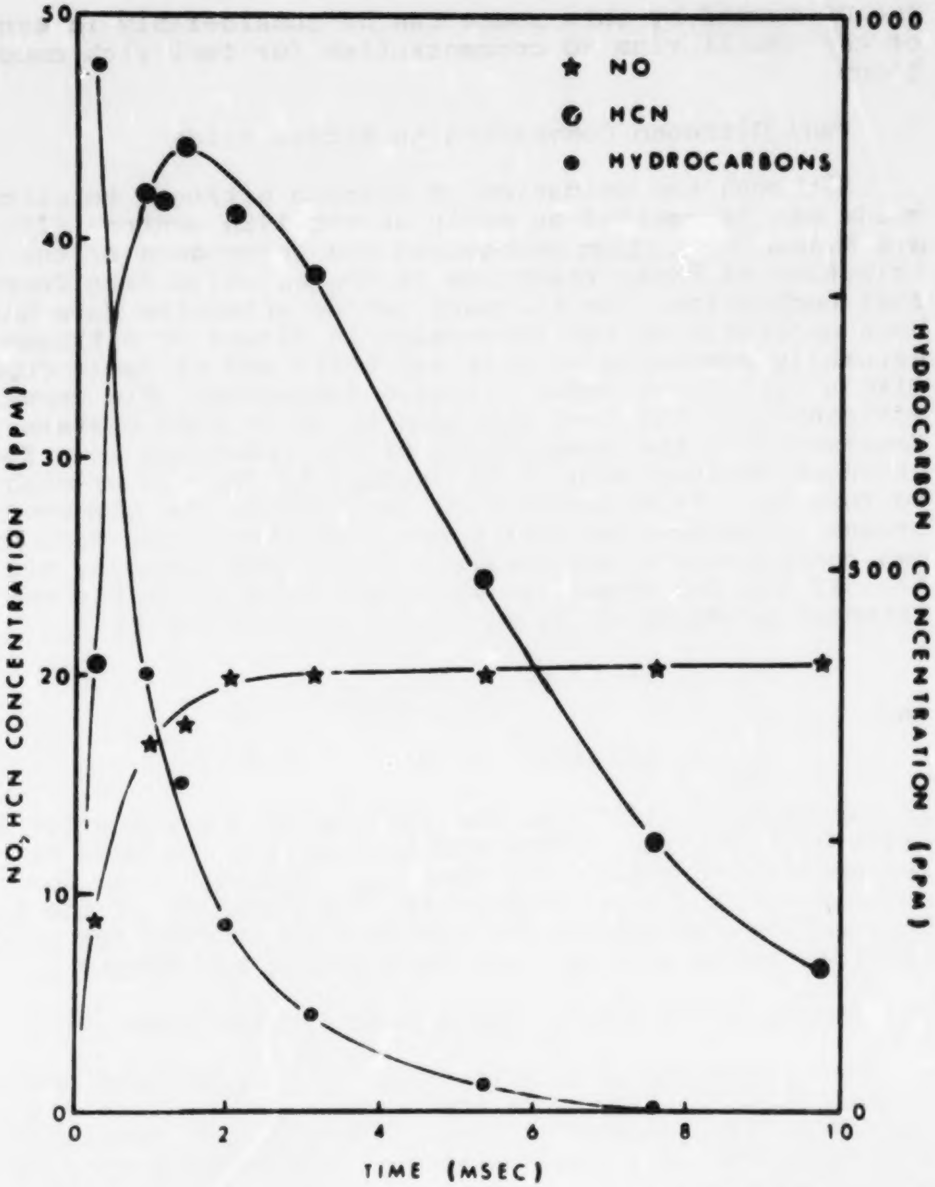

FIG. 5 Measured profiles of NO, HCN, and hydrocarbons in an ethylene-air flame, $\phi = 1.64$, $T = 2040°K$. (from Ref. 14)

The NO formed by this route can be considerably in excess of the equilibrium NO concentration for fuel rich conditions.

C. Fuel Nitrogen Conversion to Nitric Oxide

Although the oxidation of organic nitrogen to nitric oxide was recognized as early as the 19th century (15), Shaw and Thomas (16), first recognized the importance of the contribution of these reactions to NO_x emission from fossil-fuel combustion. In the past decade extensive data has been generated on the conversion in flames of nitrogen naturally occurring in oils and coals and of fuels doped with a variety of model nitrogen compounds. The conversion efficiency of the fuel nitrogen to NO in such systems is determined by the competition of the reactions of a fuel nitrogen derivative with an oxidant to form NO or with NO to form N_2. This competition can explain the observed decrease in conversion efficiency with increasing fuel nitrogen concentration and fuel/air ratio (for example, see Fig. 6). If the two competing reactions leading to the end nitrogen products of N_2 and NO are represented by

$$RN + OX \rightarrow NO + RX \qquad (5)$$

and

$$RN + NO \rightarrow N_2 + RO \qquad (6)$$

it can be shown (8) that the maximum NO concentration is given by $k_5(OX)/k_6$. This simple relation was used by Fenimore to correlate his results. Although numerous postulates have been offered for the identity of the key intermediate RN, additional mechanistic studies are needed in order to resolve present conflicting statements.

D. Reduction of Nitric Oxide with Hydrocarbons

The reduction of nitric oxide by hydrocarbons has been demonstrated by Sternling and Wendt (17), Myerson (18), De Soete (19), amongst others. The probable mechanism is the formation of a bound nitrogen intermediate by a reaction such as

$$HC + NO \quad HCN + O \qquad (7)$$

followed by the partial reduction of the fuel nitrogen intermediate to N_2. The results by De Soete shown in Fig. 7 demonstrate quite clearly the occurrence of such a

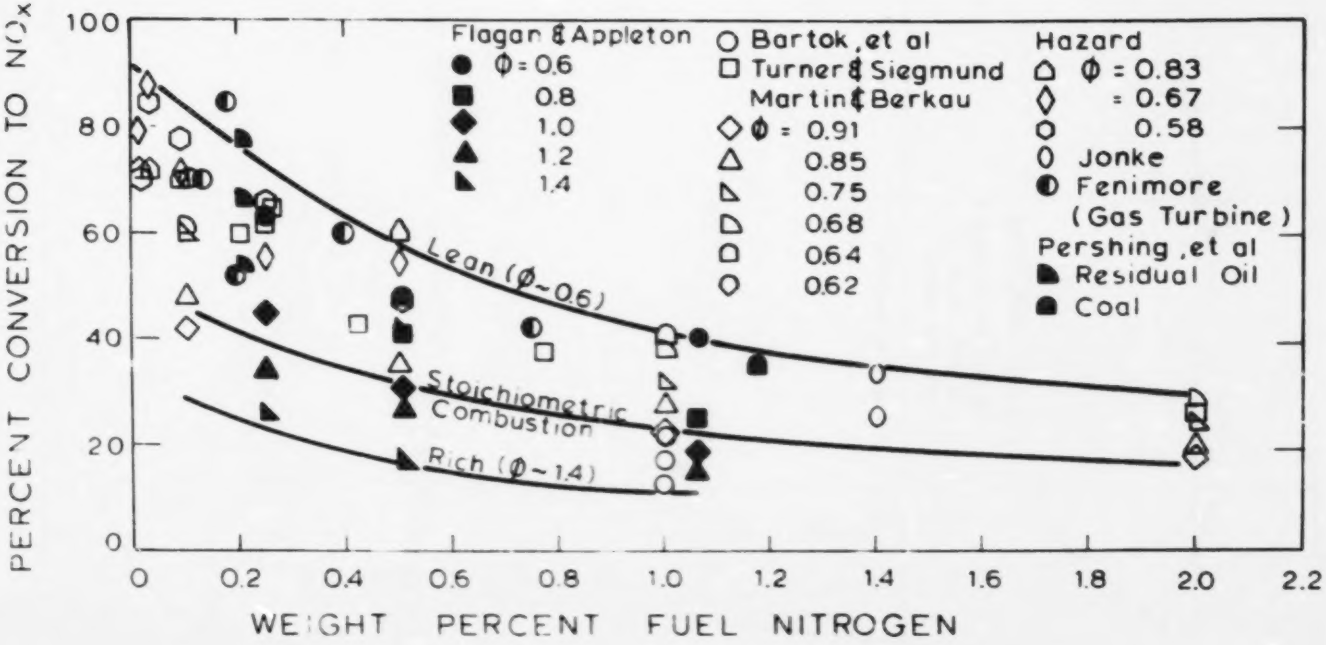

Figure 6 Conversion of Fuel-Nitrogen to NO_x in Combustors
(compiled by R. C. Flagan from selected references)

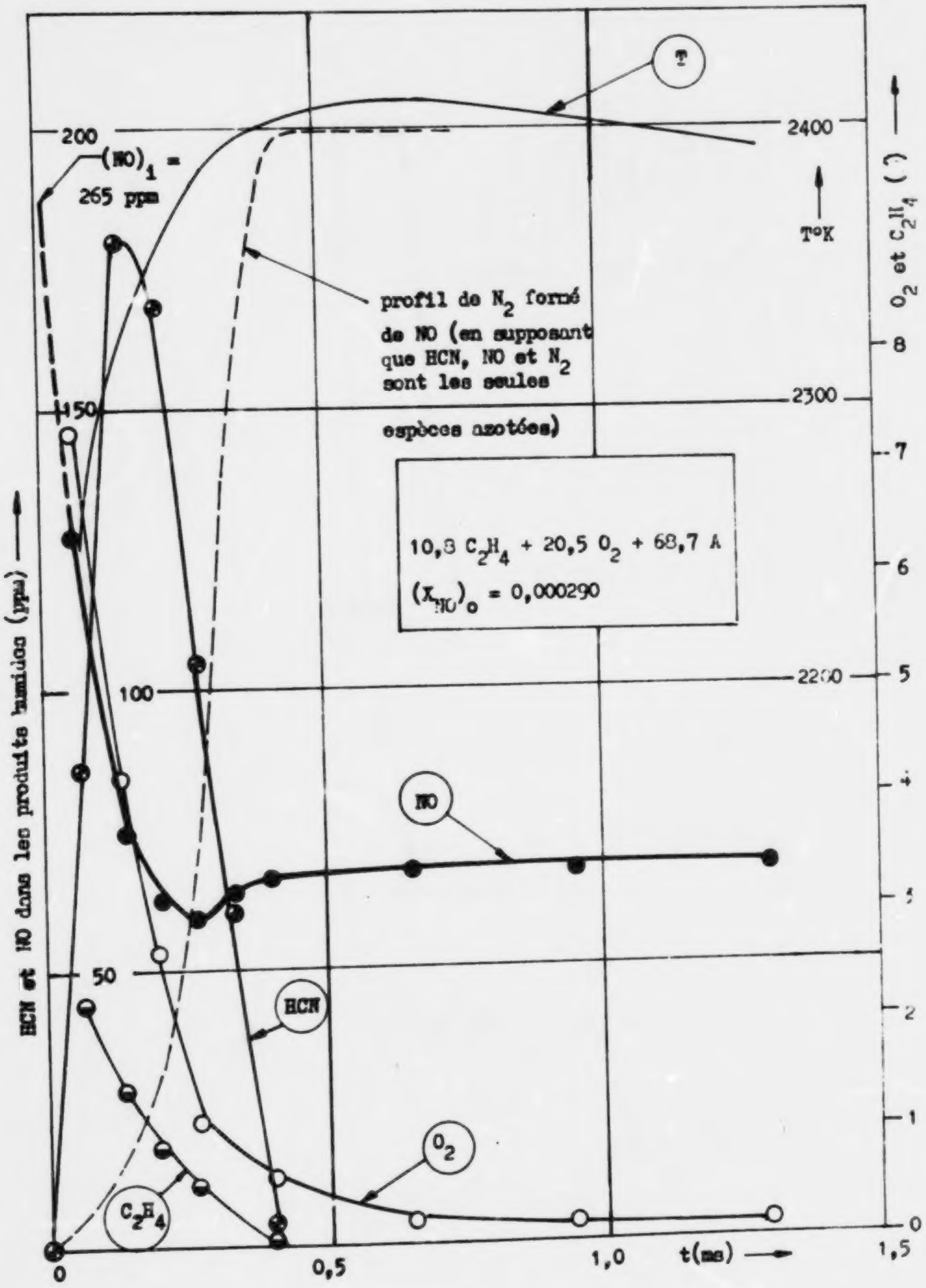

Fig. 7 Concentration profiles in a $C_2H_4/O_2/A$ flame to which NO has been added (from Ref. 19)

sequence of reactions. The NO injected into an ethylene/oxygen/argon flame is converted to HCN, which in turn is partially reduced to N_2. The HCN intermediate may also be converted to nitric oxide in the tail of the flame, particularly under fuel lean conditions (19).

E. NO_2 Formation in Flames

Until recently periodic reports of significant NO_2 formation in flames was discounted as being due to probe errors. It now appears probable that NO_2 is formed in high concentrations by reactions of NO with HO_2 and/or OH, and that the NO_2 may be subsequently reduced by reactions with O atoms. Evidence for this is provided by Merryman and Levy (20), one of whose profiles is reproduced in Fig. 8, and by the numerical simulations by Kendall et al. (This Symposium). In most practical systems NO_2 accounts for less than 5 percent of the NO_x in the exhaust but higher values can be encountered when flames are rapidly quenched.

F. Catalytic Reduction of NO

Probe effects in NO sampling provide a good example of the catalytic reduction of NO (21). The combustion system most amenable to the exploitation of catalytic reduction is the fluidized bed combustor because the bed substrate provides a high specific surface area. Indeed, heterogeneous reduction of NO in fluidized beds has been reported by Hammond and Skopp (22), Jonke (23), and Pereira et al. (24).

G. Complete Kinetic Models for NO Formation

Detailed kinetic models of the reactions in flames leading to NO formation have been developed for a few well-defined systems. An example of such modelling is the study of Engleman et al. (15) of NO formation in a well-stirred reactor. They obtained excellent agreement between calculations and measurements for CO/air and H_2/air mixtures for all the stoichiometries studied but found that, for rich hydrocarbon/air mixtures, the measured NO_x levels were higher than predicted. Later calculations by Tyson and Heap (26) suggest that the discrepancies for hydrocarbon/air mixtures are attributable to the HC + N_2 reaction.

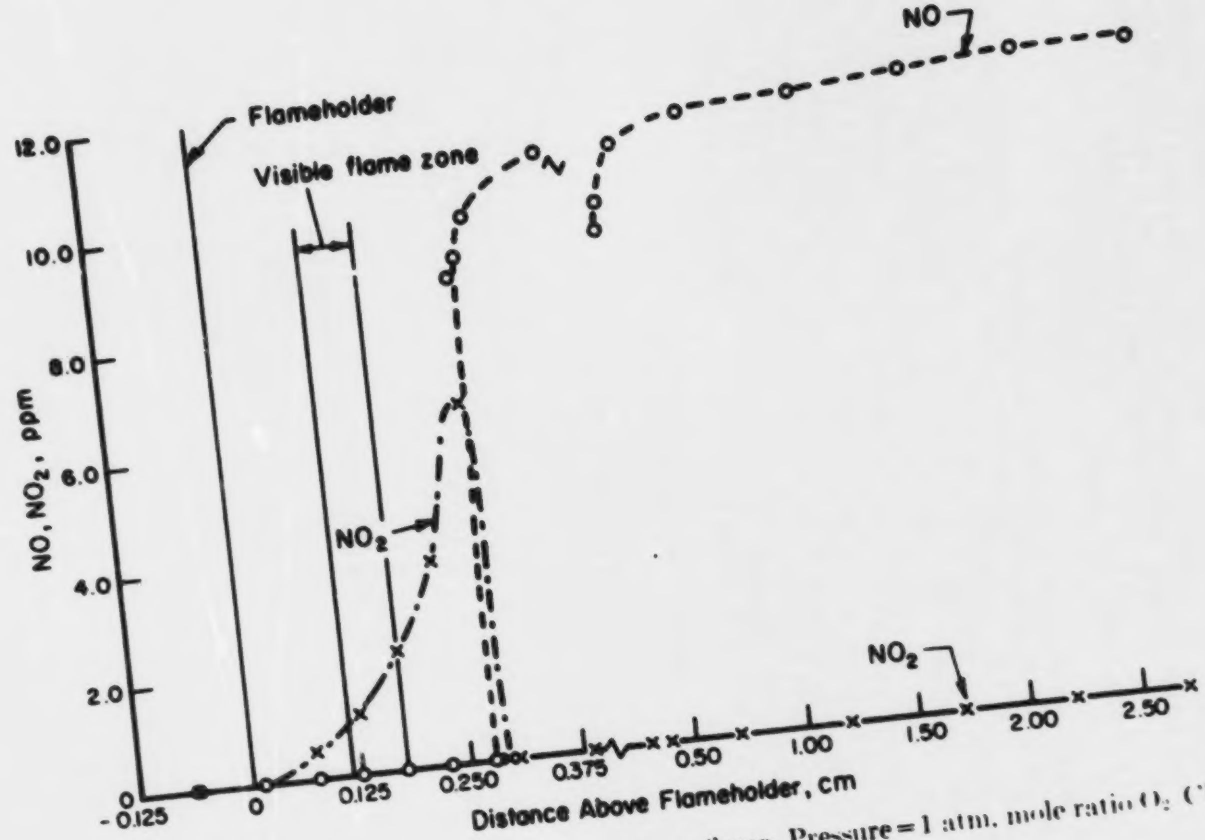

FIG. 8 Formation of NO and NO_2 in a fuel-rich methane flame. Pressure = 1 atm, mole ratio O_2:CH_4 = 1.8.

H. Developing Combustion Process Modification for NO_x Control

The understanding of the mechanism for NO formation, although incomplete, is sufficient to permit the development of optimized control strategies for aerodynamically simple systems. Unfortunately, in many practical combustors the complexities introduced by the turbulent mixing processes and recirculation leads to an enormous number of possible paths for NO formation and destruction (shown schematically in Fig. 9) and optimization is difficult. It is for this reason that the full potential for NO_x reduction by combustion process modification has not been achieved.

Pollutants Other Than NO_x

Of the emissions from stationary sources, the nitrogen oxides have justifiably received the greatest attention since they both pose a critical environmental problem and are amenable to control by combustion process modifications. A listing of other combustion-generated pollutants is provided in Table I derived from the study by Locklin et al. (27). Many of these pollutants involve complex molecules whose formation chemistry is poorly understood. With the probable trend toward the burning of more coal, coal-derived fuels, and possibly shale oils it is apparent that the future problems of modelling combustion kinetics will be associated with the chemistry of larger molecules, having lower H/C ratios, and possibly higher nitrogen and sulfur concentrations. In addition the chemistry of ash behavior may become increasingly important. The gaps in the chemical kinetics pertinent to the combustion of coal and heavy oils that we should strive to fill include:

- solid and liquid phase pyrolysis: the rates and mechanisms of formation of volatiles, carbonaceous cenospheres and tar; and the distribution of critical trace elements
- gas phase pyrolysis: the competitive and sequential reactions leading to the formation of soot, tars, polycyclic aromatic hydrocarbons, and light constituents
- catalytic effects on the above: the modification of the rates of the pyrolysis reactions by free radicals or solid catalysts

TABLE I

CONTRIBUTION TO COMBUSTION-GENERATED EMISSIONS BY DIFFERENT FUELS*

(Percentages Derived for the Period 1970-1990 assuming no advances in technology)

Pollutant	Products of Incomplete Combustion					Fuel Contaminants				Fuel Additives			Combustion Generated Pollution	
Fuel	CO	HC	POM PNA	Odor	Combustible Particles	Ash	SO_x	NO_x from Fuel N	Heavy Metals	Pb	Ba	Mn	NO_x from Atmos. N	Combustion Noise
Coal	1.2	1.7	79.9	-	48	98	88.3	$26.4x_1$					$26.4(1-x_1)$	
Oil	97.6	95.1	15.2	100	44.6	2	11.7	$56.7x_2$		100	100	100	$56.7(1-x_2)$	
Gas	1.2	3.2	3.9	-	7.4	-	-	-					16.9	
Estimated 1970 Emissions (10^6 tons/yr.)	147	35			25		34	$23x_3$					$23(1-x_3)$	

x_1, x_2, x_3: fractions of NO_x emissions contributed by fuel nitrogen

---

*Derived from 27

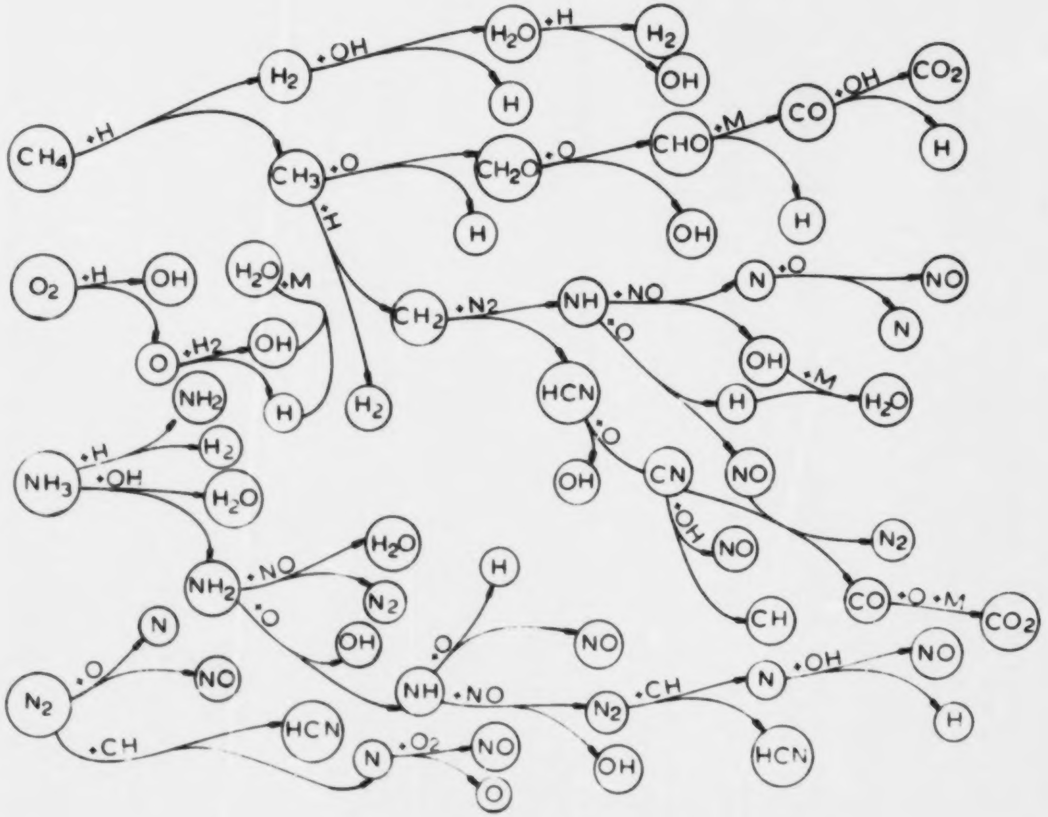
CH4
•H
H2
•OH
H2O
•H
H2
OH
H
CH3
•O
CH2O
•O
CHO
•M
CO
•OH
CO2
H
H
OH
H
•H
O2
•H
OH
O
•H2
OH
H
H2O
•M
H2
CH2
•N2
NH
•NO
•O
N
•O
NO
N
OH
•M
H2O
H
HCN
•O
OH
CN
•OH
NO
CH
NO
N2
CO
•O •M
CO2
NH3
•H
•OH
NH2
H2
H2O
NH2
•NO
•O
H2O
N2
OH
N2
•O
N
NO
•CH
HCN
N
•O2
NO
O
NH
•O
H
NO
•NO
N2
•CH
OH
N
•OH
NO
H
HCN

Figure 9 Schematic of Some of Many Possible Interactions in Hydrocarbon, Oxygen, Nitrogen, Bound Nitrogen System in the Presence of Inhomogeneities and Back-Mixing

- solid reactions: reactions such as the reduction of metal and mineral oxides, e.g., $SiO_2 + C \rightarrow SiO + CO$, which can lead to the augmentation of the vaporization of the oxides and subsequent recondensation as submicron particles.

Literature Citations

1. Longwell, J. P., and Weiss, M. A., Ind. Eng. Chem., 47, 1634 (1955).
2. Spalding, D. B., Combustion and Flame, 1, 287 (1957).
3. Smithells, A., and F. Dant, Chemical Society Journal Transactions, 65, 603 (1894).
4. Sarofim, A. F., and J. H. Pohl, Fourteenth Symposium (International) Combustion, p739, The Combustion Institute, Pittsburgh (1973).
5. Lavoie, G. B., Heywood, J. B., and Keck, J. C., Combustion Science and Technology, 1, 313-326 (1970).
6. Lange, H. B., Jr., "NO_x Formation in Premixed Combustion: A Kinetic Model and Experimental Data," Air Pollution and Its Control, AIChE Symposium Series 126, Vol. 68, p17 (1972).
7. Baulch, D. L., D. D. Drysdale, D. G. Horne, and L. C. Lloyd, "Critical Evaluation of Rate Constants for Homogeneous, Gas Phase Reactions of Interest in High Temperature Systems," Dept. of Physical Chemistry, The University of Leeds, England, Report No. 4, December, 1969.
8. Fenimore, C. P., Thirteenth Symposium (International) on Combustion, p373, The Combustion Institute, 1971.
9. Thompson, D., T. D. Brown, and J. M. Beer, Combustion and Flame, 19, 69 (1972).
10. Livesey, J. B., A. L. Roberts, and A. Williams, Combustion Sci. Tech., 4, 9(1971).
11. Williams, G. C., A. F. Sarofim, and N. Lambert, Proc. General Motors Symposium on Emissions from Continuous Combustion Sources, p141, Plenun Press, 1972.

12. Sarofim, A. F., G. C. Williams, A. Padia, "Control of NO_x Emission by Partial Quenching," Presented at Central States Section Meeting of the Combustion Institute, Champaign, Ill., March, 1973.

13. Mitchell, R. E., and Sarofim, A. E., "Nitrogen Oxide Formation in Laminar Methane Air Diffusion Flames," Paper 75-3, Western Sections Meeting, Combustion Institute, October, 1975.

14. Haynes, B. S., Iverach, D., and Krov, N. Y., Fifteenth Symposium (International) on Combustion, Combustion Institute, Pittsburgh, 1975, p103.

15. Berthelot, M., Ann. Ohm. Phys., 5, 433 (1875), and Later works.

16. Shaw, J. T., and Thomas, A. C., 7th International Conference on Coal Science, Prague, June 10-14, 1965.

17. Wendt, J.O.L., Sternling, C. V., and Matovich, M. A., (1973), Fourteenth Symposium (International) on Combustion, Combustion Institute, Pittsburgh (1973).

18. Myerson, A. L., Fifteenth Symposium (International) on Combustion, Combustion Institute, Pittsburgh (1975), p1085.

19. De Soete, G., and A. Muerand, Institute Francois du Petrol, Report No. 21.381, May, 1973.

20. Merryman, E. L., and Levy, A., Fifteenth Symposium (International) Combustion, p1073, The Combustion Institute, Pittsburgh (1975).

21. Halstead, C. J., and A.V.E. Munro, "Sampling, Analysis and Study of the Nitrogen Oxides Formed in Natural Gas/Air Flames," Presented at 1st AGA-IGT Conference on Gas Research and Technology, Chicago, Ill., (1971).

22. Hammons, G. A., and A. Skopp, "NO_x Formation and Control in Fluidized Bed Coal Combustion Processes," ASME Paper No. 71-WA/APC-3, Presented at ASME Winter Annual Meeting, Washington, D. C., November - December (1971).

23. Jonke, A. A., G. J. Vogel, L. J. Anastasia, R. L. Jarry, D. Ramaswami, M. Haas, C. B. Schoffstou, J. R. Pavlik, G. N. Vargo, and R. Green, "Reduction of

Atmospheric Pollution by The Application of Fluidized-Bed Combustion," Report No. ANL/ES-CFN-1004, Annual Report July 1970 - June 1971 by Chemical Engineering Division Argonne National Laboratory, Ill.

24. Pereira, F. J., J. M. Beer, B. Gibbs, and A. B. Hedlye, Fifteenth Symposium (International) Combustion, p1149, The Combustion Institute, Pittsburgh, 1975.

25. Engleman, V., S., W. Bartok, and J. P. Longwell, Fourteenth Symposium (International) Combustion, p755, The Combustion Institute, Pittsburgh, (1973).

26. Heap, M. P., and Tyson, T. J., Reaction Screening for Methane/Air Combustion," EPA Contractors Meeting, SRI, Palo Alto, Calif., June, 1975.

27. Locklin, D. W., et al., Air Pollution and Its Control, AIChE Symposium Series, 126, Vol. 68, (1972).

4:25 p.m.
Combustion Chemistry and Modeling: An Overview
Adel Sarofim, Massachusetts Institute of Technology

Q: I do not think that NO is strictly necessary in order to form N_2 from fuel nitrogen. Reactions that will produce N_2 additional to that of NO plus NR are those of two NR's or NR plus N. Four center reactions proposed to explain the formation of N_2 would be expected to be slow, i.e., have a high activation energy.

A: The primary reactions that form N_2 from fuel nitrogen in flames are not well established. That the fuel nitrogen conversion is determined by competition between reactions involving NO to form N_2 and an oxidant to form NO is supported by the successful correlation of data using such simplified models. There is, however, need for more detailed studies of mechanisms and rates of the dominant reactions.

Q: The formation of HCN by the reaction of a CH radical with N_2 should not be labeled fuel nitrogen. Although such reactions can explain the formation of prompt NO under fuel-rich conditions, their kinetics are not as well understood as the reactions leading to NO formation under fuel-lean conditions.

A: Agreed.

Q: In a boiler furnace with water walls at, say, 450° F, flame temperatures of 2000 to 2200° F, and a luminous wrinkled flame, there is evidence of a black space between the burned gases and the walls. Would you hazard a comment on the nature of the soot or soot-like products in the black space?

A: The most likely constituents are soot and unburned char for coal-fired boilers and soot and carbonaceous cenospheres for boilers fired with residual fuel oils. At flame temperatures the soot and carbonaceous particles would be expected to contribute to the flame luminosity. Dark spaces are usually confined to cooler regions, close to the burner nozzle or where non-uniform mixing has led to quenching of partially burned combustion products.

THE MATHEMATICAL MODELING

OF

COMBUSTION DEVICES

By:

T. J. Tyson

Ultrasystems, Inc.
2400 Michelson Drive
Irvine, California 92715

1.0 INTRODUCTION

The mathematical modeling of combustion devices to predict pollutant formation involves the detailed description of molecular transport and chemical kinetics in regions which are small in comparison to the total device volume and where reactant concentrations are determined by macroscale mixing. This contrasts with the prediction of heat transfer in these same devices where the fine detail of heat release can often be ignored for practical design purposes. This paper has three objectives:

- To review the status of mathematical modeling of combustion physics and chemistry, and the engineering analysis of practical combustion devices.
- To discuss the potential for the development of analytical tools which could be of value to the combustion engineer faced with the development of advanced environmentally acceptable combustors for fossil and alternate fuels.
- To suggest areas in which future efforts should be concentrated in order to ensure that the maximum use can be made of mathematical models for the solution of engineering problems.

The subject area is exceedingly broad and the paper cannot be considered as an overview but rather as a discussion of what might reasonably be expected in the near and long term from mathematical models. In assessing the present status and prospects for the future, modeling will be examined both from its mathematical (computational) aspects and from the adequacy of the imbedded physics and chemistry.

There exists a broad spectrum of combustion models with regard to their mathematical and physical sophistication, complexity, accuracy, cost both to develop and use, and applicability. Such models may, on the one hand, be suitable only for the detailed analysis of a specific phenomena occurring within a combustion device or under idealized laboratory conditions such as droplet burning, coal particle devolatilization, or the kinetics of complex chemical systems. On the other hand, the engineer also needs in his inventory of modeling tools, techniques which are suitable for the analysis of complete practical combustion devices which represent the arena for a multitude of complex physical and chemical phenomena. Mathematical models are not necessarily restricted to those which are totally predictive in nature, that is, models which allow the prediction of the entire behavior of a given combustion device and hence allow the synthesis of new designs through parametric variations. There is another important, and often mathematically simpler, class of models for use in the analysis of experimental observations. Such models can be used to deduce the nature of physical and chemical processes which have not been, or cannot be, directly measured.

2.0 BACKGROUND

2.1 Role of Mathematical Modeling

Before addressing the three objectives stated above it is necessary to recognize how an engineer utilizes mathematical modeling techniques in the design and development process and to realize the limitations of these techniques. As in the case of many other engineering endeavors the utility of mathematical analysis in the development of combustion devices can be very substantial. However, the maximization of this contribution will only come about through a realistic appraisal of what can and cannot be accomplished with present-day and near-future analytical tools. It is wishful thinking, for example, to suppose that three-dimensional elliptic codes will be available in the near future for the satisfactory detailed analysis of complex turbulent flame behavior. To suggest that this is possible provides a disservice to the combustion engineering community since failure to achieve anticipated results will only lead to a lack of enthusiasm for the application of techniques which do have potential for success. On the other hand the academic community should not be discouraged from developing such codes since only then can their limitations be exposed and corrected.

Seldom, if ever, is one faced with an engineering task that can be solved in its entirety through the straightforward application of a mathematical model to synthesize an optimum design by the systematic variation of operational and design parameters. This situation is especially apparent in the field of combustor design. The reasons are three-fold: (1) the fundamental phenomena associated with the dominant physical and chemical processes are not sufficiently well understood; (2) the mathematics of numerical solution techniques and the capabilities of modern computational machines are not sufficiently advanced; and (3) the design parameter definitions and variations are either unknown or too numerous at the outset of the synthesis process to allow a systematic treatment. These factors are, of course, intimately coupled and advances in any one area relate strongly to the requirements imposed upon the others. For example, as is so often the case, physical behavior may be well understood on the molecular level while gross physical phenomena which are a consequence of this behavior are difficult to correlate with easily identified physical observables. Taking turbulent transport as an example, the time dependent Navier-Stokes equations adequately describe the continuum physics of fluid motion except for the unusual situation of highly rarified gases. These equations are based upon an understanding of behavior at the molecular level. However, because of computational limitations it is impossible today, and maybe for the next several decades, to solve these equations of fluid physics. Thus the model is forced to adopt cruder "phenomenological" descriptions of turbulent transport which are based upon examination of time-averaged motion over periods which are long compared to the unsteady turbulent fluctuation periods which characterize fluid motion at high Reynolds numbers. Satisfactory phenomenological descriptions of turbulence have defied the very substantial efforts of physicists and engineers for all but the very simplest of flows. Thus we have sacrificed understanding in one area in order to accommodate limitations in another.

Perhaps the most useful contribution of mathematical modeling to the design of combustors in the near-future will come from the analysis of so-called "limit-case" situations in which some single aspect of the physics or chemistry dominates and the remaining phenomena can either be ignored or modeled by simple idealized processes. Fundamental laboratory experiments are generally designed to fit this situation and the availability of mathematical models with which to analyze the results are of considerable value. "Limit-case" analysis serves another useful function in that it often allows an estimation of the upper bounds of performance of a combustion device as limited, for example, only by fundamental chemical constraints. Such an analysis provides a significant yardstick by which to measure the performance of various design concepts which may be limited in performance by fluid mechanical and heat transfer constraints.

2.2 Classification of Mathematical Models

In order to appreciate the breadth of the domain referred to as "mathematical modeling of combustion behavior" it is useful to classify the various model types according to their engineering functions as follows:

- Data Analysis. Procedures which allow the extraction of the maximum amount of information from experimental data. For example, mean (time averaged) flow field and concentration measurements contain implicit information about the nature of turbulent transport and chemical production which can be obtained through rather straightforward analysis.
- Prediction of Behavior of Fundamental Laboratory Experiments. Here the models and experiments focus in considerable depth on some limited aspects of the physical or chemical behavior of flames with the complications of other phenomena being eliminated by careful design. Examples are the modeling of well stirred and plug flow chemical reactors, flat molecular diffusion flames, spherically symmetric particle flames, and cold flow experiments.
- Empirical and Order-of-Magnitude Analysis of Engineering Devices. This important category covers analytical techniques ranging from "back-of-the-envelope" estimates to extensive correlations of empirical evidence cast into relatively simple models for predicting energy release, heat transfer, internal flow behavior, fuel burn-out, pollutant formation, flame stability, ignition characteristics, etc.
- Development of Engineering Intuition, Guidance of Experiments, and the Synthesis of Design Concepts. Many types of engineering analysis tools fall into this category. "Limit-case" models which treat certain limiting situations in considerable detail can establish bounds on the performance of a device. Such analysis can lead, through numerical experimentation, to an intuitive feel for the influence of significant design and operational parameters on performance and scaling.

2.3 Some Physical Aspects of Combustion Modeling

The modeling of combustion devices is amongst the most difficult of all the classical engineering problems in continuum mechanics. This is primarily due to our lack of basic understanding of the phenomena of turbulence. Virtually all combustion devices involve turbulent flow. In those instances where fuel and air are admitted separately to the combustion chamber the rate of heat release is controlled by turbulent mixing. It is difficult to give a precise definition of turbulence, texts rather list the characteristics of turbulent flows(1). Turbulent flows are irregular and dissipative, their diffusivity causes rapid mixing. Turbulence is rotational and three-dimensional and is a continuum phenomenon governed by the equations of fluid mechanics. Even the smallest scales occurring in turbulent flows are ordinarily far larger than any molecular length scale. From the viewpoint of combustor modeling the most important characteristic of turbulent flows is that they are flows.

Turbulence is a property of the flow and not a property of the fluid. It has been well characterized for only a few classical situations which can be divided into two groups. One group consists of boundary influenced turbulence and the other group consists of boundary-free or "free" shear layers. The latter includes planar and axisymmetric jet mixing and free mixing layers in which two fluids of different velocity and large lateral extent merge. To a much lesser degree turbulence measurements have been made in other types of flows such as boundary layer separation and reattachment zones and in internal recirculation regions.

Provided that the mean flow gradients are not too large the turbulent behavior is dependent on the local velocity distribution over a region of the scale of the largest turbulent eddies. Such a condition is referred to as equilibrium turbulence and represents a condition where turbulence production and dissipation are in balance. In flows where the mean flow gradients are very large this equilibrium condition is violated and turbulence generated upstream may be convected to the point under consideration without experiencing equilibration. Similarly local turbulence production may lag far behind in a rapidly accelerating flow leaving the region "laminarized." Under these circumstances of rapid mean flow variations a nonequilibrium (or so-called "history dependent") turbulence model is required to predict the local turbulence energy and length scale. Such a model must contain a description of equilibrium turbulence in such a way that when the mean flow gradients decay the turbulence proceeds asymptotically to the equilibrium value.

Figure 1 presents a schematic of a typical combustor flow field with swirl induced recirculation. For the purposes of discussion the mean flow gradients are assumed to be sufficiently small that the turbulence has an equilibrium distribution. The

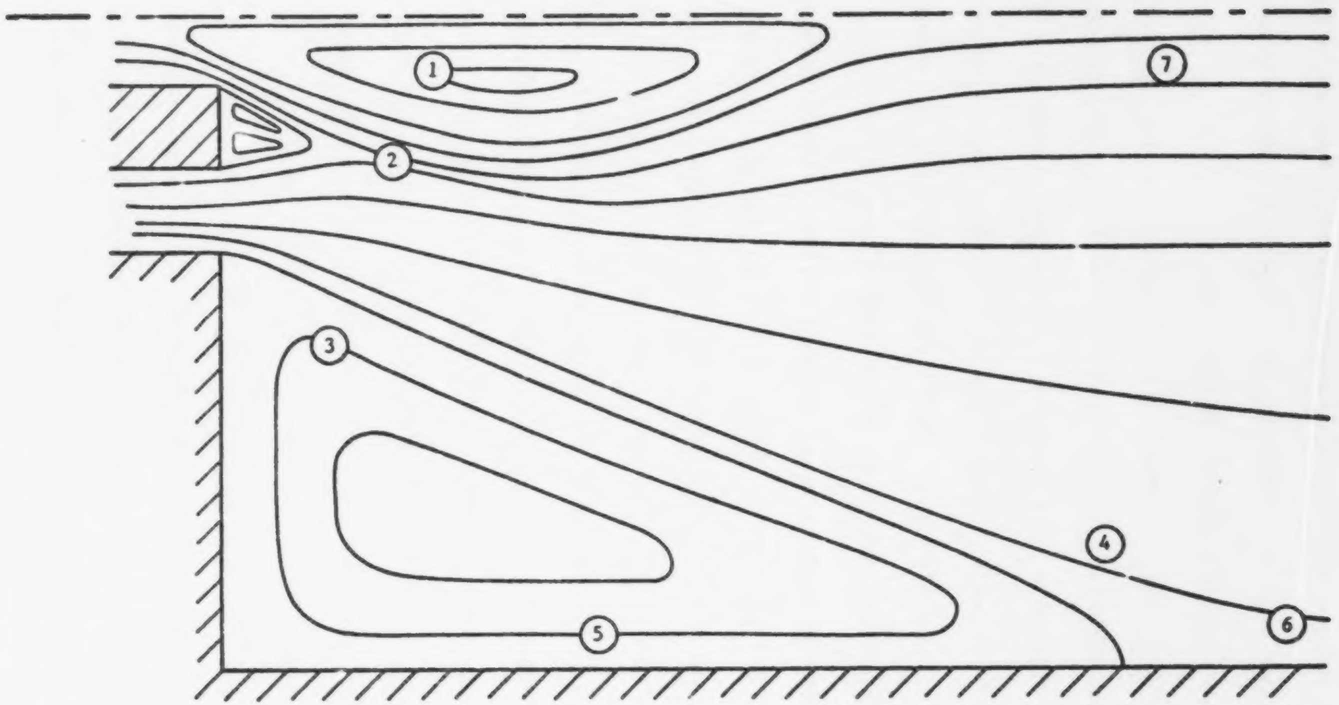

Fig. 1 Schematic of Typical Combustor Flow Field With Swirl Induced Recirculation. Numbers Indicate Regions of Different Turbulence Character.

circled numbers indicate regions where the equilibrium turbulence levels probably take on a distinctly different dependence on the local conditions due to the different mean flow character. The regions can be distinguished as follows:

Region 1 - Internal recirculation

Region 2 - Typical of confined planar jet mixing

Region 3 - Typical of planar free shear layer

Region 4 - Boundary layer reattachment

Region 5 - Recirculation zone boundary layer

Region 6 - Conventional wall boundary layer

Region 7 - Axisymmetric jet mixing

Hopefully measurements taken in flow environments typical of these will yield the appropriate relationship between turbulent viscosity and the local flow kinematics.

The physics of turbulent transport is described by the time dependent Navier-Stokes equations for which no solutions have yet been obtained and these equations will probably continue to defy mathematical solution for several decades. In an attempt to overcome this dilemma the modeler wishing to predict such flow fields as shown in Figure 1 is forced to solve the time averaged Navier-Stokes equations. This approach entails the "phenomenological" or "empirical" modeling of turbulent transport which can be undertaken at various levels of sophistication and mathematical complexity. Unfortunately very little data from detailed physical observations exists to guide these efforts. The result, all too often, is the substitution of complexity for reality in order to hide our ignorance of turbulent transport. Thus "history dependent" turbulence models may be substituted when classical mixing length theories prove inadequate because of a lack of understanding of the relationship between turbulent transport and the local kinematics of the flow in slowly varying mean flow fields.

Another aspect of turbulent behavior which adds greatly to the complexity of combustion phenomena is the unmixedness on a molecular scale which exists throughout the combustion field. This unmixedness is a consequence of the marble-cake like structure associated with the large scale turbulent eddies which entwine fluid originating from different parts of a mixing zone and which dominate the mass trasport process. These eddy structures are in themselves unstable and a cascading process ensues with breakdown to smaller and smaller eddies. This process is eventually terminated by molecular diffusion eliminating the last traces of unmixedness. It is only in this final stage of the mixing process that chemical action and energy exchange can take place between the originally separate reactants. This delay time between "macromixing" on the turbulent scale and "micromixing" on the molecular scale must be compared with the characteristic times for chemical reaction in order to qualitatively assess the significance of this segregation of material.

For large low velocity combustion systems the eddy break-up time tends to be long and the significance of this "turbulence-kinetics" interaction can be substantial. The phenomena effects the rates of energy release, pollution formation, and combustion product quenching which in turn can effect the ultimate levels of nitrogen oxides and incomplete products of combustion. No adequate treatment of turbulence-kinetics coupling exists at present for even the simplest flow and chemical systems. However, it is not unreasonable to expect progress in the near future in this area based on relatively simple models allowing for turbulent macromixing in conjunction with segregation on the microscale which decays with time. Adequate modeling here awaits the generation of a definitive set of experiments.

Two-phase flow and spray combustion behavior adds enormously to the complexity of any analysis approach which attempts to solve for the detail structure of the combustion field. Vaporization and burning histories of droplet clouds are very different from the simple idealized case of single drops burning in a quiescent non-vitiated and unconfined environment. Droplet and solid fuel behavior can be strongly coupled to the local relative Reynolds number between the particle and the gas if the particles are large and the gas phase undergoes substantial acceleration. Any model which attempts a detailed treatment of two-phase combustion must integrate the particle ballistics equations in order to establish gas-particle velocity lags and to locate the particle trajectories within the combustion flow field. This is particularly important during the initial injection period even for the smallest particles. The degree to which particles participate in turbulent motion is poorly understood and yet may be crucial to their combustion behavior. In general, for large combustion systems particles tend to follow the turbulent motion. That is, an eddy is likely to carry its particulate content with it as it moves. For small systems, on the other hand, particles tend to follow the mean motion. The velocity lags associated with turbulence tend to be higher in small systems giving rise to a larger dependence of vaporization and burning rates on turbulence intensity. Figure 2, taken from Beér and Chigier(2) and McCreath and Chigier(3), illustrates the complexities of spray combustion in swirl and bluff body stabilized flames.

2.4 Some Mathematical Implications of Various Modeling Approaches

Before examining the current status and future potential for modeling it is appropriate to anticipate some of the mathematical problems which must be adequately handled by the numerical techniques employed. To place these mathematical problems in perspective it should be noted that the two areas which will undoubtedly pace advances in mathematical modeling for some time to come are improvements in numerical computational capability and advances in the understanding of turbulent behavior.

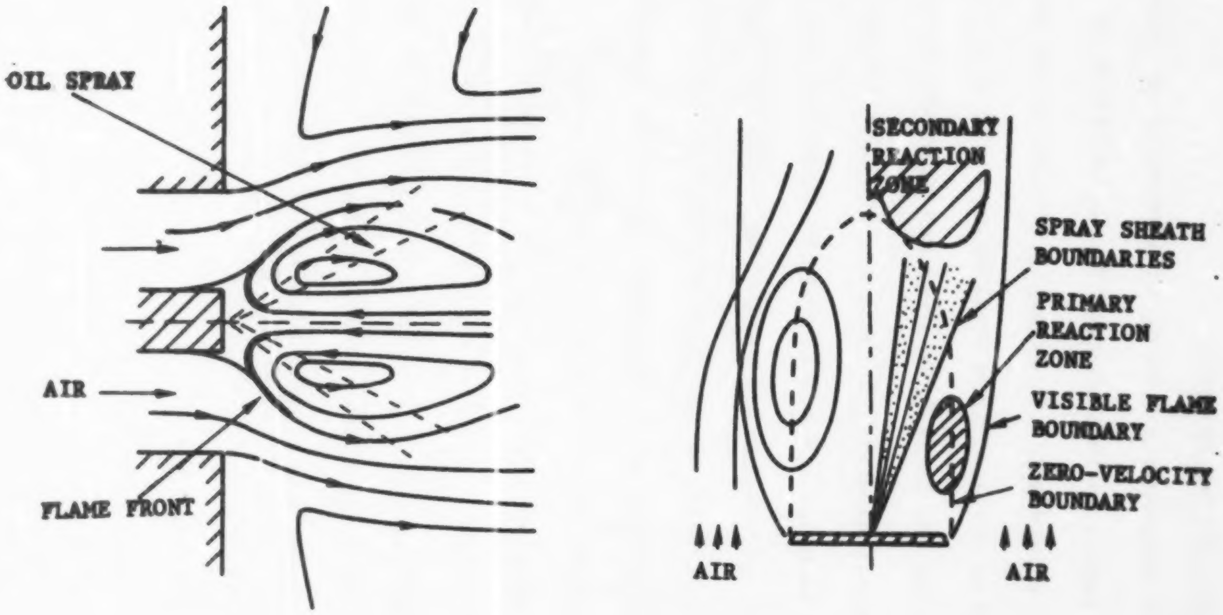
OIL SPRAY
AIR
FLAME FRONT
SECONDARY REACTION ZONE
SPRAY SHEATH BOUNDARIES
PRIMARY REACTION ZONE
VISIBLE FLAME BOUNDARY
ZERO-VELOCITY BOUNDARY
AIR
AIR

Fig. 2 Illustration of the Complexities of Spray Combustion (Following Beer and Chigier(2) and McCreath and Chigier(3)

2.4.1 Near Equilibrium Behavior

Several phenomena occurring in combustors are often of a "near equilibrium" nature in that an equilibrium condition is rapidly approached at a rate which is strongly coupled to the degree to which the system deviates from equilibrium. The equilibrium state is determined by the local kinematics and thermodynamics of the system. Chemical kinetics, turbulence, and particle dynamics can all exhibit this behavior. The differential equations governing these approaches to equilibrium are said to be "stiff" in that any disturbance from equilibrium is met by a strong restoring "force." The numerical integration of coupled stiff equations requires special attention in order to avoid numerical instabilities(4,5). Implicit integration techniques are required which can contribute to very long computational times.

2.4.2 Characteristics of Full Equations of Fluid Motion

In general the time-averaged low-speed Navier-Stokes equations have the following features in addition to the nonequilibrium behavior discussed above:

- Nonlinearity
- "Singular" limit solutions as the effective Reynolds number becomes large
- Thin flame (energy release) zones in the limit of rapid chemical kinetics
- Elliptic behavior
- Small pressure differences, i.e., $\Delta P/P \ll 1$

These features have implications regarding the numerical solution treatment and provide motivation to attempt simplifications. Nonlinearity rules out "general" solutions and superposition of solutions. It also introduces further complexity into numerical convergence schemes. The singular nature of high effective Reynolds number solutions refers to the fact that the limiting solutions, as the effective viscosity approaches zero, are not the same as zero "viscosity" solutions. This is reflected in the existence of thin regions of high turbulent transport such as boundary layers and boundary-free mixing layers. The presence of these thin zones has significant numerical implications. They suggest the need for a fine numerical mesh in certain regions of the flow where the gradients are large whereas a coarse mesh would suffice elsewhere. The possible existence of thin flame zones imbedded within mixing layers carries similar implications with regard to numerical mesh size control.

The elliptic nature of the problem refers to the short-range turbulent-transport (diffusion) coupling and pressure wave coupling between an element of fluid and its surrounding neighbors. One consequence of the turbulent diffusion of momentum is the possible presence of large scale recirculation zones. These vortex structures provide strong convective "upstream influence." Such a situation is properly set as a "boundary-value" problem because all boundaries can influence the entire flow and downstream behavior can effect upstream processes through convective signalling. Again this has strong implications for the type of numerical procedures to be employed.

All numerical procedures replace the differential equations with fully coupled algebraic equations linking the unknowns at every node point in the numerical mesh. It is the numerical solution of this coupled set of nonlinear algebraic equations that presents the difficulties. The iterative method of solution amounts to obtaining successive approximations through a procedure of uncoupling the node points to a greater or lesser degree depending upon the method. After each iteration an error component or "residual" is calculated for each subset of uncoupled nodes which represents a correction to the coupling terms. This residual is then used to adjust the solution and the cycle is then repeated. As can be inferred from the "singular" nature of the problem it is not surprising that the physics of the element-to-element coupling plays an important role in the convergence of any scheme based on partial uncoupling. As high effective Reynolds numbers are approached the diffusive coupling allows for solutions with very large gradients over very short distances (thin layers). Such solutions are needed to accommodate wall boundary conditions and mixing layers discontinuities. The analogue to this behavior in the finite difference numerical iteration scheme is that the reaction to a small error at a node point is a large gradient to eliminate or diffuse away that error. However, if the grid size is too large the analogy of a "thin" high gradient region does not hold. The numerical scheme applies the large gradient over a large distance and introduces an error at the adjacent grid point which is larger than the original error. This leads to exponential error growth. Hence for numerical stability we require a small mesh size when the turbulent viscosity becomes small. In fact, a careful analysis shows that the "cell Reynolds number" must be small to ensure stability. The numerical values of this critical cell Reynolds number depends upon the degree to which the nodes are uncoupled in the iterative solution process. The greater the coupling the greater the numerical stability. This is the motivation behind going to so-called "block", "line", and "alternating direction" relaxation procedures.

One approach to achieve numerical stability without the need to use an excessively small grid mesh is to introduce an artificial viscosity which satisfies the critical cell Reynolds number criteria. Meteorologists originally introduced the concept of "weather" differencing which provides such an artificial viscosity. More commonly called "upwind" differencing this technique biases the numerical estimate of the convective terms to the values existing on the upstream side of the node point in question. The numerical error introduced by this procedure is equivalent to an additive diffusion term with an artificial Reynolds number on the order of 2.0. This in turn is equivalent to introducing additional "turbulent eddies" into flow whose size is of the order of the grid spacing. This poses no serious problem when the real eddy scale is substantially larger than the grid spacing necessary for accuracy in regions of steep gradients such as those which exist in mixing layers. However, outside the thin boundary and mixing layer zones in the so-called "outer" regions of the flow the turbulence scale is very small and the gradients are gentle. In these regions it is desirable to use a coarse grid. In doing so, however, one introduces a substantial error through the artificial viscosity.

The numerical procedure that is typically followed at present is a combination of the above approaches. The alternating direction line relaxation or so-called ADI (Alternating Direction Implicit) method first introduced by Peaceman and Rachford(6) is employed to maximize the value of the critical Reynolds number. The cell size is then reduced to avoid violation of this criteria. In addition, some codes still invoke a partial upwind differencing to gain stability. Finally, the method of iteration to achieve convergence of the ADI procedure is related to cell Reynolds number and stability. Briley(7) at UARL has developed a method of maximizing the convergence rate for a given cell Reynolds number.

2.4.3 Characteristics of the Parabolic Equations of Motion

Great simplification of the mathematical and numerical treatment can be achieved if the classical Prandtl "thin shear layer" assumptions can be invoked. The necessary conditions are that:

- There is no reverse flow.
- The flow has a single dominant direction along one set of coordinate lines with the velocities in the lateral plane small compared to the streaming velocity.
- The laminar or effective turbulent Reynolds number be large, say greater than 10 (this condition is satisfied by typical turbulent free shear layers which have effective Reynolds numbers in the range 15-35 based on the length of the shear layer).

The significant implications of these assumptions are:

- Shear layers, boundary or free, will be thin compared to the streamwise length) and lie close to the principal coordinate lines.
- Derivatives in the streamwise direction (x) are much smaller than in the lateral direction (y,z) and as a consequence $\partial/\partial x\ (\tau_{xx}, \tau_{xy}, \tau_{xz})$ are small compared with other stress terms and can be set equal to zero.
- The pressure field can be represented by

  $$P = \overline{P}(x) + \varepsilon P'(y,z)$$

  where $\varepsilon \ll 1$. This implies that the pressure gradient in the streamwise direction is approximately independent of the position in the lateral plane.

As a consequence of these implications regarding the flow behavior the overall governing equations reduce to parabolic form which means they are properly posed as an "initial value" problem. That is, the solutions exhibit no upstream influence and the equations can be integrated by "marching" downstream from known conditions at an upstream starting point. This is an enormous simplification which allows two-dimensional flows to be treated almost with the simplicity of one-dimensional problems and three-dimensional flows to be solved with machine times comparable to the iterative solution of two-dimensional elliptic problems. Hence it is important to try to recognize those regions in combustion devices which may satisfy the necessary conditions stated above. Figure 3 suggests two possibilities. The lower schematic represents the combustion field of a fuel-staged device where fuel is injected in such a way that it penetrates far downstream from the initial heat release zone. If the ignition region can be solved in an approximate fashion, then such a solution could be used as the initial condition for a parabolic two-dimensional (axisymmetric) procedure for the remainder of the reaction zone. The upper schematic in Figure 3 represents one possible model of flow in the secondary (S) and tertiary (T) zones of a gas turbine combustor. Here it is assumed that the (S) or (T) air jets can be modeled by aerodynamically clean "source bodies" immersed in the flow which circumvents the problem of calculating the jet penetration behavior (which is done in this case as a preliminary to the calculation by simple jet penetration theory). Under these assumptions the three-dimensional jet interaction problem can be solved with a three-dimensional parabolic procedure.

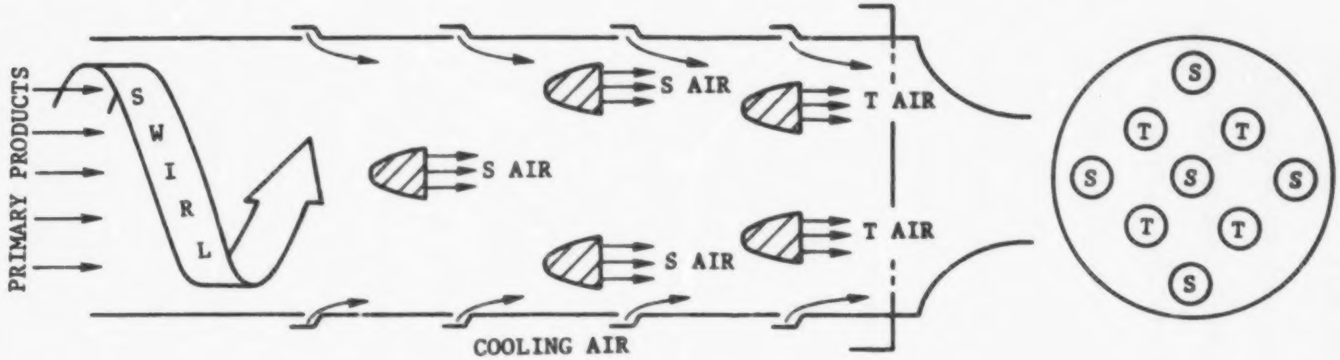
PRIMARY PRODUCTS
S W I R L
S AIR
S AIR
S AIR
T AIR
T AIR
COOLING AIR
S
T
T
S
S
S
T
T
S

APPLICATION OF 3-D PARABOLIC FORMULATION TO GAS TURBINE

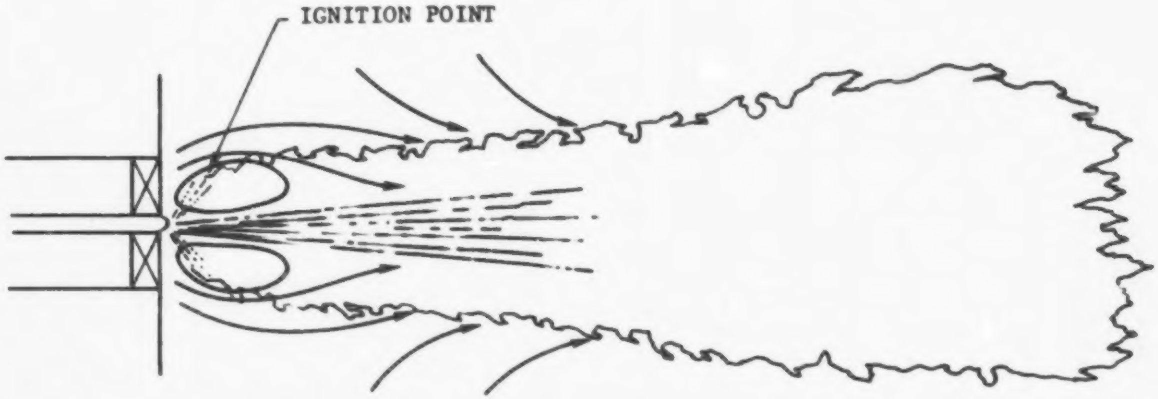
IGNITION POINT

APPLICATION OF 2-D PARABOLIC FORMULATION TO UNCONFINED LONG FUEL STAGED DIFFUSION FLAME

Fig. 3

3.0 STATUS OF CURRENT MATHEMATICAL MODELING PROGRAMS

This section presents a brief review of the current status of several combustor device modeling programs which have been supported by the EPA either in whole or in part. The comments are limited to modeling of continuous combustion devices. None of the EPA-sponsored work on reciprocating internal combustion engines is discussed. The review is not comprehensive either in depth or in breadth and is only intended to provide some general insight into the type of investigations which are being pursued. In addition to these efforts brief mention is made of other pertinent non-EPA-sponsored work.

3.1 One-Dimensional Diffusion Flames

3.1.1 The Aerotherm Flat Flame Code

Kendall and Kelly(8) have developed the PROF code at Aerotherm for the analysis of premixed flat flames. The code couples an arbitrarily large set of finite rate chemical reactions with molecular diffusion. Only solutions for low-speed combustion waves are sought and hence the assumption of constant pressure can be invoked. The problem is properly set as a boundary value problem and utilizes matrix inversion techniques to solve the fully coupled set of finite difference equations. For the constant area duct computation the flame speed becomes the eigenvalue for which a steady state solution exists. An alternative to the eigenvalue formulation is to perform the calculations in a duct of slowly varying cross section which diverges in the direction of the flow. A stable flame will stand at the station corresponding to the appropriate flame speed. Such a flame deviates slightly from one in a constant area channel due to the small divergence. The primary purpose of the code is to examine flat flame data in order to extract information regarding the kinetic mechanism of NO_x formation in flames. Of particular interest is to establish to what degree there is a deviation from the simple Zeldovich theory, and to elucidate the mechanisms of this "prompt" NO formation in hydrocarbon flames.

Figure 4 presents a comparison between the carbon monoxide flat flame data of Merryman and Levy(9) and the prediction of the species distributions. The agreement is excellent. Figure 5 shows a comparison between predicted and measured H_2/air flame speeds.

3.1.2 The Rocketdyne Spherically Symmetric Particle Diffusion Code

Nurick(10) and co-workers at Rocketdyne have developed a set of spherically symmetric diffusion codes for the prediction of:

- Droplet fractional distillation history
- Coal devolatilzation and surface reaction history
- Pollutant formation in the near field of particles with emphasis placed on the fate of fuel nitrogen compounds

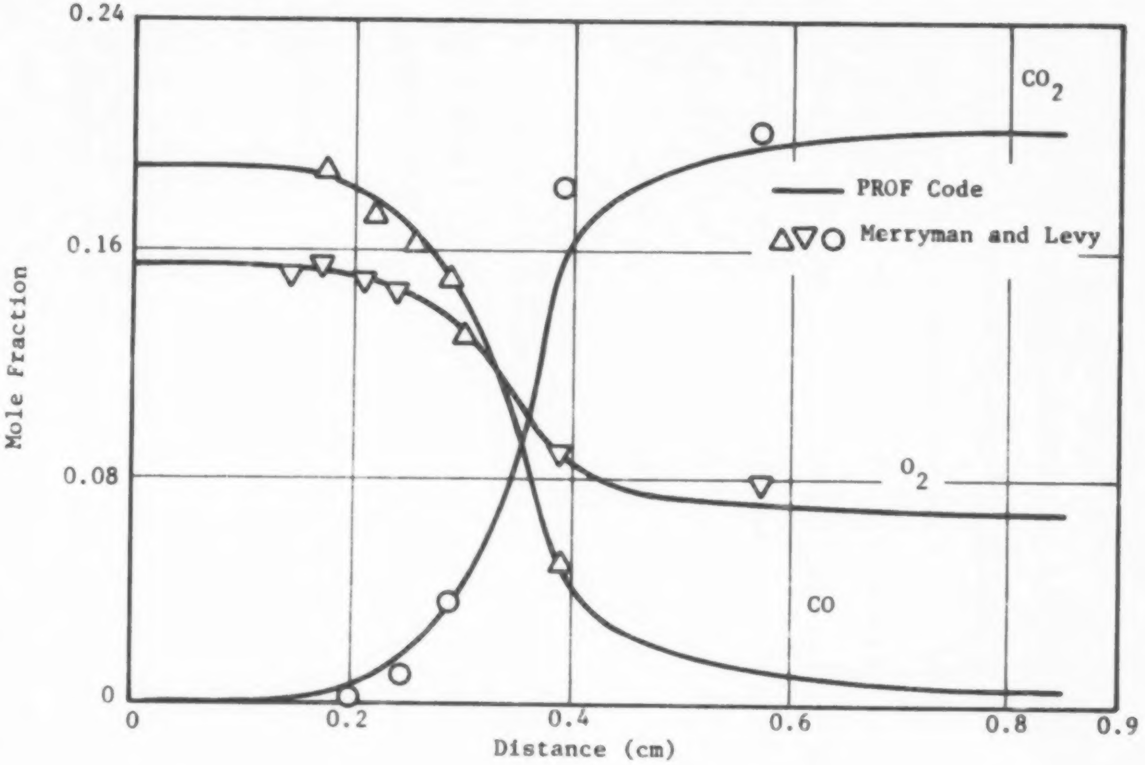

Fig. 4 Aerotherm PROF Code - Comparison of Predicted and Experimental Major Specie Concentrations Through a $CO/O_2/N_2/H_2O$ Flame

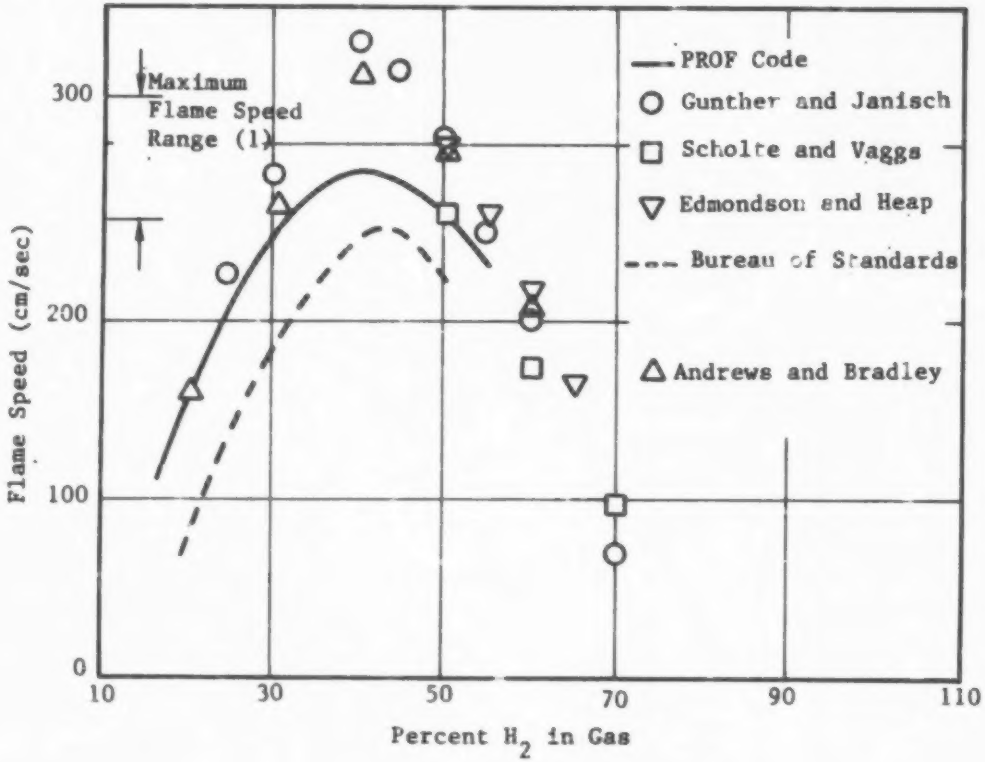

Fig. 5 Aerotherm PROF Code - Comparison of Predicted and Experimental H_2/Air Flame Speed Variation With Percent H_2 in Gas

Four diffusion models were developed. They are:

- Droplet Vaporization
- Droplet Thin Flame
- Coal Combustion
- Finite Rate Kinetics-Diffusion

Figure 6 illustrates the Finite Rate Kinetics Model. Preliminary numerical experiments have been made with the coal combustion model. Comparison of predicted fixed carbon and volatile matter loss with time against measured values are given in Figure 7 . The two calculated curves were obtained with the upper and lower bounds of reaction rate data available in the literature. The agreement appears to be good.

3.1.3 One-Dimensional Limit-Case Solution from Two-Dimensional Codes

Both two-dimensional elliptic and parabolic formulations contain the one-dimensional premixed flat flame as limiting cases. The elliptic programs can be set up as one-dimensional by using only one line of node points and specifying the lateral boundary conditions as zero-shear (rather than zero velocity) and zero heat-flux. It would be a worthwhile exercise to run the UARL CRISTY program in this fashion as a numerical check-case and as an investigation of the limitations of CRISTY imposed by the use of completely uncoupled

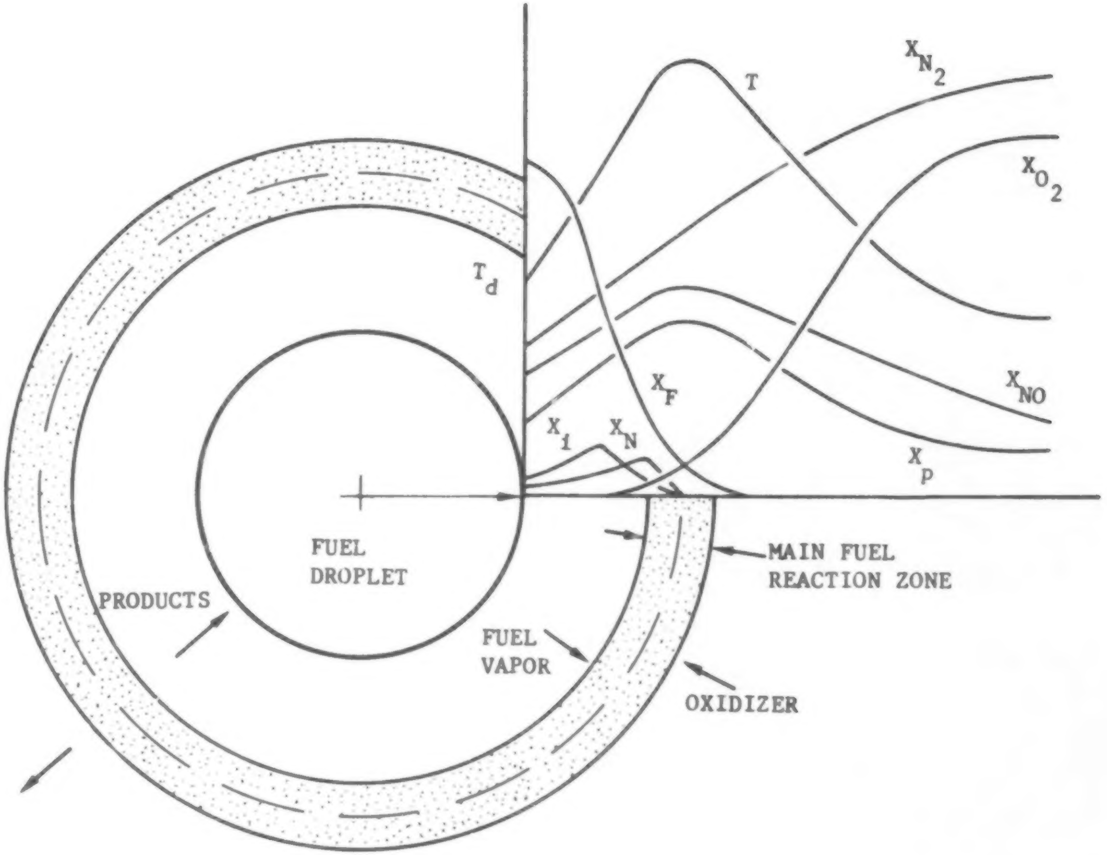
X_{N_2}
T
X_{O_2}
T_d
X_F
X_{NO}
X_i
X_N
X_p
FUEL DROPLET
MAIN FUEL REACTION ZONE
PRODUCTS
FUEL VAPOR
OXIDIZER

Fig. 6 Rocketdyne Droplet Diffusion Model with Finite Rate Chemistry

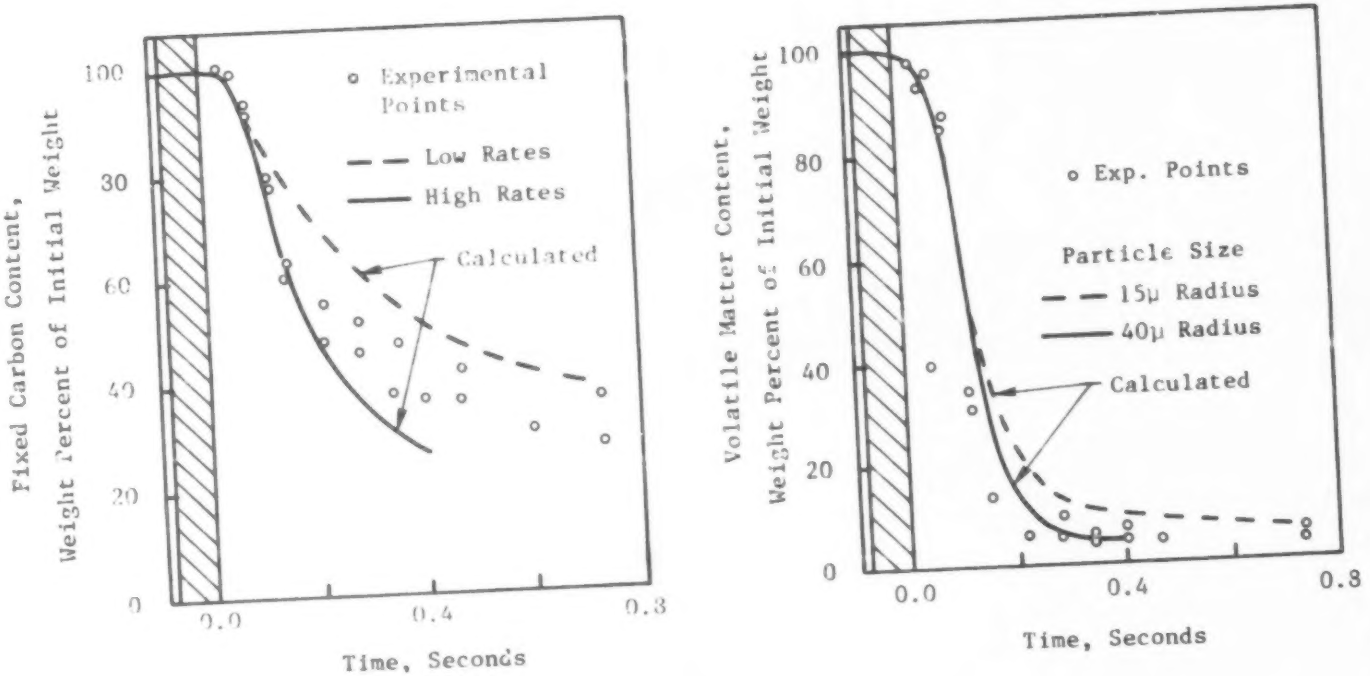

Fig. 7 Rocketdyne Coal Combustion Diffusion Model

chemical kinetics. As discussed below CRISTY relies on diffusion-coupling to stabilize the stiff uncoupled chemical equations. If this procedure works adequately (which seems unlikely for situations involving complex chemistry) then the one-dimensional CRISTY calculations will be much faster than the PROF code.

A parabolic two-dimensional code can be set up to handle the flat flame calculation by using the initial condition option for planar free-shear-layer mixing. In this case the initial conditions would be unburned pre-mixed air/fuel on one side and burned pre-mixed on the other. The flame structure will develop out of this discontinuity as the asymptotic solution for fully developed flow. A small error is introduced since diffusion is allowed only on the lateral-coordinate direction. This can be made arbitrarily small by increasing the streaming velocity such that the flame lies flat alongside the axis of flow. A fully implicit parabolic code will yield flat flame solutions in the same computational time as a one-dimensional code by rapid convergence on the asymptotic solution through the use of large streamwise steps. Again such cross-check calculations between different codes are useful as a verification of sound numerical procedures.

3.2 Chemical Kinetics and Modular Modeling Codes

3.2.1 The Ultrasystems Kinetics Code

The IKAP kinetics program is capable of treating large chemical systems in stirred reactors or generalized plug flow situations. It is based on a chemical kinetics analysis procedure developed at TRW Systems by Tyson(5) which, through fully implicit integration, allows the rapid solution of complex chemical systems. A principal feature of the program is its ability to determine which reactions dominate in the production or destruction of a particular species under various reactor conditions dictated, for example, by residence times, heat transfer and mixing histories. This procedure known as "reaction screening" has been used in the course of establishing a definitive reaction set for the prediction of NO production and destruction in combustion devices. Figure 8 shows a comparison between prediction from this set and the experimental stirred reactor results obtained by Bartok, et al(11) at the Exxon Laboratories.

3.2.2 Modular Modeling Programs

The modeling of chemical processes by a collection of well - stirred and plug-flow chemical reactors has been a standard chemical engineering approach for many years(12). During the last five years the practice has been extended to the analysis of combustion devices by a number of investigators(13,14,15). Ultrasystems has, to a limited degree, automated the coupling of elemental kinetics modules

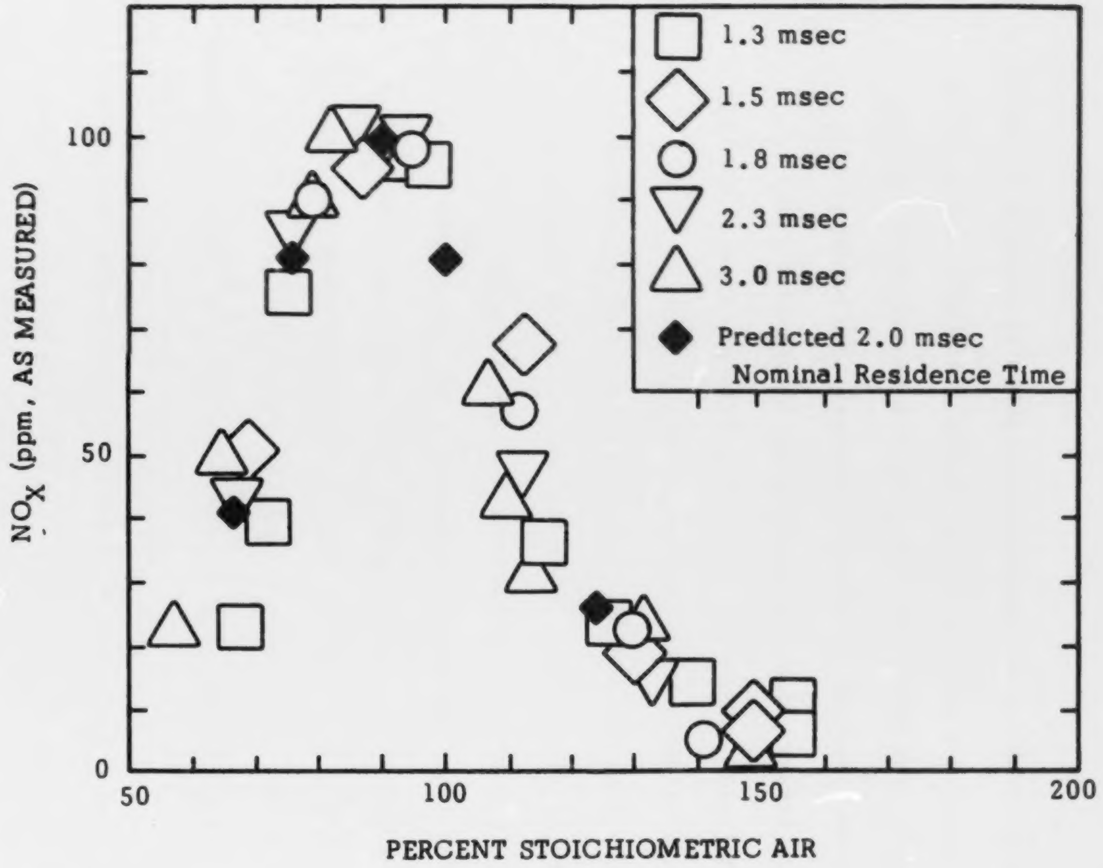

Fig. 8 NO_X EMISSIONS IN JET-STIRRED COMBUSTOR METHANE-AIR to form an integrated engineering analysis code referred to as MKAP.

The basic coupling arrangements are shown in Figures 9 and 10 . As indicated these are represented by series, feedback, and parallel coupling arrays. The most time consuming are the feedback elements which require an iterative solution procedure. The estimate of exchange rates between elements requires an independent fluid mechanical analysis or direct experimental evidence from flow field measurements or stimulus-response tracer studies.

MKAP has been applied to conventional gas turbine combustors as illustrated in Figure 11 . Here the recirculation zone which stabilizes the primary is modeled with a stirred reactor. This in turn is coupled in a feedback fashion to a plug flow simulation of the streaming flow around the recirculation zone. The plug flow element receives combustion air from the swirler as well as from the primary stabilization ports. Fuel enters both the SR and the PFR. The remainder of the system is simulated as shown by a PFR with distributed air addition.

MKAP has also been used in a study of gas turbine combustors utilizing low-Btu coal derived gas. In this instance the secondary combustion stage diffusion flame was modeled as shown in the upper sketch of Figure 10 . The thin flame zone was represented by short residence time well stirred zones with near stoichiometric equivalence ratios. The residence times were determined by estimates of the flame

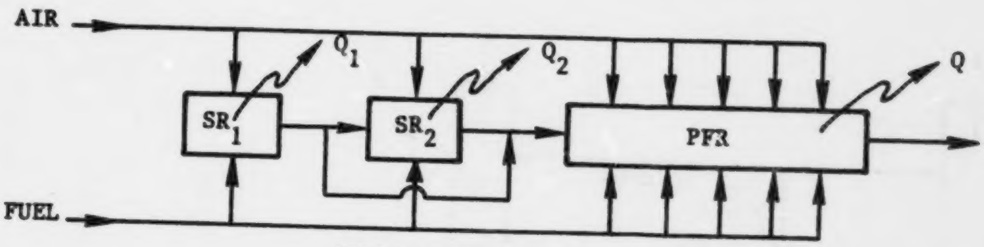
AIR
FUEL
SR1
SR2
PFR
Q1
Q2
Q

SERIES CONNECTED

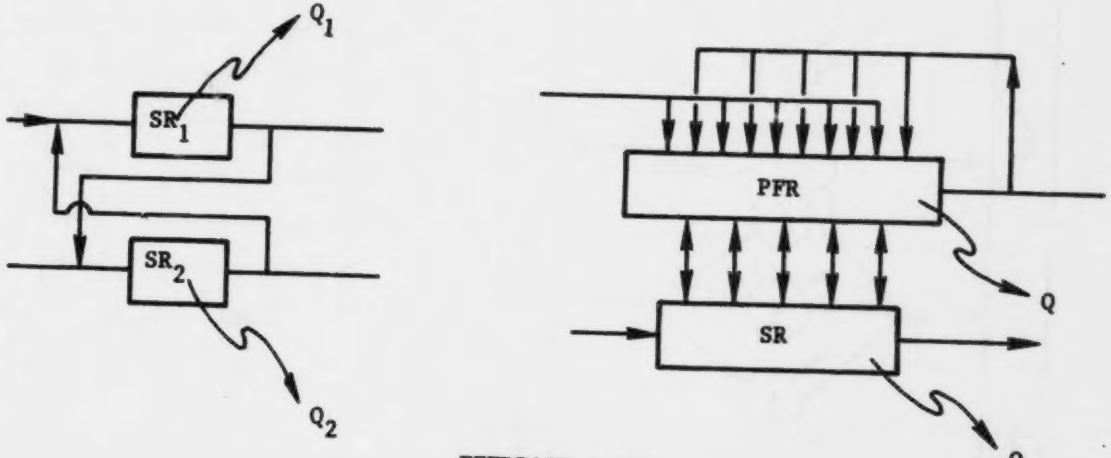
SR1
SR2
Q1
Q2
PFR
SR
Q
Q

FEEDBACK LOOPS

Fig. 9 Examples of Basic Elements for Modular Analysis

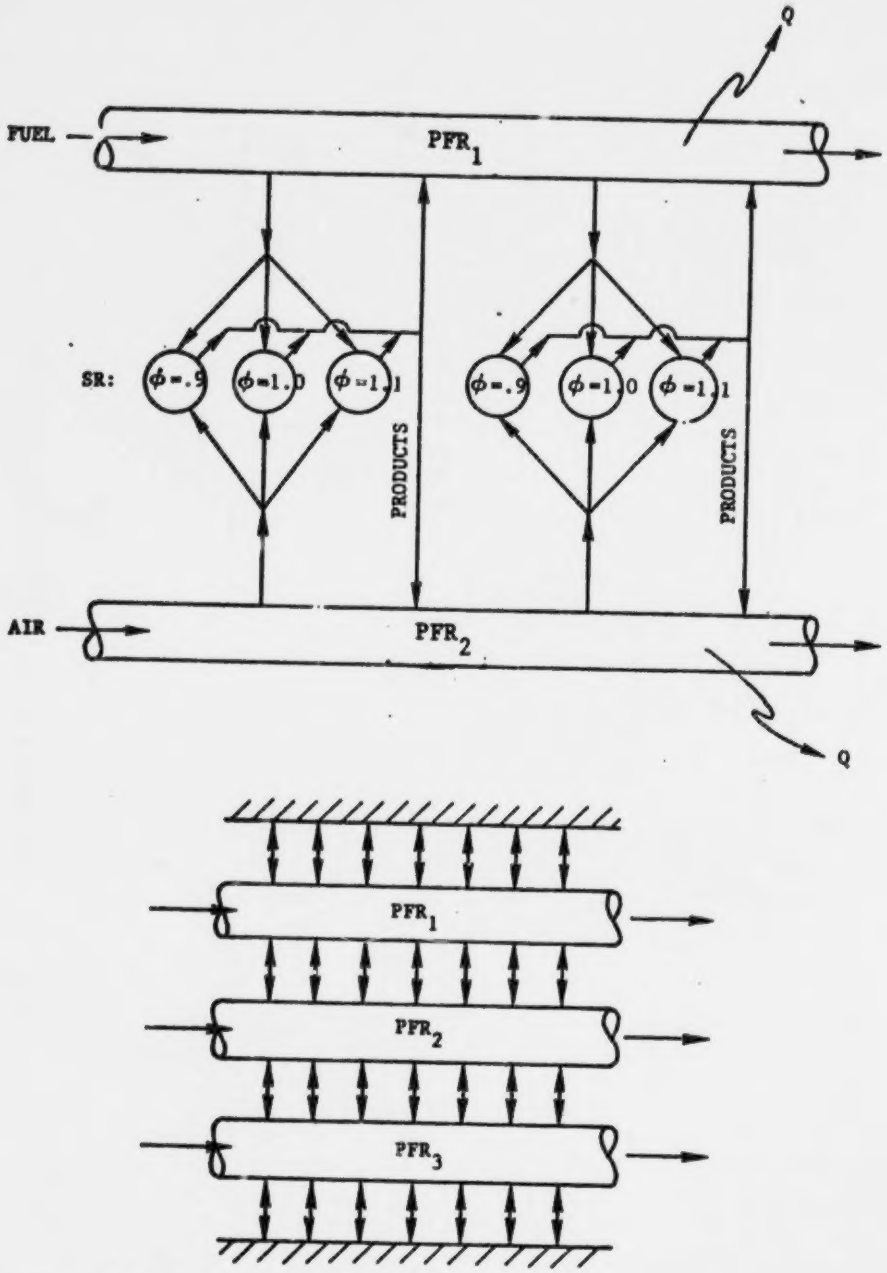
FUEL
PFR$_1$
Q
SR:
ϕ=.9
ϕ=1.0
ϕ=1.1
ϕ=.9
ϕ=1.0
ϕ=1.1
PRODUCTS
PRODUCTS
AIR
PFR$_2$
Q
PFR$_1$
PFR$_2$
PFR$_3$

Fig. 10 Examples of Parallel Coupled Elements for Modular Analysis

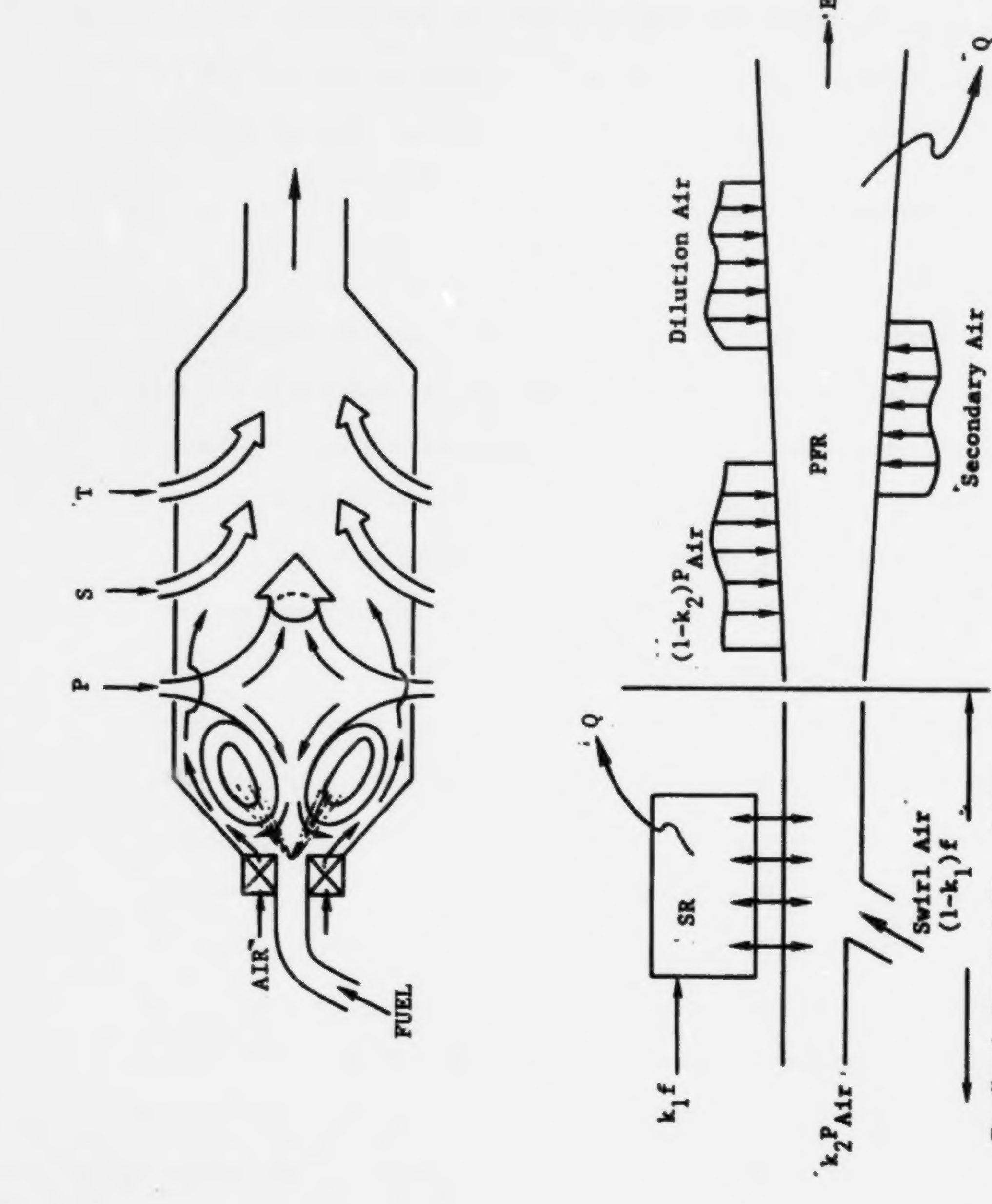
AIR
FUEL
P
S
T
SR
Q
$k_1 f$
$k_2 P_{Air}$
Swirl Air
$(1-k_1)f$
$(1-k_2)P_{Air}$
PFR
Dilution Air
Secondary Air
Exit
Q

Feedback Coupled SR and PFR

Fig. 11 Modular Gas Turbine Model

zone volume and diffusion flame mixing rate. The flame was divided into three axial zones (only two are shown in the sketch). The products of combustion from the flame zone were returned to both the fuel/products PFR and the air/products PFR for further chemical reaction.

3.3 Two-Dimensional Codes

3.3.1 Parabolic

Numerous boundary-layer and free-shear-layer parabolic two-dimensional programs have been developed for chemically reacting flows. Aerotherm, GASL, AeroChem, Ultrasystems, Sandia, TRW Systems, Avco, General Electric, The Rocket Propulsion Establishment in England, and Spalding's group at Imperial College have all, for example, developed such computational methods. These programs have resulted from the investigation of: reentry vehicle flow fields, rocket plume afterburning, ramjet and afterburner propulsion, and chemical lasers. In general the existing programs suffer from a variety of problems which may include: excessive computation times, inability to handle thin high energy release rate flame zones, and inadequate description of turbulent transport. The best available programs for free-shear layer computations, known to the author, are those developed at AeroChem by Mikatarian, Kau, and Pergament(16) and at the Rocket Propulsion Establishment in England by Jensen and Wilson(17). Partially implicit integration techniques are employed and considerable attention is paid to the description of turbulent transport. Jensen and Wilson, however, make a common error in assuming that because simple mixing-length concepts are inadequate to describe the distribution of equilibrium turbulence the situation necessarily calls for a "two-equation" nonequilibrium model.

3.3.2 Two-Dimensional Elliptic Programs

In the area of combustion device modeling the principal contributions to the two-dimensional numerical solutions of the full elliptic Navier-Stokes equations have come from the Imperial College group(18-22) under Spalding and the United Aircraft group under McDonald(23-25). In addition several investigators have used the Gosman, et al(19) code in a variety of numerical calculations(26,27).

In many ways the two groups, having proceeded down separate paths in the course of developing their respective methodologies, are now at a point where the programs share many common features.

Both programs are applicable to furnace situations which are:

- Roughly cylindrical in shape as, for example, would be the case for a typical industrial boiler.
- Aerodynamically controlled by the burner design as distinct from furnace designs which have discrete staging (air or fuel) along the length of the combustor which in turn introduce three-dimensional effects.

Both programs have essentially the same embedded physics and chemistry. Turbulent transport is predicted through the use of a two-equation nonequilibrium model. Radiant heat transfer is predicted by means of a four-flux formulation. Two-phase flow is modeled on the assumption of zero velocity and temperature lag and the particles are assumed to participate in turbulent transfer to the same extent the gas phase does. Finite rate chemical kinetics is allowed in both models. Various versions of the Gosman-type programs have appeared with different dependent variables, i.e., vorticity/stream function variables or primitive velocity and pressure variables. Contrary to the arguments that are generated by this issue there appears to be little sound basis for the choice of one formulation over the other.

3.3.2.1 Numerical Procedures

It is in the numerical methods where the two programs show the greatest difference in character. Yet even here there are definite signs of eventual convergence to the same general approach.

Both programs have gone to an ADI type of alternating direction line relaxation procedure in order to increase the value of the critical cell Reynolds number. At this point, however, the programs differ in the iteration technique whereby the ADI procedure is brought to convergence. The UARL code uses a modification of the Peaceman and Rachford(6) acceleration parameter to achieve optimum convergence for a given cell Reynolds number and in this regard has a definite advantage over the Gosman code. This advantage is reflected in two related ways. First, the Gosman procedure apparently still requires the use of partial upwind differencing in order to maintain stability. Secondly, the optimum ADI convergence method used in CRISTY will yield shorter computation times.

Both the Gosman and UARL programs uncouple all of chemical kinetics equations in the ADI iteration procedure. This relies on the stabilizing effect of the diffusion coupling to maintain stability of the kinetics integration. It is unlikely that this procedure will work for complex chemistry and the equations will necessarily have to be coupled thus increasing the computation times by a large factor. The ratio of computational times between uncoupled and coupled systems of equations goes roughly as the square of the number of equations.

Both codes are forced by computation time consideration to use a relatively coarse node point mesh as illustrated in Figure 12. For the ADI procedure the computation time is proportional to the number of node points provided the number of iterations required for convergence remain constant.

3.3.2.2 Computational Results

Unfortunately these codes have had little opportunity to be adequately tested against reliable furnace data. Nor has there been the opportunity to perform the necessary numerical experiment to establish the solution dependence of various physical and numerical parameters. Some comparisons have been made between the UARL FREP

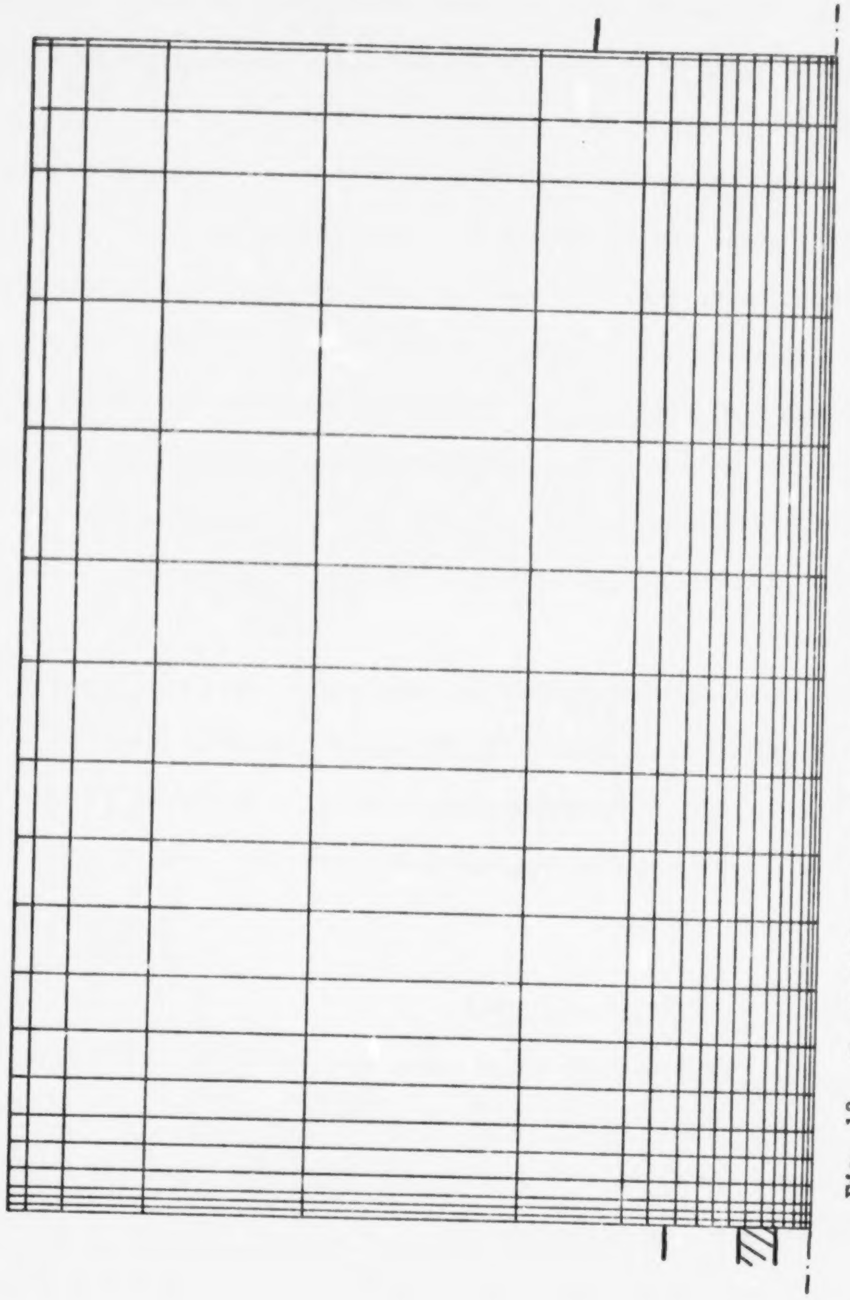

Fig. 12 Typical Numerical Mesh for Flow Field Calculation (After Khalil and Whitelaw(21)). Flow Enters From the Left Through a Double Concentric Port. Low Boundary is the Axis of Symmetry.

Code (predecessor to CRISTY) and cold swirling turbulent flow data(25). For low to moderate degrees of swirl the comparisons showed good agreement based on calculations using a sample Prandtl mixing length hypothesis. For higher swirl levels which yielded internal recirculation the simple turbulence model still appeared to give reasonable agreement with the data.

Gosman and Lockwood(22) have reported some comparisons between calculated behavior and the gas fired "M1 Trials" carried out at the International Flame Research Foundation at Ijmuiden. A partially burned gaseous fuel-air mixture enters a square cross section furnace along the centerline. Additional air enters in a concentric duct located around the centerline duct. Figure 13 shows comparisons between predicted and measured temperature profiles and streamline patterns. The agreement can only be considered fair.

3.4 Three-Dimensional Program

3.4.1 Elliptic

Both the United Aircraft Research Laboratories(28) and Imperial College(20) groups are developing three-dimensional elliptic programs for the stated purpose of analyzing combustion devices. In the author's opinion, the practical application of this type of program will be at least a decade off and will require dramatic advances in computer capability.

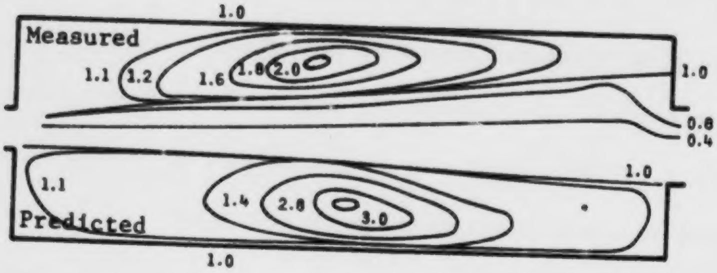
1.0
Measured
1.1
1.2
1.6
1.8
2.0
1.0
0.8
0.4
1.1
1.0
1.4
2.8
3.0
Predicted
1.0

Fig. 13a. Comparison of the Predicted and Measured Streamline Patterns - from Gosman and Lockwood(22)

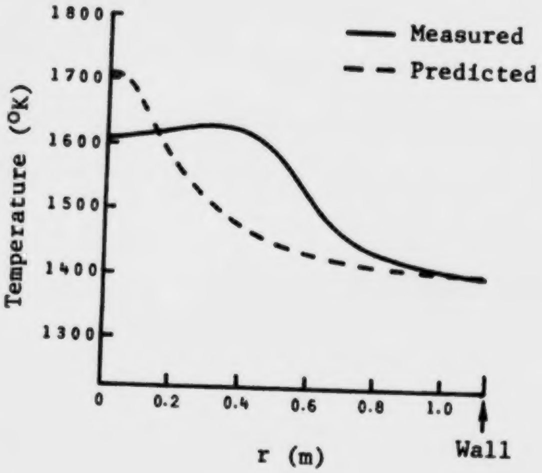

Fig. 13b. Comparison of Predicted and Measured Radial Temperature Profiles - from Gosman and Lockwood(22)

3.4.2 Parabolic

As mentioned earlier this type of program holds promise for those three-dimensional situations in which no upstream influence exists and in which the mixing regions lie along the coordinate lines. The turbulent transport laws for two-dimensional boundary and free shear layers can probably be generalized with some degree of confidence to this type of situation. The numerical problems are comparable to those encountered in two-dimensional elliptic problems. Hence if a satisfactory resolution is found in the two-dimensional case it should carry over to the three-dimensional situations.

Several three-dimensional laminar boundary layer programs have been developed over the last ten years. With straightforward modifications to the boundary conditions these codes can be immediately generalized to the three-dimensional combustor containing free-mixing layers. Patankar and Spaulding(29) have made such a modification and illustrate its use by applying the method to the developing laminar flow and heat transfer in a duct of square cross section with a laterally-moving wall as shown in Figure 14 . The asymptotic cross flow solution obtained when the flow becomes fully developed is identical to the two-dimensional flow in a square cavity with a moving wall. Patankar and Spalding compare their fully developed solution with those obtained by others for the two-dimensional case. (see Figure 14)

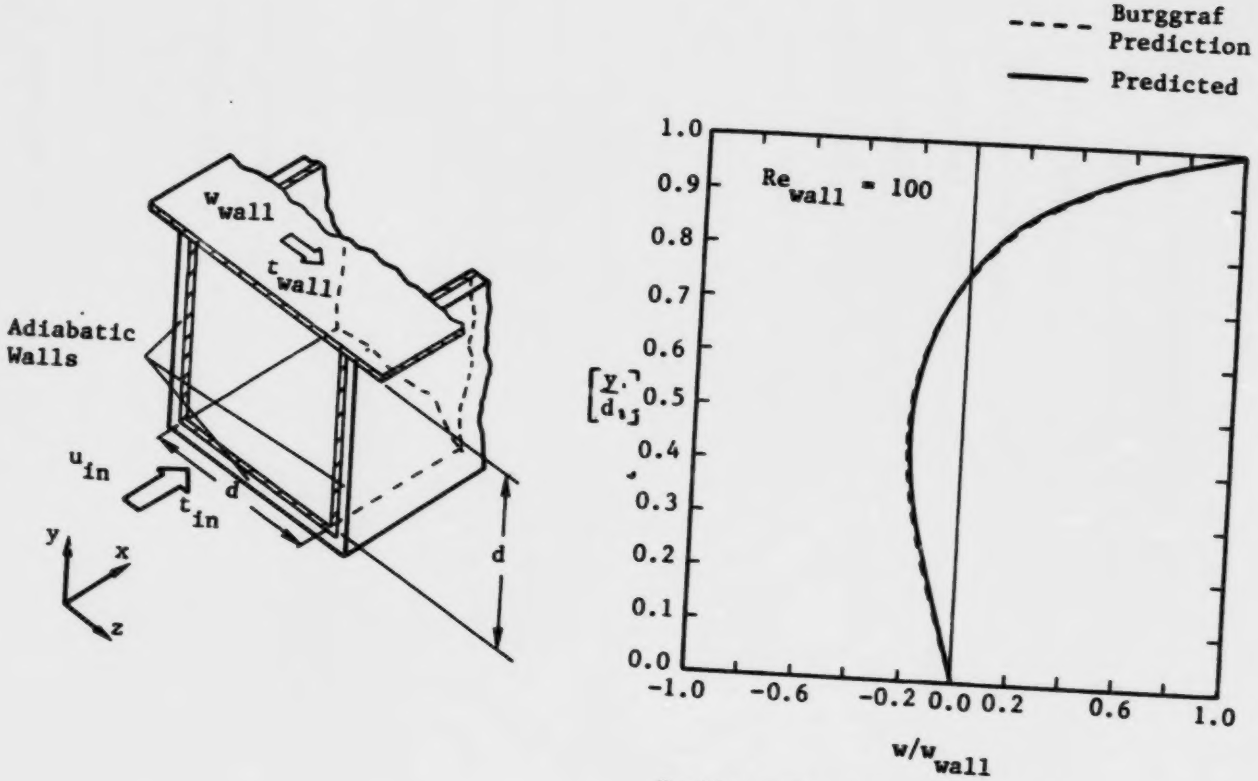

Profile of a Cross-Stream Velocity in the Fully-Developed Region

Fig. 14 Illustration of Three-Dimensional "Parabolic" Numerical Code (After Patankar and Spalding(29))

3.5 Data Analysis Codes

3.5.1 Deduction of Turbulent Transport and Chemical Source Distributions From Mean Flow Measurements

In recent years a considerable body of experimental data has been obtained on the time averaged temperature, velocity and concentration fields in various combustion devices. This experimental data does not generally lead to an intuitive understanding of the phenomena of turbulent mixing, heat release and the sources and sinks of trace species such as pollutants. Latent in the measured maps is a great deal of information regarding time-averaged turbulent transport of species, momentum, and energy. This information along with a description of the species source strength distributions can be extracted through the integration of the conservation principles of mass momentum and energy using the measured mean flow distributions.

Sadakata and Beér(49) have recently utilized a program of this type to calculate local NO formation rates in swirling turbulent methane-air flames. The NO formation rates in the reaction zone were found to be 3 to 5 times higher than those in the post flame region. Work is presently under way at Ultrasystems to develop such a program to evaluate flame data generated by the IFRF, IGT and others.

3.6 Radiative Heat Transfer

In any enclosure where the temperature and distribution of radiating species is known the prediction of radiation exchange to all points within that enclosure can be considered in two parts:

(1) Evaluation of radiative exchange between all points within the enclosure if the absorption, emission and scattering characteristics of the material within the enclosure and its bounding surfaces are known.

(2) Evaluation of the absorption, emission and scattering characteristics from a knowledge of the temperature and concentration of radiating species.

Theoretically an accurate solution of radiative exchange within any enclosure, at equilibrium, can be obtained by summation over the spectrum of the multiple reflection, absorption and scattering of an infinite number of emitted monochromatic beams. However, spectral information is not readily available for real solid surfaces(30) and only limited information is available concerning emission and absorption characteristics of flame gases which may contain solid particles(31,32). Consequently these limitations plus those associated with computational capabilities necessitated the development of different techniques for the evaluation of radiative exchange.

The various methods available for the evaluation of radiant heat exchange in combustors have recently been reviewed by Bartelds, et al(32) amongst which are:

- The Monte Carlo Method. This method includes a statistical approach to radiative exchange processes in which Monte Carlo sampling techniques are used to examine the action of small bundles of energy, rather than attempting to simultaneously solve for the behavior of all the energy involved in the process. If other numerical techniques are available to solve the problem under consideration Howell(34) does not recommend the use of Monte Carlo methods.

- Zone Method(35,36). In this method the enclosure is divided into several gas and surface zones and exchange between each zone pair is evaluated from the radiative transfer equation. The method has been successfully applied to furnaces(37,38,39) where acceptable predictions of heat flux to the walls and heat sinks have been reported. However, predictions of gas temperature profiles within the enclosure are not good. This can be attributed to coarse zoning or incorrect allowance for the emission/attenuation characteristics of the flame gases. In principle, the zone method is not limited to coarse zoning, computation times normally limit the number of of zones making it unacceptable for application to problems requiring definition of steep temperature gradients.

- Electrical Analogue Methods. Oppenheim(40) developed a technique in which the radiative quantities (emission, heat flux, etc.) are replaced by analogeous electrical quantities (potential current, etc.) in a network. The method has not been used extensively although advances in hybrid computing techniques could encourage further development and use.

- Flux Methods(39,41,42). In flux methods, the solid angle of 4π steradians surrounding a point is divided into a number of solid angles in which the intensity of radiation is assumed to be a specific function. The exact integro-differential equations of radiative transfer are replaced by approximate differential ones and can be easily solved by standard finite difference techniques. Consequently flux methods are ideally suited for coupling with the elliptic or parabolic flow field analysis programs discussed earlier. Results of this type of coupling have been presented by Gosman and Lockwood(43) and Lowes, et al(39). Bartelds(32) has recently developed two and four flux models which can be conveniently coupled with either physical or mathematical models to allow furnace performance to be predicted. Bartelds has increased the accuracy of these flux models by considering the intensity distribution around a point to be a continuous function rather than being constant over a given solid angle.

3.7 Spray Combustion Programs

3.7.1 One-Dimensional

Rocketdyne and Ultrasystems have developed one-dimensional spray combustion programs under sponsorship by the Air Force and NASA. These programs consider the dynamics, evaporation, and flame-mantle burning of liquid fuels. The gas phase is assumed to be in chemical equilibrium. Whether the droplet is burning with a flame mantle or evaporating with the vapor burning in the wake is determined by a criteria which is a function of the droplet relative Reynolds number and the thermodynamic state of the gas phase. The process rates are, of course, also dependent on these same variables. The droplet velocity lag and hence Reynolds number is dictated by the acceleration of the gas phase. The programs accept, as initial conditions, the droplet size distribution and initial injection velocities.

The codes have been applied in combustion systems analyses to determine approximate droplet lifetimes and the effective fuel source distribution for use in more complex nonequilibrium gas phase chemistry calculations. In those cases where the droplet spray initially crosses streamlines an independent estimate must be made of the degree of droplet consumption before they become "locked" into streamtubes. The initial distribution of drops by size and quantity as a function of streamtube location must then be specified.

3.7.2 Two-Dimensional Parabolic Codes

Considerable work has been done, under Department of Defense support, by Smoot and his co-workers(44-46) at Brigham Young University in the development of parabolic two-dimensional, two-phase combustion programs. The particle dynamics have been treated for a distribution of particle sizes without the assumption of zero velocity or zero temperature lag. For small particles these equations have the same "stiff" behavior as near equilibrium chemistry. In general it has been assumed that the particles respond to the mean motion only. Some consideration has been given to the turbulent particle diffusion in those cases for which the particles are small and eddy scale is large. To date there has been no application of this type of two-dimensional analysis to practical industrial furnaces.

3.7.3 Two-Dimensional Elliptic Codes

Spalding(20) and McDonald, et al(23) have employed a relatively simple model to predict the behavior of droplet clouds in two-phase combustion systems governed by two-dimensional elliptic behavior. These models have been incorporated into the Imperial College and UARL codes. The basic assumption is, that from a transport point of view, each size class of particles can be considered to behave as another gas phase species. These particle "species" are taken to have infinite "molecular weight" and hence do not contribute to the thermodynamic pressure. The particles are assumed to enter into convective motion with zero velocity lag and exhibit the same turbulent transport behavior as the gas phase. The net source (or sink) strength of each droplet size group is determined by a droplet evaporation or burning law. This mass loss behavior depends on local conditions as described in 3.7.1 above.

The shortcomings of such a model are certainly obvious and yet the numerical complexities of the model described in 3.7.2 combined with the elliptic nature of the flow make the resolution of this problem formidable. In the limiting situation of large particles and small eddy scale the assumptions made above break down completely. That is, the velocity lags are substantial and relative Reynolds number effects dominate the evaporation or burning rates. Also under these circumstances the particle paths will not necessarily coincide with mean flow lines and the particles will tend not to participate in the fluctuating eddy motion.

Perhaps the greatest drawback of this type of analysis is its inability to handle the initial behavior of a liquid fuel spray as it penetrates across stream lines. In this sense the model is similar to the one-dimensional methods described in 3.7.1 and requires similar auxiliary treatment.

3.8 Engineering Models of Furnace Behavior

The ultimate test of the value of any model of a combustion device is the degree to which it aids in the construction of such a device. Since furnaces have been built without the aid of models for some time the accuracy of any useful model must be at least equivalent to the empirical based design standards it was developed to supplant. Due to the complex nature of the problem useful engineering models will almost certainly contain adjustable empirical constants which restrict the model to particular furnace types. An excellent example of this type of model is that developed by Beuters, et al(47) at Combustion Engineering.

The analysis of the heat flux distribution and nitric oxide formation in a tangential fired boiler represents a problem of not trivial proportions. Figure 15 presents a schematic of a tangential fired boiler. Beuters(48) has described in detail the development of a program to predict the performance of the lower furnace. The furnace is divided into a series of horizontal strips with an arbitrarily assigned heat release distribution in the firing zone. The products of combustion "created" in each slice are directly proportional to the fraction of heat release and to the recirculation or backmix flow. Thus the flow originates in the heat release zone, circulates through the hopper region and "peels-off" to rejoin the exit stream (see Figure 15). The empirical factors included in the model have been established by extensive field testing. The gas emissivity factor (F_e), for example, takes account of the emission/absorption characteristics of the combustion gases and is fuel dependent. It also contains a correction for convective heat transfer. The lower

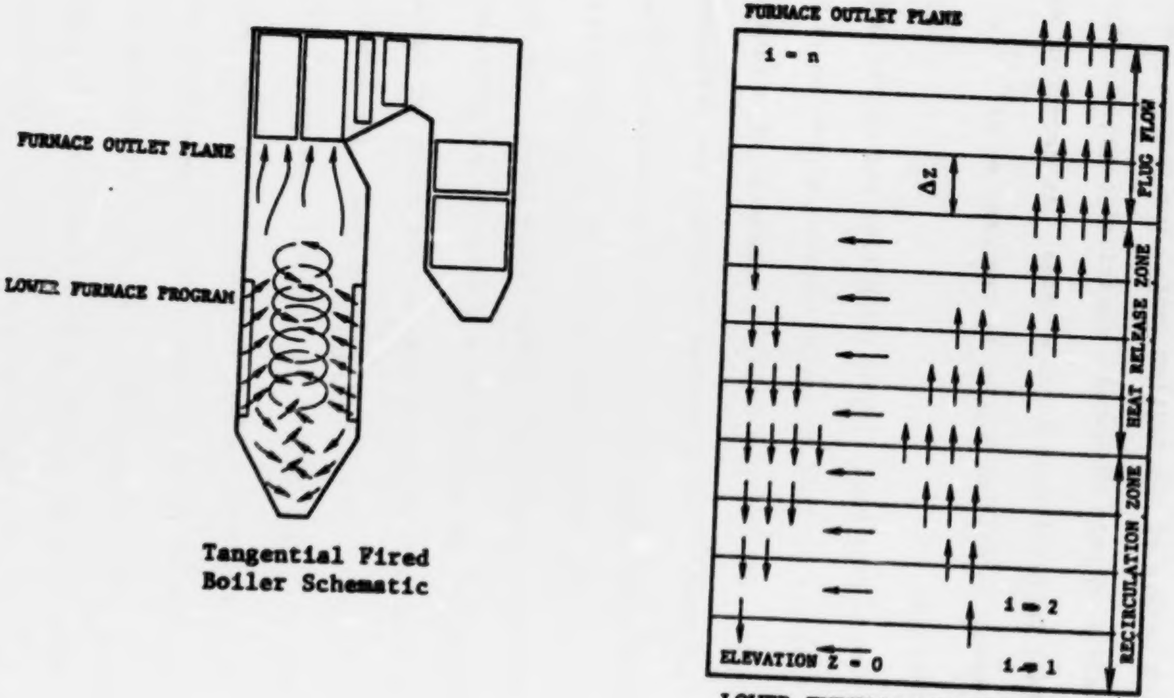
FURNACE OUTLET PLANE
LOWER FURNACE PROGRAM
FURNACE OUTLET PLANE
i = n
Δz
PLUG FLOW
HEAT RELEASE ZONE
RECIRCULATION ZONE
i = 2
i = 1
ELEVATION Z = 0

Tangential Fired
Boiler Schematic

LOWER FURNACE PROGRAM SAMPLE
GAS RECIRCULATION PATTERN

Lower Furnace Program Recirculating Model

Fig. 15 Furnace Model for Tangential Fired Boiler (Bueters$^{(47)}$)

furnace model has been modified to allow it to predict NO_x formation based upon the Zeldovich mechanism. The success of this empirical engineering model can be judged from the comparisons between measured and predicted wall absorption rates and NO_x emissions for oil fired utility boilers shown in Figure 16 . The Bueters model has been included as one example of several empirical models which can be successfully used to predict furnace behavior over restricted ranges.

4.0 CONCLUSIONS AND RECOMMENDATIONS FOR FUTURE ACTIVITIES RELATED TO MATHEMATICAL MODELING

From the "catalogue" of Section 3 it is certainly clear that a great deal of thoughtful work has gone into the development of mathematical models in recent years. It would be premature to judge the product of these efforts completely on the basis of what has been accomplished to date in the way of successful engineering application. Such a judgement would necessarily yield a low grade since most of the tools are still in the development stage and there has not been the opportunity to adequately test them against reliable measurements.

Nevertheless a few general conclusions can be reached regarding the achievements. The advancement in numerical analysis techniques should be applauded. The work at United Aircraft on the improvement

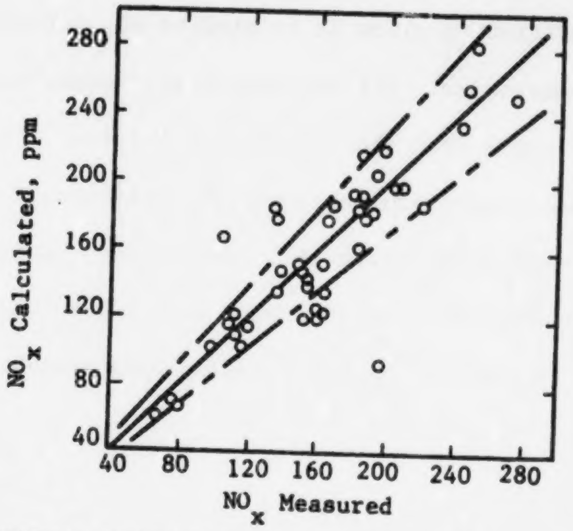

Nitric Oxide Emissions - Predicted vs Measured Values on Oil-Fired Units

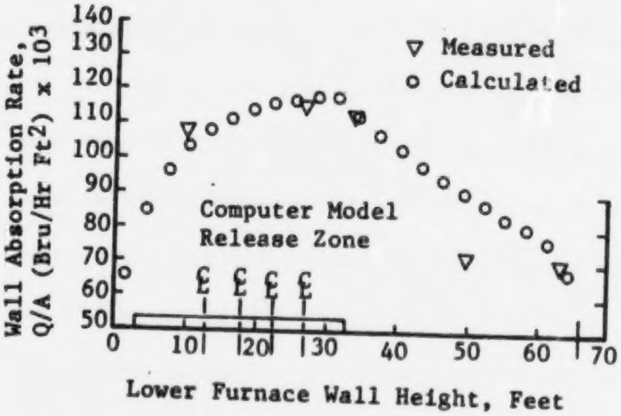

Wall Absorption Rate vs Lower Furnace Wall Height. Predicted vs Measured Values for Utility Unit A (Oil Fired)

Fig. 16 Comparisons of Predictions with Measured Values for an Empirical Engineering Model of Furnace Behavior (Beuters, et al$^{(48)}$

in numerical convergence techniques for the elliptic Navier-Stokes equations without the need to artificially introduce significant errors is a good example. The large increase in the number and type of models available today for both numerical experimentation and those with which to attempt engineering analysis tasks represent a significant contribution. The success of numerical manipulations of large sets of chemical reactions in helping to sort out the significant chemistry of pollutant formation is a notable accomplishment. Related to this is the ability, in certain cases, to establish the lower bounds on pollutant formation that are set by chemical considerations.

The single most important area that needs further investigation in order to dramatically improve our ability to predict combustor behavior is the physics of turbulent transport. Without a knowledge of this fuel/air contacting behavior on the "macro" scale there is little that can be accomplished with a more refined knowlege of the other physical and chemical aspects of combustion. In this regard several well designed experimental programs could be of great help. These would be designed to obtain the following information:

- Detailed mean flow and fluctuation measurements in types of flow regimes which are similar in character to the distinguishable regions of practical combustion devices. This would provide an empirical coupling between the turbulence level and the kinematics of the mean flow.

- Stimulus-response measurements with inert tracers introduced into various regions of typical combustion devices - this would provide gross coupling parameters for use in modular modeling.
- Determination of nonequilibrium turbulence parameters by stimulus-response measurements using a disturbance of the inflow turbulence level as the stimulus and measuring the decay of this disturbance within the system.

The second category of experiments could lead to a significant body of empirical data upon which to build a sound modular modeling capability. In light of the difficulties in obtaining a more detailed understanding of turbulent transport this empirical approach may prove to be the most promising of all. Possibly second only to macromixing in importance is the attainment of a better understanding of turbulence/kinetics coupling. An experiment is called for in which the eddy breakdown time can be varied for a well defined nonpremixed flow using reactants which have a simple and well understood chemistry.

Since the two-dimensional elliptic modeling techniques have significant potential for assisting in the design process, if the physics can be improved, there is considerable motivation to improve the numerical techniques. Some areas which deserve further investigation are:

- Automatic mesh control where grid size is linked to the gradients in the system
- Combined ADI iterations and iterations to "update" the nonlinear coefficients

- Further research to improve the ADI convergence rate for a given cell Reynolds number

There is a need for the smallest possible chemical reaction sets for use in complex fluid mechanical codes. Numerical experiments using simple stirred and plug flow reactors should be conducted to sort out these "reduced" sets. Improvements in "reaction screening" procedures are needed to accomplish this and to identify reaction rates which need further definition.

REFERENCES

1. Tennekes, H. and Lumley, J.L., A First Course in Turbulence. The MIT Press, 1972.

2. Beer, J.M., and Chigier, N.A., Combustion Aerodynamics, John Wiley & Sons, Inc., 1972.

3. McCreath, C.G., and Chigier, N.A., Fourteenth Symposium (International) on Combustion, p. 1355, The Combustion Institute, 1972.

4. Curtiss, C.F., and Hirschfelder, J.O., "Integration of Stiff Equations," Proceedings of the National Aeronautical Society, Vol. 38, pp. 235-243, 1952.

5. Tyson, T.J., "An Implicit Integration Method for Chemical Kinetics," TRW Systems Report 9840-6002-RU000, Sept. 1964.

6. Peaceman, D.W., and Rachford, H.H., Jr., Journal of the Society of Industrial and Applied Mathematics, Vol. 3, 1965.

7. Briley, W.R., "A Numerical Study of Laminar Separation Bubbles Using the Navier-Stokes Equations," Report J110614-1, United Aircraft Research Laboratories, East Hartford, Conn., 1970.

8. Kendall, R.M., and Kelly, J.T., "Premixed One-Dimensional Flame Code (PROF) - Its Formulation, Manipulation, and Evaluation," Aerotherm TR-75-158, July 1975.

9. Merryman, E.L., and Levy, A., Fifteenth Symposium (International) on Combustion, p. 1073, The Combustion Institute, 1974.

10. Nurick, W.H., Private communication.

11. Bartok, W., Engleman, V.S., and del Valle, E.G., "Laboratory Studies and Mathematical Modeling of NO_x Formation in Combustion Processes," ESSO Research and Engineering Co., Report GRU.3GNOS.71.

12. Levenspiel, O., Chemical Reaction Engineering, Second Edition, John Wiley & Sons, Inc.

13. Mellor, A.M., "Current Kinetic Modeling Techniques for Continuous Flow Combustors," presented at the Symposium on Emissions from Continuous Combustion Systems, pp. 23-55, September 1971.

14. Hammond, D.C., Jr., and Mellor, A.M., Combustion Science and Technology, Vol. 4, pp. 101-112, 1971.

15. Swithenbank, J., Poll, I., Vincent, M.W., and Wright, D.D., Fourteenth Symposium (International) on Combustion, p. 627, The Combustion Institute, 1972.

16. Mikatarian, R.R., Kau, C.J., and Pergament, H.S., "A Fast Computer Program for Nonequilibrium Rocket Plume Predictions," AFRPL-TR-72-94, 1972.

17. Jensen, D.E., and Wilson, A.S., Combustion and Flame, 25, pp. 43-55, 1975.

18. Runchal, A.K., and Wolfshtein, M., Journal of Mechanical Engineering Science, Vol. 11, No. 5, 1969.

19. Gosman, A.D., Pun, W.M., Runchal, A.K., Spalding, D.B., and Wolfshtein, M., "Heat and Mass Transfer in Recirculating Flows," Academic Press, New York, New York, 1969.

20. Spalding, D.B., "Mathematical Models of Continuous Combustion," p. 23, Emissions From Continuous Combustion Systems, Proceedings of the Symposium on Emissions from Continuous Combustion Systems, September 1971, Plenum Press, New York, London.

21. Khalil, E.E., and Whitelaw, J.H., "The Calculation of Local-Flow Properties in Two-Dimensional Furnaces," Imperial College of Science and Technology, HTS/74/38, November 1974.

22. Gosman, A.D., and Lockwood, F.C., Fourteenth Symposium (International) on Combustion, p. 661, The Combustion Institute, 1972.

23. McDonald, H., et al., Draft Final Report on Two-Dimensional Elliptic Program for Combustor Flow Field Analysis (CRISTY) - Developed under EPA Contract - August 1975.

24. Anasoulis, R.F., McDonald, H., and Buggein, R.C., "Development of a Combustor Flow Analysis, Part I: Theoretical Studies," AFAPL-TR-73-98, Technical Report, January 1974.

25. Anasoulis, R.F., and McDonald, H., "A Study of Combustor Flow Computations and Comparison with Experiment," EPA Report EPA-650/2-73-045, December 1973.

26. Quan, V., Bodeen, C.A., and Teixeira, D.P., Combustion Science and Technology, 7, pp. 65-75, 1973.

27. Samuelsen, G.S., and Peck, R.E., "Pollutant Formation in Reacting Flows with Recirculation," Paper presented at Western States Section, The Combustion Institute, October 1972.

28. Gibeling, H.J., McDonald, H., and Briley, W.R., "Development of a Three-Dimensional Combustor Flow Analysis," Volume I: Technical Report, United Aircraft Research Laboratories, R75-911850-18, July 1975.

29. Patankar, S.V., and Spalding, D.B., Fourteenth Symposium (International) on Combustion, p. 605, The Combustion Institute, 1972.

30. Hottel, H.C., and Sarofim, A.F., Radiative Transfer, McGraw-Hill, New York, 1967.

31. Sparrow, E.M., and Cess, R.D., Radiation Heat Transfer, Brooks/Cole, Belmont, USA, 1970.

32. Lowes, T.M. and Heap, M.P., Emission/Attenuation Coefficients of Luminous Radiation, Second Members Conference, I.F.R.F., IJmuiden, 1971.

33. Bartelds, H., Heap, M.P., and Lowes, T.M., Prediction of Radiative Exchange Within Furnace Enclosures, Vol. II, Final Report, EPA Contract 68-02-0202.

34. Howell, J.R., Application of Monte Carlo to Heat Transfer Problems, Advances in Heat Transfer, 5, p. 1-54, Academic Press, New York, 1968.

35. Hottel, H.C., and Cohen, E.S., Radiant Heat Exchange in a Gas-Filled Enclosure: Allowance for Non-uniformity of Gastemperature, AIChE Journal, 4, p. 3-24, 1958.

36. Hotell, H.C., and Sarofim, A.F., Theory and Fundamental Research in Heat Transfer (ed. J.A. Clark), p. 139-160, Pergamon Press, New York, 1963.

37. Johnson, T.R., and Beér, J.M., Fourteenth Symposium (International) on Combustion, p. 639, The Combustion Institute, 1973.

38. Latsch, R., Mathematisches Modell für eine turbulente Diffusionsflamme und deren zylindrischen Brennraum, Dissertation, University Karlsruhe, 1972.

39. Lowes, T.M., Bartelds, H., Heap, M.P., Michelfelder, S., and Pai, B.R., Prediction of Furance Heat Transfer, I.F.R.F. Document K20/a/72, August 1974.

40. Oppenheim, A.K., Trans. A.S.M.E., 78, p. 725-735, 1956.

41. Viskanta, R., Radiative Transfer and Interaction of Convection with Radiation Heat Transfer, Advances in Heat Transfer (eds. Irvine, T.F. and Hartnett, J.P.), 3, p. 175-252, Academic Press, New York, 1966.

42. Siddall, R.G., Flux Methods for the Analysis of Radiant Heat Transfer, Fourth Symposium on Flames and Industry, British Flame Research Committee I.F.R.F. and Inst. of Fuel, London, 1972.

43. Gosman, A.D., Lockwood, F.C., Fourteenth Symposium (International) on Combustion, p. 661, The Combustion Institute, 1973.

44. Smoot, D.L., and Allred, L.D., "Particle-Gas Mixing in Air-Breathing Ducts with Nonparallel Air Injection," AIAA Paper No. 74-1158, AIAA/SAE 10th Propulsion Conference, October 1974.

45. Smoot, L.D., Douglas, R.A., Simonsen, J.M., and Tufts, L.N., "A Model for Mixing and Combustion of Compressible, Particle-Laden Ducted Flows," Paper 70-736, AIAA Conference, 1970.

46. Hedman, P.O., "Particle-Gas Dispersion Effects," Ph.D. Dissertation, Brigham Young University, Provo, Utah, August 1973.

47. Bueters, K.A., and Habelt, W.W., "NO_x Emissions from Tangentially Fired Utility Boilers - A Two Part Paper," Part I - Theory, Presented at 66th Annual AIChE Meeting, November 1973.

48. Bueters, K.A., Cogoli, J.G., and Habelt, W.W., Fifteenth Symposium (International) on Combustion, p. 1245, The Combustion Institute, 1974.

49. Sadakata, M., and Beér, J.M., "Spatial Distribution of Nitric Oxide Formation Rates in a Swirling Turbulent Methane-Air Flames," The Combustion Institute European Combustion Symposium, 1975.

4:25 p.m.
The Mathematical Modeling of Combustion Devices
Thomas J. Tyson, Ultrasystems, Inc.

Q: I should like to elicit a comment from Dr. Tyson concerning the use of time-smoothed equations of motion in large furnaces containing thin flame zones.

A: The question raised is a major area requiring further clarification, and is related to the questions of macroscale turbulent transport; particle ballistics, evaporation, and combustion in turbulent flows; and turbulence/chemistry coupling. Large furnaces have less confined flames where the gross motion of the mixing zones can be influenced by the large scale low frequency turbulent motion of the furnace as a whole. Time averaging on this scale undoubtedly is questionable. Nevertheless, I think the macromizing associated with fuel/air contacting on the scale of the active flame zone can be predicted by time-averaged behavior even though the precise location of the flame is uncertain. With regard to the thin flame zones, I don't believe this is a more critical issue than for smaller-sized combustors. During the time that fuel and air are initially entwined in a large eddy the opportunity for molecular diffusion is small even in small devices. Chemical action awaits the cascading breakdown process to smaller eddies. Similarly, the "hold up" period after hot products become entwined with cooler zones but still continue to be chemically active is dictated by the eddy breakdown rate. Since this breakdown time is longer in large furnaces and the quenching is more severe following breakdown, the issue of turbulence kinetics coupling is indeed more important in large furnaces; hence the time-averaged equations should come under greater scrutiny.

I believe the resolution to this, however, will not be to abandon the time-averaged formulation, but rather to develop a phenomenological eddy "hold-up" model.

Q: The situation of modeling flames often involves attention to the local scale -- reactions are occurring locally -- either in the shear layers or around droplets. In many instances the modeler is trying to define the conditions under which this local action is occurring -- be it NO formation or soot formation. One interesting way to do this and one which has met with some success, is to feign ignorance of the total flow field and the exact distribution of temperature and equivalence ratio. In many instances they are too hard to define. Heywood and others have met with some success by specifying a distribution of reaction zone equivalence ratio.

A: I sympathize with this approach, which was suggested some twenty years ago by Corrsin in describing the statistical behavior of unmixedness decay in a turbulent field and developed by Heywood for combustion devices. It stems from a desire to simplify the task of predicting furnace performance. However, I find it very difficult to know how to do this. To employ this approach one needs to describe, in some statistical fashion, the environment in which the local chemical action is taking place. For example, the statistical quantities defining the "background" stoichiometry and temperature fields (say mean and deviation from the mean parameters) must be modeled in some manner. How, for example, does the deviation from the mean of overall fuel/air ratio decay with distance down a complex combustion device? I would rather gamble on the development of a mechanistic approach, based on a fluid mechanical description of the device, to describe this behavior rather than on an ad hoc statistical description. I agree with the implication of your question that attention may need to be focused on local scale high temperature thin molecular diffusion layers within eddies or around drops or droplet clouds. However, in considering the importance of such zones in comparison with adjacent locally well mixed regions, one must consider relative scales, residence times, compositions, and temperatures. The lifetime and contribution from thin molecular diffusion zones within large scale eddies is, for example, dictated by the eddy breakdown rate which is such that the diffusion layer becomes of less significance as the combustor size increases.

DEVELOPMENT OF FEDERAL STANDARDS OF PERFORMANCE

By:

Stanley T. Cuffe

Environmental Protection Agency

Research Triangle Park, N.C.

DEVELOPMENT OF FEDERAL STANDARDS OF PERFORMANCE

I am pleased to have been invited to participate in this Stationary Source Combustion Symposium. My comments will include a summary of the procedures used to develop standards of performance, typical problem areas we have encountered in the past, sources we are presently working on, and new sources we will survey.

As many of you know, the authority of the U.S. Environmental Protection Agency (EPA) to control the discharge of pollutants into the atmosphere is provided by the Clean Air Act, as amended in 1970.

Section 112 of the Act directs the Administrator to issue national emission standards for air pollutants which cause an increase in mortality or an increase in a serious, irreversible, or incapacitating reversible, illness. Standards for hazardous pollutant emissions are designed to provide an ample margin of safety to protect public health. Hazardous pollutant standards have been issued for 13 sources of asbestos, beryllium and mercury, as noted in Table 1.

Most of our efforts in developing federal standards, however, have been for sources covered under Section 111 of the Act. This section requires the establishment of standards of performance for new stationary sources of air pollution which "... may contribute significantly to air pollution which causes or contributes to the endangerment of public health or welfare." The Act requires that standards of performance for such sources reflect "... the degree of emission limitation achievable through the application of the best system of emission reduction which (taking into account the cost of achieving such reduction) the Administrator determines has been adequately demonstrated."

During the past several years of developing new source performance standards, EPA staff have generally used the following guidelines:

1. Source test data on existing well-controlled plants are the most desirable basis for setting emission limits for new plants. Most of these data are obtained from EPA source tests on best controlled plants.

2. Interpretation of test results from any single best-controlled plant must consider (a) representativeness of the plant tested (feedstock, operation, size, age, etc.); (b) age and maintenance schedule for the control equipment tested; and (c) design uncertainties for the type of control equipment being considered and the "safety factor" that must be used to ensure meeting the emission standard.

3. For sources where emerging technology is significant, consideration is given to (a) test data from pilot and prototype installations and application of reasonable engineering judgment to these data; (b) vendor guarantees; (c) existing design contracts; and (d) foreign technology.

4. Cost of control is related to the cost of the new industrial installations and the economic impact on the industry, not in reference to air quality improvements or the economic benefits of such improvement.

5. Where possible, standards should be able to be met through the use of more than one control technique or licensed process. (Electrostatic precipitators or fabric filters can meet standards for cement plants.)

6. Where possible, standards should encourage, or at least permit, the use of process modifications or new processes in place of add-on air pollution control systems, i.e. use of low sulfur fuel.

7. Where possible, standards should allow the use of control systems capable of controlling other pollutants (i.e., scrubbers versus electrostatic precipitators on steam electric generators).

8. Where possible standards should allow the use of control systems that can minimize the impact on other aspects of the environment.

9. Where appropriate, visibility standards are established which are compatible with mass emission standards. A prime purpose of this type of standard is to facilitate surveillance and enforcement.

The timetable in the Clean Air Act requires that EPA first publish a list of source categories for which it intends to establish performance standards. Within 120 days after the list is published in the Federal Register, the Agency must propose standards for those categories. Within 90 days following their proposal, EPA must promulgate the standards. As required by the Act, time is provided for interested parties to comment on the proposed standards and for the Agency to review and react to the comments prior to promulgation. The standards are effective upon promulgation; however, a source is subject to the standards if construction or modification is begun after the date the applicable standards are proposed.

The procedures which are followed by EPA project officers or by their contractors in preparing a standards support and environmental impact document (SSEID) and in having the document reviewed prior to proposal of standards of performance in the Federal Register include:

1. Available background data (particularly emission control technology) is gathered by conducting literature searches, and short term screening studies, and by meeting with representatives of industry trade associations, industrial plants, air pollution control agencies, and with vendors of air pollution control equipment.

2. Field inspections are made of candidate plants which have more efficient processes and/or emission control systems.

3. After an evaluation of the inspected facilities, specific processes and/or emission control systems are selected for source testing pollutants of concern. Emission measurements are then made at selected facilities by EPA staff or their contractors.

4. Letters are forwarded to owners or operators of specific plants requesting information on performance of their emission control systems and on the capital and annual costs of these systems. In sending the letters, EPA normally invokes Section 114 of the Clean Air Act which requires that the owners or operators provide this information to the Administrator of EPA. The letters are usually a primary source of data on emission control costs and a secondary source of emission data.

5. After the gathering of these data is completed, a standards support and environmental impact document (SSEID) is written. This report details the performance and costs of alternate emission control systems and the rationale for the proposed standard of performance. Also discussed are the environmental effects of water pollution, solid waste, noise and particularly the energy requirements if the proposed performance standard were adopted. Up to this point, the gathering of data and the writing of the SSEID will require between 12 and 16 months.

6. The SSEID then undergoes a series of reviews and proposal of standards for a period of about one year before a final standard of performance is promulgated.

Initial review is provided within EPA by a working group composed of representatives from Enforcement, Research, Water Pollution, Solid Waste, Economic Analysis, and the Office of General Counsel. Outside of EPA, the proposed standards of performance are reviewed in detail by two advisory committees to EPA. The first of these, The National Air Pollution Control Techniques Advisory Committee, has 16 members representing industry, control equipment manufacturers, air pollution control agencies, consultants specializing in air pollution control and environmental groups. To assist the committee, several individuals with specialized expertise related to the specific source categories being considered are asked to attend the meetings as technical consultants. Next a steering committee composed of Assistant Administrators of each office within EPA reviews the SSEID. Prior to proposal of performance standards in the Federal Register, the document is then reviewed by other Federal agencies such as the Departments of Commerce, Interior & Defense. This review is coordinated by the President's Office of Management and Budget. After proposal in the Federal Register, usually several hundred comments on the proposed standards are received from interested industries, citizens groups, control agencies, universities and research institutes. These comments are made known to the Advisory Committee to obtain their comments before the proposed standards become law.

During the data gathering phase of developing a standard, several main types of problems are encountered which have resulted in extended time schedules. One expensive and time consuming area is the locating of candidate "best systems of emission reduction." This has been a particular problem in the category of metallurgical processes. During the past three years our project engineers have inspected ferroalloy and by-product coke plants in Europe and Japan to gather information on efficient particulate control systems. Inspections of copper smelters in Europe were also made to assess efficient systems for control of sulfur dioxide. Municipal incinerators equipped with efficient particulate collectors were also visited in Europe. For most other types of industrial processes, however, we have been able to locate candidate "best controlled plants" in the United States.

Although many well controlled sources are located in the United States, the control systems are often not well maintained and operated. Dense plumes of particulate emissions have been observed from fabric filters and electrostatic precipitators of efficient design. Screens on centrifugal pumps serving packed scrubbers have been partially plugged as have spray heads within the scrubber. Proper maintenance must be performed before emission measurements are made or else these specific installations are not tested.

A second problem area is the lack of demonstrated control technology for oxides of nitrogen and for hydrocarbons. As noted in this symposium, control techniques for nitrogen oxides have been applied to fossil fuel burning steam generators. However, these techniques have apparently not been applied to fossil fuel fired kilns, dryers, process heaters and incinerators. For the control of hydrocarbons, particularly solvents, the most commonly used method of control is an afterburner or incinerator where recovery of heat is not practiced. Other types of control systems, which are not energy intensive, have had limited use in controlling hydrocarbons.

The third problem area is a lack of standard methods of measurement for emissions of atmospheric pollutants. Fugitive emissions of gaseous and particulate pollutants from charging coal into and pushing coke from by-produce coke ovens are not amenable to conventional methods of emission measurement. Emissions from coke oven charging holes, standpipes and covers, chuck and end doors often occur over a period of several minutes and cannot reasonably be captured to determine the mass rates of pollutant emissions. For other industrial sources, particulate emissions from centrifugal scrubbers and from screens serving grain dryers are usually not amenable to isokinetic, traverse type sampling procedures. Also the measurement of condensible hydrocarbons to determine particulate and gaseous portions have been a problem in the measurement of emissions from asphalt roofing plants. In another area, standard techniques for measuring asbestos emissions from taconite beneficiation plants are not available.

To date, standards of performance for new stationary sources have been set for pollutants from 17 source categories (see Table 2). The preparation of SSEID has been completed for 14 other sources (see Table 3). Engineers in our Industrial Studies Branch are presently gathering information for development of standards of performance for 17 other sources (See Table 4). Stationary fossil fuel combustion sources which are covered in this data gathering phase include 1) combined coal-municipal refuse fired steam generators, 2) stationary internal combustion engines, 3) stationary gas turbines and 4) intermediate size boilers.

For the combined firing of coal and municipal refuse, emission measurement results from the Union Electric Power Plant (the only commercial size operating unit) show some increase in emissions of particulate when firing coal and refuse over that from burning coal alone. As expected, however, no increase in emissions of nitrogen or sulfur oxides was noted. A performance standard for particulate emissions will therefore be proposed. The demonstrated control technology for particulate is an electrostatic precipitator which in order to maintain the same particulate emission limit will generally be slightly larger than that for firing coal alone. A draft SSEID has been written and has undergone review by the NAPCTAC. A standard of performance for this source should become law by next summer.

For stationary internal combustion engines, emission measurement results for nitrogen oxides (and also carbon monoxide and hydrocarbons) are being obtained from natural gas and diesel oil-fired engines tested in manufacturer's laboratories. The various control techniques for nitrogen oxide which are used alone or in combination include:

1. Turbo charging and reduced compression ratio
2. Spark retard
3. Changed air to fuel ratio
4. Increased engine speed
5. Modified injectors
6. Exhaust gas recirculation
7. Engine derating
8. Water injection

Many of these control techniques cause some increase in fuel consumption, particularly retard and engine derating. A compromise between reduction of NO_x and increased fuel consumption will therefore be considered. Also, because promulgated standards could not be implemented immediately by engine manufacturers, time will be provided to incorporate control techniques into their production engines. A draft SSEID should be available by this coming December or January. Performance standards for this source category should be forthcoming in about a year.

Regarding stationary gas turbines, the primary emissions when firing oil or gas are nitrogen oxides and carbon monoxide. Sulfur dioxide can also be a problem when firing oil. The nitrogen oxides can be controlled by a) dry techniques such as external combustion, variable geometry combustors, catalytic combustors and exhaust gas recirculation and b) water or steam injection into the combustion chamber. Although sulfur oxides can be controlled by using low sulfur fuels, in some cases, desulfurization of oil will be required. Some of the problems which have been encountered to date in developing proposed performance standards are:

1. Lack of treated water at remote locations for treatment of nitrogen oxides.

2. Availability of low sulfur fuel.

3. High content of bound nitrogen in the fuel.

4. Increased emissions of nitrogen oxides with increased turbine efficiency.

A draft SSEID should be available by April 1976 while performance standards for turbines should be promulgated about 10 months later.

A study of intermediate size boilers (smaller than 250×10^6 Btu/hr heat input) will be started by a contractor in about 3 months. Information will be developed on the performance of control techniques for particulates, nitrogen oxides, sulfur oxides, hydrocarbons, and carbon monoxide. After a survey has been completed in about a year, suitable types and sizes of boilers and specific pollutants will be selected for development of standards of performance.

Source categories involving the processing of fossil fuels which are presently being surveyed include a) sulfur recovery plants in petroleum refineries and in natural gas fields and b) the gasification of coal. Pollutants of concern from the sulfur recovery plants include sulfur dioxide (SO_2), hydrogen sulfide (H_2S), carbon disulfide (CS_2) and carbonyl sulfide (COS). Efficient control systems for these pollutants include the Wellman Lord, Scott and Beavon. The Wellman Lord system consists of incineration followed by scrubbing of SO_2. For the other two systems, sulfur compounds are converted to H_2S and removed by scrubbing. Several of these processes have been tested by EPA staff or contractors at petroleum refineries in the United States. A Stretford system is scheduled for testing at a natural gas field plant in Texas. A SSEID has been completed and is undergoing review for control of sulfur plants in petroleum refineries. A draft SSEID for control of sulfur compounds from natural gas fields should be complete by April, 1976.

Conversely, there are no commercial size coal gasification plants operating in the United States. To define basic components of exit gas streams from lurgi coal gasification plants and the performance of systems to recover sulfur compounds, the EPA project officer inspected and obtained data from coal gasification plants in South Africa, Germany and Scotland. The pollutants of primary concern are sulfur oxides, sulfides and mercaptans, hydrocarbons and particulates. A draft SSEID for coal gasification plants should be complete by February, 1976.

Finally, the source categories which will be surveyed during the next two years to determine the magnitude of emissions and the availability of demonstrated control technology for the probable development of standards of performance are:

1. Power plant boilers $>250 \times 10^6$ Btu/hr
2. Cement plants
3. Explosives
4. Steel foundries
5. Industrial surface coatings
6. Charcoal manufacture
7. Ethylene oxide
8. Coal liquefaction
9. Industrial & Commercial incineration
10. Fibers (Nylon & Acetate)
11. Plywood manufacture
12. Beer & whiskey processing

Standards of performance were promulgated in December of 1971 for pollutants from power plant boilers and cement plants. However, recent information indicates that revised standards are needed for particulates and nitrogen oxides from power plants and that standards should be developed for nitrogen and sulfur oxides from cement kilns. Most of the other industries, e.g. industrial surface coatings, charcoal manufacture, ethylene oxide, coal liquefaction, nylon and acetate fibers and beer and whiskey processing, are significant sources of hydrocarbon emissions. Because of the widespread problem of photochemical oxidants, which may extend into rural as well as urban areas, it is apparent that maximum control of all new hydrocarbon sources nationwide will be an important factor in controlling the oxidant problem.

TABLE I

SUMMARY OF HAZARDOUS POLLUTANT STANDARDS

Pollutant	Affected Facility	Limitation
Mercury	Mercury ore processing facilities Mercury cell chlor-alkali plants	Not more than 2300 gm/day for the entire facility.
Beryllium	Extraction plants, foundries ceramic manufacturing plants beryllium waste disposal incinerators propellant plants, machine shops processing alloys with >5% Be.	Not more than 10 gm/day (Option of meeting ambient level of 0.01 ugm/m^3 if three years of ambient data available).
	Rocket testing facilities	Limited to 75 ugm-min/m^3
Asbestos	Asbestos mills, manufacturing operations	No visible emissions or use control equipment meeting specific performance characteristics
	Spraying of asbestos fireproofing and insulation that contains more than 1% asbestos on buildings, structures, pipes and conduits.	Banned
	Spraying of asbestos fireproofing and insulation that contains more than 1% asbestos on equipment and machinery.	No visible emissions
	Use of asbestos mill tailings on roadways	Banned except on asbestos ore deposits
	Demolition operations	Good control practices are required

TABLE 2

SUMMARY OF STANDARDS FOR NEW OR SUBSTANTIALLY MODIFIED SOURCES

1. Steam Generators [>250 million Btu/hour heat input]

   (a) Particulate Matter:
   - (1) 0.1 lbs. per million Btu heat input (0.18 grams per million calorie)
   - (2) No more than 20% opacity visible emissions, except for two minutes in any hour visible emissions may be as great as 40% opacity.

   (b) Sulfur Dioxide:
   - (1) 0.8 lbs. per million Btu heat input (1.4 grams per million calorie) when oil is fired.
   - (2) 1.2 lbs. per million Btu heat input (2.2 grams per million calorie) when coal is fired.

   (c) Nitrogen Oxides (as NO_2):
   - (1) 0.20 lbs. per million Btu heat input (0.36 grams per million calorie) when gas is fired.
   - (2) 0.30 lbs. per million Btu heat input (0.54 grams per million calorie) when oil is fired.
   - (3) 0.70 lbs. per million Btu heat input (1.26 grams per million calorie) when coal is fired.

2. Incinerators [>50 tons per day charging rate]

   Particulate Matter:
   0.08 grains per standard cubic feet corrected to 12% CO_2 (0.18 grams/NM^3)

3. Portland Cement Plants

   Particulate Matter:

   - (1) 0.30 lbs. from the kiln per ton of feed to the kiln (0.15 kg per metric ton of feed).
   - (2) 0.10 lbs. from the clinker cooler per ton of feed to the kiln (0.05 kg per metric ton of feed).
   - (3) No more than 10% opacity visible emission from kiln and cooler.
   - (4) Less than 10% opacity visible emission from all other sources in the plant.

4. Nitric Acid Plants

Nitrogen Oxide (as NO_2):
(1) 3 lbs. per ton of acid produced (1.5 kg per metric ton).
(2) Less than 10% opacity visible emissions.

5. Sulfuric Acid Plants

(a) Sulfur Oxide:
4 lbs. per ton of acid produced (2 kg per metric ton).
(b) Acid Mist:
(1) 0.15 lbs. per ton of acid produced (0.075 kg per metric ton).
(2) Less than 10% opacity visible emission.

6. Asphalt Concrete Plants

Particulate Matter:
(1) 0.04 grain per dry standard cubic foot (90 mg/dscm).
(2) Less than 20% opacity visible emissions.

7. Petroleum Refineries

(a) Particulate Matter
(1) 1.0 pound per 1000 pounds of coke burnoff in a FCC catalyst regenerator.
(2) Less than 30% opacity except for 3 minutes in any one hour.
(b) Carbon Monoxide
0.05% by volume in gases from a FCC catalyst regenerator
(c) Sulfur Dioxide
No fuel gas shall be burned which contains H_2S in excess of 0.10 gram per dry standard cubic foot (230 mg/dscm).

8. Storage Vessles for Petroleum Liquids

Hydrocarbons:
(1) If the true vapor pressue of the petroleum liquid, as stored, is equal to or greater than 78 mm Hg (1.5 psia) but not greater than 570 mm Hg (11.1 psia), the storage vessel shall be equipped with a floating roof, a vapor recovery system, or their equivalents.
(2) If the true vapor pressure of the petroleum liquid as stored is greater than 570 mm Hg (11.1 psia), the storage vessel shall be equipped with a vapor recovery system or its equivalent.

9. Secondary Lead Smelters

Particulate Matter:
(1) 0.022 grain per dry standard cubic foot (50 mg/dscm).
(2) Less than 20% opacity visible emissions.

10. Secondary Brass and Bronze Plants

Particulate Matter:
(1) 0.022 grain per dry standard cubic foot (50 mg/dscm).
(2) Less than 20% opacity visible emissions.

11. Iron and Steel Plants

Particulate Matter:
0.022 grain per dry standard cubic foot (50 mg/dscm) from a basic oxygen furnace.

12. Sewage Treatment Plants

Particulate Matter:
(1) 1.30 pounds per ton of dry sludge input (0.65 g/kg).
(2) Less than 20% opacity visible emissions.

13. Wet Process Phosphoric Acid Plants

Total Fluorides:
0.020 pound per ton of equivalent P_2O_5 feed (10.0 g/metric ton).

14. Super-Phosphoric Acid Plant

Total Fluorides:
0.010 pound per ton of equivalent P_2O_5 feed (5.0 g/metric ton).

15. Diammonium Phosphate Plants

Total Fluorides:
0.060 pound per ton of equivalent P_2O_5 feed (30 g/metric ton).

16. Triple Superphosphate Plants

Total Fluorides:
0.20 pound per ton of equivalent P_2O_5 feed (100 g/metric ton).

17. Granular Triple Superphosphate Storage

Total Fluorides:
5.0×10^{-4} pound per hour per ton of equivalent P_2O_5 stored (0.25 g per hour per metric ton).

TABLE 3
SOURCES FOR WHICH DRAFT SSEID HAVE BEEN COMPLETED AND REVIEW INITIATED

	Source	Affected Facility	Pollutant
1.	Copper smelters	Roasters, reverberatory furnaces, converters, or metallurgically equivalent	Particulates Sulfur Dioxide
2.	Lead smelters	Sintering machines, roasters or metallurgically equivalent	Particulates Sulfur Dioxide
3.	Zinc smelters	Sintering machines, roasters or metallurgically equivalent	Particulates Sulfur Dioxide
4.	Aluminum reduction plants	Pot lines	Fluorides
5.	Ferroalloy plants	Furnaces	Particulates
6.	Iron and steel mills	Electric furnaces	Particulates Carbon Monoxide
7.	Coal cleaning plants	Air tables, thermal dryers	Particulates
8.	Polyvinyl chloride plants	Entire process	Vinyl chloride
9.	Lignite-fired steam generators	Boiler	Nitrogen oxides
10.	Grain elevators	Truck, railcar, barge and ship unloading and loading operations, and conveyors, cleaners and dryers.	Particulates
11.	Sulfur recovery plants in petroleum refineries	Sulfur recovery plant	Total reduce sulfur and sulfur dioxide
12.	Kraft pulp mills	Recovery furnace, lime kiln, smelt dissolving tank, digester and multiple effect evaporators, pulp washer, black liquor oxidation tanks, and condensate stripping system.	Total reduced sulfur and particulates

	Source	Affected Facility	Pollutant
13.	By-product coke ovens – charging operation	Truck, railcar, barge and ship unloading and loading operations, and conveyors, cleaners and dryers	Particulates
14.	Crushed stone plants	Crushers, screens, conveyor transfer points, surge and storage bins, and drilling operations	Particulates

TABLE 4

SOURCE CATEGORIES BEING SURVEYED

	Source	Pollutants
1.	Primary aluminum - 111-d	Fluorides
2.	Kraft pulp mill - 111-d	Total reduced sulfur
3.	Chlor-alkali plants	Mercury
4.	Electric furnaces in grey iron foundries	Particulates
5.	Carbon black plants	Hydrocarbons, carbon monoxide & particulates
6.	By-product coke ovens - pushing	Particulates & hydrocarbons
7.	Lime plants	Particulates & sulfur dioxide
8.	Phosphate rock processing	Particulate
9.	Drycleaning	Hydrocarbons
10.	Sintering plants in iron and steel mills	Particulate
11.	Solvent degreasing	Hydrocarbons
12.	Sulfur recovery plants in natural gas fields 111-d	Sulfur dioxide
13.	Asphalt roofing plants	Particulates & hydrocarbons
14.	Low grade iron ore beneficiation	Asbestos
15.	Lead battery manufacture	Lead
16.	Gasoline additive manufacture	Lead
17.	Lead typesetting plants	Lead

AN OVERVIEW OF REGIONAL FUEL COMBUSTION REGULATIONS:
PARTICULATE MATTER AND SULFUR OXIDES

By:

G. T. Helms

Deputy Director, Air and Hazardous Materials Division

United States Environmental Protection Agency

Region IV

Atlanta, Georgia

INTRODUCTION

The Clean Air Amendments of 1970 provide the basis for current national efforts to control air pollution. This legislation requires the Administrator of the Environmental Protection Agency (EPA): 1) to designate air pollutants that have an adverse effect on public health and welfare; 2) to publish and periodically update monographs, known as air quality criteria documents, which accurately summarize current scientific knowledge of the effects of designated pollutants; 3) to issue documents summarizing control technology applicable to designated pollutants, and 4) to propose and promulgate national ambient air quality standards for designated (criteria) pollutants. Primary standards are to be sufficiently stringent to protect public health, allowing an adequate margin of safety, while secondary standards are to protect public welfare. Thus far, six criteria pollutants have been designated: particulate matter, sulfur dioxide (SO_2), nitrogen oxides, carbon monoxide, hydrocarbons, and oxidants. This paper deals principally with two of these pollutants, SO_2 and particulate matter.

Under Section 110 of the Clean Air Act, states are required to adopt and submit for EPA's approval plans which provide for the implementation, maintenance, and enforcement of the national ambient air quality standards. Such plans are to be approved by EPA if they provide for the attainment of primary standards by mid-1975. The plans must include "emissions limitations, schedules, and timetables for compliance with such limitations, and such other measures as may be necessary to insure attainment and maintenance of such primary or secondary standard." The emission limitations developed under Section 110 apply to existing air pollution sources and once approved by EPA become by that fact Federally enforceable. New air pollution sources are governed by emission limits set pursuant to Section 111 of the Act. These "New Source Performance Standards" are set independently of air quality considerations and represent the best available control technology considering economics.

CONTROL STRATEGY TESTING

EPA's regulations governing the preparation of Section 110 State Implementation Plans were promulgated in the August 14, 1971, Federal Register. These regulations, now known as 40 CFR Part 51, provided a rather rough and ready guidance by which states could develop emission limits adequate to assure attainment of the national standards. Section 51.13(d), Control Strategy for Particulates and SO_2, allowed the use of the so-called "example region" approach to control strategy testing. In practice, the use of this approach meant that states could develop regulations for general application on the basis of the degree of control needed only in the most polluted areas of the state. The resulting emission limits in some cases were unnecessarily stringent when applied to sources outside these heavily polluted areas. In Florida, for example, fuel combustion SO_2 limits needed to meet standards in Hillsborough County were applied to sources in all other parts of the State as well. States like Kentucky, where limits varied according to an Air Quality Control Region's (AQCR) priority classification, were the exception.

40 CFR 51.13(e) provided for the adequacy of states' regulations to be tested either by a proportional model, generally referred to as the rollback technique, or by diffusion modeling. Since the rollback method was easier and faster to use, many states developed their regulations in this way. The major flaw in the rollback method, aside from the crudeness of the formula itself, is that rollback neither considers the special distribution of air pollution sources nor the meteorological conditions influencing atmospheric dispersion.

As a result of improved expertise and less restrictive time frames, a shift has taken place toward the use of diffusion models to estimate the effects of emissions and emission reductions. For fuel combustion sources, the most commonly used diffusion models are EPA's Air Quality Display Model (AQDM) and 24-hour power plant model. As its name implies, the latter is concerned with predicting short-term concentrations in the vicinity of power plants under varying meteorological conditions and terrain configurations. The AQDM is a multi-source, long-term urban dispersion model which is used to determine the impact of a wide variety of stationary source categories on annual average concentrations of SO_2 and particulate matter. Basic inputs are a comprehensive emission inventory, including both point and area sources, a joint frequency distribution of wind speed, wind direction and stability classes, and an annual average mixing height.

REGULATORY REVISIONS

The increasing sophistication of mathematical models has been in part spurred by the desire to remove some of the excessive stringency in SO_2 emission limiting regulations adopted by the states in 1972. With the energy crisis of 1973, and the low-sulfur fuels shortage, EPA responded with its Clean Fuels Policy, which sought to reserve the use of low-sulfur fuels for areas where they were needed to meet health standards. Also, the Energy Supply and Environmental Coordination Act

(ESECA) of 1974 required that state implementation plans be examined to determine if changes could be made in emission limits applicable to fuel-burning sources without jeopardizing the attainment of ambient air quality standards. Before the passage of ESECA, EPA Region IV had already received SO_2 revisions from Alabama, South Carolina, and Tennessee. These have since been approved, except for the immediate vicinity of three TVA plants.

Tennessee is currently preparing a further revision of its SO_2 limits for fuel-burning sources. EPA has just announced receipt of Florida's ESECA revision and called for public comment on it by means of a notice in the Federal Register. Kentucky has developed an ESECA SO_2 revision with the assistance of EPA Region IV. In the Kentucky revision, virtually all the power plants in the State were subjected to diffusion modeling. The resulting emission limits are contained in a five-tiered structure coupled with a county classification system. The limits are in a few cases more stringent than the old ones, but in general far less restrictive than those the State originally developed in 1972.

SUMMARY OF STATE REGULATIONS

With the help of visual aids, I would like now to give you a summary of Region IV state regulations applicable to particulate and SO_2 emissions from existing fuel combustion sources. Particulate regulations have remained essentially unchanged since their development in early 1972. Except for those of one state, all take the general form shown in Figure 1. They provide for varying degrees of emission control as a function of the heat input of a boiler or boilers. States vary in the application of this regulation, some employing the rated capacity of each individual boiler to arrive at an allowable emission limit, while others use the total heat input for all boilers at a plant or facility.

Table 1 contains a summary compilation of all the applicable Region IV particulate emission limits for existing stationary fuel combustion sources. As can be seen, the limits range from 0.8 lbs. per million BTU of heat input for small sources in Class II counties in Alabama to 0.10 lbs. per million BTU for larger sources in North Carolina, Tennessee, and Florida.

Particulate emissions from new sources are governed by the Federal New Source Performance Standards contained in 40 CFR 60.42 which contain a limit of 0.10 lbs. per million BTU.

Regarding SO_2 emissions, EPA's clean fuels policy and ESECA have caused emission limiting regulations to undergo numerous and continuing modifications. The SO_2 regulations currently federally enforceable for existing fuel combustion sources are presented in Table 2. As can be seen, many states have gone beyond the example region approach and tailored their limits to specific air quality considerations.

Table 3 presents additional SO_2 regulation changes currently under review by EPA. These proposed changes represent a further refinement and tailoring to reflect the air quality and economic needs of individual states.

New fuel combustion sources are again governed by the Federal New Source Performance Standards as contained in 40 CFR 60.43. This required compliance with SO_2 limits of 1.2 lbs. per million BTU and 0.8 lbs. per million BTU respectively for coal and oil burning facilities with heat inputs of 250 million BTUs per hour or greater.

SUMMARY

I have attempted to provide an insight into the Clean Air Act and the methods and techniques employed to establish fuel combustion limiting regulations for particulate matter and SO_2. Currently applicable particulate and SO_2 emission limiting regulations (Tables 1 and 2) were discussed along with changes (Table 3) that Region IV states are presently considering.

For more detail on the regulations which were presented today, I have appended a listing of the State Air Pollution Control Directors. I suggest that you contact them about the applicability of any regulation.

FIGURE 1

MAXIMUM ALLOWABLE PARTICULATE EMISSIONS FROM FUEL COMBUSTION SOURCES

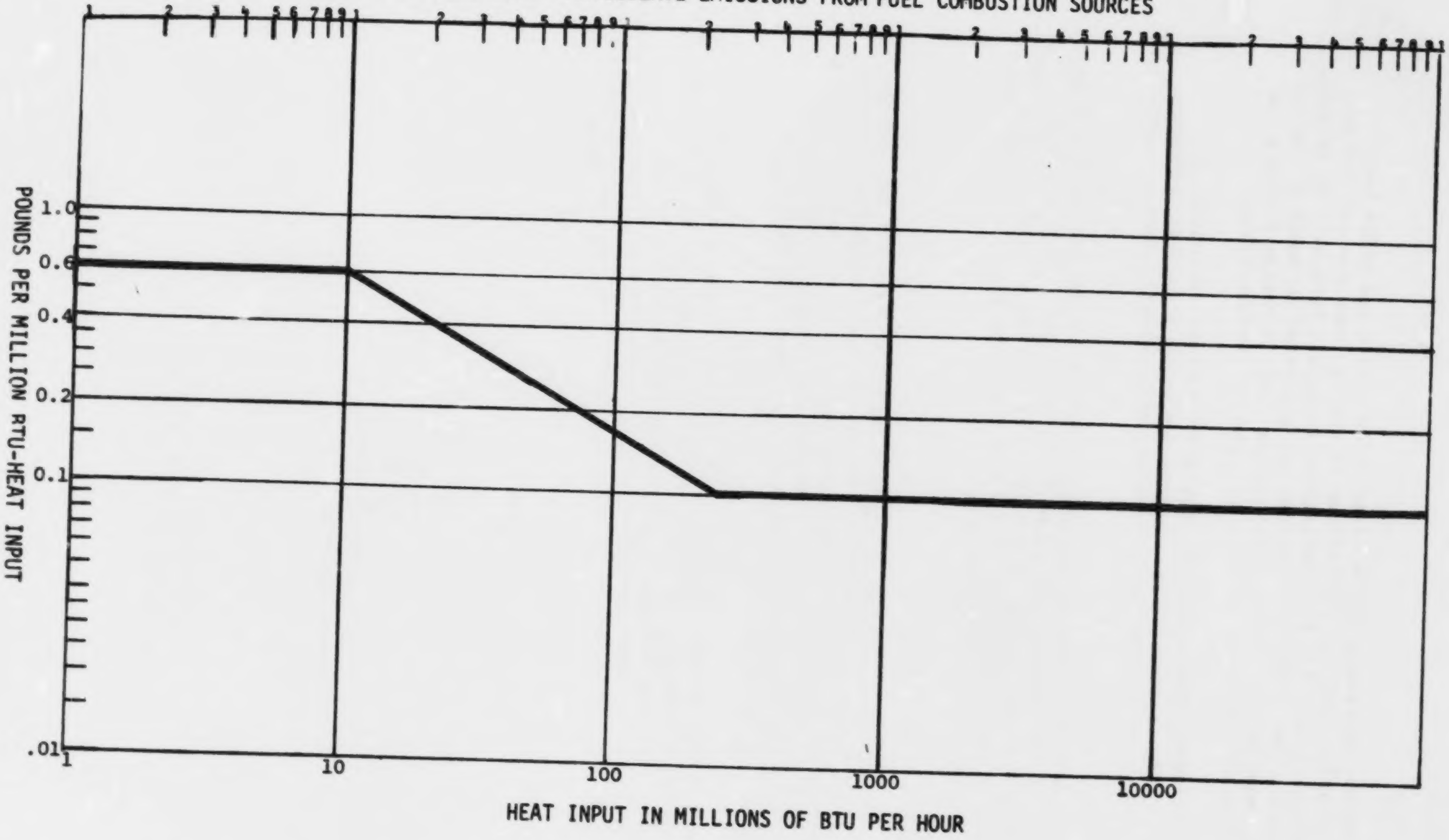

TABLE 1
APPLICABLE PARTICULATE EMISSION LIMITS
Existing Fuel Combustion Sources
(lbs particulate/MM BTU)

State \ Heat Input	<10 MM BTU/HR	10 to 250 MM BTU/HR	250 to 10,000 MM BTU/HR	>10,000 MM BTU/HR
Alabama[c]				
Class I	0.5	$E=1.38\ H^{-0.44}$	0.12	0.12
Class II	0.8	$E=3.109\ H^{-0.589}$	0.12	0.12
Florida[d]	LRACT[a]	LRACT[a]	0.10	0.10
Georgia	0.7	$E=1.1145\ H^{-0.202}$	$E=1.1145\ H^{-0.202}$[f]	0.24
Kentucky b, d				
Priority I	0.56	$E=0.9634\ H^{-0.2356}$	$E=0.9634\ H^{-0.2356}$	0.11
Priority II	0.75	$E=1.2825\ H^{-0.2330}$	$E=1.2825\ H^{-0.2330}$	0.15
Priority III	0.80	$E=1.3152\ H^{-0.2159}$	$E=1.3152\ H^{-0.2159}$	0.18
Mississippi[d]	0.6	$E=0.8803\ H^{-0.1665}$	$E=0.8803\ H^{-0.1665}$	0.19
North Carolina[d]	0.6	$E=1.0903\ H^{-0.2594}$	$E=1.0903\ H^{-0.2594}$	0.10
South Carolina[c]	0.6	0.6	Equation dependent on stack height	Equation dependent on stack height
Tennessee d, e	0.6	$E=1.0903\ H^{-0.2594}$	$E=1.0903\ H^{-0.2594}$	0.10

E = Allowable emission rate, lbs. particulate per million BTU heat input
H = Heat input in MM BTU's per hour
MM = 1×10^6

a - Latest reasonably available control technology (LRACT) as defined by the state.
b - Regulations allowed less stringent limits (old Regulation 7) for sources that installed control equipment prior to 11/27/69.
c - Heat input figured on a unit-by-unit basis.
d - Heat input is the total plant heat input.
e - Not applicable to Chattanooga, Nashville, Knoxville, and Memphis.
f - $E=1.1145\ H^{-0.202}$ up to 2,000 MM BTU per hour, then a constant limit of 0.24 # per MM BTU.

TABLE 2

APPLICABLE SULFUR DIOXIDE EMISSION LIMITS

Existing Fuel Combustion Sources

(lbs SO_2/MM BTU Unless Otherwise Indicated)

State \ Heat Input	10 MM BTU/HR		< 10 to 250 MM BTU/HR		>250 MM BTU/HR	
	COAL	OIL	COAL	OIL	COAL	OIL
Alabama						
Category I Counties	1.8	1.8	1.8	1.8	1.8	1.8
Category II Counties	4.0	4.0	4.0	4.0	4.0	4.0
Florida [a], [b]	LRACT	LRACT	LRACT	LRACT	1.5#/10^6 BTU	1.1#/10^6 BTU
Georgia [c]	2.5%S	2.5%S	2.5%S to 100 MM BTU/HR, then 3.0%S	2.5%S to 100 MM BTU/HR, then 3.0%S	3.0%S	3.0%S
Kentucky[a]						
Priority I	4.0	2.5	Sliding Scale	Sliding Scale	1.2	0.8
Priority II	4.0	2.5	Sliding Scale	Sliding Scale	2.0	Sliding Scale to 500 MM, then 1.5
Priority III	4.0	2.5	Sliding Scale	Sliding Scale	3.5	Sliding Scale to 1000 MM, then 2.0
Mississippi	4.8	4.8	4.8	4.8	4.8	4.8
North Carolina	2.3	2.3	2.3	2.3	2.3	2.3
South Carolina						
Class I Counties	3.5	3.5	2.3	2.3	2.3	2.3
Class II Counties	3.5	3.5	3.5	3.5	3.5 to 1000 MM BTU/HR then 2.3	3.5 to 1000 MM BTU/HR then 2.3
Class III Counties	3.5	3.5	3.5	3.5	3.5	3.5
Tennessee[a]						
Class I Counties	1.6	1.6	1.6	1.6	1.6	1.6
Class II Counties	3.0	3.0	3.0	3.0	3.0	3.0
Class III Counties	4.0	4.0	4.0	4.0	4.0	4.0

MM= 1 X 10^6

a - State limits changing. EPA currently reviewing the changes.

- Sources<250 MM BTU/HR must meet Latest Reasonably Available Control Technology (LRACT) as defined by state. Stack Height regulation applicable also. More restrictive of the two governs.

TABLE 3
PROPOSED CHANGES TO SULFUR DIOXIDE EMISSION LIMITS
Existing Fuel Combustion Sources
(lbs SO_2/ MM BTU)

State \ Heat Input	< 10 MM BTU/HR		10 to 250 MM BTU/HR		> 250 MM BTU/HR	
	COAL	OIL	COAL	OIL	COAL	OIL
Florida						
Hillsborough Co.	6.17	1.1	6.17	1.1	6.17[a]	1.1
Duval Co.	6.17	2.5/1.65[b]	6.17	2.5/1.65[b]	6.17	2.5/1.65[b]
All Other Counties	6.17	2.75	6.17	2.75	6.17	2.75
Kentucky						
Class I	5	3	Sliding Scale	Sliding Scale	1.2	0.8
Class II	6	4	Sliding Scale	Sliding Scale	1.8	1.2
Class III	7	4.6	Sliding Scale	Sliding Scale	3.2	2.1
Class IV	8.0	5.4	Sliding Scale	Sliding Scale	5.2	3.5
Class V	9.0	6.0	Sliding Scale	Sliding Scale	6.0	4.0
Tennessee						
Class I	1.6	1.6	1.6	1.6	1.2[c]	1.2
Class II	5.0	5.0	5.0	5.0	1.2[c]	1.2
Class III	1.6	1.6	1.6	1.6	1.6	1.6
Class IV	4.0	4.0	4.0	4.0	4.0	4.0
Class V	5.0	5.0	5.0	5.0	5.0	5.0

MM = 1 X 10^6

a - Limit of 6.17 lbs/MM BTU applies to all coal fired sources except Units 5 & 6 at Plant Gannon (limit of 2.4) and at Big Ben (limit of 6.5)

b - 2.5 lbs/MM BTU for sources south of Hecksher Drive., and 1.65 lbs/MM BTU for all other sources.

c - Limit begins at 1000 MM BTU/HR Heat Input, below this lesser limit applies.

APPENDIX

REGION IV STATE AIR POLLUTION CONTROL DIRECTORS

Mr. James W. Cooper, Director
Division of Air Pollution Control
State of Alabama Department of Public Health
645 S. McDonough Street
Montgomery, Alabama 36104

Mr. Joseph W. Landers, Jr., Secretary
Florida Department of Environmental Regulations
2562 Executive Center Circle East
Tallahassee, Florida 32301

Mr. Robert H. Collom, Jr., Chief
Air Protection Branch
Environmental Protection Division
Georgia Department of Natural Resources
270 Washington Street
Atlanta, Georgia 30334

Mr. John T. Smither, Director
Division of Air Pollution
Kentucky Department for Natural Resources
and Environmental Protection
West Frankfort Office Complex
US 127 South
Frankfort, Kentucky 40601

Mr. Jerry M. Stubberfield, Chief
Division of Air Pollution Control
Mississippi Air & Water Pollution Control Commission
P.O. Box 827
Jackson, Mississippi 39205

Mr. J. A. McColman, Chief
Air Quality Section
Division of Environmental Management
North Carolina Department of Natural & Economic Resources
P.O. Box 27687
Raleigh, North Carolina 27611

Mr. William G. Crosby, Director
Bureau of Air Quality Control
Department of Health and Environmental Control
2600 Bull Street
Columbia, South Carolina 29201

Mr. Harold Hodges, Director
Division of Air Pollution Control
Tennessee Department of Public Health
256 Capitol Hill Building
Nashville, Tennessee 37219

COMMON METRIC CONVERSION FACTORS

1#/10^6 BTU = 1.8g/10^6 Calories

BTU X 0.252 = Kilogram - Calorie

THE PAST, PRESENT AND FUTURE OF STATE AIR POLLUTION REGULATIONS FOR COMBUSTION SOURCES

By:

Robert H. Collom, Jr.

Air Protection Branch
Georgia Department of Natural Resources
Atlanta, Georgia

Preceding page blank

As has already been discussed by EPA representatives, the 1970 amendments to the Clean Air Act required a good deal of short-term and specific action from the federal, state and local governments. The end result of all this hurried activity was the State Implementation Plans which, at a minimum, had to be adequate to attain and maintain national ambient air quality standards for the six criteria pollutants. Almost all States felt it feasible to meet the primary and secondary air quality levels at the same time (July 1975).

To achieve the ambient sulfur dioxide standards many States elected to utilize sulfur limitations in fuel as their emission regulation of choice. Others adopted the approach of specifying an allowable sulfur emission in pounds per hour or pounds per million BTU's from a fuel-burning boiler. There was almost no attention given to sulfur dioxide emissions from any sources other than fuel burning.

Due to the fuels crisis and the economic crunch we are now facing, EPA has deemed it necessary to suggest to the States that if possible, they relax their emission standards and tailor them more specifically to those limits actually needed to achieve national sulfur dioxide ambient standards. The Energy Supply and Environmental Coordination Act of 1974 required that EPA review all State Implementation Plans with this goal in mind.

Control of particulate matter from fuel-burning sources was more uniformly approached, and based on proven control systems such as electrostatic precipitators. Technical understanding in this area was much more available to the sources, and the particulate regulations have been more readily complied with throughout the country.

During the development of the Georgia Implementation Plan it was determined that the State's air quality levels for sulfur dioxide were generally much better than the national standards required. This coupled with a need for a margin of safety and a desire to maintain good air quality brought about adoption of a State ambient regulation lower than the national standard. It was determined through computer modelling of two "example regions" in the State that the use of readily available 2.5 or 3.0 percent sulfur in fuel (depending on boiler size), coupled with minimum stack height requirements, that the State ambient standard could be achieved. This has been proven out by subsequent ambient air sampling throughout the State.

Since the State plans were submitted to EPA and approved by them in early 1972, a number of significant developments have transpired. Most significant of these are the fuels crisis, the supreme court decision (or lack thereof) in relation to significant deterioration, and a suit brought by NRDC against EPA for having approved certain portions of the Georgia Plan (specifically those utilizing stack height and dispersion).

In February of 1974 the Fifth Circuit of Appeals made a partial ruling on the case involving use of stack heights. It was made clear that dispersion techniques are not allowed under the Clean Air Act as a means to achieve national ambient air standards. Emission reducing regulations are the only acceptable means of meeting the national standards. However, stack heights or any other techniques are acceptable to achieve a better air quality than national air standards re quire. A final decision is pending from the Fifth Circuit concerning this point. Computer modelling has shown that the emission limiting regulations of the Georgia Plan are adequate by themselves to meet national standards. Therefore, it should be permissible for the State to use dispersion techniques to achieve the State ambient air standards.

At the present time there is no legally or nationally uniform policy as to acceptable stack heights. It is necessary that a technically and legally acceptable approach to stack heights be developed as soon as possible since the States and EPA are now facing the need to project into the future, through the use of modelling, to determine any necessary amendments to regulations needed to attain and maintain air standards. Not necessarily accepting the need for it, the requirement to not exceed a specified air quality increment for non-significant deterioration purposes, will be next to impossible unless acceptable stack heights are established.

A newly-resurrected concern has appeared on the scene, namely that of suspended sulphates and their effects upon human health and vegetation. The various reports and publications in this area tend to agree that suspended sulphates can produce such effects, but there is a total lack of agreement on the levels of concern and the sources and/or mechanisms of formation of the sulphates themselves. A more thorough understanding and grasp of these issues is necessary before any definitive action of a significant nature is initiated.

It is likely that a future area of concern which will require additional knowledge is that of the potential harmful effects from oxides of nitrogen from fuel combustion. There have been some suggestions about cancerous properties of nitrogen dioxide in the atmosphere. Our knowledge about photochemical oxidant formation and the role which oxides of nitrogen play does not appear to be as well defined as we once thought. I notice that the agenda for this seminar includes many technical papers on formation of oxides of nitrogen and their propagation and control in a boiler. Hopefully, the attention being addressed to this matter will provide industry and government experts with enough technical understanding to take logical control action, if needed at a future time. We have too many times in the past had to act to meet legal deadlines on very complicated problems, with only a limited amount of knowledge.

Thus far I think it is reasonable to say that the preparation of State Implementation Plans and enforcement of emission regulations has generally produced the hoped for results indicated in the Clean Air Act. However, it would be imprudent not to take into account for future actions and legislation the knowledge which we have gained over the recent past. I would hope that the emotional basis for action, the so-called "Chicken Little" approach, is behind us. The air quality improvements which present programs have produced should allow us to take more deliberate and knowledgeable action in the future in dealing with more refined air pollution issues.

Statement by H. W. Poston, Commissioner
Chicago Department of Environmental Control
before the EPA Combustion Symposium
September 24, 1975, Atlanta, Georgia

MEETING AND MAINTAINING ENVIRONMENTAL STANDARDS THROUGH PRODUCT CONTROL

When in the late '60's we became aware of the status of our environment, we sought the advice of engineers and chemists. This was natural enough. They were the ones who had designed the automobiles, steel mills, furnaces and boilers, air conditioners and phosphate detergents - - all the symbols of an affluent society. Our task was to reverse a situation that, if not restrained, could destroy the very progress these things had brought about. A balance was clearly needed which continued to encourage growth and at the same time encouraged conservation and preservation. It was not feasible in the beginning of our endeavor to merely close all sources of emissions and build "clean" facilities. So we hired engineers to design controls for every conceivable emission their products had created. This pattern of attacking the problem still prevails for the most part. The majority of beverage containers used continue to be throw away bottles and aluminum cans; the internal combustion engine remains our predominant form of transportation. Recycling centers and catalytic converters were developed to cure the problems. The problems remained largely unsolved.

Obviously new approaches were needed to solve age old problems. Environmental standards had to be attained and maintained. Controls had to be implemented but in a manner that would not require costly installations, additional bond issues and increased taxes to our citizens. The controls had to be placed on the products that were causing the environmental assault.

The experiences of the Chicago Department of Environmental Control can well serve as an example of product control to attain standards. When, in 1970, the Clean Air Act mandated air quality standards for certain pollutants, the sulfur dioxide levels in the city were greater than .03 parts per million (the 1975 federal annual average to be achieved for that pollutant) at almost half of the department's monitoring sites. A survey taken by the department determined that the major source of coal burning came from older apartment buildings in residential areas. The Chicago City Council enacted an ordinance in 1970, which limited the sulfur content of fuels to one per cent, for all processes, by 1972. In addition to the use of low sulfur coal, owners switched to low sulfur fuel oil and applied for natural gas hookups. Negotiations between the Department of Environmental Control and Peoples Gas Company produced an agreement whereby residential users were given first priority as more gas became available. Industrial emitters were required to employ control devices in addition to the use of low sulfur fuels and the largest cumulative source of sulfur dioxide emitters was eliminated. The result was dramatic. By the end of 1973, every monitoring site had an annual arithmetic mean of .03 parts per million or below and only two of the 23 sites had an annual average above .022 - - the secondary standard. In 1974, progress continued and only one monitoring site exceeded .022 parts per million.

It might seem as if all this were accomplished without a hitch. But shortly after the ordinance for low sulfur fuel took effect in 1970, an organization representing some 45 coal dealers filed an appeal for a variance from the limitations of the ordinance. In its appeal for a variance, the association claimed, among other things, that solid fuel containing less than two per cent sulfur by weight was very difficult to obtain in any quantity in the City of Chicago. The association listed such factors as railroad car shortages, foreign shipments, union problems, the demand for low sulfur fuels by utility companies, the reluctance of mine owners to open new mines and the threat of conversions of coal burning equipment to competing fuels.

While some of the factors may have been valid, the department brought in expert testimony to state that low sulfur coal was indeed available for Chicago and that adequate railroad facilities were available to transport low sulfur fuel from the west to Chicago.

The corporation counsel for the city filed a motion with the Appeal Board to dismiss the association's petition for a variance on the grounds that the Appeal Board had jurisdiction only to grant "individual variances." The petition as submitted by the Chicago Coal Merchants Association did not enumerate any individual petitioner or coal dealer a party to the proceeding.

Other interested parties, including the Attorney General of the State of Illinois and the Environmental Law Society of the University of Chicago, also filed motions to dismiss the petition by the association.

The association itself filed a motion to withdraw its petition. Its motion to dismiss was based on the ground that the "... Appeal Board did not have jurisdiction to entertain its said petition because petitioner and its members are not individual users, owners or operators of coal burning equipment in the City of Chicago, but are suppliers to those individuals . . ."

On October 28, 1970 the Appeal Board ordered that the motion be allowed and the petition was withdrawn.

Subsequent to this action, no individual company sought a variance before the Appeal Board and the availability of low sulfur fuel did not pose a problem for the '70 - '71 heating season nor in the years that followed.

Control at the source has been successful in another of the department's concerns with the pollution of our waterways. At its treatment plants the Metropolitan Sanitary District removes 90 per cent of the effluent pollution. The district serves the metropolitan Chicago area and would have to spend over $27 million each year to remove excess phosphorus and to reduce the biochemical oxygen demand (BOD) and suspended solids to acceptable levels. In October of 1970, the Chicago City Council passed an ordinance limiting the amount of phosphates in household laundry detergents to 8.7 per cent by February 1971 and after June 1972 the phosphorus content was reduced to zero or trace amounts of phosphorus.

The reduction to 8.7 per cent had marked results. At one plant the Metropolitan Sanitary District recorded phosphorus concentrations of its effluent ranging from 1.6 to 3.5 milligrams per liter in 1971. For the period of July through December 1972, the average effluent was .65 milligrams per liter. Therefore, without additional treatment the facility was in compliance with the State of Illinois water quality standard for phosphate concentrations.

Not only was this standard met, but additional benefits were realized when BOD levels dropped to less than 10 milligrams per liter and suspended solids to less than 12 milligrams per liter and at a savings in excess of $27 million.

Once again, the ordinance did not go unchallenged.

The constitutionality of the ordinance was challenged in the federal district court on the grounds it imposed an impermissible burden on interstate commerce. On March 6, 1973, the court ruled ". . . the entire ordinance, including the labeling and enforcement provisions, is of no effect."

The local U.S. Court of Appeals upheld the city's ordinance classifying it as ". . . a slight burden on interstate commerce" on January 15, 1975.

Following this reversal, Procter & Gamble and the FMC Corporation petitioned the U.S. Supreme Court to review the earlier court proceedings. This court's refusal in effect upheld the city ordinance.

Penalties range from $100 to $300 for the first violation and from $300 to $500 for additional offenses within a six-month period.

Enforcement of Chicago's phosphate ban in household laundry detergents was resumed in Chicago stores on August 19. The enforcement action came 90 days after the U.S. Supreme Court refused to hear an appeal of a lower court ruling which upheld the city law.

Zero phosphate limitations apply to household cleaning compounds except those used in automatic dishwashers. Other cleaning products exempted until December 31, 1975 include food processing and dairy equipment cleansers; phosphoric acid products such as sanitizers, acid cleaners and metal conditioners; and laundry detergents used exclusively by the food and dairy industries and institutional health care facilities.

These exemptions are similar to those granted by other jurisdictions in the country with phosphate controls on cleaning products. During the grace period, department engineers will assess the technological developments by industry in developing phosphate substitutes for these products.

Product control such as this eliminates the need for tertiary treatment, eliminates the problem at the source and saves the citizen tax dollars.

Suspended particulate levels were also above the ambient air quality standard of 75 micrograms per cubic meter. We attacked this situation in much the same way as sulfur dioxide. An ordinance enacted in 1970 prohibited burning refuse in boilers and leaf burning. Single chamber incinerators were prohibited in 1971 which encouraged the use of compactors. Industrial pollution control programs were made mandatory for all major emitters. Our results have been substantial. In 1971, only 10 per cent of the land area of Chicago had a concentration below 75 micrograms per cubic meter. By May of this year, 51 per cent of the land area met the standard. Likewise, concentrations were reduced substantially in areas not presently meeting the standard. Forty-one per cent of the land area had concentrations over 100 micrograms per cubic meter in 1971. Today this has been reduced to five per cent.

In the area of noise pollution, the city's ordinance prohibits the sale of motor vehicles which emit excessive noise. The determination of noise is made by acoustical instruments. It is the manufacturer's obligation to certify that vehicles sold in the city meet specific standards. Because motor vehicles constitute the major urban noise source, the ordinance attempts to solve noise problems at the source without building costly sound barriers or tunnels to mask the source of noise. Beginning in 1980, no motor vehicle emitting more than 75 dB(A) as it comes off the assembly line can be sold in the city of Chicago.

Thus, by product control which controls pollution at the source, the city has been successful in meeting standards that a decade ago seemed impossible to attain.

SUSPENDED PARTICULATE

CITY - WIDE YEARLY RUNNING GEOMETRIC MEAN

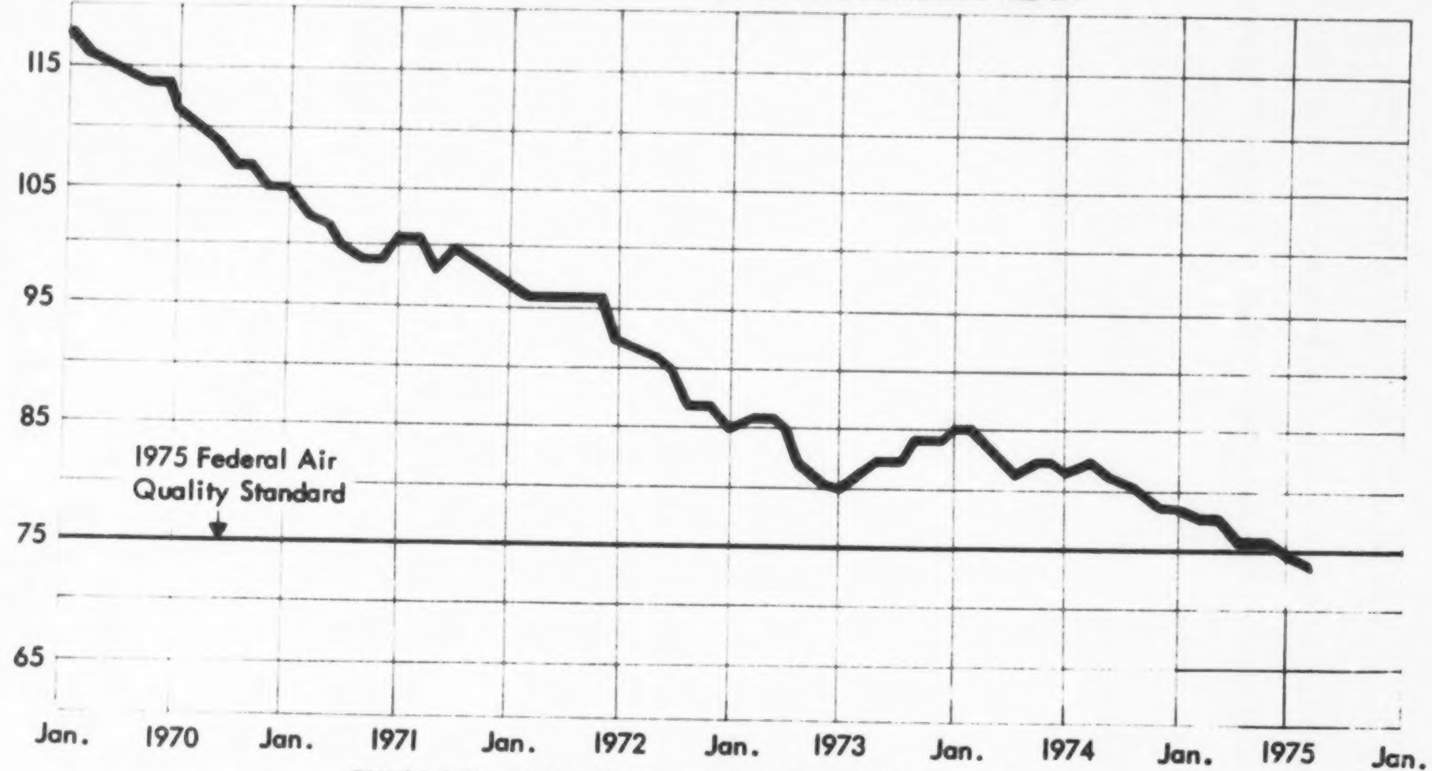

CHICAGO DEPARTMENT OF ENVIRONMENTAL CONTROL

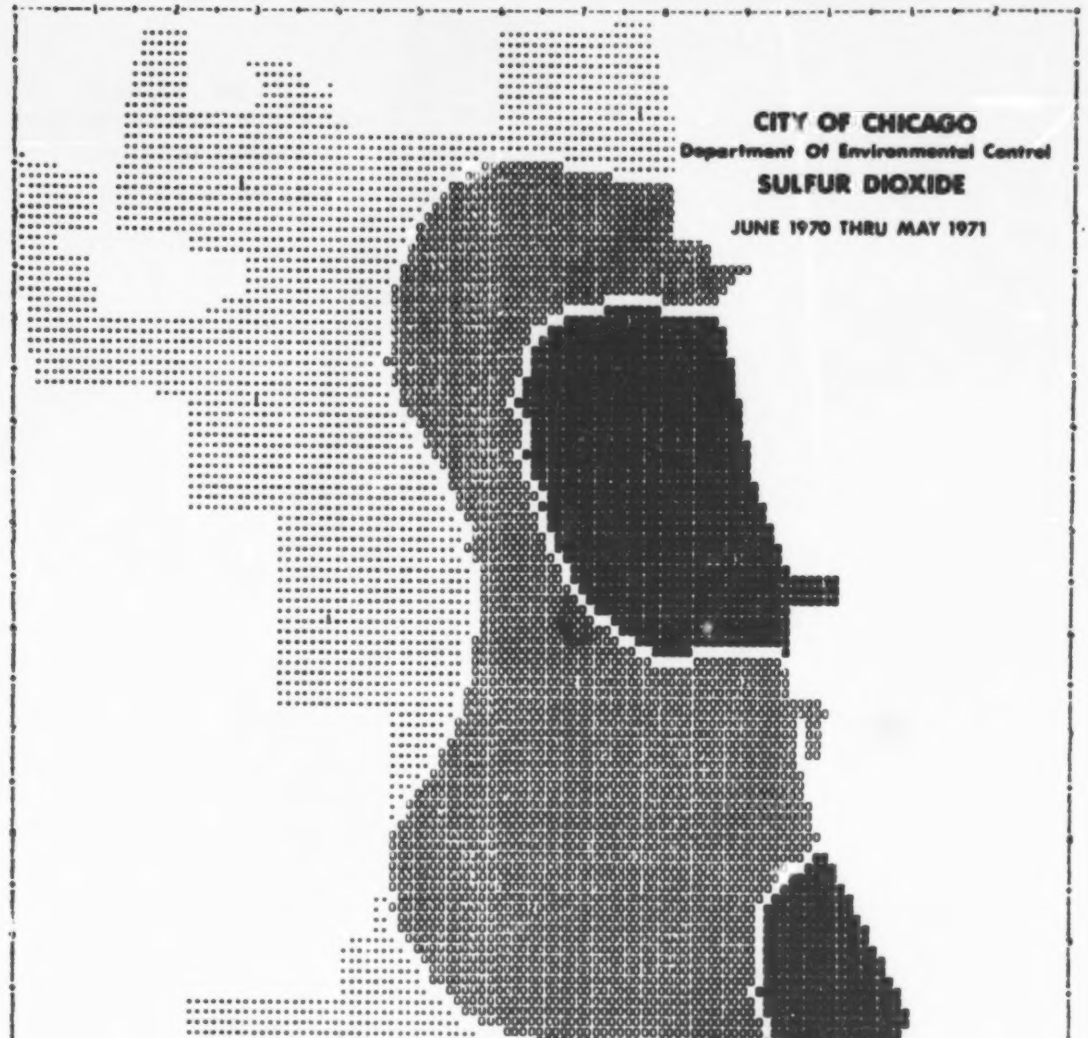
CITY OF CHICAGO
Department Of Environmental Control
SULFUR DIOXIDE
JUNE 1970 THRU MAY 1971
CODE:
In Parts Per Million
Percent Of Land Area For Each Level
.022 AND UNDER
.023 TO .030
OVER .030
71%
22%
7%
FEDERAL AIR QUALITY STANDARD - .030

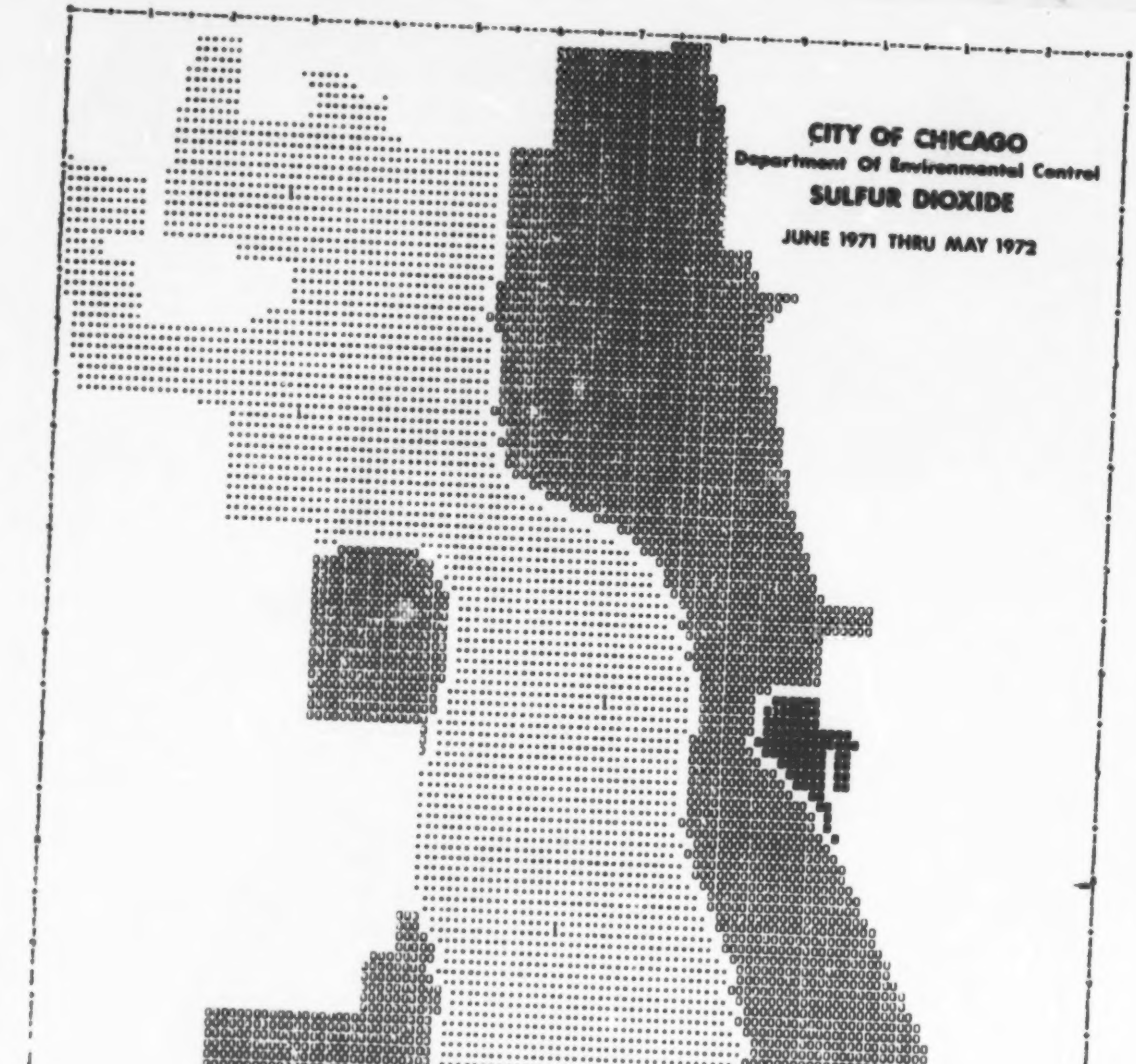

CITY OF CHICAGO
Department Of Environmental Control
SULFUR DIOXIDE
JUNE 1971 THRU MAY 1972

CODE:
In Parts Per Million
Percent Of Land Area For Each Level
.022 AND UNDER
78%
.022 TO .030
21%
OVER .030
1%
FEDERAL AIR QUALITY STANDARD - .030

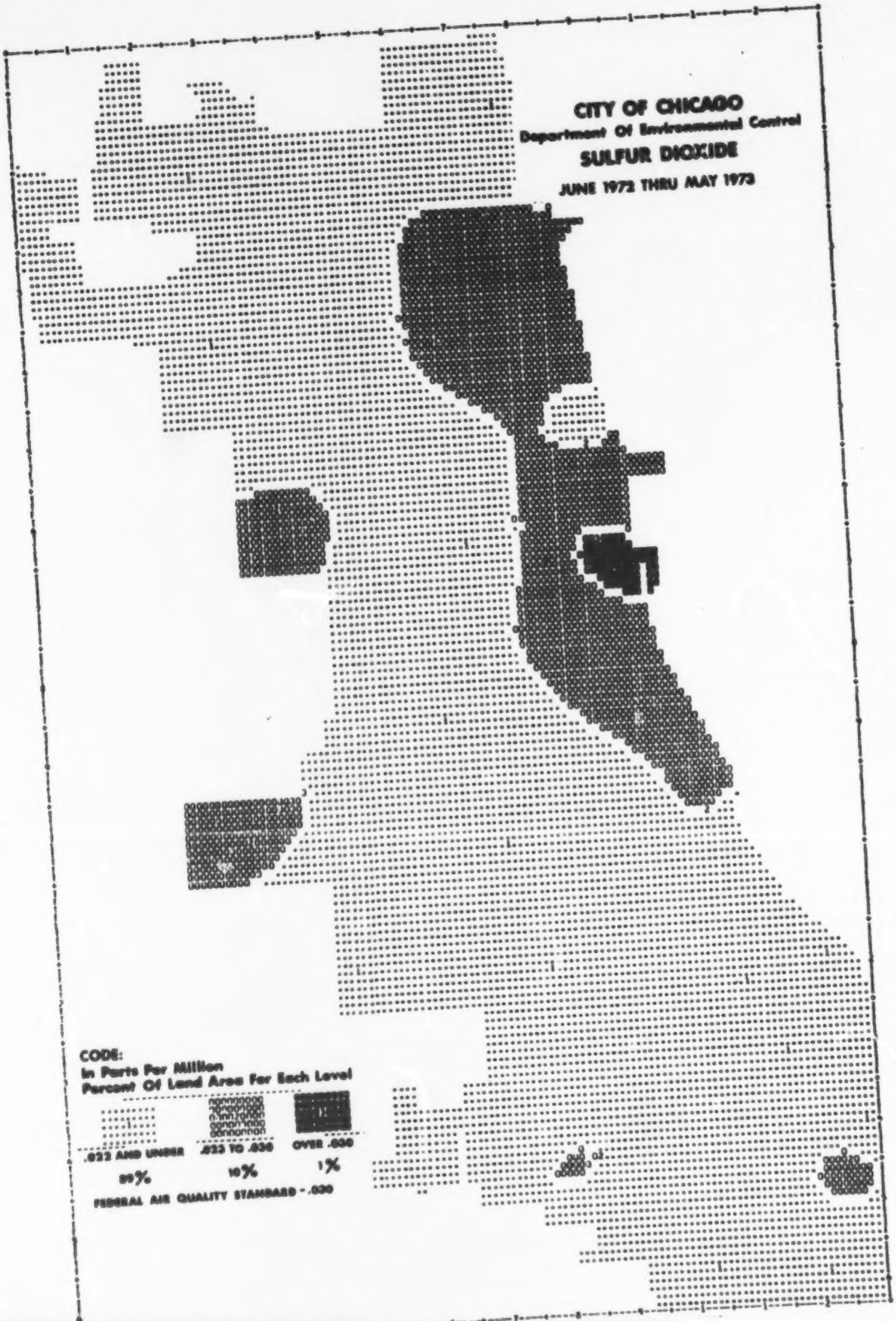
CITY OF CHICAGO
Department Of Environmental Control
SULFUR DIOXIDE
JUNE 1972 THRU MAY 1973
CODE:
In Parts Per Million
Percent Of Land Area For Each Level
.022 AND UNDER
.022 TO .030
OVER .030
89%
10%
1%
FEDERAL AIR QUALITY STANDARD - .030

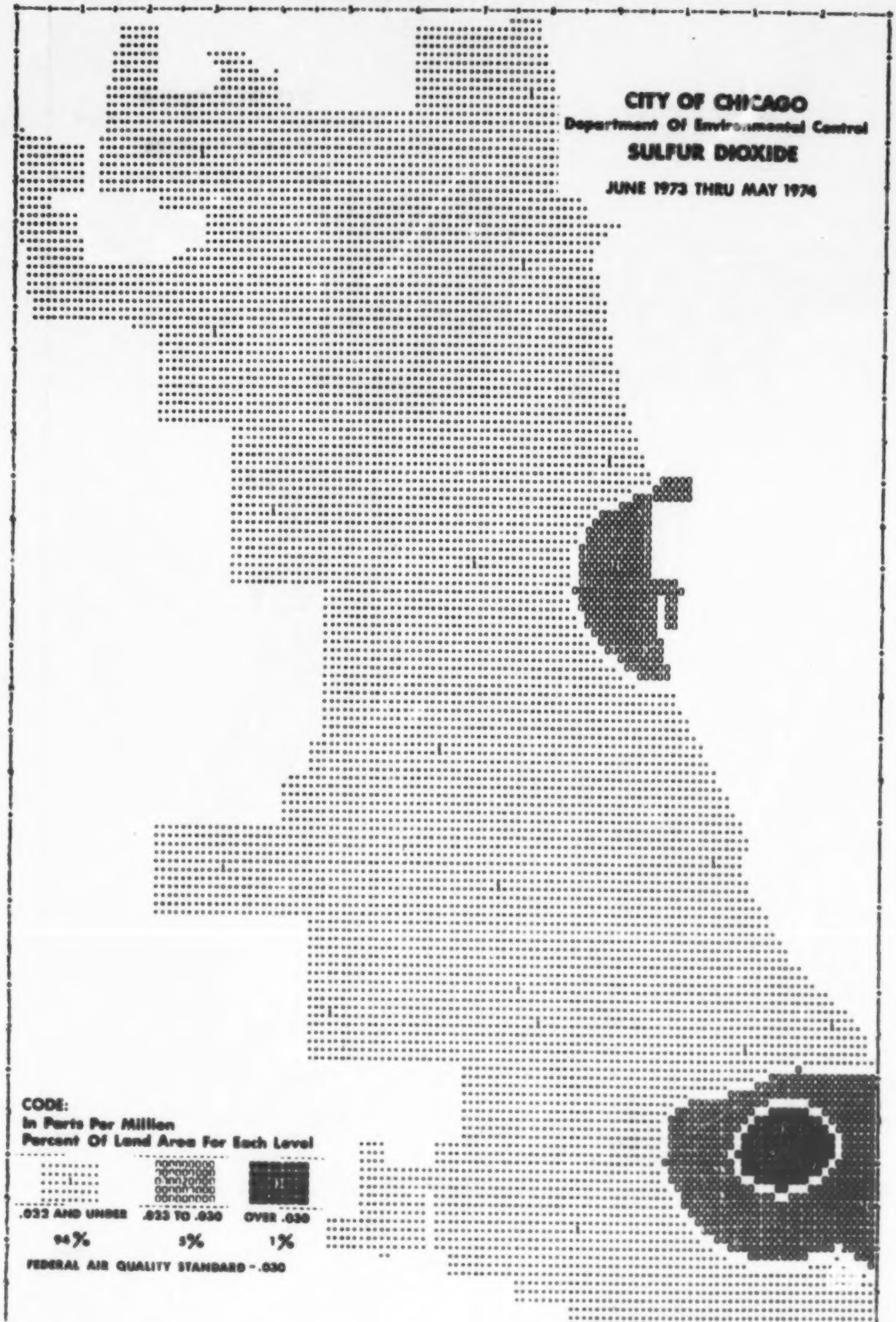

CITY OF CHICAGO
Department Of Environmental Control
SULFUR DIOXIDE
JUNE 1973 THRU MAY 1974

CODE:
In Parts Per Million
Percent Of Land Area For Each Level
.022 AND UNDER
94%
.023 TO .030
5%
OVER .030
1%
FEDERAL AIR QUALITY STANDARD - .030
SYMAP

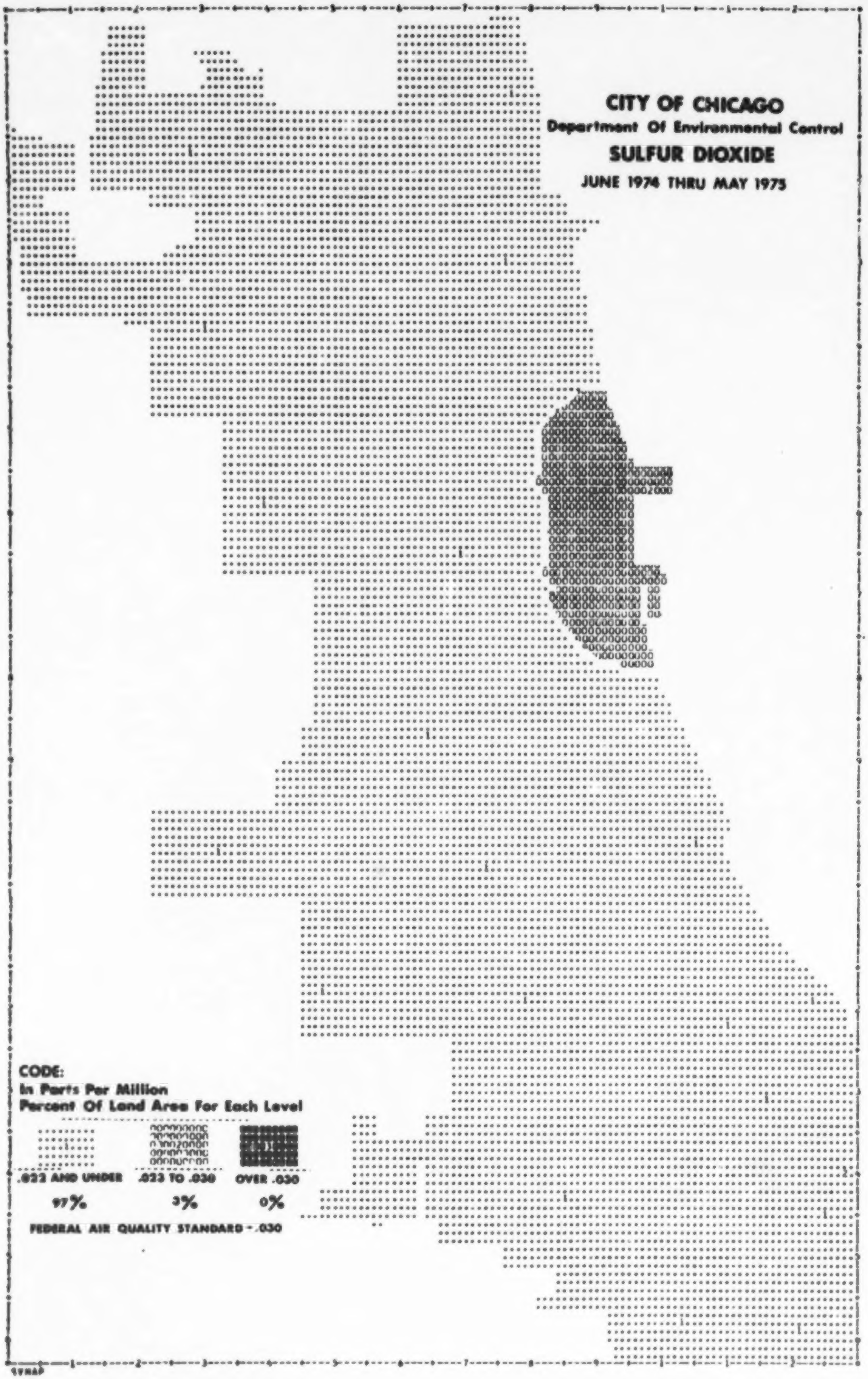

CITY OF CHICAGO
Department Of Environmental Control
SULFUR DIOXIDE
JUNE 1974 THRU MAY 1975

CODE:
In Parts Per Million
Percent Of Land Area For Each Level

.022 AND UNDER	.023 TO .030	OVER .030
97%	3%	0%

FEDERAL AIR QUALITY STANDARD - .030

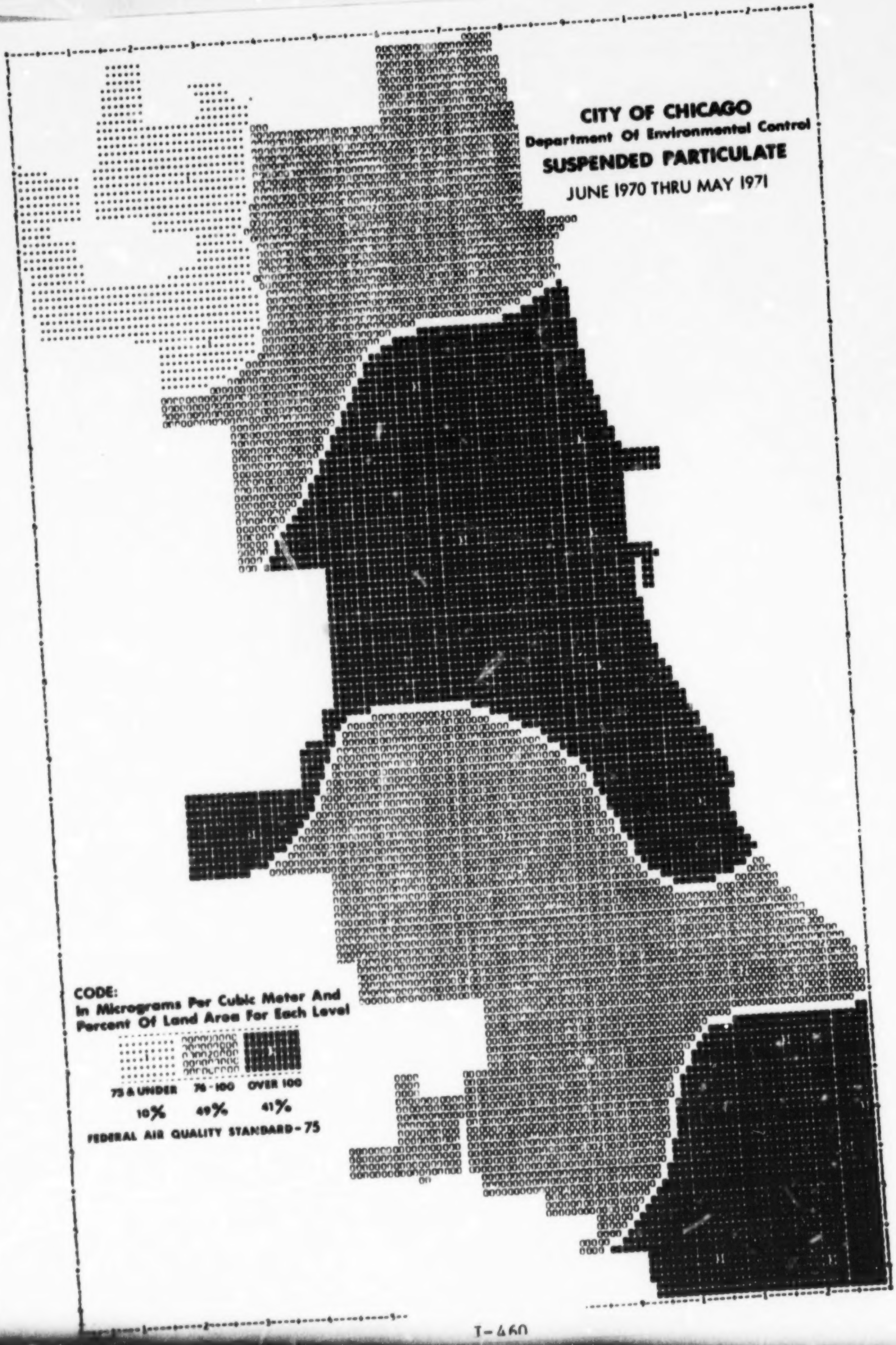

CITY OF CHICAGO
Department Of Environmental Control
SUSPENDED PARTICULATE
JUNE 1970 THRU MAY 1971

CODE:
In Micrograms Per Cubic Meter And Percent Of Land Area For Each Level
75 & UNDER
76 - 100
OVER 100
10%
49%
41%
FEDERAL AIR QUALITY STANDARD - 75

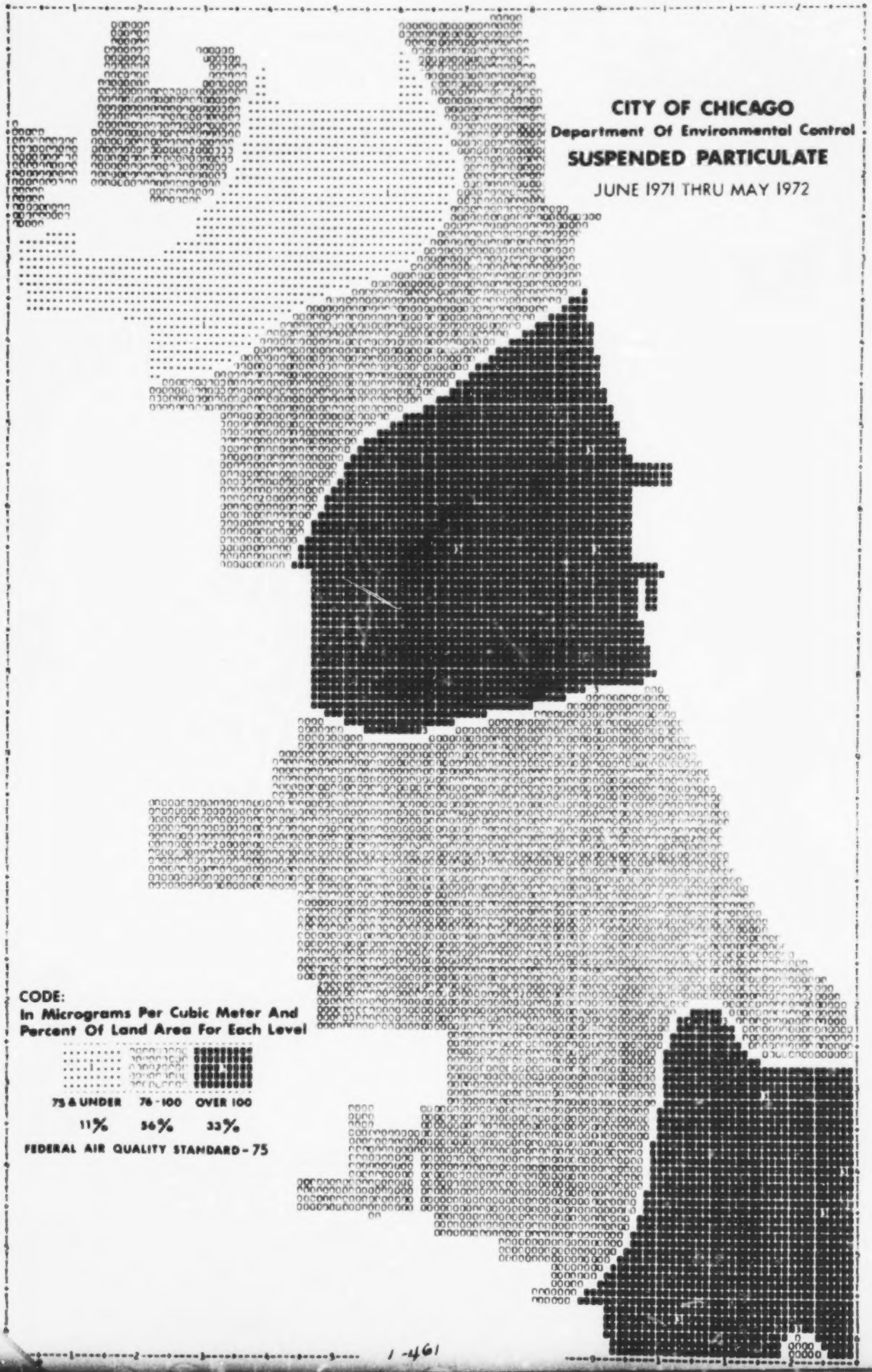

CITY OF CHICAGO

Department Of Environmental Control

SUSPENDED PARTICULATE

JUNE 1971 THRU MAY 1972

CODE:
In Micrograms Per Cubic Meter And Percent Of Land Area For Each Level

·	○	●
75 & UNDER	76 - 100	OVER 100
11%	56%	33%

FEDERAL AIR QUALITY STANDARD - 75

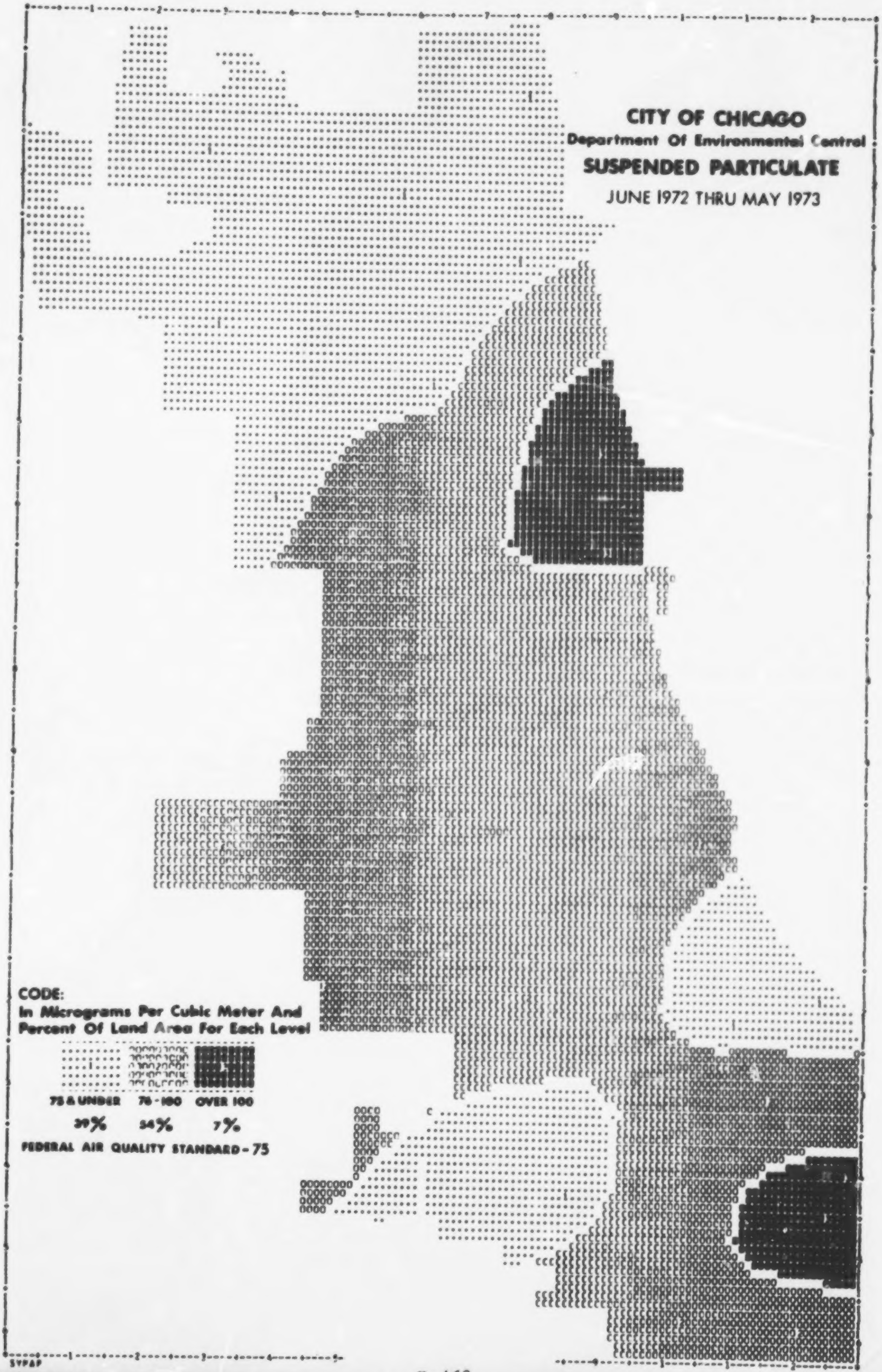

CITY OF CHICAGO

Department Of Environmental Control

SUSPENDED PARTICULATE

JUNE 1972 THRU MAY 1973

CODE:
In Micrograms Per Cubic Meter And Percent Of Land Area For Each Level

75 & UNDER	76 - 100	OVER 100
39%	54%	7%

FEDERAL AIR QUALITY STANDARD - 75

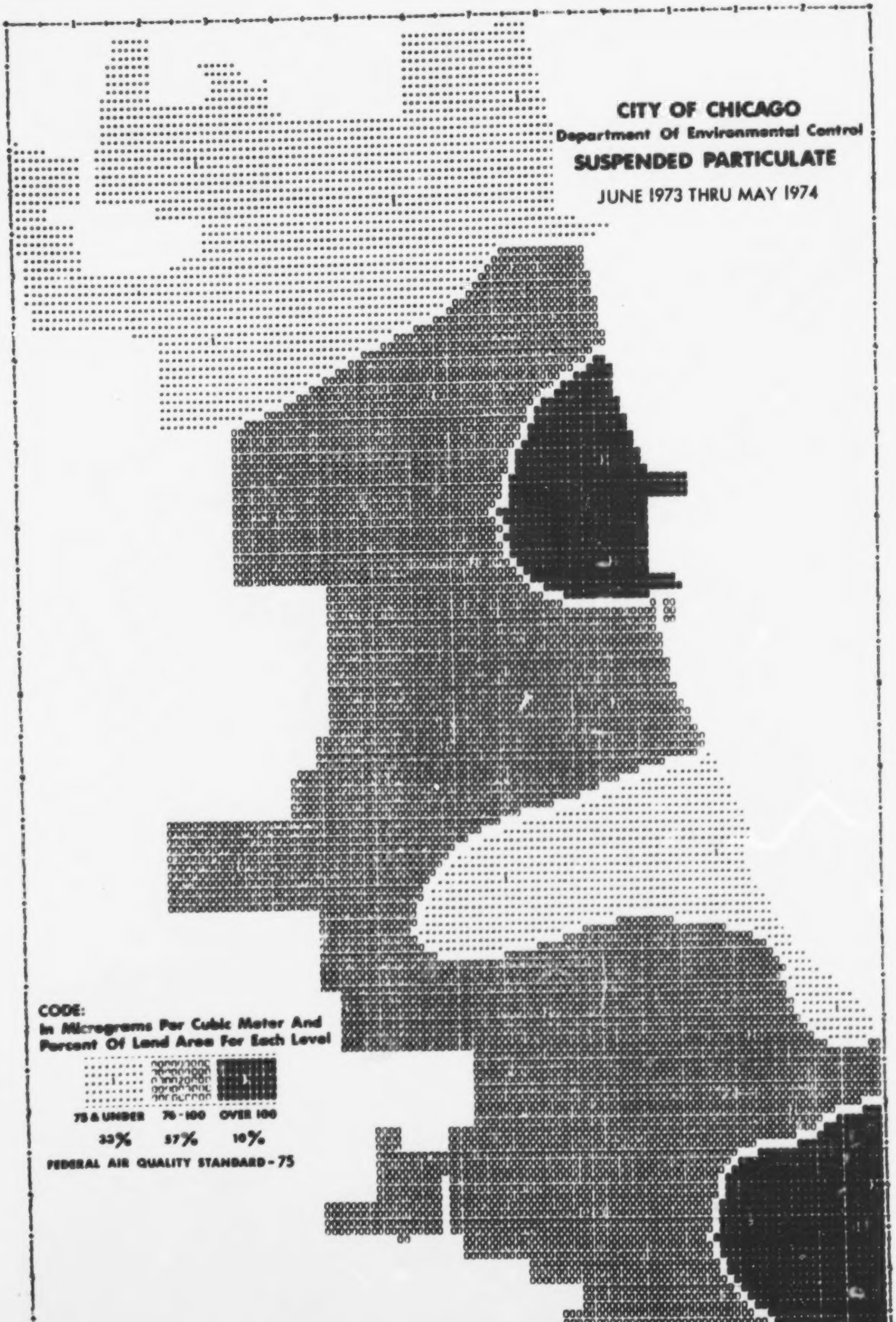

CITY OF CHICAGO
Department Of Environmental Control
SUSPENDED PARTICULATE
JUNE 1973 THRU MAY 1974

CODE:
In Micrograms Per Cubic Meter And Percent Of Land Area For Each Level
75 & UNDER
76 - 100
OVER 100
33%
57%
10%
FEDERAL AIR QUALITY STANDARD - 75

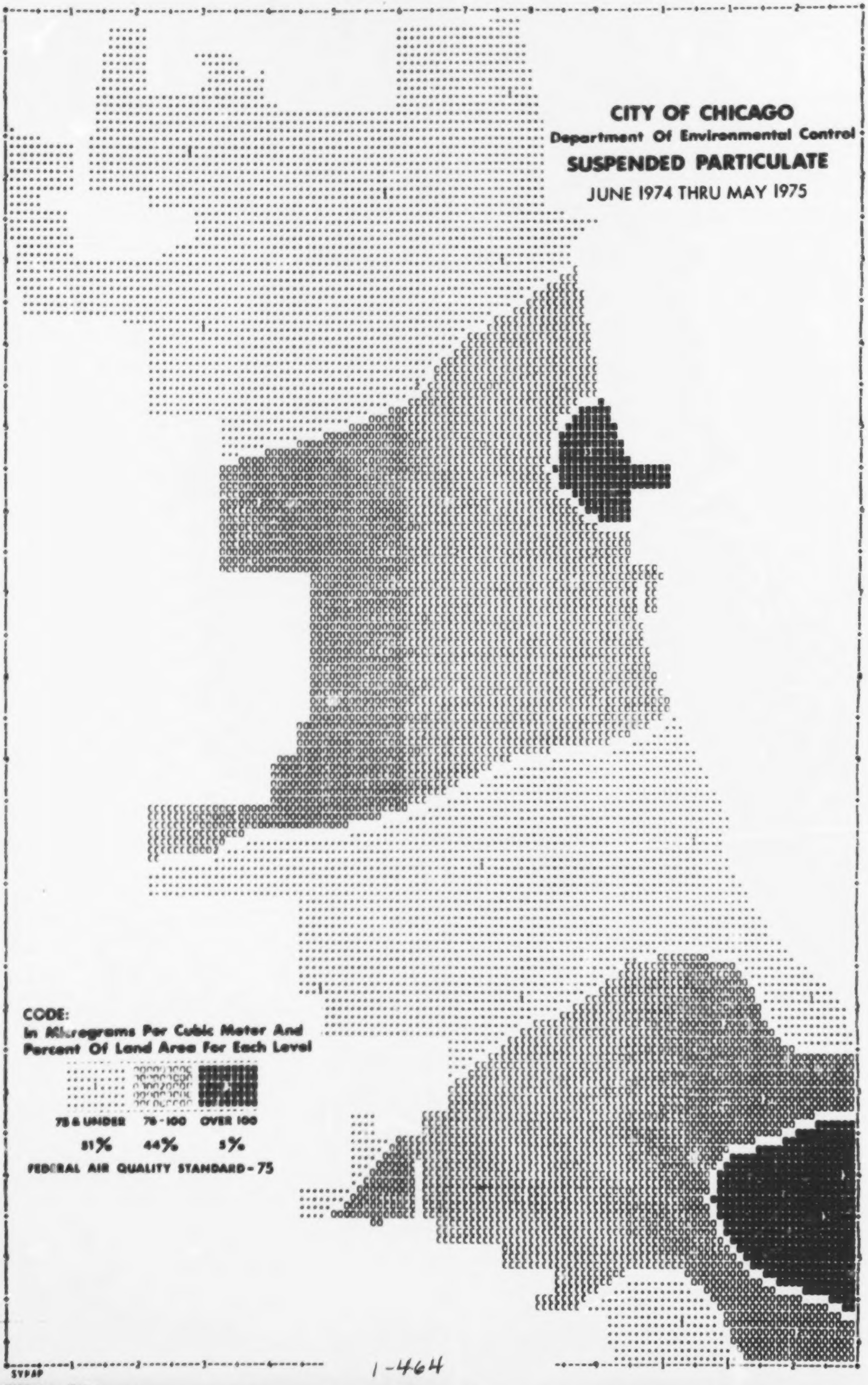

CITY OF CHICAGO
Department Of Environmental Control
SUSPENDED PARTICULATE
JUNE 1974 THRU MAY 1975

CODE:
In Micrograms Per Cubic Meter And Percent Of Land Area For Each Level

⠿	▨	■
75 & UNDER	76 - 100	OVER 100
51%	44%	5%

FEDERAL AIR QUALITY STANDARD - 75

SPEAKER LIST

(NOTE: To facilitate their identification, speakers are listed alphabetically together with the name of the organization they represent. The complete address of each organization represented at the conference appears at the end of the list of attendees.)

LIST OF SPEAKERS

Name	Representing
Axworthy, Dr. Arthur E.	Rockwell International, Rocketdyne Division
Bittner, James D.	Massachusetts Institute of Technology
Bowen, Dr. Joshua A.	EPA, IERL, Combustion Research Branch
Bowman, Dr. Craig T.	United Technology Research Center
Brown, Richard A.	Acurex, Aerotherm Division
Burchard, Dr. John K.	EPA, IERL
Cato, Glenn A.	KVB, Inc.
Collom, Jr., Robert H.	State of Georgia, Department of Natural Resources
Combs, L. Paul	Rockwell International, Rocketdyne Division
Crawford, Allen R.	Exxon Research and Engineering
Cuffe, Stanley T.	EPA, Office of Air Quality Planning and Standards
Dykema, Owen W.	The Aerospace Corporation
England, Dr. Christopher	Jet Propulsion Laboratory
Engleman, Dr. Victor S.	Exxon Research and Engineering
Giammar, Robert P.	Battelle-Columbus Laboratories
Hall, Robert E.	EPA, IERL, Combustion Research Branch
Heap, Dr. Michael P.	Ultrasystems
Helms, G. Thomas	EPA, Region IV, Air and Hazardous Materials Division
Hollinden, Dr. Gerald A.	Tennessee Valley Authority
Kason, T.T.	City of Chicago, Department of Environmental Control
Kendall, Dr. Robert M	Acurex, Aerotherm Division
Kesselring, Dr. John P.	Acurex, Aerotherm Division
Ketels, Peter	Institute of Gas Technology
Lachapelle, David G.	EPA, IERL, Combustion Research Branch
Lanier, W. Steven	EPA, IERL, Combustion Research Branch
McDonald, Henry	United Technology Research Center
Maloney, Dr. Kenneth L.	KVB, Inc.
Manny, Erwin H.	Exxon Research and Engineering
Martin, G. Blair	EPA, IERL, Combustion Research Branch
Muzio, Dr. Lawrence J.	KVB, Inc.
Pohl, John H.	Massachusetts Institute of Technology
Poston, H. Wallace	City of Chicago, Department of Environmental Control
Princiotta, Frank	EPA, Energy Processes Division
Rosenberg, Dr. Robert B.	Institute of Gas Technology
Sarofim, Dr. Adel F.	Massachusetts Institute of Technology
Selker, Ambrose P.	Combustion Engineering
Shaw, Dr. Robert	Stanford Research Institute
Shoffstall, Dr. Donald R.	Institute of Gas Technology
Tyson, Dr. Thomas J.	Ultrasystems
Wasser, John H.	EPA, IERL, Combustion Research Branch
Wendt, Dr. Jost O.L.	University of Arizona

PARTICIPANTS LIST

(NOTE: To facilitate their identification, participants are listed alphabetically together with the name of the organization they represent. The complete address of each organization represented at the conference appears at the end of the list of attendees.)

LIST OF PARTICIPANTS

Name	Representing
Alvey, Courtney D.	Baltimore Gas & Electric
Anderson, Dr. Larry W.	Acurex, Aerotherm Division
Axtman, William H.	American Boiler Manufacturers Association
Bagwell, Fred A.	South California Edison
Baker, Burke	Shell Development Company
Ban, Stephen D.	Battelle-Columbus Laboratories
Barrett, Richard E.	Battelle-Columbus Laboratories
Barsin, Joseph	Babcock & Wilcox
Bartok, William	Exxon Research & Engineering
Batra, Sushil K.	New England Electric Systems
Bauman, Robert D.	EPA, Office of Air Quality, Planning & Standards
Beals, Rixford A.	NOFI
Beatty, James D.	Procter & Gamble
Bennett, Dr. Robert	Apollo Chemical
Blandford, Jr., J.B.	Englehard Industries
Blythe, R. Allen	International Boiler Works
Buechler, Lester	Systems Research Labs
Bonne, Ulrich	Honeywell
Booth, Michael R.	Ontario Hydro
Bowman, Barry R.	Lawrence Livermore Laboratories
Bueters, K.A.	Combustion Engineering
Carpenter, Ronald C.	Armstrong Cork
Cernansky, Dr. Nicholas P.	Drexel University
Christiano, John P.	EPA, Office of Air Quality, Planning & Standards
Chu, Richard R.	EBASCO
Clark, Norman D.	C-E Air Preheater
Cleverdon, R.F.	Chevron Research Company
Cotton, Ernest	American Petroleum Institute
Creekmore, Andrew T.	EPA, Control Programs Development Division
Daughtridge, Jimmy T.	Pratt & Whitney Aircraft
Degler, Gerald H.	Systems Research Labs
Demetri, E.P.	Northern Research and Engineering Corporation
DeWerth, D.W.	American Gas Association Labs
Dingo, T.T.	General Motors
Donaldson, Thomas M.	EPA, Office of Air Quality, Planning & Standards
Dowling, Daniel J.	Union Carbide
Downey, Thomas A.	Gamlen Chemical Company
Dyer, T. Michael	Sandia Laboratories
Dygert, J.C.	Shell Development Company

LIST OF PARTICIPANTS (CONT'D)

Name	Representing
Dzuna, Eugene R.	Gulf Research & Development Company
Erskine, George	Mitre Corporation
Feng, C.L.	Selas Corporation of America
Fennelly, Paul F.	GCA/Technology Division
Fletcher, James	Industrial Combustion
Fletcher, Roy J.	Peabody Engineering Corporation
Freelain, Kenneth	Federal Energy Administration
Frisch, Dr. N.W.	Research-Cottrell
Fuhrman, Jr., Theodore C.	Erie City Energy Division
Gibbs, Thomas	EPA, Region IV
Goetz, Gary	Combustion Engineering
Goodley, Allan R.	California Air Resources Board
Graham, David J.	EPA, Office of Research and Development
Greene, Jack H.	EPA, Administrative Office
Grimshaw, Vincent C.	Process Combustion
Grossman, Ralph	Ralph Grossman, Ltd.
Hangebrauck, Robert P.	EPA, Energy Assessment and Control Division
Heck, Ronald	Englehard Industries
Hensel, Thomas E.	Turbo Power and Marine Systems
Holden, Edward A.	General Foods Corporation
Honea, Dr. Franklin I.	Midwest Research Institute
Howard, Jack B.	Massachusetts Institute of Technology
Hudson, Jr., James L.	Tampa Electric Company
Jackson, Dr. A.W.	Ontario Hydro
Jepson, Dr. A.F.	Environmental Measurements, Inc.
Karas, Dennis T.	East Chicago Air Quality Control
Kemmerer, Jeffrey	Fuller Company
Khan, M. Ali	East Chicago Air Quality Control
Khoo, Dr. S.W.	Canadian Gas Research Institute
Kloecker, J.F.	Erie City Energy Division
Kykendal, William	EPA, Process Measurement Branch
Lahre, Thomas	EPA, Office of Air Quality, Planning & Standards
Lange, Dr. Howard	Babcock & Wilcox
Lavoie, Raymond C.	Rohm & Haas Company
Lee, James E.	Facilities Engineering Command (U.S. Navy)
Lenney, Ronald J.	Ronald J. Lenney Associates
Levy, Arthur	Battelle-Columbus Laboratories
Lewis, F. Michael	Stanford Research Institute
Lii, Dr. C.C.	EPA, Combustion Research Branch
Lin, Donald J.L.	Forney Engineering Company
Locklin, David W.	Battelle-Columbus Laboratories
Lord, Harry C.	Environmental Data Corporation
Loweth, Carl	The Trane Company
Marshall, David	Babcock & Wilcox
Marshall, John H.	Combustion Engineering

LIST OF PARTICIPANTS (CONT'D)

Name	Representing
Marton, Miklos B.	IBM
Mayfield, D. Randell	EPA, Region IV
Meier, John G.	International Harvester, Solar Division
Moore, Douglas S.	Chevron Research Company
Moore, Edward E.	Eclipse, Inc.
Morton, William J.	E. Keeler Company
Moscowitz, Charles	Monsanto Research Corporation
Mosier, Stanley A.	Pratt & Whitney
Newton, Charles L.	Colt Industries
Nurick, W.H.	Rockwell International, Rocketdyne Division
Pantzer, Karl	Babcock & Wilcox
Pershing, David W.	University of Arizona
Pertel, Dr. Richard	Institute of Gas Technology
Renner, Ted	Fuel Merchants Association of New Jersey
Riley, Joseph	EPA, Region IV
Robert, J.	Canadian Department of Environment
Roberts, Dr. George	Englehard Industries
Robertson, J.F.	Crystal Petroleum Company
Roffe, Gerald	General Applied Science Laboratories
Rosen, Meyer	Union Carbide
Ross, Marvin	Lawrence Livermore Laboratory
Rulseh, Roy	Cleaver-Brooks
Sadowski, R.S.	Riley Stoker Corporation
Samples, J.R.	Union Carbide
Scott, Donald R.	Columbia Gas System Service Corporation
Sheffield, E.W.	TRW
Slack, A.V.	SAS Corporation
Smith, Lowell L.	KVB, Inc.
Spadaccini, L.J.	United Technology Research Center
Sterman, Sam	Union Carbide
Sullivan, Robert E.	General Motors
Swearingen, W.E.	Koppers Company
Takacs, Dr. L.	General Motors
Taylor, Barry R.	Massachusetts Institute of Technology
Utterback, Paul M.	Babcock & Wilcox
Van Grouw, Sam J.	KVB, Inc.
Vatsky, Joel	Foster-Wheeler Energy Corporation
Vershaw, Jim	The Trane Company
Watson, Raymond A.	Florida Power & Light Company
Webb, R.	The Trane Company
Weiland, J.H.	Texaco, Inc.
Weinberger, Dr. Lawrence	Mitre Corporation
White, David J.	International Harvester, Solar Division
White, James H.	Coen Company
White, Phil	Ventura Company

LIST OF PARTICIPANTS (CONT'D)

Name	Representing
Wiedersum, George C.	Philadelphia Electric Company
Wilhelm, Ronald	Aqua-Chem, Inc.
Wilson, Jr., R.P.	Arthur D. Little, Inc.
Winters, Harry K.	Ray Burner Company
Wittig, Dr. Sigmar L.K.	Purdue University
Woolfolk, Dr. Robert	Stanford Research Institute
Wright, Richard	Industrial Combustion
Young, Dexter E.	EPA, Control Programs Development Division
Ziarkowski, Stanley	Gamlen Chemical Company
Zielke, Robert L.	Tennessee Valley Authority
Zirkel, Eric C.	Armstrong Cork

LIST OF ORGANIZATIONS REPRESENTED

Name (Represented By)	Address
Acurex Corporation, Aerotherm Division (Mr. Anderson)	485 Clyde Avenue Mountain View, California 94042
American Boiler Manufacturers Association (Mr. Axtman)	1500 Wilson Boulevard, Suite 317 Arlington, Virginia 22209
American Gas Association Labs (Mr. De Werth)	8501 East Pleasant Valley Road Cleveland, Ohio 44131
American Petroleum Institute (Mr. Cotton)	1801 K Street, N.W. Washington, D.C. 20006
Apollo Chemical (Dr. Bennett)	35 South Jefferson Road Whippany, New Jersey 07981
Aqua-Chem, Inc. (Mr. Wilhelm)	P.O. Box 421 Milwaukee, Wisconsin 53201
Armstrong Cork Company (Mr. Carpenter, Mr. Zirkel)	Liberty & Charlotte Streets Lancaster, Pennsylvania 17604
Babcock & Wilcox (Mr. Barsin, Mr. Lange, Mr. Moore)	20 South Van Buren Avenue Barberton, Ohio 44203
(Mr. Utterback, Mr. Pantzer, Mr. Marshall)	P.O. Box 2423 North Canton, Ohio 44720
Baltimore Gas and Electric Company (Mr. Alvey)	2012 Gas and Electric Building Baltimore, Maryland 21203
Battelle-Columbus Labs (Mr. Ban, Mr. Barrett, Mr. Levy, Mr. Locklin)	505 King Avenue Columbus, Ohio 43201
C-E Air Preheater (Mr. Clark)	Andover Road Wellsville, New York 14895
California Air Resources Board (Mr. Goodley)	1709 11th Street Sacramento, California 95814
Canadian Department of Environment (Mr. Robert)	351 St. Joseph Boulevard Houll, Quebec, Canada
Canadian Gas Research Institute (Dr. Khoo)	55 Scarsdale Road, Don Mills Ontario, M3B2R3, Canada
Chevron Research Company (Mr. Cleverdon, Mr. D. Moore)	P.O. Box 1627 Richmond, California 94802

LIST OF ORGANIZATIONS (CONT'D)

Name (Represented By)	Address
Cleaver-Brooks (Mr. Rulseh)	3707 North Richards Street Milwaukee, Wisconsin 53201
Coen Company (Mr. J.H. White)	1510 Rollins Road Burlingame, California 94010
Colt Industries (Mr. Newton)	701 Lawton Avenue Beloit, Wisconsin 53511
Columbia Gas System Service Corporation (Mr. Scott)	1600 Dublin Road Columbus, Ohio 43215
Combustion Engineering (Mr. Bueters, Mr. Goetz, Mr. Marshall)	1000 Prospect Hill Road Windsor, Connecticut 06095
Crystal Petroleum Company (Mr. Robertson)	P.O. Box 4180 Corpus Christi, Texas 78408
Drexel University (Dr. Cernansky)	Philadelphia Pennsylvania 19104
EBASCO (Mr. Chu)	145 Technology Park Norcross, Georgia 30071
East Chicago Air Quality Control (Mr. Karas, Mr. Khan)	900 East Chicago Avenue East Chicago, Indiana 45312
Eclipse, Inc. (Mr. E. Moore)	1100 Buchanan Rockford, Illinois 61101
Englehard Industries (Mr. Blandford, Dr. Heck, Dr. Roberts)	Middlesex Turnpike, Wood Avenue Edison, New Jersey 08876
Environmental Data Corporation (Mr. Lord)	608 Fig Avenue Monrovia, California 91016
Environmental Measurements, Inc. (Dr. Jepsen)	2 Lincoln Court Annapolis, Maryland 21401
Environmental Protection Agency EPA - Administrative Office (Mr. Greene)	Research Triangle Park North Carolina 27711

LIST OF ORGANIZATIONS (CONT'D)

Name (Represented By)	Address
EPA - Combustion Research Branch (Dr. Bowen, Mr. Hall, Mr. Lachapelle Mr. Lanier, Dr. Lii, Mr. Martin, Mr. Wasser)	Research Triangle Park North Carolina 27711
EPA - Control Programs Development Division (Mr. Creekmore, Mr. Young)	Research Triangle Park North Carolina 27711
EPA - Energy Assessment & Control Division (Mr. Hangebrauck)	Research Triangle Park North Carolina 27711
EPA - Office of Air Quality, Planning, and Standards (Mr. Bauman, Mr. Christiano, Mr. Donaldson, Mr. Lahre)	Research Triangle Park North Carolina 27711
EPA - Office of Research and Development (Mr. Graham)	Washington, D.C. 20460
EPA - Process Measurement Branch (Mr. Kuykendal)	Research Triangle Park North Carolina 27711
EPA - Region IV (Mr. Biggs, Mr. Mayfield, Mr. Riley)	1421 Peachtree Street, N.E. Atlanta, Georgia 30309
Erie City Energy Division (Mr. Fuhrman, Mr. Kloecher)	1422 East Avenue Erie, Pennsylvania 16502
Exxon Research & Engineering Company (Mr. Bartok)	P.O. Box 8 Linden, New Jersey 07036
Federal Energy Administration (Mr. Freelain)	1200 Pennsylvania Avenue, N.W. Washington, D.C. 20461
Florida Power & Light Company (Mr. Watson)	P.O. Box 013100 Miami, Florida 33101
Forney Engineering Company (Mr. Lin)	P.O. Box 189 Addison, Texas 75001
Foster Wheeler Energy Corporation (Mr. Vatsky)	10 South Orange Avenue Livingston, New Jersey 07039
Fuel Merchants Association of New Jersey (Mr. Renner)	66 Morris Avenue Springfield, New Jersey 07081

LIST OF ORGANIZATIONS (CONT'D)

Name (Represented By)	Address
KVB Engineering, Inc. (Mr. L. Smith, Mr. Van Grouw)	6624 Hornwood Drive Houston, Texas 77036
E. Keeler Company (Mr. Morton)	Williamsport Pennsylvania 17701
Koppers Company, Inc. (Mr. Swearingen)	Koppers Building Pittsburgh, Pennsylvania 15219
Ronald J. Lenney Associates (Mr. Lenney)	2001 Palmer Avenue Larchmont, New York 10538
Arthur D. Little, Inc. (Mr. R.D. Wilson)	Acorn Park Cambridge, Massachusetts 02140
Lawrence Livermore Laboratories (Mr. Bowman, Mr. Ross)	P.O. Box 808 Livermore, California 94550
Massachusetts Institute of Technology (Mr. Howard, Mr. Taylor)	Massachusetts Avenue Cambridge, Massachusetts 02139
Midwest Research Institute (Dr. Honea)	425 Volker Boulevard Kansas City, Missouri 64110
Mitre Corporation (Dr. Weinberger, Mr. Erskine)	Westgate Research Park 1820 Dolly Madison Boulevard McLean, Virginia 22101
Monsanto Research Corporation (Mr. Moscowitz)	Station B. Box 8 Dayton, Ohio 45407
NOFI (Mr. Beals)	New York, New York
Naval Facilities Engineering Command, Southern Division (Mr. J. Lee)	2144 Melbourne Street P.O. Box 10068 Charleston, South Carolina 29411
New England Electric Systems (Mr. Batra)	20 Turnpike Road Weston, Massachusetts 01581
Northern Research & Engineering Corporation (Mr. Demetri)	219 Vassar Street Cambridge, Massachusetts 02139

LIST OF ORGANIZATIONS (CONT'D)

Name (Represented By)	Address
Fuller Company (Mr. Kemmerer)	124 Bridge Street Catasauqua, Pennsylvania 18032
GCA/Technology Division (Dr. Fennelly)	Burlington Road Bedford, Massachusetts 01730
Gamlen Chemical Company (Mr. Downey, Mr. Ziarkowski)	299 Market Street Saddle Brook, New Jersey 07662
General Applied Science Laboratories (Mr. Roffe)	Merrick & Stewart Avenues Westbury, New York 11790
General Foods - Technical Center (Mr. Holden)	250 North Street White Plains, New York 10625
General Motors Corporation (Mr. Sullivan)	5735 West 25th Street Indianapolis, Indiana 46224
(Mr. Dingo, Mr. Takacs)	Technical Center Warren, Michigan 48090
Gulf Research and Development Company (Mr. Dzuna)	P.O. Box 2038 Pittsburgh, Pennsylvania 15230
Honeywell, Inc. (Mr. Bonne)	Bloomington Minnesota 55420
IBM (Mr. Marton)	1000 Westchester Avenue White Plains, New York 10604
Industrial Combustion (Mr. Wright, Mr. Fletcher)	4465 North Oakland Milwaukee, Wisconsin 53211
Institute of Gas Technology (Dr. Pertel)	3424 South State Street Chicago, Illinois 60616
International Boiler Works (Mr. Blythe)	P.O. Box 498 East Stroudsburg, Pennsylvania 18301
International Harvester, Solar Division (Mr. Meier, Mr. D.G. White)	2200 Pacific Highway San Diego, California 92119

LIST OF ORGANIZATIONS (CONT'D)

Name (Represented By)	Address
KVB Engineering, Inc. (Mr. L. Smith, Mr. Van Grouw)	6624 Hornwood Drive Houston, Texas 77036
E. Keeler Company (Mr. Morton)	Williamsport Pennsylvania 17701
Koppers Company, Inc. (Mr. Swearingen)	Koppers Building Pittsburgh, Pennsylvania 15219
Ronald J. Lenney Associates (Mr. Lenney)	2001 Palmer Avenue Larchmont, New York 10538
Arthur D. Little, Inc. (Mr. R.D. Wilson)	Acorn Park Cambridge, Massachusetts 02140
Lawrence Livermore Laboratories (Mr. Bowman, Mr. Ross)	P.O. Box 808 Livermore, California 94550
Massachusetts Institute of Technology (Mr. Howard, Mr. Taylor)	Massachusetts Avenue Cambridge, Massachusetts 02139
Midwest Research Institute (Dr. Honea)	425 Volker Boulevard Kansas City, Missouri 64110
Mitre Corporation (Dr. Weinberger, Mr. Erskine)	Westgate Research Park 1820 Dolly Madison Boulevard McLean, Virginia 22101
Monsanto Research Corporation (Mr. Moscowitz)	Station B. Box 8 Dayton, Ohio 45407
NOFI (Mr. Beals)	New York, New York
Naval Facilities Engineering Command, Southern Division (Mr. J. Lee)	2144 Melbourne Street P.O. Box 10068 Charleston, South Carolina 29411
New England Electric Systems (Mr. Batra)	20 Turnpike Road Weston, Massachusetts 01581
Northern Research & Engineering Corporation (Mr. Demetri)	219 Vassar Street Cambridge, Massachusetts 02139

LIST OF ORGANIZATIONS (CONT'D)

Name (Represented By)	Address
Ontario Hydro Corporation (Mr. Booth, Dr. Jackson)	620 Union Avenue Toronto, Ontario, Canada M561X6
Peabody Engineering Corporation (Mr. R. Fletcher)	835 Hope Street Stamford, Connecticut 06907
Philadelphia Electric Company (Mr. Wiedersom)	2301 Market Street, S10-1 Philadelphia, Pennsylvania 19101
Pratt & Whitney Aircraft (Mr. Daughtridge, Mr. Mosier)	P.O. Box 2691 West Palm Beach, Florida 33402
Process Combustion Corporation (Mr. Grimshaw)	1675 Washington Road Pittsburgh, Pennsylvania 15228
Procter & Gamble Company (Mr. Beatty)	610 South Center Hill Road Cincinnati, Ohio 45224
Purdue University (Mr. Wittig)	West Lafayette Indiana 47907
Ralph Grossman, Ltd. (Mr. Grossman)	P.O. Box 70, Town of Mt. Royal Montreal, Canada H3P 3B8
Ray Burner Company (Mr. Winters)	1301 San Jose Avenue San Francisco, California 94112
Research-Cottrell, Inc. (Dr. Frisch)	P.O. Box 750 Boundbrook, New Jersey 08805
Riley Stoker Corporation (Mr. Sadowski)	9 Neponset Street Worcester, Massachusetts 01613
Rockwell International Corporation, Rocketdyne Division (Mr. Nurick)	6633 Canoga Avenue Canoga Park, California 91304
Rohm & Haas Company (Mr. Lavoie)	P.O. Box 584 Bristol, Pennsylvania 19007
SAS Corporation (Mr. Slack)	RFD #1 Sheffield, Alabama 35660

LIST OF ORGANIZATIONS (CONT'D)

Name (Represented By)	Address
Sandia Laboratories (Mr. Dyer)	Livermore California 94550
Selas Corporation of America (Mr. Feng)	Dresher Pennsylvania 19025
Shell Development Company (Mr. Dygert, Mr. Baker)	P.O. Box 481 Houston, Texas 77001
South California Edison (Mr. Bagwell)	P.O. Box 800 Rosemead, California 91770
Stanford Research Institute (Dr. Woolfolk, Mr. Lewis)	1611 North Kent Street Arlington, Virginia 22209
Systems Research Labs (Mr. Buechler, Mr. Degler)	2800 Indian Ripple Road Dayton, Ohio 45440
TRW, Inc. (Mr. Sheffield)	1 Space Park - R4/2020 Redondo Beach, California 90278
Tampa Electric Company (Mr. Hudson)	P.O. Box 111 Tampa, Florida 33601
Tennessee Valley Authority (Mr. Zielke)	524 Power Building Chattanooga, Tennessee 37401
Texaco, Inc. (Mr. Weiland)	P.O. Box 509 Beacon, New York 12508
The Trane Company (Mr. Loweth, Mr. Vershaw, Mr. Webb)	3600 Pammel Creek Road La Crosse, Wisconsin 54601
Turbo Power and Marine Systems (Mr. Hensel)	1690 New Britain Avenue Farmington, Connecticut 06032
Union Carbide Corporation (Mr. Rosen, Mr. Sterman)	Tarrytown Technical Center Tarrytown, New York 10591
(Mr. Dowling)	Box 180 Sistersville, West Virginia 26175

LIST OF ORGANIZATIONS (CONT'D)

Name (Represented By)	Address
Union Carbide Corporation (Mr. Samples)	Box 4361 South Charleston, West Virginia 25353
United Technologies Research Center (Mr. Spadaccini)	400 Main Street East Hartford, Connecticut 06040
University of Arizona (Mr. Pershing)	Tucson Arizona 85721
Ventura County A.P.C.D. (Mr. P. White)	740 East Main Street Ventura, California 93001

*U.S. GOVERNMENT PRINTING OFFICE: 1976-641-317/5514 Region No. 4